IAEA Nuclear Energy Series

No. NP-T-4.2

Hydrogen Production Using Nuclear Energy

IAEA
International Atomic Energy Agency

IAEA NUCLEAR ENERGY SERIES PUBLICATIONS

STRUCTURE OF THE IAEA NUCLEAR ENERGY SERIES

Under the terms of Articles III.A and VIII.C of its Statute, the IAEA is authorized to foster the exchange of scientific and technical information on the peaceful uses of atomic energy. The publications in the **IAEA Nuclear Energy Series** provide information in the areas of nuclear power, nuclear fuel cycle, radioactive waste management and decommissioning, and on general issues that are relevant to all of the above mentioned areas. The structure of the IAEA Nuclear Energy Series comprises three levels: **1 — Basic Principles and Objectives; 2 — Guides; and 3 — Technical Reports.**

The **Nuclear Energy Basic Principles** publication describes the rationale and vision for the peaceful uses of nuclear energy.

Nuclear Energy Series Objectives publications explain the expectations to be met in various areas at different stages of implementation.

Nuclear Energy Series Guides provide high level guidance on how to achieve the objectives related to the various topics and areas involving the peaceful uses of nuclear energy.

Nuclear Energy Series Technical Reports provide additional, more detailed, information on activities related to the various areas dealt with in the IAEA Nuclear Energy Series.

The IAEA Nuclear Energy Series publications are coded as follows: **NG** — general; **NP** — nuclear power; **NF** — nuclear fuel; **NW** — radioactive waste management and decommissioning. In addition, the publications are available in English on the IAEA's Internet site:

http://www.iaea.org/Publications/index.html

For further information, please contact the IAEA at PO Box 100, Vienna International Centre, 1400 Vienna, Austria.

All users of the IAEA Nuclear Energy Series publications are invited to inform the IAEA of experience in their use for the purpose of ensuring that they continue to meet user needs. Information may be provided via the IAEA Internet site, by post, at the address given above, or by email to Official.Mail@iaea.org.

HYDROGEN PRODUCTION USING NUCLEAR ENERGY

The following States are Members of the International Atomic Energy Agency:

AFGHANISTAN
ALBANIA
ALGERIA
ANGOLA
ARGENTINA
ARMENIA
AUSTRALIA
AUSTRIA
AZERBAIJAN
BAHRAIN
BANGLADESH
BELARUS
BELGIUM
BELIZE
BENIN
BOLIVIA
BOSNIA AND HERZEGOVINA
BOTSWANA
BRAZIL
BULGARIA
BURKINA FASO
BURUNDI
CAMBODIA
CAMEROON
CANADA
CENTRAL AFRICAN REPUBLIC
CHAD
CHILE
CHINA
COLOMBIA
CONGO
COSTA RICA
CÔTE D'IVOIRE
CROATIA
CUBA
CYPRUS
CZECH REPUBLIC
DEMOCRATIC REPUBLIC OF THE CONGO
DENMARK
DOMINICA
DOMINICAN REPUBLIC
ECUADOR
EGYPT
EL SALVADOR
ERITREA
ESTONIA
ETHIOPIA
FIJI
FINLAND
FRANCE
GABON
GEORGIA
GERMANY
GHANA
GREECE
GUATEMALA
HAITI
HOLY SEE
HONDURAS
HUNGARY
ICELAND
INDIA
INDONESIA
IRAN, ISLAMIC REPUBLIC OF
IRAQ
IRELAND
ISRAEL
ITALY
JAMAICA
JAPAN
JORDAN
KAZAKHSTAN
KENYA
KOREA, REPUBLIC OF
KUWAIT
KYRGYZSTAN
LAO PEOPLE'S DEMOCRATIC REPUBLIC
LATVIA
LEBANON
LESOTHO
LIBERIA
LIBYA
LIECHTENSTEIN
LITHUANIA
LUXEMBOURG
MADAGASCAR
MALAWI
MALAYSIA
MALI
MALTA
MARSHALL ISLANDS
MAURITANIA
MAURITIUS
MEXICO
MONACO
MONGOLIA
MONTENEGRO
MOROCCO
MOZAMBIQUE
MYANMAR
NAMIBIA
NEPAL
NETHERLANDS
NEW ZEALAND
NICARAGUA
NIGER
NIGERIA
NORWAY
OMAN
PAKISTAN
PALAU
PANAMA
PAPUA NEW GUINEA
PARAGUAY
PERU
PHILIPPINES
POLAND
PORTUGAL
QATAR
REPUBLIC OF MOLDOVA
ROMANIA
RUSSIAN FEDERATION
RWANDA
SAUDI ARABIA
SENEGAL
SERBIA
SEYCHELLES
SIERRA LEONE
SINGAPORE
SLOVAKIA
SLOVENIA
SOUTH AFRICA
SPAIN
SRI LANKA
SUDAN
SWAZILAND
SWEDEN
SWITZERLAND
SYRIAN ARAB REPUBLIC
TAJIKISTAN
THAILAND
THE FORMER YUGOSLAV REPUBLIC OF MACEDONIA
TOGO
TRINIDAD AND TOBAGO
TUNISIA
TURKEY
UGANDA
UKRAINE
UNITED ARAB EMIRATES
UNITED KINGDOM OF GREAT BRITAIN AND NORTHERN IRELAND
UNITED REPUBLIC OF TANZANIA
UNITED STATES OF AMERICA
URUGUAY
UZBEKISTAN
VENEZUELA
VIETNAM
YEMEN
ZAMBIA
ZIMBABWE

The Agency's Statute was approved on 23 October 1956 by the Conference on the Statute of the IAEA held at United Nations Headquarters, New York; it entered into force on 29 July 1957. The Headquarters of the Agency are situated in Vienna. Its principal objective is "to accelerate and enlarge the contribution of atomic energy to peace, health and prosperity throughout the world''.

IAEA NUCLEAR ENERGY SERIES No. NP-T-4.2

HYDROGEN PRODUCTION USING NUCLEAR ENERGY

INTERNATIONAL ATOMIC ENERGY AGENCY
VIENNA, 2013

COPYRIGHT NOTICE

Marketing and Sales Unit, Publishing Section
International Atomic Energy Agency
Vienna International Centre
PO Box 100
1400 Vienna, Austria
fax: +43 1 2600 29302
tel.: +43 1 2600 22417
email: sales.publications@iaea.org
http://www.iaea.org/books

Printed by the IAEA in Austria
March 2013
STI/PUB/1577

IAEA Library Cataloguing in Publication Data

Hydrogen production using nuclear energy. — Vienna : International Atomic Energy Agency, 2013.
p. ; 29 cm. — (IAEA nuclear energy series, ISSN 1995–7807 ; no. NP-T-4.2)
STI/PUB/1577
ISBN 978–92–0–135110–4
Includes bibliographical references.

1. Nuclear energy — Industrial applications. 2. Hydrogen as fuel — Research. I. International Atomic Energy Agency. II. Series.

IAEAL 13–00792

FOREWORD

One of the IAEA's statutory objectives is to "seek to accelerate and enlarge the contribution of atomic energy to peace, health and prosperity throughout the world." One way this objective is achieved is through the publication of a range of technical series. Two of these are the IAEA Nuclear Energy Series and the IAEA Safety Standards Series.

According to Article III.A.6 of the IAEA Statute, the safety standards establish "standards of safety for protection of health and minimization of danger to life and property". The safety standards include the Safety Fundamentals, Safety Requirements and Safety Guides. These standards are written primarily in a regulatory style, and are binding on the IAEA for its own programmes. The principal users are the regulatory bodies in Member States and other national authorities.

The IAEA Nuclear Energy Series comprises reports designed to encourage and assist R&D on, and application of, nuclear energy for peaceful uses. This includes practical examples to be used by owners and operators of utilities in Member States, implementing organizations, academia, and government officials, among others. This information is presented in guides, reports on technology status and advances, and best practices for peaceful uses of nuclear energy based on inputs from international experts. The IAEA Nuclear Energy Series complements the IAEA Safety Standards Series.

Nuclear generated hydrogen has important potential advantages over other sources that will be considered for a growing hydrogen share in a future world energy economy. Still, there are technical uncertainties in nuclear hydrogen processes that need to be addressed through a vigorous research and development effort. Safety issues as well as hydrogen storage and distribution are important areas of research to be undertaken to support a successful hydrogen economy in the future.

The hydrogen economy is gaining higher visibility and stronger political support in several parts of the world. In recent years, the scope of the IAEA's programme has been widened to include other more promising applications such as nuclear hydrogen production and higher temperature process heat applications. The OECD Nuclear Energy Agency, Euratom and the Generation IV International Forum have also shown interest in the non-electric applications of nuclear power based on future generation advanced and innovative nuclear reactors.

This report was developed under an IAEA project with the objective of providing updated, balanced and objective information on the current status of hydrogen production processes using nuclear energy. It documents the state of the art of the development of hydrogen as an energy carrier in many Member States, as well as its corresponding production through the use of nuclear power. The report includes an introduction to the technology of nuclear process heat reactors as a means of producing hydrogen or other upgraded fuels, with a focus on high temperature reactor technology to achieve simultaneous generation of electricity and high temperature process heat and steam. Special emphasis is placed on the safety aspects of nuclear hydrogen production systems.

This publication was compiled by K. Verfondern (Germany) based on evaluations of officially issued reports and published papers and presentations from major international conferences. The draft report was reviewed by the experts named at the end of the report. The IAEA officer responsible for this publication was I. Khamis of the Division of Nuclear Power.

EDITORIAL NOTE

This report has been edited by the editorial staff of the IAEA to the extent considered necessary for the reader's assistance. It does not address questions of responsibility, legal or otherwise, for acts or omissions on the part of any person.

Although great care has been taken to maintain the accuracy of information contained in this publication, neither the IAEA nor its Member States assume any responsibility for consequences which may arise from its use.

The use of particular designations of countries or territories does not imply any judgement by the publisher, the IAEA, as to the legal status of such countries or territories, of their authorities and institutions or of the delimitation of their boundaries.

The mention of names of specific companies or products (whether or not indicated as registered) does not imply any intention to infringe proprietary rights, nor should it be construed as an endorsement or recommendation on the part of the IAEA.

CONTENTS

SUMMARY

Energy has been universally recognized as one of the most important inputs for economic growth and human development. Economic growth implies the availability of cost effective and environmentally benign energy sources. A future energy economy will need to replace oil and reduce greenhouse gas emissions (GHGs) for climate protection. The worldwide interest in hydrogen as a clean fuel has led to comprehensive research, development and demonstration activities whose main objective is the transition from a fossil based to a "CO_2 lean" energy structure.

In fact, a major hydrogen economy already exists and is expected to grow at a rate of 4–10%/a. Current global hydrogen production is estimated at around 7×10^{18} J/a, corresponding to ~52.6 million t/a (higher heating value (HHV)) or ~630 billion Nm^3/a (as of 2006), which is about 2% of the world's total energy consumption. Significant amounts of hydrogen are produced in the fertilizer industry for the manufacture of ammonia. In the near future, hydrogen will play a large and growing role in the refining of petroleum products where the reserves of high quality light sweet crude oils are declining and the available crude stocks are becoming progressively heavier. These heavier crudes as well as the increasing share of 'dirty fuels' (heavy oils, coal, oil shale, tar sands) require larger amounts of both process heat and hydrogen to produce cleaner burning end point fuels with a higher hydrogen to carbon ratio.

A secondary market to develop in the medium term is that for hydrogen as a means of storing electrical energy, for example, the steadily increasing amounts of electricity produced by intermittent renewable energy sources. Hydrogen can be used to store this 'intermittent energy' during periods of weak consumption and to restore them during times of peak power demand.

The projection of the European Commission High Level Group shown in Fig. 1 offers a realistic scenario of the hydrogen market and the application areas.

The figure clearly shows that the largest near term markets will be the petrochemical industries, requiring massive amounts of H_2 for the conversion of heavy oils, tar sands and other low grade hydrocarbons, as well as the fertilizer and steel industries. Anything to liquid (XTL) processes for fuel production for the transportation sector have been gaining attention in recent years. However, the generation of Fischer–Tropsch liquid fuels from synthesis gas (H_2 + CO) — for example, derived from coal — produces significant CO_2 emissions. These could be reduced with carbon capture and storage (CCS) at the plant, with the net GHG emission rate being approximately the same as that for the crude oil products displaced.

Furthermore, it can be seen that the decrease of hydrogen consumption in these areas after 2025 coincides with the market introduction of new hydrogen applications such as in the transportation sector or as a distributed

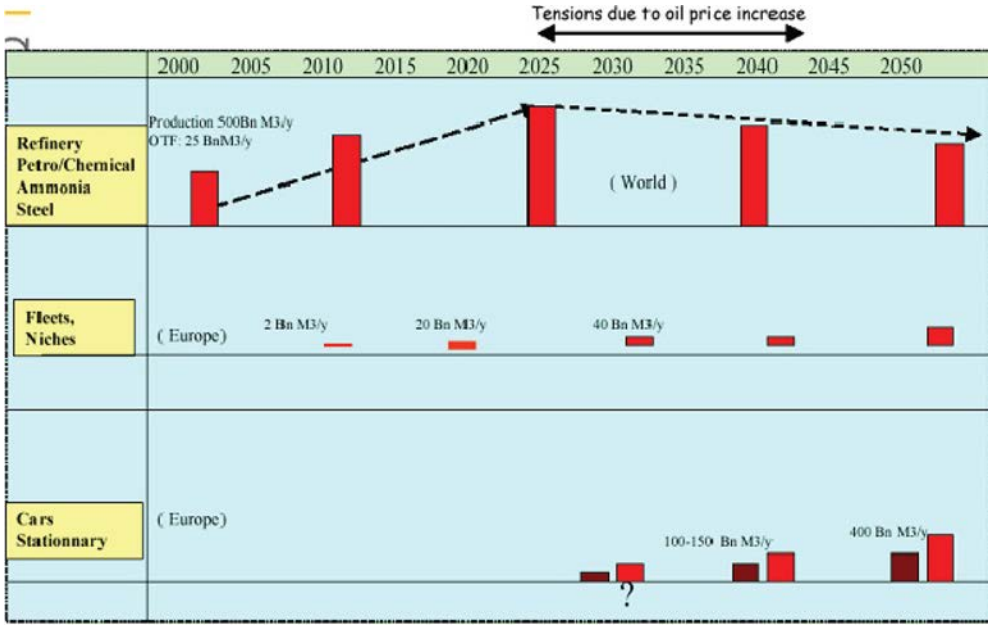

FIG. 1. Hydrogen production roadmap [1].

electrical energy source through the use of fuel cells. Liquid biofuel production needs external energy sources (heat and/or H_2). Hydrogen can be an energy storage system, an energy carrier or feedstock to liquid fuels production.

Hydrogen is omnipresent but not readily available: energy is required to extract it from chemical compounds. If hydrogen is to play a major role in a future energy economy, the whole spectrum of primary energies (fossil, nuclear, renewable) for its production must be considered. Different hydrogen production methods are given in Table 1, which lists the benefits and barriers of the different technologies.

The first step toward a hydrogen economy will always be based on existing technologies and established processes. In the near and medium terms, fossil fuels are expected to remain the principal source of hydrogen. Natural gas, the 'cleanest' fuel among the hydrocarbons, is expected to have advantages as a starting point for the initial hydrogen market (in the transition phase) as a source of hydrogen in terms of environmental impact (highest H:C ratio), availability and economy. In the long term, hydrogen production technologies will be strongly focused on CO_2 neutral or CO_2 free methods.

Hydrogen could provide a link between the electricity and liquid fuels markets. It can be generated from excess electricity produced by means of technologies with low operating costs and stored until needed. Hydrogen produced from off-peak electricity can be used for premium markets where the unique characteristics of hydrogen add value [2]. Peak electricity production from stored hydrogen can be provided today from gas turbines, which may be replaced in the future with high temperature fuel cell plants and/or liquid hydrogen (LH_2)–LOX steam generator cycles.

TABLE 1. BENEFITS AND BARRIERS OF HYDROGEN PRODUCTION TECHNOLOGIES [1]

Technology	Benefits	Barriers
Steam reforming: Splitting of hydrocarbons with heat and steam.	Well understood at large scale; commercially available with proven technology; widely available feedstock; highly economic at present; CO_2 sequestration at large scale; ideal for centralized production.	Small scale units not commercial; CO_2 emissions; H_2 contains some impurities; primary fuel may be used directly; subject to natural gas price fluctuations; in distributed form not yet verified.
Gasification: Splitting of heavy hydrocarbons and biomass into hydrogen and other gases for reforming.	Well understood at large scale; can be used for solids and liquids; abundance of (coal) resources.	Less hydrogen-rich than methane; lower efficiency; High levels of CO_2 emissions from coal; feedstock requires pretreatment; H_2 requires cleaning prior to use; biomass gasification still at pilot plant scale; low energy density of biomass.
Electrolysis: Splitting of water using electricity.	Well understood; commercially available with proven technology; high purity hydrogen; modular; convenient for renewable electricity; ideal for distributed production.	Electricity price strongly impacts cost of H_2; efficiency of whole chain is low; need for development of durable HTSE cells; competition with direct use of renewable electricity.
Thermochemical cycles: Splitting of water using inexpensive high temperature heat from nuclear or solar.	Potentially massive production at low cost; no GHG emissions; high efficiency (~50% expected); International collaboration on R&D and deployment.	Not commercial; aggressive chemistry; much R&D work still needed on process and materials technology; high capital cost; high temperature nuclear reactor deployment needed.
Biological production: Algae and bacteria produce hydrogen directly under certain conditions.	Potentially large resource; no feedstock required.	Slow hydrogen production rates; large area needed; low efficiency; appropriate organisms not yet found; still at R&D level.

Similar to electricity, hydrogen decouples the energy demand from the energy resources. It can enhance energy supply security in that individual countries can choose their own sources of energy. But hydrogen is not always an ideal vector to carry energy from its place of production to the end user, because a fairly high amount of energy is lost during handling, storage and transportation (Table 2). If the hydrogen is packaged in liquid synthetic fossil fuels, the overall energy consumption can be considerably lower [3].

Centralized energy production in large quantities favours the use of nuclear plants, which should operate as the baseload power source, whereas conventional plants would cover peak load. A principal advantage of a nuclear based energy supply is eliminating supply uncertainty and the sensitivity of energy prices to volatility of natural gas and other fuel prices. Nuclear, with virtually no emissions of airborne pollutants, appears to be an ideal option for large scale centralized H_2 production (Fig. 2).

TABLE 2. ENERGY AVAILABILITY [3]

Hydrogen stages of application		Energy cost in % of HHV
Production:	electrolysis	43
	on-site production	65
Packaging:	compression 20 MPa	8
	compression 80 MPa	13
	liquefaction	40
	chemical hydrides	60
Distribution:	road, 20 MPa, 100 km	6
	road, liquid, 100 km	1
	pipeline, 1000 km	10
Storage:	liquid, 10 d	5
Transfer:	20 MPa to 20 MPa	1

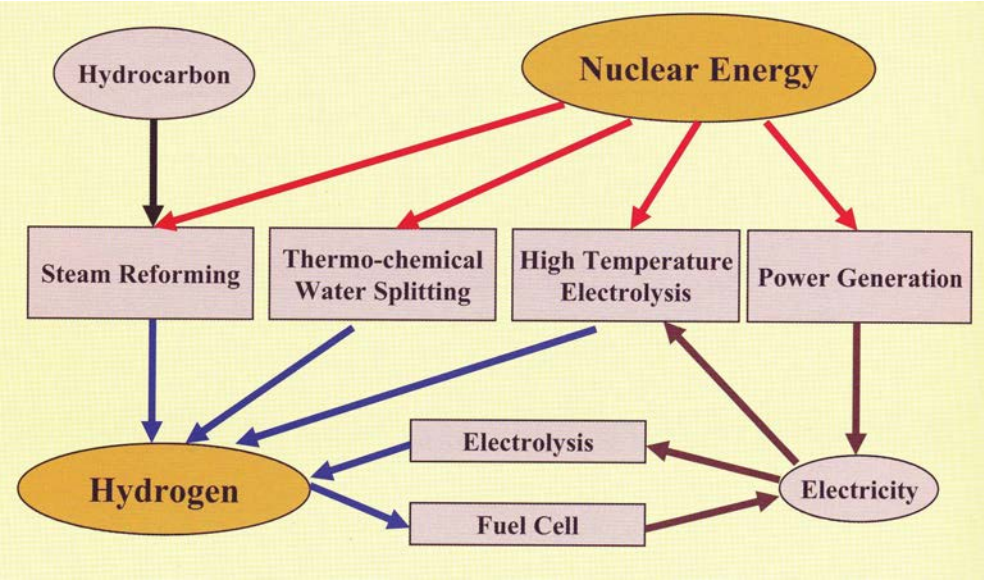

FIG. 2. Routes for nuclear assisted hydrogen production [4].

The future for hydrogen and the potential for nuclear generated H_2 will be driven by major factors such as:

— Production rates of oil and natural gas;
— Societal and governmental decisions on global climate change gases and CO_2 emissions;
— Need for savings of fossil resources for later use in environmentally friendly applications;
— Energy security from extended fuel reserves and independence of foreign oil uncertainties;
— The economics of large scale hydrogen production and transmission.

It is strongly recommended to extend the scope of future industrial activities on the market introduction of nuclear reactors within the spectrum of petrochemical processes. Nuclear cogeneration of heat and power (NCHP) can be considered, as a near term step, for a variety of existing industrial processes, which need electricity and large quantities of steam at different pressure and temperature (up to ~600°C) levels. High temperature gas cooled reactors (HTGRs) are the nuclear energy option to displace the use of natural gas and petroleum for industrial process heat and to reduce dependence on imported petroleum when integrated with coal conversion processes such as coal-to-liquid (CTL) to produce synthetic fuels. With the achievability of coolant outlet temperatures up to 950°C, HTGRs could expand the application range beyond electricity and steam generation to high temperature process heat, which is not directly open to other reactor types. The main incentive for the R&D work on the very high temperature reactor (VHTR) is its potential for industrial process heat applications, up to 850°C with the existing technology and higher temperatures in the longer term.

The introduction of a nuclear heat/steam source into an existing refinery consisting of many units promises enormous CO_2 reductions and resource savings, but requires on the other hand tremendous efforts. Heating furnaces must be adjusted or even replaced. The existing, highly optimized energy and mass flow structures must be reorganized. An important first step must be the successful operation of a chemical process plant coupled with a nuclear heat source and demonstration of the potential benefits. While this first step of using high temperature nuclear heat in refineries and chemical plants would primarily replace the existing use of natural gas as a heat source, next-step applications of high temperature nuclear heat could produce commodity chemicals such as hydrogen.

The main challenge at present is to include the production of hydrogen and combined heat and power applications by means of nuclear energy into the general energy strategies and to establish transition technologies from present industrial practice or emerging new resources (“dirty fuels”) in order to stabilize the cost for energy. The question of which energy source is to be utilized will ultimately be decided by the individual country in line with its domestic resources and methods on how to guarantee energy security. Cogeneration HTGR systems produce electricity, high temperature process heat for hydrogen production or other applications, and low temperature process steam if coupled with a desalination system. Reactor power is shared for electricity generation and process heat supply (Fig. 3).

If nuclear power as a substitute for traditional fossil fuels is to be realized in the future, further work is needed to enable nuclear technology to accommodate the various industrial needs. There is, however, no standard solution; each potential industrial customer needs a specific solution. Apart from demonstrating the economics of production and end use, requirements need to be met in terms of the consumer’s perception of availability and convenience, and last but not least, social acceptance both by the population and by the industry itself. A nuclear reactor operated in the heat and power cogeneration mode must be located close to the consumer and thus must have a convincing safety concept for the combined nuclear/chemical production plant. Both parts will be separated from each other by employing an intermediate heat exchanger as an interface component between the primary helium circuit of the reactor and the heat consuming system, e.g. a steam reformer/steam generator facility. The intermediate circuit serves the safety related purpose of preventing the primary coolant to flow through the conventionally designed heat-consuming plant and, on the other hand, allowing the gas produced to enter the nuclear reactor building. At the other end of the intermediate circuit, the thermal energy of the coolant is transferred to the hydrogen production plant through a process heat exchanger. For economic reasons, all necessary heat exchanger plants on the process side should be built, maintained and repaired according to conventional, not nuclear, specifications.

Although this assessment is mainly devoted to hydrogen production methods, it must be noted that, due to the complex interaction of the different chemical processes optimized to a very high degree, the potential supply of energy by nuclear power may not be dedicated to a specific process, but rather would cover the overall cogeneration of process steam, process heat and electricity. Any substitution of process heat in large scale industrial productions

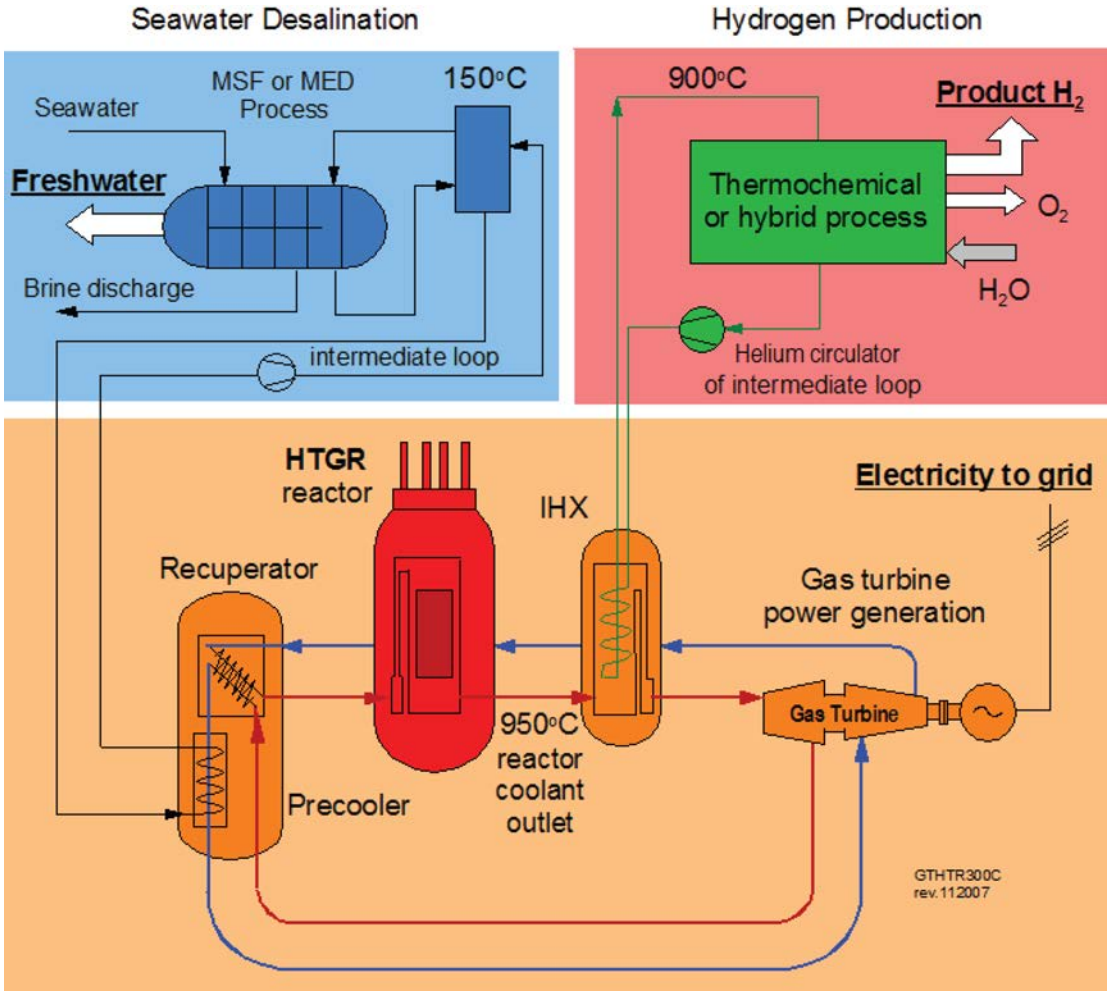

FIG. 3. HTGR cascade energy plant for efficient cogeneration of electricity, hydrogen, and fresh water.

by nuclear energy results in a complicated restructuring of the on-site energy supply system. But it promises significant CO_2 reductions and savings of fossil resources at competitive costs, which is the dominant challenge for future energy systems. This will include the generation of process steam and sensible heat for a variety of applications beyond dedicated hydrogen production.

A near term option of nuclear hydrogen production which is readily available is conventional low temperature electrolysis using inexpensive off-peak electricity from existing nuclear power plants. This, however, is available only if the share of nuclear in power production is large. But as fossil fuel prices increase, the use of nuclear outside baseload becomes more attractive. The main disadvantage is the very low efficiency from today's reactors, making it unattractive for H_2 production, although it is a proven and clean technology. Optimization and adaptation of the electrolysis process in combination with HTGR may improve the relatively low thermal efficiency of the electrolysis path. To demonstrate the order of magnitude: a 500 000 kg/d H_2 generation plant capable of serving around 1 million fuel cell vehicles, if based on nuclear power and low-temperature electrolysis, would require 500 of the largest electrolyser units available today consuming a total of about 1 GW of electric power.

Nuclear steam reforming is another important near term option for both the industrial and the transportation sectors, since development of the principal technologies and their demonstration in pilot-scale plants was done in Germany and Japan. It promises a saving potential of some 35% of methane feedstock but is surely not a sustainable method. In connection with the steam reformer development, the closed-cycle EVA/ADAM chemical energy transportation system based on H_2 was successfully demonstrated.

The competitiveness of nuclear steam reforming will benefit from the increasing cost of natural gas. It is compatible with a realistic evolution of actual industrial practice and could fully meet the process heat

requirements. The economics of this process will be much more favourable compared with electrolysis as long as natural gas is available at a reasonable cost. Although the process is not free of CO_2 emissions, it is justified within a medium (for natural gas importing countries) to long term transition period toward a less polluting approach with inherently higher cost.

Coal is a viable option for making hydrogen in large, centralized plants [5]. Nuclear coal gasification for conversion of coal into substitute natural gas (SNG) for direct use, synthesis gas for the production of methanol or other hydrocarbons, heating gas for residential heating purposes, reduction gas, e.g. for the direct reduction of iron ore, or hydrogen as a raw material and universal energy carrier can be used economically under certain conditions depending mainly on the location, the cost of coal, and the product and its price compared with the competitors, natural gas and crude oil. A wide variety of coal gasification processes has been developed and demonstrated. Allothermal steam–coal gasification simulating the nuclear heat source has been examined in numerous experiments up to pilot scale.

A CO_2 emission free option is high temperature electrolysis, which reduces the electricity needs up to about 30% and could make use of high temperature heat and steam from an HTGR. This needs a much more complex economic evaluation as compared to dedicated hydrogen and dedicated electricity producing plants and opens room for significant cost reductions. Research and development needs for HTSE will surely capitalize on the solid oxide (high temperature) fuel cell development, having some technology elements in common. In addition, coupling of the HTSE process to CTL is of advantage because it provides both hydrogen and oxygen at elevated temperatures, where the O_2 can be directed to a gasifier and the H_2 could be used to reduce the excess CO_2 produced via the reverse shift reaction.

Coupling to HTGRs is feasible and possesses optimization potential toward allothermal high temperature electrolysis and more efficient combined cycle HTGR designs. The use of nuclear generated electricity in off-peak periods from existing LWRs may become economically competitive, but the stranded capital costs of the electrolysers during periods of peak electricity prices may be prohibitive.

With respect to thermochemical water splitting cycles, the processes which are receiving the most attention are the sulphur–iodine (S–I), the Westinghouse hybrid and the calcium-bromine (UT-3) cycles. Efficiencies of the S–I process are in the range of 33–36% if operated at 950°C which is judged as a feasible upper temperature limit for the reactor and related heat transfer devices. Under the same conditions, the Brayton cycle may reach ~50% and could be combined with electrolysers having a conversion ratio greater than 90%. Thus, this process will have an overall efficiency of greater than 45% depending on the electrolyser performance.

Process optimization and material qualification still require considerable R&D efforts with regard to the potential of higher efficiencies and more compact chemical reactors to be optimized for commercial use. The S–I process will benefit from the medium term progress in HTGR and materials technology as well as from non-nuclear activities on thermochemical water splitting (e.g. by solar energy) thus remaining a long term option for commercial applications and a typical Generation IV R&D objective.

Both thermochemical and HTSE processes introduce new considerations into the design, licensing and operation of combined nuclear–chemical plants that must also be considered in the technology selection process. Many supporting systems will be common to both the nuclear and hydrogen plants, while the high temperature heat exchanger and the materials associated with thermal transfer will be specific to each production process. The final decision on which water splitting cycle is the one with lowest cost and lowest technical risk will be dependent on efficiency and complexity, but also on factors like excessive temperature or pressure requirements, and highly toxic or corrosive materials. Technical and economic feasibility, however, remains to be demonstrated, since these H_2 production processes have not yet been tested beyond the pilot plant scale. The study of other heat transfer media like molten salts or liquid metals may help to adopt the chemical processes better to HTGR applications. For the evaluation of efficiencies, both thermochemical processes and electricity generation in combination with electrolysis are finally governed by the Carnot law, meaning that operational temperatures of the process and the heat source should be as high as technically feasible. This makes HTGRs more appropriate than other reactor types, because heat requirements ideally fit with heat available from the reactor.

The most significant product that an HTGR can deliver in the near term is steam to be used in various industries. Steam pressure is much higher than what is normally produced by LWRs and thus gives a significant advantage to HTGRs. Decoupling of process steam can be done via a steam–steam intermediate heat exchanger, the so-called steam converter. The average heat process needs for applications in the steam class are more in the low power range of 20–40 MW(th) for a single process. An HTGR unit in the order of 250–600 MW(th) would be used

to supply a steam network. Nuclear process steam production from an advanced HTGR may actually represent a reasonable first step to be demonstrated on a commercial scale, before tackling the more ambitious goal of nuclear hydrogen from high temperature electrolysis or thermochemical cycles.

In industrial processes, energy supply is of the utmost importance. The market for process heat is huge and hardly penetrated by nuclear. With respect to the large variation in the quantity of energy demand and to the wide spectrum of operational parameters, a small modular type size and a flexible design of a nuclear unit are necessary to meet customers' requirements. Also the security of energy supply is essential, demanding a very high degree of reliability and availability. Particularly in large establishments, the supply of heat/steam must be highly reliable, with basically not more than a month of maintenance within a five year operation period for the petrochemical and refining industries. This can only be ensured by sufficient reserve capacity, which makes a modular arrangement of electricity or heat producing plants appropriate.

There will also be a strong demand of high reliability for desalination plants, but it will be lower compared to process heat. Methanol, as an example, is a convenient energy carrier to handle. If the CO_2 needed for its synthesis is taken from other processes where it was released ('double use of CO_2'), CO_2 emissions could be further reduced.

Coolant outlet temperatures of up to 1000°C have been discussed but are considered to be beyond the current capability of metallic materials. A reasonable interim step in VHTR development is a plant at a reduced gas outlet temperature of 750°C. Reduction in the outlet temperature to 750°C relieves the impact on materials and changes the safety margins for fuel quality compared to the higher temperatures. Higher temperatures may be considered but will be at the expense of a significantly reduced lifetime for the respective components.

A new, perhaps revolutionary nuclear reactor concept of the next generation will offer the chance to deliver, besides the classical electricity, also non-electrical products such as hydrogen or other fuels (e.g. methanol). In a future energy economy, hydrogen as a storable medium could adjust to a variable demand for electricity by means of fuel cell power plants and also serve as spinning reserve. Both together offer much more flexibility in optimizing energy structures (e.g. substitution of natural gas fired peaking plants by hydrogen). Prerequisites for such systems, however, would be competitive nuclear hydrogen production, large scale (underground) storage at low cost and economic fuel cell plants. The utilization of oxygen (rather than air) co-produced in the water splitting processes would improve the efficiency of fuel cell operation significantly, thus further reducing costs.

In various countries, ambitious programmes are ongoing within the Generation IV International Forum (GIF) initiative, with the main objective being to bring nuclear hydrogen production to the energy market. Numerous institutions are active in the first stage of demonstrating the viability of nuclear hydrogen production, to be followed by the stages of performance testing and demonstration of the pursued technologies. Both China and Japan are operating HTGR test reactors and offer international collaboration on utilizing these tools to further demonstrate HTGR principles and, at a later stage, nuclear hydrogen production.

Future activities on nuclear process heat could also benefit from a re-evaluation of the studies conducted in the past on HTGR process heat applications by comparing against current technologies and market conditions. The goal should be to select promising applications under the current industrial practice within existing and evolving markets. Superior safety features and high reliability are considered prerequisites for the introduction of nuclear process heat and nuclear combined heat and power.

The coupling of a nuclear reactor to a hydrogen production plant located in a chemical complex requires special attention with regard to safety, regulatory aspects and licensing. There is a need for nuclear process heat reactors to have a common international approach to safety issues related with hydrogen such as explosions and fires, confinement and limits of contaminants (e.g. tritium); and reliable isolation of both nuclear and chemical plants. To minimize tritium contamination, it will be essential to keep the fraction of defective/failed TRISO coated fuel particles and the level of ^{3}He and Li impurities as low as possible, and to properly design the purification system capacity. Current safety requirements, basically orientated to LWR nuclear plants, must be modified to Generation IV and new reactors for hydrogen production which are inherently safe, reliable and simple to operate. This will help the industrial deployment, coordinate the licensing process, and reduce the uncertainties to obtain agreement by national and local authorities of the hydrogen/nuclear facilities.

The introduction of nuclear energy into the heat or combined heat and power (CHP) market is of a global dimension, since both nuclear and potential end users are already global players. Thus, the demonstration of the coupling of a nuclear heat source to an industrial complex should take place on a global level. This needs political and co-funding support for R&D and efforts to establish an international public/private partnership and to overcome the 'cultural gap' between the nuclear and the end user communities.

Whatever the nuclear technological and political challenges are, the public needs to be assured that the highest standards of safety, security and environmental protection will continue to be applied. This is achieved through extensive research, development, demonstration and deployment programmes conducted by an alliance of researchers, vendors, operators, customers and politicians.

1. INTRODUCTION

1.1. WORLD ENERGY SITUATION

In 2007, the world's total primary energy supply was more than 12 billion tonnes of oil equivalent (toe)[1]. The breakdown by energy resources as given in Fig. 4 (left) shows a dominant contribution of 81% by the fossil fuels. Nuclear represented 6% of the total energy supply, thereby reducing global CO_2 emissions by nearly 10%, which means that worldwide more than 80% of the total primary energy consumption increased CO_2 emissions. From the total amount of primary energy supply, about 8.5 Gtoe was transformed into final consumption energy, the remainder being conversion and distribution losses or use by the energy industries. Breakdown of the final energy consumption was mainly accounted for by the transport sector (28%), the domestic sector (34%) and the industrial sector (36%). In terms of fuels consumed, the share of oil is on the decline (43%), while electricity generation is strongly rising, having reached a share of 17% in 2007 [6]. All countries have their own specific energy requirements, which differ in demand, growth, alternatives, financing options and preferences, and therefore prefer their own energy mix.

The role of electricity is increasing because it is an extremely versatile energy carrier which can be generated from a wide range of fuels. The world's total electricity generation in 2007 was about 19 800 TW·h with fuel shares of 41% from coal, 20% from gas, 6% from oil, 14% from nuclear, 16% from hydro and the remaining 2% from other renewables (Fig. 4 (right)). These figures also show a strong carbon based economy character, with worldwide 67% of the electricity generated from fossil fuels, and thus increasing CO_2 emissions. According to the reference energy scenarios of the International Energy Agency (IEA), coal will remain the dominant fuel worldwide, but natural gas based electricity generation will rapidly increase. In the Organisation for Economic Co-operation and Development (OECD) countries, about 2000 GW of new generating capacity will be needed, with about one third to replace old plants.

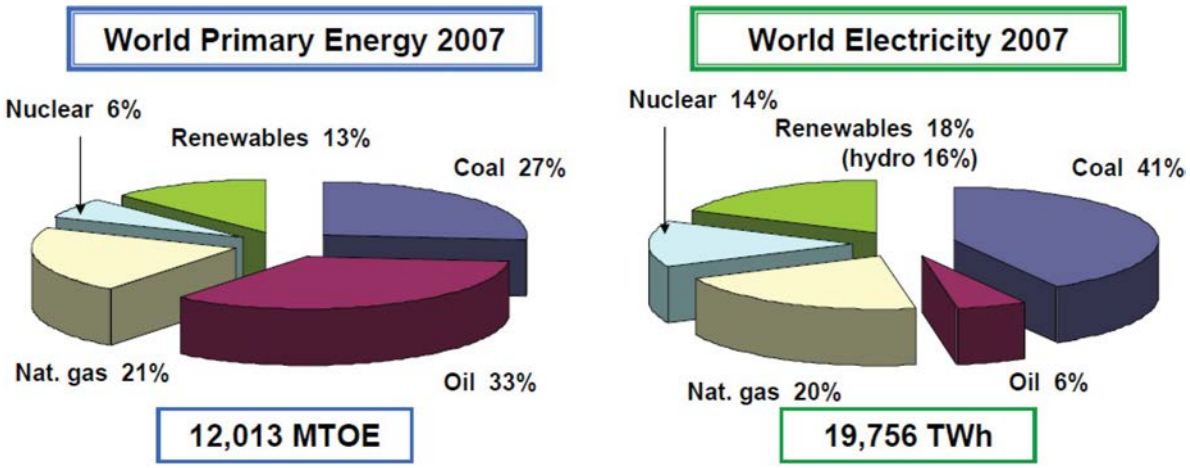

FIG. 4. IEA key world energy statistics 2007 [7].

[1] 1 toe corresponding to the energy content of 7.4 barrels of oil = 1.428 tce (tonne of coal equivalent) = 39.68 million Btu (British thermal unit) = 41 868 MJ = 11 630 kW·h.

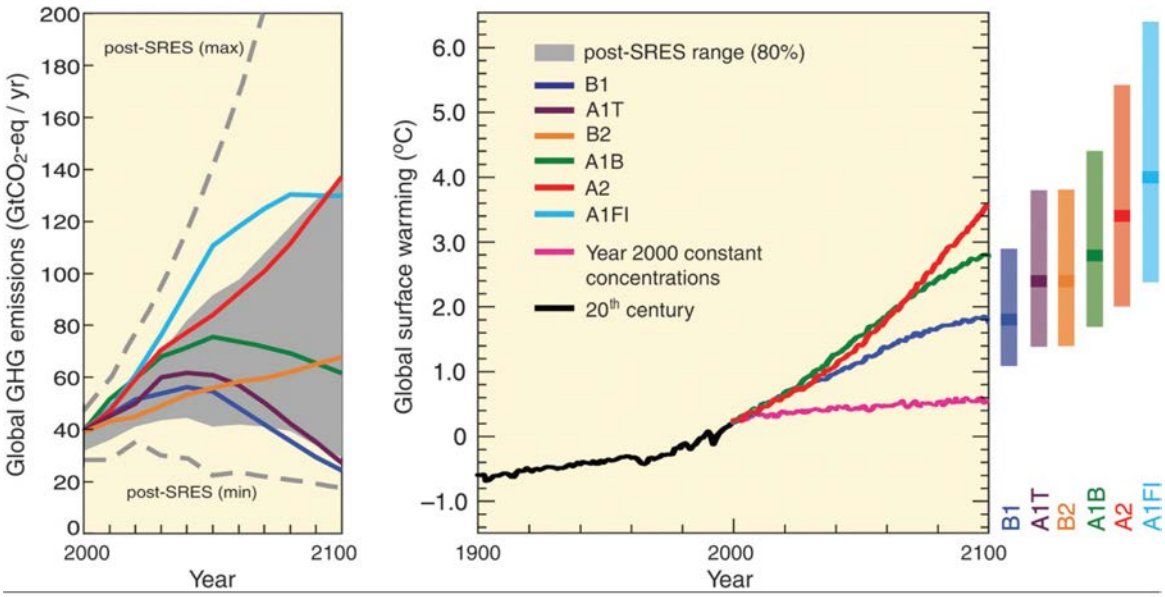

A1: rapid economic growth and rapid introduction of new and efficient technologies
(A1F1: fossil-intensive; A1T: non-fossil resources; A1B: balance across all sources)
A2: high population growth, slow economic development, slow technological change
B1: more rapid changes in economic structures toward a service and information economy
(SRES = IPCC Special Report on Emissions Scenarios, 2000)

FIG. 5. Global emission of GHGs (CO_2, CH_4, N_2O, F gases) (left); average of surface warming projection (right) for six IPCC emission scenarios which do not include climate policies in addition to current ones [8].

Since the electricity share in final energy consumption is less than 20% worldwide, as mentioned above, CO_2 emission free sources of energy may find new markets, for example, in the transportation sector, whether directly (electric cars) or indirectly (fuel cells). Nuclear power may play here a major role in the non-electric sector in delivering electricity, but also may become important as a provider of process heat in a great variety of industrial processes, including the large scale production of hydrogen.

Energy demand in the world depends on population growth and economic development; it will therefore be inhomogeneous in terms of quantity and quality. World primary energy breakdown by application is 18% electricity, 55% heat and 27% transportation. Energy sources have to be considered from the perspectives of pollution, the gradual depletion of natural resources and import dependency. The most realistic scenario of the IEA for 2050 is as follows: the world population will be approximately 8.5 billion and the primary energy supply will almost double, compared to 2007, to reach 23 Gtoe.

The strong influence of global energy use on economic development became obvious with the global financial crisis in 2008–2009 and the subsequent recession. World energy demand, and consequently CO_2 emissions, plunged with the economic contraction, for the first time since 1981. Under current policies, however, it will quickly resume its long term upward trend once economic recovery is under way.

Greenhouse gas emissions are being studied by the Intergovernmental Panel on Climate Change (IPCC), which was established by the World Meteorological Organization and the United Nations Environment Programme to assess scientific, technical and socioeconomic information relevant for understanding climate change, its potential impacts, and options for adaptation and mitigation. With publishing their 4th assessment report in 2007 [8], intensive public debates were restarting on the effects of anthropogenic emissions of GHGs on the climate. Based on continued current climate policies with a dominant role of fossil fuels, the IPCC emission scenarios project a further growth of GHG emissions of 25–90% between 2000 and 2030. For some of the scenarios, this would result in a global warming at a rate of 0.2°C per decade by 2030 (Fig. 5) [8].

According to the IPCC, the total primary energy consumption means releasing into the atmosphere approximately 7.25 billion t of energy related CO_2 per year. From this amount, about half remains in the atmosphere (today: 380 ppm, compared to 280 ppm before 1750) and half comes back to the earth. This anthropogenic CO_2 release exceeds the balancing effect of sinks and results in a gradual accumulation in the atmosphere.

The CO_2 release from energy consumption has its geographical origin in the OECD countries (53%), in transition economies (36%) and in developing countries (11%). The emissions per sector of human activity are 40% in electricity production (primarily coal fired plants); 21% in transport; 14% in buildings; 17% in industry; and 8% in other sectors.

CO_2 emissions have increased greatly since the turn of the century (Table 3). Some of the industrial and emerging countries are showing high growth rates. Two countries, China and the USA, account for 42% of the total CO_2 emissions, while only a few of the EU Member States and the Russian Federation exhibit decreasing rates. And global CO_2 emissions will continue to increase. With 31.5 billion t of CO_2 emissions in 2008, the tenth world record in a row was set [9].

The Copenhagen Accord of December 2009 confirmed the continuation of the Kyoto Protocol and the United Nations Framework Convention on Climate Change. It set a maximum of 2°C average global temperature rise, and states that a review by 2016 should consider if it will be necessary to limit warming to 1.5°C. Countermeasures for a reduction in CO_2 would include increasing the use of non-fossil energies such as nuclear and renewable energy. Currently under investigation is the development of new technologies for carbon capture and sequestration, but also for carbon capture and reuse (CCR) as a chemical feedstock in different applications [10].

1.2. HYDROGEN AS AN ENERGY CARRIER

Hydrogen has been used as a chemical for decades, can be produced from various resources, and is used in many different applications. In the world energy economy of the future, it may serve as a universal energy carrier, where it will compete with electricity and hydrocarbons. These three energy carriers will coexist, but most certainly with changing ratios. During the transition period toward a hydrogen based economy, the production of synthetic hydrocarbon fuels will certainly still be dominating. This intermediate stage will be characterized by enhanced production of synthetic fuels through the conversion of fossil fuels. Adding hydrogen into the transformation process improves the CO_2 balance.

The general requirements for an innovative energy system are availability, economic production, transportability, storability, transformability into other forms of energy and environmental friendliness. Hydrogen is an alternative energy carrier that meets most of these requirements. Hydrogen can contribute to both energy security and environmental compatibility. A market for hydrogen already exists for specific industrial energy needs (fertilizer production, oil refining, etc.) and is growing at a rapid pace. Markets may grow further in the future with the expansion of cogeneration of heat and power and to use as a fuel in fuel cell applications. Important benefits of hydrogen are expected from the operation of zero-emission vehicles for local (urban) air quality improvement and from its use as flexible, autonomous energy supply in remote areas or for portable/mobile applications.

TABLE 3. THE TEN LARGEST CO_2 EMITTING COUNTRIES AS OF 2008 [9]

Country	CO_2 in 1990 (million t)	CO_2 in 2008 (million t)	Relative change 1990–2008 (%)	Kyoto goal by 2012 (%)
China	2452	6809.7	+178	—
USA	5461	6369.8	+17	–7[a]
Russian Federation	2369	1687.6	–29	0
India	626	1408.5	+125	—
Japan	1179	1391.5	+18	–6
Germany	1029	857.3	–17	–21
Republic of Korea	257	663.5	+158	—
Canada	485	658.3	+44	–6
United Kingdom	625	581.8	–7	–12.5

[a] The USA participated in the Kyoto Summit in 1999 but did not ratify the Kyoto protocol.

Both electricity and hydrogen will become highly important energy carriers in the future. Both are efficient and easy to handle, and have near-zero emissions when used, assuming they are of non-fossil origin. Electricity (electrons) and hydrogen (protons) form complementary and synergetic options for transferring and storing energy for different end uses. They are in a certain way exchangeable, although conversion losses occur. Both together are also complementary to each other in that either one is superior to the other in certain aspects, offering much more flexibility in optimizing energy structures on a macro scale (e.g. substitution of hydrogen for natural gas fired peaking plants). Hydrogen combined with the reuse of abundantly available CO_2 to produce liquid synthetic fuels may also contribute to a reduction of CO_2 emissions. Hydrogen or hydrogen-rich liquid fuel (e.g. methanol) can be converted to electricity for transport purposes via fuel cells. Decentralized hydrogen production systems can be established via electrolysis if inexpensive (CO_2 free) electricity is available (e.g. off-peak nuclear power). A new hydrogen market may be first introduced and prepared via the electricity sector.

But hydrogen will also be able to take on a role in energy storage. Due to the steadily increasing share of wind and solar energy, with their distributed and intermittent character, the resulting fluctuations in electricity generation will require efficient management to balance the power system, which becomes more complex as the number of power sources grows. Therefore intelligent solutions for large scale storage are required in a future energy economy [11]. Also for transportation of energy to the consumer, it will, under certain circumstances, be practical to convert the energy to hydrogen.

Water and biomass are expected to be the main sources for hydrogen in the future, with the necessary process heat for extracting the hydrogen to be provided by CO_2 emission free energy sources. With respect to hydrogen production on a large scale at a constant rate, nuclear energy may play an essential role.

But before a major introduction of a new form of energy into the market will take place, it must be accepted by the consumer. The typical consumer of energy expects a decent energy supply system that provides energy any time and any place, in any quantity and of any type, in a safe, user friendly and environment friendly way. Plus, it must be inexpensive.

1.3. NUCLEAR ENERGY

It is more than 50 years ago, in 1954, that the first commercial nuclear power station, the Obninsk reactor near Moscow, started its operation, producing 5 MW(e). Five decades of development since then have made nuclear power an industrially mature and reliable source of energy and a key component in the world's energy economy (Fig. 6). In 31 of the 191 United Nations Member States, nuclear power plants are being operated for commercial electricity production. According to the World Nuclear Association, as of 1 October 2010, 441 nuclear power plants, with a total capacity of 376.3 GW(e) were in operation, with 58 more nuclear stations and an additional capacity of 60.5 GW(e) under construction [12]. Of 31 newly constructed nuclear plants, 11 were small or medium-sized plants. More than 44 GW of nuclear capacity have gone on-line since 1990, and many countries are currently considering nuclear as a realistic option within their national energy policy.

Six countries — the United States of America (USA), France, Japan, Germany, the Russian Federation and the Republic of Korea — produce about 70% of the nuclear electricity in the world. In 16 countries, nuclear power provides more than 25% of the electricity. Nuclear is a proven technology that provides clean electricity at predictable and competitive prices with approximately 14 000 reactor-years (as of 2010) of accumulated operating experience, generating a total of some 6000 TW·h.

Nuclear expanded steadily until the mid-1980s, when it began levelling out or even declining (Fig. 6). As an example, in October 2007, 15 of the 27 countries of the European Union (EU27) operated 146 reactors, down from 151 units in 2003 and 177 reactors in 1989. The major reasons were [14]:

— Energy efficiency improvements in power plant operation;
— Economic restructuring;
— A significant drop in electricity demand;
— Excess generating capacity;
— Oil price collapse;
— Highly efficient gas turbine technology;
— Liberalization and privatization of electricity market;

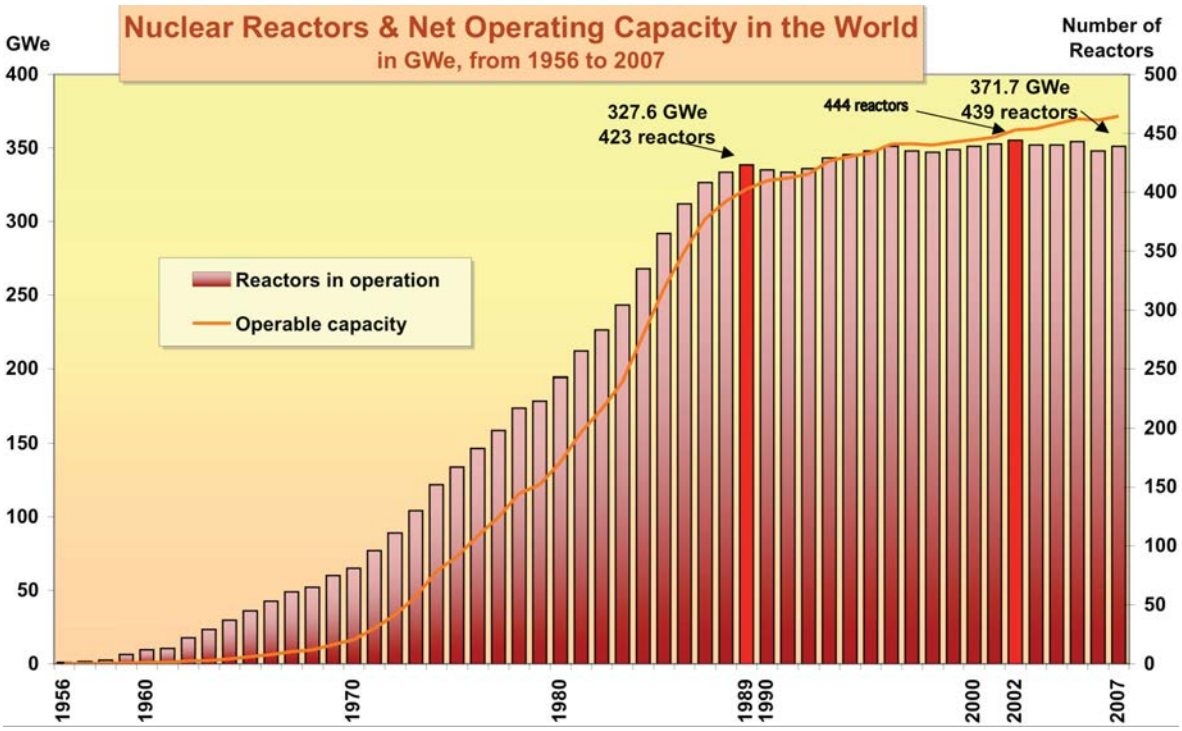

FIG. 6. Nuclear reactors in operation worldwide [13].

— Regulatory intervention after the accident at Three Mile Island;
— The accident at Chernobyl.

The flattening was compensated by increased availability corresponding to 34 virtual LWRs. There are, however, signs of rising expectations in the past few years. At present, nuclear power output grows in all major regions except Europe, but its share in world electricity generation is decreasing slightly. According to an IAEA projection for 2030, the expected nuclear capacity is 473 GW(e) for the "IAEA low projection" and ~750 GW(e) for the "IAEA high projection" [14].

Economic baseload production of electricity makes nuclear energy competitive with fossil fuelled power plants, with the comparatively low fuel cost helping to stabilize the price of electricity within the energy mix. It helps to save fossil fuel resources and to extend their availability. As an energy source with no GHG emissions and as a means to improve national energy security, nuclear thus contributes to 'sustainable' development.

To keep the nuclear option alive in a longer term perspective, the nuclear industry not only has to continue operating the existing plants at that high level of safety and reliability, it also has to steadily develop the next generation of nuclear power plants to meet the more and more insistent concerns of the public about safety. Studies show that there is a high potential for innovative nuclear techniques, systems and concepts that can offer socially acceptable, environmentally benign and competitive solutions.

1.4. DRIVERS FOR NUCLEAR ASSISTED HYDROGEN PRODUCTION

Centralized energy production in large quantities favours the use of nuclear plants, which should operate in baseload mode, with conventional plants covering peak load. Nuclear emits virtually no airborne pollutants. Therefore, it appears to also be an ideal option for large scale centralized hydrogen production. Figure 7 shows the broader picture of where nuclear energy fits in into the major energy sectors, with the aim of reducing CO_2.

The future of hydrogen and the potential for nuclear generated H_2 will be driven by major factors such as:

— Production rates of oil and natural gas.
— Societal and governmental decisions concerning global climate change due to GHG emissions.

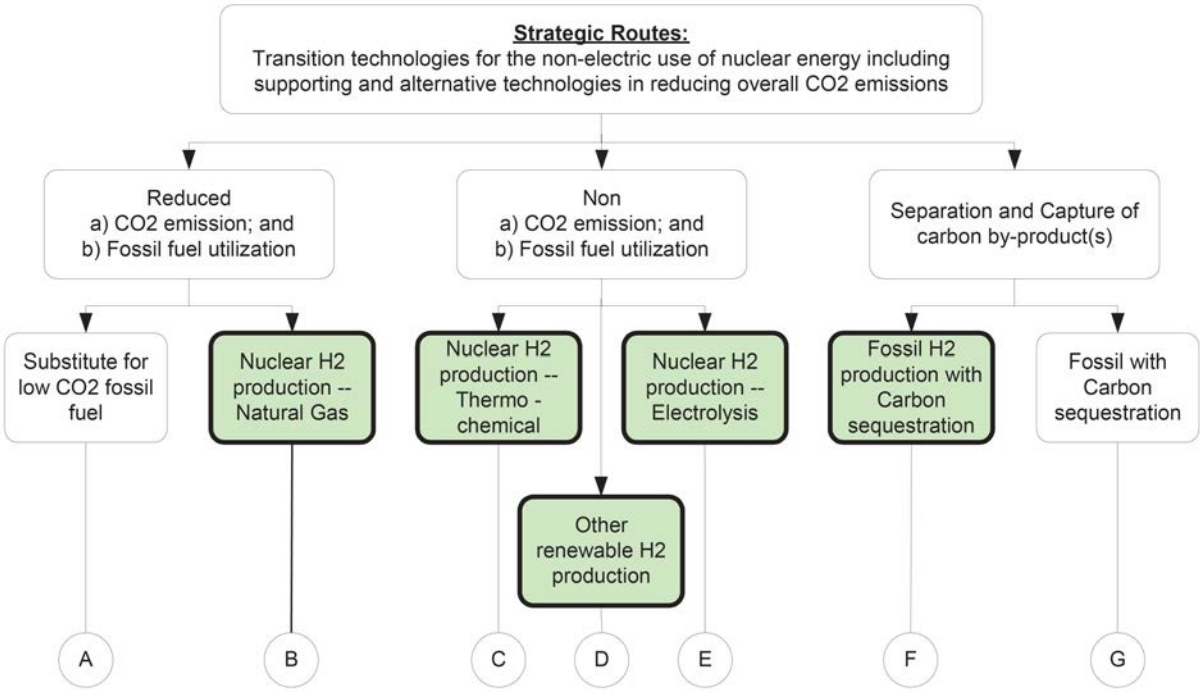

FIG. 7. Strategic routes for energy technologies for hydrogen production to reduce overall CO_2 emissions [15].

— The need to save fossil resources for use in environmentally friendly applications (substitution of nuclear for conventional process heat production would allow resource savings of up to 40%).
— If the cost of nuclear heat is sufficiently low, it may help to meet growing rates of energy use, replace expensive electricity generation with fossil fuels and replace old plants.
— Energy security from extended fuel reserves and independence from foreign oil uncertainties.
— Economics of large scale hydrogen and synthetic fuels production and transmission.

1.5. SCOPE OF THE REPORT

This report includes an overview of the current status and the recent progress made on hydrogen production using nuclear energy. Starting with a short description of the world energy situation, with a focus on nuclear energy, hydrogen as a promising energy carrier in the future, and arguments that favour nuclear assisted, large scale hydrogen production, Section 2 provides an outline of the specific energy situation and the national R&D programmes for nuclear hydrogen production currently under way in various Member States. Sections 3 and 4 describe the principal hydrogen production methods and the present status of R&D activities for conventional production methods under nuclear conditions and advanced methods concentrating on the water splitting processes of electrolysis at high temperatures and thermochemical cycles. Section 5 deals with the concepts of nuclear process heat reactors, with a strong focus on HTGRs, which allow the achievement of high coolant outlet temperatures for process heat/steam production. The coupling of a nuclear heat source and the chemical process is described in Section 6, including materials aspects and potential types of coolant. Section 7 is dedicated to the safety aspects that arise with the combination of a nuclear and chemical plant describing potential hazards and the R&D efforts conducted so far to contribute to an appropriate safety concept. The final sections cover present and future markets for hydrogen and the hydrogen infrastructure, and also present some thoughts on the economic aspects of future large scale hydrogen production. The characteristic physical and chemical features of hydrogen are described in the Appendix.

2. NATIONAL AND REGIONAL PROGRAMMES ON THE PRODUCTION OF HYDROGEN USING NUCLEAR ENERGY

A number of countries have established or are establishing road maps to a hydrogen economy. Among them are various countries that are considering the option of using nuclear energy to produce the hydrogen at a large scale and have started comprehensive R&D programmes. These national and international activities will be outlined in the following sections, including their embedment in national energy policies.

2.1. CANADA

2.1.1. Energy situation in Canada

Canada has considerable natural resources and is one of the world's largest producers (ranking 5th) and exporters of energy. Since 1980, Canada's total energy production has almost doubled, reaching 486 Mtoe in 2006, while its total energy consumption has increased by only 44%. Almost all of Canada's energy exports go to the USA.

In 2006, the largest source of energy consumption in Canada was oil (32%), followed by hydroelectricity (25%) and natural gas (24%). Both coal (10%) and nuclear (7%) constitute a smaller share of the country's overall energy mix. Electricity production in Canada has been dominated by hydroelectricity, with nuclear and fossil fuels holding a 15–25% share each over the past two decades.

Canada has the second-largest petroleum deposits in the world (after Saudi Arabia). Its oil sands produce 1.3 million bbl/d of oil today, up from 600 000 bbl/d in 2000. But the development of oil sands projects has been sharply criticized for its impact on the environment and its intensive use of both water and natural gas. The growth in oil sands exploitation is one of the reasons that Canada has failed to contain its GHG emissions in recent years despite its commitment to do so.

The nuclear industry in Canada dates back to 1942 when a decision was made to develop a design for a heavy water based nuclear reactor and to build Canada's first nuclear power plant. The so-called Nuclear Power Demonstration Reactor, a 20 MW(e) plant, started operation in 1962 and successfully demonstrated the unique concepts of on-power refuelling using natural uranium fuel, and heavy water as a moderator and coolant. These features formed the basis for the now more than 60 year evolutionary development of CANDU power reactors built and successfully operated in Canada and elsewhere.

Currently, nuclear power provides about 15% of Canada's electricity from 18 units with a capacity of 12.7 GW. Canada's nuclear energy production peaked in 1994 at 102.4 TW·h, declined to 67 TW·h by 1998 as reactors were mothballed, and increased to 85.6 TW·h in 2005 due to improved reactor performance and refurbishment. Recently renewed interest in nuclear energy is spurred by increasing demand and the desire to comply with Canada's Kyoto Agreement obligations.

Hydrogen is currently produced in Canada at a rate of 3 million t/a. Of this hydrogen, 35% is used for chemical products, 24% for refining, 23% for heavy oil upgrading and 18% for chemical by-products [16]. Hydrogen R&D activities have been initiated within the Fuel Cell and Hydrogen Programme by the National Research Council and managed by Natural Resources Canada since 1985. Prominent successes were, among others, the world's first demonstration of a fuel cell bus in 1993 based on Ballard's polymer electrolyte membrane (PEM) fuel cells, and the Hydrogenics low temperature water electrolyser.

2.1.2. R&D activities on nuclear hydrogen production in Canada

Canada, a founding member of the Generation IV International Forum (GIF) has selected and is developing the Generation IV supercritical water reactor (SCWR) based on the successful CANDU system. The use of the Canadian ACR (Advanced CANDU Reactor) for hydrogen production is considered a realistic short term approach. Its modular design would make it adaptable to various power requirements. The success of such a concept using

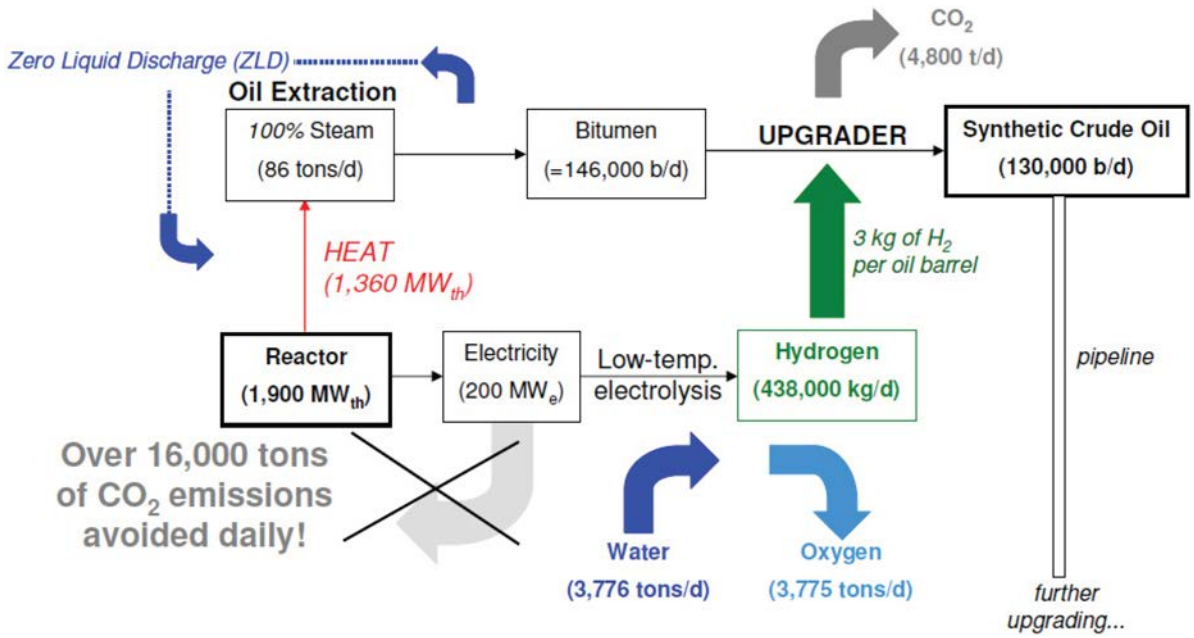

FIG. 8. Schematic of nuclear syncrude production with ACR-700 [18].

electricity and heat (to produce hydrogen and steam, respectively) would represent a first step toward the development of cogeneration applications from nuclear power.

In tertiary oil recovery, the biggest cost factor is energy for steam, electricity and hydrogen production, which is currently provided by natural gas. Its replacement with nuclear energy was found in a study to be competitive. A candidate nuclear system is the ACR-700, a pressurized heavy water reactor design developed in Canada (see Section 5.3.6.1). The thermal power of the reference design was 2034 MW(th) with an electric output of 703 MW(e). Assuming high temperature steam electrolysis (HTSE) as the hydrogen production method, two ACR-700 units would be needed to meet the demand of a 100 000 bbl/d syncrude reference plant for electricity, steam and hydrogen [17].

Due to the enormous steam demand in tertiary oil recovery, nuclear process steam generation is considered a good option for coupling to a synthetic crude oil plant. The example shown in Fig. 8 is based on the ACR-700 nuclear plant with a thermal power of 1900 MW(th). The diagram shows the various associated operations with the typical production rate of a synthetic crude oil plant, taken to be 130 000 bbl/d. While most of the nuclear thermal power is used for steam generation, the remaining part of 540 MW(th) is used to generate 200 MW(e) of electricity to be used in low temperature electrolysis for hydrogen production.

The refining of the extracted bitumen by hydrogenation is required for transformation into a lighter product (with lower density and viscosity) that can be transported to refineries via pipelines. The 86 t of steam flow can be maintained at a fairly constant level with the use of the ‘zero liquid discharge crystallizer’ system (instead of the traditional deep well injection) that enables virtually 100% recycling of the water in a closed cycle. Still, the process consumes large amounts of water. The 16 000 t of CO_2 avoided represent a 77% decrease in emissions.

In close cooperation with the Argonne National Laboratory (ANL) in the USA and the University of Ontario Institute of Technology (UOIT) and other universities, Atomic Energy of Canada Limited (AECL) is investigating the copper–chlorine family of thermochemical cycles with maximum temperatures that can be provided by the CANDU Mark 2 SCWR (see also Sections 4.6.1 and 5.3.6.1). The coolant exit temperature of 625°C meets the maximum temperature criterion of the Cu–Cl thermochemical cycle, which is a promising cycle that could be coupled in the future with the Generation IV CANDU-SCWR [19]. In the process, high quality waste heat following the expansion of reactor coolant to 300 kPa will be useful for the thermal drying requirements in the Cu–Cl cycle. But apart from that cycle, AECL research includes investigating the use of direct resistive heating of catalysts for SO_3 decomposition in the S–I process where nuclear electricity is used to provide the high temperature required that cannot be delivered from the SCWR [20].

2.2. CHINA

2.2.1. Energy situation in China

Due to its large population and its strong economic growth in recent years, China's demand for energy is rising rapidly. Since 2003, China ranks second after the USA in the consumption of primary energy and also in the consumption of oil. China is the third largest energy producer in the world, after the USA and the Russian Federation.

In 2007, China's total energy consumption was 1970 Mtoe, up from 872 Mtoe in 1990 [21]. In the period 2000–2007, the average growth rate of energy consumption was 8.9% per year. Coal makes up the bulk of China's primary energy consumption (66% in 2007) and will remain the dominant energy source in the next decades. Other energies consumed are oil (18%) and hydropower (12%). Natural gas production currently accounts for only 3%, with most reserves located far away from the demand sites.

China is the largest producer and consumer of coal in the world, which has made the country one of the world's largest emitter of GHGs. The present energy policy calls for greater energy conservation measures and a move away from coal toward cleaner energy sources including oil, natural gas, renewable energy, nuclear power and hydroelectric resources. A new energy law calls for 10% of its energy to come from renewable energy sources by 2020. China has abundant cellulosic biomass resources, with an estimated 220–380 Mtoe available for bioenergy production (e.g. ethanol, synthetic liquid fuels) each year [22].

The total electricity consumption in China in 2007 was 3318 TW·h, an increase by a factor of five compared to 1990, with more than 80% covered by coal and 15% by hydropower [21]. The consumption of electricity tends to further grow by over 4% per year through 2030, which will require huge investment in electricity infrastructure to meet the demand. In 2004 and 2005, the newly installed power capacity was ~60 GW(e)/a, and it was 100 GW(e) in 2007 [23].

China has an ambitious nuclear power programme for the next decades. At present, 13 commercial nuclear power units with a total capacity of 10.2 GW(e) are in operation, representing ~1% of the total power capacity. Nuclear energy output in 2009 was 70 TW·h, representing ~2% of the total energy consumption. There are 25 more units with 27.6 GW under construction. According to the "State Medium-Long Term (2005–2020) Development Programme of Nuclear Power" of 2007, the power capacity goal is 40 GW(e) by 2020 plus an additional 18 GW(e) under construction. With regard to the types of nuclear plants, a wide variety has been chosen, showing obvious interest in different technological developments. In 2007, orders were given for Generation III reactors (two EPRs, four AP1000) and a fuel reprocessing plant [23].

Hydrogen activities have been enhanced by the Chinese government in recent years, with the main objective of improving air quality in major cities. This led to the first national hydrogen project, on Fundamental Research for Hydrogen Production, Storage and Transportation in Large Scale Fuel Cells.

2.2.2. R&D activities on nuclear hydrogen production in China

2.2.2.1. High temperature reactor development

The development of HTGRs is an important part of the national nuclear programme. Its role is, on the one hand, to supplement PWRs for electricity generation with more flexibility and, on the other hand, to provide process steam for heavy oil recovery or the petrochemical industry, and to serve as a process heat source for coal gasification and liquefaction as well as hydrogen production.

The Chinese HTR-10 with a pebble bed core producing a power of 10 MW(th) is one of the two HTGRs currently in operation. Like the Japanese HTTR, it is also basically a research tool. First criticality in the HTR-10 was achieved in 2000. The active core consists of some 27 000 fuel spheres producing a coolant outlet temperature of 700°C. The reactor core and steam generator are housed in two steel pressure vessels in a side-by-side arrangement. The HTR-10 is planned to be equipped later with a gas turbine cycle (HTR-10GT). Numerous safety demonstration tests have been conducted in the HTR-10 demonstrating the safety features of small HTGRs.

A follow-on demonstration plant HTR-PM will consist of two nuclear steam supply system modules, each comprising a single zone 250 MW pebble bed modular reactor (PBMR) and a steam generator. Both modules feed one steam turbine to generate an electric power of 200 MW. The HTR-PM power plants are intended to be a series of commercial plants, beginning with a demonstration plant. All project activities including investment, design,

construction and operation are required to follow market rules. Work on the HTR-PM project can be divided into four categories: technical design, marketing, project, and organization. Concerning the technical design, the main work is to find and optimize an HTR-PM standard design which is based on the enveloping or reference site conditions. The kernel of the organization team is the Institute of Nuclear and New Energy Technology (INET) of Tsinghua University, responsible for research, design and technology development of the nuclear island of the HTR-PM. The second level is an architecture and engineering company, called CHINERGY, responsible for the engineering design, main components supply and construction. The third part is the Chinese utility China HUANENG Group, the Chinese Nuclear Engineering and Construction Corporation (CNECC) and other local investors. The utility will be responsible for all issues of marketing, financial, site selection, etc.

For the demonstration plant, three parallel lines of the project are being followed: (i) standard design of the HTR-PM, (ii) site selection for the demonstration plant, and (iii) a fuel plant for the HTR-PM. The standard design of the HTR-PM envelops all possible site conditions in China. The purpose of a standard design is to accelerate the design process and to improve the design quality. The work for the fuel plant aims to expand the capacity of the plant, to stabilize the mass production processes, and to produce fuel elements for initial loading and operation of the demonstration plant and future follow-on plants.

2.2.2.2. Nuclear hydrogen production

R&D on hydrogen production through water splitting using HTGR as a process heat source was initiated in 2005 as one component of China's HTR-PM demonstration project. Both the S–I thermochemical cycle and high temperature steam electrolysis have been selected as potential processes for nuclear hydrogen production. Beginning with preliminary studies, the R&D programme, now part of the HTR-PM project, will be conducted in phases:

— Phase one (2005–2009): verification of nuclear hydrogen production;
— Phase two (2010–2012): bench-scale testing;
— Phase three (2013–2020): pilot-scale testing, R&D on coupling technology with reactor, nuclear hydrogen safety;
— Phase four (after 2020): commercialization of nuclear hydrogen production.

2.3. EUROPEAN UNION

2.3.1. Energy situation in the European Union

The European Union comprises highly industrialized countries with extended urban agglomerations, and therefore needs to rely on a secure and economically competitive supply of energy. As of 2007 the European Union, with 7.5% (or 496 million) of the world population, consumed 15% (1757 Mtoe) of the total energy and 18% (3325 TW·h) of the total electricity [21], and was responsible for 14% (4100 million t) of the total CO_2 emissions. Primary energy by fuel share is 19% coal (down from 28% in 1990), 35% oil, 25% natural gas, 14% nuclear and 8% renewables. The respective electricity shares are 31% coal, 28% nuclear, 22% natural gas, 9% hydro, 6% other renewables and 3% oil [21].

The production of oil and natural gas in the European Union has been decreasing for a few years. The situation in the European Union as projected for the next 30 years is characterized by a growing demand for energy by 2 %/a and, at the same time (after 2010), decreasing domestic energy production. In 2030, if no additional measures are taken, 70% of the energy demand will have to be covered by imports. In addition, this development will push CO_2 emissions up 14% compared to the 1990 level, far off the Kyoto commitment of an 8% reduction. For these reasons, all energy options should be left open for the future [24].

In 2007, principal energy and climate policy targets for the European Union were redefined by the European Council (the decision making organ of the European Union) to be attained by the year 2020, which are characterized by the 'three twenties':

— A 20% reduction of GHGs compared to the 1990 level;
— A 20% share of renewable energies of end use (compared to 8.5% at present);
— A 20% efficiency of energy use.

The four areas selected by the GIF as technology goals (namely, sustainability, economics, safety, and reliability, proliferation resistance and physical protection) correspond exactly to the priorities set above by the energy policy for Europe [25]. An important issue for any energy policy is the correct evaluation of the new industrial needs. Besides electricity production, other industrial requirements are addressing high temperature heat production for (the petrochemical) industry, synthetic fuel production for transportation, and hydrogen production from water. In this way, nuclear energy will penetrate the global energy market through cogeneration of heat and power, thus reducing the dependence on fossil fuel supply.

Also in the light of the 2006 Ukrainian gas crisis, the European Union has set energy security at the top of the agenda, with the objectives being to strengthen energy markets, secure imports, improve efficiencies, and increase the degree of self-sufficiency.

Nuclear power is a major energy source in Europe, covering approximately 30% of the total electricity demand and providing a significant source of reliable and secure baseload power. As of October 2010, a total of 195 nuclear reactors (including the 32 plants in the Russian Federation, of which 5 units are located in the Asian part of the Russian Federation) were operating in Europe with a net capacity of 170 GW(e), and 19 more units with 16.9 GW(e) were under construction. Within the European Union, 143 nuclear plants with 131 GW(e) of capacity were operated, located in 14 of the 27 Member States are being operated representing 35% of the installed nuclear capacity in the world. The nuclear share, however, varies significantly between countries: while some countries completely refrain from nuclear power, in other countries the nuclear shares range between ~3% for the Netherlands to ~78% for France. In many EU countries, the possibility of a 'nuclear renaissance' is being discussed and first new construction projects (Generation III+ European Pressurized Reactors (EPRs)) are under way in Finland and France. Long term intensive cooperation already exists among the nuclear vendors, utilities and research organizations, not only aiming at an evolutionary development of existing nuclear technology, but also searching for innovative concepts of power plants and components with improved safety characteristics and different applications.

With the recent worldwide increased interest in hydrogen as a clean fuel of the future, Europe has also embarked on comprehensive research, development and demonstration activities, with the main objective of moving from a carbon-based economy toward a CO_2 emission free energy structure. Due to the growing demand for hydrogen in the petrochemical, fertilizer and refining industries, however, the near and medium terms will be characterized by coexistence between the energy carriers hydrogen and hydrocarbons.

2.3.2. EU research policy

EU energy policy is characterized by diversity in national energy policies and the tendency among the EU member countries to consider their energy strategies as a matter of national security. Therefore, closer collaboration among the EU countries is required to provide a balanced choice of energy supply technologies while achieving the principal objectives of energy supply security, sustainable development, and economic competitiveness. Of particular importance are Europe's R&D efforts in the field of nuclear fission, which is deemed an essential part of the solution in a balanced energy mix, at the same level as other developments, such as clean fossil and renewable sources as well as rational use of energy. Since a worldwide increase in the use of nuclear energy is expected, a potential for economic benefits in maintaining and developing the technological lead of the European Union is seen in this field.

Under Framework Programme 6 (FP-6) (2003–2006), two new instruments have been created and are being further developed in FP-7 (2007–2013): a Network of Excellence (NOE) with long term joint planning, and Integrated Projects (IPs) to develop new knowledge, new technologies and demonstration activities with a planned total budget of €48 billion for EU research and €3 billion for Euratom, a 40% increase compared to FP-6. The so-called European Technological Platforms are another new element, of which numerous have been founded in the meantime. These Technological Platforms are forums bringing together stakeholders of a strategic area to define strategic research agendas, set up industrial deployment strategies, analyse potential markets and prepare the legal and political framework. The Platforms propose so-called joint technology initiatives (JTIs), large projects in public–private partnership with a great deal of autonomy. The first JTIs became active in 2008, among them is the JTI on Fuel Cells and Hydrogen.

In the European Union, there are no explicit research activities dedicated to nuclear hydrogen production. The research programmes either concentrate on the nuclear aspects or on the hydrogen aspects. There is, however, a

little overlap of both areas in such a way that research on innovative nuclear reactor designs also takes into consideration one of their most pronounced features, which is the possibility of penetrating the non-electricity market with hydrogen production as a major issue. On the other hand, research projects which deal with large scale H_2 production methods of the future may also include the option of nuclear power to provide the required primary energy.

2.3.3. Euratom activities on nuclear process heat

2.3.3.1. Nuclear technology networks and platforms

Between the 1960s and 1980s, Europe played a leading role in the development of HTGRs with the successful construction and operation of the test reactors DRAGON (UK) and AVR (Germany), the extensive exploration of the possibilities for process heat applications, and later the introduction of a modular concept. Starting in 2000 with the foundation of the European High Temperature Reactor Technology Network (HTR-TN), by industrial and research actors, major activities were resumed dedicated to the development of base generic HTR technologies and to the exploration of advanced solutions for improving the performances for future VHTR.

The main incentive for the foundation of the MICHELANGELO Network (2001–2005) within FP-5 was to move away from the fragmentation and isolation of national research efforts and elaborate a common European position on the priorities of future R&D for the sustainable use of nuclear energy within the worldwide activities in this area. The principal results were the establishment of a consistent strategy of European nuclear R&D, a dynamic, long term R&D partnership between the main European organizations of the nuclear industry, and research in the form of a stable network in an international frame. In particular, a strong European partnership in the 'Generation IV' initiative was deemed crucial in order to obtain a benefit for Europe. But this also holds for other international initiatives like the INPRO initiative by the IAEA (see Section 5.1.3), the Three Agency Study (IAEA, IEA, OECD/NEA) or the United States Department of Energy (USDOE) Nuclear Energy Research Initiative NERI, as well as for national programmes like the HTTR in Japan or the HTR-10 in China.

The network has made proposals for the orientation of future Euratom R&D Framework Programmes, including new aspects of nuclear energy like combined heat and power, desalination, and hydrogen or other fuel production as a complement to other CO_2 free energy sources. Nuclear driven steam reforming or coal gasification may well serve as a bridge to the water splitting processes such as thermochemical cycles or high temperature electrolysis. In both cases, the complexity of the processes implies that capital and maintenance costs would be higher than for low temperature electrolysis, and even further increased because they are non-proven processes.

The activities of the MICHELANGELO Network are now continued by the Sustainable Nuclear Energy Technology Platform (SNE-TP), which prioritizes the deployment of Generation III reactors and the development of Generation IV systems, both fast neutron reactors with fuel multi-recycling for sustainable electricity generating capability and (very) high temperature reactors for other applications of nuclear, such as production of hydrogen or biofuels.

2.3.3.2. The RAPHAEL integrated project

Among the nuclear projects of FP-6 with a certain relationship to hydrogen, the most important was the 'IP RAPHAEL (Reactor for Process Heat, Hydrogen, and Electricity Generation). Starting in 2005 and terminated in 2010, the IP consisted of 33 partners from 10 countries, with the main objectives being, on the one hand, a study of advanced gas cooled reactor technologies needed for industrial reference designs, but also benefiting from the existing demonstrator projects in Japan and China. On the other hand, RAPHAEL aimed at exploring options for the new nuclear generation with 'very high temperature' applications, i.e. at coolant exit temperatq IP comprised efforts in all VHTR sections, including reactor physics, thermodynamics, fuel, back end, materials and components development, safety, and system integration, building upon the successful HTGR projects of previous FPs.

In the European Union, it is recognized that for the introduction of hydrogen energy into the future energy market, political support (e.g. by public funding of research projects) is an essential key to long term success. Hydrogen production technologies are strongly focusing on CO_2 neutral or CO_2 free methods as represented by, for example, biomass conversion or water splitting processes or reforming of fossil fuels plus CO_2 sequestration. Primary energy sources include nuclear and renewable energies.

While RAPHAEL was fully concentrated on the development of a VHTR, five more activities were launched in the form of Specific Targeted Research Projects (STREPs) to deal with the other Generation IV reactor systems:

— RAPHAEL — Reactor for Process Heat, Hydrogen, and Electricity Generation (VHTR), 2005–2010;
— GCFR — Gas Cooled Fast Reactor (GFR), 2005–2009;
— HPLWR — High Performance Light Water Reactor (SCWR), 2006–2010;
— ELSY — European Lead Cooled SYstem (LFR), 2006–2010;
— EISOFAR — Road map for European Innovative Sodium Cooled Fast Reactor (SFR), 2007–2008;
— ALISIA — Assessment of liquid salts for innovative applications (MSR), 2007.

2.3.3.3. The EUROPAIRS project

After several years of joint European research dedicated to base HTGR technologies, HTR-TN has proposed to develop a demonstrator plant coupling an HTGR with industrial process heat applications. Such a development requires a close partnership with the end user industries, since their needs will certainly be different from those of utilities in terms of power and temperature. Typically, nuclear designers are not familiar with industrial process heat needs. But also the end users themselves, accustomed to integrating heat supply needs in the global optimization of their processes through heat recovery from these processes, burning of exhaust gases, etc., are not used to considering the availability of an external, massive, inexpensive (nuclear) heat source [26]. For the demonstration, the coupling should involve a full scale proven industrial process with high reliability of the nuclear heat supply to the process. A schedule for the European demonstrator HTR/VHTR is suggested in Fig. 9.

The project EUROPAIRS (End user Requirements for Industrial Process Heat Applications with Innovative Nuclear Reactors for Sustainable Energy Supply) is a so-called Coordination and Support Action (CSA) within FP-7 that started in 2009. This project intends to take into account the advice of RAPHAEL's Industrial User Advisory Group (IUAG) and could eventually transfer valuable input to the so-called Confirmation of Key Technologies phase, as defined by the SNE-TP, considering VHTR systems.

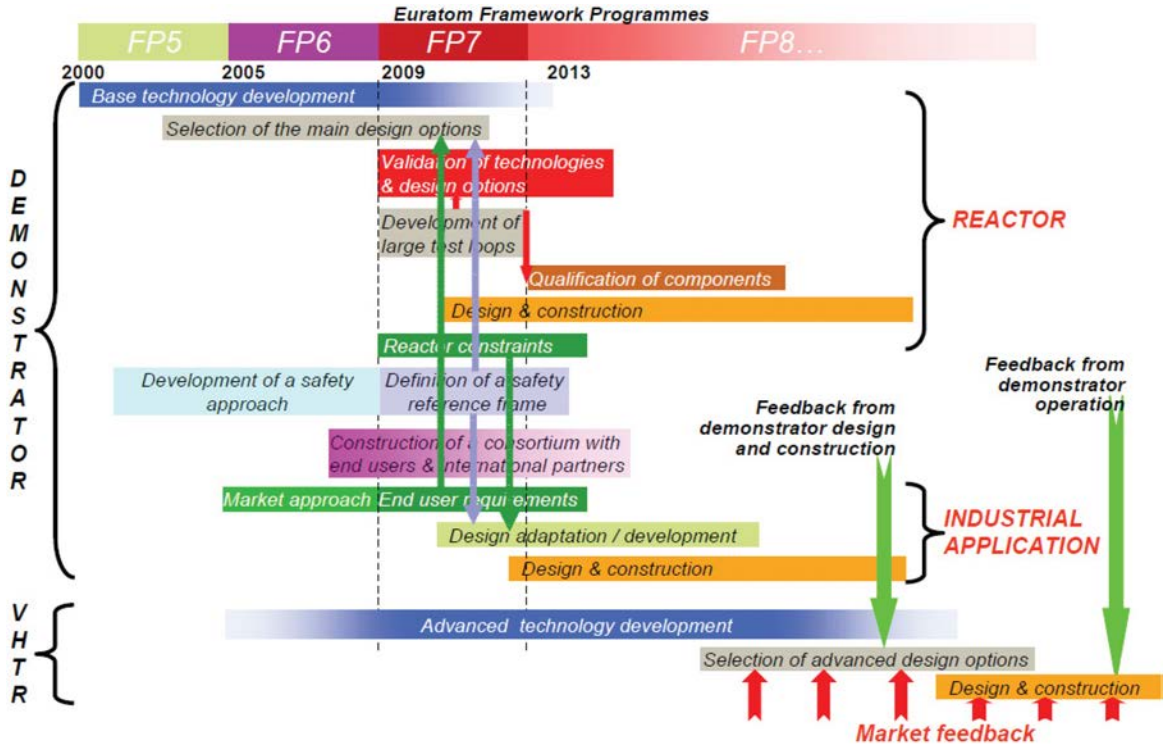

FIG. 9. Suggested schedule for the development of a demonstrator HTR/VHTR for industrial process heat applications [26].

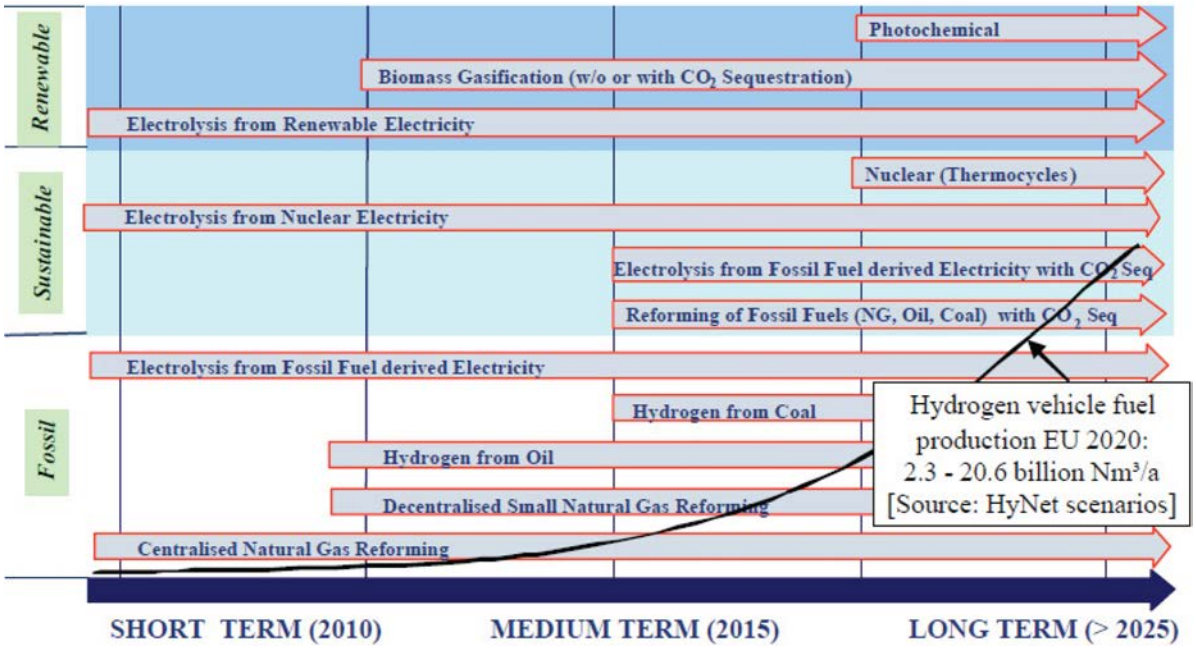

FIG. 10. HyNet timeline for hydrogen production technologies [27].

EUROPAIRS has the following main objectives:

— To identify the main applications for nuclear process heat;
— To determine the viability of combining a nuclear heat source with conventional industrial processes and CHP applications;
— To elaborate a programme for the development of a coupled demonstrator between a VHTR and industrial processes that require heat supply;
— To form a strategic alliance between nuclear industry and process industries.

An essential prerequisite for the success of this project is the significant involvement of private companies in the form of industrial participation to develop and deploy innovative energy supply systems.

2.3.4. European Union activities on hydrogen

2.3.4.1. European hydrogen road map

The hydrogen network HyNet is the analogue to MICANET on the hydrogen side. HyNet became active from 2001 to 2004 as a 'thematic network' within FP-5 with 12 contractors and more than 70 interested partners. It was working on the development of strategies for the introduction of a European hydrogen fuel infrastructure road map (Fig. 10).

In 2002, a so-called High Level Group on Hydrogen and Fuel Cells (HLG) was established by the European Commission (EC). Its principal task is to initiate strategic discussions for the development of a European consensus on the introduction of hydrogen energy. The group strongly recommended the development of an integrated European strategy on hydrogen energy through the creation of a political framework consisting of a partnership of major private and public hydrogen stakeholders. The International Partnership for a Hydrogen Economy (IPHE) was launched in 2003, representing 15 countries and the European Union. Work is done here on the governmental level to foster international collaboration on policy and research programmes and thus to accelerate the transition to a hydrogen economy, with the H_2 to come from multiple sources: renewables, nuclear and fossil plus sequestration.

In 2004, the EC started another policy group, the European Hydrogen and Fuel Cell Technology Platform (HFP). Key elements of the integrated European strategy to be deployed include a strategic research agenda with performance targets, timelines, lighthouse demonstration projects and a deployment strategy or road map for Europe. General EU targets for 2020 are a 10–20% supply of the hydrogen energy demand by CO_2 free or CO_2 lean sources and a 5% hydrogen fuel market share.

HyWays is an IP proposed by HyNet which has elaborated a fully validated European Hydrogen Energy Roadmap as a synthesis of national road maps from the participating Member States. It comprises a comparative analysis of regional hydrogen supply options and energy scenarios including renewable energies. The study includes the investigation of the technical, socio–economic and emission challenges and impacts of realistic hydrogen supply paths as well as the technological and economical needs, and details the steps of an action plan necessary to move toward greater use of hydrogen. According to the HyWays road map, an estimated 16 million hydrogen cars will exist in 2030. The study has also found that introducing hydrogen into the energy system would reduce the total oil consumption by the road transport sector by 40% between now and 2050. Regarding large scale hydrogen production, in the early phase up to 2020, hydrogen production will rely on steam reforming of natural gas, electrolysis and by-product contribution. In the longer term, by 2050, production will be based on centralized electrolysis and thermo–chemistry from renewable feedstocks and CO_2 free or CO_2 lean sources (coal and natural gas with carbon capture and sequestration, and nuclear) [28].

Hydrogen production is deemed a crucial element for the introduction of hydrogen into the energy sector. Hydrogen production from fossil feedstock, mainly natural gas, is a mature technology for the chemical industry. Research efforts were to be concentrated on the further improvement of known reforming and gasification methods, also with regard to high temperature primary energy systems such as Generation IV nuclear reactors and solar–thermal concentrating systems; on the development of CO_2 sequestration systems; on gas separation technologies; and on the efficiency improvement of hydrogen liquefaction technologies and system integration with hydrogen production facilities [29].

With CHRISGAS, SOLREF, HYTHEC and Hi2H2, projects started in 2004 dedicated to the hydrogen production by biomass gasification, steam reforming, thermochemical cycles, high temperature steam electrolysis. Another IP, HYVOLUTION, started in 2006 to deal with biological processes of hydrogen production.

The integrated project CHRISGAS (Clean Hydrogen-rich Synthesis Gas), with a duration of five years, had the goal of developing and optimizing an energy efficient and cost efficient method to produce hydrogen rich gases from biomass. The gas can then be upgraded to commercial quality hydrogen or to synthesis gas for liquid fuels production. The core of the project is a (solid) biomass fuelled integrated gasification combined cycle (IGCC) pilot plant facility in Värnamo, Sweden. New process equipment has been developed and tested, and has been implemented in a pilot facility to produce hydrogen-enriched gas. Studies included the conditioning of the synthesis gas to the quality required for the production of transportation fuels.

In the Hi2H2 STREP, it was proposed to develop a low cost, compact high temperature water electrolyser with very high electrical efficiencies of more than 90%. The project makes use of technological developments that have been made in the field of high temperature fuel cells and evaluates a solid oxide water electrolyser with a target cost of €400/kW(e) considered feasible. Experimental work is concentrating on the performance of two types of planar solid oxide fuel cell (SOFC) designs. Steam electrolysis was successfully demonstrated at high current densities and high efficiency on single cells (see also Section 4.5.2).

HySafe was conceived as a Network of Excellence running from 2006 to 2009. The main objectives were to strengthen, integrate and concentrate existing capacities and fragmented research efforts aiming at the removal of safety related barriers to the large scale introduction of hydrogen as an energy carrier. By harmonizing methodologies for safety assessment, the focus is on studies of fire and explosion safety, mitigating techniques and detection devices. In this way, the network contributes to promoting public awareness and trust in hydrogen technology. Essential HySafe activities are continued in the newly founded International Association of Hydrogen Safety.

2.3.4.2. The HYTHEC STREP and HycycleS project

High Temperature Thermochemical Cycles (HYTHEC) was a STREP with six partners starting in 2004 and running over almost four years. Its main objective was to evaluate the potential of thermochemical processes, focusing on the S–I cycle to be compared with the Westinghouse hybrid (HyS) cycle. Nuclear and solar were

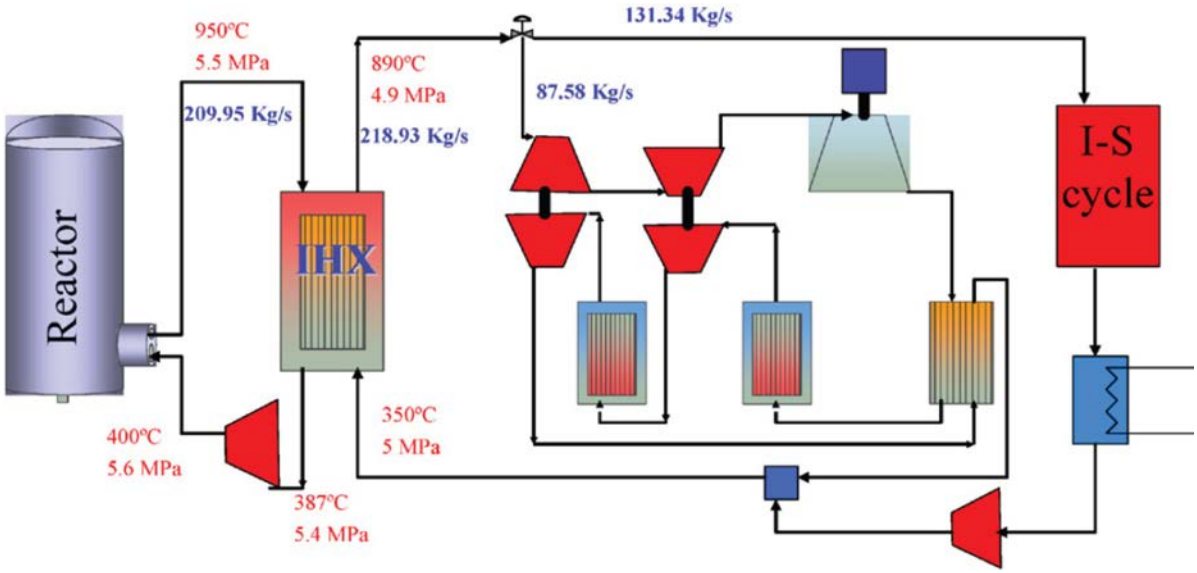

FIG. 11. Coupling of a 600 MW VHTR nuclear reactor to the sulphur–iodine cycle [30].

considered as the primary energy sources, with a maximum temperature of the process limited to 950°C. The HYTHEC activities comprised, apart from the coupling to high temperature heat sources, the modelling, chemical analysis, process flowsheeting and experimental studies of the H_2 and O_2 production steps. The project also included industrial scale-up studies for the investigation of the feasibility of the main components, the safety aspects and cost [30].

A preliminary reference sheet of the S–I cycle has been reviewed and optimized to a 'reference' flowsheet with coupling to a single 600 MW indirect cycle VHTR (Fig. 11). The reactor, fully dedicated to hydrogen production, is designed as a 'self-sustaining concept" delivering both electricity to meet the plant's own total power demand and heat to run the H_2 production process at a rate of 110 t/d and an overall plant efficiency of ~35%. The heat of the 890°C hot primary helium is decoupled in an IHX to secondary helium which partially serves a Brayton power cycle at 5 MPa and the endothermic sections of the S–I cycle. A specific study was dedicated to the performance of candidate membranes for separation processes in the HI_x section to further improve the thermochemical cycle efficiency.

A large scale solar furnace was used as an experimental tool in HYTHEC to study the chemical reactions common to both cycles at VHTR temperatures (~900°C) and also at a higher level (1100–1200°C). The receiver reactor was qualified for the solar decomposition of H_2SO_4. Maximum conversion rates were observed with a Pt catalyst, but significant catalytic activity was also found for uncoated SiSiC absorbers. Both nuclear and solar can be adjusted to the typical thermal power sizes of present modular power plant designs of up to 600 MW. It will thus support the design of novel components up to an industrial scale, which are required in allothermal reforming processes as well as in high temperature electrolysis, or in thermochemical processes. A preliminary evaluation of the hydrogen production costs based on solar, nuclear and hybrid operation led to following results: small plants are powered most favourably by solar energy, while nuclear plants are most economical at high power levels (> 300 MW(th)); hybrid systems may have their niche in the midrange of 100 to 300 MW(th).

The 2015 targets defined for high temperature thermo–electrical–chemical processes with solar–nuclear heat sources are a reduction of CO_2 emissions for fossil reforming by more than 25% and hydrogen production cost of less than €2/kg [31].

HycycleS is a new European project within FP-7 that started in 2008 involving nine European and four international associated partners [32, 33]. Following in the footsteps of the HYTHEC project, the three year project HycycleS (2008–2010) is aimed at the qualification of ceramic materials and reliability of components for the essential reactions in thermochemical cycles. The focus is on the decomposition of sulphuric acid as the central step of the hybrid-sulphur (HyS) cycle and the S–I cycle. The final aim is to bring thermochemical water splitting closer to realization by improving the efficiency, stability, practicability and economic viability. Work includes the design,

modelling, realization and testing of a large compact plate SiC heat exchanger for thermal SO_3 decomposition. Dense oxygen transport membranes are being tested under severe conditions for efficient O_2 separation in the SO_3 decomposition step. A criterion of thermal efficiency of more than 85% has been set, and the mock-up suitability will be tested under realistic thermal conditions (850°C). The results will lead to recommendations for a pilot-scale H_2SO_4 decomposition reactor in the several kW range.

2.3.4.3. The INNOHYP project

Innovative High Temperature Routes for Hydrogen Production (INNOHYP) was a 'Coordination Action' within FP6 starting in 2004 to run over four years. Its main objectives were the collection and coordination of information describing the options for hydrogen production at high temperatures and the identification of further research efforts. From all the routes to hydrogen considered, 17 were identified as important, for which conversion efficiencies and their influence on various operating parameters have been studied. Some results are shown in Section 10.6. Also, a categorization of primary energy sources was made. While nuclear is a 'high density' energy source with maximum process temperatures limited to ~900°C, solar energy appears to be a key primary energy source in the 'low density' category for high temperatures up to ~1600°C [34].

2.4. FRANCE

2.4.1. Energy situation in France

Consumption of primary energy in France amounted to 278 Mtoe in 2005, with an average increase of 1.3%/a between 1990 and 2005. The breakdown of primary energy is 42% nuclear energy, 33% oil, 15% natural gas, 6% renewables and 4% coal.

France is comparatively poor in domestic energy resources. French coal production, which was still around 40 million t/a at the end of the 1970s, was terminated in 2004. Also, domestic natural gas contributes not more than 2% of France's primary energy production. With the general objectives being to control energy demand, diversify sources of energy, increase research into energy, and provide methods of transporting and storing energy, the French energy policy has given priority to the development of a national energy supply with a strong focus on nuclear energy and renewable energies. These energies are seen to provide a reliable long term supply without GHG emissions and to ensure stable electricity prices.

The first nuclear power plants built in France were gas cooled reactors and the country also participated in the OECD Dragon project. Today France is the world's second largest producer of nuclear energy (after the USA) with an electricity share of 78%. France operates 58 nuclear power stations with a total capacity of 63.2 GW. One Gen-III reactor (EPR) is currently under construction. Since nuclear energy is not always fully used, interest is growing in using excess nuclear electricity, apart from export, for hydrogen production to regulate the electricity production.

As was approved by the French Government in 2005, the nuclear R&D strategy in France is concentrating on the development of fast reactors with a closed fuel cycle in succession to the Phénix and Superphénix projects, innovative LWRs, and the promotion of nuclear hydrogen production and very high temperature process heat supply to industry. France participated in the activities on the GIF VHTR system as well as the different European programmes on HTGR and hydrogen production. In 2006, however, France announced plans to phase out VHTR activities and to instead pursue the aim of constructing a sodium cooled nuclear fast reactor of the 4th generation and to study, as an alternative, the helium cooled fast reactor. The current goals are the construction of a 250–600 MW(e) prototype SFR 'Astrid' by 2020 and the preconceptual design for a 75 MW(th) GFR 'Allegro'. A cornerstone of this policy is the existing infrastructure for reprocessing to be increasingly used in the civilian business of reprocessing and fabricating new reactor fuel from the uranium and plutonium present in spent fuel.

2.4.2. R&D activities on nuclear hydrogen production in France

Although emphasis was on the rapid expansion of PWR technology, some work on the HTGR continued within European Union FPs. The French AREVA NP company is developing the concept of the ANTARES reactor, a full-size HTGR design, and is a partner in the US/Russian GT-MHR project. The reference design is based on the

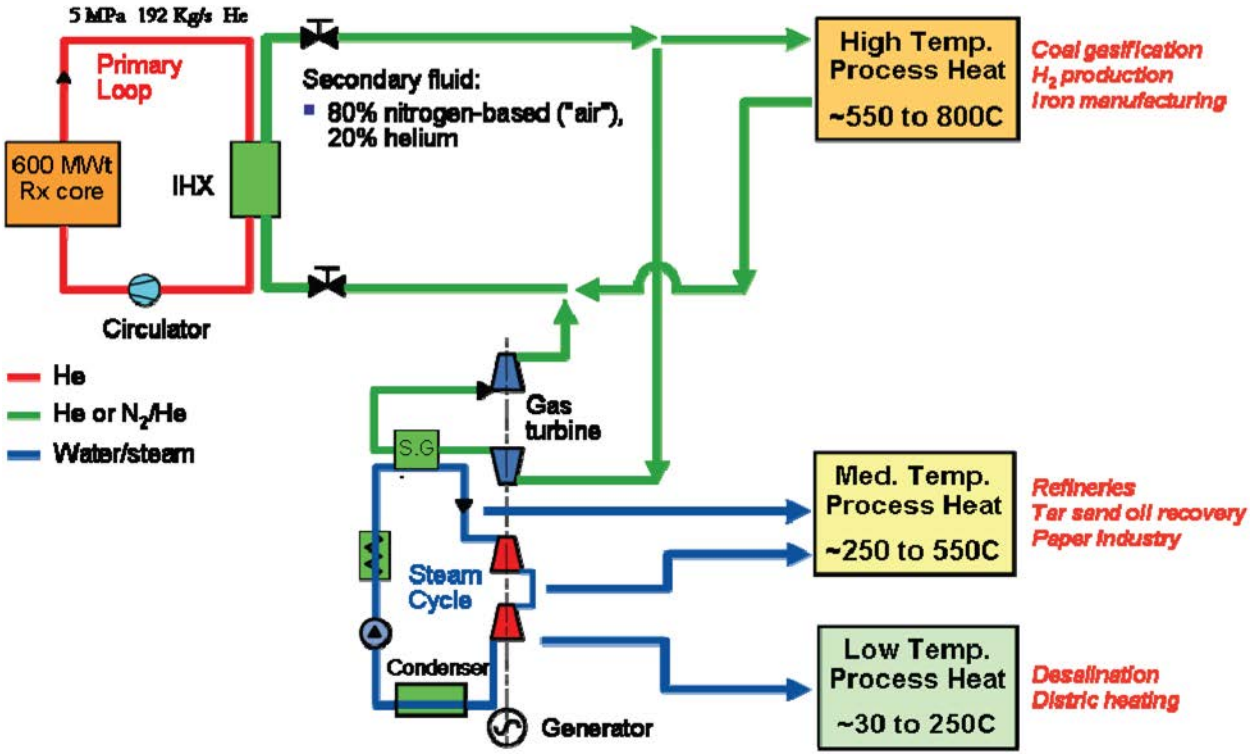

FIG. 12. Flexible reference design of ANTARES with heat applications in a wide temperature range [38].

GT-MHR of General Atomics of a 600 MW(th) reactor with prismatic block fuel and a core outlet temperature of up to 850°C for the advanced HTGR version, or ~1000°C for a VHTR version. It uses an indirect cycle, possibly with a helium–nitrogen mix in the secondary system.

The IHX is the only novel component that needs further development for the considered operation range. Options are, besides the 'conventional' tubular concept (as a fall-back solution), the plate machined heat exchanger (PMHX) and the plate fin heat exchanger (PFHX) designs, which should be capable of also sustaining higher temperatures typical for direct cycle applications (Fig. 12). An extensive R&D and testing programme is necessary, and has started already, to investigate appropriate materials [35, 36].

The AREVA company has also been developing an HTGR design within the USDOE's Next Generation Nuclear Plant (NGNP) programme. A comprehensive evaluation programme for the ANTARES concept was completed, with a VHTR version for electricity generation and another one for process heat applications (see Section 5.3.6.3). Following the change of the NGNP project goal to near term deployment with a greatly reduced technology development and project risk, a new proposal was made, benefitting from the experience of past HTGR projects, but also from the progress made since. Based on the previous ANTARES reactor, the new concept is a 625 MW(th) prismatic block reactor with a two-loop modular steam supply system which could be designed as a multiple module plant depending on the applications and the customer's needs [37].

With the withdrawal of Westinghouse from the bidding with a pebble bed reactor, AREVA is organizing a concept design team from various suppliers and may still become a pebble bed vendor based on the German HTR-Modul design.

2.5. INDIA

2.5.1. Energy situation in India

India's energy consumption has been increasing at a rapid pace in recent years due to population growth and economic development. In terms of primary energy consumption, at 595 Mtoe in 2007, despite a low per capita

energy consumption rate, India ranks fifth in the world, accounting for about 3.5% of the global commercial energy demand in 2003. Until the end of the 1980s, India's energy policy was mainly based on the availability of indigenous resources.

Coal, oil and natural gas are the three primary commercial energy sources. India has the world's third largest coal reserves after the USA and China; still, the existing demand exceeds the supply. Coal accounts for 41% (as of 2007) of India's total energy consumption, followed by renewables including hydroelectric power (29%), oil (24%) and natural gas (6%) [21]. Although nuclear power comprises only 1% of total energy consumption, it is expected to increase in the future. A large share of the total energy requirement is met by non-commercial energy sources, which include wood, crop residue and animal waste. But commercial energy of a much higher quality and efficiency are steadily replacing the traditional energy resources being consumed mainly in the rural sector. Of India's total energy needs, 30% are met through imports.

About 75% of the coal in the country is consumed in the power sector. The poor quality of Indian coal, coupled with a lack of infrastructure to clean it, poses a major environmental threat. Oil consumption accounts for roughly a third of India's energy use. Due to limited domestic resources, most of the demand for crude oil and petroleum products must be met with imports; since recently, this is the case for coal as well. Natural gas consumption has risen at the rate of about 6.5% during the past 10 years, thus faster than any other type of energy source. The import of liquefied natural gas (LNG) is being considered as one of the possible solutions for India's expected gas shortages. Part of India's long term strategy is also to look at unconventional sources such as gas hydrates, coal bed methane, underground coal gasification and use of coal for SNG production.

India's electricity consumption totalled 792 TW·h in 2007 with 68% covered by coal and 8% by gas plants, 16% by hydropower and 2% by nuclear [21]. The electric system has proven highly inefficient. There is an at least a 30% loss of power along the delivery chain. Unreliable power grids cause regular blackouts. In order to meet its goals for poverty eradication, India must at least triple its primary energy supply and quintuple its electrical capacity from 160 GW currently to ~800 GW by 2030. The electricity demand by 2050 is estimated to be 13 000 GW, with a nuclear share of about 20%.

India now envisages increasing the contribution of nuclear power to overall electricity generation capacity from 4.2% to 9% within 25 years. In 2010, India's installed nuclear power generation capacity will increase to 6000 MW with plans for construction of nine more units, including two EPRs being constructed by France's AREVA. Indigenous atomic reactors include TAPS-3 and -4, both of which are 540 MW reactors. India's fast breeder reactor programme started in the 1980s with a 40 MW(th) test reactor. A follow-on plant, a 500 MW(e) prototype fast breeder reactor, is currently under construction at the Indira Gandhi Centre for Atomic Research (IGCAR) at Kalpakkam.

India boasts a quickly advancing and active nuclear power programme. The country has 19 nuclear power plants in operation, generating 4.2 GW, and six more reactors under construction and expected to generate an additional 3160 MW. Due to dwindling domestic uranium reserves, electricity generation from nuclear power in India declined by 13% from 2006 to 2008. The country is expected to have 20 GW of nuclear capacity by 2020. Most of the nuclear programme is domestic development. India, being a non-signatory of the Treaty on the Non-Proliferation of Nuclear Weapons, has been subjected to a de facto nuclear embargo from members of the Nuclear Suppliers Group cartel. This has prevented India from obtaining commercial nuclear fuel, nuclear power plant components and services from the international market, thereby forcing India to develop its own fuel, components and services for nuclear power generation. Use of heavy water reactors has been particularly attractive for the nation because it allows uranium to be burned with little to no enrichment capabilities. India's nuclear technology road map will be strongly based on the closed fuel cycle and on the utilization of thorium, of which India has nearly one third of the world's reserves [39].

2.5.2. R&D activities on nuclear hydrogen production in India

In the Indian nuclear programme, the utilization of thorium has been given high priority. Among the initiatives for thorium utilization are new nuclear reactor concepts currently under research and development at the Bhabha Atomic Research Centre (BARC) such as the advanced heavy water reactor, the so-called KAMINI reactor at IGCAR, the only one in the world that is successfully operated with thorium and ^{233}U fuel, the fast breeder thorium reactor (FBTR), and the high temperature nuclear reactor to supply process heat in the 600–1000°C temperature range.

While there is a need to find ways to optimize utilization of raw material, especially related to nuclear materials, options for nuclear energy assisted hydrogen production are being considered. To meet such large demands in a sustainable way, India has plans to employ a closed nuclear fuel cycle with large scale thorium utilization. The magnitude of the demand will call for nuclear reactors with advanced designs. The other specifications for a suitable nuclear reactor for hydrogen generation would obviously depend on the process selected for hydrogen production.

Considering these aspects, India has prepared a road map for development of reactors for generating nuclear hydrogen. Keeping in focus the long term objective, the current R&D activities in BARC are targeting challenging technologies for high temperature nuclear reactors using thorium based fuel and capable of supplying process heat at 1000°C.

India has also started to work on a National Hydrogen Energy Road Map with the main targeted sectors of transportation and power supply and the longer term goal of replacing fossil fuels with hydrogen.

BARC has started a research programme on nuclear hydrogen production through water splitting based on the S–I thermochemical process. Theoretical and experimental studies are being conducted, currently concentrating on the Bunsen and the HI decomposition sections of the S–I cycle.

2.6. JAPAN

2.6.1. Energy situation in Japan

Japan has shown tremendous economic growth in the post-war period and is now one of the world's leading industrial countries. Japan has virtually no domestic oil or natural gas reserves and is the second-largest net importer of crude oil and largest net importer of liquefied natural gas in the world. Including nuclear power, Japan is only 16% energy self-sufficient (neglecting uranium imports).

Japan's total primary energy demand in 2007 was 514 Mtoe [21]. Oil is the most consumed energy resource in Japan (45% as of 2007), although its share of total energy consumption has strongly declined from 57% in 1990. Coal, with 22% (versus 17% in 1990), continues to account for a significant share of total energy consumption, although 99% of the coal must be imported. Natural gas (16%) and nuclear power (13%) are increasingly important sources.

Total electricity production in Japan amounted to 1123 TW·h in 2007, with the largest share of 35% (up from 20% in 1990) from natural gas. The share of nuclear power is 32%, followed by coal (28%), oil (19%), hydro (9%) and other renewables (3%) [21].

The commercial nuclear era in Japan started in 1966 with the operation of the 166 MW(e) gas cooled reactor of the Tokai power plant. Later, light water reactors (LWRs) were introduced from the USA. With 55 nuclear reactors and a total capacity of 47.3 GW, Japan has become the third largest consumer of nuclear power in the world (after the USA and France). The Japanese government has maintained strong support for nuclear power. The LWR Improvement and Standardization Programme launched by the Ministry of International Trade and Industry (MITI) and the nuclear power industry has led to the improvement of operation and maintenance of the existing BWR and PWR designs and, later, with the introduction of the 'advanced BWR', to an increase of reactor size to 1300–1400 MW(e), making considerable design changes. After several incidents in nuclear power plants (Tokai-mura, Mihama, Monju, Kashiwasaki), however, the government-funded research institutions were reorganized and stricter controls were enforced. While the number of reactors is expected to increase, the focus of new developments will shift to the advanced fuel cycle and next generation plants such as the 'super-safe, small and simple' (4S) nuclear battery system, which is a sodium cooled reactor with a steam cycle that is capable of three decades of continuous operation without refuelling, or the GTHTR300, a helium cooled VHTR for future large scale hydrogen production.

The commitment made by Japan at the Kyoto conference was a reduction of GHG emissions by 6% below the 1990 level. The reality, however, is an observed increase of 8% in 1995, and of 12% in 2002. This would require an 18% GHG reduction by 2008–2012. Measures to help meet this goal are energy savings by the public, strengthened plans for renewables, energy efficient vehicles and appliances, expanded use of natural gas, and last but not least the construction of new nuclear power plants.

Because of enhanced and actively promoted R&D projects financially supported by the Government, Japan has become a strong player in the development of a hydrogen economy. It is, besides the USA, the leading country in fuel cell research, with large investments by both the Government and the car industries. Since Japan's transportation sector accounts for 20% of all CO_2 emissions, fuels for 'clean' fuel cell vehicles (FCVs) were chosen to be methanol and/or compressed H_2 gas at present, gasoline reforming in the near term, and hydrogen plus advanced storage options in the long term [40].

The present H_2 consumption in Japan is about 162 million Nm^3 per year, mainly produced via steam reforming of natural gas. The demand for hydrogen in the future was projected by METI's Agency for Natural Resources & Energy (ANRE) to rise to 54.4×10^9 Nm^3 in 2030 [41], with by far the largest share dedicated to stationary fuel cells. But it will be only after 2020 that the use of H_2 will show its CO_2 reducing effect.

2.6.2. Hydrogen R&D activities in Japan

2.6.2.1. The Sunshine, Moonlight, New Sunshine and WE-NET projects

In 1974, shortly after the first energy crisis, the Agency of Industrial Science and Technology (AIST) in MITI (known since 2001 as the Ministry of Economy, Trade and Industry (METI)) of the Japanese Government initiated the Sunshine project to develop new energy technologies and reduce environmental pollution. The project was followed in 1978 by the Moonlight project to focus on energy saving and energy conversion technologies and in 1979 by the project on environmental technology. Due to the strong interrelations between new sources of energy, energy conversion, and environmental technology, the New Sunshine project was started in 1993, merging all previous projects to contribute to an international system based on environmentally friendly energy technologies. The New Sunshine project has become the largest non-nuclear R&D programme supported by the Japanese Government. In 1997, the Law Concerning Promotion of the Use of New Energy went into force, providing subsidies in the area of new energy electric power generation with the main goal being to meet 3.1% of the domestic energy supply using new energy sources by 2010, thus lowering the dependency on fossil fuels.

As a part of the New Sunshine project, the so-called International Clean Energy Network Using Hydrogen Conversion, or World Energy Network (WE-NET), was established in 1993. The project was directed by NEDO (New Energy and Industrial Technology Development Organization), an implementing agency of the Japanese Government. Originally conceived as a 28 year project to demonstrate all aspects of a future hydrogen economy, WE-NET was terminated after ten years and replaced with more specific projects on hydrogen applications. The WE-NET project is described in more detail in Section 8.4.2.

2.6.2.2. The Japan Hydrogen and Fuel Cell demonstration project

The new Japan Hydrogen and Fuel Cell (JHFC) demonstration project was designed to consist of three phases [42]:

— In a first R&D stage until 2005, demonstration projects of H_2 infrastructure, also a discussion of international and a review of domestic codes and regulations;
— In the phase from 2005 to 2010, the gradual establishment of the fuel supply system and promotion of fuel cell cars and buses;
— And, finally, after 2010, the diffusion of H_2 technologies, leading to self-sustained growth and the promotion of fuel cell systems in the private sector.

Starting with the so-called Koizumi Initiative, a success of the JHFC demonstration programme was the delivery of the first generation of commercially released H_2-fuelled FCVs by Toyota and Honda in December 2002 in both Japan and California. Since then, quite a number of FCVs are being in test operation [43]. The Government also issued the world's first FCV safety and environmental standards, in force since April 2005 [44].

A large scale demonstration of stationary fuel cell systems started in 2005 on numerous sites all over Japan using a polymer electrolyte fuel cell (PEFC) from several manufacturers and applying different fuels under various conditions. By 2006, more than 1000 PEFC systems in the power range of 0.7–1 kW were being operated for residential use. Tests will expand to ≥5 kW systems for business use in a second stage of the project [43, 45].

2.6.2.3. The stationary fuel cell demonstration project

Fuel cells for mobile, but also for stationary, applications are being investigated. Various demonstration projects have been starting, particularly as part of complete energy systems based on renewable primary energy. Within the Millennium project coordinated by the Japan Gas Association, companies are moving to the large scale production of 1 kW power units for households. Unlike the USA or Europe, Japan is basically looking at PEM technology [42, 46].

As part of the infrastructure, 10 hydrogen refuelling stations were constructed in the Tokyo–Kanagawa area based on different H_2 sources, with the aim being to compare the various options and investigate their well-to-wheel efficiencies.

2.6.3. Nuclear hydrogen production concepts in Japan

2.6.3.1. Hydrogen production with high temperature gas cooled reactor

The Basic Plan for Energy Supply and Demand of October 2003 as part of the Basic Law on Energy Policy Making explicitly states that hydrogen is a clean energy carrier and that commercialization of hydrogen production systems by means of nuclear, solar and biomass, but not fossil fuels, is desired. With the construction and operation of the 30 MW(th) high temperature engineering test reactor, or HTTR (which achieved first criticality in 1998), the Japan Atomic Energy Agency (JAEA), formerly JAERI, has laid the basis for utilization of nuclear process heat for hydrogen production. The reactor allows a coolant outlet temperature of 950°C outside the reactor vessel to provide process heat at 905°C through the intermediate heat exchanger, which was demonstrated in 2004 for the first time in the world.

Over several years, steam reforming of methane was considered the top candidate method to be connected to the HTTR. The steam reforming process was successfully demonstrated in an out-of-pile facility under nuclear conditions (see Section 4.1.3). Potential hazards of the combined system have been comprehensively investigated in theoretical and experimental studies [47].

In recent years, JAEA has undertaken extensive R&D on the thermochemical cycles based on the UT-3 and S–I processes for H_2 production. It is most advanced in the study of the S–I cycle, with the successful operation of a bench-scale facility having achieved a hydrogen production rate of 30 NL/h in continuous closed cycle operation over one week. This process is now considered the prime candidate for the demonstration of nuclear assisted hydrogen generation. The next step, which started in 2005, is the design and construction of a pilot plant with a production rate of 30 Nm^3/h of H_2 under the simulated conditions of a nuclear reactor. Helium is heated by a 400 kW electrical heater [48]. While the efficiency was ~10% for the bench-scale plant, the goal for the pilot plant is ~40%. The backup hydrogen production method is high temperature electrolysis, which was also investigated, but has not yet gone beyond lab-scale testing [49].

Development of the so-called HTTR-IS system began in 2005 with a conceptual design study, where the available structure and heat mass balance of the system were evaluated [50]. The HTTR-IS (Fig. 13) will be operated at gas temperatures of 395–950°C with a 10.2 kg/s coolant flow rate. A thermal power of 8.5 MW(th) will be taken from the IHX and transferred to the secondary helium gas at the intermediate heat exchanger. The secondary helium supplies heat to the chemical reactors of the S–I process such as a SO_3 decomposer, H_2SO_4 vaporizer and HI decomposer. Finally, after cooled by a steam generator and helium cooler, secondary helium is circulated by a helium circulator back to the IHX through the annular pipe of the concentric hot gas duct. Chemical impurities in the secondary helium are removed by the secondary helium purification system to allow for an H_2 production rate of 1000 Nm^3/h with an expected efficiency of 43.6% [51]. The S–I process will be designed as a 'non-nuclear' grade plant, however, backup nuclear-graded equipment is available for cases of S–I abnormal conditions [52].

Based on the experience with the construction and operation of the HTTR, JAEA has developed the conceptual design of a commercial scale HTGR hydrogen cogeneration system, GTHTR300C [53–55]. The baseline concept is the GTHTR300, which employs a helium cooled, graphite moderated prismatic core with 600 MW of thermal power and a helium outlet temperature of 850°C, and a gas turbine electricity generation system [56, 57]. The GTHTR300 employs fully passive reactor safety, high fuel burnup, a conventional steel reactor pressure vessel, non-intercooled direct Brayton cycle power conversion, a horizontal single shaft gas turbine

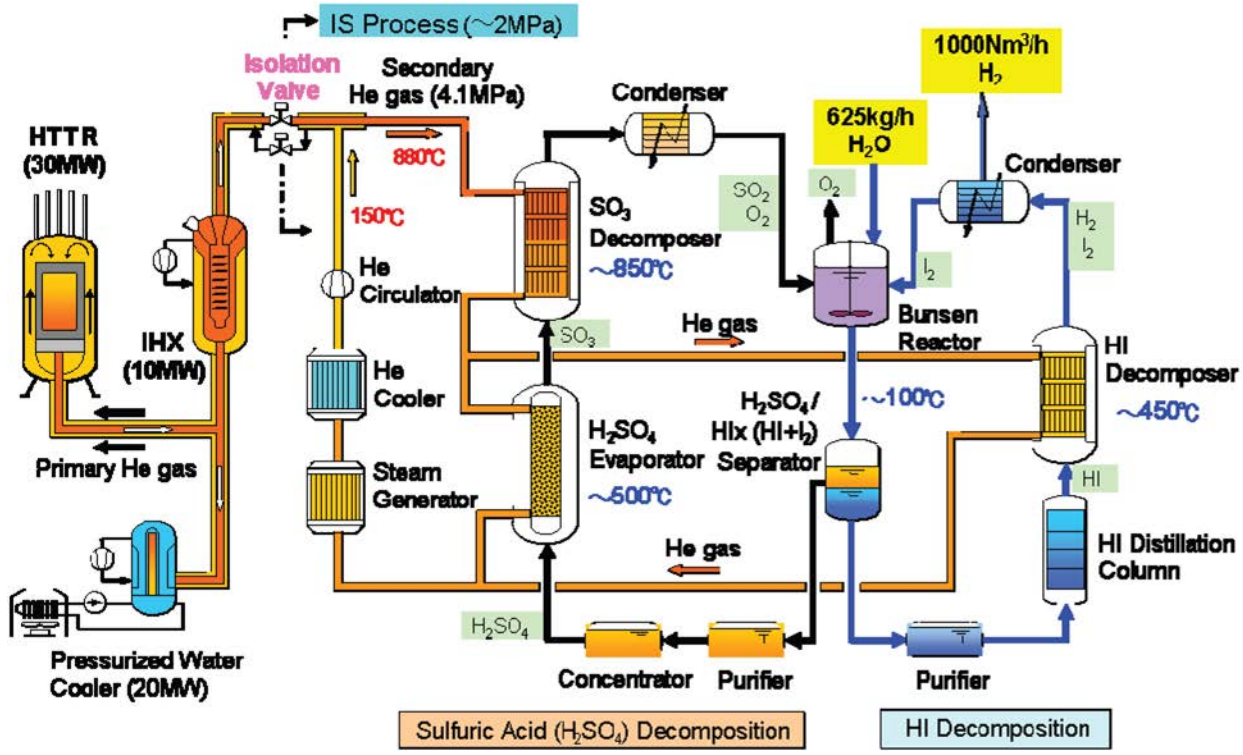

FIG. 13. Demonstration plant for nuclear hydrogen production with sulphur–iodine cycle connected to HTTR [53].

and electric generator, and a modular system arrangement. The reactor coolant temperature is limited to 850°C to avoid turbine blade cooling and to allow the use of conventional turbine blade materials. The elimination of an intercooling system reduces the power generation efficiency by 2%. But the system arrangement is simplified and the cost of construction becomes lower.

For the GTHTR300C (Fig. 14; see also Section 5.3.6.6), the thermal power provided to the hydrogen system can be increased from 170 to 370 MW if more hydrogen is needed. A total of 30 GTHTR300C could produce hydrogen to operate 5.9 million FCV which is about 8% of the assumed vehicle fleet of 75 million, while the 370 MW version could provide hydrogen for 12.6 million FCV [55].

2.6.3.2. Hydrogen production with sodium cooled fast reactors

According to the Science and Technology Basic Plan by the Council for Science and Technology Policy of 2006, the fast breeder reactor cycle technology was selected as one of the key technologies of national importance. Toshiba and CRIEPI developed the concept of the '4S Reactor', a sodium cooled pool type reactor with 30 or 135 MW(th) power output, passive safety features, and underground construction as an additional safety measure. The advanced fast reactor concept with sodium as a coolant is designed for 410 MW(e) power output. Its special feature is a double-wall steam generator to avoid construction of an intermediate circuit [58].

JAEA is also studying the concept of a sodium cooled reactor to produce hydrogen in the so-called Thermochemical and Electrolytic Process or JNC process. Since the maximum temperature remains below approximately 500°C because electrolysis is applied, a fast reactor can be employed. It is designed for a power of 395 MW(th) to provide primary sodium at 550°C and secondary sodium at 540°C. The electrolytic steps require an electric power of 18 MW for the SO_3 electrolysis and 56 MW for the SO_2 electrolysis. Hydrogen is yielded at a rate of 47 000 Nm^3/h [59].

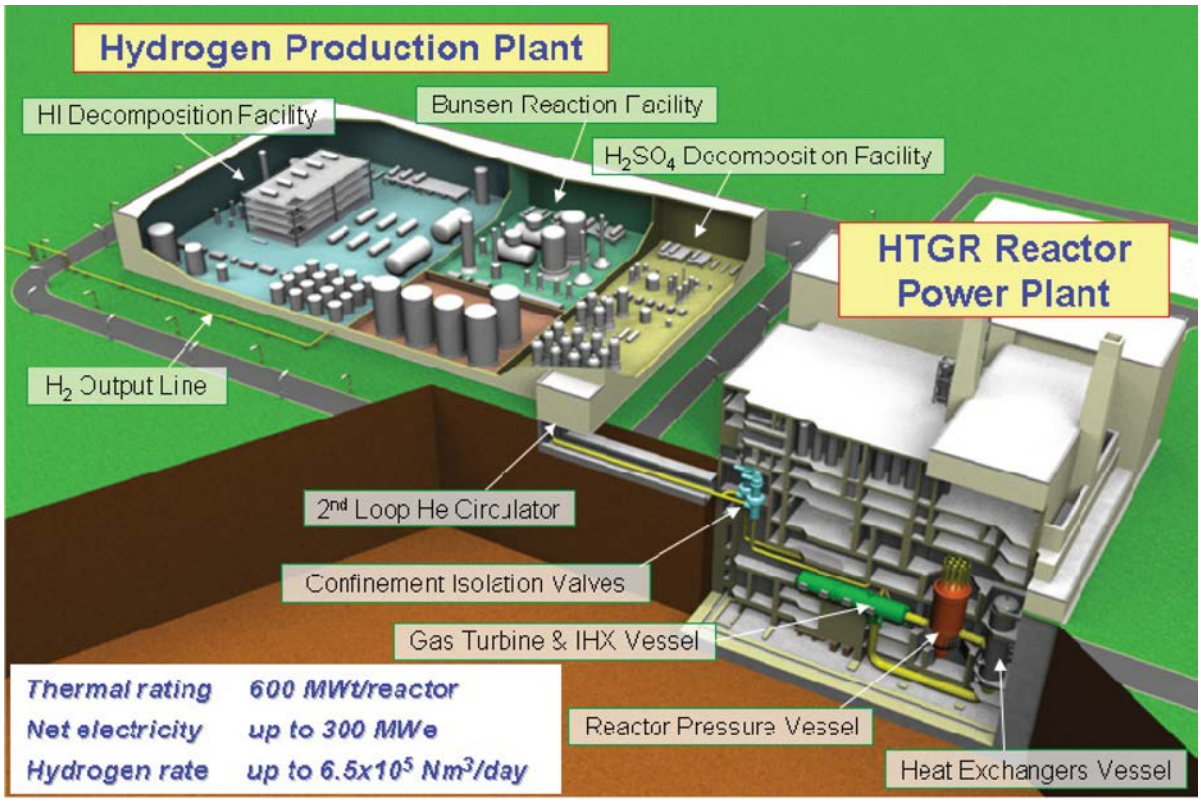

FIG. 14. Design of Japan's VHTR system GTHTR300C for hydrogen production with sulphur–iodine cycle [54].

2.6.3.3. Hydrogen production with water cooled reactors

Toshiba of Japan has proposed that steam reforming of dimethyl-ether (DME), a derivative of fossil fuels or biomass, could be used to produce hydrogen with 300°C heat from water cooled reactors (see also Section 3.2.3.3). With 40 MW of heat supply, production of approximately 230 t/d of hydrogen is possible, which is of the same scale as the largest hydrogen production unit existing. To date, the demonstrated production rate is 4.10 kg/d of hydrogen [60].

2.7. REPUBLIC OF KOREA

2.7.1. Energy situation in the Republic of Korea

The total primary energy consumption of the Republic of Korea in 2006 was 233 Mtoe (ranking ninth in the world), with 43% petroleum, 24% coal, 16% nuclear, 14% LNG, 2% renewables and 1% hydro. Energy consumption is expected to grow significantly in the future. The country lacks domestic energy resources and currently has to import 97% of its primary energy demand. The Republic of Korea is the sixth largest and fastest growing CO_2 emitter of the OECD countries. The total installed electrical generation capacity is 61.4 GW(e), of which 17.5 GW(e) is from nuclear. As of 2006, 36% of the electricity was generated by nuclear, 38% by coal, 20% by LNG, 5% by petroleum and 1% by hydropower. The Republic of Korea is a small country with a high population density where the use of low-density renewable energies is limited and not a practicable solution.

Commercial scale nuclear power generation started at the Kori-1 plant in 1978, and another 19 reactor units have since been built using a mixture of CANDU (4 reactors) and PWR (16 reactors) technologies. The total nuclear capacity amounts to 17.7 GW. Eight more plants are planned to come on-line in the period from 2010 to 2016, adding another 9.4 GW. According to the 'National Energy Basic Plan' of 2008, the share of nuclear in the

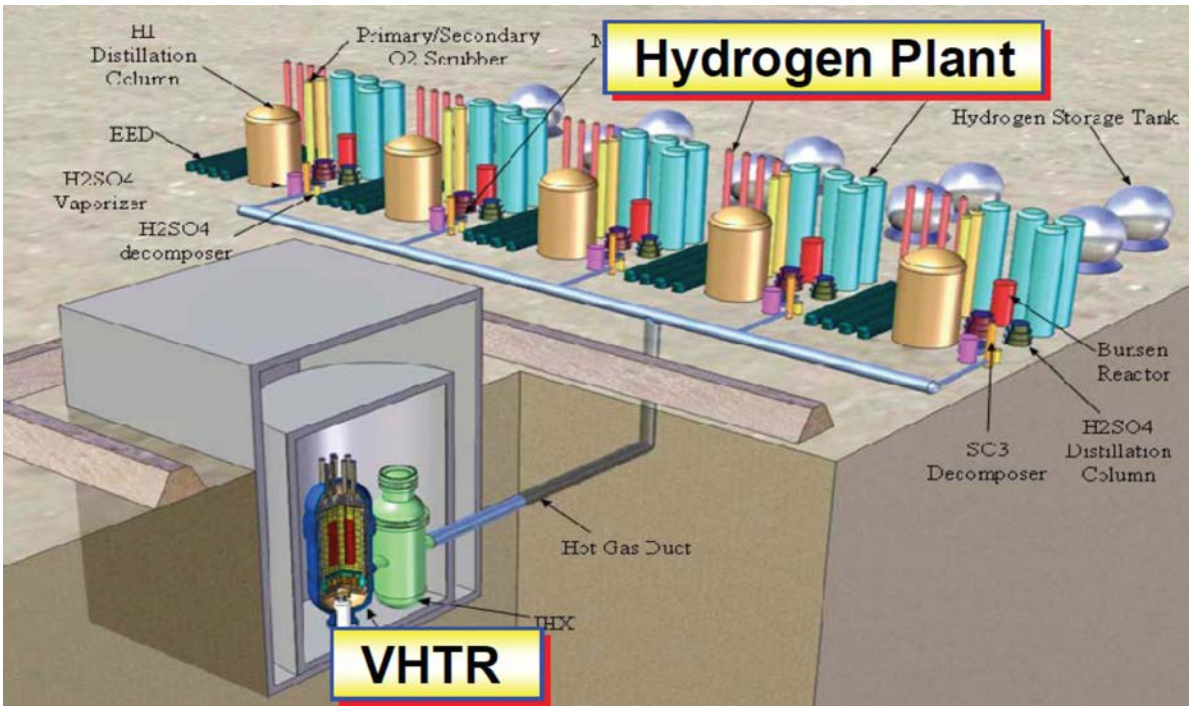

FIG. 15. Korean design of a VHTR for hydrogen production with S–I cycle [64].

primary energy should grow to 33% provided by 32 units. Nuclear power research in the Republic of Korea is very active with investigation into a variety of advanced reactors, including the Korea Atomic Energy Research Institute (KAERI) small system-integrated modular advanced reactor (SMART), a 330 MW(th) pressurized water reactor with integral steam generators and advanced safety features, and designed for generating electricity (up to 100 MW(e)) and/or for thermal applications such as seawater desalination. Other advanced reactor concepts under development are a liquid metal fast/transmutation reactor and a high temperature hydrogen generation design.

The Ministry of Science and Technology (MOST) initiated systematic research on the production, storage and utilization of hydrogen and started a fundamental fuel cell technology development programme. The hydrogen supply in the Republic of Korea was ~1 million t/a in 2008 and will increase to 3.6 million t/a or 7% of the total energy share in 2030 and 11.8 million t/a (15%) in 2040, respectively [61]. Of the anticipated 2040 hydrogen demand, 25% is projected to be generated with nuclear energy, for which about 50 nuclear hydrogen units will be required.

2.7.2. R&D activities on nuclear hydrogen production in the Republic of Korea

2.7.2.1. Nuclear hydrogen development and demonstration project

The Government of the Republic of Korea established a long term vision for the transition to a hydrogen energy economy [62] where nuclear energy will play an essential role in the hydrogen production at a large scale (Fig. 15). The main steps of this plan are to develop the technologies for production, storage and supply of hydrogen fuel by 2020, to demonstrate these technologies by 2030, and then to commercialize them on the basis of a Generation IV nuclear system [63].

In March 2004, MOST started the Nuclear Hydrogen Development and Demonstration (NHDD) project. Its main goal is the design, construction and demonstration of nuclear based hydrogen production technology and the achievement of commercial nuclear hydrogen production by the middle of the 2020s to cover 20% of the total vehicle fuel demand, corresponding to 3.3 million t/a of hydrogen [65, 66]. While the Government is leading the programme in the design phase, industrial participation is required from early on, to later take the lead in the construction of a demonstration nuclear plant.

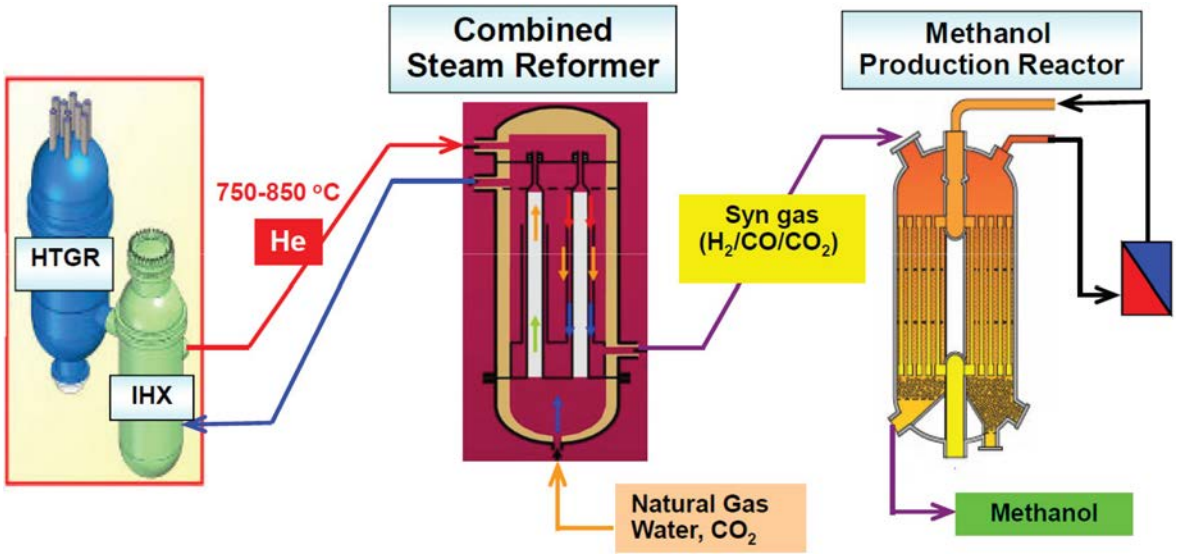

FIG. 16. Republic of Korea's concept for nuclear methanol production [68].

2.7.2.2. Nuclear hydrogen key technologies development project

A nuclear hydrogen key technologies development project was starting in 2006 as a 12 year national programme to develop and demonstrate the technologies required for the future nuclear H_2 system. The institutions involved in the project are KAERI for the nuclear part, and the Korea Institute of Energy Research (KIER) and the Korea Institute of Science and Technology (KIST) for the hydrogen part. These national activities are in parallel with the Generation IV VHTR R&D. Research and development is concentrating on HTGR technology. A two-step approach has been decided which foresees in the first step the deployment of an advanced HTGR (AHTGR) with a moderate coolant outlet temperature of 850°C to be connected to a steam–methane reforming system with the syngas used in iron ore reduction or methanol production. The final step will be the more challenging VHTR with a coolant outlet temperature of 950°C [61].

The steel industries in the Republic of Korea, which need a large amount of energy (currently 11% of the country's total energy consumption), are particularly considered for the introduction of nuclear energy from HTGRs. The introduction of nuclear would offer here the chance to reduce CO_2 emissions by substituting fossil fuel based processes and to produce the hydrogen needed for the direct reduction of iron ores [67]. Another example is methanol production in the chemical industries (Fig. 16).

2.8. RUSSIAN FEDERATION

2.8.1. Energy situation in the Russian Federation

The Russian Federation, one of the world's big energy superpowers, is rich in natural energy resources. It has the largest known natural gas reserves of any country on earth, representing 32% of the world's proven reserves. Furthermore, it has, with 157 billion t, the world's second largest coal reserves (10% of the explored coal reserves). The Russian Federation is the largest oil producer of the non-OPEC countries, and the second largest in the world after Saudi Arabia. It has the biggest oil shale reserves in Europe, equal to 35.47 billion t of shale oil. Last but not least, it possesses 8% of the proven uranium reserves.

In recent years, the Russian Federation has identified the gas sector as being of key strategic importance. The share of natural gas as a primary energy source is remarkably high compared with the rest of world. Gazprom has a monopoly for the natural gas pipelines and has the exclusive rights to export natural gas, and thus controls their access to the European market.

The total primary energy consumption in the Russian Federation was 665 Mtoe in 2007, down from 871 Mtoe in 1990, with 55% covered by natural gas, 20% by oil and 15% by coal [21]. It is the world's fourth largest electricity producer after the USA, China and Japan. In 2007, it produced 1013 TW·h of electricity. Roughly 67% of the Russian Federation's electricity is generated by thermal plants, 17% by hydropower and 17% by nuclear reactors. The Russian Federation is the world's leading net energy exporter and a major supplier to the European Union. In the Russian Federation, about 40% of electric power and 85% of heat supply, mainly in cogeneration, is covered by regional power industries with power plant units of ~300 MW(th) [69].

With the approval of the Kyoto Protocol by the Russian Federation in November 2004, the Accord could finally be brought into force 90 days after Russian ratification (16 February 2005). The Russian Federation's commitment is not to exceed the 1990 emission level. Its GHG emissions, however, fell well below the 1990 baseline due to a drop in economic output after the breakup of the Soviet Union. The actual Russian energy strategy is currently determined to find ways of reaching a better quality of fuel and energy mix by concentrating on energy safety, energy effectiveness, budget effectiveness and ecological energy security.

In the Russian Federation, three big nuclear reactor technology lines have been developed: the pressurized water reactor WWER, the boiling water reactor RBMK (which has been abandoned in the meantime), and the sodium cooled fast reactor. As of 2010, ten nuclear power plants with 32 nuclear units and a total installed capacity of 24.2 GW(e) were in operation, with four more units to be commissioned by 2013 [70].

The major objectives of the current programme are providing accelerated development of the nuclear power industry with the commissioning of new standardized serial nuclear units. For the near term, a modification of existing nuclear units is envisaged to extend their lifetime, as well as completion of construction of nuclear plants at the advanced construction stage. The announced target for future nuclear power generation is to provide 23% of the electricity needs by 2020. The Russian Federation has made plans to almost double the number of reactors in operation to 59. Older reactors will be maintained and upgraded, including RBMK units. Preparation for the construction of new nuclear plants based on the advanced WWER reactor unit with 1170 MW(e) is in progress. Also, the fast breeder reactor BN-800 with 2100 MW(th) and 880 MW(e) is currently under construction.

Based on several decades of experience with lead cooled or Pb–Bi cooled reactors, a large lead cooled fast reactor concept has been proposed with the Russian BREST reactor, designed for a power generation of 300 MW(e) (pilot scale) and 1200 MW(e) (commercial scale), with a primary coolant outlet temperature of 540°C and employing nitride fuel and a supercritical steam cycle.

In cooperation with the USA and Japan, the Russian Federation is currently developing the GT-MHR for disposition of surplus weapons-grade plutonium. Alternative fuel cycles for the Russian concept are also being investigated.

2.8.2. R&D activities on nuclear hydrogen production in the Russian Federation

Starting in the 1960s, the HTGR programme of the Russian Federation focused on the so-called VG reactors, including the pebble bed reactor concepts VGR-50, VG-400, VGM and VGMP, for which detailed designs have been elaborated, mainly by the OKBM. At present, the focus is on the block type GT-MHR, which is a cooperative effort with the USA.

Due to the vast amount of domestic natural gas resources and the anticipated need for large amounts of hydrogen in the future, steam reforming of methane will remain the dominant hydrogen production method in the first stage before being replaced with water splitting production processes. Since there is the potential for considerable savings of natural gas resources when utilizing nuclear energy as a heat source for the steam reforming process, the Russian Federation has developed an increased interest in utilizing modular type HTGRs for hydrogen production.

The reactor project MHR-T (see also Section 5.3.6.8) has been designed as a nuclear energy complex with a thermal power output of 600 MW(th). The complex includes a chemical–technological sector for hydrogen production plus necessary infrastructure. In the case of steam–methane reforming as the short term option, nuclear heat is considered to be directly transferred from the primary coolant to the chemical process, while for high temperature steam electrolysis, both two- and three-circuit plant configurations are being considered [71].

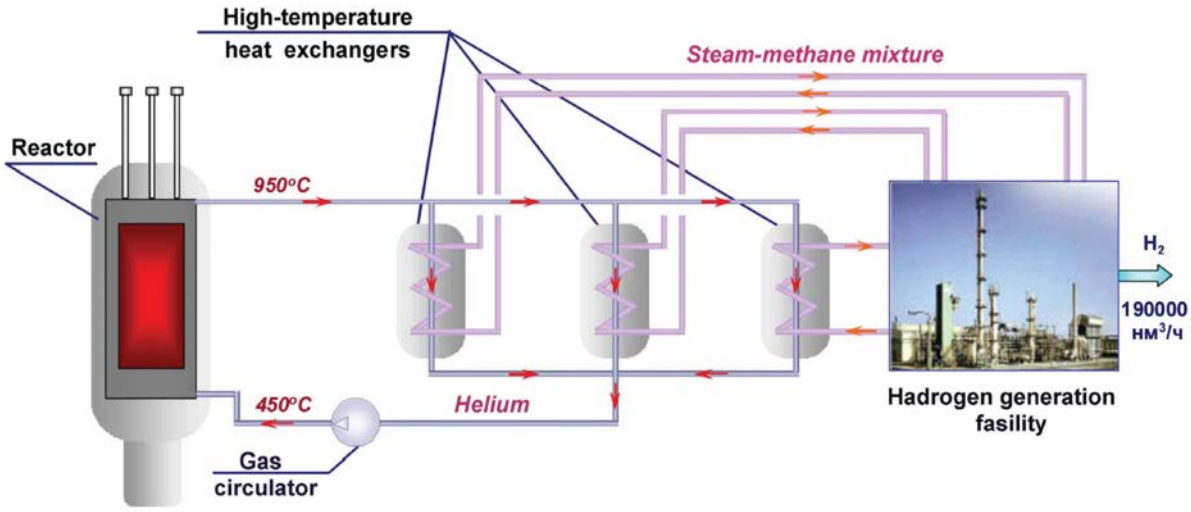

FIG. 17. Schematic of MHR-100SMR for hydrogen production by steam-methane reforming [69].

2.8.2.1. Nuclear steam–methane reforming

Based on the preconceptual design of the MHR-100 with a thermal power of ~215 MW and an electric power of 100 MW, the steam–methane reforming version, MHR-100SMR, is operated with a coolant outlet temperature of 950°C. The hot helium then enters the steam reformer which is composed of three heat exchangers (Fig. 17; see also Section 4.1.4).

Besides the production of pure (≥99.99%) hydrogen from steam–methane reforming, a modified process would also allow the production of methane–hydrogen mixtures in one process step (rather than by subsequent mixing). The mixture is like hythane (see Section 8.2.6.3), but with much higher hydrogen fractions of up to 48%, to be used, for example, as a cleaner transportation fuel [71].

Another technology of hydrogen production by methane thermal disintegration has been developed using advanced liquid metal cooled fast reactors [72], which is described in more detail in Section 5.3.6.8.

2.8.2.2. Nuclear hydrogen from high temperature steam electrolysis

In the MHR-100SE for high temperature steam electrolysis (Fig. 18), the helium coolant flows at a rate of 126 kg/s through the gas turbine for electricity production, while another part of the helium, at a rate of 12.1 kg/s, is used for the generation of steam at a pressure of 4.82 MPa. In the nuclear system to be used in the refinery industries, it is foreseen to employ an additional intermediate helium circuit to transfer the nuclear heat to the petrochemical plant, while all other concepts use a two-circuit system.

2.9. SOUTH AFRICA

2.9.1. Energy situation in South Africa

South Africa has only small deposits of oil and natural gas and relies on coal production for most of its energy needs. South Africa's economy is structured around large scale, energy-intensive mining and primary minerals industries having a high commercial primary energy intensity. The supply of primary energy in 2007 was 128 Mtoe at a growth rate of 4.4 %/a. The main shares were given by coal (68%), crude oil (19%), renewables (8%), nuclear (3%) and natural gas (2%).

South Africa accounts for a major fraction of the CO_2 emissions of the whole continent. Due to its large coal deposits, South Africa is one of the cheapest electricity suppliers in the world. The main reason is its coal based power generating capacity, whose share is 79% (of ~40 GW(e)), followed by crude oil (10%), renewables (6%),

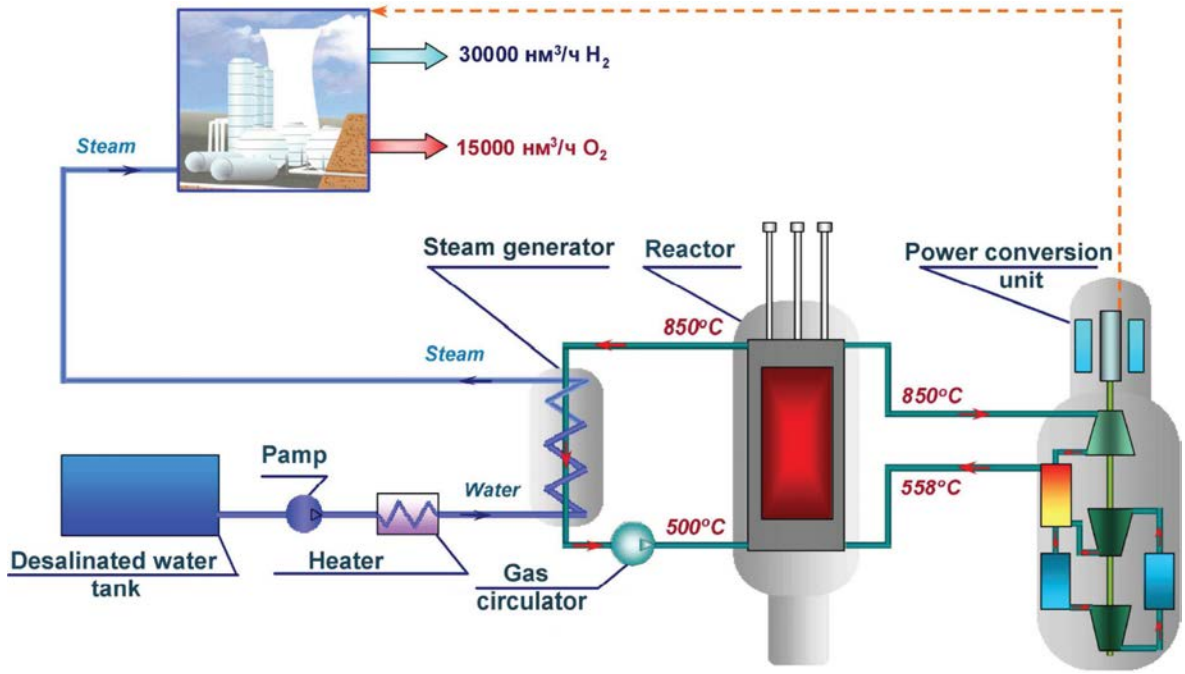

FIG. 18. Schematic of MHR-100SE for hydrogen production by HTSE.

nuclear (3%) and natural gas (2%). Eskom Holdings Ltd, the State owned power utility that supplies 95% of South Africa's electricity, is planning to increase the current generation capacity of 40 GW by 4%/a to 80 GW by 2025. The power supply crisis in January 2008, which forced shutdowns at mines, has accelerated recognition of the need to diversify the energy mix, such as with nuclear power and natural gas, as well as various forms of renewable energy.

Starting in 1984, the national utility ESKOM has been successfully operating the Koeberg nuclear power station consisting of two 900 MW(e) PWR units which generated ~6.5% of the electricity needs. In addition, ESKOM has been pursuing the project of modular HTGRs for electricity production to meet the demand of its growing economy.

In 2007–2008, the demand for electricity in South Africa started to exceed supply when the economy was growing and, at the same time, existing plants went out for maintenance. As a result, ESKOM and the South African Government decided to request proposals for new nuclear capacity and to expand the nuclear component in the energy supply mix of the country. In the strategic plan for the development of a national nuclear policy in 2007, South Africa decided for the promotion of an ambitious nuclear power plant construction programme. It has been projected that an additional 40 GW of electricity will be required over the next 20 years in South Africa. By 2030, nuclear energy should provide 30% of electricity in South Africa, from a fleet of LWRs and HTGRs.

2.9.2. R&D activities on nuclear process heat in South Africa

The main drivers for a larger scale national nuclear hydrogen programme are the significant domestic resources of uranium (10% of the global reserves) and the broad nuclear expertise (including HTGRs); domestic resources of platinum group metals (75% of the global reserves), required as catalyst material for fuel cells; and those of coal, providing the link to the country's highly developed CTL technologies. In 2007, a National Hydrogen and Fuel Cell Strategy was approved to develop local, cost competitive hydrogen production solutions on the basis of nuclear coal gasification with HTGRs.

In 2004, the PBMR project was officially launched and announced as a National Strategic Project. In 2009, when the project was hit hard by the world economic crisis and lost its financial backing by the Government, a number of technical achievements had been made. These include different reactor designs with the supporting nuclear engineering and safety analysis, with the latest reference concept being a 400 MW(th) pebble bed reactor

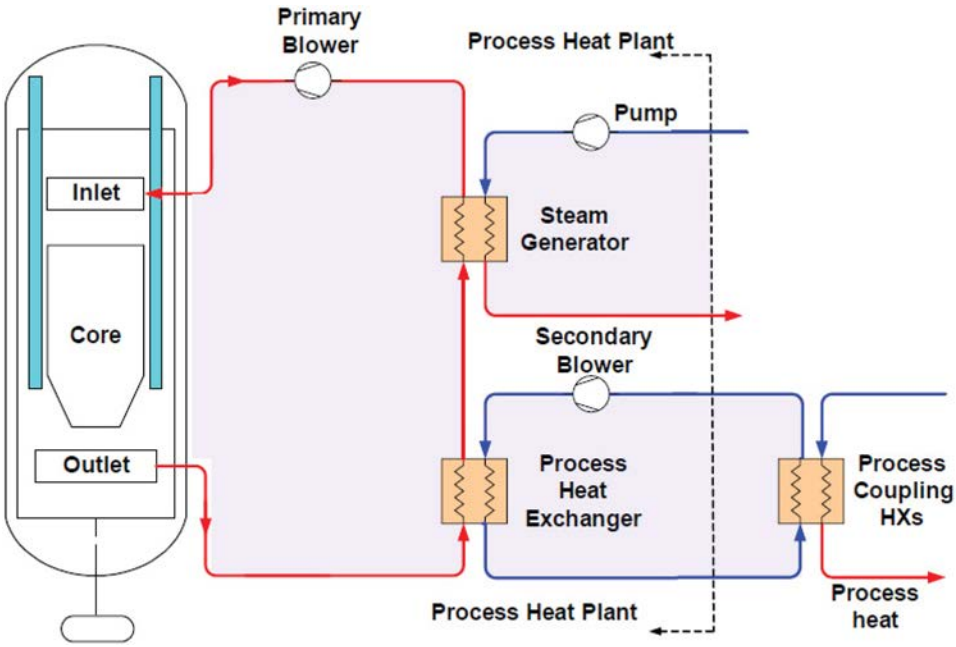

FIG. 19. Process scheme of steam–methane reforming with nuclear process heat plant [77].

with annular core geometry and utilizing a recuperative direct Brayton cycle to produce a nominal net electrical output of 165 MW(e). The manufacturing capability of pebble fuel including quality control has been managed such that the high quality of the latest German fuel production could be reproduced. Numerous test facilities and experiments accompanied by modelling methods and software development discussed with national and international nuclear regulators resulted in a wealth of expertise in nuclear engineering being gathered [73].

In 2008, as a result of the sudden increase of the oil price on the world market, a re-orientation took place. The PBMR company changed its business strategy and reactor design by concentrating on near term market opportunities to serve both electricity and process heat markets with nuclear steam cycle plants and smaller scales. Potential customers are the South African petrochemical company SASOL for delivery of process steam and, at a later stage, hydrogen, or oil sands producers in Canada. The most recent design has been scaled back to a 200–250 MW thermal steam cycle plant with a 200 MW(th), 80 MW(e) demonstration plant at the nuclear site in Koeberg.

In cooperation with Westinghouse, PBMR has developed the preconceptual design of an NGNP plant (see also Section 5.3.6.9). It employs a PBMR reactor for the production of hydrogen [74]. At a later stage, PBMR was concentrating on the design of a 200 MW(th) plant (DPP200) for steam production to be delivered to the chemical industries (see also Fig. 116). The final stage would be a process heat cogeneration plant with a coolant outlet temperature of 900°C, and steam of 550°C. The combination of a Brayton cycle with a Rankine cycle promises efficiencies of greater than 50%. A proposal was submitted in 2009 to the USDOE NGNP programme based on two 200 MW(th) reactors linked to an indirect steam cycle, but the participation in the NGNP programme ended with the withdrawal of the consortium from the project in 2010 [75].

PBMR developed the conceptual design for steam methane reforming under the heat delivery conditions provided by an HTGR (Fig. 19). Hot secondary helium enters the process plant at 900ºC and about 9 MPa, and exits at about 660ºC. Temperatures are somewhat below optimum reformer performance, but still it is believed that an HTGR can economically replace a natural gas heat source under certain conditions of high (and volatile) gas prices and the need for major reductions in CO_2 emissions [76, 77].

Other nuclear hydrogen production methods considered by PBMR were high temperature steam electrolysis and the thermochemical cycles, with a preference for the Westinghouse HyS hybrid cycle (Fig. 20). The fastest route to a design was to take the German HTR-Modul concept as basis and to develop a concept design for a 200–250 MW(th) plant which can be used for process heat only, electricity only, or both [73].

An environmentally friendly CTL technology is given if nuclear hydrogen from water splitting processes is taken for upgrading the fuel chains which result from the coal liquefaction processes. A nearer term solution would

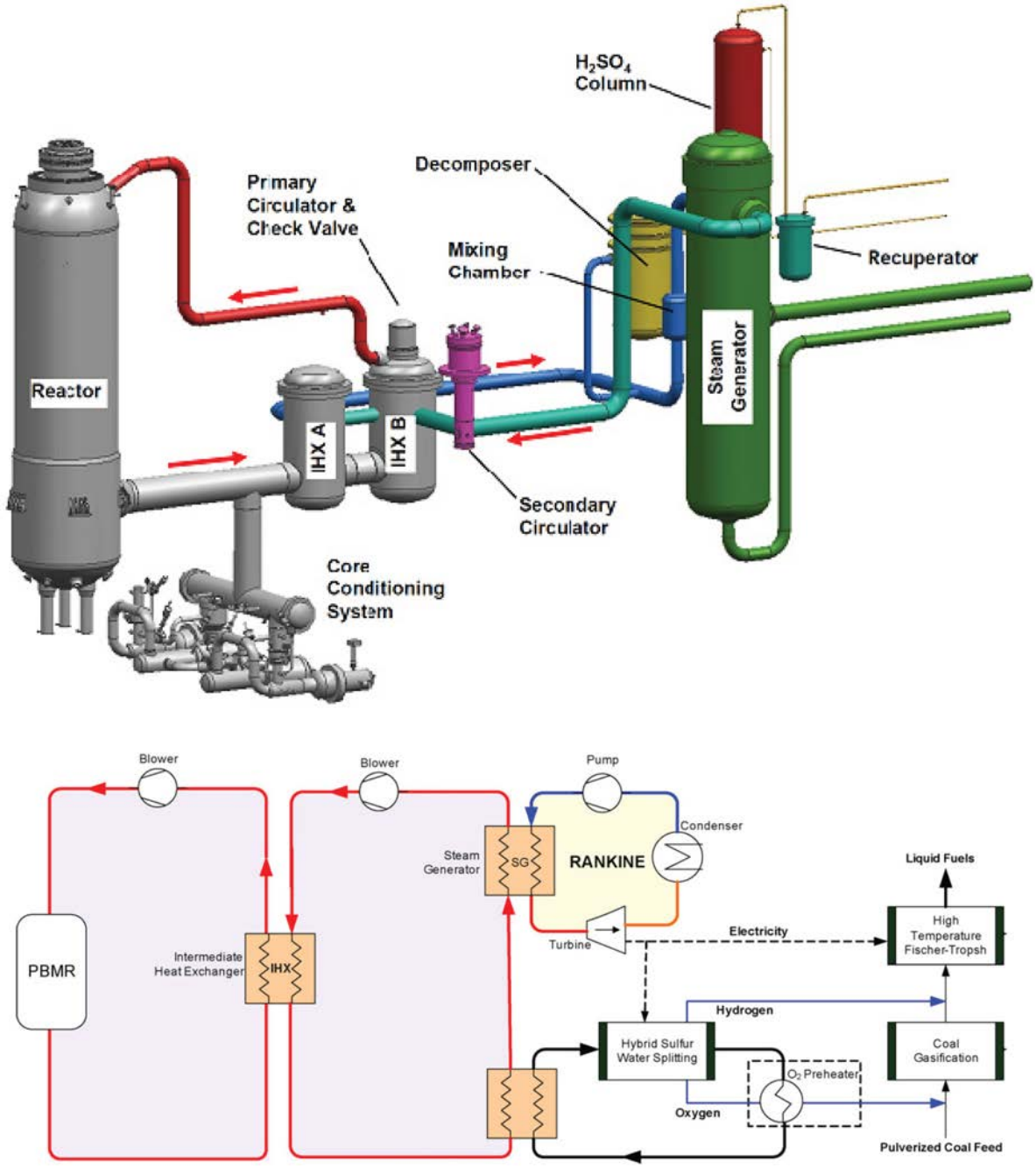

FIG. 20. Schematic (top) and process scheme (bottom) of nuclear CTL with PBMR and hydrogen from the HyS process [74].

be the delivery of nuclear-produced process steam, to be used in the petrochemical industries for CTL processes or oil sands recovery. At a later stage, also hydrogen may be delivered from PBMR plants to serve not only the chemical industries, but also the future transportation fuel market. In addition to process steam, cogeneration and water desalination options are also being pursued [78].

The idea of collocating a 400 MW(th) PBMR plant within a chemical complex to supply process heat for ethylene production is elaborated in Ref. [79]. Ethylene can be produced from different feedstocks by thermal cracking of hydrocarbons (pyrolysis) at ~750°C in the presence of steam and subsequent separation by multiple distillation steps at low temperatures. The power output of 400 MW(th) corresponds to the demand for the pyrolysis step (consuming 75% of the total energy needed) in a large ethylene production train. As the heat transport medium to the chemical process, the fluoride salt Flinak was selected. One coupling option suggested was to transport the

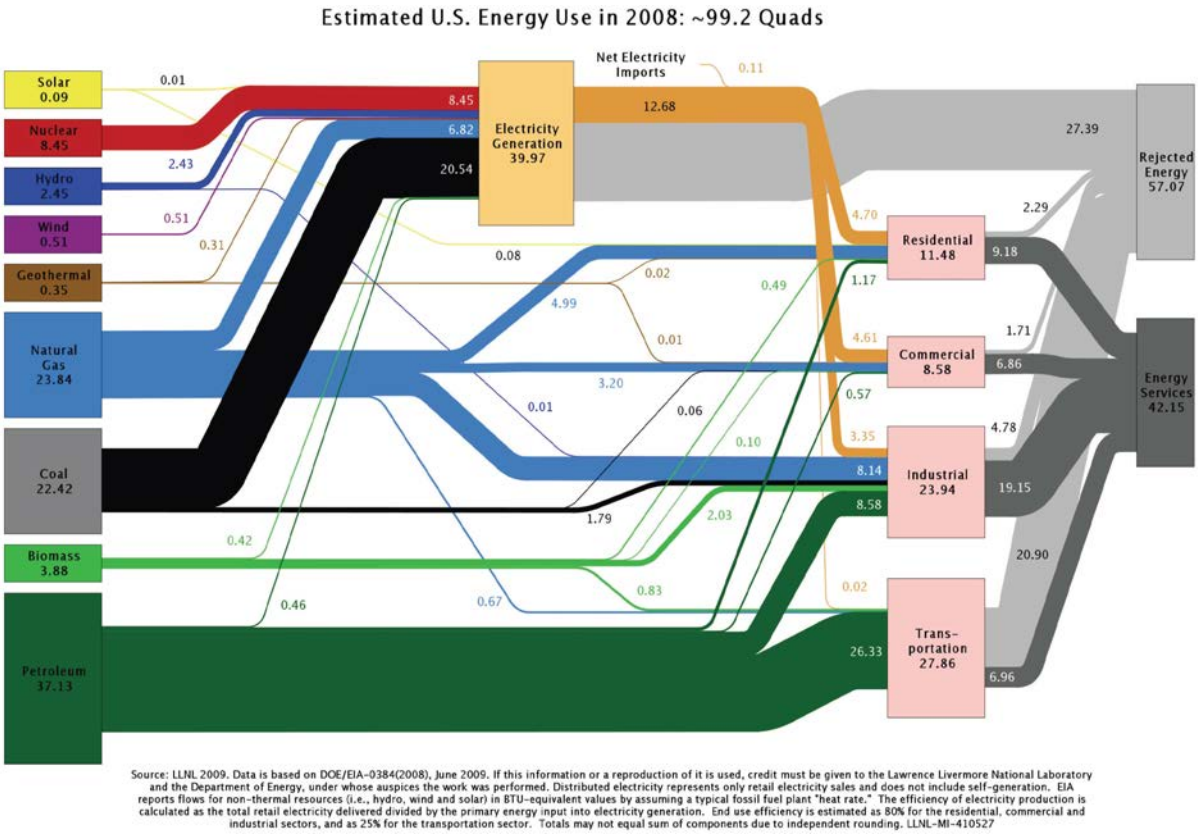

FIG. 21. Estimated energy use in the USA in 2008 [80].

hydrocarbon feedstock near the nuclear plant for conduction of the high temperature pyrolysis step and to return the cooled cracking products to the chemical site for distillation.

2.10. UNITED STATES OF AMERICA

2.10.1. Energy situation in the United States of America

The USA uses more energy than any other country in the world. Energy consumption exceeds domestic supply, which continuously declines. Currently, 27% of the energy needs are imported, a share which will rise to 31% by 2020. In 2007, the USA consumed in total 2337 Mtoe of primary energy [21]. An estimate of the energy use in 2008 is given in Fig. 21 [80]. The country's largest source representing 39% of the energy demand is crude oil, of which 60% must be imported. About 66% of the oil is consumed in the transportation sector and 24% in the industrial sector, while the remainder is used for residential and commercial heating. The USA is also the largest consumer of natural gas, with 27% of the world's annual production. Natural gas is increasingly used for electricity production (almost doubled to 21% in 2007 compared to 1990) and will remain in the nearer term the fuel of choice for new electric power plants. About 16% of the natural gas consumed is imported, partly in the form of LNG. Regasification of LNG is a growing industry. Coal is the most abundantly available energy resource in the USA. About 50% of the electricity production is from coal, which is responsible for a relatively high level of pollutant emissions. The USA will need approximately 400 GW of new power generation capacity by 2020.

In 2007, nuclear energy accounted for 837 TW·h or 19% of the total electricity production from the operation of 104 nuclear reactors with a capacity of 101.2 GW(e). To maintain this nuclear share, the equivalent of 30 1000 MW nuclear reactors will have to be built. Renewables are basically used for electricity production with a share of 9% (with 6% from hydro and 3% from other renewables).

In recent years, there has been a renewed interest in nuclear power in the USA. This has been facilitated in part by the Federal Government with the Nuclear Power 2010 Programme and the Energy Policy Act. By March 2009, the US Nuclear Regulatory Commission (NRC) had received applications for permission to construct 26 new nuclear power reactors, with applications for another seven expected. Types of reactors include ABWR, AP-1000, ESBWR and US-EPR. To achieve energy security and stability, the US Energy Policy Act of 2005 (EPAct) defined a strategy to demonstrate an HTGR.

The USA has the fourth largest uranium reserves in the world. Domestic production increased until 1980, after which it declined sharply due to low uranium prices. In 2001 the United States mined only 5% of the uranium consumed by its nuclear power plants. The remainder was imported, principally from the Russian Federation and Australia. After 2001, however, uranium prices were steadily increasing, which prompted enhanced production and revived domestic mines.

In the American Clean Energy and Security Act of June 2009, it was foreseen to define, for the first time in the USA, upper limits of GHG emissions with the goal of a 17% reduction of the 2005 emissions by 2020. At present, the transportation sector accounts for one third of fossil fuel GHG emissions; 16% are from industrial applications.

US process energy demand is in the order of 49 Mtoe in the process temperature range of 250–500°C, of which more than 90% is used for various petroleum products and Canadian oil sands; 41.5 Mtoe in the range of 500–700°C for petroleum products and ammonia; and about 9 Mtoe in the high temperature range of 700–950°C for ethylene, propylene and hydrogen production [81]. Synthesis gas production in the USA amounted to 6700 MW of thermal equivalent in 2005, delivered from 20 coal gasification plants [81].

The annual production of hydrogen was 11 million t in 2006, representing ~49 GW(e) (HHV) or ~1% of the primary energy. Of all hydrogen, 90% is produced by steam–methane reforming, consuming 5% of the natural gas used in the USA [82]. This quantity would be sufficient to power 60 million FCVs. Demand for hydrogen in the USA has been increasing by 10%/a [83] and is expected to grow to more than 30 million t/a by 2030 [84]. Since 1982, there has been a 59% expansion of on-site refinery-owned hydrogen plant capacity in the USA, an average growth rate of 1.2%/a. Currently, the largest sources of hydrogen production capacity in the USA are associated with the nation's 145 operating oil refineries. Three major potential hydrogen markets seen in the USA are transportation, electric power, and production industries. R&D activities have been or are being supported by the Hydrogen Fuel Initiative of 2003, the Hydrogen, Fuel Cells and Infrastructure Development Programme, the Multi-Year Research, Development and Demonstration Plan of 2005, and the Roadmap for Manufacturing R&D on the Hydrogen Economy of 2005.

2.10.2. Nuclear hydrogen production R&D programme in the United States of America

The USDOE has initiated a Global Nuclear Energy Partnership (GNEP), to offer a framework for worldwide use of nuclear power while reducing the risks of nuclear proliferation and the impacts of radioactive waste. US participation in GIF is on sodium cooled fast reactors and very high temperature reactors.

2.10.2.1. The Nuclear Hydrogen Initiative

The goal of the Nuclear Energy Research Initiative (NERI) is to demonstrate the commercial scale production of hydrogen using nuclear energy by 2017. The modular helium reactor (MHR) has been suggested as the Generation IV reference concept for nuclear hydrogen generation on the basis of either the S–I thermochemical cycle or HTSE.

As part of the national hydrogen research programme, the USDOE created the Nuclear Hydrogen Initiative (NHI) with the objective being to advance nuclear energy for the support of a future hydrogen economy. The frame was widened with the start of the International Nuclear Energy Research Initiative (I-NERI) for bilateral or multilateral international cooperation supporting R&D activities for Generation IV, the NHI and the advanced fuel cycle R&D.

The objectives of I-NERI include the development and demonstration of technologies which enable the nuclear powered production of hydrogen by non-fossil based water splitting H_2 production processes. The USDOE cost goal for hydrogen (as of 2005) is US$2–3 per gge (gallons of gasoline equivalent), independent of the pathway of H_2 production and delivery [85]; 1 gge corresponds to 1.004 kg of H_2 [86]. Thermochemical cycles that were selected by a screening effort within the NHI are listed in Table 4.

TABLE 4. USDOE NUCLEAR HYDROLOGY INITIATIVE SELECTED THERMOCHEMICAL CYCLES

	Thermochemical cycles
Highest priority baseline cycles	Sulphur–iodine (S–I)
	Hybrid sulphur (HyS)
	Suphur–bromine hybrid
Next priority cycle	Calcium–bromine
Promising alternatives	Copper–chlorine hybrid (Cu–Cl)
	Iron–chlorine (Fe–Cl)
	Copper–sulphur hybrid
	Vanadium–chlorine (V–Cl)

Between 2003 and 2008, the USDOE promoted nuclear hydrogen programmes in the USA which concentrated on:

— Hybrid sulphur thermochemical cycle development at Savannah River National Laboratory (SRNL);
— High temperature electrolysis development at the Idaho National Laboratory (INL);
— S–I process development at General Atomics.

In a down selection activity in 2009, led by INL, to systematically evaluate and select the best technology for deployment with NGNP, HTSE was judged as the most appropriate advanced nuclear hydrogen production technology that presents the greatest potential for successful deployment and demonstration at NGNP. But it was also stated that both HyS and S–I processes exhibit attractive attributes for hydrogen production, which supports not abandoning either technology for future consideration [87, 88].

The Nuclear Hydrogen Initiative ended in 2009.

2.10.2.2. Nuclear gas cooled reactor concepts

(A) Next Generation Nuclear Plant (NGNP)

As a part of the Energy Policy Act of 2005, the USA has been designing a Next Generation Nuclear Plant (NGNP). This government sponsored demonstration programme of a VHTR Generation IV system is to be conducted by an alliance of suppliers of the technology, nuclear plant owner/operators, other support technology companies, and potential industrial end users of the technology. This alliance in partnership with the USDOE would provide the private sector perspective and support the selection of the specific operating conditions and configuration for the NGNP [89]. A licensing strategy is required to be developed with the NRC.

The NGNP project's objective is to develop and demonstrate a first of a kind nuclear system with the capability to generate electrical power and produce process heat for hydrogen production and other applications. The nuclear plant is based on a 400–600 MW(th) full scale prototype gas cooled reactor using an indirect cycle with intermediate circuit to provide electricity and process heat at 950°C. From the total thermal power, a part is planned to be consumed for hydrogen production using either the S–I process or the HyS cycle or high temperature steam electrolysis (Fig. 22).

Preconceptual design studies for the NGNP project have been developed by three contractor teams with the team leaders Westinghouse Electric Company LLC, AREVA NP Inc., and General Atomics (Table 5). With the decision of the US Secretary of Energy in March 2010, both a pebble and block type reactor design will be subjected to continued work on a conceptual design. The selections will support the development of conceptual designs, cost and schedule estimates for demonstration project completion and a business plan before a final decision will be made to proceed to Phase 2, which would entail detailed design, licence review and construction of a demonstration plant.

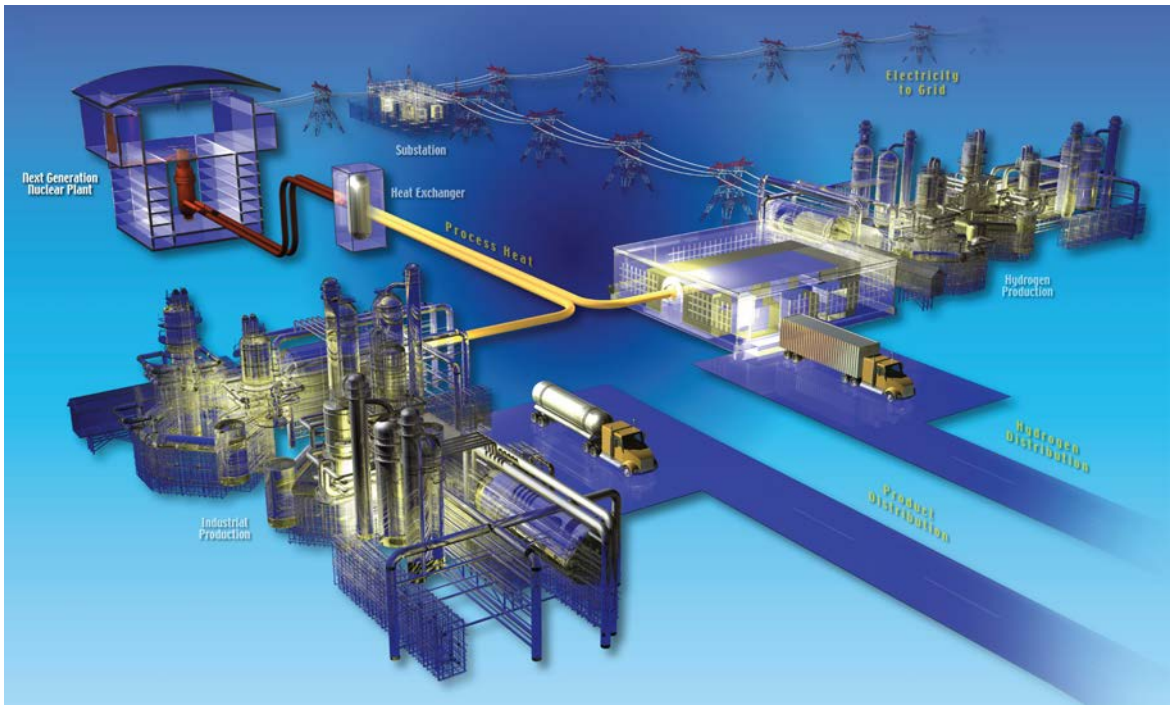

FIG. 22. NGNP combined with both S–I and HTSE systems [90].

Because the NGNP is a prototype plant, and in order to reduce the technology development risks, it is likely that initial operation will start at less than full design conditions (e.g. lower coolant outlet temperature) with a subsequent proof of principle operating period which will be used to verify design assumptions as plant operating conditions are gradually expanded to the full design point. Baseline fuel design for the first modules will be low enriched uranium (LEU) TRISO coated particle fuel in a once-through fuel cycle. The initial operating period will also demonstrate general technical performance and reliability of the primary and support structures [89]. More specifically, the use of a high temperature helium direct Brayton cycle has been suggested to be replaced with a primary helium cycle and a secondary Rankine steam cycle. Potential materials problems are met in the modified reference design by a reduced outlet fluid temperature of 750–800°C.

The hydrogen production technology will interface with the NGNP via an intermediate heat exchanger or steam generator. The interface parameters are [87]:

— Utilize up to 50 MW(th) total reactor power with any electric conversion at 40%;
— He IHX outlet to the hydrogen process at 700°C and 7 MPa pressure;
— Outlet temperature from steam generator up to 550°C at 15 MPa pressure.

The potential for tritium contamination of the hydrogen production process loop is minimized by the employment of an additional process heat exchanger [91].

While the original NGNP mission goal was for the project to be built at INL, interested industries favour the co-location of the demonstration facility with an existing commercial chemical plant. In the modified version of cogeneration of process steam and electricity, General Atomics suggested a 350 MW(th) MHR with a prismatic LEU UCO core in a single primary helium loop at 750°C outlet temperature, and a single secondary water/steam loop to produce steam at 540°C, 17.3 MPa. Electricity generation will be done via Rankine cycle, while process steam generation will be conducted in a tertiary system via steam-to-steam heat exchanger [92].

TABLE 5. PRECONCEPTUAL DESIGNS FOR NGNP [89]

	Westinghouse	AREVA	General Atomics
Reactor core	Pebble bed	Prismatic	Prismatic
Cycle configuration	Indirect Rankine	Indirect Rankine PCS and H_2 process	Direct Brayton
Power size (MW(th))	500	565	550–600
Reactor inlet/outlet temperature (°C)	350/950	500/900	490/≤ 950
Fuel	TRISO UO_2	TRISO UCO	TRISO UCO
Secondary fluid	He	He–N_2 to PCS He to H_2 process	He
IHX	2-stage PCHX	PCS, 3-helical coil shell & tube	
PHX		PCHX or PFHX	1-stage PCHX
Hydrogen production	HyS, HTSE	HTSE, later S–I	HTSE, later S–I
Hydrogen plant power	10% of total power	10% of total power	5 MW(th) for HTSE 60 MW(th) for S–I

(B) Modular helium reactor for hydrogen production (H2-MHR)

The GT-MHR design with a prismatic and annular core design (see Section 5.3.6.10) is a General Atomics development which should go up to 600 MW(th) with direct gas turbine cycle and filtered confinement. For commercial use, the GT-MHR of 600 MW(th) power will use an LEU fuel cycle. It is designed for averaged coolant inlet/outlet temperatures of 590/950°C working with an efficiency of 48–52% for electricity production [93]. The option for cogeneration of electricity and process heat is also studied (see Section 5.3.6.10). In cooperation with the Russian Federation, a parallel GT-MHR design is being developed for surplus weapons plutonium disposition. The GT-MHR project coordinating committee decided that before final design development starts, all efforts and funds should be concentrated on technology demonstration. The GT-MHR for hydrogen production is referred to as H2-MHR.

INL has conducted system analyses of commercial-size nuclear hydrogen production plants based on HTSE (Fig. 23) [94, 95]. Flowsheet studies were made for a 600 MW(th) reference HTGR operated at 7 MPa with coolant inlet/outlet temperatures of 540/900°C. The HTSE section operating ideally at 5 MPa consists of 4 million electrolysis cells, each with an active cell area of 225 cm^2 requiring 300 MW(e) as direct current.

The overall thermal-to-H_2 conversion efficiency was assessed to be 47.12%, corresponding to a hydrogen production rate of 2.356 kg/s. The process analysis tool UniSim was used to develop realistic flow diagrams for three different advanced nuclear reactors, a direct cycle helium cooled HTGR with 900°C outlet temperature, a CO_2 cooled SCWR with 650°C outlet temperature, and a sodium cooled FBR with 550°C outlet temperature, all connected to a power cycle and an integrated HTSE loop. On the hydrogen side, the cell area was assumed to be 225 cm^2. The results have shown that reasonable H_2 production rates can be achieved at efficiencies in the range of 45–50% for the HTGR, 42–44% for the SCWR and 33–34% for the FBR.

The same code UniSim was also applied to a 600 MW(th) and 300 MW(e) co-electrolysis plant for dedicated synthesis gas production. Such a system is conceivable in combination with a biomass plant to deliver the feedstock CO_2 and with Fischer–Tropsch conversion to synthetic liquid fuels [96]. For the nuclear reactor concept, a coolant exit temperature of 900°C and a direct Brayton cycle is foreseen. The feed stream to the electrolyser cell is a mixture of CO_2, H_2 and synthesis gas with a share of 10% recycled from the product stream. The mixture receives its cell operation temperature from nuclear heat in an IHX. The hot product stream flows through a recuperator to

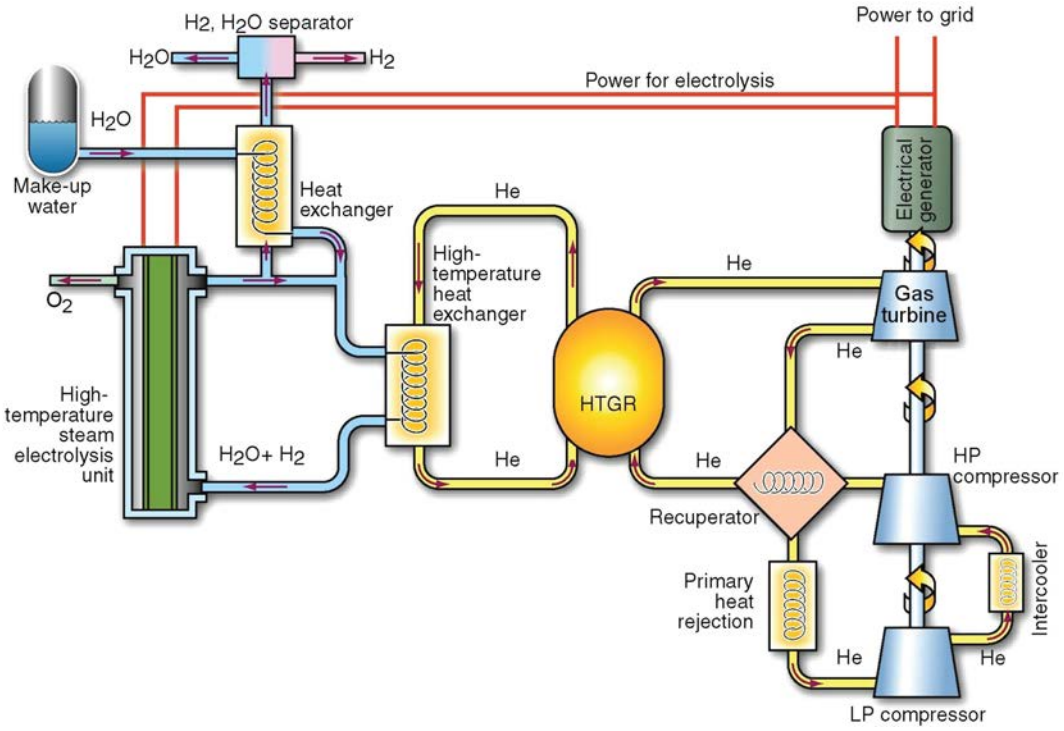

FIG. 23. MHR coupled to high temperature steam electrolysis [86].

preheat the feed stream. Air is used as sweep gas to dilute and remove the hot excess oxygen. The efficiency is estimated to be 48.3% to result in a synthesis gas production of ~10 kg/s or 78 000 Nm^3/h.

Initial analysis of the latest INL reference design using the HYSYS process analysis software results in a hydrogen production rate of 1.75 kg/s at an overall efficiency of 40.4% with a reactor power source of 600 MW(th) operating at a reactor outlet temperature of 750°C. The electrolysis stack is assumed to consist of 1.057 million electrolysis cells operating at a current density of 0.6969 A/cm^2 and a steam utilization rate of 66.67% [91].

2.10.2.3. The liquid salt cooled advanced high temperature reactor

A reactor system that did not survive the selection process for Generation IV type reactor concepts was the advanced high temperature reactor (AHTR). It is a reactor concept that combines four existing technologies in a new way [97]: (i) coated particle fuel in matrix graphite; (ii) high temperature Brayton power cycle with coolant outlet temperatures between 700 and 1000°C; (iii) passive safety systems and plant designs from liquid metal cooled fast reactors; and (iv) low pressure liquid salt coolants with boiling points far above the maximum coolant temperature. The AHTR uses technologies from VHTRs, GFRs and MSRs, but it is not an MSR where the fuel is dissolved in a molten salt. It is actually viewed as a follow-on concept for the VHTR, therefore also called LS-VHTR. It should be economically competitive with LWRs or modular HTGRs.

2.10.2.4. The STAR-H2 reactor

Another project as part of the USDOE NERI is the Secure Transportable Autonomous Reactor Hydrogen (STAR-H2) project (Fig. 24), characterized by passive safety features. The concept was originally based on the Russian submarine reactor technology demonstrated at ~500°C. STAR-H2 is designed as a heavy liquid metal cooled, mixed U–TRU–nitride fuelled fast reactor with a power of 400 MW(th) supplying heat at a maximum of 800°C. The primary coolant, lead, circulates by natural convection and transfers its heat to a molten salt coolant (FLiBe = containing F, Li and Be) in a low pressure intermediate circuit. The salt then transfers heat to a hydrogen production system based on a variant of the Ca–Br (UT-3) thermochemical cycle.

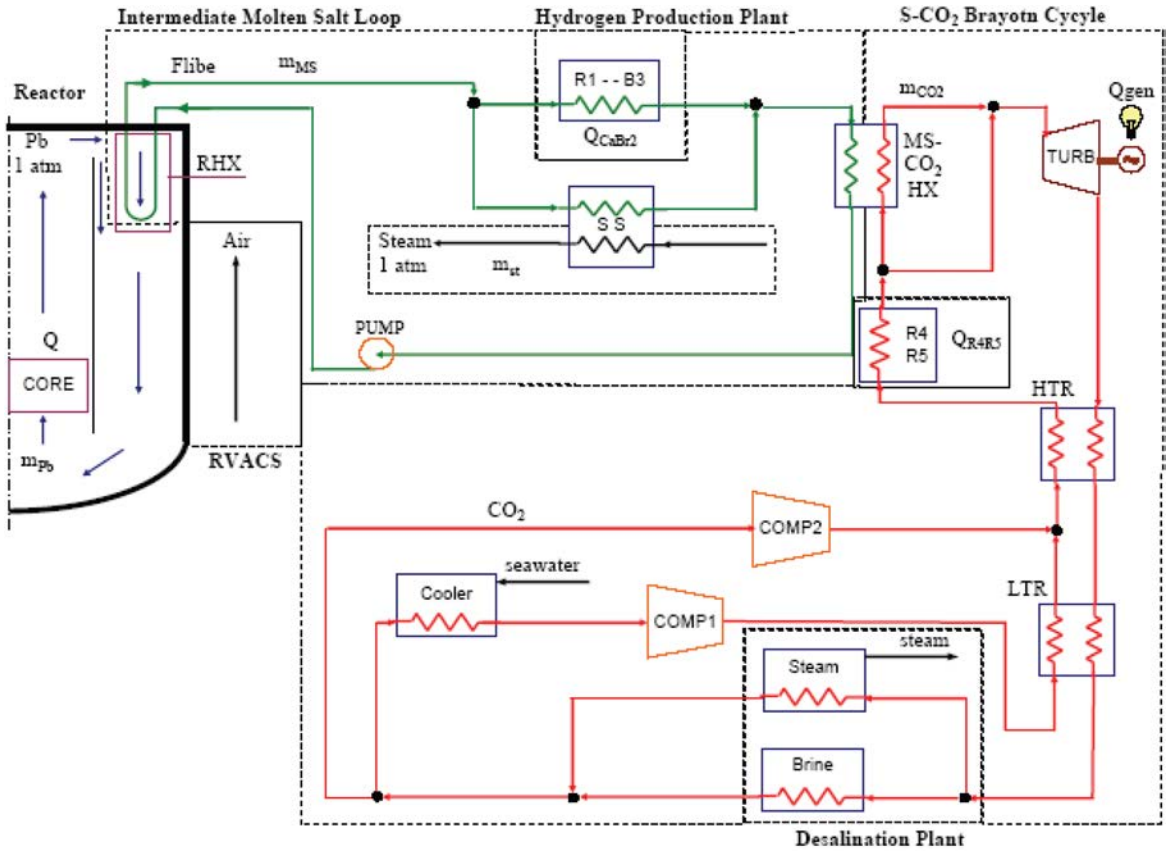

FIG. 24. STAR-H2 concept [98].

The Ca–Br (star) cycle operates at atmospheric pressure employing a single-stage HBr dissociation step:

$$2\,HBr + plasma \leftrightarrow Br_2 + H_2$$

This production process rejects heat at ~600°C, which — plus some heat from the FLiBe — is used for electricity production in a supercritical CO_2 Brayton cycle. Rejected heat from the Brayton cycle (< 125°C) can be used in an MED desalination plant with a capacity of 8000 m^3/d of potable water [99]. The operation of a liquid metal reactor above 600°C poses extensive materials problems yet to be solved.

The liquid salt cooled fast reactor (LSFR) has a design similar to that of the AHTR. The coolant is a fluoride salt such as sodium–zirconium salt, to minimize neutron moderation. Operating temperatures are 700–800°C, limited by fuel clad materials. The high temperature metal cladding also has to withstand the corrosive environment and the fast neutron radiation.

In a molten salt breeding reactor (MSBR), all fissile, fertile and fission product materials are dissolved in the coolant, which flows to a primary heat exchanger to transfer heat to a secondary liquid salt coolant. For the 1000 MW(e) plant concept, the primary coolant temperatures are 565°C at the inlet and 705°C at the outlet at atmospheric pressure. A molten salt reactor technology (MOST) project aimed at investigating the potential of MSRs as breeders or burners. The critical aspects are neutronic stability, viability of the reprocessing scheme and mechanical integrity of the primary circuit structures.

3. METHODS OF HYDROGEN PRODUCTION

3.1. INTRODUCTION

Current global hydrogen production has been estimated at around 7×10^{18} J/a, corresponding to ~52.6 million t/a (HHV) or ~630 billion Nm^3/a, which is about 2% of the world's total energy consumption [100]. Almost all hydrogen on earth is found in compounds, mainly in combination with oxygen as water or in combination with carbon as organic substances.

Contemporary industrial hydrogen production is primarily based on extraction from fossil resources, foremost the reforming of natural gas (48% of the world's production), but also processes like partial oxidation (POX) of oil and off-gas from refinery processes in the chemical industries (30%) and the gasification of coal (18%) [101]. Electrolysis contributes 3.9%, with about 2% being generated as a side product in chlorine–alkaline electrolysis. Still at a minor scale and in the demonstration phase is biomass gasification to produce a hydrogen and/or methane rich fuel gas. The various process paths from primary energy to the end product and secondary energy carrier, hydrogen, are illustrated in Fig. 25, encompassing both the CO_2 emitting extraction processes from hydrocarbons and the CO_2 emission free water splitting processes.

In the future, new production processes will be needed to supply hydrogen to the energy market, including the use of biomass and CO_2 free or CO_2 neutral primary energies.

3.2. HYDROGEN FROM FOSSIL FUEL PROCESSING

The principal conversion product of hydrocarbons is synthesis gas, a mixture of hydrogen and carbon monoxide, mainly resulting from the processes of steam reforming, POX or autothermal reforming. The process is,

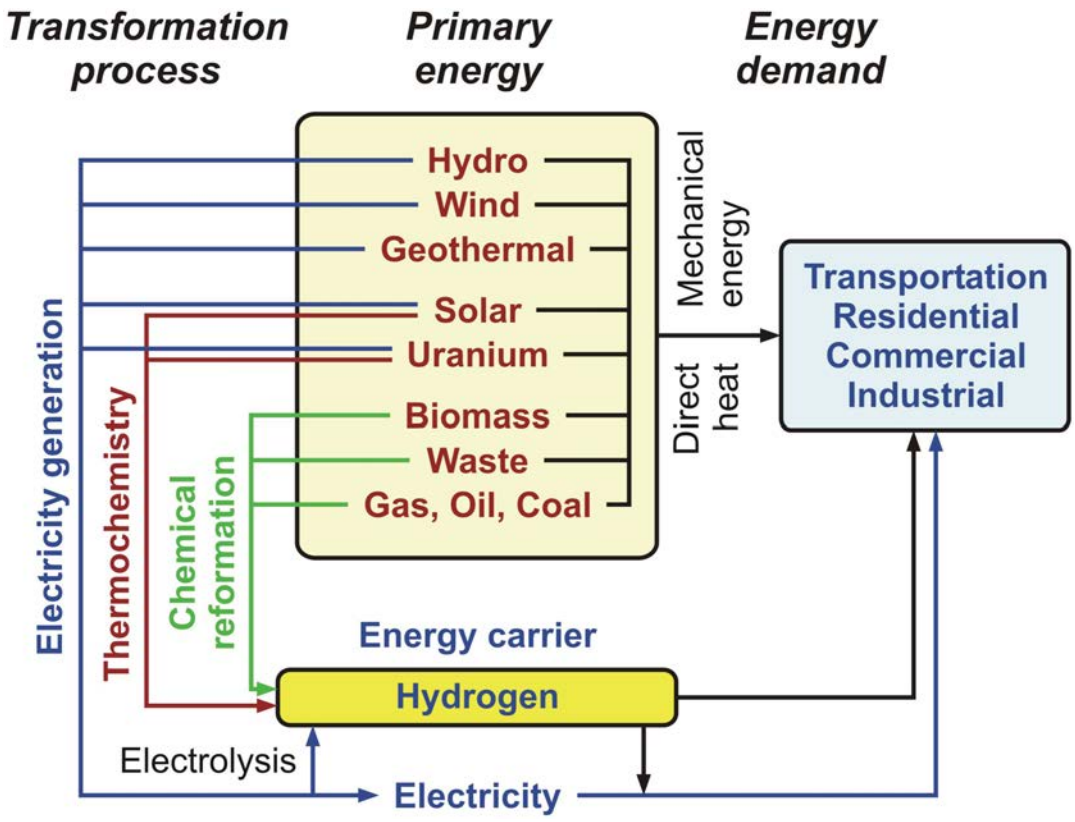

FIG. 25. Routes of hydrogen production [102].

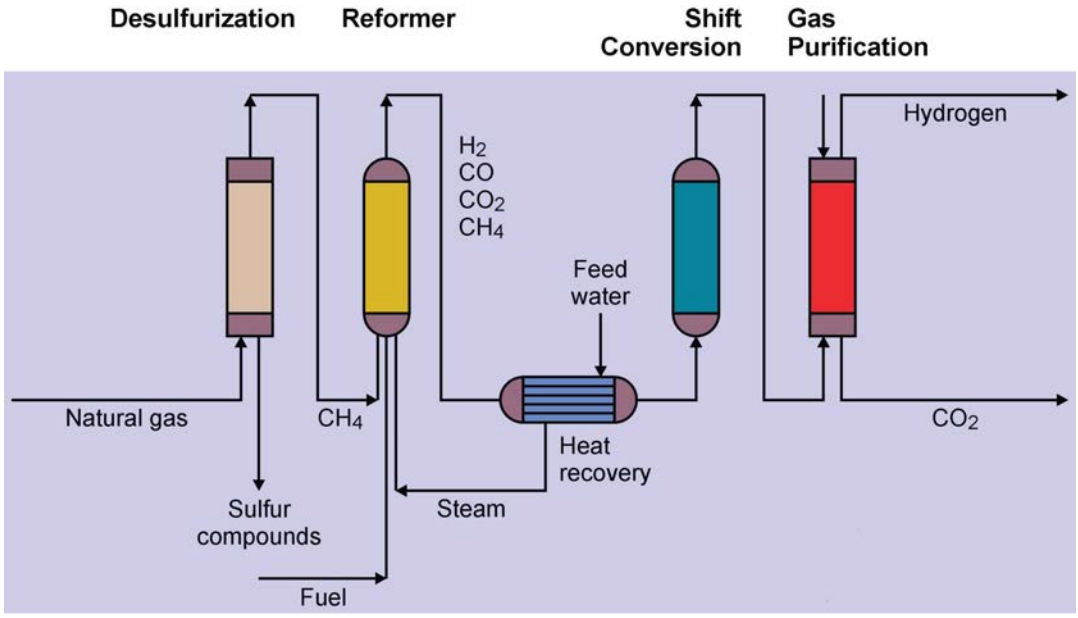

FIG. 26. Processing scheme of steam–methane reforming.

in most cases, a reaction of the feedstock hydrocarbon, steam and air/oxygen taking place at high temperatures. The hydrogen produced originates from both the hydrocarbon and the steam. If the hydrogen product is to be maximized, the conversion processes are followed by the water gas shift reaction. The final processing step is the separation and purification of the hydrogen.

3.2.1. Steam/CO_2 reforming of natural gas and light hydrocarbons

3.2.1.1. Steam reforming

The steam reforming process is the catalytic decomposition of light hydrocarbons (e.g. methane, natural gas, naphtha) to react with superheated steam, resulting in a hydrogen rich gas mixture. A processing scheme is given in Fig. 26.

The reforming reactions are endothermic, running at high temperatures of greater than 500°C. Steam–methane reforming (SMR) typically takes place at 850°C, and at pressures of greater than 2.5 up to 5 MPa in the presence of an iron or nickel or ruthenium catalyst:

$$C_nH_m + n\,H_2O \leftrightarrow (n+m/2)\,H_2 + n\,CO \quad \text{(endothermic)}$$

$$C_nH_m + 2n\,H_2O \leftrightarrow (2n+m/2)\,H_2 + n\,CO_2 \quad \text{(endothermic)}$$

And for methane:

$$CH_4 + H_2O \leftrightarrow 3\,H_2 + CO \quad -206\ \text{kJ/mol}$$

$$CH_4 + 2\,H_2O \leftrightarrow 4\,H_2 + CO_2 \quad -165\ \text{kJ/mol}$$

Since the number of moles is increased during the conversion, high temperatures and low pressures generally are favourable for this process. Pressures of up to 5 MPa are chosen to save compression energy for the large amounts of synthesis gas generated. In order to increase the output of hydrogen and to avoid carbon deposition due to the Boudouard reaction, the carbon monoxide is catalytically converted in the slightly exothermic water gas shift reaction with steam according to:

$$CO + H_2O \leftrightarrow H_2 + CO_2 \quad +43.3\ \text{kJ/mol}$$

The shift reaction is generally done in industrial processes via two steps at different temperature levels, the first at 350–450°C using an iron-oxide catalyst, and the second at 150–250°C using a copper–zinc or aluminium catalyst. The result is more H_2 and a lower CO concentration, which can be reduced to 0.5–2% of the dry gas. The feedgas is desulphurized to protect the catalyst inside the reformer tubes. The reformer tubes in the furnace are heated from the outside by burning a part of the natural gas (Fig. 26). The main processes of heat transfer are radiation and convection. Flue gas at a temperature above 1300°C passes the furnace and is used in a waste heat utilization step to produce steam and to preheat the feedgas.

The average equilibrium composition of the dry reformer gas, i.e. without steam, is 75% H_2 (about half of which is from the shift reaction), 13% CO, 10% CO_2 and 2% CH_4. It is strongly dependent on the fuel characteristics, steam-to-carbon ratio, outlet temperature and pressure, which are chosen according to the desired products. High reforming temperatures, low pressures and high steam-to-methane ratios favour a high methane conversion. A minimum H_2O:CH_4 ratio of around 2 is necessary to avoid carbon deposition on the catalyst, which would be deactivated. If excess steam is injected, typically 300% away from the stoichiometric mixture, the equilibrium is shifted toward more CO_2 at temperatures of 300–400°C, increasing the hydrogen yield and reducing the undesired production of carbon by the Boudouard reaction:

$$2\ CO \quad \leftrightarrow \quad CO_2 + C \qquad +172\ kJ/mol$$

Another unwanted reaction is thermal cracking of hydrocarbons which produces soot or carbon black. The reaction is dependent on the operating temperatures and the steam to carbon ratio.

$$C_nH_m \quad \leftrightarrow \quad 0.5m\ H_2 + n\ C$$

The hydrogen gas needs to pass further purification steps to realize a purity of >99% before being used, e.g. in fuel cells. The unwanted constituents CO_2 and others are removed from the gas mixture by pressure swing adsorption (PSA), i.e. adsorption on beds of molecules, sieves, or by membrane separation. Another efficient method for cleaning the H_2 product gas developed by AECL is a methanator, which converts the still available CO to methane, reducing concentrations to below the parts per billion level. An alternative method of removing CO is by PSA [20]. Tail gases may be used for heat requirements. The CO_2 generated is contained in the PSA reject gas and usually vented to the atmosphere.

Higher hydrocarbons are more reactive and can easily be reformed, the only limitation being sulphur poisoning. If light hydrocarbons are used as fuel, a pre-reformation is sometimes helpful to operate the tubes under the same conditions with methane as feedgas. Naphtha based plants are applying a pre-reforming step at a lower temperature and using a more active catalyst, partially converting the hydrocarbons to methane, hydrogen and carbon oxides. This allows alternate feed operation and makes better use of heat in the overall process. Feed and fuel consumption savings are approximately 5% [103]. Steam reforming of heavier hydrocarbons is possible, but it requires more complex process equipment and is therefore only rarely applied.

Steam reforming of natural gas is a technically and commercially well established technology on the industrial scale and currently the most economical route. Reforming technology is mainly used in the petrochemical and fertilizer industries for the production of ‘on-purpose’ hydrogen. Large steam reformer units with up to about 1000 splitting tubes with a typical diameter of 100 mm and a length of 10 m have a production capacity of around 130 000 Nm^3/h (Fig. 27). At the Fortum refinery in Porvoo, Finland, a hydrogen plant with a capacity of 180 000 Nm^3/h or 16.2 t/h of H_2, corresponding to a stored power of 645 MW (based on HHV), which started operation in 2007, is one of the largest one-line steam reforming hydrogen plants in the world. This plant is flexible in feedstock in that, besides natural gas, it can also convert refinery off-gas or liquid propane. Future reformer plants are designed to produce 237 000 Nm^3/h. Commercial large scale SMRs produce hydrogen at an efficiency of about 75% and a CO_2 intensity of 9.5 kg per kg of H_2 produced [104].

Modern steam–methane reformers often use more than one catalyst at different temperatures to optimize the H_2 output. Heat losses and thermodynamic (Carnot) limitation lead to an overall efficiency of about 80%. Catalytic autothermal reforming is ideal for fuel cell systems due to its simple design, low operation temperatures, flexible load and high efficiency.

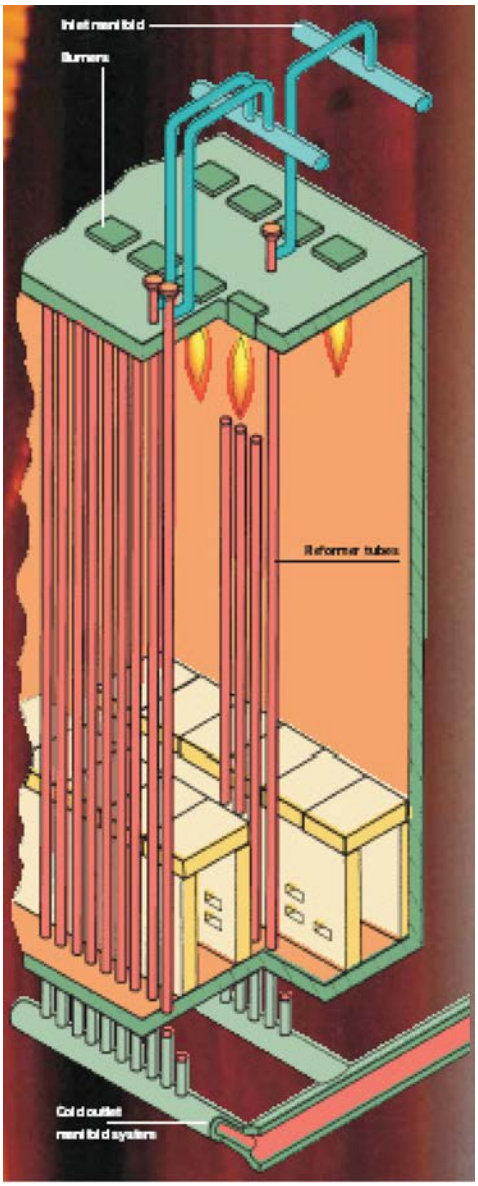

FIG. 27. Uhde steam reformer for light hydrocarbons [103].

In plate type reformers, plates are arranged in a stack, with one side coated with a catalyst and supplied with the reactants. These reformers are of a more compact design and show faster startup and better heat transfer, and therefore a higher conversion efficiency.

Advanced reforming techniques will operate at reduced reaction temperatures by means of microporous ceramic membranes. Membrane modules made of palladium based alloy and a nickel based catalyst can drive the steam reforming reaction, shift reaction and H_2 separation simultaneously (Fig. 28), i.e. without shift converter and PSA stages. Therefore, the system is compact and provides higher efficiencies. The simultaneous processes allow a lower reaction temperature down to around 550°C, posing less stringent requirements to the materials. The temperature reduction is possible because part of the heat for the endothermic reforming reaction is provided by the exothermic shift reaction. The net heat required is 165 kJ/mol. The technical feasibility of a methane-combusting membrane reforming system was demonstrated in 2004–2005 by the Tokyo Gas Company, Japan, at a hydrogen fuelling station in Tokyo [105]. The system performance, efficiency and long term reliability were confirmed by the production of >99.99% hydrogen at 3.6 kg/h for more than 3000 h with a hydrogen production efficiency of about 68% (lower heating value) [106]. Catalysts and the separation membranes are the key components with potential for further improvement and optimization.

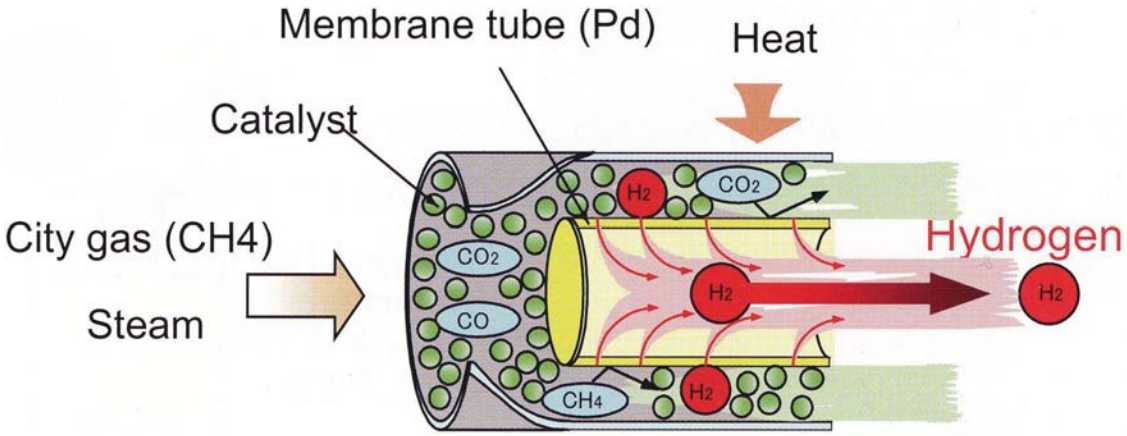

FIG. 28. Membrane reformer [105, 108].

For the high temperature range, inorganic membranes (ceramics, metals) are under development. They allow new concepts that may make the stages of air separation, POX or PSA obsolete. Ion transport membranes (ITMs), with their stable oxygen defect crystal structure, are operated at greater than 700°C and allow only oxygen ions to move through the membrane, which is gas-tight for all other gases. Due to the charge separation, the material must be conducting at the same time. Palladium coated metal composite membranes promise advantages in terms of mechanical strength, higher hydrogen flux, high selectivity and reduced materials costs. Hydrogen permeation through a palladium membrane is a complex multi-step activated process typically in the range of 300–600°C. Palladium membranes combine the separation unit and shift reaction in one stage, which is particularly advantageous for small reformers [107]. Conceptual designs promise cost reductions in the generation of high pressure hydrogen.

A novel approach of allothermal steam–methane reforming has been proposed [109]. External heat, e.g. from nuclear power, is supplied via an IHX to a three-step reforming and membrane module system, where — in contrast to a membrane reactor — the membrane stage is separated from the reforming reactor (Fig. 29). Reforming is done at temperatures of 600–650°C in three steps, reaching a conversion ratio of ~90%. The reactors are heated by hot air, which itself is heated in a heat exchanger and from purge gas combustion. The main advantage is that the subsequent external membrane separation step can work at lower temperatures of ~450°C, which is beneficial with respect to the stability, lifetime and maintenance of the membrane. A highly reliable, reproducible, hydrogen selective membrane is essential. Research is focused on palladium based composites with thin palladium films (0.5–3 μm) on porous metallic substrates, promising sufficient mechanical strength, hydrogen permeability and selectivity.

There is only limited potential for further improvements in the large scale steam reforming process. Such improvements may be brought about by the optimization of heat integration and recovery, and the removal of the CO_2 in the shift reactor or the replacement of the PSA unit with the selective catalytic removal of CO, assuming appropriate membranes and catalysts have been developed. With such improvements, an increase in overall efficiency of approximately 4% might be achievable by 2020 [110].

For decentralized hydrogen production, small scale steam reformers are also commercially available, with capacities of 500–700 Nm^3/h. These reformers are characterized by efficiencies of up to 65% (LHV) within a wide range of operating conditions (load changes between 40 and 100%), small size, short cold startup times and automated operation. Smaller scale designs with capacities in the range of 100 Nm^3/h appear to be cost competitive solutions for refineries and applicable in hydrogen refuelling stations. A significant potential for further improvements is seen in the optimization of compressors and storage vessels, size and cost reductions, and an increase in reliability and availability [110].

In the 1980s, AECL demonstrated the concept of electro-steam reforming of methane, which appears to be attractive for small scale hydrogen production. The catalyst on a metal substrate is heated, bypassing electricity [20].

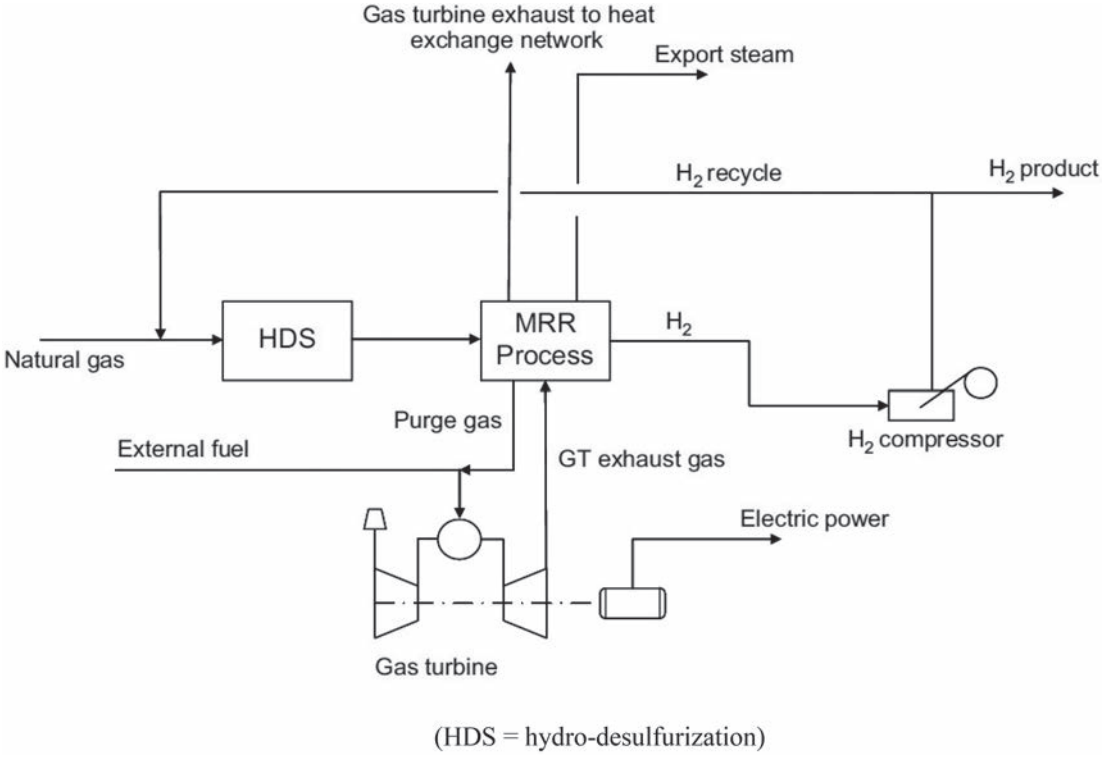

FIG. 29. Schematic of the membrane reforming reactor (MRR) [109].

3.2.1.2. CO_2 reforming

If the steam is completely or partially replaced with CO_2, the process is called 'dry reforming'. The strongly endothermic reaction proceeds at high temperatures of 800–1000°C with a nickel based catalyst [10]:

$$CH_4 + CO_2 \leftrightarrow 2\ H_2 + 2\ CO \qquad -206\ kJ/mol$$

The composition of the synthesis gas is shifted toward a larger CO fraction, with a H_2:CO ratio of ~1 or lower, compared with greater than 3 in the syngas from steam reforming of CH_4, making it ideal for production of synthetic liquid fuels through the Fischer–Tropsch process. The ideal H_2:CO ratio for methanol production, however, is ~2 [111]. Desired ratios can be obtained by combining the CO_2 reforming of CH_4 and steam reforming of CH_4, so-called bi-reforming:

$$3\ CH_4 + 2\ H_2O + CO_2 \rightarrow 8\ H_2 + 4\ CO \rightarrow 4\ CH_3OH$$

The CO_2 can be either imported or taken from the reformer outlet. The catalytic reforming of methane with CO_2 offers an environmental advantage, because two GHGs are combined, resulting in a product gas mixture which might be more favourable for certain applications, such as the synthesis of oxygenated chemicals.

The main drawback of dry reforming is the formation of coke from the Boudouard reaction, resulting in a rapid deactivation of conventional reforming catalysts. Coking is also a problem with steam reforming, but it is less severe since the carbon formed can be volatilized. Only at increased temperatures above 900°C is carbon deposition minimized during dry reforming. Catalysts based on noble metals were found to be less sensitive to coking than were nickel based catalysts for dry reforming, but their disadvantage is the high cost and limited availability.

The formation of synthesis gas by dry reforming of methane could provide a substantial use for CO_2 from industrial and natural sources. New methods of combined POX and dry reforming considerably improve the energy economy for synthesis gas production [10].

3.2.2. Partial oxidation and autothermal reforming of hydrocarbons

3.2.2.1. Partial oxidation

POX of carbonaceous feedstock in the presence of water is also a conversion process at high pressures and high temperatures (950–1100°C), where the reaction heat is provided by partial combustion of the feedstock. POX produces synthesis gas and maximizes the hydrogen yield if followed by the water gas shift reaction. The hydrogen mainly originates from the water, while the carbon in the feedstock provides the energy to split the water. By adding oxygen, a part of the feedstock is burned in an exothermic reaction. It can be noted for alkanes:

$$C_nH_m + 1/2\ n\ O_2 \leftrightarrow 1/2\ m\ H_2 + n\ CO$$

$$C_nH_m + n\ O_2 \leftrightarrow 1/2\ m\ H_2 + n\ CO_2$$

And for methane:

$$CH_4 + 1/2\ O_2 \leftrightarrow 2\ H_2 + CO \qquad -38\ kJ/mol$$

$$CH_4 + O_2 \leftrightarrow 2\ H_2 + CO_2$$

Downstream equipment is needed to remove the heat generated. The oxygen required is typically provided by an air separation plant. POX can easily be performed without the presence of a catalyst. Non-catalytic POX needs high temperatures of 1200–1450°C and pressures of 3–7.5 MPa (Texaco process) to ensure high conversion rates. The catalytic partial oxidation (CPOX) reaction, however, after premixing of the reactants, can take place at lower temperatures (~900°C in the hot zone), produces less NO_x and may lead to a significantly enhanced H_2 yield from the fuel.

The POX process has the advantage of accepting all kinds of heavy hydrocarbon feed, such as oil, residues, coal or biomass. In comparison to steam reforming, the hydrogen yield is smaller, meaning that larger reactors for the shift reaction are required if H_2 is the desired product. But the resulting synthesis gas with a H_2:CO ratio of ~2 (versus greater than 3 for SMR) makes methanol synthesis an ideal follow-on process. POX allows for compact equipment and easy maintenance, since there is no need for external heating or steam supply. Efficiencies of about 70% are somewhat lower than those for SMR (80–85%) because of the higher temperatures involved and problems with the heat recovery. The disadvantages are its high energy consumption and the need for large amounts of oxygen, catalyst deactivation due to carbon deposition, the by-product CO, which requires the shift reaction, the need for gas purification stages to remove CO_2 (and nitrogen), and, if methane is used as feed, the possibility of runaway reactions due to hot spot formation. POX can be scaled down to 10 kW(e) units.

Catalytic POX of heavy oil and other hydrocarbons is a commercially applied, large scale H_2 production method, used, for example, in refineries where synthesis gas is generated from residual heavy oil fractions, coal or coke. The lower feedstock prices of heavy residues are at the expense of higher capital costs and more demanding operating conditions. The process may become more economical when inexpensive oxygen is available. It can be conducted in both monolith reactors and in fluidized bed reactors, but also in fixed bed microreactors. Large scale plants usually include also air decomposition with unit sizes which may reach about 100 000 Nm^3/h. Available commercial technologies include the gasification processes of Texaco and Shell. Small units of POX reforming for mobile applications are currently in the R&D and demonstration phase, with the aim being to find the optimal conditions of feedstock and catalyst.

3.2.2.2. Autothermal reforming

The combination of the POX process with endothermic steam reforming may lead to internally heat balanced reactions in a single fixed bed reactor without heat input from the outside. This method is called autothermal reforming (ATR). It can be described with the following reaction equations, here especially for oxygen containing hydrocarbons:

$$C_nH_mO_l + (n - l)\ H_2O \leftrightarrow (n - l + 0.5m)\ H_2 + n\ CO_2$$

$$C_nH_mO_l + 0.5(n - l)\ O \leftrightarrow m\ H_2 + n\ CO$$

And for methane:

$$CH_4 + 3/2\ O_2 \leftrightarrow 2\ H_2O + CO \qquad -520\ kJ/mol$$

$$CH_4 + H_2O \leftrightarrow 3\ H_2 + CO \qquad +206\ kJ/mol$$

For alkanes, the overall reaction equation is

$$C_nH_m + x\ O_2 + y\ H_2O \leftrightarrow (2n - 2x + 0.5m)\ H_2 + n\ CO_2 + (y + 2x - 2n)\ H_2O$$

where x is the molar oxygen to carbon ratio and y is the molar steam to carbon ratio in the input mixture. Typical ratios in the reactions are 0.2–0.6 for the oxygen to carbon ratio and 1.0–3.0 for the steam to carbon ratio [112]. The reaction heat is ideally zero (thermo-neutral) to achieve maximum fuel reforming efficiency. In practice, however, side reactions such as reverse shift or methanation or incomplete conversion result in additional components in the reformate. The use of a catalyst allows for lower operation temperatures.

ATR technology has been under development since the late 1970s, with the goal being to have the reforming step in a single adiabatic reactor. Preheated feedstock is gradually mixed and burned in the combustion chamber at the top where POX takes place. Steam is added to the feed to allow premixing of CH_4 and O_2. In such a reformer, the reactor consists of a combustion zone where the heat-up reaction gas mixture is directly transferred into a fixed bed catalytic steam reforming zone, which is implemented in the lower part of the same reactor vessel. Once the reactions have started, no separate heater or heat exchanging devices are necessary to transfer heat to the process stream for the reforming step.

Downstream processing is needed for cooling, purification and separation of the hydrogen from the reformate. When atmospheric air is used, the nitrogen must be removed from the product stream. The hydrogen content in the reformate can be as high as 50–55%. PSA allows the level of CO or CO_2 impurities to be reduced to a few parts per million. The soot/carbon formed can be removed in separate soot scrubber systems. Various characteristics of an ATR contribute to the overall performance of the reformer system such as the mixing and reforming process, fuel composition, thermodynamic conditions, the ratios of steam to carbon and oxygen to carbon, catalysts, coke/soot formation and other pollutants. An overall evaluation of important features of these reforming processes is given in Fig. 30.

	Steam reforming	Autothermal	Partial oxidation
Startup	Slow	⟷	Fast
Size	Large	⟷	Small
Hydrogen content	High	⟷	Low
Temperature control	Easy	⟷	Difficult
Emissions	Low	⟷	High
Efficiency	High	⟷	Low
Complexity	High	⟷	Low
Hydrogen quality	High	⟷	Low
Cost of large plant	Low	⟷	High
Cost of small plant	High	⟷	Low

FIG. 30. Evaluation of reforming processes.

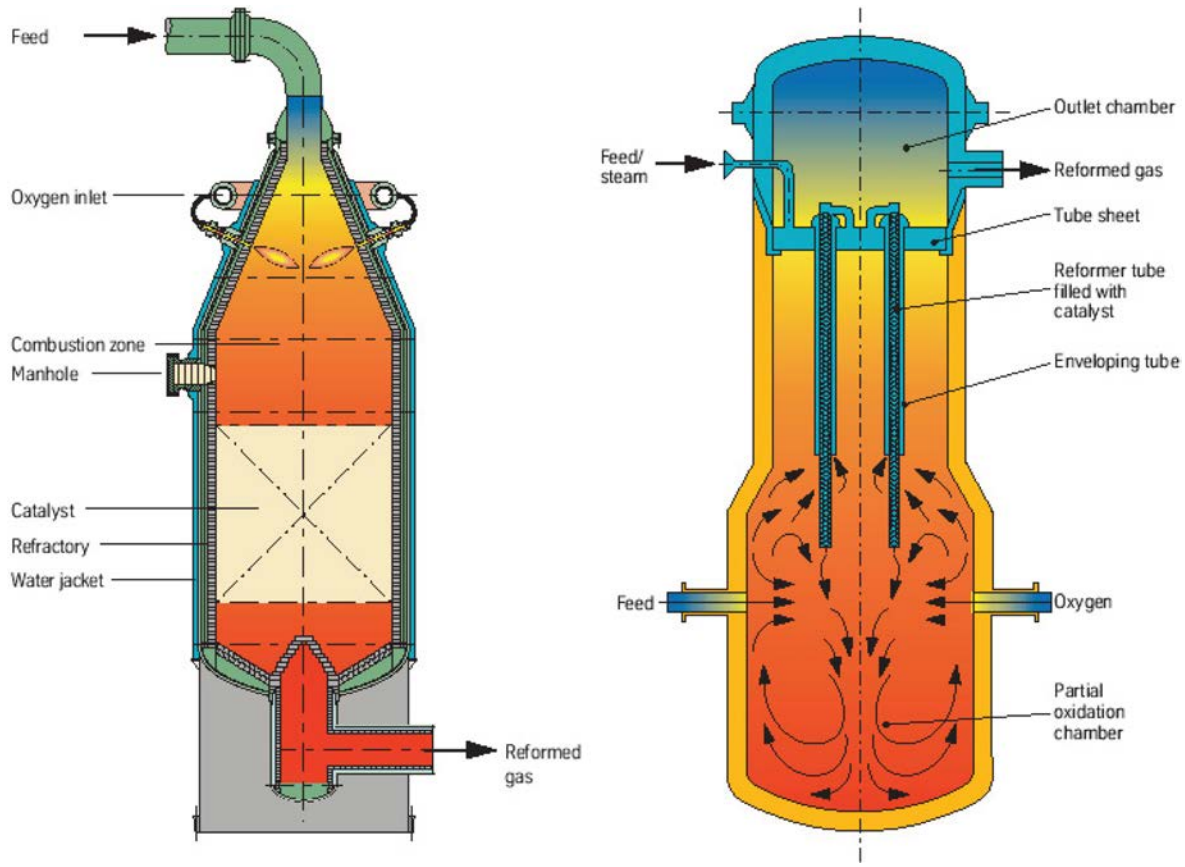

FIG. 31. Autothermal reformer (ATR) (left); tandem system (right) [103].

ATR is mainly used in large scale plants for gas-to-liquid (GTL) applications, with an important cost factor again being the oxygen. Typical capacities of combined autothermal reformers, however, are between 4 000 and 35 000 Nm^3/h, a range where 'normal' steam reforming exhibits high specific investment. But there are also smaller units for local H_2 production with a capacity around 150 Nm^3/h. Research in reforming technologies is concentrating on finding the right balance of fuel, air and water flows for optimal processing. If CO_2 capture technology should be added, ATR has an advantage in that the CO_2 is recovered from a separation step which works optimally at 0.3 MPa, thus saving compression costs.

If a distributed generation system with a typical plant size of 480 kg/d of hydrogen is to be used for mass production, it must be optimized to maximize operating efficiency, to provide buffer storage for a variable hydrogen demand and to meet the purity requirement, e.g. for fuel cell applications. Whether POX or autothermal reforming will be applied in such a system may depend on the way the oxygen can be provided, since conventional oxygen supply (by cryogenic separation) will have increasing costs with reduced unit size [5].

Tandem reforming is the combination of a gas heated reformer and an oxygen fired autothermal reformer (Fig. 31). If neither oxygen nor steam is available, the facility needs air separation and steam generator units.

There was also increasing interest in using ATR in the fuel processing technology, e.g. for automotive applications, to convert hydrocarbons such as gasoline, diesel, bioethanol, or methanol into a hydrogen rich gas for fuel cell applications. The hydrogen here is defined as 'short lived hydrogen'. For on-board reforming, multifuel processors in the 50 kW range have been developed. Methanol appears to be an attractive fuel, because it operates at lower temperatures and is more tolerant of intermittent demand. Gasoline or LPG reforming would be even more practicable, since this infrastructure exists already and could allow the introduction of vehicles even at a lower number. The types of reactors for small scale applications are the fluidized bed reactor, membrane reactor, short contact reactor, heat exchange reactor and microreactor. Reformer units in the very low power range such as for mobile/portable fuel cell applications are currently being developed and tested. A key aspect of fuel processing is the removal of sulphur and CO from the product gas prior to its entering the fuel cell system.

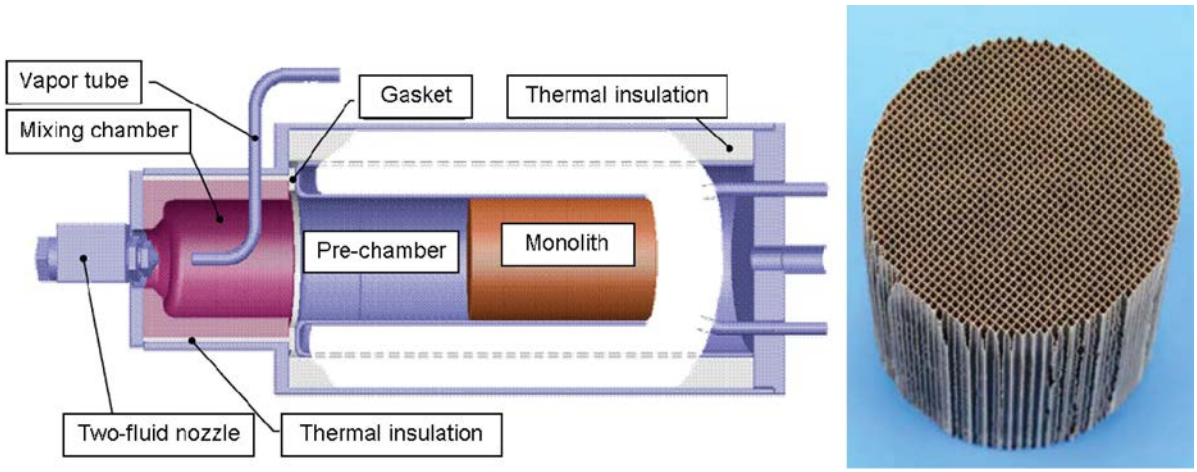

FIG. 32. Schematic of the fifth generation of ATR development at FZJ [113].

On-board reforming is currently being investigated in smaller units of ~5 kW(e) to provide the on-board electricity in a fuel cell based auxiliary power unit (APU). The fuel cell system can be either a high temperature solid oxide fuel cell or a low temperature PEM fuel cell. An example is given from the activities at the Research Centre Jülich (FZJ), which have the objectives of designing, constructing and testing ATR systems at the power level of ~5 kW(e) and focusing on the reforming of diesel fuel. Figure 32 shows the ATR-5A from the fifth generation of ATR development at FZJ [113]. A part of the airstream is mixed with the fuel and injected through a two-fluid nozzle to deliver tiny fuel droplets into the mixing chamber where the fuel is vaporized and mixed with steam and air to form the educt gas mixture. The heart of the ATR is a monolith where the catalytic reforming process takes place. The monolith has a diameter of ~50 mm and a length of 85 mm. POX is dominant in the first part of the monolith. Typical operational parameters are flows of 3 kg/h of air, 1.6 kg/h of water, and 0.7 kg/h of fuel. An essential prerequisite is to obtain a homogeneous mixture of fuel, steam and air for the reforming process. Therefore, a proper design of the mixing chamber is required whose function is to provide a uniform flow to the catalyst.

The FZJ autothermal reformer of the ninth generation, ATR 9.2, has been specifically designed for the conversion of synthetic fuels and produces hydrogen with a thermal power of 28 kW. Here, geometry and injection of the feedstock are arranged such that a homogeneous, slightly exothermic pre-reaction between oxygen and fuel in the mixing chamber is favoured, which eases the complete evaporation of the fuel. Other improvements are an integrated heat exchanger device for steam production and a one-fluid nozzle for fuel injection [114].

A modification of the POX steam reforming process has been suggested which leads to an inherent capture of the CO_2 generated during fuel combustion. The principle of the so-called chemical looping combustion (CLC) is to have separate reactors, an ‘air reactor’ where oxygen is extracted from air by means of a solid oxygen carrier, typically a metal, and a ‘fuel reactor’ where the metal oxide is reduced to its initial state and recirculated. CLC has the advantage of reducing the exergy loss during fuel combustion, while the generated CO_2 is separated from the (diluted) air steam and thus can easily be sequestrated [115].

3.2.3. Reforming of other hydrocarbons

3.2.3.1. Methanol

The production of hydrogen from methanol is attractive because it generates high quality H_2. Methanol has a high hydrogen to carbon ratio, can be easily produced in large quantities, and can be easily stored and transported. It can be activated at temperatures below 300°C and it is free of sulphur and other impurities and therefore ideally suited for low temperature fuel cell applications. Extraction of hydrogen from methanol is usually done either by POX or steam reforming of methanol. POX is characterized by an exothermic reaction and high reaction rates. Steam reforming of methanol is, although endothermic, advantageous because of its direct decomposition, which takes place at moderate temperatures in the range of 250 to 350°C:

$$CH_3OH + H_2O \leftrightarrow CO_2 + 3\ H_2$$

Catalysts typically used in POX with suppressed CO formation are Cu–Zn based. They have, however, the drawbacks of fast deactivation, poor thermal stability and pyrophoric characteristics. Platinum catalysts are more stable, but produce much more CO [116]. A steam to methanol ratio of greater than 1 (good: 1.5) results in a mixture of H_2, CO_2 and CO as the only significant products.

Present methanol reformers are of fixed bed type. The drawbacks are hot and cold spots and slow response due to slow heat transfer. Improvement has been achieved by using wash-coated heat exchangers. If applied in a hydrogen refuelling station, methanol reforming needs a hydrogen purification stage. Small scale reformers for on-board fuel processors in fuel cell vehicles have been developed as an alternative to on-board storage of hydrogen. Various types include the plate and membrane concepts for compact design. A reasonable choice for portable fuel cell applications is the employment of microreactors for methanol reforming. Microreactors are those having channel sizes with a cross-section of 1000 μm × 230 μm plus a 33 nm thick Cu layer as the catalyst.

3.2.3.2. Ethanol

Interest has also increased in catalytic reforming of biomass derived, CO_2 neutral ethanol, which is produced in large quantities worldwide. A total of six moles of H_2 per mole of ethanol reacted can ideally be obtained according to the endothermic process:

$$CH_3CH_2OH + 3\ H_2O \leftrightarrow 2\ CO_2 + 6\ H_2 \qquad -173.4\ kJ/mol$$

followed by the water gas reaction and a purification of the product gases. An ethanol steam reforming process might be well suited for decentralized stationary hydrogen production.

3.2.3.3. Dimethyl ether

Dimethyl-ether (DME), generally produced from methanol, is an organic compound with properties similar to LPG. Combustion of DME leads to low emissions of particulate matter, NO_x and CO. It is promising as a clean-burning hydrocarbon fuel for diesel engines or gas turbines, as synthetic biofuel and as a useful precursor to other organic compounds. DME is gaseous at ambient conditions and easy to liquefy, highly soluble in water, relatively non-toxic and flammable.

The reforming reaction is [60]:

$$CH_3OCH_3 + H_2O \rightarrow 2\ CH_3OH$$

$$2\ CH_3OH + 2\ H_2O \rightarrow 6\ H_2 + 2\ CO_2$$

The hydrogen is produced at temperatures of 285–300°C, much lower than those with the reforming of methane. This was made possible by the development of a DME reforming catalyst, Cu–Zn/Al_2O_3, which gives 98% conversion of DME to hydrogen at 285°C. An additional advantage is the simpler processing, with no need for desulphurization or CO transformation. DME steam reforming is particularly interesting for on-board reforming, since the reforming temperature is low and DME is less toxic than methanol. Furthermore, it represents an option for nuclear assisted hydrogen production using conventional LWRs [60].

3.2.3.4. Benzene

Benzene can be used to extract the hydrogen to be consumed as fuel in a fuel cell. The decomposition of benzol by steam reforming takes place at temperatures above 700°C and in the presence of a catalyst.

$$C_6H_6 + 12\ H_2O \leftrightarrow 6\ CO_2 + 15\ H_2 \qquad -458\ kJ/mol$$

3.2.4. Gasification of coal

Because of its abundance on earth, coal has become a major source of energy, accounting for about 27% of the world's primary energy consumption and 41% of the world's electricity production (as of 2007) [6]. More than 90% of the existing coal reserves are concentrated in eight countries: Australia, China, India, Kazakhstan, the Russian Federation, South Africa, Ukraine and the USA. The largest among them (China, the USA and India) have even become coal importing countries. It is anticipated that China and India will account for about two thirds of the worldwide increase in demand for coal by 2030, mainly for the production of electricity.

The coke furnace process was already in use more than 100 years ago for the production of low Btu gas (5–12.7 MJ/m^3), synthesis gas (~12.7 MJ/m^3), town gas (16.7–20 MJ/m^3) or SNG (25–42 MJ/m^3). In Germany, hydrogen rich (~50%) coal gas was fed as town gas into the municipal gas grids [117] and later played an important role in the production of synthetic fuels. Gasification of coal is the oldest hydrogen production technology but still plays an important role today. For practically all processes for coal refinement, the technological development was undertaken in Germany. Today, the conversion of coal to gaseous or liquid fuels is being applied commercially worldwide.

Unlike combustion in a coal fired power plant, gasification is regarded as a clean coal technology, producing synthesis gas and hydrogen, and with the potential for easy separation of a high concentration CO_2 stream. Numerous process variants have been developed to effectively gasify coal by adjusting to the different grades and qualities of coal and to the product composition and undesired interim products. Despite its comparatively low hydrogen content, and thus higher cost, steam–coal gasification is currently used to produce 18% of the world's hydrogen. At present, about 45 million t of coal are converted by gasification worldwide per year [118].

Coal is a solid with a high carbon content and an approximate 5% content of hydrogen. If expressed in carbon and hydrogen, coal can be described with the formula ~$(CH_{0.8})_n$. For the production of higher grade hydrocarbons, either the carbon must be reduced or hydrogen must be added. The conversion of coal into a gas is realized by means of a gasification agent, which reacts with the coal at temperatures greater than 800°C, similar to an incomplete combustion (since much less oxygen is used). All organic constituents will be converted at long enough residence times.

Gasification agents can be steam, oxygen, air, hydrogen, carbon dioxide or a mixture of these. The gasification agent steam (steam–coal gasification) belongs to the most important reactions of commercial interest. If air or oxygen is injected into the gasifier, a part of the coal is directly burned (POX), allowing for an autothermal reaction. The processes have in common that high pressures are needed to achieve a high methane yield, whereas for an optimal output of synthesis gas, high temperatures and low pressures are required. Effective gasification means to retain as much of the energy of the coal as possible in the gas.

At present, 20 000 MW of synthesis gas is being produced by coal, mainly for chemicals and power generation. However, its importance for hydrogen production is decreasing and its use for ammonia synthesis in the fertilizer industry or for methanol synthesis with large scale production facilities, particularly in the developing countries, is growing. Air-blown plants have lower capital costs than oxygen-blown plants, but they suffer from much higher separation costs. Future hydrogen production plants will most probably tend to be based on oxygen-blown designs. Other important criteria for applicability and economic viability of coal gasification are the characteristics of the coal to be gasified. The (geologically) older the coal, the smaller is its reactivity and the higher is the temperature required. Major improvements of efficiencies could be achieved with the development of improved gas separation and purification techniques like the use of membranes.

3.2.4.1. Steam–coal gasification

Steam gasification of coal has long been a mature and well established technology practised on an industrial scale. In the conventional steam–coal gasification process, a part of the coal is partially oxidized before, in the much slower heterogeneous water gas reaction, the residual organic solids are converted to synthesis gas with some CO_2 and steam.

In the steam–coal gasification process, two consecutive processes take place, the POX or pyrolysis reaction, and the water gas reaction. The first step is the pyrolysis reaction during the heat-up phase (400–600°C), where all volatile constituents of the coal are rapidly expelled. The gasification reaction with the agent 'steam' is given by the

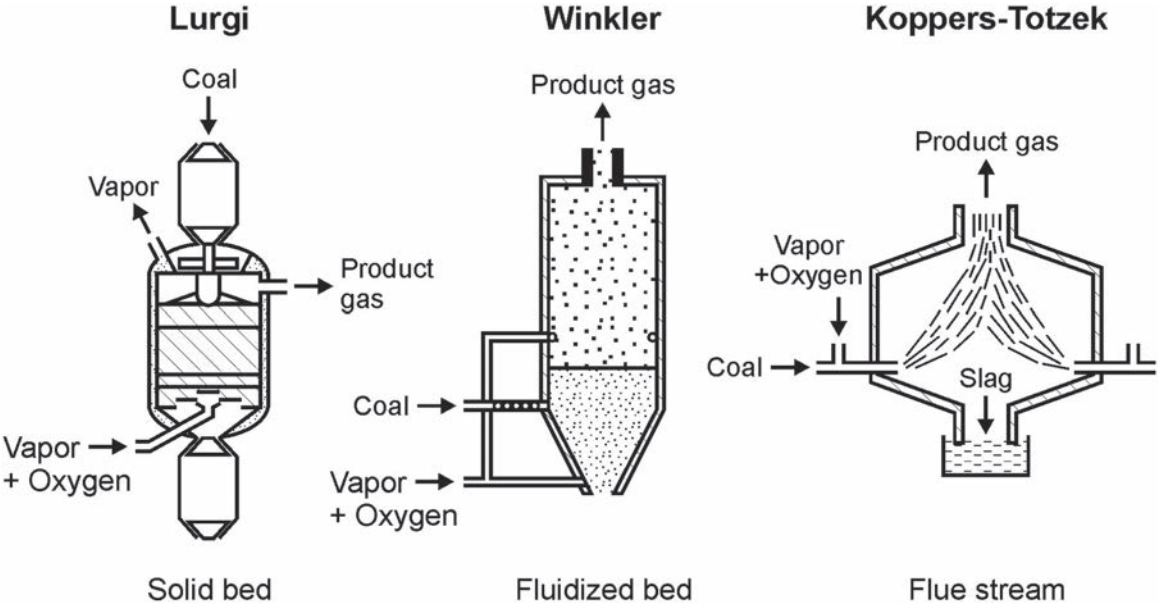

FIG. 33. Three principal lines of steam–coal gasification [119].

heterogeneous water gas reaction and the homogeneous shift reaction with a further increase of the H_2 fraction where residual organic solids are converted to synthesis gas with some CO_2 and steam:

$$C + H_2O \leftrightarrow H_2 + CO \qquad -118.5 \text{ kJ/mol C}$$

$$CO + H_2O \leftrightarrow H_2 + CO_2 \qquad +43.3 \text{ kJ/mol C}$$

This is followed by a methanation step if the desired end product is SNG. Synthesis gas output is optimal at high temperatures and low pressures. Heat must be quickly withdrawn to avoid reverse chemical reactions:

$$CO + 3\,H_2 \leftrightarrow CH_4 + H_2O \qquad +206.0 \text{ kJ/mol C}$$

Gasification processes are classified according to the type of reactor. The principal lines used today are those by Lurgi (since 1931), Winkler (since 1922) and Koppers–Totzek (since 1941). These all were developed in Germany and exist at a large scale (Fig. 33). Modified process variants, such as Texaco, Shell–Koppers and many others, have been developed aiming at an adjustment to the feedstock quality, optimization of the product gas composition and, of course, efficiency improvements. Variants differ by temperature and pressure range, grain size of the coal, and residence time.

POX of pulverized coal by oxygen/air (pure O_2 for hydrogen production) and steam in a fluidized bed takes place at about atmospheric pressure, where 30–40% of the coal is transformed to CO_2 to supply splitting energy of water. The reaction rate strongly increases with temperature; typically temperatures up to 2000°C and pressures up to 3 MPa are selected. Commercial scale plants usually run in an autothermal mode. Depending on the customers' requirements, downstream processing allows the optimized generation of hydrogen, methane or synthesis gas. Coal conversion is estimated to be around 95%, and the total efficiency (based on HHV) is estimated to be ~70%. The main disadvantages of coal gasification are the handling of solid material streams and the large amounts of CO_2, SO_2 and ash, requiring a complex cleaning system. New coal gasification techniques, however, can also be linked with a CLC process to reduce the impurity level in the synthesis gas. Table 6 lists some of the major characteristic features of the different types of steam–coal gasification processes [117, 120].

Autothermal gasification reactors are of relatively simple design in that they do not need heat input or heat exchanging devices. Higher temperatures are possible and thus higher reaction velocities which result in a higher

TABLE 6. CHARACTERISTIC FEATURES OF STEAM–COAL GASIFICATION PROCESSES

	Lurgi	Winkler	Koppers–Totzek
Reactor	Moving solid bed	Fluidized bed	Flue stream
Grain size (mm)	10–30	0.5–8	<0.09
Steam-to-oxygen ratio	9–5	2.5–1	0.5–0.02
Movement of reactants, products	Countercurrent flow	Vortex-co-current flow	Co-current flow
Residence time of fuel (min)	60–90	15–60	<0.02
Requirements to fuel	Must not cake or decay	Highly reactive, must not decay	Melting point of ash <1450°C
Maximum gas outlet temperature (°C)	370–600	800–950	1400–1600
Pressure (MPa)	2–3	0.1 (also <1)	0.1 (also <8)
Composition of product gas (vol%)			
$CO + H_2$	62	84	60 + 29
CH_4	12	2	0.1
By-products	Tar, oil, phenols, gasoline, wastewater	Little dust, tar	None

coal throughput. A disadvantage is the larger specific CO_2 generation, since part of the feedstock is burned to provide the process heat for the gasification reactions. This is not a problem if a, external, CO_2 emission free heat source is applied (allothermal gasification). For example, with an HTGR, the heat provided by the hot helium coolant can be introduced directly into the gas generator, another part being used for the steam production, with the rest still usable for electricity production.

According to their flow geometry, gasifiers are classified into several generic variants [121].

(A) Solid bed

In Lurgi pressure gasification, a solid bed of coal moving from top to bottom is preheated, dried, pyrolyzed, gasified and combusted by adding steam and oxygen from the bottom at a pressure of 1.5–3 MPa, forming different reaction zones at different temperatures. The highest temperatures (~1300°C for dry ash gasifiers) are reached in the combustion zone, where the remaining char is finally completely burned. The amount of methane generated is dependent on the pressure, temperature, oxygen to steam ratio, reactivity of the coal, and contents of volatile substances in the coal. In a solid bed, the coal should be in smaller pieces (but not too small) and must not cake to allow for a sufficient permeability of the gases. The countercurrent flow arrangement leads to higher conversion rates and thermal efficiencies. A drawback is that, before exiting, the product gases pass through a zone of fresh coal (which is given to the reactor from top), where it receives a significant load of tar and higher hydrocarbons, and therefore requires extensive purification. Of all variants, the moving bed gasifier is the most mature technology developed to the industrial scale.

The ‘RUHR-100’ reactor is a Lurgi design from 1979 with a coal throughput of 170 t/h, where the ‘100’ (bar) refers to the increased pressures of up to 10 MPa at which the reactor can be operated. The raised pressure increases the methane yield in the product gas from 9 to 16 vol%. A test facility was operated in Dorsten, Germany. The Lurgi gasifier is the only one operated under pressure at a large technical scale, producing synthesis gas for the Fischer–Tropsch process.

The SASOL company in South Africa is the world’s largest commercial applier of coal conversion technology, operating a total of 97 units. Most Sasol–Lurgi standard fixed bed reactors have an inner diameter of 3.85 m (‘Mark IV’), able to produce 65 000 Nm^3/h of dry gas with a raw coal throughput of 54 t/h. This capacity,

corresponding to about 200 MW(th) (based on HHV), appears to represent the upper limit. SASOL is also operating a 4.7 m diameter reactor (Mark V) with a capacity of 100 000 Nm^3/h [122, 123]. The plants in Secunda and Sasolburg convert more than 30 million t/a of bituminous coal to yield about 5.1 million Nm^3/h of pure synthesis gas (containing 56% H_2, 32% CO, 11% CH_4), corresponding to almost 30% of the world's production. It is the basis of manufacture of numerous fuels and chemicals [124].

(B) Fluidized bed

Fluidized bed combustion systems are operated either under atmospheric conditions or under pressurized conditions, and are further classified into bubbling or circulating systems. Atmospheric combustors exist up to a power of 250 MW(e), while pressurized systems are currently at a demonstration stage.

The high temperature Winkler (HTW) process takes place in a fluidized bed where fine-grain brown coal is reacted with oxygen and steam, which are fed in at the bottom at high speed. The fluidized bed has no reaction zones but rather forms a homogeneous distribution of solids. Operational conditions are high temperatures, which are uniformly distributed due to a high degree of back-mixing. The temperature, however, must be below the ash melting point to prevent a softening and agglomeration of the ash, which would lead to a collapse of the fluidized bed. The product gas composition changes with height and contains almost no higher hydrocarbons at the exit. It carries, however, a large amount of dust, which can be recirculated to the reactor to further raise the carbon conversion rate, reaching up to 95%. Still, treatment of the solid remainder is necessary. Sorbents such as limestone help decrease the H_2S concentration in the product gas and reduce corrosion effects. An important advantage is that fluidized bed gasifiers are highly flexible, since they can be operated at variable load.

The Winkler gasification is characterized by simple coal pretreatment, low oxygen consumption and good performance over a broad load range. HTW was proven successful for highly reactive coal grades. It was developed in Germany under the specific consideration of the domestic lignite resources. A test facility was operated in Frechen, Germany, at 1 MPa and 1100°C with a dry coal throughput of 1.3 t/h. Several large scale plants were constructed in Germany and other countries with coal throughputs of up to 35 t/h. Industrial scale is up to 750 MW(th) (~360 000 Nm^3/h of synthesis gas) based on HHV [118]. Any type of coal can be applied. Following the atmospheric Winkler process, the gasification was later carried out at higher pressures of up to 1 MPa in order to raise unit capacity and gas quantity, and to save compression energy for the product gas. Gasifier plants have shown simple startup and shutdown as well as good partial load behaviour and high reliability. Also advantageous is the low oxygen consumption.

(C) Flue stream

In the flue stream or entrainment flow gasifier, dry coal dust is mixed with steam and oxygen/air and gasified at atmospheric pressure in an autothermal way. The reaction zone is limited to the flame area with a co-current flow of coal and gasification agent. The Koppers–Totzek process runs at very high temperatures above the ash melting point. It has the advantage that tar formation is suppressed and other organic substances are destroyed. At the same time, the injected steam serves as a coolant, as it is injected between the flame and reactor wall. The conversion rate is at almost 100%, with a methane content in the product of < 0.1%.

Industrial plant capacities are in the range of 500–1000 MW(th), corresponding to 140 000–280 000 Nm^3/h based on HHV [118]. The Shell process applies the Koppers–Totzek principle under pressures of up to 4 MPa. Gasification temperatures achieved are up to 2000°C, as was demonstrated in a test plant in Oberhausen, Germany, with a throughput rate of 160 t/d of coal. In the Texaco gasification process, fine-grained coal is mixed with water to a suspension. The oxygen is added at the burner. The reactor operates at pressures of ~5.5 MPa and high steam contents. Due to the high operation temperatures, the carbon conversion rate is about 99% and the thermal efficiency is about 92%. The synthesis gas typically contains 34% H_2 and 48% CO. Hydrogen can be obtained with a purity greater than 97% and at a pressure of 4 MPa.

Flue stream coal gasifiers are the most commonly used gasifiers. Their main advantage is that they accept both solid and liquid fuels. The high operation temperatures and pressures, on the other hand, require high quality materials for burner and heat exchanger. In the Japanese so-called ECOPRO process, for "efficient co-production with coal flash hydro-pyrolysis", a two-stage flue stream reactor is used, where, after injection of coal, oxygen and steam, gasification takes place in the lower part, while more coal and hydrogen are given to the upper part of the reactor to allow for partial coal hydro-pyrolysis [118].

(D) Iron bath

Coal can also be gasified in a bath of liquid iron. In the MIP (molten iron process) of KHD Humboldt–Wedag AG, fine-grained coal (<2 mm) is blown pneumatically at the bottom into the molten iron at 1400–1450°C and 0.3–1 MPa. Oxygen is also added. The carbon dissolves in the iron and reacts to CO, while the hydrogen contained in the coal is liberated. The reactor operates almost continuously. With the Klöckner steel–gas process, coke, oxygen and iron ore are processed in the iron bath. In the Sumitomo method, coal, lime and a gasification agent are blown from the top onto the liquid iron ,where the gasification reactions take place basically at the surface.

3.2.4.2. Hydrogasification

In the hydrogasification process of coal, the agent 'hydrogen' is added to convert the coal into a methane-rich raw gas, ideal for the production of SNG. The hydrogen can be provided either by taking the coke left from the hydrogasification and converting it with oxygen and steam in an HTW process, or by taking a part of the product methane for steam reforming. Both processes requires high temperatures (>600°C), which could be — in an allothermal process — provided by nuclear. The gasification reaction with hydrogen and the main product, methane, is given through a hydrogenating reaction which is strongly exothermic:

$$C + 2\,H_2 \quad \leftrightarrow \quad CH_4 \qquad\qquad +87.5\ \text{kJ/mol C}$$

The kinetics of the process are more complex than those of steam gasification. The above reaction runs in several steps, a pyrolytic step where primary methane is formed, plus volatile hydrocarbons, which also react with H_2 to methane. The remainder is a highly reactive coke ("C^+") which either reacts with H_2 to methane or converts to slowly reacting coke ("C^-"), which then undergoes a hydrogenating gasification to form methane. The other chemical reactions are the endothermic steam–methane reforming and again the water gas shift reaction, both of which serve the purpose to provide the gasification agent.

A high gasification degree can be obtained with relatively short residence times of 9–80 min. In order to obtain a high conversion rate of coal, the methane fraction should not be more than 5%, which requires a low temperature separation step. The advantage of hydrogasification compared with steam–coal gasification is its 200 K lower preheating temperature, which reduces potential corrosive attack. A major drawback, however, is the low conversion rate, i.e. the large amount of residual coke of up to 40%. But again, subsequent processes would allow the generation of SNG or methanol. In contrast to steam gasification, the hydrogasification process still needs to be demonstrated at a larger commercial scale.

With regard to the exothermic character of the above hydrogenation reaction, if wet coal were applied and steam added, it would be possible to compensate the heat generation with parallel endothermic steam gasification to make it an autothermal process.

3.2.4.3. Clean coal technologies

The integrated gasification combined cycle (IGCC) is currently considered the cleanest and most efficient coal fuelled technique for power generation. A schematic is shown in Fig. 34.

The first step is the gasification of the coal, followed by the Boudouard reaction to produce H_2 and CO_2. The 'entrained flow gasifier' in an IGCC usually operates at high pressures of 2–3 MPa and high temperatures greater than 1400°C to achieve high reaction rates and residence times in the order of seconds. Gasification is done with oxygen ('oxyfuel process') rather than with air to eliminate the presence of nitrogen. Unlike in conventional plants, a wide variety of coal grades can be used. After separation and cleaning of dust, sulphur and other impurities, the hydrogen is combusted in a gas turbine for power production. The hot exhaustion gases can then be used in a waste heat boiler, where steam is generated to drive a steam turbine for further electricity production. With its gas turbine step prior to the oxygen/steam process and its intermediate stage of synthesis gas, this technique allows the removal of most carbon components before combustion. The stream of CO_2, which can be easily processed from the flue gas through rectification or distillation, is of high purity and at high pressure, and therefore suited for capture. The thermal efficiency achieved can be up to 50%.

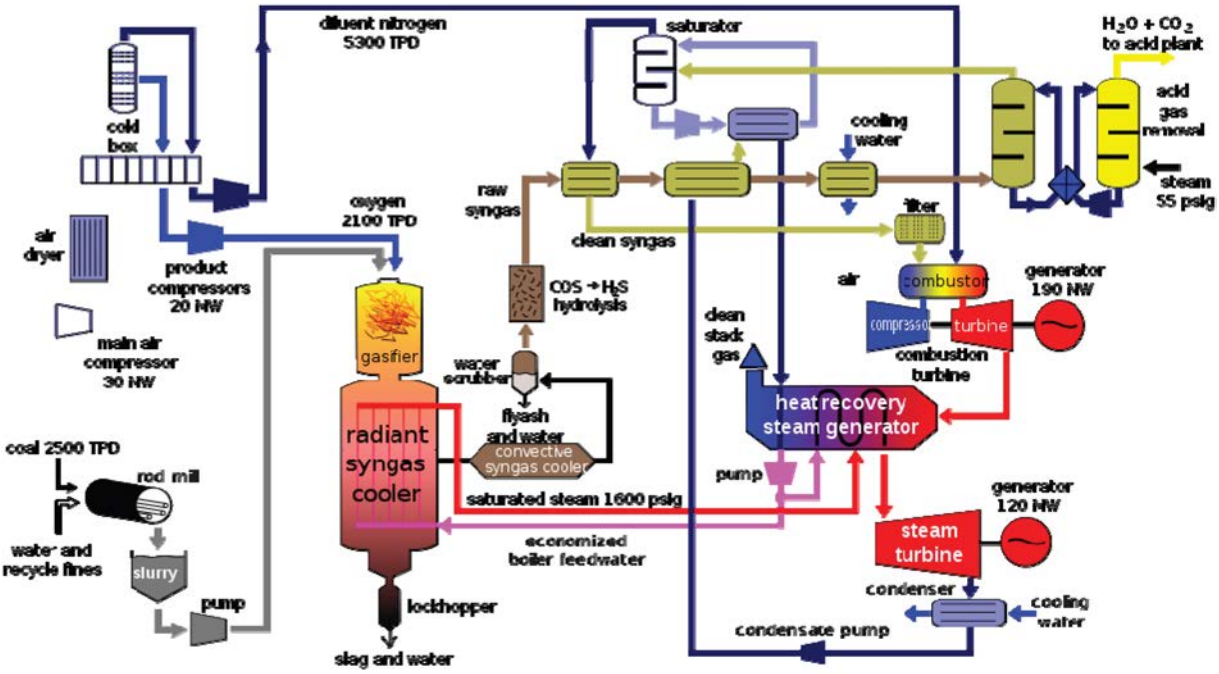

FIG. 34. IGCC flow diagram (Stan Zurek, 2006).

The 'cleaner' technology of IGCC was demonstrated in the 1980s with POX, where the oxygen was distilled from air. Other facilities on a pilot plant scale followed in Germany and the USA. Clean coal technology with removal of contaminants during gasification could largely eliminate the emissions of SO_x, NO_x and particulates. Thermal efficiency is expected to improve by 10% over conventional coal fired steam turbines. But also other solid wastes can be gasified with the IGCC technology. For example, the "Schwarze Pumpe" plant in Germany treats a wide variety of solid (~1200 t/d) and liquid (~200 t/d) wastes, ranging from waste plastic to tires, sewage sludge and household garbage for the generation of electricity, steam, synthesis gas and methanol (100 000 t/a) [125]. IGCC technology represents the most advanced and efficient solution where the carbon in the fuel is removed and hydrogen is produced in a pre-combustion process [126].

Under 'normal' conditions, IGCC is not competitive with steam–methane reforming. As of 2003, commercial IGCC plants in the power range of 250–350 MW and with efficiencies of 37.5–41.5% were being operated in the USA, the Netherlands, Spain and Japan. The most powerful coal based IGCC plants in Europe are the 400 MW(th) plant in Vresova, Czech Republic (since 1996) for lignite, and the 350 MW(th) plant in Puertollano, Spain (since 1998) for coal and pet coke. The total IGCC capacity in Europe is 2745 MW(e), of which 1075 MW(e) is coal based [127]. More commercial scale demonstration and R&D efforts aiming at gas turbine improvement, lower cost air separation and material research are required, to further this technology [121].

The USDOE goal within FutureGen is the verification of a zero-emission, coal fuelled facility for H_2 and electricity cogeneration coupled with CO_2 sequestration with an overall efficiency of 60%. The facility is also intended to be used as a large scale test bed for innovative technologies. The FutureGen programme is now in the early stages of planning. Germany is also planning the construction of a 400–450 MW, CO_2 free IGCC plant, with the CO_2 storage system to be developed in parallel. In the Japanese EAGLE project, a coal gasification system is being investigated that integrates, in addition to a gas turbine and a steam turbine, a fuel cell system fuelled by the produced gas. Certain requirements have to be met regarding the purity level of the fuel gas. This integrated coal gasification fuel cell combined cycle (IGFC) promises an efficiency improvement to greater than 55% and a 30% CO_2 emission reduction. In an advanced design, waste heat from high temperature fuel cells could be recovered and utilized in the endothermic steam gasification reaction [128].

An improved performance is expected if coal gasification is performed in a two stage, double line process [129]. The employment of two separate reactors for combustion and for gasification avoids the use of pure oxygen and still produces synthesis gas free of nitrogen. The two reactors operating in a continuous mode are linked by

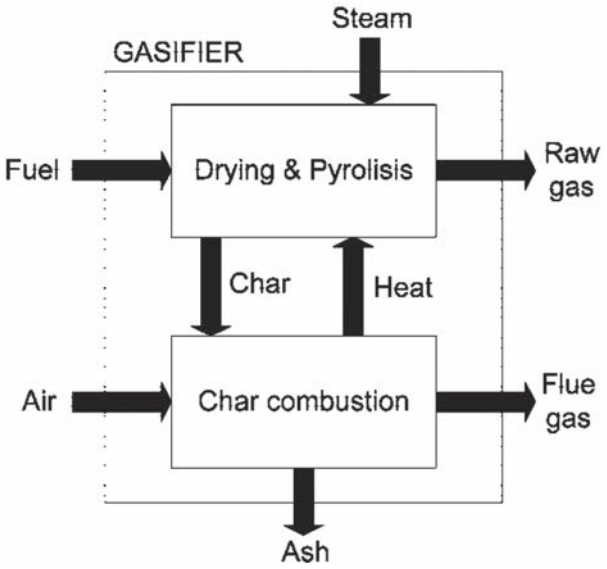

FIG. 35. Schematic of a two-stage coal gasification process [129].

process heat transfer to the gasification plant by an inert solid continuously moving between the two sections, and by charcoal transfer to the combustion system (Fig. 35). This principle was successfully tested with biomass gasification where the heat transferring medium was sand.

In syngas chemical looping (SCL) combustion following the gasification process, hydrogen enrichment and solids regeneration take place in a fixed bed reactor at atmospheric pressure. Metal oxide, preferably Fe_2O_3, used as an oxygen carrier for the combustion, is reduced to the metal (Fe, FeO) in a low temperature reactor, where the oxygen combines with carbon to form CO_2 and steam. Condensing the steam leaves the CO_2 for sequestration. The Fe_2O_3 particle size is 2–10 mm. In a second reactor, the metal is oxidized at 500–700°C and 3 MPa with the oxygen from moistened air and recycled to the first reactor, while 99% pure H_2 is produced from the water. The gasification step prior to the chemical looping allows for easier handling of the solids (no contact of coal with the metal oxide).

In a process called coal direct chemical looping (CDCL), a fuel reactor is employed where the coal is not gasified, but reacts directly with the metal oxide and oxygen to generate metal and CO_2 ready for sequestration. The metal is oxidized with steam to produce hydrogen. The residence time of the coal in the fuel reactor is between 30 and 90 min. The advantage is reduced oxygen consumption, and a significantly higher conversion rate of the solid fuel. Problems may be given by the high temperatures destabilizing the metal oxide and the control of the reaction rates [130].

Looking for even higher efficiencies and lower emitting processes, a highly favoured clean coal technology is the so-called ultra super critical (USC) power cycle characterized by an improved conceptual boiler design resulting in a longer product lifetime and steam of 600°C and 30.5 MPa. Double reheating has been introduced in order to increase the efficiency. The final live steam temperature and pressure goals by the year 2020 are 760°C and 38.5 MPa, respectively, raising the efficiency to more than 48% [131].

The Zero Emission Coal Alliance (ZECA) initiative, founded in 2000 in the USA, is pursuing a concept developed at the Los Alamos National Laboratory. It integrates hydrogasification of coal, a CaO driven reforming step with simultaneous CO_2 separation, an SOFC for electricity production, and heat recovery. This process showing no air emissions and producing a stream of liquid CO_2 ready for sequestration promises an efficiency of about 70% (HHV) of fuel energy into electricity [132].

The so-called hydrogen production by reaction integrated novel gasification (HyPr-RING) process proposed in Japan in 1999 uses the sorbent CaO to fix CO_2 as $CaCO_3$. Reaction of the CaO with steam provides reaction heat for the coal gasification. The overall reaction is exothermic:

$$C + 2\,H_2O + CaO \quad \leftrightarrow \quad CaCO_3 + 2\,H_2 \qquad +88\ \text{kJ/mol C}$$

The CO_2 fixation was found to enhance the hydrogen production reactions. HyPr-RING runs at a temperature of 800–900°C. Experiments in a fluidized bed with a throughput of 50 kg/d of coal resulted in a product gas with a H_2 concentration of more than 80%. Concentrations of CO and CO_2 were found to decrease with increasing pressure and reached a level below 1% at pressures above 3 MPa [133].

Similarly, in the so-called lime enhanced gasification (LEGS) process, the stages of catalytic steam reforming, shift reaction and CO_2 removal are performed in one reactor, with the result of almost pure hydrogen in one reaction step. Lignite and other low rank coals appear to be perfect fuels for LEGS. CaO or other lime is used as a sorbent for the CO_2. The solid product generated, consisting of limestone, CaO, char, ash and CaS, is separated from the gas and regenerated to produce a high purity CO_2 stream. LEGS is applicable to a wide range of carbonaceous fuels, including biomass, sewage sludge and solid organic waste [134].

Another advanced method is the HYDROCARB coal cracking process. The coal is decomposed in a thermal cracker to carbon black as a clean fuel and hydrogen as a by-product fuel. The commodity carbon black outweighs the poor efficiency of 17% for this method.

Coal gasification can also be done directly in situ [135]. In this underground coal gasification (UCG) process, oxygen (or air) and hot steam are given through injection boreholes to the coal-containing layers where the coal seams are ignited and burn at about 1200°C. After conversion, the synthesis gas is captured through another borehole and brought to the surface. Further treatment is required to remove pollutants such as particulate matter and H_2S gas. With this method, coal resources can be exploited to a larger extent compared to traditional methods. It also avoids solid waste discharge. Remote directional drilling equipment is necessary to create a network of gasification channels, injection wells and production wells. UCG was carried out on the industrial scale in the Soviet Union beginning in the 1930s, with several commercial plants being operated in the 1960s. The largest UCG plant today is a 100 MW(e) steam turbine plant operated in Uzbekistan. Currently the most extensive programme is ongoing in China with renewed interest also in the UK, the USA and Australia. The overall amount of synthesis gas produced up to now by underground coal gasification corresponds to approximately 15 million t of coal [135].

3.2.5. Gasification of biomass

Biomass is classified into massive biomass (dedicated bioenergy crops, process residues, harvest residues, energy crops), which can be directly converted thermochemically to hydrogen, and organic biomass (liquid manure, sludge, process residues), where the hydrogen is produced indirectly by anaerobic fermentation. The amount of hydrogen in biomass is in the range of 6–7 wt%.

Steam gasification of biomass is generally conducted in two steps. First, thermochemical decomposition of the biomass takes place with cracking and reforming of volatiles, and the production of tar, char and gasification of the char. In the second step, hydrocarbon gases and carbon in the biomass react with CO, CO_2, H_2 and H_2O, leading to more light gases. Dry gas yield, carbon conversion efficiency and the hydrogen fraction in the product gas increase with increasing temperatures (from ~25% to ~50% if the temperature increases from 600 to 900°C).

The conversion of biomass such as peat, wood and agricultural residues in a thermal process leads to a hydrogen-containing gas mixture. Its H_2 content is dependent on the fuel/feedstock, the availability of steam and oxygen, and the process temperatures. Processes for decomposition of the organic substances are gasification or pyrolysis with subsequent autothermal or allothermal steam reforming. The gasifiers are usually indirectly heated or oxygen-blown to avoid nitrogen in the product gas, and are operated at low pressures. The autothermal gasification in a fluidized bed results in a synthesis gas with typically 30% H_2, 30% CO, 30% CO_2 and 5–10% CH_4 plus some higher hydrocarbons. A shift reaction again converts CO to increase the hydrogen fraction. Anaerobic fermentation of wet biomass leads to a CH_4 rich gas with only little hydrogen, which, however, at a certain quality could be used in higher temperature fuel cells (MCFC, SOFC). Although the conversion rate of biomass is high, hydrogen production is an expensive and thermodynamically highly inefficient process [5]. Due to the relatively low specific energy content of the biomass, only 0.2–0.4% of the total solar energy is converted to hydrogen.

The gasification of biomass or microbial hydrogen production by converting organic wastes is limited to mid-sized plants (<40 MW(th)) for decentralized applications. The reasons for this are the distributed nature of biomass and the low energy density ($\leq$3.7 GJ/m^3) connected with high transportation costs where economies of scale do not apply. For example, a 1.25–2.5 MW(e) biomass gasification plant requires a catchment area with a 60 km diameter [136]. Facilities for wood treatment are on the verge of achieving commercial status [137]. The transportation issue

could be eased with the conversion of the biomass to a bio-oil as an interim product that can be stored and reformed to hydrogen as needed.

Demonstration of biomass gasification in pilot plants is being performed in various countries and has reached power sizes in the range of several tens of megawatts [138]. Some plants apply an autothermal process and use air instead of oxygen. More advanced concepts perform gasification in supercritical water or apply thermochemical cycles. Concepts based on circulating fluidized bed gasification seem to be the most promising. Their overall efficiency is likely to be in the range of 50–60%. Despite the development of a broad variety of system components and designs, it still needs further improvements in feedstock preparation and raw gas handling, ash removal, and synthesis gas cleanup. Plant capacities should reach an appropriate scale in the range of ~57 000 Nm^3/h of hydrogen [110].

Still, biomass conversion appears to be less convenient if dedicated to hydrogen production and is instead employed for heat and electricity production, helping to reduce CO_2 emissions. Furthermore, biomass can easily be converted to a variety of valuable chemicals and liquid fuels like methanol. Fast pyrolysis of biomass for liquids production has been under research and development for nearly 20 years and has now achieved commercial status. In that time, a wide range of reactor configurations have been devised to achieve the basic process requirements that give high liquid yields. The focus of research activities is now on the improvement of oil quality. Further areas of potential improvement include pretreatment of feed to improve liquid quality and liquid collection systems. Issues raised in connection with biofuel production are land use allocation and food crop displacement, but also the need to transport very large volumes of biomass feedstock due to the inherently low energy density. An external energy source for bio-refineries could be provided by nuclear energy.

3.3. HYDROGEN FROM WATER SPLITTING BY ELECTROLYSIS

Apart from classic alkaline electrolysis, he types of electrolysis that are being considered for employment on an industrial scale are PEM electrolysis using a hydrogen ion conducting polymer electrolyte membrane (or proton exchange membrane), both operating at low temperatures, and high temperature steam electrolysis (HTSE) using oxygen conducting ceramics. Electrolysis is the most straightforward approach currently available to produce hydrogen directly from water.

3.3.1. Low temperature electrolysis

There are principally two classes of low temperature electrolysis based on either a liquid electrolyte (most commonly potassium hydroxide, KOH) or a solid polymer electrolyte. In both cases, the water molecule is dissociated by applying an electrical current.

In an alkaline electrolysis cell containing an aqueous caustic solution with usually 20–40% KOH or NaOH (typically 30%), electrical energy is applied to two electrodes which are plates made of nickel (anode) or chromium–nickel steels. Water decomposes at the cathode to H_2 and OH^-, where the latter migrates through the electrolyte and a separating diaphragm and discharges at the anode, liberating the O_2.

$$4\ H_2O \leftrightarrow 4\ H^+ + 4\ OH^-$$

$$4\ OH^- \leftrightarrow O_2 + 2\ H_2O + 4\ e^- \quad \text{Oxygen electrode}$$

$$4\ H^+ + 4\ e^- \leftrightarrow 2\ H_2 \quad \text{Hydrogen electrode}$$

The hydrogen gas is dissolved in the water and extracted in a separating chamber with high purity. Operation temperatures are limited to less than 150°C due to corrosion problems; typically ~90°C is used. A schematic is shown in Fig. 36.

The ideal reversible cell potential needed to split water is 1.229 V at 25°C and 0.1 MPa, which corresponds to a theoretical dissociation energy of $\Delta G^o = 237$ kJ/mol or an electricity demand of 3.56 $kW \cdot h/Nm^3$ of H_2. Because of irreversible processes in the reaction mechanism to account for gas expansion at the electrodes and to maintain the operation temperature, however, realistic cell voltages are 1.7 to 2.1 V. Requirements to the electrodes for water

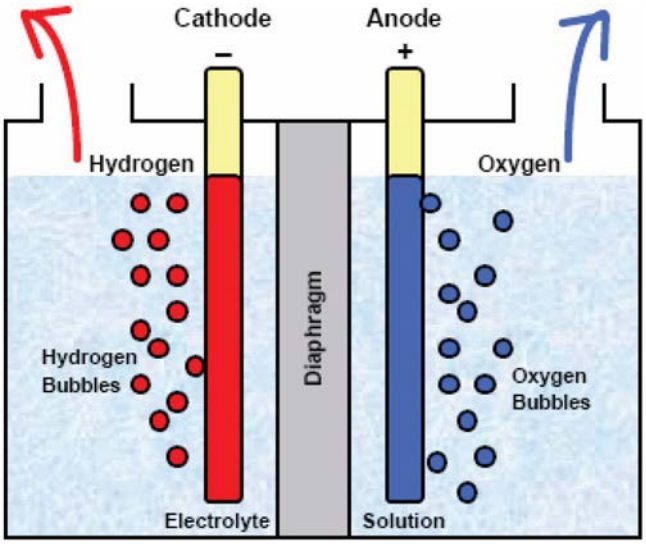

FIG. 36. Standard low temperature alkaline electrolysis.

electrolysis are a large active surface area, electrochemical stability, high corrosion resistance, good electrical conductivity, low over-potential, selectivity, ease of use and low cost. The electrical energy requirement is in the order of 4–4.5 kW·h/Nm^3 of H_2, corresponding to an efficiency of 80% and higher. Norsk Hydro Electrolysers (NHE) estimates that electrical costs make up about 65% of the operational costs. The water demand is theoretically 0.8 L/Nm^3 of H_2, in practice 1.0 L/Nm^3. The water should be as clean as possible to prevent deposition and electrode corrosion.

High pressure electrolysis working at pressures of up to 3 MPa allows the saving of compression energy if hydrogen is stored as a pressurized gas or transported in pipelines, thus reducing the specific consumption of electricity. A disadvantage is the necessary pressure control and the bulky design of the pressure containment. After first commercialization of a 3 MPa electrolyser by Lurgi in Germany, low temperature, high pressure electrolysis has become a well established technology on the industrial scale worldwide, covering about 3.9% of the world's production.

In chlorine–alkaline water electrolysis, the hydrogen is actually a by-product of chlorine production and mostly used as the thermal energy source and a substitute for natural gas. A solution of salt in water is decomposed into hydrogen and soda lye (mercury cathode) and chlorine (graphite anode):

$$2\ NaCl + 2\ H_2O \quad \leftrightarrow \quad (Cl_2)_g + (2\ NaOH)_l + (H_2)_g$$

The oldest process is the amalgam electrolysis where a mercury film a few millimetres thick (as the cathode) flows along an inclined surface. The initially formed sodium is dissolved as an amalgam before it reacts with water and decomposes to hydrogen and sodium hydroxide. Other processes are diaphragm electrolysis, mainly used in the USA, where gases are separated from the other products by migration through a fine-pore wall, and membrane electrolysis which is the most environmentally friendly and economical method, using an extremely strong and resistant synthetic foil. The annual production of chlorine worldwide today is approximately 68 million t from about 550 chlorine plants, mainly in China and other countries in Asia and North America, with ~40 billion Nm^3 of hydrogen being generated.

The first alkaline electrolysers for hydrogen production were developed by Norsk Hydro in Norway, where inexpensive electricity from hydropower could form the basis for this process. The large hydro electrolyser units have a capacity of 485 Nm^3/h (or ~1 t/d) at an availability of greater than 98% and with an energy consumption of 4.1 kW·h/Nm^3 [139] (Fig. 37). They usually operate at about atmospheric pressure and allow unmanned remote operation. Today's alkaline units are available across a range of capacities — between 4 kW and 100 MW. The largest electrolyser units produce ~760 Nm^3/h with multiple units being combined to larger capacities.

FIG. 37. Standard low temperature alkaline electrolysis [140].

Overall efficiencies achieved at that scale are about 63% LHV. Efficiencies are principally independent of cell or cell stack size, which make them appropriate for small scale use. Additional components are necessary such as purification of water and products, cooling/heating/compressing devices, gas drying, and reprocessing of alkaline solution. Other features are a lifetime of over 30 years, a hydrogen purity of greater than 99.8%, and H_2 produced at 3 MPa, the latter, however, at the expense of bringing the efficiency down to about 59%. Pressurized systems operating at higher pressures help to save compression energy resulting in higher efficiencies. Pressurized electrolysis up to 3 MPa is state of the art; operation at pressures up to 14 MPa has been demonstrated in prototypes [104].

Norsk Hydro is the world largest producer of technical electrolysers. It describes in a publication an atmospheric plant for the production of 46 560 Nm^3 of H_2/h having an electrical power consumption of 230 MW. The plant has an area requirement of ~27 000 m^2 and thus is not designed or optimized for less area demand or offshore use. The largest integrated installation is currently in Aswan, Egypt, with a production capacity of around 35 000 Nm^3/h. Low output electrolysers with less than 100 Nm^3/h are typically used in the electronics, agricultural or food industries. Chlorine–alkali electrolysis can be beneficial to the development of seawater electrolysers, which might be considered for hydrogen production from offshore wind farms. Characteristic data of various units of different sizes are given in Table 7.

Both alkaline electrolysis and PEM electrolysis are characterized by good dynamic performance. Therefore, they are suited for applications with fluctuating power plants (primarily renewables). At present, the more advanced method is the solid polymer electrolyte water electrolysis (SPEWE) or PEM electrolysis using an acidic, proton conducting (exchange) PEM as the diaphragm, thus making an additional electrolyte unnecessary. Here the hydrogen ions are migrating from the anode through the membrane and recombine at the cathode with electrons to hydrogen molecules. The oxygen remains in the water. The SPEWE can be operated at higher pressures and at higher current densities due to the compact design compared with cells with a KOH electrolyte. Typical operation temperatures are 200–400°C; pressures may go up to several tens of MPa. PEM electrolysis is simpler in its design, safer and promises higher power densities and a longer lifetime and a higher efficiency of ~90%. The electricity requirement will be reduced to values below 4 kW·h/Nm^3 of H_2.

Today, PEM electrolysers can be regarded as a well established industrial technology. They exhibit efficiencies of around 50%, somewhat lower than KOH electrolysis; this is, however, compensated by the lower requirements for purification and compression. High pressure systems are established in the smaller power range with pressures of 3 MPa achieved and efficiencies up to 80%. Membrane development started in the 1950s and 1960s for use in PEM fuel cells within the US space programme. The main disadvantage today, however, is the still high capital cost of membrane manufacture, which has prevented significant penetration of the hydrogen market up to now. In development are plants for pressures of up to 5 MPa. Current plant capacities are in the range of 1–20 kW. The main drawbacks are the limited lifetime and high cost of the membrane [126].

TABLE 7. SOME DATA OF INDUSTRIAL WATER ELECTROLYSIS PLANTS, DATA A–D FROM [141]

Parameter	A	B	C	D	E	F	G
H_2 production rate (Nm^3/h)	10	42	60	485			5–760
Electrolyte (%)	PEM	alkaline	alkaline	25% KOH	25% KOH	29% KOH	25% KOH
Type of cell	bipolar	bipolar	bipolar	bipolar	bipolar	bipolar	bipolar
Temperature (°C)				80	80	80	90
Pressure (MPa)	1.4	0.4–0.8	2.5	0.1	0.1	0.1	3.0
Current density (kA/m^2)				1.75	2	1.5	2
Voltage of cell (V)		2.1	2.04	1.75	2.04	1.85	1.86
Production pressure (MPa)	1.4	0.4–0.8	2.5	3.0			
H_2-purity (%)	99.999	99.9998	99.997	>99.8	≥99.8	>99.8	>99.8
O_2-purity (%)				>99.5	≥99.6	>98.5	>99.5
Energy requirement electrolyser ($kW·h/Nm^3$ H_2)	n.a.	n.a.	4. 2	4.3[a]	4.9	4.6	4.5
Energy requirement entire system ($kW·h/Nm^3$ H_2)	6.3	5.6	4.8	4.8[a]			
System power requirement (kW)	63	235.2	288	2330			
Water requirement (L/h)	8.4	42	60	485			
Conversion efficiency (%)	95	80	80	80			
System efficiency (HHV) (%)	56	63	73	73			

A: Proton HOGEN 380
B: Teledyne EC-750
C: Stuart IMET 1000
D: Norsk Hydro HPE Atmospheric Type No. 5040
E: BBC
F: De Nora
G: Lurgi (now ELT)

[a] incl. compression to 3.3 MPa.

3.3.2. High temperature electrolysis

A principal variant of electrolysis considered promising for the future is high temperature steam electrolysis (HTSE). Unlike low temperature water electrolysis, the total energy demand of electrolysis in the vapour phase is reduced by the heat of vaporization, which can be provided much more inexpensively by thermal rather than electric energy. Decreasing electricity input can be seen with increasing temperature from Fig. 38 [49], and is about 35% lower compared to conventional electrolysis in the high temperature range of 800–1000°C. Also the efficiency of electrical generation at this high temperature level is significantly better.

The HTSE process is advantageous because of its high overall thermal-to-hydrogen efficiency when coupled with high efficiency power cycles. HTSE corresponds to the reverse process of the SOFC; devices could be operated in both modes. The HTSE development may therefore benefit of ongoing R&D efforts in the SOFC area. A major difference is that a high temperature electrolyser must be coupled with a heat and power source. Nuclear plants, in particular those of the fourth generation, could provide the electricity and, in the case of a VHTR, also deliver relatively high temperatures and high net power cycle efficiencies.

3.3.2.1. High temperature electrolysis of steam

Essentially the electrolytic cell consists of a solid oxide electrolyte with conducting electrodes deposited on either side (Fig. 39). The electrolyte is an oxygen-conducting ceramic material, typically Y_2O_3 stabilized ZrO_2 (YSZ) and MgO. A mixture of steam to be dissociated and some hydrogen is supplied to the hydrogen electrode at 750–950ºC. At the hydrogen electrode–electrolyte interface, the steam is split into hydrogen and oxygen:

$$2\ H_2O + 4\ e^- \quad \leftrightarrow \quad 2\ H_2 + 2\ O^{2-}$$

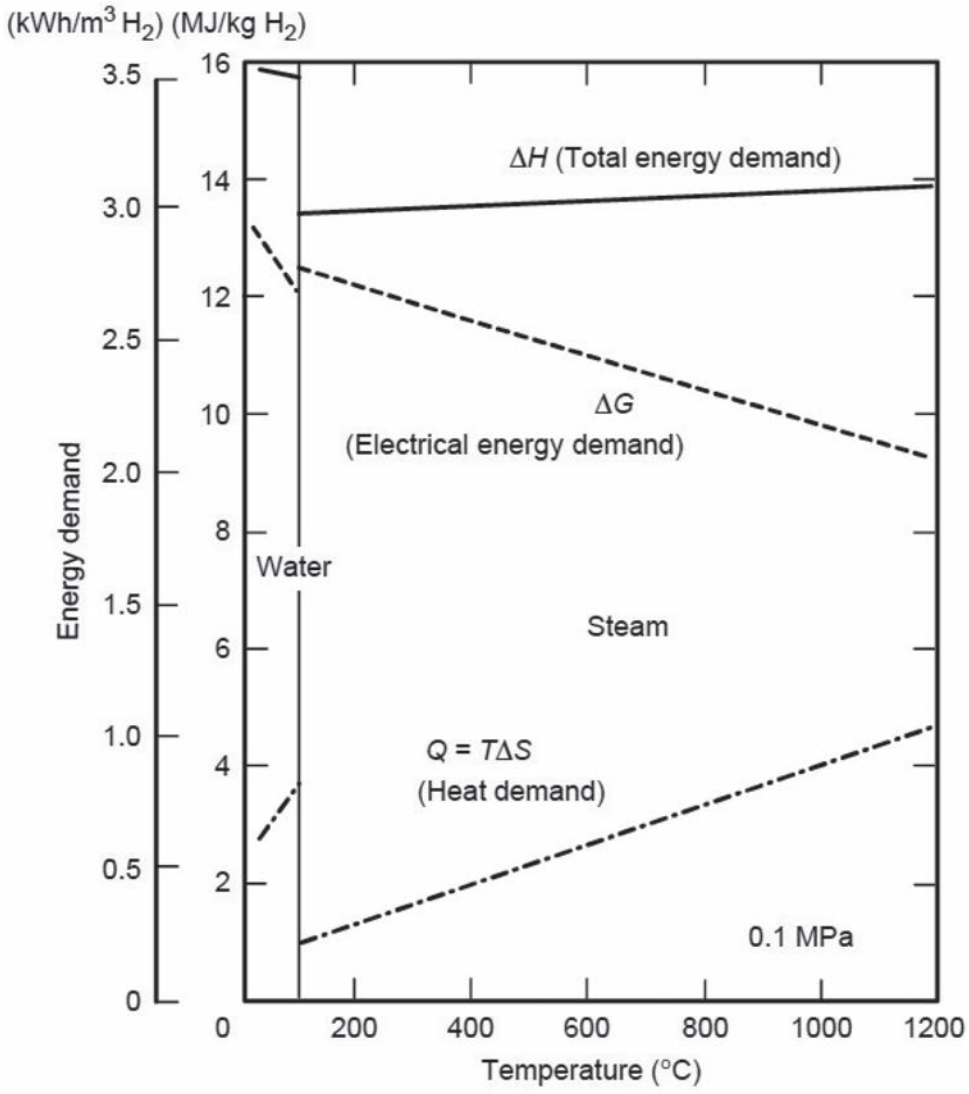

FIG. 38. Energy demand for water/steam electrolysis [49].

Oxygen ions are drawn through the ceramic electrolyte by the electrical potential of about 1.3 V, until they recombine to oxygen gas at the electrolyte–oxygen electrode interface:

$$2\ O^{2-} \quad \leftrightarrow \quad O_2 + 4\ e^-$$

The oxygen then flows along the anode, typically made of a composite of YSZ and Sr-doped lanthanum manganite (LSM)), while the hydrogen–steam mixture passes along the hydrogen electrode (Ni/YSZ cermet with ~30% porosity) on the opposite side of the electrolyte. Preheated air or steam can be used as a sweep gas to remove oxygen from the stack. The purpose of the sweep gas is to dilute the oxygen concentration and thus decrease corrosion of the oxygen-handling components. Pure oxygen can be produced by the stack and would be a valuable commodity if satisfactory materials and/or coatings could be developed for construction of the oxygen-handling components.

At these high temperatures, all reactions proceed very rapidly. The steam–hydrogen mixture exits from the stack and then passes through a separator to separate hydrogen from the residual steam. The feedgas stream to the HTSE cell contains a 10% fraction of hydrogen for the purpose of maintaining reducing conditions and avoiding oxidation of the nickel in the hydrogen electrode (Fig. 39). HTSE cells can be operated at high current densities, which allow large production capacities in comparatively small volumes. A practical electricity-to-hydrogen

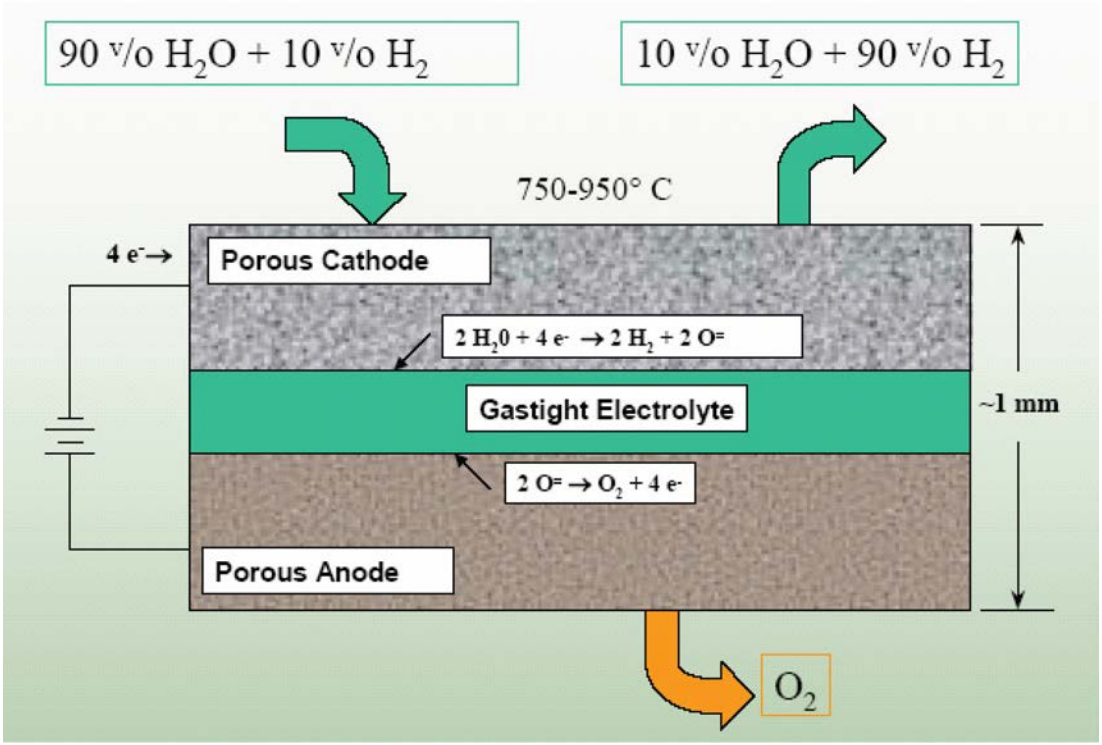

FIG. 39. Schematic of a planar steam electrolysis cell [142].

efficiency of about 90% appears to be realistically achievable. The main issue that needs further improvement remains the lifetime of the hydrogen electrode, which is limited by degradation [143].

One can clearly see on the graph in Fig. 38 that a large part of the energy demand reduction is related to water vaporization which does not require high temperature heat. Once vaporization is achieved, the extra heat necessary to reach the high temperature required to have high enough ionic conductivity in the electrolyte may be also be provided by a combination of nuclear heating, recuperation of the sensible heat of the produced hydrogen and oxygen, and self-heating of the cell due to its inherent electrical resistance.

With respect to the electricity requirements, values of 2.6–3 kW·h/Nm^3 of H_2 are expected. The heat for steam production to supply the cells, however, must be added. The process with the production of hot steam and cell operation at high temperatures requires a solid oxide membrane electrolyte. For example, Y_2O_3 stabilized ZrO_2 acting as both gas separator and electrolyte is used where oxygen ions start migrating when a voltage is applied. Steam electrolysis at about 800°C will have an overall efficiency (including the electrical conversion efficiency) in the range of 35–45%. The efficiency will even rise to around 50% at 900°C. Two major problems to be solved are the improvement of the long-duration performance of the cells and the development of techniques for manufacturing and assembling large area cells in order to reduce the overall cost of the commercial plant.

3.3.2.2. High temperature co-electrolysis of steam and carbon dioxide

The principle of high temperature electrolysis is also applicable when steam and carbon dioxide are present simultaneously. In this case, both H_2O and CO_2 can be co-electrolysed to hydrogen and CO. A mixture of CO_2 and steam is electrolytically decomposed at a required cell voltage of 1.48 V (if no external heat source is available), resulting in the production of synthesis gas that may be subsequently used for synthetic fuel production. The quantities produced are dependent on the quantities of H_2O and CO_2 in the feedstream, the electrolysis current applied, and the reverse water gas shift reaction. The net reaction of CO_2 electrolysis is:

$$2\,CO_2 \quad \leftrightarrow \quad 2\,CO + O_2 \qquad \text{at 1.47 V}$$

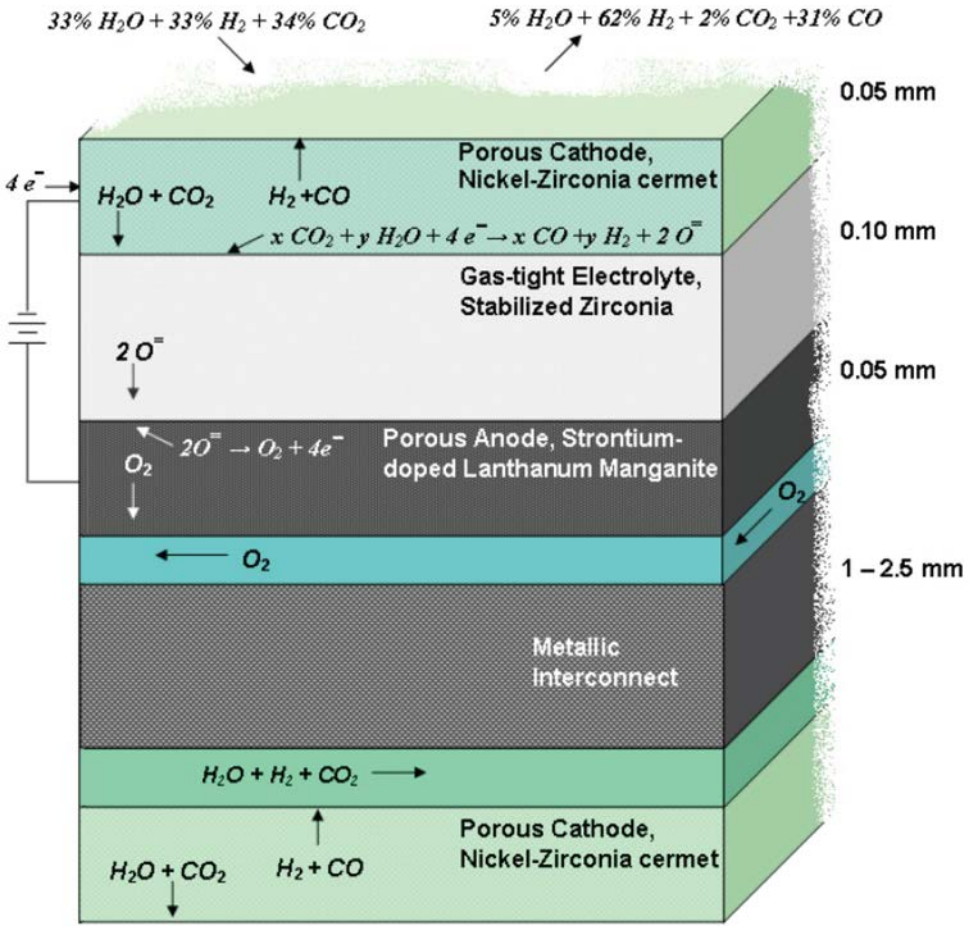

FIG. 40. Solid oxide cell used for the co-electrolysis of CO_2 and steam [144].

The solid oxide electrolysis cell (SOEC) negative electrode is usually made of a Ni–YSZ composite, where the Ni serves directly as a catalyst. As for the electrolyte, a higher ionic conductivity and a lower ohmic loss are the focus of research, and new materials (ScSZ, LSGM, LSGMC) are being looked into as alternatives to YSZ.

The process taking place is more complex than pure steam electrolysis, since it involves several reactions. Also in a co-electrolysis cell (Fig. 40), about 10% of the product (here synthesis gas) is recycled and added to the feed stream to maintain reducing conditions at the steam/H_2 electrode. The mixture then enters the electrolysis cell, where the oxygen is removed electrolytically and the product stream is enriched in synthesis gas.

Two design concepts are possible: planar and tubular. The tubular design pursued in Germany and the USA was first selected for its mechanical stability and because fabrication of thin-walled ceramic parts with large surfaces was not state of the art. The tubes were vertically deployed on support tracks which contained steam input and hydrogen output ducts. Tubular cells have the advantage of achieving a high degree of leaktightness, while planar cells can be fabricated with a larger active area per volume.

3.4. HYDROGEN FROM WATER SPLITTING BY THERMOCHEMICAL CYCLES

3.4.1. Overview

Besides high temperature electrolysis, high temperature water splitting has been identified as another potential method for producing large amounts of hydrogen, and the thermochemical process is currently under investigation worldwide.

The most straightforward way of splitting water would be one-step direct thermal decomposition. This, however, would require temperatures of greater than 2500°C for reasonable quantities, which industrially is not

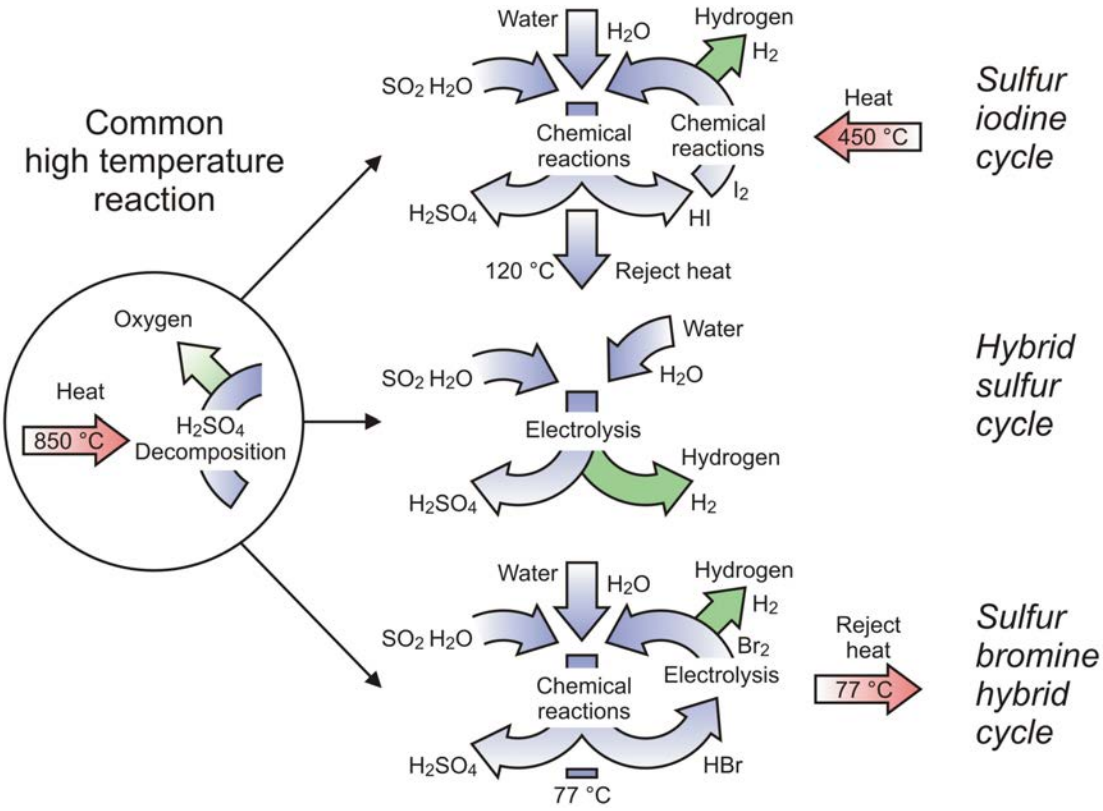

FIG. 41. Thermochemical cycles of the sulphur family [146].

feasible. Therefore, multistep processes are being considered. A thermochemical cycle is a process consisting of a series of thermally driven chemical reactions where water is decomposed into hydrogen and oxygen at moderate temperatures. Supporting intermediate chemical compounds are taken to run a sequence of chemical and physical processes and are regenerated and recycled internally, and remain — ideally — completely in the system. The only input is water and high temperature heat. Therefore, these cycles have the potential for better efficiency compared with low temperature electrolysis and hence promise to significantly reduce the production cost. A hybrid cycle combines the benefits of thermochemical and electrolytic reactions. Here, the low temperature reaction, while thermodynamically unfavourable, is forced electrochemically. Thermochemical cycles are being investigated mainly with regard to solar or nuclear primary heat input.

Numerous thermochemical cycles have been proposed in the past and checked against features such as reaction kinetics, thermodynamics, maximum temperature, heat transfer, separation of substances, side reactions, material stability, toxicity, corrosion problems, processing scheme, thermal efficiency and cost analysis [145]. Some have sufficiently progressed to be experimentally demonstrated and proven their scientific and practical feasibility. All cycles, however, have design challenges, and none has actually reached the commercial scale. In all studies that systematically examined thermochemical cycles, those of the sulphur family — sulphur–iodine, hybrid sulphur, sulphur–bromine hybrid — have been identified as the potentially most promising candidates with higher efficiency and a lower degree of complexity (in terms of number of reactions and separations) [86]. All three have in common the thermal decomposition of sulphuric acid at high temperatures (Fig. 41).

A major challenge in thermochemical cycles is to obtain maximum yields while reducing the amount of any excess reagents used to drive the reactions in the desired directions. Optimization of heat flows is important for high energy conversion efficiency in thermochemical cycles.

After the principle of a thermochemical cycle was discovered by Funk and co-workers in the mid-1960s [147], various process suggestions have been made. The first major programme [148] directed by the Joint Research Centre (JRC) of the European Community in Ispra, Italy, began in the late 1960s and ended in 1983. The goal of this work was to identify potential thermochemical cycles to be coupled with a high temperature gas cooled reactor. In a first step, mercury, manganese and vanadium based cycles were studied. Later, nine cycles based on

iron and chlorine were investigated. These cycles were abandoned because of difficulties in decomposing the iron chloride. Finally several cycles of the sulphur family were studied, which eventually resulted in a laboratory demonstration loop of the sulphur bromine process. Associated with this experimental effort, the JRC had an important activity in the field of corrosion, the design of large scale equipment and the development of industrial scale flowsheets.

Japan has focused its efforts on two cycles: the UT-3 cycle (iron, calcium and bromine) and the S–I cycle. In both cases, the reactions were studied separately and demonstration loops were successfully operated. Japan maintains activity in the S–I cycle. In the USA, particularly the S–I cycle was extensively studied with respect to individual reactions, corrosion, bench scales of the three parts of the cycle and full scale flowsheet [149]. Later the Gas Research Institute (GRI) funded a long term systematic programme to evaluate some 200 distinct thermochemical cycles, out of which 125 cycles were selected on the basis of thermodynamic criteria. Eighty of the most promising were tested in a laboratory, 15 were found to be feasible using batch techniques with chemical reagents, and eight were demonstrated successfully with recycled materials. Within the Nuclear Energy Research Initiative (NERI), a three year programme was conducted to evaluate the feasibility of thermochemical cycles for efficient, cost effective, large scale nuclear H_2 production. After various screening processes on a total of 115 cycles, the number of cycles considered worth investigating in more detail boiled down to two: S–I and UT-3 [150]. The Russian Federation also undertook some major research on the thermochemical cycles and finally constructed and operated a small demonstration loop of the hybrid sulphur (HyS) process.

In the following subsections, some thermochemical cycles are described in more detail. They refer to those cycles that have been recently identified within the USDOE NHI as worth further investigating (see also Section 2.10.2).

3.4.2. Sulphur–iodine cycle

3.4.2.1. Reactions and processes

One cycle considered with a high priority is the S–I process (also known as the Ispra Mark 16 cycle) originally developed by the US company General Atomics and later taken up and modified by different research groups such as the JAEA. It basically consists of three chemical reactions. According to the General Atomics stoichiometry, the S–I process is an all-fluid cycle and can be split into the following steps [151]:

(1)	$(9I_2)_l + (SO_2)_g + (16H_2O)_l$	→	$(2HI+10H_2O+8I_2)_l + (H_2SO_4+4H_2O)_l$	(120°C)
(2)	$L_2 = (2HI + 10H_2O + 8I_2)_l$	→	$(2HI)_g + (10H_2O+8I_2)_l$	(230°C)
(3)	$(2\ HI)_g$	→	$H_2 + (I_2)_l$	(330°C)
(4)	$L_1 = (H_2SO_4 + 4H_2O)_l$	→	$(H_2SO_4)_l + (4H_2O)_l$	(300°C)
(5)	$(H_2SO_4)_l$	→	$(H_2SO_4)_g$	(360°C)
(6)	$(H_2SO_4)_g$	→	$(SO_3)_g + (H_2O)_g$	(400°C)
(7)	$(SO_3)_g$	→	$(SO_2)_g + 0.5\ O_2$	(870°C)

The temperatures in parentheses are approximate values and depend upon the pressure, which is not necessarily uniform in the different parts of the cycle.

The S–I cycle is, of all thermochemical cycles, the one with the highest efficiency quoted. The theoretical limit of efficiency for the total process is assessed to be 51% assuming ideal reversible chemical reactions. Analytical studies anticipate efficiencies of 40–50%. As the result of a flowsheet analysis in 1982, General Atomics estimated the process thermal efficiency to be 47% [152]. A best estimate was found to be around 33–36% [153]. A schematic of the S–I cycle is shown in Fig. 42.

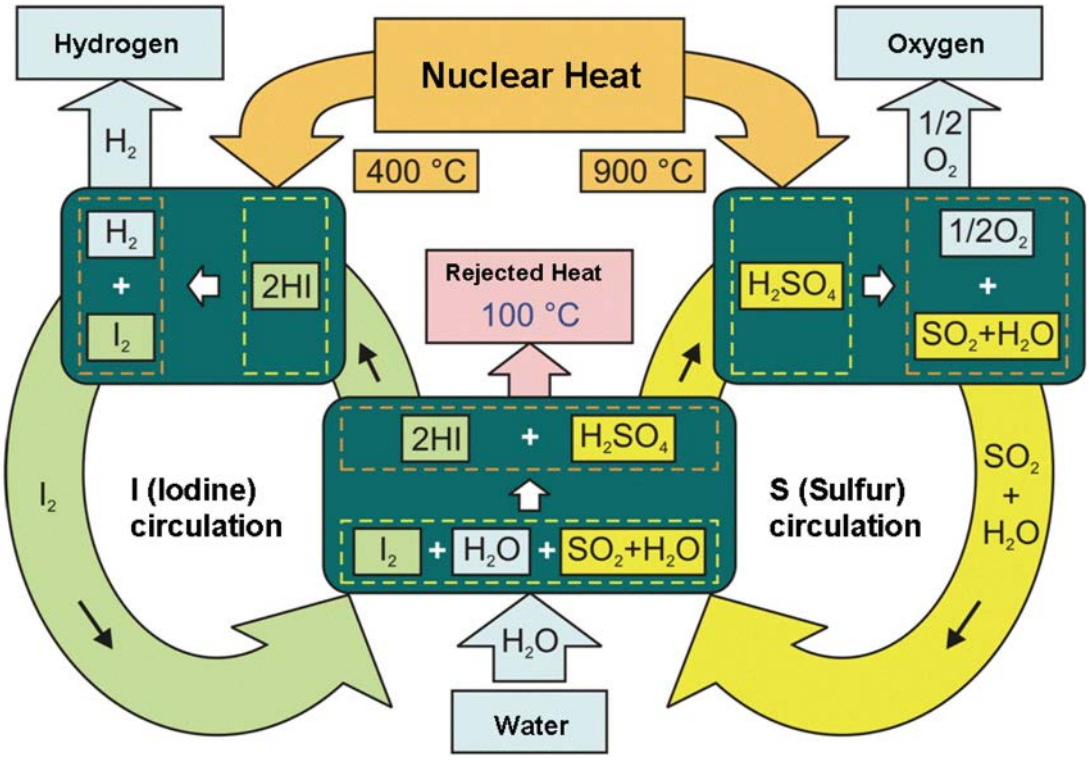

FIG. 42. Schematic of sulphur–iodine thermochemical water splitting cycle.

After separation, purification and further concentration, both acids are decomposed. The heavier HI part is sent to the section of reaction (3), the endothermic decomposition of the HI resulting in the production of hydrogen, while the lighter H_2SO_4 part is sent to the section of reaction (4), the endothermic decomposition of the H_2SO_4 resulting in the production of oxygen. This separation is the most critical phase and is difficult because of the partial decomposition into H_2 and I_2 and the presence of an azeotrope[2] in the ternary mixture.

The most energy consuming parts of the S–I cycle are the separation processes, where optimization decisively determines the potential and economics of this cycle. Heat requirements for concentration and purification of the two acids influence the thermal efficiency. Figure 43 shows the equilibrium conversion of the two acids as a function of temperature, showing the need for high excess iodine due to the low HI conversion ratio of about 20%.

3.4.2.2. Bunsen section

The Bunsen reaction represents an essential part of the S–I cycle. Its reaction products and their composition have a strong influence on the energy consumption in the subsequent reaction steps and therefore need to be optimized. Due to the exothermic nature of the Bunsen reaction, through which some amount of heat is rejected, this section does not need a connection to an external heat source. The reaction system consisting of SO_2, H_2O, I_2, HI and H_2SO_4 has a very complex solution chemistry due to strong electrolytic behaviour, the formation of tri-iodides (I_3^-), poly-iodides (I_4^{2-}, I_5^-, etc.) and solvation reactions. The system displays partial miscibility behaviour [155], as can be seen in Fig. 44.

As can be seen from reaction (1), a considerable excess of iodine is necessary in practice to observe the splitting of the acids into immiscible aqueous solutions through a spontaneous (and slow) separation process. Also, water is added in excess to keep the overall reactions exothermic and spontaneous. Those excesses become a burden in the downstream sections where they have to be recovered and sent back to the Bunsen section, requiring energy for heating, separating, concentrating, cooling, pumping and recycling, thus decreasing the overall

[2] An azeotrope is a mixture that cannot be separated by normal distillation since compositions of the liquid phase and the gas phase are equal.

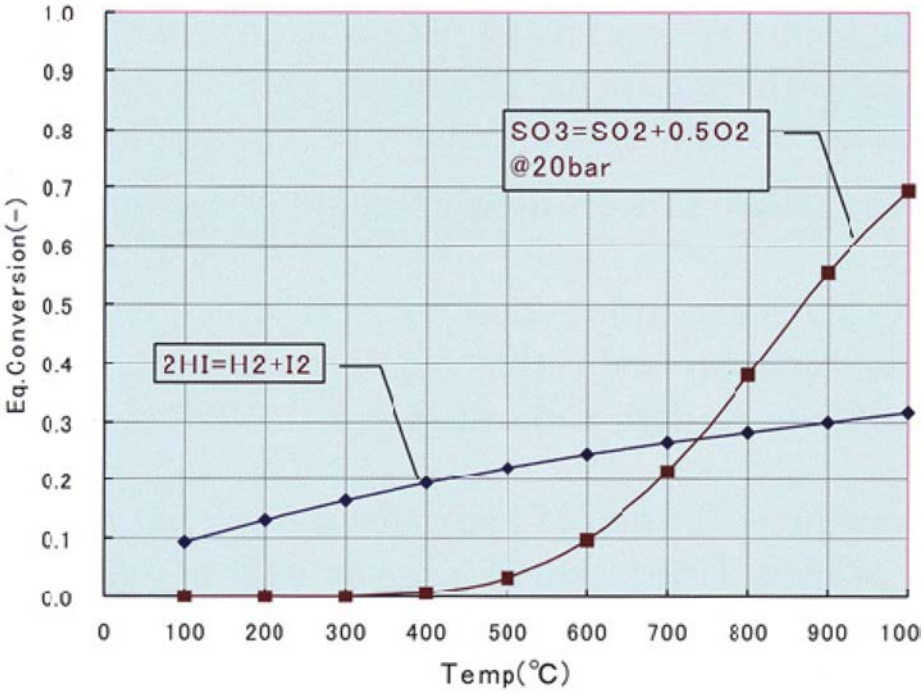

FIG. 43. Sulphur–iodine process equilibrium conversion [4].

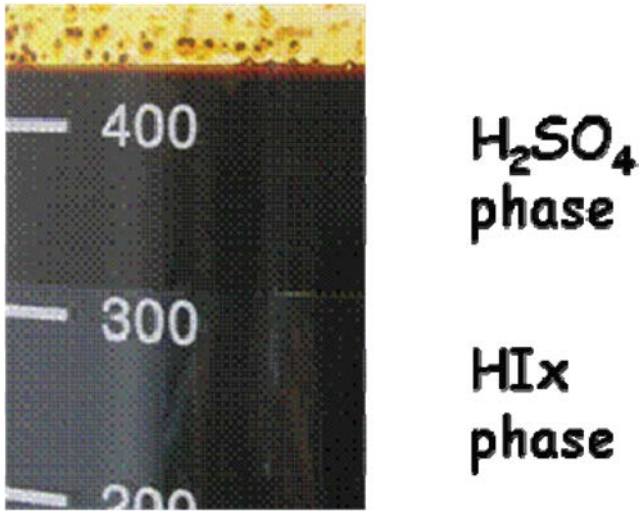

FIG. 44. Two immiscible aqueous acid phases resulting from the Bunsen reaction [154].

efficiency. Efforts are directed at minimizing excess quantities and/or seeking alternative routes to carry out process operations in various sections. It is very important to find the optimal composition ratio of chemicals for the Bunsen reaction. A large excess is typically connected with side reactions which lead here to the formation of S and H_2S according to:

$$H_2SO_4 + 8\ HI \rightarrow 4\ I_2 + 4\ H_2O + H_2S$$

$$H_2SO_4 + 6\ HI \rightarrow 3\ I_2 + 4\ H_2O + S$$

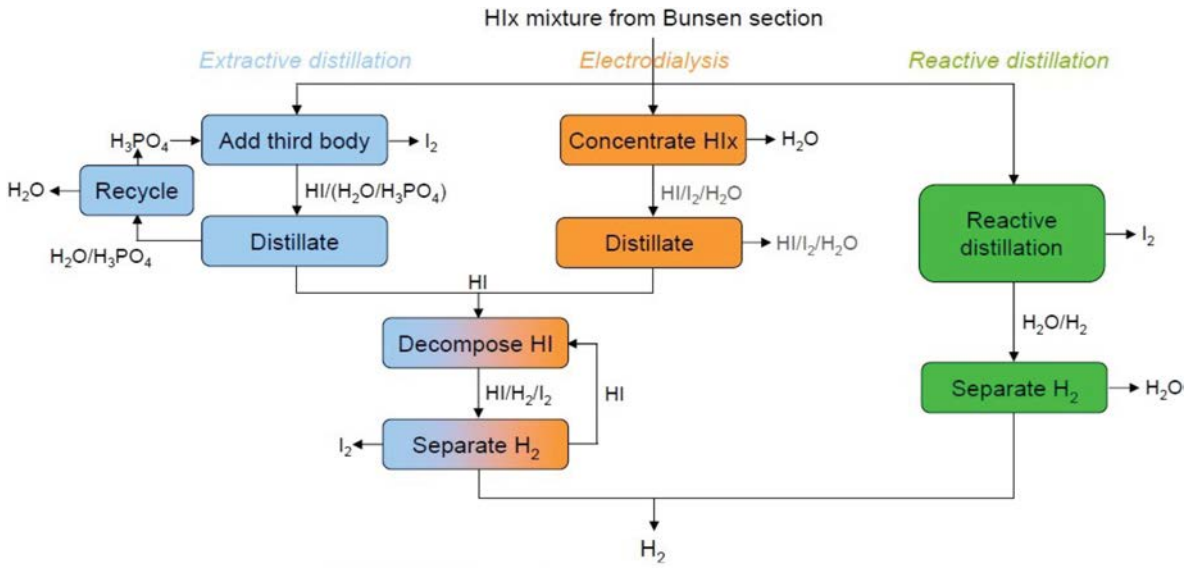

FIG. 45. Options of HI_x decomposition [151].

3.4.2.3. HI decomposition section

The steps of HI concentration, i.e. the separation of HI from water and excess iodine, and of HI decomposition to H_2 and I_2 are key parts in terms of further cycle optimization because the:

(1) Concentration of HI in the HI_x solution is highly energy intensive due to the presence of a homogeneous azeotrope in the binary system HI–H_2O;
(2) Decomposition into H_2 and I_2 is slow and thermodynamically limited (22% equilibrium conversion ratio at 450°C), implying large amounts of products to be recirculated;
(3) Separation of H_2 from still unreacted HI requires a dedicated unit including an I_2 distillation column and HI condenser at low temperature;
(4) Energy exchange is large due to the large heat capacity of the HI_x mixture.

For the difficult process of separation of large amounts of water from HI (to be recycled to the Bunsen section), efficient distillation is not viable due to the azeotropic character of the HI-H_2O mixture. Three methods (Fig. 45) are currently being investigated [156]: extractive distillation, electro–electrodialysis and reactive distillation.

(A) Extractive distillation

In extractive distillation (Fig. 46), pursued in the USA, a third body — phosphoric acid (H_3PO_4) — is added to destroy the azeotrope by separating the iodine before the HI is distilled and decomposed with the hydrogen separated by using membranes [157].

(B) Electro–electrodialysis

In electrodialysis and electro–electrodialysis (EED) (Fig. 47), pursued by Japan, the Republic of Korea and China, water is removed in the HI_x purifier to concentrate the HI_x mixture. Purified HI_x is sent to the EED section, where, in the cathode cell, HI is concentrated by electrochemical reduction of I_2 to I^-, while in the anode cell, HI is diluted by electrochemical oxidation of I^- to I_2. Excess HI can be removed by simple distillation using ion exchange membranes under the driving force of electric potential difference. H^+ is transported from anode to cathode through a Nafion 117 proton permeation-selective membrane [159, 160].

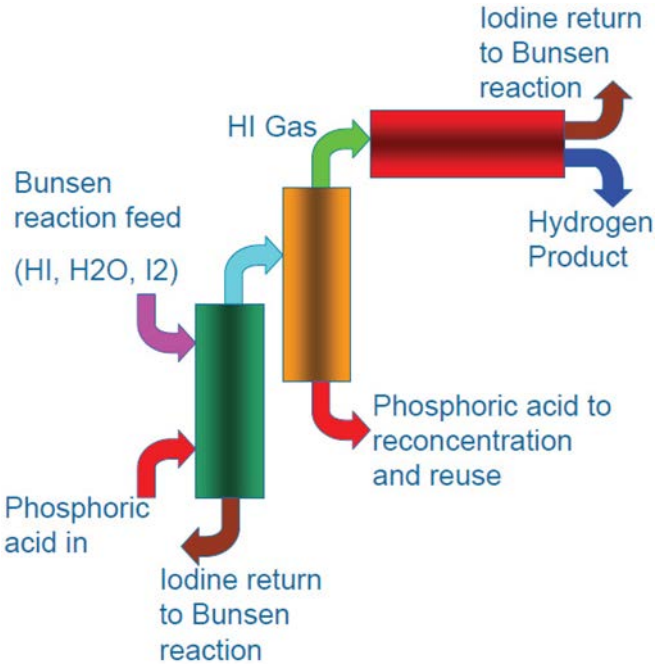

FIG. 46. Principle of extractive distillation [158].

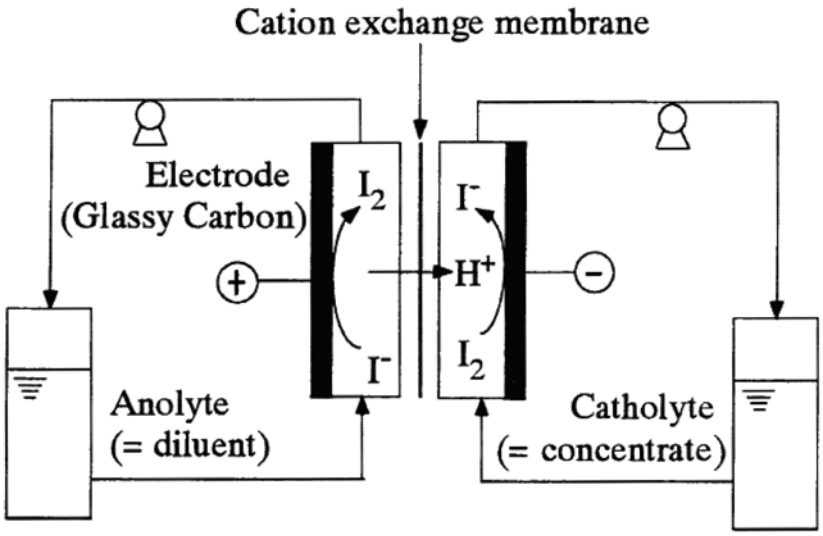

FIG. 47. Principle of electro–electrodialysis [161].

(C) Reactive distillation

Reactive distillation (Fig. 48), pursued by France, is based on the idea of shifting the azeotropic composition at elevated pressures (~2 MPa). The HI_x is distilled in a pressurized distillation column where, after vaporization, the HI_x passes through a catalyst bed with the HI being decomposed to a gas mixture of I_2, H_2, HI and H_2O. HI_x distillation and HI decomposition take place in the same reactor, leading to a liquid–gas column with I_2 dissolved in the lower, liquid phase and H_2 plus water to be gained from the upper, gaseous phase [153]. The pressurized hydrogen gas is removed from the stream by condensation and released, while the unreacted species are sent back to the EED reservoir tank. Iodine at the distillation bottom is recycled to the Bunsen reactor to close the cycle.

HI distillation columns have been proposed so far for operation at ~2.2 or ~5.0 MPa [156]. The HI_x environment is extremely corrosive, and the severity increases with temperature.

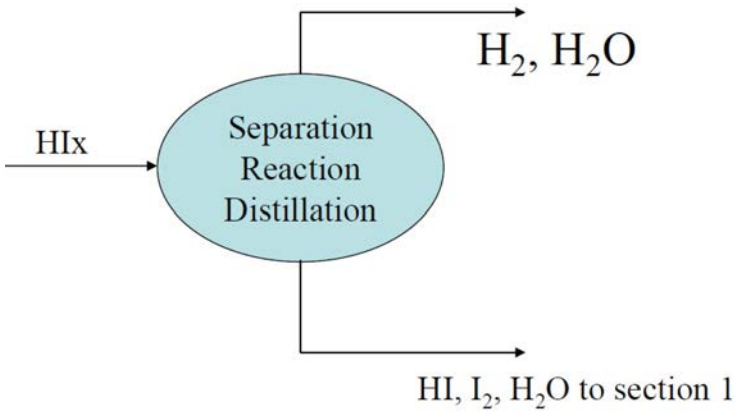

FIG. 48. Principle of reactive distillation [158].

3.4.2.4. H_2SO_4 decomposition section

In the S–I cycle reactions (5)–(7), sulphuric acid is decomposed in two endothermic stages. One of the key components in this section is the decomposer of H_2SO_4, which, at a concentration of greater than 90 wt%, is vaporized and decomposed to SO_3 and H_2O at temperatures between 300°C and 500°C. In the second stage, the SO_3 further decomposes at high temperatures of 800–900°C and in the presence of a catalyst into oxygen and sulphur dioxide. Sulphur dioxide, water and iodine are then recycled in L_1. The H_2SO_4 decomposition reactions proceed smoothly with almost no side reactions.

More complex heat exchanger configurations are needed for the second stage, the SO_3 decomposition, because both primary and secondary streams are gas phases. Sulphur trioxide decomposition was observed to be satisfactory only at temperatures above 800°C. Several designs of ceramic high temperature heat exchangers have been suggested. They include the application of catalyst coatings to the inner walls of the decomposer channels.

The high temperatures and pressures required make the unit operation technologically challenging due to the harsh corrosion characteristic of H_2SO_4 under such conditions. According to the temperatures required in the different components of this section, the helium coolant has to pass in series the SO_3 decomposer, the H_2SO_4 decomposer and the H_2SO_4 vaporizer. Heat exchange between hot fluids from the nuclear reactor and process fluids needs to be carried out effectively. One type of innovative heat exchanger reactors considered is PCHX having catalyst coated small semicircular flow channels. Another one is a self-catalysing heat exchanger reactor made of platinum (1–5 wt%) incorporated Alloy 800H, Inconel 617, etc. These compact designs allow for effectively carrying out multiple operations like heat exchange or chemical reaction. Corrosion-resistant membrane reactor–separator–heat exchanger units are also being developed.

3.4.3. The Westinghouse (hybrid sulphur or HyS) cycle

The hybrid-sulphur (HyS) process [162] originally studied at the Los Alamos Scientific Laboratory and further developed by Westinghouse in 1973–1983, also known as the Ispra Mark 11 cycle, is a variation of the S–I process which consists of only two reaction steps and where sulphur is the only other element involved apart from hydrogen and oxygen:

(1) $(H_2SO_4)_g \rightarrow (SO_2)_g + (H_2O)_l + 0.5\ O_2$ (~850°C)

(2) $(SO_2)_g + (2\ H_2O)_l \rightarrow H_2SO_4 + H_2$ (20–110°C, 0.17 V, 0.2–1 MPa)

Reaction (1) is conducted in two stages: first the decomposition of the sulphuric acid into SO_3 and H_2O at 500–600°C, followed by the SO_3 gas catalytic decomposition, where the SO_3 is then reduced in a high temperature step to SO_2 and O_2. The products are sent through various heat exchangers for heat recovery and cooling to allow phase separation. A series of flash evaporators are used to separate oxygen from the rest of the liquid species,

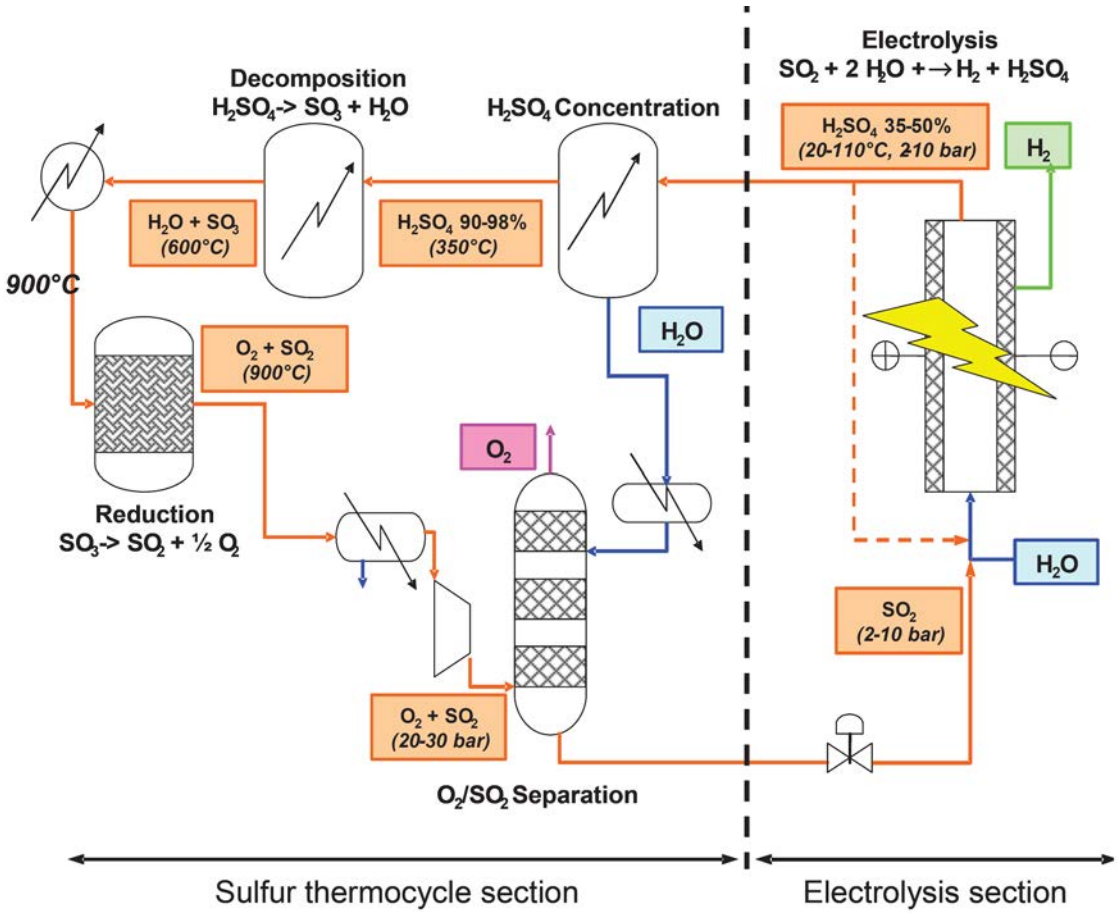

FIG. 49. Schematic of Westinghouse hybrid-sulphur cycle [164].

resulting in almost pure oxygen. The rest of the mixture, consisting of mainly SO_2, sulphuric acid and water, is sent to the electrochemical section. The mixture of SO_2 and water is reacted in an electrolytic cell at lower temperatures to produce H_2 and a sulphuric acid aqueous phase. The electrolytic step offers the advantage of having a theoretical cell potential for SO_2 anode depolarized electrolysis of only 0.17 V per cell. In practice, SO_2 electrolysers may require ~0.29 V, i.e. no more than 25% of the electricity needed in the low temperature water electrolysis [163], however, at the expense of the need to decompose H_2SO_4 at high temperatures in order to recycle the SO_2 for cycle completion. Still, the net thermal energy requirement is significantly less than that for conventional water electrolysis. The Westinghouse process (Fig. 49) is simpler in design, because the use of corrosive halides is not required.

The first reaction equation, sulphuric acid splitting, is common to all cycles of the sulphur family. After the oxygen is removed from the system, the SO_2 and H_2O are combined with make-up H_2O and routed to the electrolyser cell. The SO_2 is then electrochemically oxidized at the anode to form H_2SO_4, protons and electrons, while the protons migrate through the electrolyte and produce H_2 gas at the cathode.

The raw material flow is quite limited when compared with other thermochemical cycles. Optimum efficiency was observed at a 65% concentration of sulphuric acid in water. The main advantages of this cycle are the fact that there are only two reactions, and the ability to have the hydrogen production separated from the nuclear plant. The overall process efficiency, taking into account the thermal energy required both for the electricity production in step 1 and for step 2, is estimated to be around 50% (based on HHV).

A major task is the optimization of the cell design (Fig. 50), materials selections and operating conditions to improve performance and overall durability. The most important issue for increasing the competitiveness of this cycle is the reduction of the cell voltage (currently about 0.6 V against a theoretical demand of 0.17 V) and the cost of the SO_2 electrolyser. The challenge is that SO_2 must react with water to produce hydrogen in the presence of strong sulphuric acid under elevated temperature and pressure.

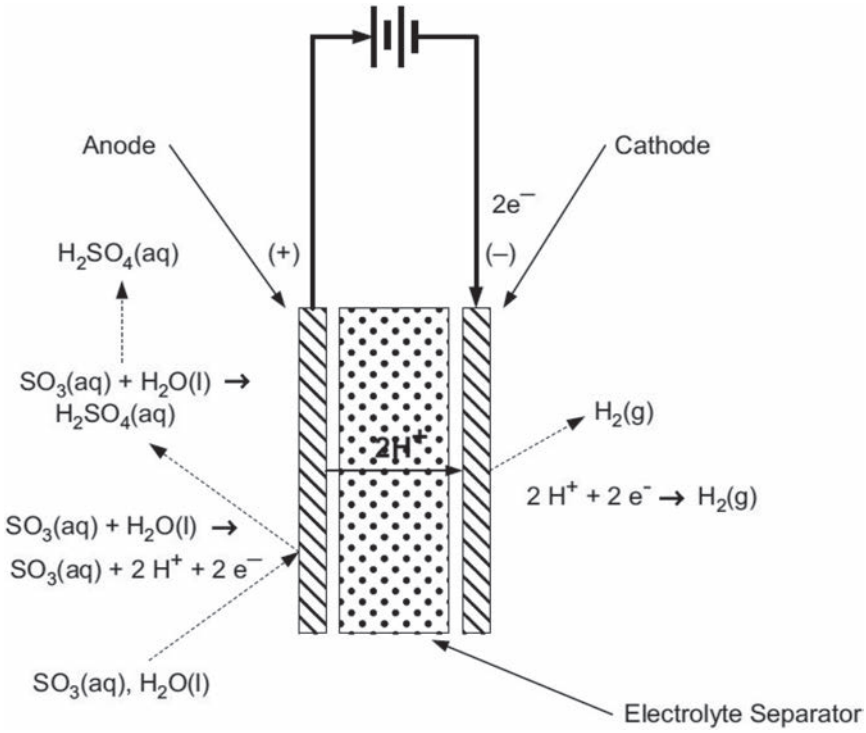

FIG. 50. Schematic of an SO_2-depolarized electrolyzer [165].

Other technical issues to be dealt with are the sulphuric acid decomposition step and the SO_2/O_2 separation system. Various design suggestions for the SO_3 decomposer are currently being investigated, including the bayonet type, plate type, direct contact, compact, and shell-and-tube type heat exchangers (see also Section 4.6). Special caution has to be taken to avoid sulphur deposition on the anode or H_2S formation in the electrolytic step, which requires the use of SO_2 perm-selective membranes.

3.4.4. Sulphur–bromine hybrid cycle

Developed as the Mark 13 cycle at JRC Ispra, this sulphuric acid–bromine hybrid cycle, the third of the sulphur family, uses bromine instead of iodine. The reactions steps are

(1a)	H_2SO_4	→	$H_2O + SO_3$	(700–1000°C)
(1b)	SO_3	→	$SO_2 + 0.5\ O_2$	(700–1000°C)
(2)	$SO_2 + Br_2 + 2\ H_2O$	→	$2\ HBr + H_2SO_4$	(20–100°C)
(3)	$2\ HBr$	→	$H_2 + Br_2$ – electricity	(80–200°C)

with reaction (3) as the electrochemical step. The S–Br hybrid cycle uses only liquid or gaseous species. In the electrochemical step, the voltage required is, at 0.8 V, slightly higher than that for the HyS cycle (0.6 V). The cycle was successfully tested in 1978 at a laboratory scale facility at JRC Ispra, demonstrating a hydrogen production rate of 100 L/h over 150 h with an efficiency of 37% [166]. The system was also operated with a 1 kW solar heat source. The main task currently seen is reducing the energy requirement for the electrochemical step [86].

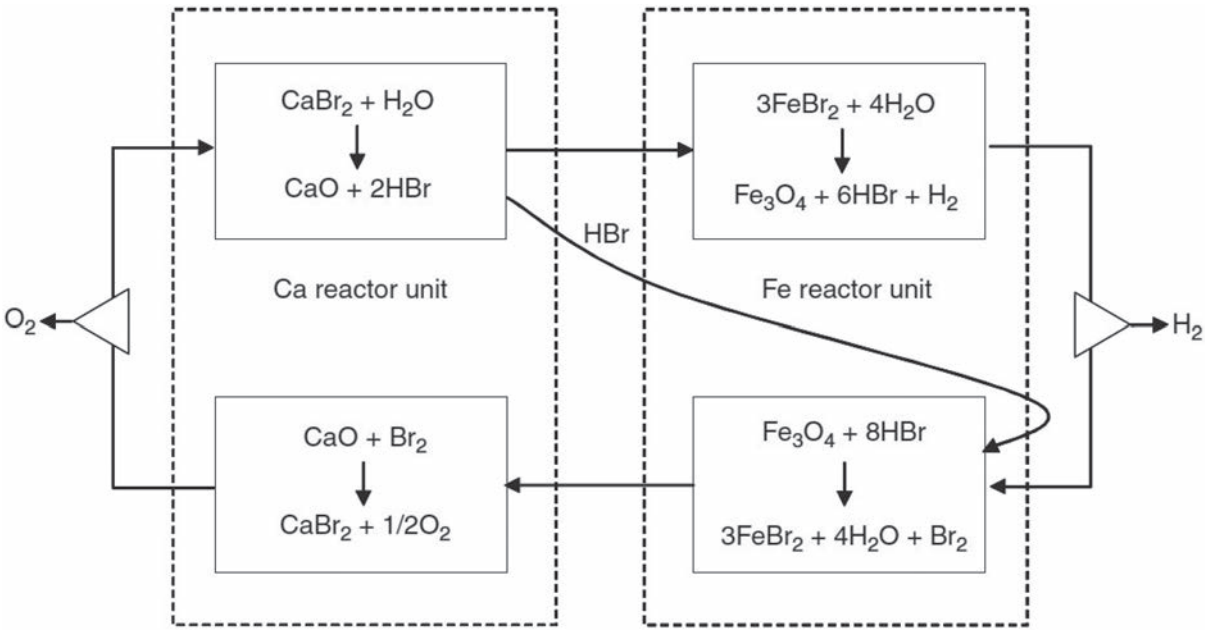

FIG. 51. Schematic of the UT-3 thermochemical process [168].

3.4.5. Calcium–bromine (UT-3) cycle

Another promising thermochemical process is the calcium–iron–bromine or UT-3 cycle which was developed at the University of Tokyo some decades ago [167]. The process consists of four gas–solid reactions which include hydrolysis and bromination of calcium and iron compounds:

(1)	$(CaBr_2)_s + (H_2O)_g$	→	$(CaO)_s + (2\ HBr)_g$	(700–750°C)
(2)	$(CaO)_s + (Br_2)_g$	→	$(CaBr_2)_s + (0.5\ O_2)_g$	(500–600°C)
(3)	$(Fe_3O_4)_s + (8\ HBr)_g$	→	$(3\ FeBr_2)_s + 4\ H_2O + (Br_2)_g$	(200–300°C)
(4)	$(3\ FeBr_2)_s + 4(\ H_2O)_g$	→	$(Fe_3O_4)_s + (6\ HBr)_g + (H_2)_g$	(550–600°C)

The process takes place in four separate reactor furnaces containing the solid reactants $CaBr_2$, CaO, Fe_2O_3 and $FeBr_2$, which are present as spherical pellets. Only the heat-carrying gases are passed through the reactors, which eases material flow control. The solid–gas reactions are connected with volume changes in each cycle step. The maximum heat input required is up to 750°C, lower than that for the sulphur cycles. Hydrogen and oxygen are removed from the recirculating streams via semi-permeable membranes. A major drawback is the still low reaction rate [169]. The reactors are connected in series in a loop as is shown in Fig. 51. Stages (1) and (3) produce reactants for stages (2) and (4). After one cycle, the reactors are switched and the direction of the cycle is reversed.

Reactions (1) and (4) are endothermic and therefore require heat, which must be supplied from an external heat source such as an HTGR. The gaseous products O_2 and H_2 from reactions (2) and (4) are separated by condensation. A condensed mixture of hydrogen bromide and steam can be utilized as gas reactant for reaction (3). The thermodynamics of the above reactions are considered favourable; the overall efficiency, however, is limited to about 40% due to the melting point of $CaBr_2$ at 760°C [170].

The physico-chemical approach forecasts some difficulties because of the sintering of the solid reactants [171]. With regard to the second and the last reaction, thermodynamics require operation at very low pressure and at high temperature, which is in contradiction with the volatility of the bromides. One way could be to operate with over-stoichiometric conditions, which assumes a large amount of gases and will probably lead to too large reactors because of the too low pressure level required by thermodynamics.

The UT-3 cycle was successfully operated for a few hours in the pilot plant MASKOT (Model Apparatus for the Study of Cyclic Operation in Tokyo) [172]. But problems were seen in the cycling behaviour of the solids and in the coupling with a permanent constant heat source because of the variations of the temperature and heat demand of the four reactors. It was found to be difficult to extrapolate to a large scale.

Another major difficulty is given by the toxicity of the reactants (bromide). To overcome this problem, a new flowsheet was developed by the Atomic Energy Commission (CEA) of France (now the French Alternative Energies and Atomic Energy Commission), which employed two asymmetrical torus reactors with fluidized beds of solid reactants in each leg. This has the advantage of avoiding the energy intensive reactant preparation step and also improves the reaction kinetics [173].

At the Argonne National Laboratory, a modified UT-3 cycle, a three step Ca–Br hybrid cycle, is being investigated. In the first step, the $CaBr_2$ is reacted with steam of 1050 K (181.5 kJ/mol heat of reaction) in a solid–gas reaction to split the water. The dry product HBr is then delivered to a plasmatron where in an endothermic reaction the HBr is decomposed by electricity into the products H_2 as a gas and Br_2 as a liquid, which are expected to be easily separable:

$$(2\ HBr)_g \rightarrow (H_2)_g + (Br_2)_g \qquad (\sim 60°C)$$

In the exothermic oxygen production step, the initial $CaBr_2$ is regenerated [174].

One advantage is the fact that more than half of the thermodynamic requirement is supplied as heat rather than electricity. Experiments on the laboratory scale have shown that the direct injection of steam into the molten bath of $CaBr_2$ promptly yields HBr in a stable and continuous operation, which is then electrolytically decomposed to produce H_2. The conversion ratios observed were up to 19 mol% of the calcium bromide [175].

3.4.6. Copper–chlorine cycle

Several alternative thermochemical cycles for hydrogen production were investigated, which operate at moderate temperatures in the range of 500–600ºC. Lower operating temperatures reduce the costs of materials and maintenance, and can effectively use low grade waste heat, thereby improving the cycle and power plant efficiencies. Additional advantages of lower operating temperatures include ease of handling the chemical agents and reactions. The NHI identified a number of chlorine-based thermochemical cycles [19]. The copper–chlorine (Cu–Cl) cycle (the four step cycle shown in Fig. 52) can be operated at a maximum temperature of about 550°C. It requires much lower operating temperatures than other cycles, with the advantages of reduced materials and maintenance costs. Furthermore, this cycle can effectively use low grade waste heat, which improves cycle and power plant efficiencies [19].

The Cu–Cl cycle is a hybrid cycle consisting of several thermal and one electrochemical reaction. The steps involved in the five step cycle are shown below. The five step cycle promises an efficiency as high as 41% and has the advantage of employing less expensive raw materials compared with the S–I cycle. The electric energy demand was assessed to be 39% of the total energy. The viability of all reactions and, in particular, the H_2 and O_2 generation, was demonstrated at ANL on the bench scale level. What still needs to be checked are side reactions and the completeness of the reactions [176].

(1)	$(2\ Cu)_s + (2\ HCl)_g$	→	$(2\ CuCl)_l + (H_2)_g$	(430–475°C) thermal reaction
(2)	$(4\ CuCl)_{aq}$	→	$(2\ CuCl_2)_{aq} + (2\ Cu)_s$	(30–70°C) electrolysis
(3)	$(2\ CuCl_2)_{aq}$	→	$(2\ CuCl_2)_s$	(< 100°C) drying
(4)	$(2\ CuCl_2)_s + (H_2O)_g$	→	$(CuO{\cdot}CuCl_2)_s + (2\ HCl)_g$	(400°C) hydrolysis
(5)	$(CuO{\cdot}CuCl_2)_s$	→	$(2\ CuCl)_l + (0.5\ O_2)_g$	(500°C) thermal decompos.

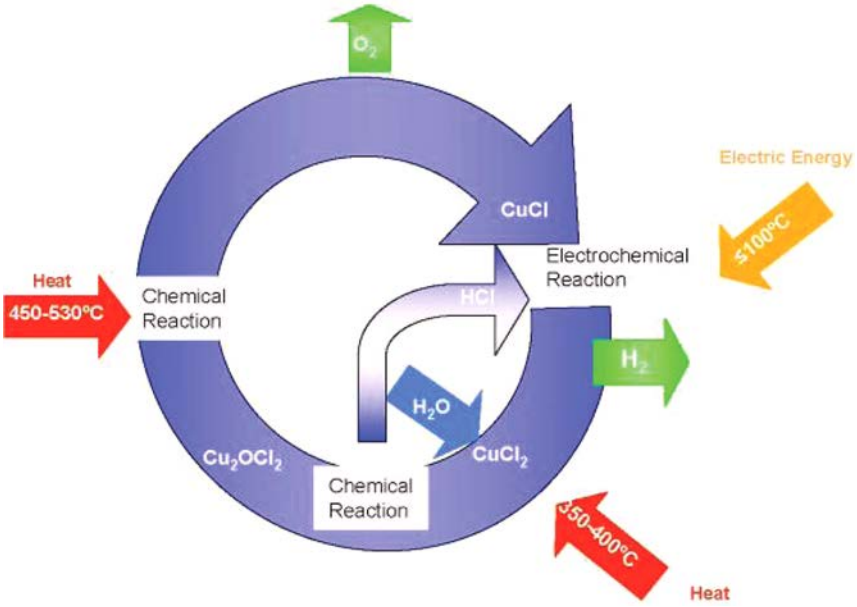

FIG. 52. Schematic of the four step copper–chlorine thermochemical water splitting cycle [177].

Reaction (1) of the cycle is a heterogeneous, exothermic and reversible reaction. HCl heated up to 475°C and solid copper are fed into a reactor. The reaction preferably takes place at temperatures greater than 425°C (i.e. above the melting point of CuCl), in order to avoid formation of solid CuCl, which would passivate the Cu metal surface. Conversion of the solid particles strongly depends on reaction rates and residence times. Particles of 3 μm size were found to result in a complete conversion, whereas larger sizes led to lower hydrogen production. Efforts are currently being made to generate hydrogen in a larger reactor at higher rates up to 3 kg/d [19]. Due to the low activation energy, catalysts might not be required.

In the electrochemical reaction (reaction (2)), aqueous CuCl enters the electrochemical cell and is electrolysed, with $CuCl_2$ formed at the anode and Cu particles at the cathode exiting the cell, possibly by a conveyer. R&D tasks include the identification of appropriate membrane and electrode materials, and of the proper operating conditions to produce small dendritic Cu particles [178].

Drying of the aqueous cupric chloride (equation (3)) is an energy intensive step that requires heat at temperatures less than 100°C. Heat requirements for the Cu–Cl cycle amount to 221 kJ/g of H_2 produced. Studies have shown that a large portion could be delivered by low grade waste heat and other heat recovery. Here, the waste heat from the moderator of a CANDU reactor could be used.

The hydrolysis step (reaction (4)) is an endothermic, non-catalytic, gas–solid reaction taking place in the temperature range 350–400°C. Here, solid $CuCl_2$ particles react with steam to generate copper oxychloride and HCl gas. The ideal operating temperature to give reasonable kinetics was found to be between 300 and 400°C. Also, excess water vapour was found to be advantageous for the hydrolysis reaction, resulting in high yields [178]. At 375°C and atmospheric pressure, the ratio is ~17 which would result in a 60–80% conversion to Cu_2OCl_2. Since high steam to copper ratios have a direct impact on the capital costs due to higher volumetric flows and larger equipment size, the main goal of the test programme at ANL is to further reduce the unwanted CuCl amount left in the solid products [179].

The endothermic oxygen production reaction (5) requires the highest temperatures. It is the thermal decomposition of solid $CuO{\cdot}CuCl_2$ which produces liquid copper monochloride and oxygen gas plus unavoidable traces of species from incomplete conversion or side reactions. This step has been experimentally demonstrated on the bench-top and laboratory scales. Unwanted agglomeration of particles during processing appeared to be a safety concern still to be solved [19].

A conceptional layout of a nuclear assisted Cu–Cl thermochemical cycle is given in Section 4.6.1 (see Fig. 81) [180].

Originally proposed in Ref. [181] as a two-step cycle, different variations of the Cu–Cl cycle have been developed in the meantime. They include the Cu–Cl cycle in four process steps [182] or in five process steps [182,

183], but also as a purely thermal reaction to produce hydrogen with low yield [184]. In the four step cycle, reactions (1) and (2) are combined to form an electrolysis step involving direct electrolysis of CuCl/HCl. Direct hydrogen production from this combined step was demonstrated for the first time by AECL. This demonstration was made possible by the use of the right type of membrane for the electrolysis. A conceptual layout of a Cu–Cl cycle is shown in Fig. 52 [180].

3.4.7. Iron–chlorine cycle

The iron–chlorine or 'Mark 9' cycle is one of the thermochemical cycles that have been extensively studied in the past. It appeared to be an appropriate cycle, since some partial reactions are well known and technically proven. The endothermic reaction (1) is the hydrogen producing step by hydrolysis of $FeCl_2$. Conversion of the solid is almost complete. The choice of the proper material is seen to be a problem, as is the coupling to a process heat source. Also, separation of the solid and gaseous reaction products appears to be difficult considering the melting point for $FeCl_2$ of 950°C and its high vapour pressure at such high temperatures. For easier separation, reaction (1) is done in two steps. The well known reaction (3) represents oxygen production by means of the reverse Deacon reaction. Reaction (2) is the chlorination of magnetite with HCl, also performed in two steps, the same as the dechlorination process of reaction (4). The latter is considered the key reaction of the cycle due to the energy consuming vaporization of the interim product Fe_2Cl_6.

(1a) $3\ FeCl_2 + 3\ H_2O \rightarrow 3\ FeO + 6\ HCl$

(1b) $3\ FeO + H_2O \rightarrow Fe_3O_4 + H_2$

(2a) $Fe_3O_4 + 3\ HCl \rightarrow FeCl_2 + FeOCl + 1/2\ Fe_2O_3 + 3/2\ H_2O$

(2b) $1/2\ Fe_2O_3 + FeOCl + 5\ HCl \rightarrow 2\ FeCl_3 + 5/2\ H_2O$

(3) $Cl_2 + H_2O \rightarrow 2\ HCl_2 + 0.5\ O_2 - \text{heat}$

(4a) $2\ FeCl_3 + CO \rightarrow 2\ FeCl_2 + COCl_2$

(4b) $COCl_2 \rightarrow CO + Cl_2$

The estimated efficiency resulting from mass and energy balances is in the range of 28–35% which is not deemed sufficiently high with regard to cycle economics [185, 186].

An analysis of the iron–chlorine cycle in terms of chemical engineering factors was conducted by detailed flowsheeting of the process, with attention given to the high and low temperature heat balances of the process. Efficiencies of 28–35% were shown to be attainable by the optimization of the HCl boiler system and by the incorporation of two paths for $FeCl_2$ hydrolysis. The irreversibility of the process was calculated to be 315 MW, most of which is produced in the separation steps. It was concluded that although the calculated efficiency is too low to guarantee the economic feasibility of the process, the further development steps needed should be valuable to other cycle studies also [186].

3.4.8. Copper sulphate hybrid cycle

The hybrid copper oxide–copper sulphate thermochemical cycle, originally derived from the Westinghouse HyS cycle, appears to be feasible with currently available technologies. The following reaction steps describe the H-5 version of the copper sulphate hybrid cycle which was simulated using Aspen Plus software [187]:

(1)	$(CuO)_s + (SO_2)_l + (6\ H_2O)_l$	→	$(CuSO_4 \cdot 5\ H_2O)_s + (H_2)_g$	(25°C)
(2)	$(CuSO_4 \cdot 5\ H_2O)_s$	→	$(CuSO_4)_s + (5\ H_2O)_l$	(208°C)
(3)	$(CuSO_4)_s$	→	$(CuO)_s + (SO_3)_g$	(850°C)
(4)	$(SO_3)_g$	→	$(SO_2)_g + (1/2\ O_2)_g$	(850°C)

Reaction (1) is the hydrogen generating step, where at 25°C and 2.17 MPa solid copper oxide and liquid sulphur dioxide is reacted in an electrolyser cell to copper sulphate pentahydrate and hydrogen. Most of the feedwater is the water recycled from reaction (2), while only a small part is fresh water. The pentahydrate is decomposed in reaction (2) at high temperatures to anhydrous copper sulphate and water. This dehydration is actually done in several consecutive steps at progressively higher temperatures (up to 320°C) where the water vapour produced is recycled for heat-up of the feed stream in the preceding steps. After cooling, the water is sent back to step (1). In reaction (3), the heated and pressurized anhydrous copper sulphate is decomposed at 850°C in a fluidized bed reactor. The fluidizing medium is oxygen gas to minimize the formation of Cu_2O. The copper oxide produced is recycled to reaction (1). The gaseous constituents of the product stream, SO_3 and O_2 are separated, which is done efficiently at elevated pressures.

The SO_3 is then heated to 850°C and decomposed in a packed bed reactor to SO_2 and oxygen (reaction (4)). The product stream contains about 20% of O_2, 40% of SO_3, and 40% of still unconverted SO_3. After separation in a distillation column, the SO_2 is recycled to the electrochemical reactor of section (1). Approximately 2% of the SO_2 is lost with the oxygen stream and must be added to the system. Oxygen purification and SO_2 recovery could be conducted more efficiently with an adequate refrigeration process. Estimated cycle efficiencies, assuming recovery and use of all rejected low quality heat, are up to ~52% [187].

3.4.9. Vanadium–chlorine cycle

The vanadium–chlorine cycle first proposed in 1964 by Funk and Reinstrom as a four step cycle, and later improved, is a purely thermochemical process. Its reaction sequence is as follows [188, 189]:

(1)	$(2\ VCl_2)_s + (2n\ H_2O)_l + (2\ HCl)_l$	→	$(2\ VCl_3 \cdot n\ H_2O)_s + H_2$	(120°C)
(2)	$(2\ VCl_3 \cdot n\ H_2O)_s$	→	$(2\ VCl_3)_s + (2n\ H_2O)_g$	(160°C)
(3)	$(4\ VCl_3)_s$	→	$(2\ VCl_2)_s + (2\ VCl_4)_g$	(766°C)
(4)	$(2\ VCl_4)_l$	→	$(2\ VCl_3)_s + (Cl_2)_g$	(200°C)
(5a)	$(1/3\ V_2O_5)_l + Cl_2$	→	$(2/3\ VOCl_3)_g + 1/2\ O_2$	(927°C)
(5b)	$(2/3\ VOCl_3)_g + (H_2O)_g$	→	$(1/3\ V_2O_5)_s + 2\ HCl$	(127°C)

In reactions (1) and (2), n ranges between 2.8 and 6.

Hydrogen generation is initiated, when an acidic V^{2+} solution is mixed with a catalyst like palladized carbon and heated up to reaction temperature. Experiments at the RWTH Aachen University have shown the feasibility of the individual reaction steps on a laboratory scale. Based on these results, the total process has been optimized. Assuming a steam power plant for the production of the electricity required, an overall plant efficiency of 42.5% has been estimated [189].

3.4.10. Very high temperature cycles

There are materials which can act as effective redox pairs in a two step water splitting process. In the first step, a metal oxide is reduced, delivering the oxygen. In the second step, the reduced compound is reacted with water, extracting its oxygen, while the hydrogen is liberated. Two-reaction processes offer the potential for high efficiencies at low cost. Pairs of materials investigated are Fe_3O_4/FeO as the most representative, but also Mn_3O_4/MnO, ZnO/Zn, CoO_3/Co-O, Ce_2O_3/CeO_2. The water splitting is done at temperatures below 650°C, whereas the reduction step requires much higher temperatures around 2000°C, which favours solar systems for primary energy supply. The advantage is the production of pure hydrogen. A major drawback is the decreasing activity over repeated oxidation/reduction cycles. The general reaction scheme is

(1) $$M_xO_y \rightarrow M_xO_{y-\delta} + \delta/2\ O_2$$

(2) $$M_xO_{y-\delta} + \delta\ H_2O \rightarrow M_xO_y + \delta\ H_2$$

Two step metal oxide cycles have been proven experimentally in laboratory scale mock-ups up to 10 kW(th). They are under investigation at the PSI, Switzerland, in connection with solar-concentrated heat input and at INET, China, in connection with nuclear heat input. Main research efforts are concentrated on finding new metal oxides with a comparatively low decomposition temperature. The most promising cycles were found to be the pairs ZnO/Zn and Fe_3O_4/FeO. Investigations by the German DLR were done on the following system to be coupled to a solar receiver:

(1) $$3\ Zn + 2\ Fe_3O_4 + 4\ H_2O \rightarrow 3\ ZnFe_2O_4 + 4\ H_2 \qquad 600°C$$

(2) $$3\ ZnFe_2O_4 \rightarrow 3\ Zn + 2\ Fe_3O_4 + 2\ H_2 \qquad 1500°C$$

INET is examining in detail MFe_2O_4 with M = Cu, Ni, Co, Mg, Zn, Mn having decomposition temperatures in the range of 800–860°C. Hydrogen generation has been demonstrated for Cu, whose cycling capability was also proven [190]. The ZnO/Zn is a promising cycle because of its comparatively low decomposition temperature. Metal–oxide cycles are often considered in connection with solar thermal reactors which can easily achieve temperatures of 1500–2500 K.

The PSI, Switzerland, has realized a 60 kW sunlight concentrating device providing a temperature of 2200°C for the water splitting process based on the metal iron with an expected efficiency of about 20%.

The steam–iron process, although based on coal, is a cycle process where hydrogen is generated from the decomposition of steam by reaction with iron oxide. The cycle is not completely closed since coal is consumed and CO_2 is emitted. The synthesis gas produced in the coal gasification process with steam is reacted to reduce the iron oxide. The input is hematite (Fe_2O_3) which can be easily reduced to magnetite (Fe_3O_4) in the presence of synthesis gas, and further reduced to either wustite (FeO) or metallic iron (Fe) depending on operating temperature. High operating temperatures (750–850°C) favour the reduction to FeO using both H_2 and CO, whereas temperatures below 550°C favour reduction to Fe using only CO. In the subsequent re-oxidation step with water, the original oxides are produced together with a hydrogen-enriched gas. The reaction equations are:

$$Fe_3O_4 + 4\ CO \rightarrow 3\ Fe + 4\ CO_2 \qquad \text{Reduction}$$

$$3\ Fe + 4\ H_2O \rightarrow Fe_3O_4 + 4\ H_2 \qquad \text{Oxidation}$$

Continuous hydrogen production is given if reduction and oxidation take place in separate reactors. This process has the advantage of producing H_2 at a high purity and the fact that renewable sources can easily be employed. A major drawback of this process is its poor efficiency. The steam–iron process was used in the early 1900s for the commercial production of hydrogen at relatively higher temperatures in the range between 750 and 850°C, but was later abandoned due to severe degradation of the iron oxide ores within a few cycles. It has regained interest due to its ability to produce pure hydrogen for fuel cell applications. With the development of a novel,

moderate temperature (400–550°C) steam–iron dual-reactor fluidized bed process, pure hydrogen by-product can be produced from coal gasification derived hot syngas in an IGCC power plant [191].

3.4.11. Heavy element halide thermochemical cycle

Another cycle currently studied at ANL is worth being mentioned because of its very low temperature requirement [106]. The cycle is based on heavy element halide chemistry with a maximum reaction temperature of 300°C, the lowest known temperature for a purely thermochemical hydrogen production cycle. The reaction sequence is composed of the following steps:

(1) $2\ UO_2Br_2{\cdot}3\ H_2O \rightarrow 2\ "(UO_3{\cdot}H_2O)_s" + 4\ (HBr)_g + 2\ (H_2O)_g$

(2) $4\ EuBr_2 + 4\ HBr \rightarrow 4\ EuBr_3 + 2\ (H_2)_g$

(3) $4\ EuBr_3 \rightarrow 4\ EuBr_2 + 2\ (Br_2)_g$

(4) $2\ "(UO_3{\cdot}H_2O)_s" + 2\ Br_2 + 4\ H_2O \rightarrow 2\ (UO_2Br_2{\cdot}3\ H_2O) + (O_2)_g$

No integrated cycle test has been performed so far, and thermodynamic data are largely unknown for this system. For reaction (1), work demonstrated that HBr was produced with the reaction going to completion at 300°C. The notation "$(UO_3{\cdot}H_2O)_s$" means that the exact stoichiometry of the species has not been determined yet. Studies on reaction (2) showed that $EuBr_2$ reacts with aqueous HBr to produce hydrogen. But reaction rates are slow, with typically several hours for completion under the experimental conditions investigated. For reaction (3), vacuum pyrolysis was employed, while for reaction (4), bromine and water were found to react to HOBr. Reactions (1) and (3) are endothermic and require application of heat at a temperature of 300°C to the drive the reaction to the desired products. Reactions (2) and (4) are expected to be exothermic and to proceed spontaneously. Further efforts are needed to enlarge the thermodynamic database for the U–Eu–Br cycle and to improve the efficiency of the system, but also including consideration of the corrosiveness of the chemicals.

3.4.12. General aspects of thermochemical cycles

3.4.12.1. Limits of number of reactions and separation energy cost

An important factor to be considered when evaluating a thermochemical cycle is the number of reactions involved. With decreasing maximum temperature, the number of required reaction steps increases. This leads to a decreasing efficiency and the need for large excess energy for separating the reaction products and of transporting the products/reactants between the reaction stages. The substantial heat usually needed to heat up and vaporize the reactants can only partly be recovered, while much of the available heat is at temperatures too low to be useful. Chemical reactions are often incomplete at low temperatures. Irreversibility and costs of each step are cumulative, quickly lowering the overall efficiency and increasing the final cost of the global process.

A minimal irreversibility (or driving force) is necessary to drive each step, especially at low temperatures, which is ~40 kJ/mol for both electrolysis and chemical reactions. To this irreversibility, minimal enthalpy needs to be added to separate the reactants from the products with a high purity (corresponding to the term of ideal mixing entropy) with a minimal amount of 20 kJ/mol in practice to achieve a purity of at least 10^{-3} molar.

In the case of low temperature exothermic reactions, this additional heat cannot be recovered in other steps of the process and has to be added to the final heat demand. Therefore the economic aspect will be an important issue in cycles with two or more exothermic chemical reactions at low temperatures or cycles with five or more reactions. The same holds for cycles with two or more electrolytic steps due to the cumulative overvoltage and large investment costs required.

The separation work required has a strong influence on the efficiency of the cycle processes. A typical separation problem is the energy needed to separate hydrogen from water vapour, for example, at the exit of a high temperature electrolysis system operating with a voltage near the theoretical reversibility point. The easiest way is

to cool the water–hydrogen mixture to ambient temperature. But doing so, the heat of vaporization of water will usually get lost and cannot be recovered directly to heat the water at the entrance of the electrolyser.

The large recirculation of materials is another major constraint of thermochemical cycles. Typically, for 1 t of hydrogen produced, the material recirculation is between 500 and 10 000 t. Recirculation can be more easily realized in cycles involving only liquids or gases and liquids, whereas transport of solid materials would be too energy consuming. Also, processes with slow kinetic steps may lead to undesired holdup of materials. affecting the plant investment costs.

Following the second law of thermodynamics, to achieve the best efficiency, heat must be provided at the highest temperature compatible with the heat source, as the efficiency of the process is limited by the Carnot law applied to all temperature levels balanced by the heat needed at these levels (and not just to the highest temperature level). Therefore endothermic reactions at low temperature levels should be avoided. The free enthalpy of each reaction must be negative or near zero to avoid apparatus dimensions that are too large (a negative example in this respect is the UT-3 process).

3.4.12.2. Heat recuperation

It is often supposed that the heat requirement for the endothermic chemical reactions is the major heat load in thermochemical cycles. But a large heat demand is always necessary to heat the chemical reactants to the reaction temperature. This amount of heat can be provided by recovering heat as higher temperature materials are cooled. This is a real challenge because of corrosion issues. The stoichiometry of the products has an impact on these energy exchanges. As the free energy change of each reaction is designed not to be too negative to avoid exergy losses that are too large, a very large recirculation rate can be needed, leading to large energy exchanges.

A typical example is the S–I cycle. First the product of the Bunsen reaction as proposed by the US company General Atomics included not only HI but also a large amount of water and iodine (2 HI with 10 H_2O and 9 I_2 in the General Atomics proposal). Furthermore, as the HI decomposition process has a positive free enthalpy, a large recirculation rate is necessary in the HI decomposition section. For example, in Ref. [153], a recirculation rate of 3 is proposed. This is equivalent to around 30 H_2O and 27 I_2 circulating to produce 1 mole of hydrogen. More than 1500 kJ must be exchanged to produce 1 mole of hydrogen (compared to the HHV of only 286 kJ/mol).

In order to keep the contribution of external energy within reasonable limits, it is necessary to recover a part of the heat rejected by exothermic reactions. This energy recuperation will be performed through heat exchangers, whose efficiencies will be dependent on their pinch values (temperature differences between the hot leg and the cold leg of a heat exchanger). The efficiencies are better, but the technical feasibility is much more difficult for low pinch values. For more than 20 years, it has been known that this should be much more of a penalty for HI decomposition than for H_2SO_4 decomposition.

3.4.12.3. Chemical elements and compounds involved in thermochemical cycles

One of the major questions in a thermochemical cycle process is whether the reactions are as expected or whether there are undesired side reactions, which are influenced by both the excess input of chemicals and by the residence time in the reactor. This can theoretically be answered by applying computer models to determine simultaneous equilibria. The fact that in some processes the low-temperature step reduces other elements rather than reducing the hydrogen has led to the proposal of using a hybrid process replacing the low-temperature step with an electrolysis step.

Computer models also allow the determination of the required excess (over-stoichiometric) masses that become necessary due to the formation of stable interim compounds but that, on the other hand, enhance side reactions. Therefore it is necessary to find a compromise between completion of reaction, phase separation, side reaction and energy loss. The weight related throughput of chemicals in use may be several orders of magnitude higher than the water to be split. Losses from the system might become economically unfavourable and also represent an ecological concern.

An often neglected aspect is the abundance of a given element. If relatively low, these rare resources may be depleted rapidly, and the cost of extraction/purification of raw material will increase significantly as supplies dwindle. The minimum maintenance cost is the flow loss running in the oxygen and hydrogen product, typically

around 0.01–0.1% of hydrogen production (lower limit of typical industrial standard in chemical industry). This gives the order of magnitude of resources needed.

Worldwide hydrogen production through thermochemical cycles should be in the order of 10^8 mole/s to have a significant influence on the transportation sector (assuming an optimistic 40% efficiency for fuel cell and transport and storage). The assumption of maintenance losses for the various chemical elements applied of (at least) ~10^3 mol/s would amount to a total annual loss of about 3×10^{10} moles. This has to be compared with the worldwide production of the respective raw material and typical worldwide reserve estimates.

Another issue is the toxicity of the various elements. Examples are the toxic gases SO_2 and SO_3 in the S–I process, and bromine in the UT-3 process. Also ,cycles that contain Hg, Se or Cd may be limited in their industrial application because of the very low allowable releases (e.g. per US EPA regulations).

For uncommon elements like iodine, a deep analysis seems necessary. As mentioned, the S–I process is practicable only when operated at over-stoichiometric mixtures with high excess of iodine (and steam). Depending on market prices, the quantity of iodine needed could represent a valuable asset, which again puts stringent limitations on the iodine loss in the S–I process with respect to the hydrogen production cost, making iodine recovery one of the key issues. The amount of iodine to be handled in a 600 MW(th) plant has been assessed to be 3000 t [151].

Iodine exists in the form of iodide ion and other iodine compounds in seawater (~0.05 ppm with a total estimated at 68.5 billion t), seaweeds, brine and minerals (niter, KNO3), as well as in the air, but its content is normally very low. The areas of the world where iodine can be economically collected are very limited. The worldwide total annual production of iodine is ~18 000 t, 50% of which is produced in Chile, 40% in Japan and 10% in the other areas.

Iodine production from brine is done through a ‘blow-out’ process taking advantage of its characteristic feature to easily evaporate. Iodine contained in brine in the form of iodine compound ions (I^-) is limited (more or less 100 ppm), and the process is suited for the extraction of iodine from such low content solution. Sand and other impurities are first removed from brine by sedimentation, an oxidant is added to it to extricate iodine (I_2) and then air is introduced to ‘blow it out’. After that, iodine is extracted, crystallized and purified.

As the iodine concentration in various types of seaweed is high (500–8000 ppm), they were used as the raw material for iodine production. Today, however, production is conducted only in areas where the iodine concentration is high in brines from oil fields and natural gas fields, and in caliche from the niter field in the Chilean nitrate industry (~1000 ppm with a total estimated 9 million t). Iodine production in Japan covers as much as approximately 30% of the total iodine production in the world. In Japan, the deposit of water-soluble natural gas/brine which stretches under Chiba prefecture is a water layer containing lots of salt and existing along with natural gas with a concentration of iodine of more or less 100 ppm. Total annual world production of iodine (as of 2006) is ~25 000 t with the big producer countries being Chile (15 500 t), Japan (8000 t) and China (360 t).

3.5. OTHER HYDROGEN PRODUCTION OPTIONS

3.5.1. Thermal cracking, plasma decomposition

Since methane belongs to the most stable organic compounds, high temperatures are required for its thermal decomposition. The search for optimal catalysts to reduce the maximum temperature has led to Ni or Fe based catalysts to decompose CH_4 in the range of 500–700°C (Ni) or somewhat higher (Fe). Activated carbon is seen as an interesting alternative for the 900–1000°C range, since it has a relatively high catalytic activity, low cost and would make an external catalyst unnecessary [192]. Process heat can be obtained either from an outside source like direct solar heating or from burning a part of the hydrogen produced.

In the plasma-arc process, methane splitting takes place at temperatures in the order of 2500°C yielding solid carbon separated from the gas stream. The efficiency was reported to be about 45% and is expected to further improve. In the so-called Kvaerner carbon black and hydrogen process, an electrically powered plasma torch is being generated in a reactor to provide the energy for the decomposition of methane into the commodity carbon black with the by-product hydrogen. Hydrogen purity is 98% prior to the cleaning step if natural gas feed is used. In principle, all kinds of gaseous and liquid hydrocarbons including heavy oils can be decomposed to hydrogen and

carbon black with almost no emissions. The main disadvantage of this process currently is its need for large amounts of expensive electricity.

Hydrogen production by catalytic methane decomposition was demonstrated in the 1960s in a pilot plant with a capacity of 7 Nm^3/h. The carbon was burned to provide process heat at 815–1093°C (emitting large amounts of CO_2). SINTEF in Norway is using a 150 kW laboratory plasma torch with coaxial graphite electrodes, but without CO_2 or NO_x emissions. In cooperation with Kvaerner, a 3 MW industrial scale plant was constructed in Canada and has been working since 1992. An input of 1000 Nm^3/h of natural gas plus 2100 kW of electric energy results in the production of 2000 Nm^3/h of hydrogen plus 500 kg of pure carbon and hot steam as a side product [193]. In 1999, the Kvaerner group started the commercial operation of its first carbon black plant in Canada, which runs on oil or natural gas and is designed for an initial annual capacity (in two units) of 20 000 t of carbon black plus 50 million Nm^3 of H_2. The hydrogen is considered here a by-product and is recirculated to the plasma burner and used as a process gas. The energy demand for the plant is said to be 1.25 $kW \cdot h/m^3$ of H_2 [194]. The conversion rate of the hydrocarbon feedstock is almost 100%. But also solar furnaces are under development using sunlight to provide the dissociation temperatures. Research efforts are concentrating on optimized concepts for gas injection, heat transfer and protection against undesired carbon deposition [195]. Ammonia is a hydrogen carrier whose cracking is an endothermic reaction with high reaction rates at above 700°C.

$$2\ NH_3 \quad \leftrightarrow \quad N_2 + 3\ H_2$$

The main impurities are NO_x and unreformed ammonia. Since PEM fuel cells need highly pure hydrogen, the recommended reaction temperature is 900°C. The reactor is of a simple design, since no H_2O co-feed or shift stage is required. The overall efficiency of an ammonia cracking fuel processor has been reported to be about 60%, with the remainder to supply the process heat and compensate for heat losses. For the production of pure H_2, efforts need to be made to separate N_2 from H_2 (which is not a problem in a fuel cell).

Splitting of sulphur hydride is developed as a by-product in different chemical processes. The endothermic reaction requires temperatures of 500–800°C.

3.5.2. Photochemical and photobiological water splitting

There are various other processes of hydrogen production currently under research and development which, however, are still on the laboratory scale. Among them are photochemical and photoelectrochemical water splitting processes. They require appropriate light absorbing materials where a species is raised into the excited state by means of radiation energy. Efficiencies achieved are still very low.

In photobiological processes, insolation is used to make algae (‘hydrogenase’) or bacteria (‘nitrogenase’) release hydrogen. Protons are reduced through electron transfer with the help of enzymes. The process is highly sensitive to the oxygen formed, which does not allow the use of higher radiation densities. The theoretical upper efficiency limit is 40.7%.

3.5.3. Hydrogen from industrial off-gases

Most off-gases in the chemical and petrochemical industries contain a large fraction of hydrogen that is usually flared or vented into the atmosphere, because its utilization is either not economical or the infrastructure for its utilization does not exist. Sources of off-gas are, for example, the processes of naphtha reforming, hydro-processing, catalytic cracking and the synthesis of methanol and ethanol. With the increased utilization of hydrogen and increasing energy prices, it has become more common to capture the hydrogen in the off-gas and sell it or use it in boilers or turbines. Recovery methods for this hydrogen are PSA, cryogenics and membrane technologies.

Industrial off-gases still represent a large potential as a hydrogen source to meet the local demand at an early stage of a hydrogen economy. For Europe, the project Roads2HyCom identified 500 industrial hydrogen production sites with an estimated surplus capacity of 2–10 billion Nm^3/a, but only a small fraction would be commercially available [136]. This hydrogen potential has been quantified for a couple of European countries to be in the order of 850 million Nm^3/a in Germany, 650 million Nm^3/a in Norway and 300 million Nm^3/a in France [11].

3.5.4. Gas emissions from geothermal fields

Geothermal fields emit gas mixtures with a high content of hydrogen in technically recoverable concentrations and quantities. The utilization of this hydrogen requires cleaning. The gas vented from the Bjarnarflag field in Iceland, for example, is composed of 40% H_2, 32% H_2S, 27% CO_2 and 1% other. It may be able to provide around 50 t/a of hydrogen. The maximum available geothermal temperature is around 350°C [196].

3.5.5. Radiolysis

Purely nuclear based production of hydrogen was observed in the 1940s in experimental nuclear reactors based on the aqueous homogeneous reactor (AHR) concept (see also Section 5.1.2.3), where the nuclear fuel is dissolved in the water coolant and circulates between reactor core and heat sink. These reactors were originally given the name 'water boiler' due to the observed bubbling of the liquid fuel. The bubbles are hydrogen and oxygen gas formed by radiolytic dissociation of the water from the ionizing radiation of energetic neutrons and fission fragments. Radiolysis is actually considered a serious problem for water reactors, since it can lead — and has led —to explosions in the reactor system.

The radiolytic yield of hydrogen was estimated to be ≤1.6 molecules of H_2 per 100 eV of absorbed energy from the fragments of ^{235}U fissioning, translating into 28.8 kg of hydrogen by-product per day per MW(th). Due to the low energy efficiency of hydrogen production, this method was not considered promising as a commercial dedicated hydrogen production method. Therefore, a proposal was made to take advantage of the radiolysis phenomenon by employing blankets around the core enriched with elements (^{10}B, ^{6}Li) that produce alpha radiation. The hydrogen would then be extracted, before it could recombine, by a mechanical gas separator system based on centrifugal forces. About 50% of the energy of fission fragments was found to be consumed in chemical transformations inside a crystal structure. This represents the upper limit for the efficiency of H_2 or CO generation if powders of substances containing H_2O or CO_2 are irradiated with fission fragments [197].

4. NUCLEAR HYDROGEN PRODUCTION METHODS

4.1. NUCLEAR ASSISTED STEAM REFORMING OF NATURAL GAS

With respect to the present dominance of steam reforming of natural gas in today's refineries, the production of process heat by an HTGR to the refining process may be an ideal starting point for nuclear power to penetrate this market in the near and medium terms, and a reasonable transition step toward fossil free hydrogen production in the long term.

4.1.1. Concept and feasibility of a nuclear steam reformer

In comparison with a conventional steam reformer, the employment of a nuclear steam reformer requires certain changes, since operational conditions of a nuclear reactor are not as flexible as those of a fossil fuelled furnace. Also, safety requirements are much more stringent than for a fossil fuelled system. It is therefore desirable to achieve the highest effectiveness in utilizing the nuclear process heat in the whole production process system. A high hydrogen production rate is achieved if the process feedgas rate and the conversion rate are high. The feedgas rate depends on the amount of heat input into the process gas and the temperature of the process gas. The conversion rate depends on the temperature and pressure of the process gas.

A principle flowsheet of an HTGR with steam reformer where all the heat for the reforming process, the steam production, gas purification and gas compression can be gained from the helium circuit is shown in Fig. 53 [198]. The stages of gas purification include the shift conversion, CO_2 scrubber, H_2 separation and a methanation reaction to remove traces of carbon oxides from the process gas.

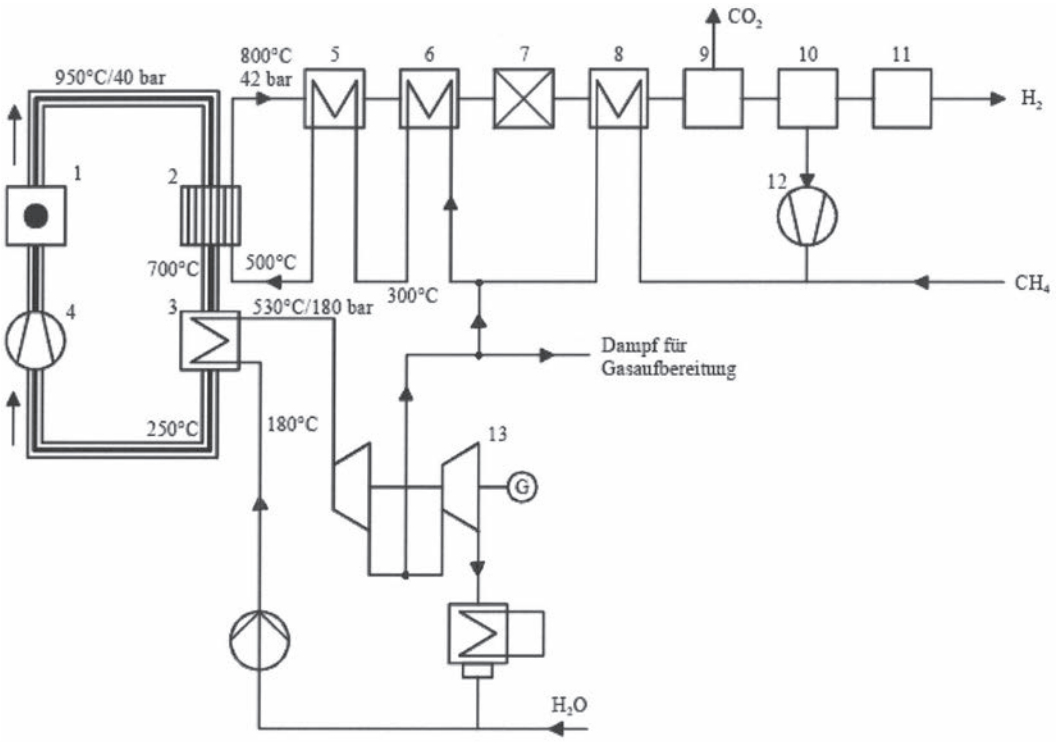

1: HTGR, 2: steam reformer, 3: steam generator, 4: He blower, 5: preheater gas, 6: preheater gas, 7: shift conversion, 8: CH_4 preheater, 9: CO_2 washer, 10: H_2/CH_4 separation, 11: methanation, 12: CH_4 compressor, 13: steam turbine plant

FIG. 53. Principal flowsheet of HTGR with steam reformer [198].

A schematic of a nuclear heated splitting tube and temperature profiles along the tube length are shown in Fig. 54. Unlike in conventional steam reforming, the splitting tube is heated from outside (allothermal) by hot helium, with an inlet temperature of ~950°C at the bottom. The process feedgas (methane) enters the splitting tube from the top at a temperature of typically ~450°C, passes through the catalyst bed, takes up heat to a final value of ~830°C, and is converted to a mixture of H_2, CO and CO_2. A special feature is the recirculation tube, which is a thin tube located inside the splitting tube to guide the process gas back to the top. By this means, not only does the countercurrent flow allow cooling of the process gas and heating of the feedgas, it also leaves the splitting tube in the area with highest thermal impact completely closed without connecting pipes and ensures free thermal expansion movement in the axial direction.

The steam reformer uses the temperature of the helium between 950 and 700°C, while the steam generator is using the part of heat between 700 and 250°C. The feedgas mixture with an H_2O:CH_4 ratio of ~3 and a pressure of ~4.0 MPa is preheated up to around 500°C and reformed at a maximum process temperature of 800°C. A fraction of 85% of the methane is then converted in this first step. Utilization of the heat of the reformer gas for preheating the feedgas, shift conversion and methanation are the steps following the reformer to finally obtain the product hydrogen. A steam turbine plant using CO generation supplies the needed steam and electrical energy for the whole process. The overall energy balance delivers roughly the following numbers:

$$1\ Nm^3\ CH_4 + 6.8\ kW(th)\ (\text{nuclear heat}) \rightarrow 4\ Nm^3\ CH_2$$

$$170\ MW(th) + 2.5 \times 10^4\ Nm^3\ CH_4/h \rightarrow 10^5\ Nm^3\ H_2/h$$

Methane as a raw material is completely converted to hydrogen; the total efficiency including the nuclear heat is around 65%. A complete life cycle analysis has even revealed that, depending on operating conditions, about 40% savings of natural gas feedstock can be achieved if nuclear is selected as the primary energy source [200].

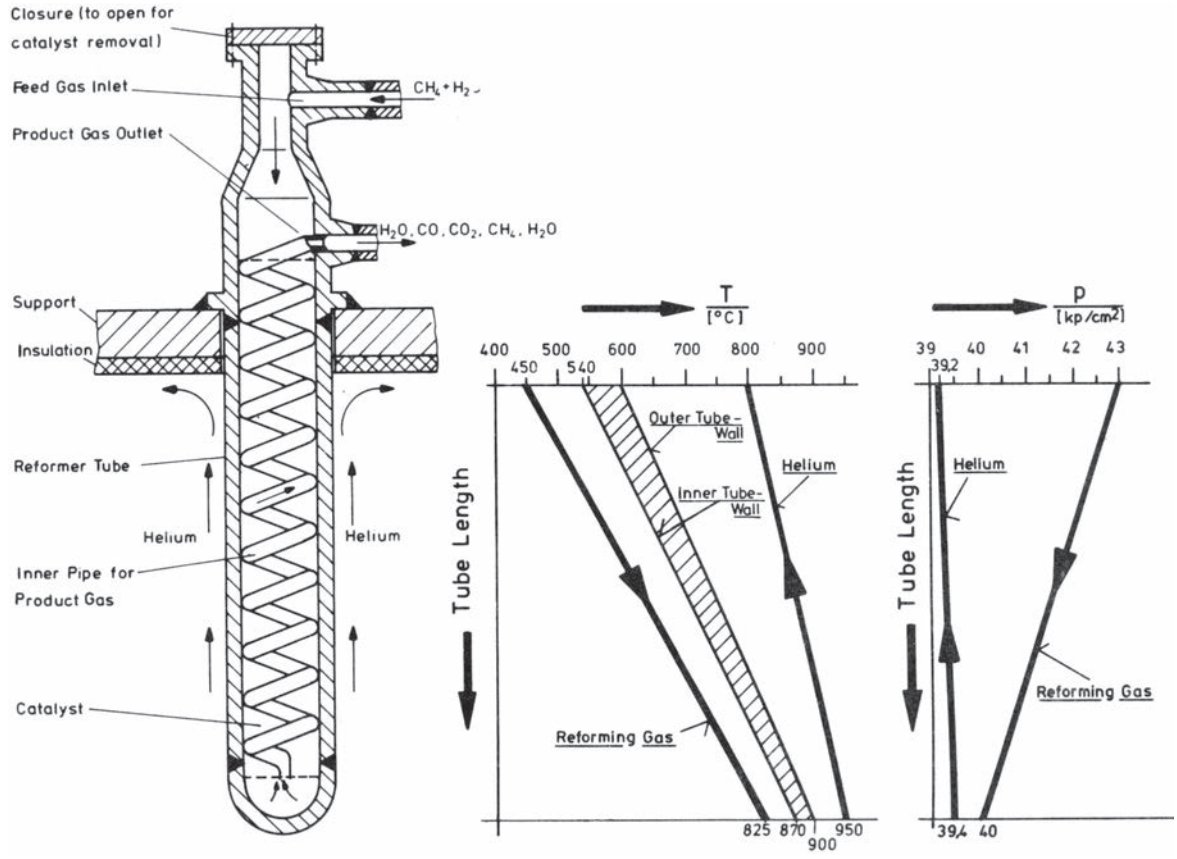

FIG. 54. Schematic of a nuclear-heated splitting tube and temperature profiles along the tube [199].

4.1.2. Germany's approach: Helium heated steam reforming

Nuclear steam reforming of methane was the subject of extensive R&D activities in Germany in the 1970–1980s. In the German Prototype Nuclear Process Heat (PNP) project, the steam reformer was an essential component of nuclear assisted hydrogasification of coal. In this concept, the nuclear steam reformer was included directly within the HTGR primary circuit. The employment of an intermediate heat exchanger (IHX) was, in those days, deemed unnecessary. Such an arrangement poses much more stringent requirements to this component and its reliability than is in the case of an indirect cycle via an intermediate heat exchanger as was pursued in the Japanese HTTR project. The direct coupling to the steam reformer, resulting in a simplified design of a process heat HTGR, may, from today's safety perspective, be regarded as a long term option.

Within the German Nuclear Long Distance Energy Transportation (Nukleare Fernenergie, NFE) project, test facilities at the megawatt scale were constructed and successfully operated at the Research Centre Jülich (FZJ), with the general aim being to demonstrate the operation of a helium heated system for steam reforming under HTGR typical conditions and to study the technical performance of the thermochemical pipeline system and its efficiency. With regard to the operational conditions, the ranges of interest were temperatures of 400–900°C, pressures of 2–4 MPa, and H:C:O ratios of 8:1:2–12:1:4 [201].

4.1.2.1. Tubular type nuclear steam reformer

(A) EVA-I reformer single tube test

The first test facility to demonstrate steam reforming of natural gas under simulated nuclear conditions was EVA-I (the German acronym for single splitting tube), which started operation in 1972 (Fig. 55) [201]. Helium was heated up to 950°C by a 1 MW electric heater and introduced at 4 MPa into the annular gap around the splitting

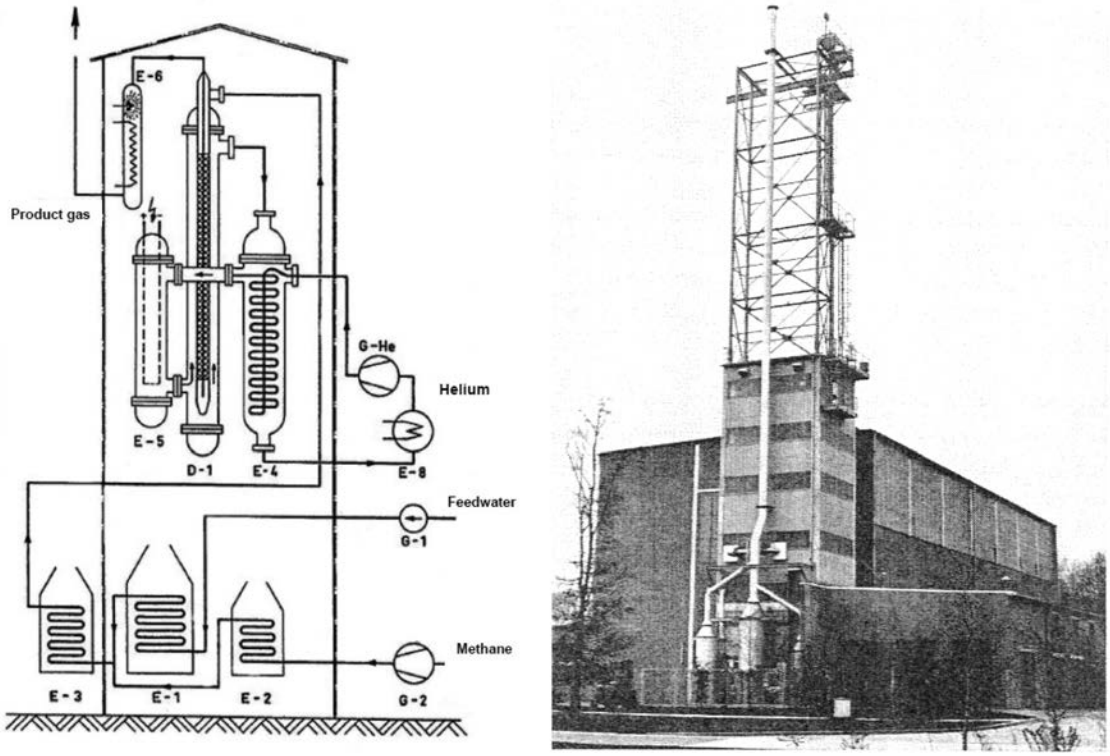

G-He: helium blower, G-1: feedwater pump, G-2: methane compressor, D-1: steam reformer,
E-1: steam generator, E-2: methane heater, E-3: steam-methane superheater,
E-4: helium heat exchanger, E-5: helium heater, E-6: product gas cooler, E-8: heat exchanger

FIG. 55. Single splitting tube test facility EVA-I at the Research Center Jülich [199].

tube. Splitting tubes of various geometries (tube diameter: 80–160 mm; heated tube length: 10–15 m) and tube materials were subjected to operational conditions covering broad ranges, as indicated in Table 8. The heat transferring inner surface of the splitting tube was between 3 and 8 m^2. Initial tests without an inner return pipe for the product gas clearly proved the advantage of the concept of internal recirculation, which has been applied since. Differently shaped inner recirculation tubes were investigated (straight, helical), as was the arrangement of more than one per splitting tube, which, however, was at the expense of ease of catalyst replacement. As a catalyst, various types of Ni Raschig rings, discs and other novel systems were examined, especially with regard to easy and rapid exchange.

The test with a double-walled splitting tube revealed the expected result of practically no transfer of hydrogen to the helium system and allowed a direct quantification of H_2 permeation rates through the Incoloy 800 tube wall to be initially 0.26×10^{-3}, later reduced to 0.013×10^{-3} $Nm^3/(m^2 \cdot h)$ at 830°C and 1.3 MPa of H_2 partial pressure on the process side.

(B) EVA-II reformer tube test bundle

The follow-on test facility, EVA-II, represented a complete helium circuit containing a bundle of reformer tubes [202]. The nuclear heat source was simulated by an electrical heater with a power of 10 MW to heat up helium gas to a temperature of 950°C at 4.0 MPa. As can be seen from the schematic in Fig. 56, the principal components of heater, reformer bundle and steam generator were housed in separate steel pressure vessels in a side-by-side arrangement. The vessels of the helium heater and steam reformer were connected by a co-axial helium duct of 5 m length.

Two reformer bundles, both with convective helium heating, were investigated in the EVA-II facility. They differed in their way of channelling the helium flow. The first bundle tested was a baffle design tube bundle for a

TABLE 8. COMPARISON OF DATA OF STEAM REFORMER IN EVA TEST FACILITIES AND IN A COMMERCIAL NUCLEAR APPLICATION [201, 202]

Parameter	Test facilities			Nuclear steam reformer for 170 MW(th) HTR-Modul
	EVA-I	EVA-II		
		Annulus design	Baffle design	
Nuclear heat input (MW(th))	~0.3	5	~6	60.2
Catalyst tube				
Outer tube diameter (mm)	80–160	120	130	120
Wall thickness (mm)	10–21	10	15	10
Length (m)	10.0–15.7	13	11.5	14
Number of tubes	1	18	30	199
Tube material	Incoloy 800H and others	Incoloy 800H and others	Incoloy 800H	Inconel 617
Primary helium				
Inlet temperature (°C)	800–950	950	950	950
Outlet temperature (°C)	~600–750	700	650	720
Inlet pressure (MPa)	4	4	4	4.987
Flow rate (kg/s)	0.15–0.45	~3.8	~3.8	50.3
Process feedgas				
Temperature inlet recuperator (°C)	460–600	330	330	347
Temperature outlet catalyst (°C)	700–850	810	800	810
Pressure inlet recuperator (MPa)	2–4	4.0	4.0	5.6
Raw gas flow rate (kg/s)	~0.01–0.04	0.62	0.62	34.8
Steam–methane ratio	2–4	4	4	4
Product gas				
Temperature inlet inner tube (°C)	~830	810	800	810
Temperature outlet recuperator (°C)	~520	457	450	480

power of 6 MW consisting of 30 tubes. The bundle was characterized by baffle structures (discs and doughnuts) on the helium side, as shown in Fig. 57, and each splitting tube was connected at the top with a separate feed and product gas line. Inside the splitting tube, the heat between 950 and 650°C was used to run the steam reforming process. The internal helical tube for recirculation of the product gas had an outer diameter of 20 mm and a wall thickness of 2.1 mm, the helix itself had a diameter of 70 mm.

The second steam reformer bundle tested was of annulus design for a power of 5 MW. It consisted of 18 tubes, with each splitting tube placed inside a guiding tube channel where the hot helium was flowing upwards through the annular gap. For both designs, tubes were hanging on a supporting plate, which allowed easy exchange of single tubes. The specific data of both tubes and catalytic systems were very similar compared with components planned for nuclear applications, as can be seen from Table 8. Also the loads imposed on the supporting structures were characteristic of the nuclear case.

In the connected steam generator, an upward boiler with forced convection and direct superheating, and composed of helical tubes for a total power of 4 MW, the remaining helium heat was used up to 350°C. Via a helium circulator, the cold helium was routed back to the electrical heater. The circuit was operated under nuclear conditions at a lower power level, but with a full scale steam reformer component. Also, the process gas handling system was the same as it would have been in a commercial scale nuclear plant.

The catalytic steam reforming reaction allows reaction rates of 10^3 Nm^3 $CH_4/(m^3_{catalyst}\cdot h)$ (related to the catalyst volume in the reformer tubes) at 800°C, 4 MPa and $H_2O/CH_4 = 4$. The overall heat transport coefficient in connection with the chosen temperature distribution on the helium side and on the process side allows an average heat flux of 60 kW/m^2 for the reformer tubes. The heat transfer coefficient on the process side was observed to be rather high. More than 1000 $W/(m^2\cdot K)$ was realized. The heat transfer coefficient on the helium side was around 500 $W/(m^2\cdot K)$, which is also relatively high. It is, however, limited by the allowable pressure drop of around 40 kPa.

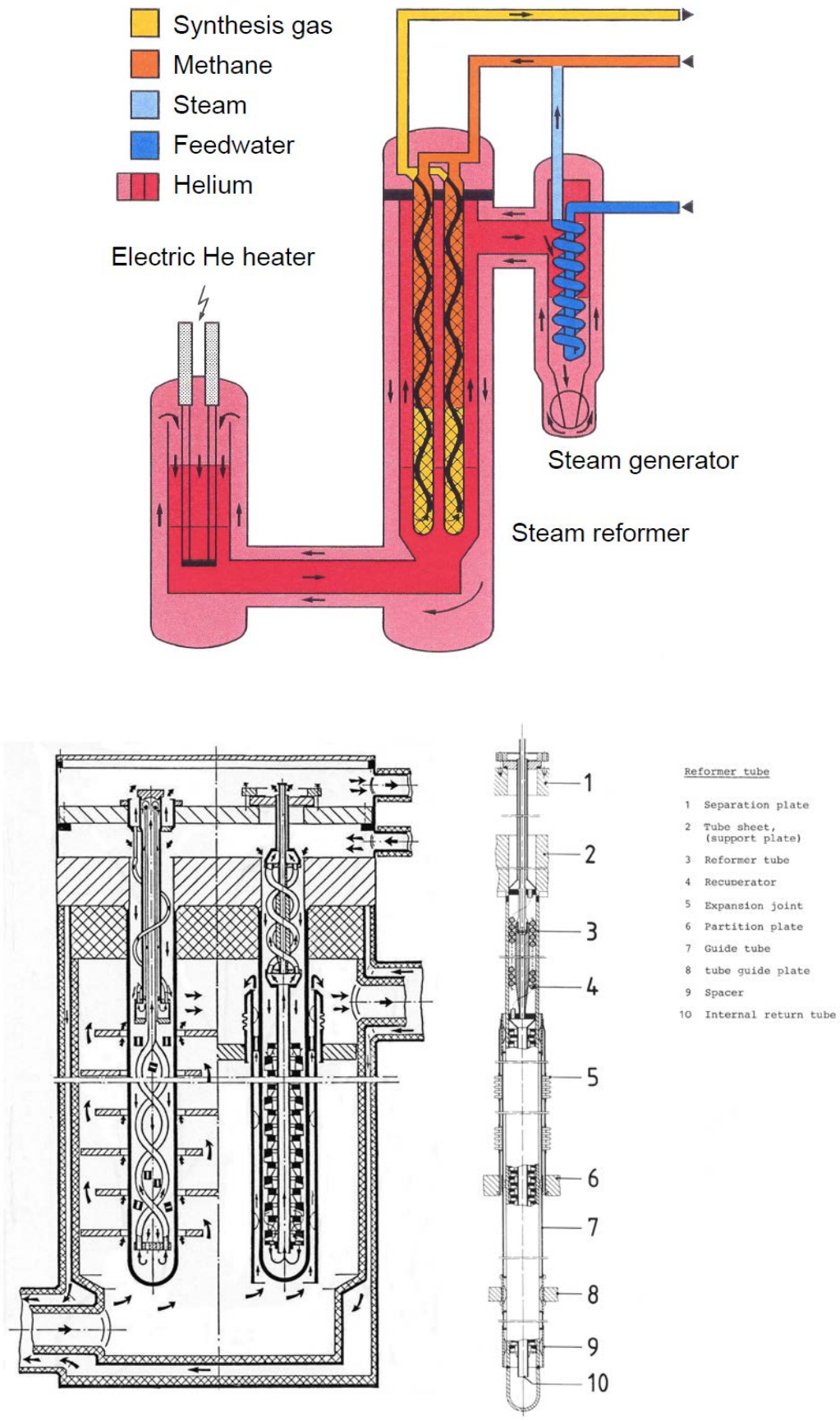

FIG. 56. Flowsheet of steam reforming test facility EVA-II [203].

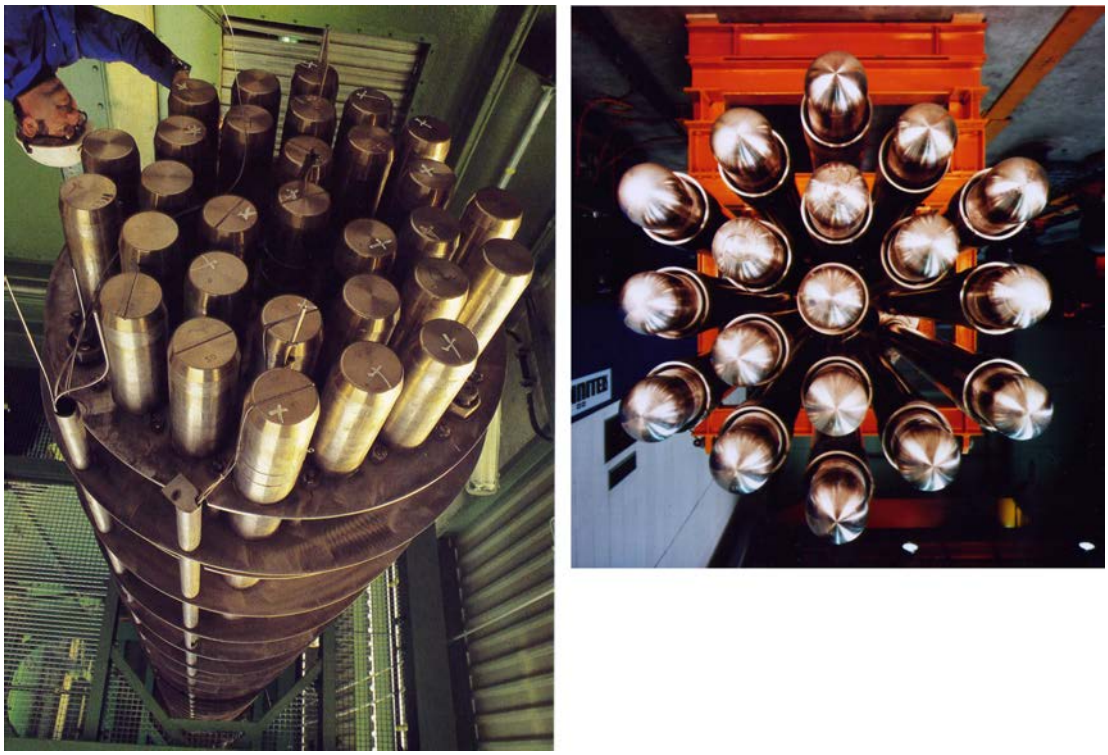

FIG. 57. EVA-II steam reformer bundle, baffle design (left); annulus design (right) [203].

During operation of the steam reforming system EVA-II, no damage was observed on reformer tubes or guiding tubes, internal recuperators or inner return pipes. The components behaved very well in terms of thermal expansion, bending of tubes, friction, fretting and vibrations caused by flow effects. The gas ducting structures, insulation and supporting structures were also operated without difficulties. Measurement and control of process parameters during operation was easy.

The efficiency of the catalyst practically did not change during some 1000 h of operation. There was no carbon deposition on the catalyst because of the chosen H_2O:CH_4 ratio of 4 in the process. The handling of different catalysts was tested with procedures which can be applied to a larger component.

Components were also tested at transient conditions, with changing rates for the temperature on the helium side of more than 10°C/min and for the pressure of more than 4 MPa/min. The rates of changes of parameters on the process side were even larger. No difficulties were encountered. The switching off of single splitting tubes within the bundle was observed to result in enhanced heat transfer for the process gas, which, however, did not compensate for the reduced heat area. The consequence was a slight reduction in the splitting temperature connected with an increased portion of unreformed methane in the product gas.

Instability in the operational behaviour was observed in the case of low helium flow rates, where an inhomogeneous temperature distribution developed, with differences of up to 150 K, causing a buckling of the vessel wall of several centimetres. Another observation was back-circulation of the helium flow in the entrance area, which resulted in inhomogeneity in the inlet temperature profile. In the reformer tube bundle of the baffle design, these differences were quickly equalized, whereas in the annulus design, differences in the inlet temperature resulted in different power rates of the single tubes.

The EVA-II helium system was operated over a total time of 13 000 h, with 7750 h at a temperature of 900°C. Both types of steam reformer were operated for more than 6000 h, each without any difficulties. The operation included steady state, partial load and transient conditions, and also special tests with tube blockage at full power operation. Post-operation inspection confirmed the integrity of all tubes.

A variant of the HTR-Modul pebble bed reactor for process heat production has been designed by Siemens-Interatom for a thermal power of 170 MW to deliver helium at temperatures of 950°C. For the version without IHX, the helium coolant is directly fed to the steam reformer, which consumes 71 MW, and to the steam generator, operated with 99 MW.

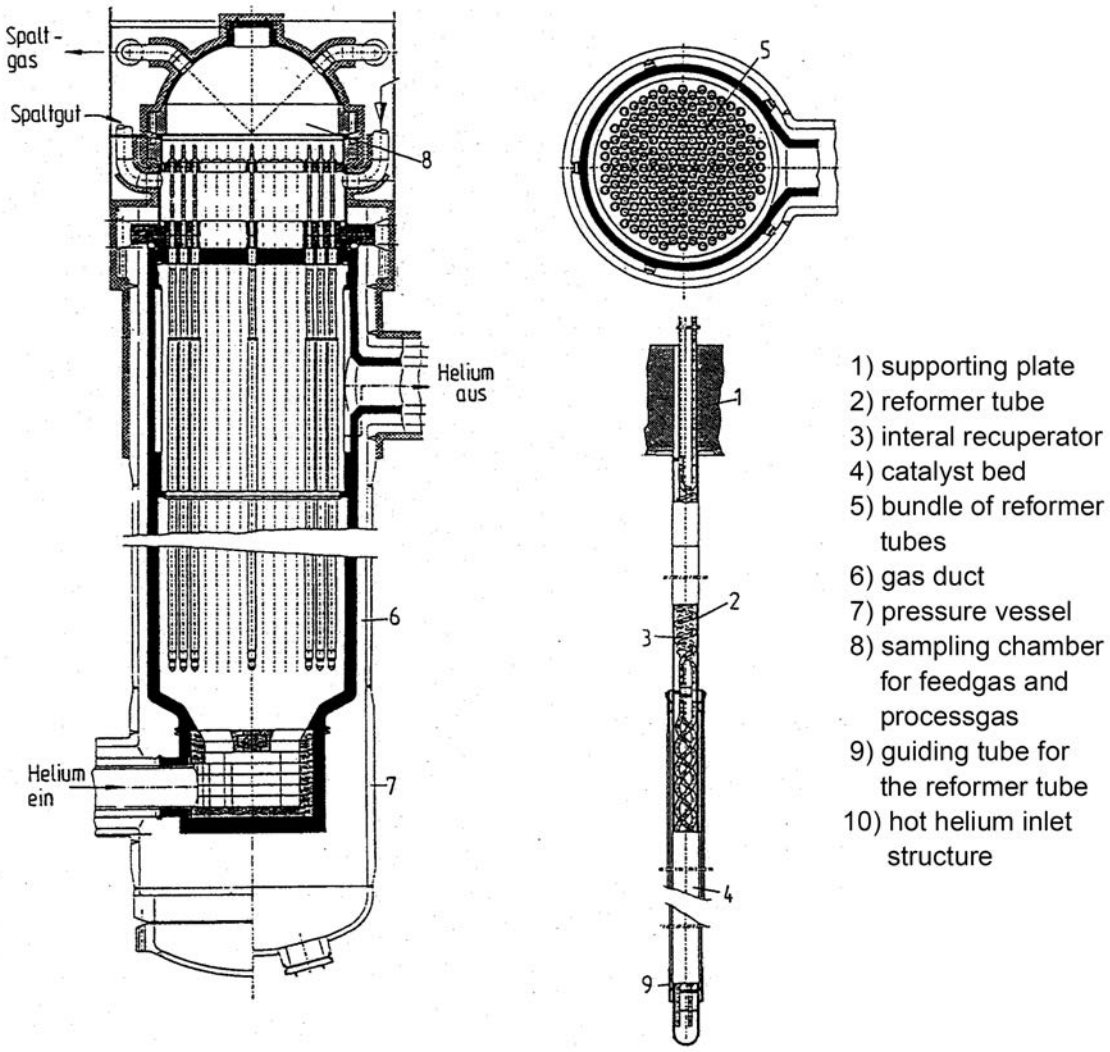

FIG. 58. Concept of a helium heated steam reformer connected to a modular process heat HTGR [202].

Details of the concept of the nuclear steam reformer are shown in Fig. 58. It is a bundle consisting of straight tubes connected to an upper supporting plate. The tubes filled with a catalyst contain an internal recuperator and an inner return duct for the hot process gas. The upper part of the component includes the collector structures for the feedgas composed of steam and methane, and for the product gas containing H_2, CO, CH_4, CO_2 and steam. Of the total heat transferred into the steam reformer, 85% is used for the reforming process, while 15% is taken to heat up the feedgas. The main characteristic data of the steam reformer component as designed by Interatom on the basis of a simple cylindrical pebble bed core with a power of 170 MW(th) are listed in Table 8.

On the basis of a broad experimental programme for nuclear steam reforming (EVA-I and EVA-II facilities, additional testing of kinetics, heat transfer, materials), it can be stated that the allothermal steam reforming process with hot helium to be supplied in the future by a process heat HTGR was successfully tested on a large scale and is well understood. The results achieved should allow, in terms of power, the extrapolation by a factor of around 10 from the EVA-II plant to a helium heated reformer connected to a modular HTGR of 170–200 MW(th). For larger powers, more reformer loops should be coupled to the reactor.

4.1.2.2. Methanation

The reverse process of steam–methane reforming is methanation. The counterpart of the EVA facility is called ADAM (Plant with Three Adiabatic Methanation Reactors). In ADAM, the original feedstock of the reforming

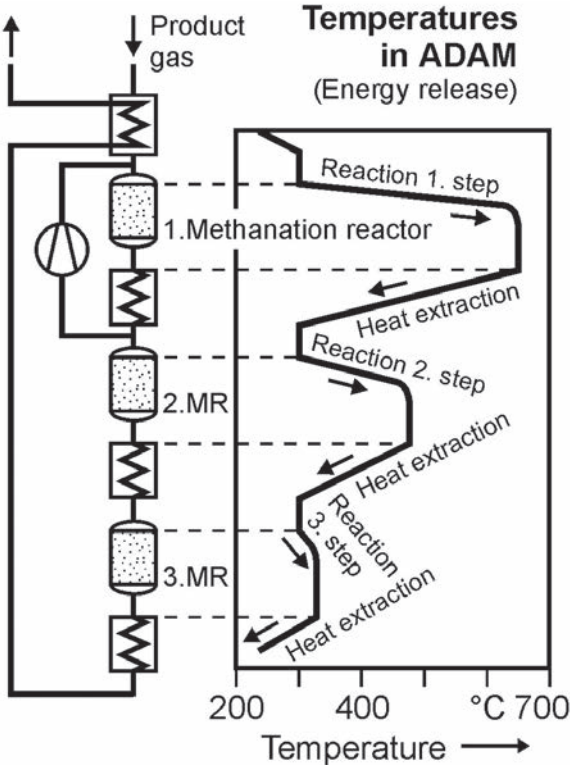

FIG. 59. Temperature profiles in the methanation system ADAM [205].

process, methane and water plus heat, can be regained. After separation, the methane can be piped back to the EVA site to close the cycle, while the steam can be used in other process applications.

From 1979, the pilot plant ADAM-I was operated where high temperature methanation takes place in a three stage process with adiabatic fixed bed reactors (Fig. 59). The three stages, including a dilution of the product gas by feedback of the already re-transformed gas, were chosen to mitigate the large heat release, to minimize soot formation and to maximize the methane output. The feedgas was synthesis gas at a rate of 600 Nm^3/h in ADAM-I. The conversion to methane leads to a release of the complete reaction enthalpy again and the realization of a 650°C gas mixture after the first methanation step, which allows for the generation of superheated high pressure steam for further use. In conjunction with EVA-I, the ADAM-I plant was tested over 2344 h and in a broad range of operational parameters [204].

For the operation of the steam reformer bundle in EVA-II, another methanation plant, ADAM-II, completing the cycle, was operated over almost 6000 h. Synthesis gas was given as feed to the plant at a rate of 9600 Nm^3/h. The conversion of methane at the reaction conditions mentioned above is in the order of 65%. This corresponds closely with the thermodynamic equilibrium. From the power input of 10.78 MW(e) into the helium, the transported energy in the pipeline was 5.72 MW(th). The heat eventually released in the ADAM plant was 5.42 MW(th) in the form of 650°C heat. With an additionally utilized heat of 2.34 MW(th), the total energetic efficiency achieved was 72%.

4.1.2.3. EVA/ADAM energy transportation system

Steam reforming reactions in combination with their reverse reaction, the methanation, can form the basis of a long distance energy transportation system using the energy carrier hydrogen. Such a system, which became known under the acronym ‘EVA/ADAM’, was first suggested in the 1970s in connection with nuclear as the primary energy source. Its principle is the storage of energy in the form of latent heat by an endothermic chemical reaction in a gas and the transportation of the gas to the consumer’s site, where in the exothermic reverse reaction the stored energy is liberated in the form of heat for further utilization (Fig. 60).

The complete EVA-II/ADAM-II system was operated at FZJ for a total time of 10 150 h. It demonstrated the chemical cycle process under the realistic conditions of industrial application with a transported power of 300 kW

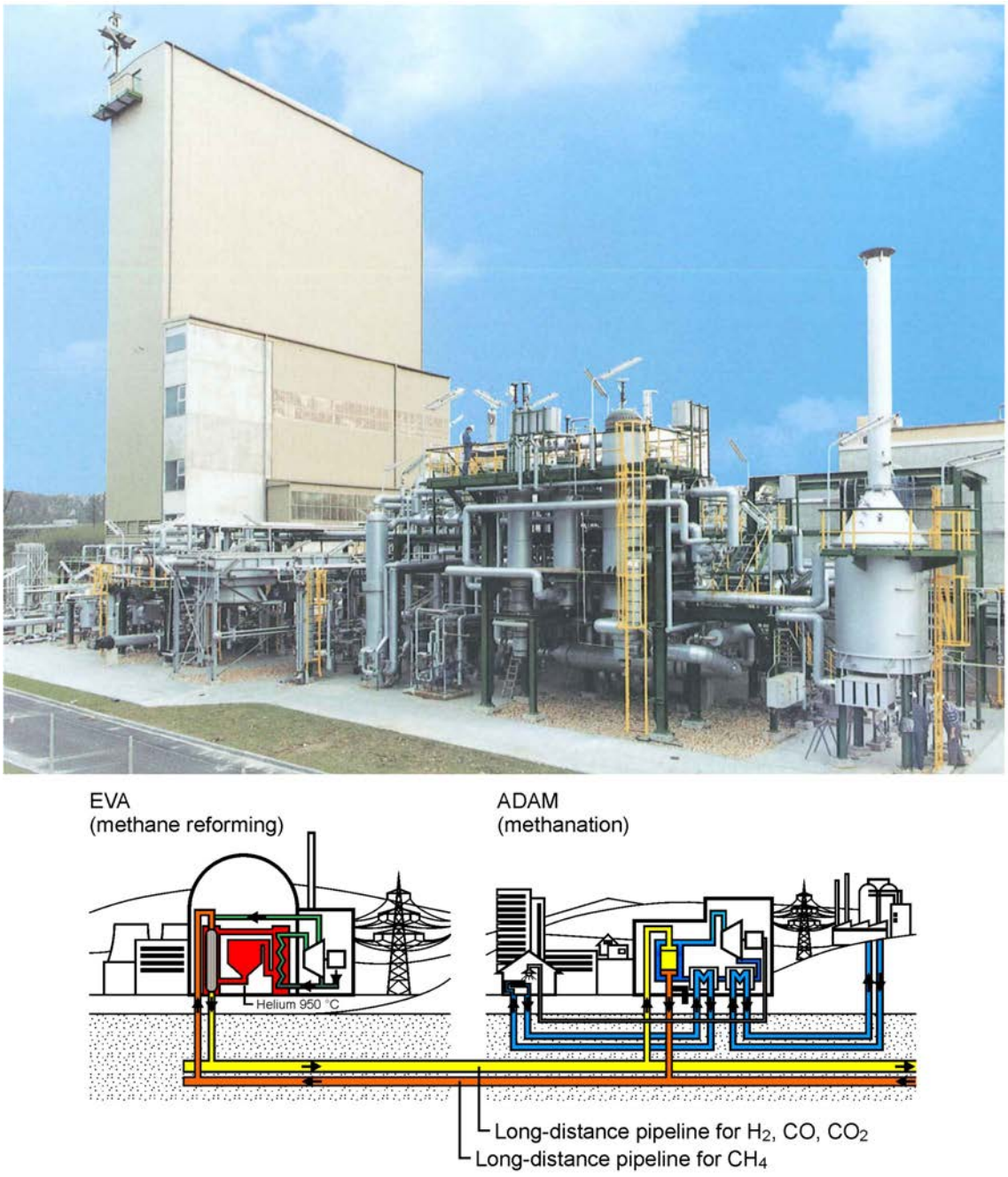

FIG. 60. EVA/ADAM energy transmission system [203, 205].

(EVA-I/ADAM-I) and of 5.4 MW (EVA-II/ADAM-II). With EVA-II/ADAM-II, it was the first time anywhere that a plant was designed, constructed and successfully operated which, in all components, process steps and auxiliary systems, represented a nuclear long-distance energy transportation system and proved its operability and reliability under nuclear heat transport conditions.

4.1.3. Japan's approach: Nuclear steam reforming

4.1.3.1. Concept of SMR for the HTTR

Unlike Germany, Japan has selected the option of coupling an HTGR to SMR by the employment of an intermediate heat exchanger for the steam reforming process. This approach has been applied in the Japanese

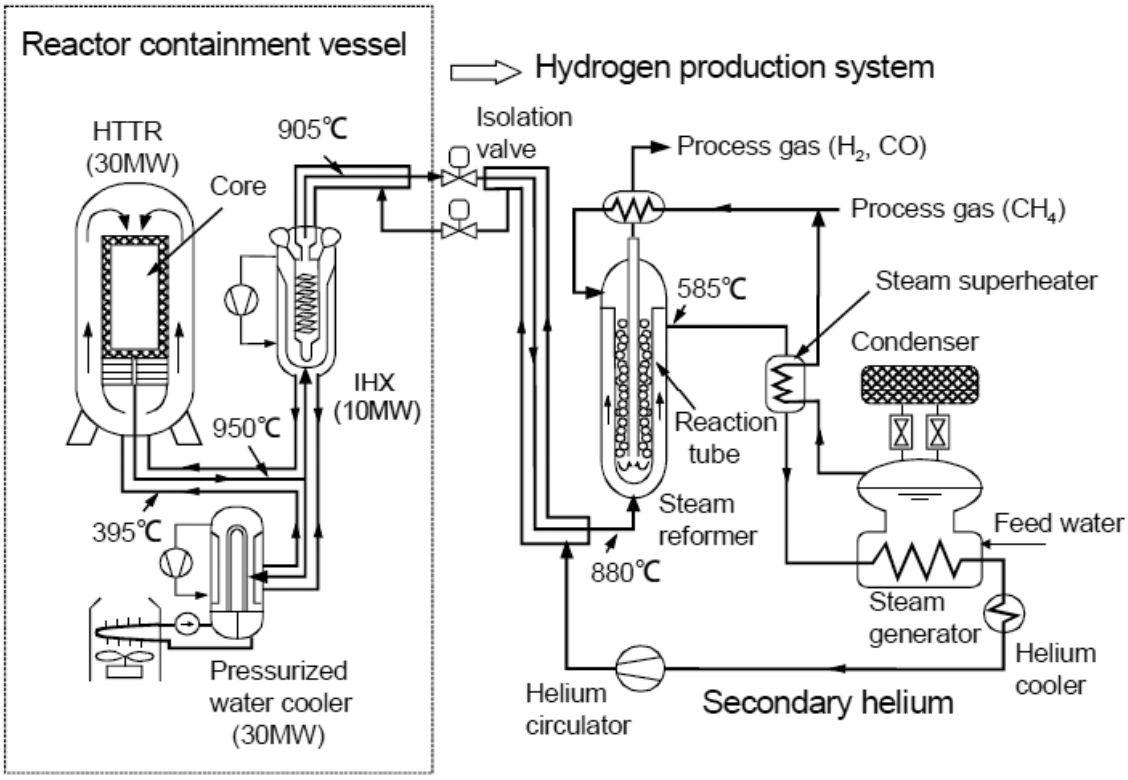

FIG. 61. HTTR coupled to a hydrogen production plant based on SMR [206].

HTTR project. A flow diagram of the hydrogen production system based on SMR and its potential coupling to the HTTR is shown in Fig. 61. The total system is subdivided by the dotted line into the existing nuclear part on the left hand side and the — not yet existing — chemical part on the right hand side.

The requirements for a system with safe operation and high hydrogen production efficiency have initiated engineering design work on key components for the nuclear steam reforming process:

— A new concept steam reformer heated by helium gas from the nuclear reactor has been designed to achieve high hydrogen production performance and competitiveness with an economical, fossil fired hydrogen production plant.
— A natural convection type of steam generator has been selected to achieve sufficient system controllability accommodating the large difference in thermal dynamics between the nuclear reactor and the steam reformer.
— An air-cooled radiator is connected to the steam generator to operate as a final heat sink during normal and anticipated operational occurrence conditions.

The separation of the primary circuit and the chemical process avoids the possibility of contamination in the steam reformer and reduces the permeation rates of hydrogen and tritium to negligible values. However, the heat fluxes in the steam reformer have values of around 40 kW/m² if the same conditions in the reforming process are fulfilled. The fabrication of the steam reformer and steam generator requires different standards than those of components that are directly integrated into the primary helium circuit.

For several years, steam reforming of methane has been considered the top candidate process to be connected to the HTTR for the world's first nuclear hydrogen production. The HTTR nuclear steam reforming system will therefore be taken as an example and described in more detail.

The HTTR steam reforming system has been designed to provide about 4200 Nm^3/h of hydrogen production using a Ni-based catalyst with 10 MW of thermal energy. A heat utilization ratio (defined as the ratio of output hydrogen energy to total input thermal energy) of 73% is expected. This value is competitive with that of the conventional system, where the heat utilization ratio is about 80%.

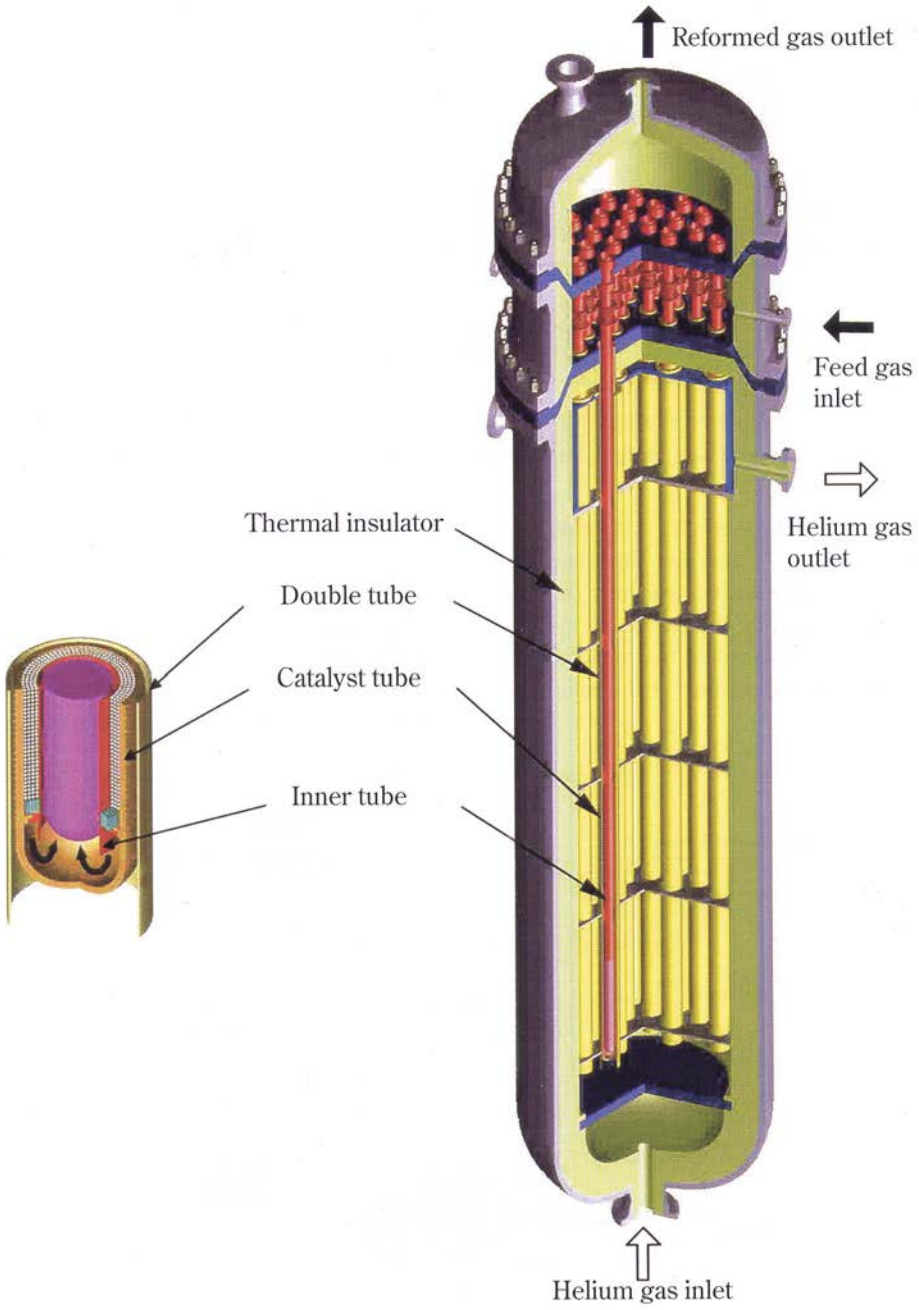

FIG. 62. Steam reformer component for connection to HTTR [206].

4.1.3.2. Design of steam reformer

The HTTR can provide high temperature helium gas of 905°C at the outlet of the IHX and, owing to further heat loss from the hot gas duct between the IHX and the steam reformer, secondary helium of 880°C at the inlet of the steam reformer. The steam reformer component is shown in Fig. 62 [206].

Helium flows into the steam reformer at the bottom and then upwards outside the catalyst tubes, squeezed by multiple plates of orifice baffles transferring heat by forced convection flow (in contrast to heat radiation in the conventional design). The catalyst tubes contain packing of Ni/Al_2O_3 reforming catalysts, through which the process feed gases (natural gas, steam) are routed. The catalyst tube wall thickness is 13 mm, meeting the requirements on design limits for pressure retaining components. Finally, the helium, which is cooled down to 585°C, exits and flows to a superheater. The main design specifications of the steam reformer are listed in Table 9.

TABLE 9. DESIGN SPECIFICATIONS OF THE STEAM REFORMER FOR HTTR AND MOCK-UP TEST FACILITY

Parameter	Steam reformer in HTTR	Splitting tube in mock-up test facility
Heat input (MW)	3.6 (nuclear) (plus 1.3 from product gases)	0.42 (electric)
Material		
Tubes	Hastelloy XR	Alloy 800H
Catalyst	Ni/Al_2O_3	
Size		
Shell diameter (m)	1.19	
Shell height (m)	14	
Catalyst tube	Bayonet type, concentric double-walled tube	Bayonet type, concentric double-walled tube
	153.8	146
Outer diameter (mm)	13	10
Wall thickness (mm)	7.9	7.0
Length (m)	60.5	
Inner tube diameter (mm)	3.9	
Wall thickness (mm)	not decided yet	
Length (m)	37	3
Number of tubes		
Secondary helium		
Inlet temperature (°C)	880	880
Outlet temperature (°C)	585	650
Pressure (MPa)	4.1	4.1
Flow rate (kg/s)	2.5	0.091
Heat transfer rate at outer surface ($W/(m^2 \cdot K)$)	1700	
Process feedgas		
Inlet temperature (°C)	450	450
Outlet temperature (°C)	580 (max.: 800)	600 (max.: 756)
Pressure (MPa)	4.5	4.5
Raw gas flow rate (kg/s)	0.39	0.012
Raw gas conversion (%)	64.2	55
Steam:methane ratio	3.5	3.5–4 (3.5)
Hydrogen production rate (Nm^3/h)	4240	120

The process feedgas mixture of natural gas and steam, after being preheated to 450°C at a pressure of 4.5 MPa, enters the steam reformer at the top and then flows downwards in an annular flow between the walls of the outer and inner tubes through the catalyst bed, where the methane and other lighter hydrocarbons together with steam are reformed. The reformed gas, having reached a maximum temperature of 830°C, then flows upwards inside the inner tubes, transferring at the same time heat to the feedgas and eventually leaving the steam reformer at a temperature of 580°C and a pressure of 4.1 MPa.

In the HTTR steam reforming system, a steam to methane ratio of 3.5 has been selected. The required steam is about 5160 kg/h at rated conditions, thus the thermal energy necessary to generate steam is 3.1 MW. The thermal energy of the product gas at the outlet of the steam reformer is only 1.9 MW. Therefore a steam generator is necessary on the secondary helium loop in order to supply this large amount of thermal energy. The superheater and the steam generator are installed downstream of the steam reformer to generate feed steam for the steam reformer. The required helium temperature at the inlet of the IHX is 160°C, requiring the addition of a feedwater preheater and a helium cooler. In the future HTGR heat application system, the outlet helium gas of steam generator will be returned to the IHX directly.

The flow rate of natural gas as a feedgas is 1290 kg/h, and the flow rate of steam is 5160 kg/h at the inlet of the steam reformer. The temperature of the product gas is about 600°C. This gas is cooled down by the water cooler and separated into steam and dry gas compositions including hydrogen, carbon oxide, carbon dioxide and residual methane in the separator. The pressure and maximum temperature of the process feedgas are 4.5 MPa and 830°C, respectively, so that the conversion ratio from methane to hydrogen is expected to be 68%. As a result, 32% of methane will remain in the product gas. In the conceptual design of the HTTR-SMR, this residual methane is burned in the flare stack together with the other combustible gases.

Furthermore, the reforming process requires a thermal heat input of 4.8 MW. In order to generate feed steam by the thermal energy of secondary helium gas, the helium gas temperature at the outlet of the steam reformer is required to be about 600°C, so that only thermal energy of 3.6 MW is supplied to the steam reformer from helium gas. This high pressure and low temperature condition is a disadvantage for the steam reforming reactions.

A new heat exchanger type concept for the steam reformer is required, to enhance the hydrogen production rate. It should allow an:

— Increased heat input into the process gas by employment of orifice baffles;
— Increased reaction temperature of the process gas at the outlet of the catalyst zone;
— Optimized reforming gas composition, to enhance the reforming rate.

The aim of reaching a heat flux density closer to that of the conventional method (Table 10) can be achieved by employing a helium heated counter-flow heat exchanger. Helium under pressure shows excellent heat transfer properties.

Assuming an infinitely long catalyst tube, the process gas temperature approaches that of the helium gas. But in general, a catalyst tube length limit of approximately 10 m is mandated from the viewpoint of seismic design. It is necessary to enhance the heat transfer rate in order to design for an adequate steam reformer size. There are several means to enhance the heat transfer, such as baffles, double tubes and fins. JAEA has performed an analytical comparison of the heat transfer rate and selected a double tube with a radially finned catalyst tube, for which the thermal radiation rate is more than 1800 W/(m^2·K).

The proposed new design of a steam reformer is shown in Fig. 63. JAEA has adopted a bayonet type of catalyst tube, a concentric, double-walled tube which can use both the outside and inside gas flow for heating up the process gas. The thermal energy input into the process gas increases from 3.6 to 4.9 MW.

These improvements are applicable not only to HTGR steam reforming systems but also to other HTGR hydrogen production systems. This is because a heat exchanger type of endothermic chemical reactor is an essential technology for the production of hydrogen through the use of nuclear heat. The heat demand drastically increases when the endothermic chemical reactions start the reforming process. On the nuclear side, the helium temperature ‘conventionally’ increases linearly with power output. Because of this mismatch between heat demand and heat supply during startup, an additional heat exchanger component, a so-called heat load controller, with a capacity of 2.8 MW is integrated into the steam reforming system. Control is achieved by adjusting the helium flow rate. Figure 64 shows the relationship between nuclear power and helium temperatures during the startup phase [207].

TABLE 10. COMPARISON OF NUCLEAR AND CONVENTIONAL DESIGN

Parameter	Steam reformer		
	Natural gas heated	Helium heated for HTTR/SMR	Helium heated improved design (bayonet type)
Process gas pressure (MPa)	1–3	>4	4.5
Maximum temperature of process gas (°C)	850–950	≤750	800
Maximum heat flux to catalyst zone (kW/m^2)	50– 80	10–20	22
Heat transfer	Radiation	Forced convection	
Efficiency (%)	80–85	50	63
CO_2 emission (t/h) (basis: 10 MW)	3	~2	

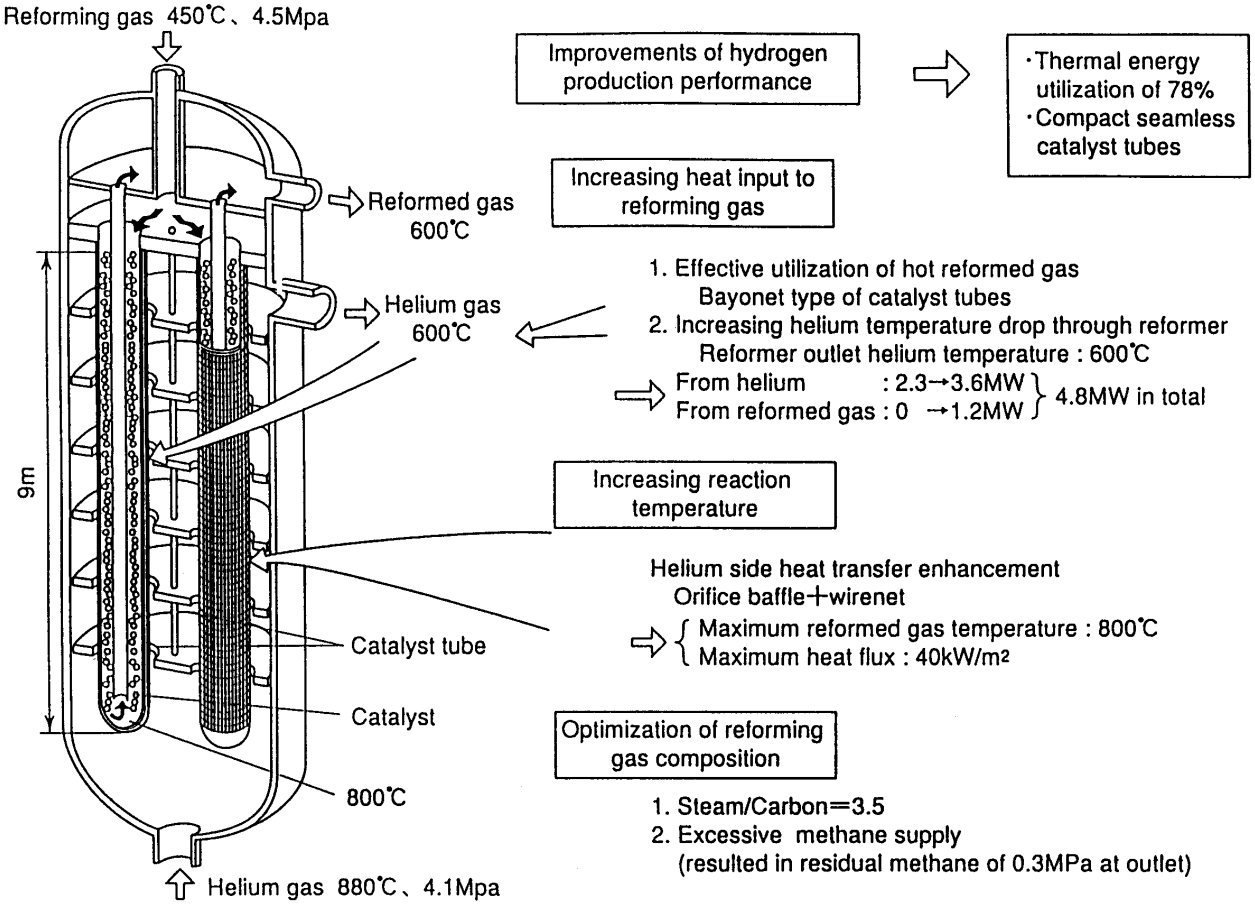

FIG. 63. New concept of a helium heated steam reformer [208].

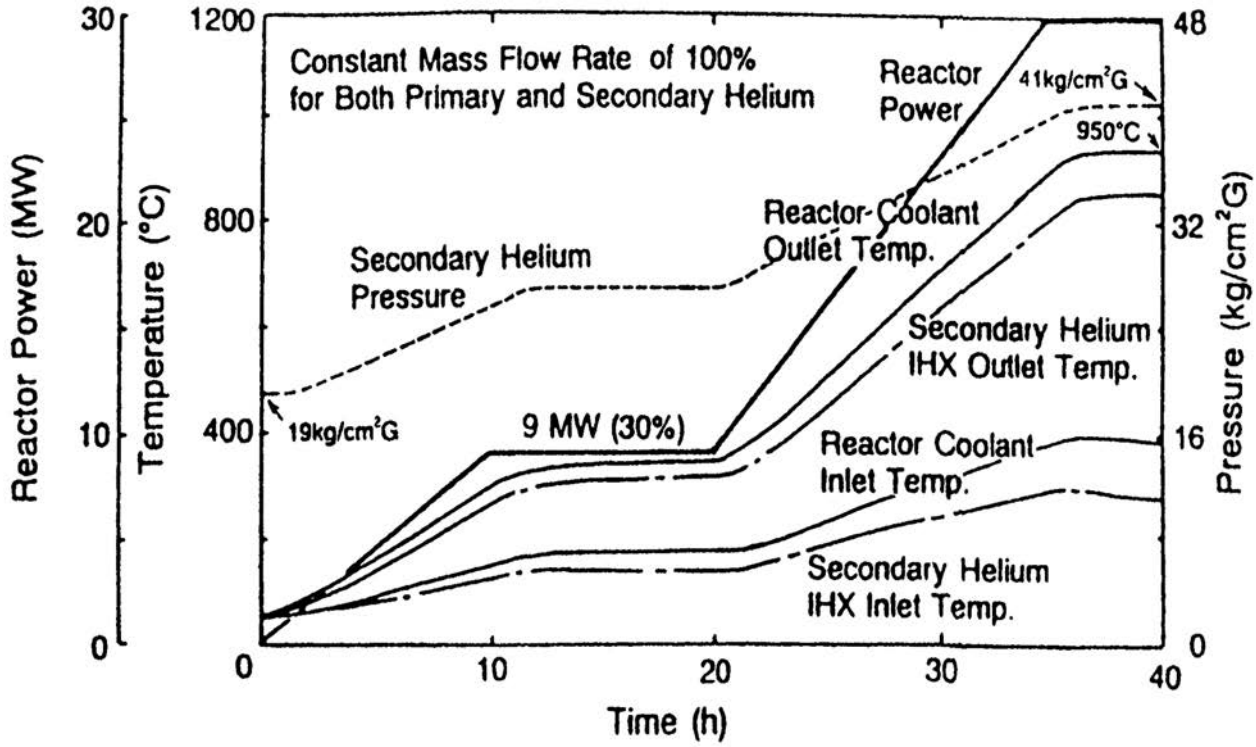

FIG. 64. Nuclear power and helium temperature during the startup phase [207].

The effective consumption of the nuclear process heat input of 10 MW can be seen from Table 11 [207].

TABLE 11. CONSUMPTION OF 10 MW NUCLEAR HEAT INPUT IN THE TEAM–METHANE REFORMING SYSTEM OF HTTR

Heat loss		0.5 MW
Air cooler		0.7 MW
Feedwater preheater		0.8 MW
Reboiler		2.7 MW
LNG preheater		0.2 MW
Superheater		1.0 MW
Process gas heater		0.5 MW
Steam reformer		3.8 MW
	Σ	10.2 MW

Partial pressure conditions of the process gas components for the catalyst zone inside the reformer tubes are given in Table 12 [207].

TABLE 12. PARTIAL PRESSURE DISTRIBUTION FOR PRODUCT GASES IN THE CATALYST ZONE

Gas component	Partial pressure (MPa) in catalyst zone	
	Inlet	Outlet
CH_4	0.82	0.28
H_2O	3.42	1.95
H_2	0.13	1.72
CO	0.03	0.27

4.1.3.3. Experiments in mock-up test facility

The steam reforming process was tested in out-of-pile experiments under simulated nuclear conditions at JAEA, Oarai [209]. For this purpose, a 1:30 downscaled mock-up facility was constructed. Schematics of the test plant and the splitting tube used are given in Figs 65 and 66. In order to enhance heat transfer from the helium through the tube walls, disc type fins of 2 mm height and 1 mm width were attached to the splitting tube, which increased the heat transfer area by a factor of 2.3 compared with a smooth surface.

The test programme started in 2002 and, after fulfilling its objectives, was terminated in 2004. The test facility was basically used to investigate the process control technology. It comprises normal startup/shutdown tests to investigate temperature and pressure fluctuations and its controllability as a function of the steam to methane ratio, in order to optimize feed flow of methane and steam according to the temperature and pressure of the helium gas. In a system controllability test, potential thermodynamic disturbances at the pressure boundary between helium and methane are examined by the stepwise change of the methane and steam flow rates, in order to optimize the control system for the pressure difference.

In steady operation, average flow rates of methane, steam and helium gas in the mock-up system were 12.0, 46.6 and 91.0 g/s, respectively [210]. The hydrogen production rate was stable and an average value between 14 and 40 h was 120.2 m^3/h. At that time, the maximum reaction temperature and pressure of the process gas were around 756°C and 4.0 MPa, respectively. The methane conversion rate observed was 55%.

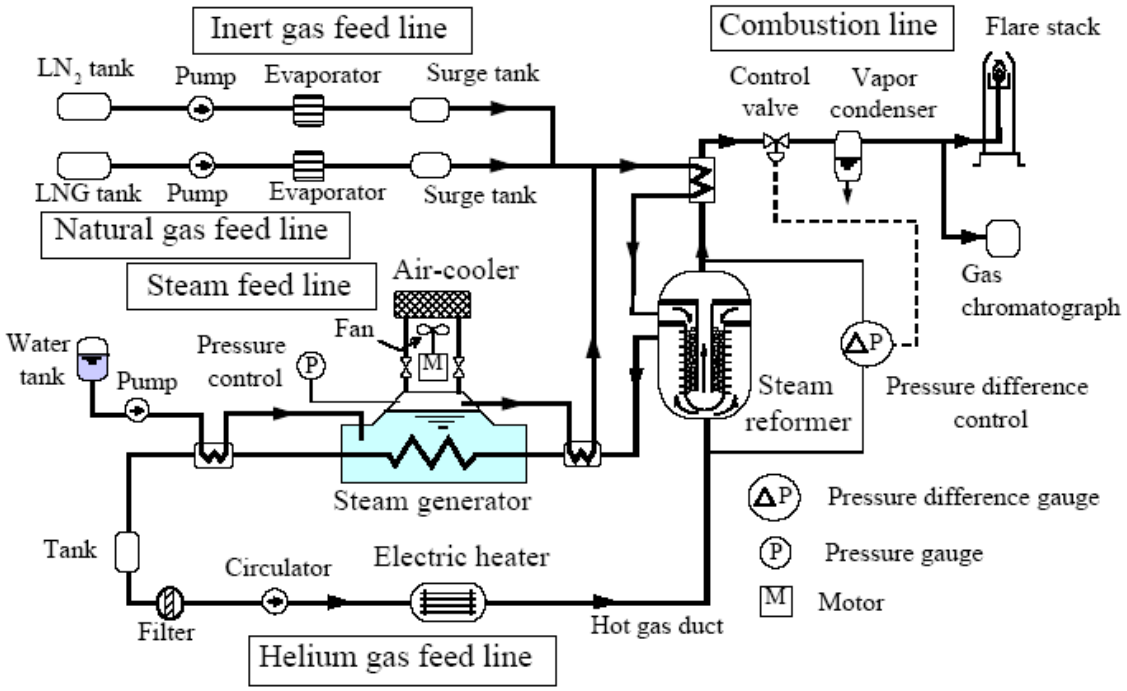

FIG. 65. Schematic of steam reforming mock-up model test facility at JAEA [210].

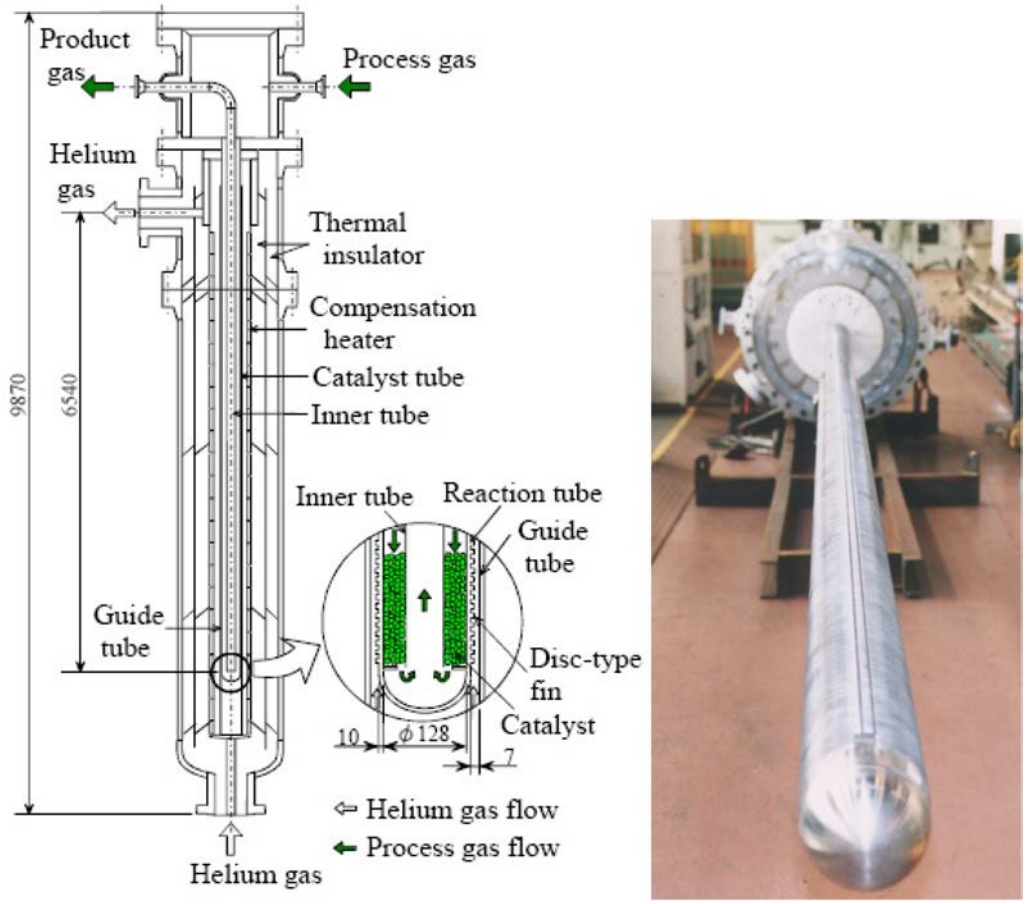

FIG. 66. Bayonet type steam reformer tube used in the mock-up facility [210].

Safety related tests were conducted with the mock-up facility to examine malfunctions and accident sequences in the process gas line, including emergency shutdown. The focus was on the examination of potential thermal turbulences from the hydrogen production system to the nuclear side. In the case of an accident in the process line, the HTTR should be shut down by the normal operation procedure rather than by a reactor scram. In such a case, the heat of the helium is to be removed via the steam generator, which limits the temperature fluctuations in the helium. Characteristic data of the splitting tube in the mock-up facility are also listed in Table 9 in comparison with the steam reformer design to be used in connection with the HTTR. Results of these safety related tests are described in more detail in Section 7.5.1.

Experimental results obtained with respect to the temperature fluctuations were as follows [211]:

Startup:	$\Delta T = 2.5$	at steam generator outlet
	$\Delta T = 110$	at steam reformer outlet
Shutdown:	$\Delta T = 0.5$	at steam generator outlet
	$\Delta T = 88$	at steam reformer outlet

The results demonstrate that the steam generator is capable of mitigating thermal disturbances arising from the chemical reactor in the form of temperature fluctuations of the helium or pressure fluctuations of the process gas. The defined target of ±10°C for the steam generator was met.

4.1.3.4. Nuclear steam reforming at lower temperatures

Another, unconventional idea of applying nuclear to steam reforming is the use of the heat of spent LWR fuel to run the endothermic process at a (lower) temperature level of 600°C. After separation of the uranium, the remaining spent fuel is packed in rods (100/80 mm outer/inner diameter) and stored in vessels (5.8 m diameter, 9 m height). Heat transferring fluids could be helium or molten salts. The decreasing decay heat production with time is compensated for by reducing the coolant flow rates to maintain the temperature level for the reforming process. The amount of 5000 t of spent fuel corresponding to about 15 MW(th) was estimated to yield ~13 000 Nm^3/h of hydrogen [212].

4.1.4. The Russian Federation's approach: Nuclear steam reforming

In the Russian Federation's concept for nuclear steam reforming of natural gas, as is suggested in Ref. [69], a 215 MW(th) nuclear plant (MHR-100SMR) provides primary helium at 950°C to the thermal conversion unit. It is composed of three individual high temperature steam reformer sections (Fig. 67) where the heat is transferred to the feedgas mixture.

The arrangement of the heat exchangers is in parallel with regard to the primary helium and in series with regard to the process gas on the secondary side. The product gas leaving the third stage, highly enriched in hydrogen and still containing a steam fraction of 55%, finally passes the usual post-processing systems (separation, purification), with the return fraction being mixed with natural gas and recycled to the thermal conversion unit. Operating conditions of the thermal conversion unit are given in Table 13.

4.1.5. China's approach: Nuclear steam reforming

The INET in Beijing has developed a concept for a hydrogen production system based on steam–methane reforming with the HTR-10 test reactor. In this case, the HTR-10 will be equipped with an IHX where primary helium of 950°C transfers heat to a secondary helium gas loop, which is then transported to the steam reformer. Characteristic operational data of the HTR-10 steam reformer are listed in Table 14.

A diagram of the steam reformer to be connected to the HTR-10 is illustrated in Fig. 68. It is a tube-shell type reformer consisting of reformer tube bundles. The process gas enters at the top with a temperature of 500°C and flows downwards through the annular catalyst bed, where the reforming reactions take place. The maximum temperature of the process gas is reached in the bottom part of the catalyst bed (840°C), before the gas flows upwards through the central tube and exits at the top. On the primary side of the reformer, the hot helium with a

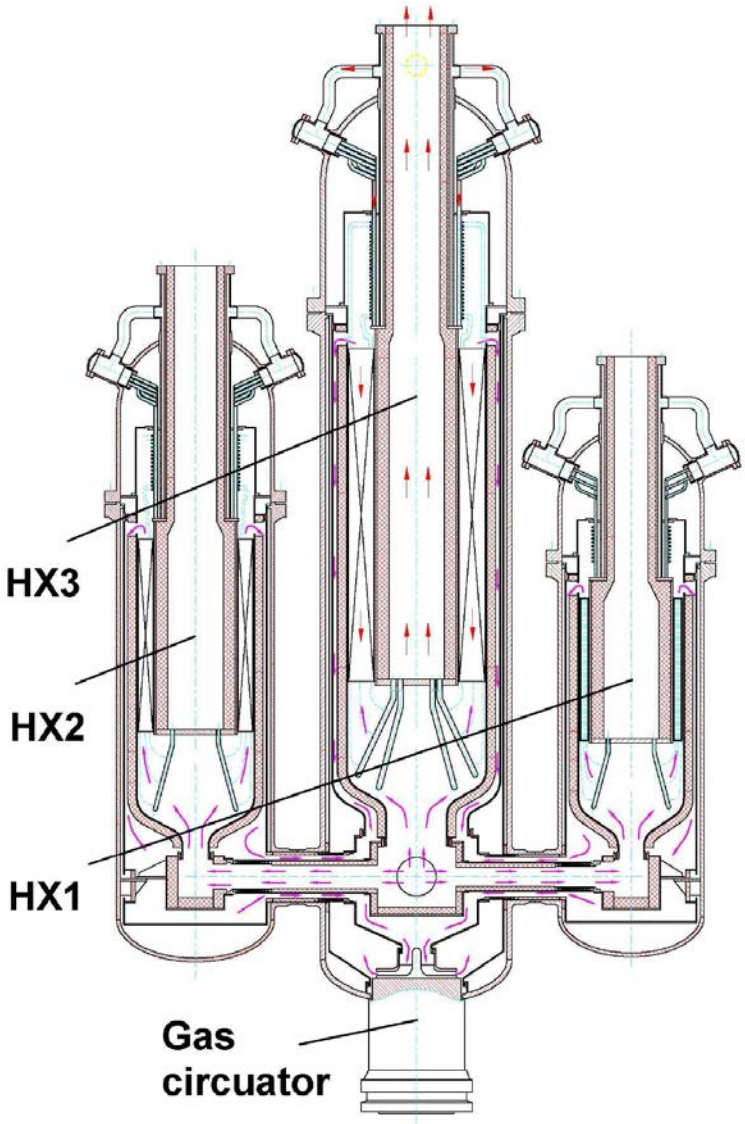

FIG. 67. MHR-100SMR thermal conversion unit with three heat exchangers for SMR [69].

temperature of 890°C enters at the bottom and flows upwards through the annular space formed by the catalyst tube and the outer guide while transferring heat to the reacting process gas. Fins are attached at the outside of the catalyst tube in order to enhance the heat transfer.

4.2. NUCLEAR-ASSISTED COAL GASIFICATION

Nuclear coal gasification has been studied in Germany within the German PNP project over more than two decades. The project was a cooperative effort between the HTGR industries (Hochtemperatur-Reaktorbau GmbH, Mannheim, and Gesellschaft für Hochtemperatur-reaktortechnik mbH, Bensberg), the coal industries (Bergbauforschung GmbH, Essen, and Rheinische Braunkohlenwerke AG, Cologne), and the Nuclear Research Centre Jülich (today: Forschungszentrum Jülich, FZJ). The project was funded by the Federal Government, the State Government of North Rhine-Westphalia, and the participating industries.

The main objective was the development, design and construction of an energy system based on a combination of coal and nuclear power, including the developing and prototype testing of a nuclear heat generating system to be operated at a 950°C gas outlet temperature, intermediate circuit, heat extraction, coal gasification processes and nuclear energy transport.

TABLE 13. MAIN PARAMETERS OF THERMAL CONVERSION UNIT IN THE MHR-100SMR [69]

	MHR-100SMR steam reforming system
Primary helium inlet temperature	950°C
Primary helium total flow rate	81.7 kg/s
HX-TCF 1	
Heat input	31.8 MW(th)
Primary helium flow rate	12.1 kg/s
Process feedgas inlet temperature	350°C
Process feedgas outlet temperature	650°C
Process feedgas flow rate	43.5 kg/s
HX-TCF 2	
Heat input	58.5 MW(th)
Primary helium flow rate	22.2 kg/s
Process feedgas inlet temperature	350°C
Process feedgas outlet temperature	750°C
Process feedgas flow rate	60.9
HX-TCF 3	
Heat input	125 MW(th)
Primary helium flow rate	47.4 kg/s
Process feedgas inlet temperature	350°C
Process feedgas outlet temperature	870°C
Process feedgas flow rate	101 kg/s

TABLE 14. MAIN OPERATIONAL PARAMETERS OF THE STEAM REFORMER FOR HTR-10 [213]

Parameter	HTR-10 steam reforming system
Primary helium circuit	
Outlet temperature	950°C
Secondary helium circuit	
Heat input	2.5 MW(th)
Inlet temperature	890°C
Outlet temperature	600°C
Pressure	3.0 MPa
Flow rate	1.6 kg/s
Process gas side	
Steam-to-carbon ratio	4
Feedgas inlet temperature	500°C
Feedgas flow rate	1.0 kg/s
Temperature in catalyst	840°C
Pressure inlet catalyst	3.7 MPa
Pressure outlet catalyst	3.2 MPa
Hydrogen yield	2500 Nm^3/h

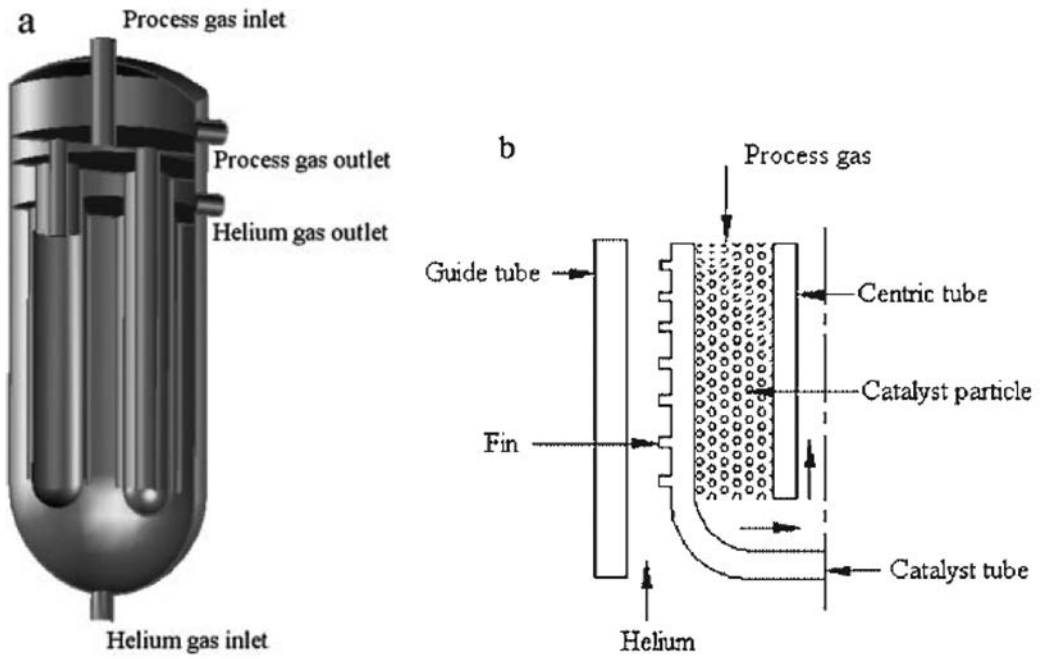

FIG. 68. Schematic of nuclear steam reformer to be connected to the HTR-10 [213].

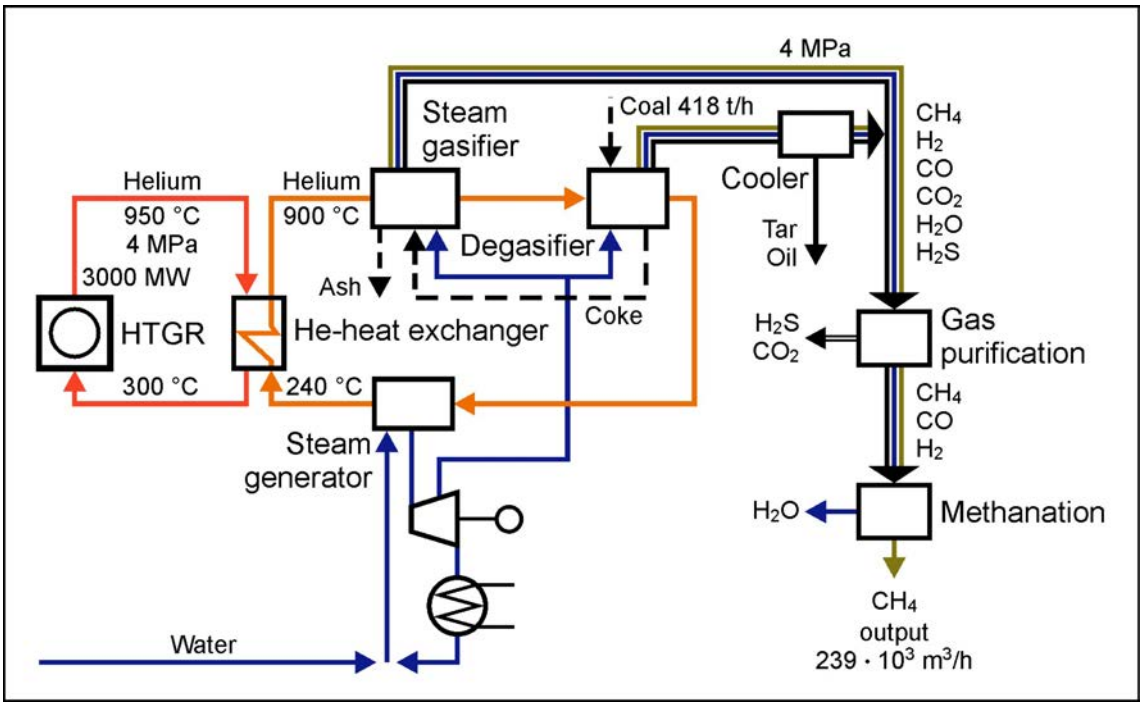

FIG. 69. Schematic of steam gasification of hard coal with nuclear process heat plant PR-3000 [216].

4.2.1. Nuclear steam gasification of coal

Figure 69 shows the flowsheet of the PNP nuclear steam–coal gasification process. For this process, the heat from the reactor coolant was foreseen to be transferred to an additional intermediate circuit via a helium–helium intermediate heat exchanger (He–He IHX). The main reason was to avoid the handling of coal and ash in the primary system of the reactor, as well as much more complex repair and maintenance work. The primary helium of

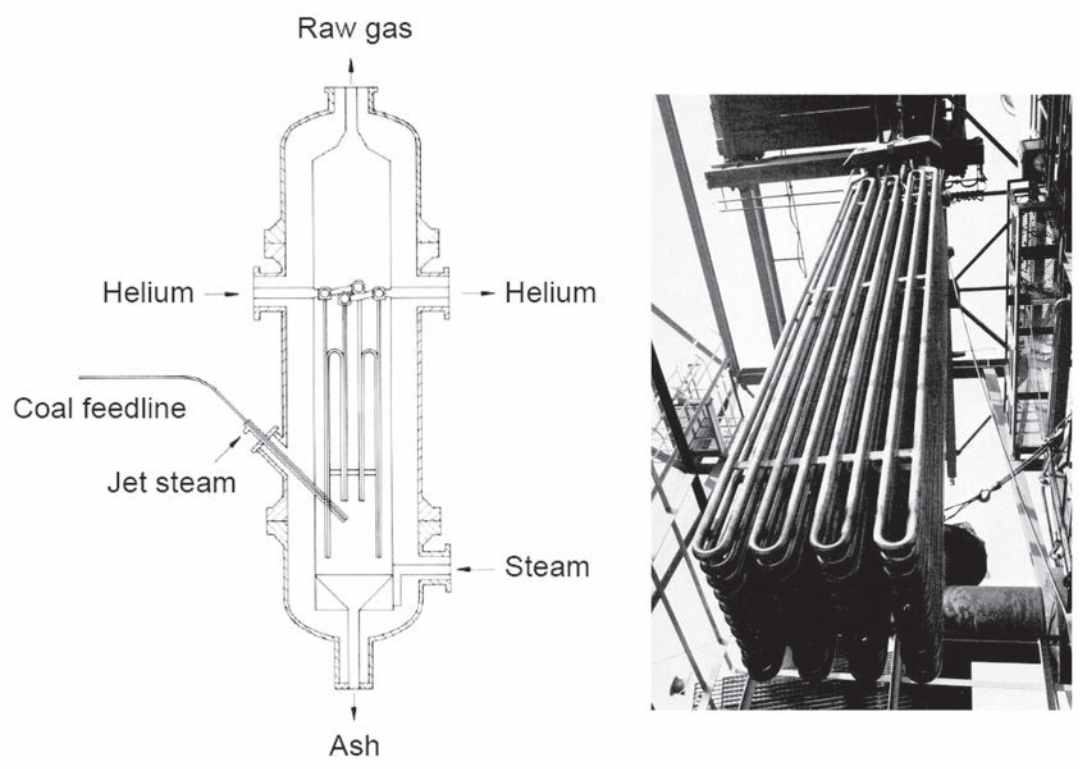

FIG. 70. Schematic of gas generator for allothermal coal gasification (left) [214]; photograph of the immersion heat exchanger (right) [217].

950°C flowing on the outside of the IHX tubes passes its heat to the secondary helium entering the steam gasifier at 900°C. Also, the pressure is slightly higher than on the primary side for the purpose of preventing radioactivity from entering the secondary circuit in the case of a leak. The hot steam produced is routed into the coal bed to be gasified. Unlike conventional fossil fuelled components, the helium heated components of the HTGR have to meet the more stringent requirements of a 'nuclear' component in terms of construction, quality assurance and scheduled retesting. They have the important function of forming a radioactivity barrier between the primary helium and the process gas.

For nuclear steam–coal gasification, a new component to be developed was the gas generator with allothermal heating. In 1973, a first device with electric heating and a volume of a few litres was tested on a small technical scale (~1 kg/h) using a fixed bed at temperatures up to 1000°C and pressures up to 7 MPa to investigate kinetics and heat transfer characteristics, gas composition and other parameters. The height of the fluidized bed was 0.37 m.

The follow-on plant, on a semi-technical scale, operated from 1976 at Bergbau-Forschung, Essen, was a first of its kind gas generator with a fluidized bed of about 1 m^2 base area and a height of up to 4 m, laid out for a coal throughput of ~200 kg/h. This unit was constructed as a vertically arranged cylindrical vessel (Fig. 70), with the outer dimensions of 7.75 m (max.) diameter and 21.13 m height, designed for pressures up to 4 MPa. Its concept differed from the conventional one in that the coal was gasified indirectly by means of a tube type immersion heater which was placed into the fluidized bed to transfer heat from a separate helium circuit. The helium was electrically heated up to 950°C, with the heat transferred at a power of 1.2 MW. The heat transfer from the hot helium to the fluidized bed was found to be about 500 W/m^2, sufficient to allow for the gasification process to be conducted in technically reasonable dimensions [214]. The conversion rate was 83%. Other characteristic data of the semi-technical plant are listed in Table 15 [215].

The semi-technical plant was used for testing components, feeding devices and insulation, investigating broad ranges of operating conditions, and applying different types of coal. Reaction rates were observed to decrease with the height of the fluidized bed, which can be explained by the inhibiting effect of the product gases, whose concentration increases with height. The operation of the immersion heat exchanger in a fluidized bed was successfully demonstrated. Due to the good heat transfer, half of the heat exchanging surface was already sufficient to decouple almost all of the heat from the helium.

TABLE 15. CHARACTERISTIC DATA OF SEMI-TECHNICAL GAS GENERATOR FOR STEAM–COAL GASIFICATION

Thermal power	1.2 MW(th)
Helium inlet temperature	<1000°C
Helium flow	1.1 kg/s
Heat exchanging surface	33 m^2
Height of fluidized bed	<4 m
Cross-section of fluidized bed	0.8 × 0.9 m^2
Density of fluidized bed	344 kg/m^3
Coal input	233 kg/h
Coal particle size	<1 mm
Steam velocity	1.13 m/s
Gasification temperature	700–850°C
Pressure	4 MPa
Raw gas production rate	816 Nm^3/h

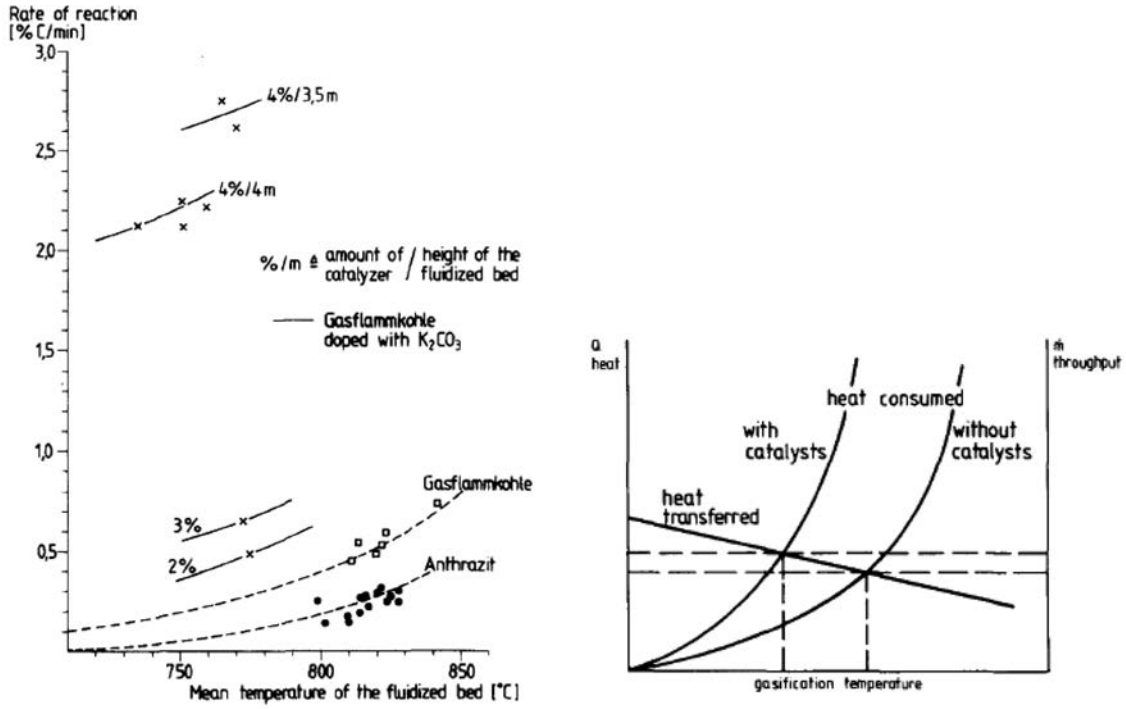

FIG. 71. Influence of catalyst on reaction rates (left); interaction between heat transfer and gasification kinetics in allothermal gas generator (right) [215].

Compared with the conventional case, the temperature provided by the helium is limited. Consequently reaction rates are slower, which, however, could be enhanced by adding a catalyst. The catalytic coal gasification was also tested in the plant (Fig. 71, left). The addition of 4 wt% of the catalyst potassium carbonate enhanced coal throughput by 44%. At the same time, the fluidized bed temperature was decreased. As the right hand side of Fig. 71 indicates, for constant helium temperature, the heat transfer decreases with increasing gasification temperature. On the other hand, heat transfer increases with increasing reaction rate (due to the addition of a catalyst). This is compensated for by a decrease in the gasification temperature [215].

TABLE 16. RESULTS FROM CATALYTIC AND NON-CATALYTIC STEAM–COAL GASIFICATION [215]

	Non-catalytic		Catalytic	
	Pyrolysis	Gasification	Pyrolysis	Gasification
Helium temperature (°C)	895		895	
Gasification temperature (°C)	805		701	
Reaction enthalpy (kJ/kg coal)	2192	5678	2058	5148
Coal throughput (t/h)	27.3		69.3	
Raw gas production rate (Nm^3/h)	234 000		659 500	
Gas composition fractions (%) H_2:	44.2	53.5	57.6	57.2
CO:	11.1	12.7	1.1	2.4
CO_2:	19.2	25.8	25.9	32.7
CH_4:	23.7	7.4	14.5	7.3

Furthermore, residence times could be reduced from 7–9 h (anthracite) down to about 1.5 h. In addition, the hydrogen production was significantly increased at the expense of CO (Table 16). The catalyst, however, was found not to be effective until a certain threshold value of ~2 wt% owing to bonding on the coal. Also, corrosion effects were enhanced, showing strong inner oxidation at temperatures above 800°C. On the other hand, adding the catalyst K_2CO_3 to the coal (as a kind of impregnation) resulted in an enhanced hydrogen permeation rate through the heat exchanger walls, obviously due to a change of quality of the protective oxide layer on the metal surface.

The semi-technical plant was in hot operation for approximately 26 600 h, with more than 13 600 h under gasification conditions (750–850°C, 2–4 MPa). The maximum capacity was 0.5 t/h of coal, and the total quantity of coal gasified was 2400 t [215]. Some results are summarized in Table 16 regarding derived reaction enthalpy and product gas composition, distinguished between the non-catalytic and the catalytic process and between the pyrolysis and the gasification phase, and also compared with the autothermal process. The results show that the primary pyrolysis products are further converted in the steam atmosphere in the gasification phase. The overall result of the semi-technical scale operation was that an industrial scale gas generator in connection with a nuclear heat source was considered feasible.

Coal conversion programmes were accompanied by a qualification programme for high temperature metallic materials. Investigations under typical steam–coal gasification conditions have shown that the degradation by corrosion is strongly dependent on the contents of chromium and other elements. A minimum chromium content was identified to be necessary for maintaining a sufficient protective layer on the metal surfaces. Thinning by corrosion in the order of 0.01 mm/a should allow a satisfactory stability.

A commercial size gas generator was considered technically feasible with a coal throughput of ~50 t/h. This size would require an estimated 4000 m^2 of heat transfer area and a 300 m^3 volume for the fluidized bed. The design that was eventually elaborated was foreseen to have a thermal power of 340 MW, requiring three units for a 1000 MW nuclear process heat plant [214]. Unlike the semi-technical plant, it was designed as a horizontal pressure vessel (Fig. 72) to contain a fluidized bed with the shape of a long, stretched channel to allow for long residence times. It consists of four parts (modules) plus the two ending pieces. The coal is introduced through several inlets in the first module, where mainly the pyrolysis process takes place. It moves longitudinally through the reactor as a plug flow. The gasification zone spreads over the other three modules. In the fourth module, the remaining ash is cooled and removed. Each module contains steam inlets in the bottom section and an immersion heat exchanger bundle, through which heat is transferred from the hot helium to the fluidized bed. For coal gasification with nuclear process steam, the steam is used for drying and preheating the reacting materials, and for generating electricity and oxygen.

From the pyrolysis to the gasification zone, a sharp increase of the fluidized bed density from 150 to 250 kg/m^3 is expected. Therefore an overflow weir is foreseen, to avoid back-mixing of the pyrolyzed coal. Also, the dust formed in the pyrolysis zone is collected in a sieve before passing on to the gasification zone and recirculated. Some characteristic data of the prototype gas generator for both the catalytic and non-catalytic version are given in Table 17.

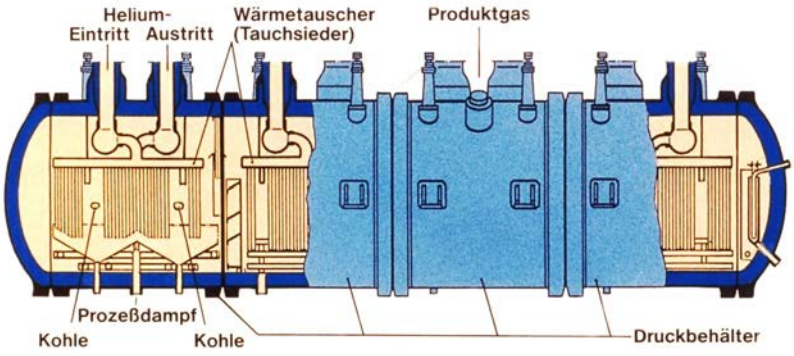

FIG. 72. Schematic of an industrial-scale gas generator for allothermal steam–coal gasification [218].

TABLE 17. MAIN DATA OF PROTOTYPE GAS GENERATOR FOR PNP STEAM–COAL GASIFICATION [218]

	Non-catalytic	Catalytic
Thermal power (MW)	340	
Length (m)	~33	
Outer diameter (m)	7.2	
Heat exchanging surface (m2)		
1st module (pyrolysis)	425	
2nd module (gasification)	535	
3rd module (gasification)	612	
4th module (gasification)	612	
Helium flow (kg/s)	94.4	
Helium inlet temperature (°C)	895	
Helium pressure (MPa)	~4.1	
Height of fluidized bed (m)	1.9–3.4	
Coal input (t/h)	27.3	69.3
Steam flow (t/h)	177	190
Catalyst (t/h)	—	3.27
Gasification pressure (MPa)	~4.3	
Gasification temperature (°C)	800–900	
Raw gas production rate (Nm^3/h)	77 923	219 818
Degree of gasification (%)	~93	

With the concept of an ‘Industrial Plant Coal Gasification Ruhr’, it was that the market introduction of nuclear take place in several steps: (i) construction of an autothermal Ruhr 100 gas generator with a coal throughput of 1 million t/a of coal for SNG production at a rate of 0.6 billion Nm^3/a; (ii) expansion to three gas generators, with one to be based on hydrogasification; (iii) connection with a 700 MW(e) coal power plant for the supply of process steam and electricity; and (iv) replacement of the coal power plant with an 1800 MW(th) HTGR to supply 400 t/h of process steam (400°C, 10 MPa) plus 600 MW of electricity.

In the 1980s, there was also a concept elaborated to convert the existing AVR reactor in Jülich to a process heat plant for steam–coal gasification. The gas generator was planned to be integrated into the confinement of the AVR. Its vertical arrangement has the advantage that in combination with a lower gasification pressure of 2 MPa less steam is required. Coal throughput was foreseen to be 7.8 t/h. Due to the low conversion rate of ~50%, a higher coal throughput and the production of a significant amount of fine coke (4.2 t/h), besides the 11 000 Nm^3/h of product gas, were expected.

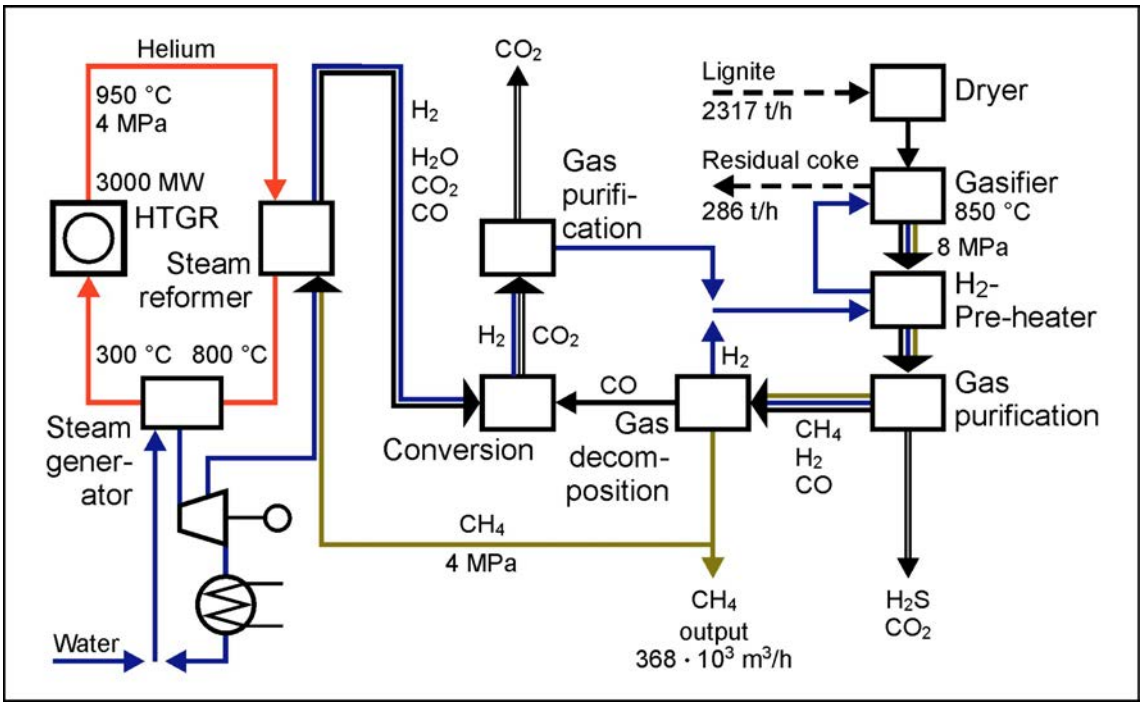

FIG. 73. Schematic of hydrogasification of lignite with nuclear process heat plant PR-3000 [216].

4.2.2. Nuclear hydrogasification of coal

The hydrogasification process can also be combined with a nuclear heat source. But unlike steam–coal gasification, the nuclear heat is not coupled directly to the gasification reactor. Different from the steam–coal gasification process, for the PNP nuclear hydrogasification of coal it was planned to directly use the steam–methane reformer for heat transfer from the hot helium to the methane–steam mixture. An intermediate heat exchanger was — at least in those days — not considered necessary. The drawback seen was the more complicated exchange of the catalyst in the nuclear steam reformer. Figure 73 shows the flowsheet of the PNP hydrogasification process.

Since two variants of hydrogen production exist, there are two alternatives of nuclear involvement [219]. The one variant is steam–methane reforming, where a part of the product gas methane is drawn off and the high temperature nuclear heat is used for the endothermic reforming reaction and to dry the lignite feed. The remaining low temperature nuclear heat is taken for steam and electricity generation. The hydrogen produced is routed at a relatively low temperature (~400°C) to the gas generator, where the gasification of coal takes place in an exothermic reaction at 800–900°C and 8 MPa. The partial pressure of the hydrogen strongly influences the methane production rate. About 40% of the H_2 reacts with the coal to methane, while 60% is recycled after gas treatment to the gasifier. The CO is added to the raw and process gas, while the methane is mixed with steam and fed to the steam reformer. Residual sulphur free coke can be either utilized as high-grade coke or further gasified in a pressurized coal gasification plant.

In the second variant, the nuclear heat is taken to preheat the hydrogen produced during the gasification process itself, i.e. by the water gas shift reaction, which occurs at 100%. Due to the endothermic character of the shift reaction resulting in much lower heat production in the reactor, the gasification agent hydrogen needs to be preheated to 800–950°C. Nuclear heat is also used for steam production and the residual power for electricity generation. Compared with the first variant, it has a simpler process scheme. A drawback is the fact that high gasification pressures (8 MPa) are needed, at least if the focus is on SNG production and high gasification rates, whereas the HTGR (PR-3000) would be operated at 4 MPa.

Between 1976 and 1982, the Rheinische Braunkohlenwerke, Wesseling, investigated the hydrogasification process in a 1.5 MW semi-technical test facility with both lignite and hard coal [219, 220]. The vertically arranged reactor of 8 m height contained a fluidized bed of 0.2 m diameter where the gasification agent hydrogen was injected. The hydrogen was electrically preheated to 750°C and could, if necessary, be further heated to 1000°C by

partial combustion. System parameters could be varied in a broader range. For temperatures between 820 and 950°C and pressures between 5.5 and 9.5 MPa, carbon gasification degrees of up to 75% and methane contents in the product gas of up to 50% were achieved. A part of the hydrogen was used as a carrier medium for the coal input. Due to the exothermic character of the reactor, a direct heat input is not required. With residence times varying between 20 and 40 min, gasification degrees (for lignite) were up to 75%. The main data of the experimental facilities and the design of a commercial size hydro-gasifier are listed in Table 18 [215].

The test facility was operated for about 27 000 h, with more than 12 000 h under gasification conditions. The throughput was 100 kg/h of carbon, corresponding to about 320 kg/h of lignite or 160 kg/h of hard coal, the total quantity gasified was 1800 t.

From 1983 to 1985, a follow-up pilot plant was operated over 8300 h, with half of the time under coal gasification conditions with high availability. Unlike the semi-technical plant, the follow-up plant included all post-processing components of gas treatment up to the stage of SNG production. The plant had a throughput of 9.6 t/h, corresponding to a total thermal power of 50 MW. Gasification of more than 38 000 t of brown coal was made to yield a total of 19 million Nm^3 of SNG, whose fraction in the raw gas was between 22 and 36%. The SNG production was at a rate of up to 6400 Nm^3/h. For catalytic gasification conditions, material problems ultimately were not solved [221].

Both the semi-technical and the pilot plant were, apart from lignite, also used for testing whether or not hydrogasification is feasible with the mostly caking hard coal using a gasification agent of either pure hydrogen or mixtures of H_2, CO and steam. Results have shown that the reaction capability of hard coal is significantly smaller than that for lignite. Due to the specific kinetics of hydrogasification, residence times for complete gasification were comparatively long. Therefore, a degree of gasification of ~65% was considered reasonable, requiring residence times of about 30 min at 9 MPa and 900°C. Beyond this value, residence times would be uneconomically long. Gasification degrees were higher for lignite and lower for anthracite coal. Caking coals were also found to lead to agglomeration near the coal inlet resulting from poor mixing with the fluidized bed and eventually preventing further operation.

TABLE 18. MAIN DATA OF HYDRO-GASIFIERS AT DIFFERENT SCALES [215]

	Semi-technical plant	Pilot plant	Large scale plant
Operation	1976–1982	1983–1985	—
Thermal power (MW)	1.5	50	3000
Length (m)	8		
Inner diameter (m)	0.2	1.0	3.2
Dry coal input (t/h)	0.32 (lignite) 0.16 (hard coal)	9.6	2200 (lignite)
Coal grain size (mm)	<1		
Residence time (min)	9–80 (lignite) 28–38 (hard coal)		
Hydrogen flow (Nm^3/h)		6 000–12 500	
Height of fluidized bed (m)	1.9–3.4	3–6	4.0
Gasification pressure (MPa)	5.5–9.5 (lignite) 8.0–8.7 (hard coal)	6.5–12	8
Gasification temperature (°C)	820–950 (lignite) 940–960 (hard coal)	850–930	850
Raw gas production rate (Nm^3/h)		<16 000	380 000 (methane)
with fraction (%) of CH_4	≤48	22–36	
Degree of gasification (%)	≤82 (lignite) ≤47 (hard coal)	50–60	<60

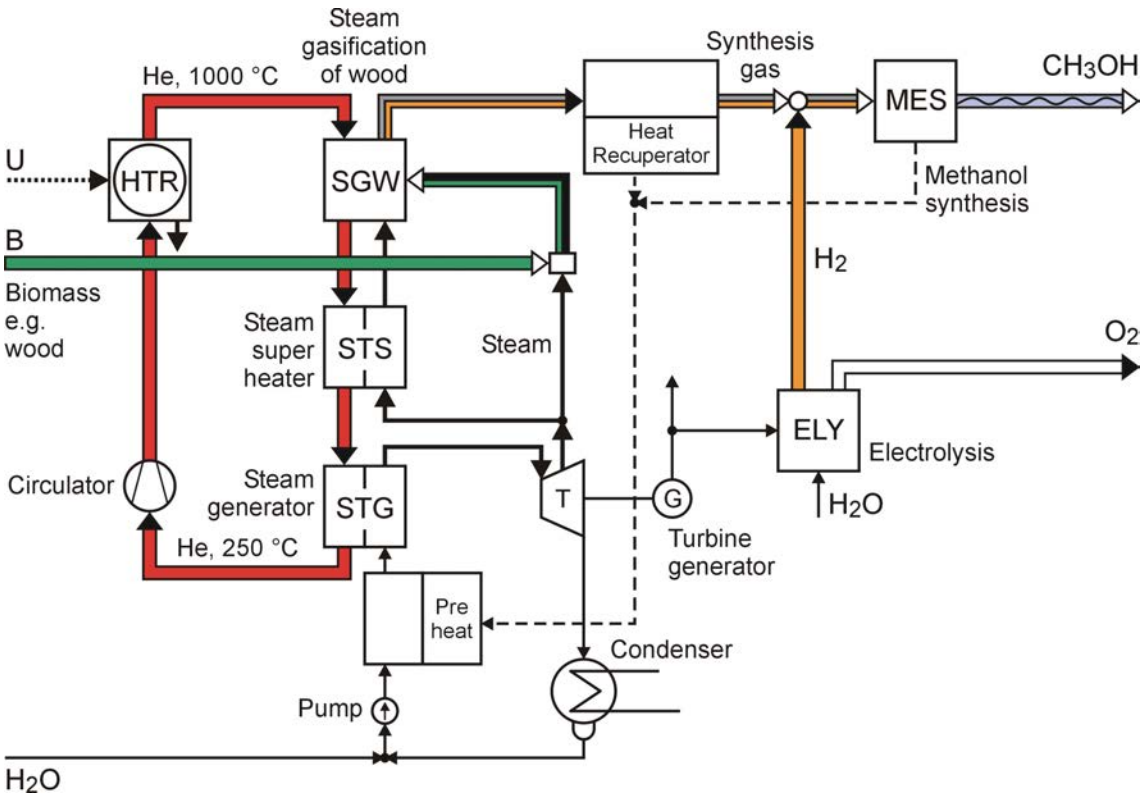

FIG. 74. Schematic of wood gasification with HTGR [222].

4.3. THERMOCHEMICAL CONVERSION OF BIOMASS WITH HTGR

As an alternative option, nuclear process heat from an HTGR can also be utilized for the production of energy alcohols from biomass, representing a CO_2 neutral production process by means of a CO_2 free primary energy input. For the generation of methanol (H:C ratio of 4) from biomass, e.g. wood (H:C ratio of 1.5), additional H atoms are needed, which means additional energy. The process could also be used for SNG production; however, energy alcohol has the advantage of being created in the user friendly liquid state.

A possible process flow scheme is shown in Fig. 74. Apart from the HTGR as the nuclear process heat source, the principal component is the gasifier for wood (SGW) heated by the primary coolant helium, and also receiving steam from the steam superheater (STS). The methanol synthesis unit (MES) receives the input flows synthesis gas from the SGW plus hydrogen from an electrolyser (ELY). The efficiency of the total process proposed has been assessed to be 52%; the product yield would be about 140% [222].

4.4. LOW TEMPERATURE ELECTROLYSIS

Nuclear energy in the form of the electricity generated from current and evolutionary water cooled reactors can be directly used for splitting water to produce hydrogen. Low temperature water electrolysis is a currently available technology (see Section 3.3.1). Since the electrolysis process can be decoupled from the power plant, electrolysis allows for decentralized production of hydrogen. Water electrolysis, however, is attractive only during off-peak hours at power plants, when electricity prices and demand are lowest, or when high-purity hydrogen is needed.

The obvious advantage of water electrolysis is the fact that the infrastructure in the form of electricity grids is already widely available and the source for the electricity can be changed without the need to replace the hydrogen production unit. Oxygen and heat by-products are considered to improve the system economy.

An option for the transition stage is small scale production of hydrogen using the hydrolysis process together with electric power systems. A blend of nuclear and wind energy (‘Nuwind’) to provide emission free and

economically feasible hydrogen production has been suggested [223]. The nuclear plant is assumed to deliver electricity in periods of low wind electricity production.

The intermittency of renewable energy sources coupled with varying demand for electricity requires a kind of energy mediator in the form of storage, conditioning and regeneration. The 'Hydrolyser' currently being developed by H2Green, Inc. can effectively mediate energy production and consumption. It uses electricity to charge materials, generates kinetic or potential energy, separates and stores the H_2 and O_2 from water, and generates heat. The intermittent peaks and valleys of electricity supply and demand can be smoothened with H_2 as a storage medium [224].

4.5. HIGH TEMPERATURE ELECTROLYSIS

In the meantime, several countries are reconsidering high temperature electrolysis of steam (HTSE) as a promising option for a future large scale hydrogen production based on nuclear energy to provide steam and electricity, and have started or resumed experimental activities in this area. Research is concentrated on the development and optimization of planar and tubular electrolysis cells, stack design, selection of appropriate materials, and finally the coupling to a nuclear heat source.

4.5.1. Experimental activities in China

In 2005, INET started a five phase R&D work programme on nuclear hydrogen production by HTSE. Phase I concentrated on project initiation and construction of the test facilities. Research activities within the second phase are mainly focused on: a demonstration of the feasibility of using planar SOEC technology for HTSE; development of new materials with corrosion resistant and high performance HTSE; analysis of degradation mechanisms of SOEC cells; optimization of electrolysis cells and cell stacks; and studies of system design to support cycle life assessment and cost analysis for HTSE plants. The achievements so far are the final determination of the fabrication process and the successful development of a single cell of 7 cm × 7 cm size. Stacks with 1, 3, and 5 cells have also been assembled, with the latter to demonstrate a hydrogen production rate of 1.7 L/h over 40 hours. The future phases include design and construction of pilot plant scale equipment to demonstrate H_2 production at a rate of 5 Nm^3/h. The final phase will be coupling of the process with a commercial HTGR plant [225–227].

Figure 75 presents the results achieved with regard to the oxygen electrode materials investigated, showing the ASR parameter, which is low for high performance of the electrode. Data reveal that the BSCF/YSZ material is a strong candidate compared with the commonly used materials LSM, LSC, and LSCF.

4.5.2. Experimental activities in the European Union

Within the European Union's FP-6, the research project Hi2H2 studied water electrolysis at high temperatures. Experimental work was concentrated on the performance of two types of planar SOFC design. Steam electrolysis was successfully demonstrated at high current densities and high efficiency on single cells. Record high values of ~2 A/cm^2 at a cell voltage below thermal-neutral voltage and ~3.6 A/cm^2 at 1.48 V in a reversely operated YSZ electrolyte based SOFC cell have been achieved so far [228]. In durability tests of up to 2500 h of operation of single cells, a maximum degradation of about 2%/1000 h at 0.5 A/cm^2 and temperatures between 800 and 950°C has been observed. Performance tests have also been conducted with electrolyser stacks of 250 and 600 cm^2 of active area for more than 3500 h at 800°C. An increase of steam content was observed to improve stack performance and to lower the degradation rate to 6% per 1000 h [229].

4.5.3. Experimental activities in France

CEA in France has been pursuing a major HTSE development programme since 2004. Both planar and 3-D cells have been manufactured and mechanical behaviour was tested under typical HTSE conditions [230]. Three experiments of more than 650 h were conducted using a 20 HTSE cell stack with 600 cm^2 of active cell surface. Problems to be investigated are the chromium evaporation, which leads to cell pollution and thus performance loss, and thermal cycling [231].

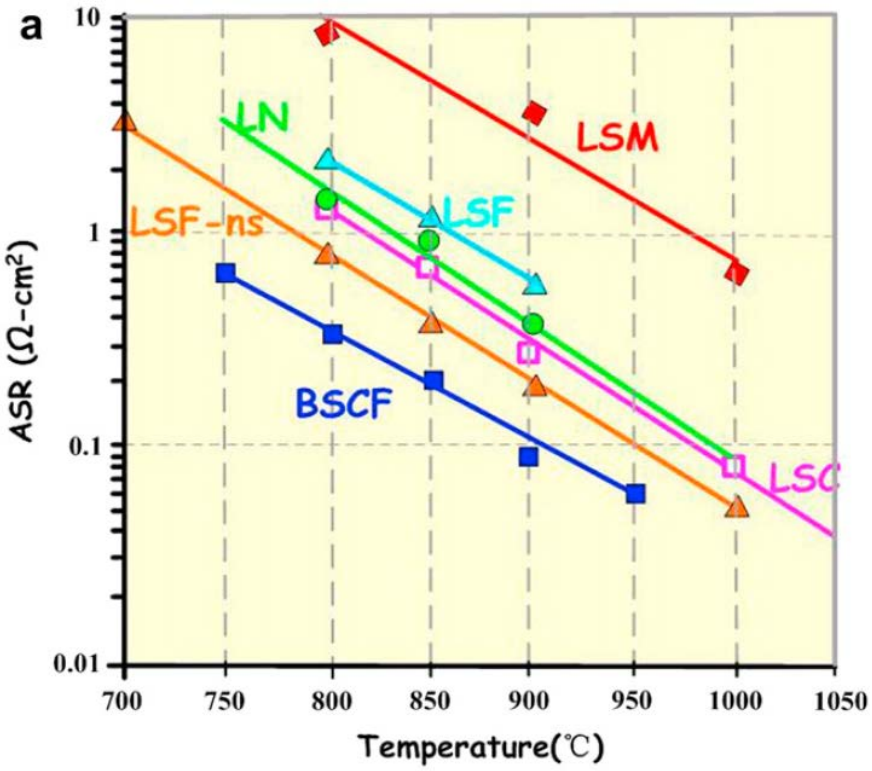

FIG. 75. Comparison of different oxygen electrodes [226].

4.5.4. Experimental activities in Germany

High temperature electrolysis of steam was investigated in the 1980s by the German company Dornier in the process called 'HOT ELLY'. An electrolysis tube consisting of 10 solid oxide cells (10 mm length each, 13 mm diameter) in series with porous thin layers as electrodes was used to produce H_2 at a rate of 6.78 NL/h at 997°C with an applied power of 21.7 W, achieving an efficiency of 92% [232, 233]. The top right part of Fig. 76 shows the German design of a 2 kW HOT ELLY module [232]. The module demonstrated longer term stability of the hydrogen electrode at 995°C with practically no degradation over 1000 h. It also confirmed the lower electricity requirements. Still, total production costs, of which 80% were for electricity, were deemed too high. As technology progressed, Dornier and others moved to the fabrication of planar electrolysis cells. The two design concepts, planar and tubular, are shown in Fig. 76.

4.5.5. Experimental activities in Japan

JAEA has tested both planar and tubular versions of high temperature electrolysis cells. The planar design appeared to be the most effective, but also the most fragile one. The limits of the performance of the tubular design were attributed to the presence of the tube, which limits the vapour flow, and ohmic losses in electrical connections. Current densities were demonstrated between 0.3 and 1 A/cm^2.

The constraint induced by thermal cycling and the variation of dilatation coefficients are major remaining problems. Also, equipment costs are still very high: current evaluation reveals investment costs to be around twenty times those for low temperature electrolysis, but these are expected to decrease rapidly.

HTSE was later also tested by JAEA in a bench scale facility, with the main aim being to test steam electrolysis under HTGR typical conditions of 850–950°C and to derive design data on the process characteristics [49]. The experiments were conducted in a serial arrangement of 12 tubular cells, each cell with a length of 19 mm, and a YSZ electrolyte between a porous Ni cermet cathode and a porous $LaCoO_3$ anode. Steam was supplied at a rate of 0.32 g/min. Hydrogen yield at a temperature of 850°C was 4 NL/h, which increased with temperature (and

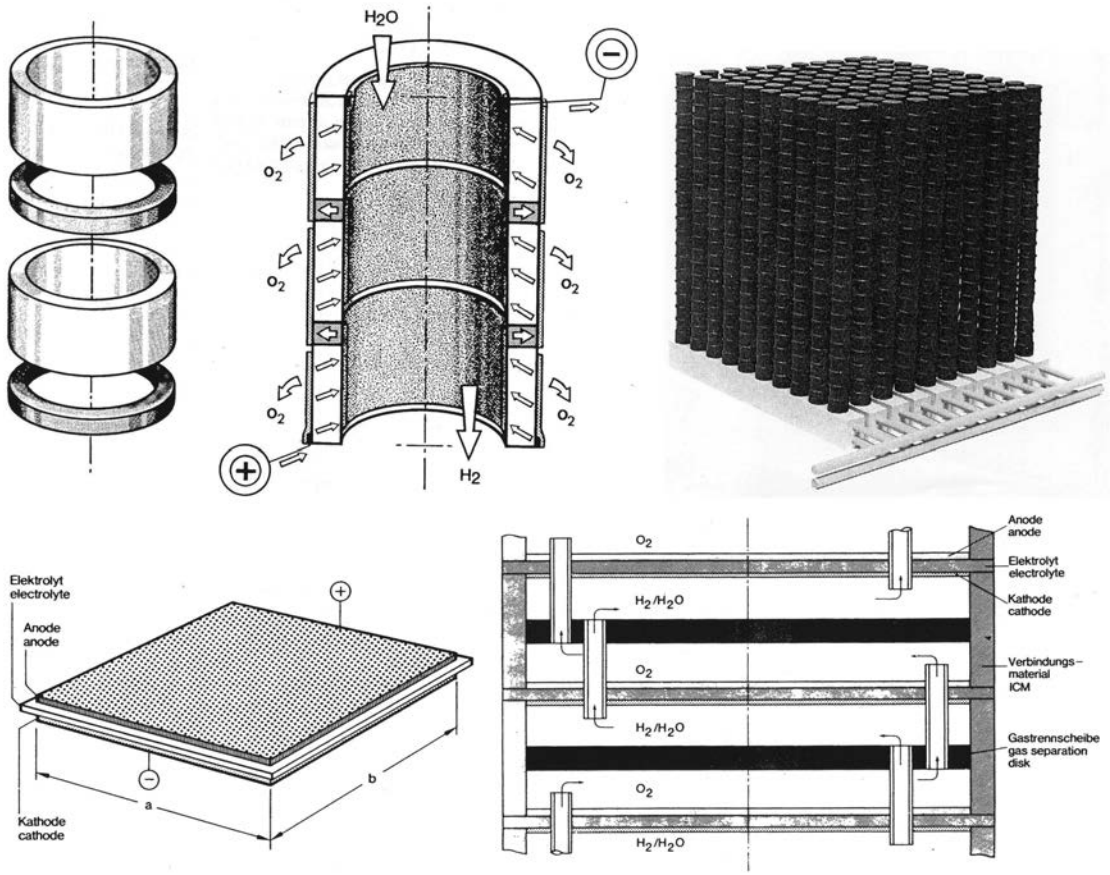

FIG. 76. Concepts of tubular (top) and planar (bottom) SOEC [232, 233].

voltage) from 3.8 NL/h at 850°C to 4.3 NL/h at 900°C and 6.9 NL/h at 950°C. The steam conversion ratio was below 40%.

Tests were also started with planar electrolysis cells. The planar cells consisted of a 0.3 mm thick, 100 mm^2 YSZ plate, with electrodes less than 0.03 mm thick attached on either side. The maximum hydrogen production rate achieved at 850°C was 2.4 NL/h; the specific production rate per cm^2 was even higher than for the tubular cell at 950°C. Efficiencies achieved were still at a very low level, e.g. from a solar furnace or a high temperature nuclear reactor. This activity at JAEA has also been terminated in the meantime.

The Toshiba company is working on an SOEC based hydrogen production plant with a nuclear reactor to deliver the steam [234]. The SOEC is of the tubular type, with an yttria-stabilized zirconia electrolyte. An appropriate hydrogen electrode catalyst for the 800–900°C operation temperature range is a mixture of metallic Ni and YSZ, while for the O_2 electrode, strontium-doped lanthanum manganite is taken. A prototype single cell with an approximate diameter of 12 mm is shown in Fig. 77. A prototype unit contains nine single cells. Each of the nine cells has an active electrode area of 50 cm^2. The hydrogen production efficiency is estimated to be ~50% at 800–900°C operating temperature.

4.5.6. Experimental activities in the United States of America

4.5.6.1. Electrolysis of steam

In the USA, INL in conjunction with the SOEC stack manufacturer Ceramatec Inc. has been conducting a comprehensive experimental programme since 2003 aimed at testing SOEC stacks combined with materials research and detailed modelling with computer fluid dynamics (CFD) codes and with process flowsheet analyses. Starting with 2 W, 2.5 cm^2 button cells, both cell and stack sizes have gradually increased. A bench scale

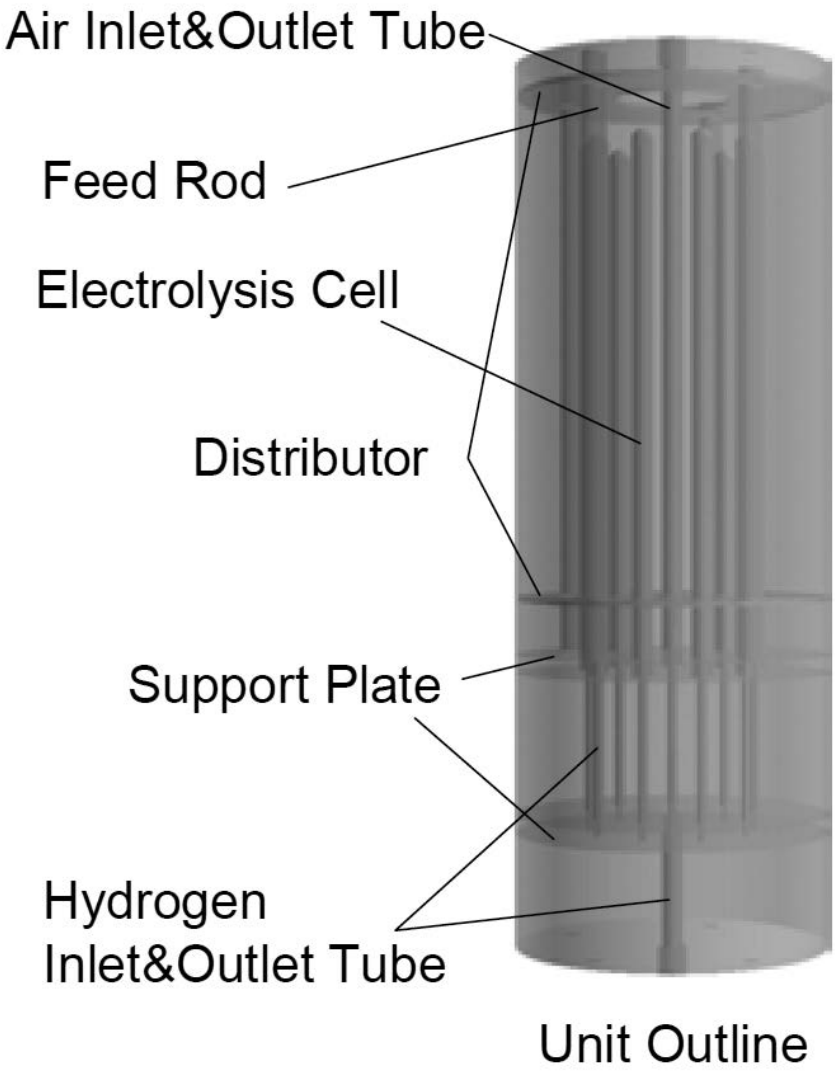

FIG. 77. Design of prototype unit with nine tubular type SOECs [234].

experimental facility has been used at INL for testing steam electrolysis and co-electrolysis in both button cells and stacks with cell surface areas of 64 cm^2 (100 mm × 100 mm) or 324 cm^2 (200 mm × 200 mm). In a test in 2005, a hydrogen production rate of 162 NL/h over 197 h could be verified using a 22 cell stack with no problem in stack performance observed. Post-experiment examination has been conducted at ANL [235]. Another test with a 25 cell stack was conducted over 1000 h at ~830°C and achieved a hydrogen production rate of 177 NL/h. The overall performance degradation observed was 20%.

Within the USDOE NHI, an integrated laboratory scale (ILS) HTSE test facility has been developed and constructed at INL. It consists of a total of 720 planar electrolysis cells in three SOEC stack modules with a total power of 18 kW. Unlike previous testing, it also addresses the integration of thermal management, such as preheating of inlet gas flow, high temperature gas handling, heat recuperation, steam generation or hydrogen recycling, and other support systems. Some of the essential parameters of a module are summarized in Table 19.

Slightly superheated steam from the steam generator is mixed with hot hydrogen (to avoid condensation) and then raised to a temperature level of 800–830°C by six electrical heaters before being routed to the electrolysis cells. The module has a cross-flow arrangement in perforated flow channels. The gas mixture leaving the SOEC is composed of at least 50% residual steam which is removed in a condenser.

In 2006, one half of an ILS module (i.e. two 60-cell stacks) was operated over 2000 h, with some parts being sent to ANL for post-test examination (Fig. 78). In 2007, initial testing operations were performed with a single module (~5 kW) over 420 h, yielding an H_2 production rate of about 0.9 Nm^3/h with a certain performance

TABLE 19. OPERATIONAL PERAMETERS OF THE HTSE-ILS [95, 236]

Number of modules	3
Number of stacks per module	4
Number of cells per stack	60
Active area per cell	64 cm^2
Operating temperature	800–830°C
Operating voltage per cell	1.283 V
Inlet stream (mole fraction)	0.9 steam + 0.1 hydrogen
Total power	18 kW
Input flow rates	160 Nl/min of steam 17.4 Nl/min of hydrogen
H_2 production rate	5.65 Nm^3/h

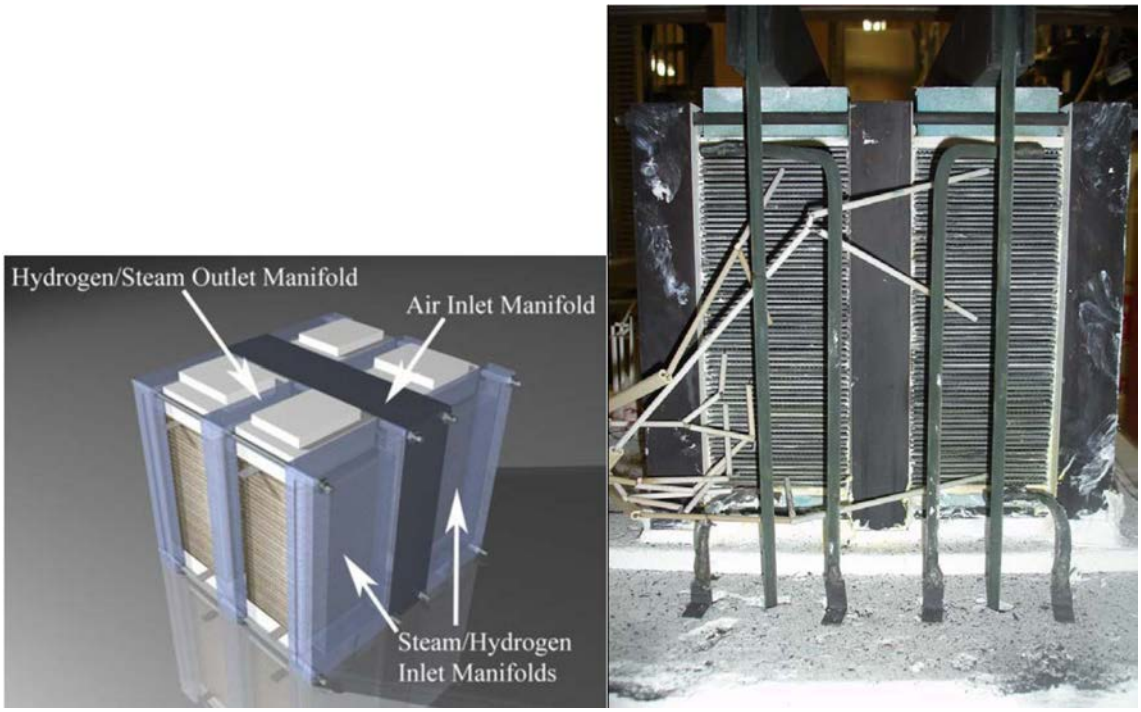

FIG. 78. Single ILS module (left), cell stacks after first test in ILS (right) [95].

degradation observed during the first 250 h and no further degradation observed afterwards [95]. In 2008, the ILS was expanded to operations with all three modules, with three parallel gas heating and delivery loops, and activation of the H_2 recycling loop. The test was conducted for 1080 h with an average H_2 production rate of 1.2 Nm^3/h peaking at 5.7 Nm^3/h after about 17 h. Degradation was observed over the first 480 h, probably due to condensation in the H_2 recycling system. The condensation led to gradual delamination of the oxygen electrode from the electrolyte, and thus to an increase in the cell resistance and a decrease in hydrogen production. After modification of the hydrogen recycling system, the degradation stopped in two modules, while it continued in the third one [83].

4.5.6.2. Co-electrolysis of CO_2 and steam

Since 2006, efforts have been made to demonstrate co-electrolysis, the simultaneous electrolysis of CO_2 and steam, to produce synthesis gas. In the 2055 h half-module test, a set-up of two stacks with 60 planar cells each

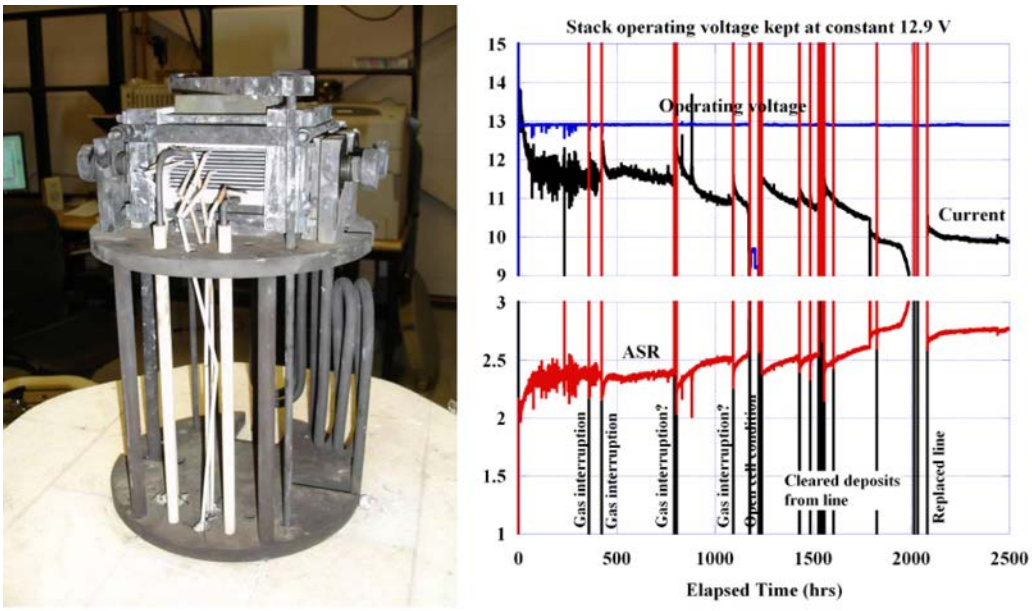

FIG. 79. Ten-cell stack (left) and its performance during a 2500 h test (right) [240].

operated initially at a temperature of 800–825°C with a steam-hydrogen-nitrogen feed stream. During the time period between 168 and 1168 h, the feed was changed by replacing half the steam with CO_2. Performance degradation was found to be ~46% over the whole test, apparently not influenced by the operation with CO_2 [237].

As part of the HYTEST programme for testing hybrid energy systems at INL, the HTSE apparatus was coupled to a new reverse shift reactor and methanation reactor to produce synthetic methane. In a first phase set-up, the total process was demonstrated over 60 h as part of a longer term HTSE test where the CO_2 was taken from a simulated flue gas stack and the H_2 produced in a 10 cm x 10 cm ten cell HTSE stack. The resulting synthesis gas was then routed to the methanation reactor. The integral test included recycling of the streams in order to attain high conversion efficiency and to investigate system dynamics and stability [238].

Extensive post-test analyses of the SOEC components from the above mentioned 1000 h and 2055 h tests have been conducted at ANL and the Massachusetts Institute of Technology (MIT) to elucidate the degradation mechanisms. It has been observed that SOEC stacks exhibit a larger degradation rate compared with SOFCs [237]. The interconnect material was recognized to be a source of different elements (Cr, Mn, Ti, Si) that can form non-conductive interlayers, which may contribute to degradation. On the oxygen side, cracks were identified in the bond layer, which may cause stack degradation. Chromium, which diffuses from the flow field into the bond layer attached to the oxygen electrode, was observed to replace cobalt in the bond material and also to react with it, thus reducing conductivity in the bond layer. Also after long term operation, the oxygen electrode was seen to have densified and delaminated together with the bond layer from the YSZ electrolyte [239].

Chromium diffusion behaviour on the oxygen electrode side of an SOEC is different from that of an SOFC. In an SOEC, oxygen emanating from the electrolyte is moving upwards to the flow field while the gaseous chromium is diffusing against the O_2 flow, meaning that the Cr is concentrating in the upper part of the bond layer. In contrast, in an SOFC, the oxygen (from the air) is moving from the flow field downwards to the electrolyte and carrying with it chromium, which may come from the flow field, deeper into the electrode material.

In 2009, 2500 h of operation of a ten cell stack (Fig. 79) with improved materials demonstrated a significantly reduced degradation rate of 8.2% per 1000 h, which is, however, still higher than that for SOFC.

For high temperature electrolysis, the research efforts were mainly focused on the development of materials for SOECs, including electrolyte and electrode materials. The immediate goal was to reduce the rate of degradation of the cells during long term operation caused by interdiffusion of materials between the electrodes and the electrolyte and by the delamination of the electrodes from the electrolytes due to the formation of oxygen-filled voids near their mutual interfaces. In addition, two key sets of instrumentation for HTSE studies were designed and constructed. One is a laboratory scale HTSE testing loop that can simulate the actual running conditions of HTSE, the other is a high temperature electrochemical analyser used to evaluate electrochemical properties of SOEC

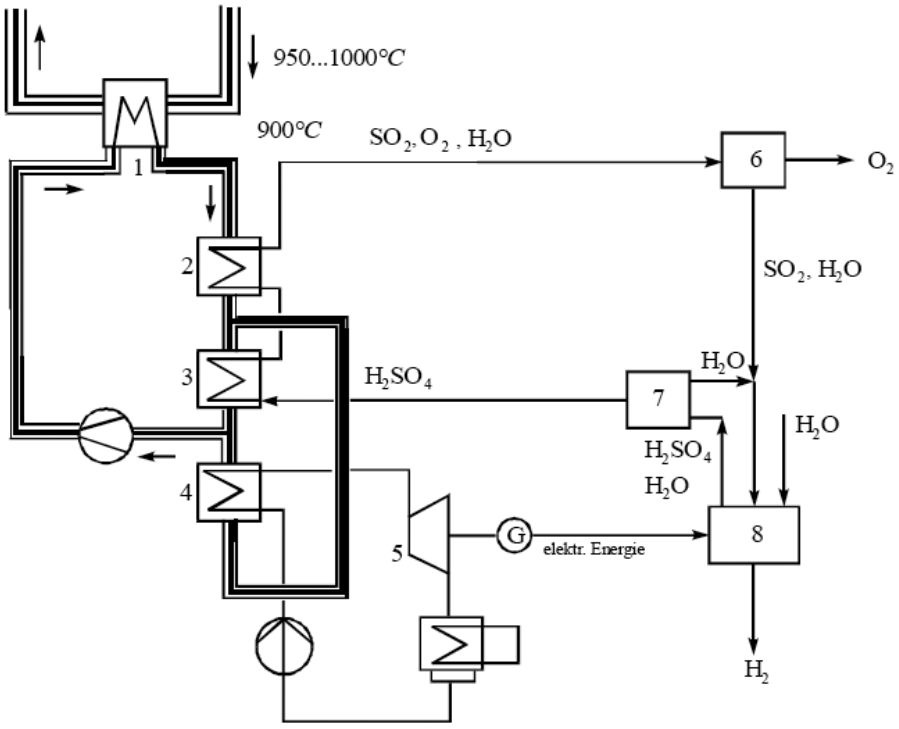

FIG. 80. Diagram of combined system of HTGR plus Westinghouse HyS cycle [198].

components at very high temperatures up to 1200°C. Future steps will be to design, construct and test a pilot scale HTSE facility in long term continuous (~2500 h) operation. Performance criteria have been set at H_2 production rates of 6, 15 and 150 kg/h of hydrogen, corresponding to power sizes of 200, 500 and 5000 kW, respectively. The pilot plant should operate at high pressures and include energy management and product purification [144].

Since the selection in the USA in 2009 of HTSE as the preferred concept for nuclear hydrogen production, various modifications and refinements have been proposed for a further improvement of the original INL reference HTSE design. These modifications include changes in plant configuration, operating conditions and individual component designs. The optimized design operates at a system pressure of 5 MPa and an electrolysis temperature of 800°C. It uses a steam sweep system instead of the original air sweep system in order to facilitate the recovery of the oxygen product gas, which represents a valuable commodity. Also, heat (from the HTGR) is delivered to the HTSE process through an intermediate helium loop to the two steam generators [91].

4.6. THERMOCHEMICAL CYCLES

Thermochemical cycle technology is at a relatively early stage, and only a few cycles have been demonstrated on the laboratory scale. Promising cycles have been or are being analysed in detail with regard to their partial reactions and also with regard to their coupling to a solar or nuclear heat source.

One cycle considered with a high priority is the S–I process (also known as the Ispra Mark 16 cycle) originally developed by the US company General Atomics and later taken up and modified by different researcher groups like the JAEA. Coupling of the HyS cycle with a nuclear power reactor appears to be easier, since heat transfer to the electrolysis cell occurs at a low temperature level. This configuration can help to improve the overall efficiency of the process. A schematic of the potential connection to an HTGR is shown in Fig. 80 [198].

Solar is an intermittent source, therefore an intermediate storage (thermal and/or chemical) would be needed for a continuous process. It would be difficult to drive a thermochemical cycle with a critical phase change. However, solar can be well suited for hybrid cycles if chemical storage at some interface is possible. The electrical part would be still driven by nuclear or another electricity source, while the thermochemical part is driven by solar. A good example is the hybrid S cycle with easy H_2SO_4 storage at the entrance of the sulphuric acid decomposition

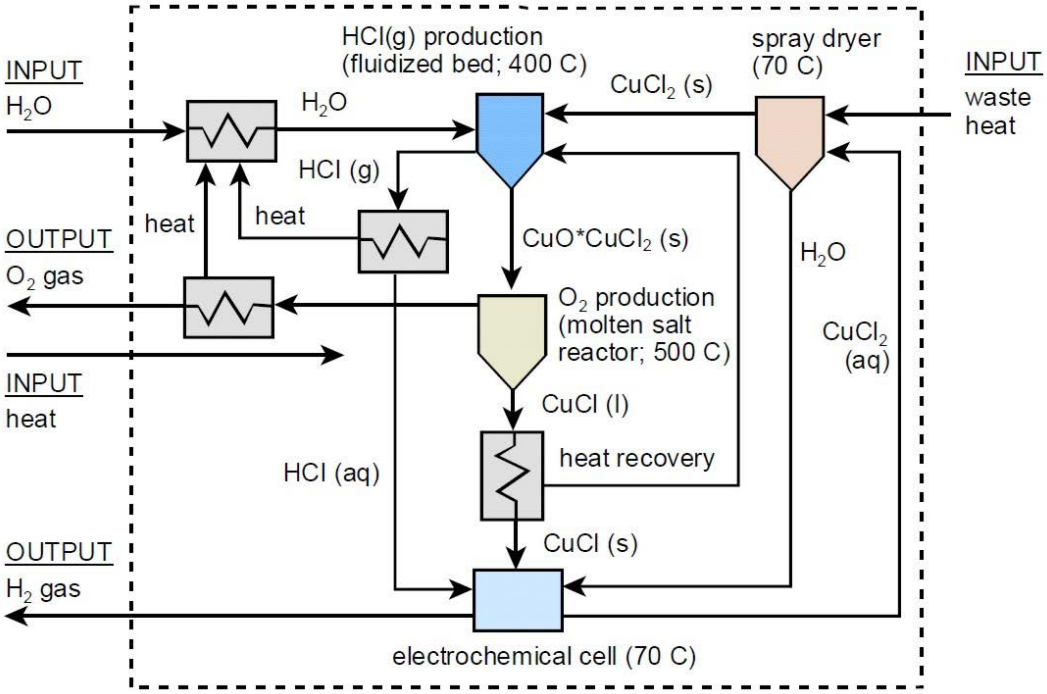

FIG. 81. Schematic of the nuclear assisted Cu–Cl thermochemical cycle [180].

section. However, the S–I cycle can not be readily adapted for use with a solar heat source because one of the reactions, the Bunsen reaction, is carried out near the solidification point of iodine.

4.6.1. Experimental activities in Canada

In a collaborative effort between AECL, the University of Ontario Institute of Technology (UOIT) and other universities, and ANL, Canada is investigating the copper–chlorine cycles for producing hydrogen from nuclear energy (Fig. 81) (or solar energy or waste heat). Cu–Cl cycles with different numbers of process steps have been examined in the laboratory, and various alternative configurations have been proposed [241]. AECL has experimentally demonstrated a CuCl electrolyser where hydrogen is produced at the cathode and Cu(I) is oxidized to Cu(II) at the anode. The reactions at the oxygen electrode worked without a noble metal catalyst, whereas the hydrogen production at the cathode required a noble metal catalyst. Cell reactions were found to be feasible at reasonably low potentials (0.7 V) and with relatively inexpensive electrode materials. One candidate material is carbon because of its high surface area and durability. A test facility with a capacity of 3 kg/d of hydrogen is currently under development [19, 224, 242]. A key component in the electrolytic step developed at AECL is the cation exchange membrane, which needs to have high conductivity for hydrogen ions but low conductivity for copper, as well as good mechanical properties to withstand the aggressive concentrated chloride environment.

ANL has shown the thermodynamic viability of all reactions of the Cu–Cl cycles. In particular, the principle of CuCl decomposition in the electrochemical step was proven in experiments. ANL developed enabling technologies for the Cu–Cl cycle and created a flowsheet of the hydrogen production plant using the Aspen Plus model [178]. An assessment with Aspen Plus yielded a heat to hydrogen efficiency of 54%, which was based on ideal heat transfers. A figure of 43%, however, might be more realistic [19].

In the ANL analysis of the Cu–Cl cycle with the above given efficiency of more than 40%, the $CuCl_2$ enthalpy of mixing with water was — in the absence of relevant data — not considered. However, based on some experimental values of the enthalpy of mixing of $CuCl_2$ with HCl in aqueous solutions [243], the missing enthalpy of mixing is estimated to range between 100 and 200 kJ/mol. This would reduce the efficiency of the cycle to a maximum value around 30%. Indeed, calculations conducted at UNLV [244] have led to a revision of the efficiency below 30%.

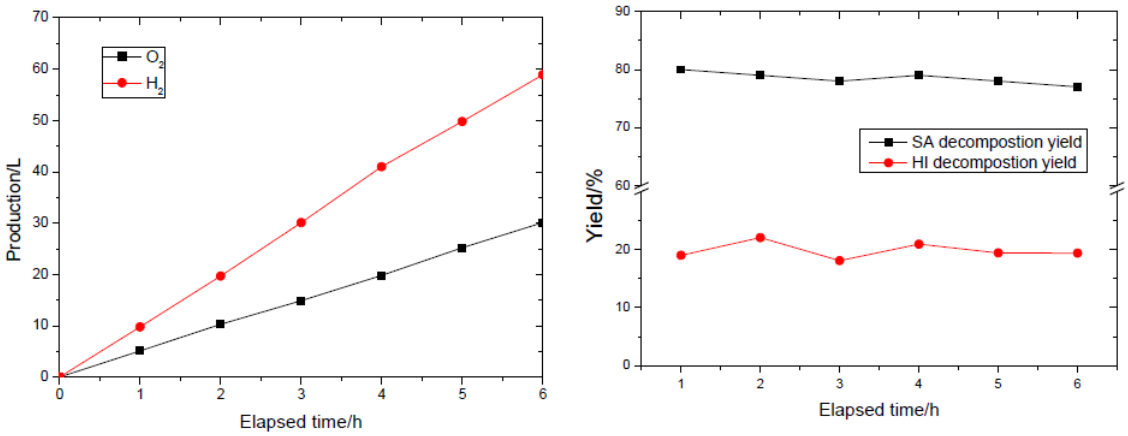

FIG. 82. H_2 and O_2 production (left) and conversion efficiencies of HI and H_2SO_4 versus time (right) in IS-10 test runs at Tsinghua University [246].

A challenge for material development is the high temperature oxidizing atmosphere in the reactor for copper oxychloride decomposition where pure oxygen is produced at 450–550°C. The most promising materials were found to be alloys with high contents of Ni–Cr, which are expected to form corrosion resistant oxide layers on the metal surfaces [19].

4.6.2. Experimental activities in China

Research efforts on the S–I cycle at the Tsinghua University in Beijing have concentrated so far on fundamental studies of the three basic reactions, and related techniques such as separation, concentration and purification are being carried out. In the Bunsen section, the kinetics, separation characteristics of the H_2SO_4 phase and HI_x phase formed and their purification were studied. In the HI section, for the concentration of HI, EED was developed; various parameters affecting the concentration effect were investigated. Platinum catalysts were loaded on different supporters by chemical plating or impregnation and used in the HI decomposition reaction to compare their catalytic effects. The catalyst containing 5 wt% Pt (with a minimum diameter of ~5 nm) supported on alumina prepared by electroless plating shows the optimum catalytic properties for HI decomposition. In the sulphuric acid section, new catalysts were developed and employed in SO_3 decomposition. A performance ranking order was observed to be Pt ≈ Cr_2O_3 > Fe_2O_3 > CeO_2 > NiO > Al_2O_3. For economic and technical reasons, however, the focus is on the development of non-Pt catalysts. Copper chromate and copper chromite with good catalytic performance to SO_3 decomposition reaction present promising catalysts.

Based on the knowledge acquired through these studies, a closed loop apparatus, named IS-10, made of glass and Teflon, with the designed hydrogen generation rate of 10 NL/h was constructed in 2007 to verify the processes for all sections of the S–I cycle. The first phase of the R&D programme has been completed with the successful demonstration of the closed cycle operation in 2009. Figure 82 shows the results of a test run over 7 h with regard to H_2 and O_2 production (left) and the achieved efficiency of 20% for the decomposition of H_2SO_4 and HI to H_2 and I_2 (right) [245]. The test was conducted at atmospheric pressure with temperatures in the Bunsen, HI and H_2SO_4 sections maintained at 80°C, 500°C and 850°C, respectively [160, 246].

Subsequent steps will be dedicated to the demonstration of the whole cycle at larger scales. Phase II will comprise bench scale testing at atmospheric pressure in glass equipment with 100 NL/h H_2 production capacity. Pilot scale testing will be done at high pressure in industrial material equipment with a 100 Nm^3/h H_2 production capacity and a design of an HTR-IS plant will be developed within phase III. Phase IV has the goal of commercialization of the process, expected after 2020 [160].

4.6.3. Experimental activities in France

In France, CEA R&D activities with regard to the Bunsen section are concentrating on a further reduction of excess H_2O and I_2 to dehydrate the HI_x phase by optimizing phase separation, and to minimize side reactions and

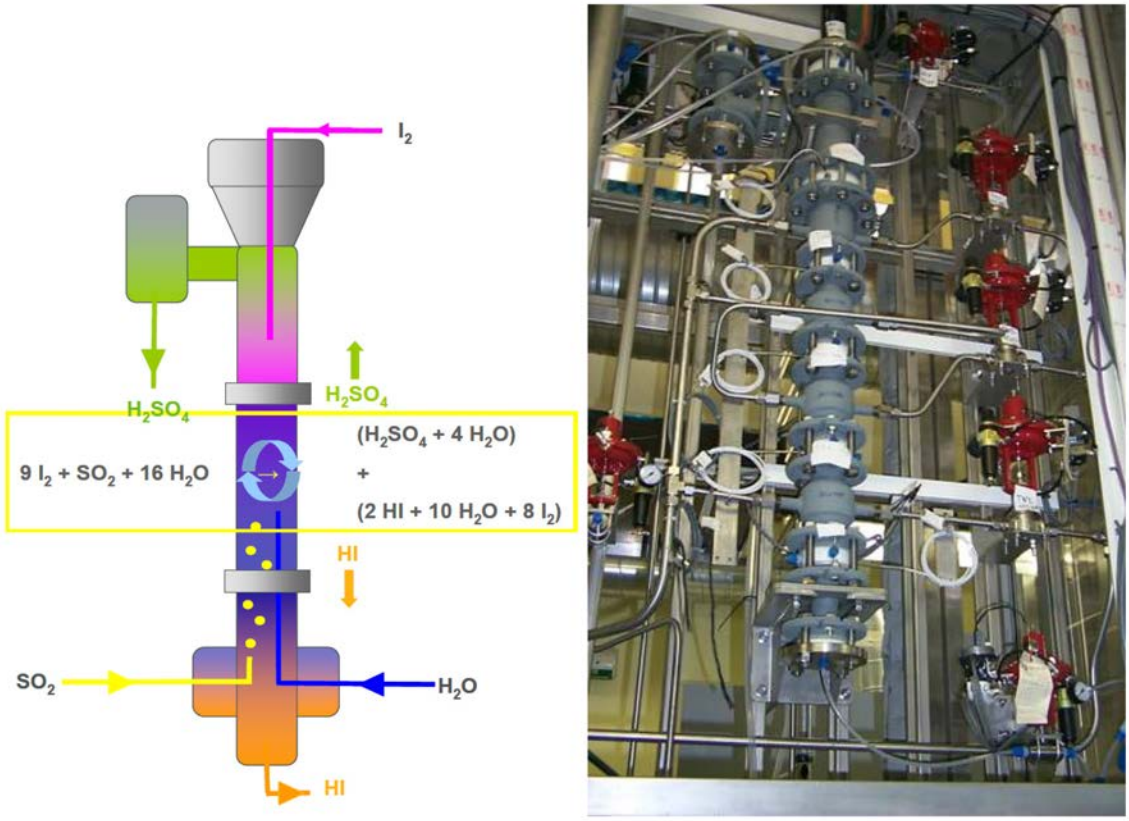

FIG. 83. New development of Bunsen section in France [230].

heat losses. Developed in 2008, a new design for the Bunsen reactor has been proposed. A characteristic feature is its operation in the countercurrent mode (Fig. 83), different from the co-current design of the Japanese and the former GA approach, by using a single reactor for the Bunsen reaction. Better yield, better purity of the phases and a lower level of side reactions are expected from the new design. Data were collected for Bunsen reactor operation at increased pressures [230].

4.6.4. Experimental activities in Germany

In Germany, the Aachen University introduced a reactive distillation column, in which concentration and decomposition processes occur simultaneously [247]. Upward along the distillation column, the HI content in the liquid phase gets richer, and so more HI molecules are likely to escape. Then the vapour phase HI content in the upper region of the column is higher than in the lower region.

4.6.5. Experimental activities in India

In India, studies of fluid mixing and heat/mass transfer in the Bunsen reaction are being conducted using two different reactor designs, a jacketed stirred vessel Bunsen reactor, made of glass, and a jacketed oscillatory baffled Bunsen reactor (OBBR), consisting of a tantalum tube in a steel jacket. In the latter type of reactor, the baffle arrangement creates turbulent eddy mixing and vortices, which lead to a radial movement of the fluid and enhanced heat/mass transfer rates to the reactor wall. The goal is the comparison of energy performance of oscillatory flow mixing versus conventional stirring and the derivation of heat transfer coefficients for the Bunsen reaction fluids [248, 249].

A multistage countercurrent contactor such as the oscillatory baffled column reactor (Fig. 84) is being considered, to enhance mass transfer, heat transfer and product purity [248, 249]. A theoretical analysis indicated better gas–liquid volume mass transfer coefficients. The preliminary design of the Bunsen reaction system can be

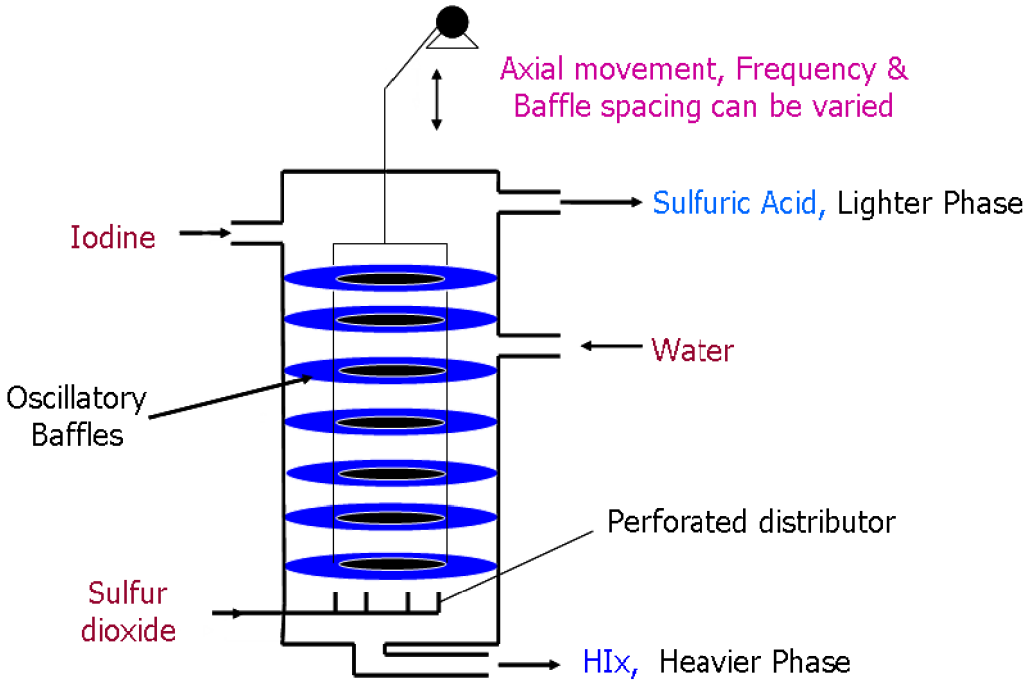

FIG. 84. Indian design of an oscillatory baffled Bunsen reactor [248].

done using simple, analytical and modelling tools, while for a detailed design and scale-up, comprehensive data on the physicochemical behaviour of the reacting system generation need to be obtained.

4.6.6. Experimental activities in Italy

Within the TEPSI project, the Italian National Agency for New Technologies, Energy and Sustainable Economic Development (ENEA) has been investigating the S–I cycle. For the purpose of demonstration of the cycle and examination of many aspects of basic and applied research, a laboratory scale integrated loop facility has been constructed, which is designed for a hydrogen production rate of 10 NL/h. The next step will be the realization of the S–I cycle at a pilot plant scale with a production rate of 80 NL/h of H_2 [250].

4.6.7. Experimental activities in Japan

4.6.7.1. S–I cycle with high temperature reactor

In the mid-1980s, Japan began R&D activities on the S–I cycle. In 1997, JAEA verified the feasibility of the S–I cycle in small scale experiments with a continuous hydrogen production rate of about 1 NL/h over 48 h [251]. In the follow-on step of bench scale testing, continuous hydrogen production in a closed loop over one week was successfully demonstrated [48]. The facility consisted of more than ten process units made primarily of glass and quartz, with a hydrogen production rate achieved of 30 NL/h at an efficiency of 6.4%. The low efficiency was mainly due to the large heat loss in the HI decomposition section. Also, an automatic control system for the Bunsen reaction was applied. The focus was on the automatic control of a long term stable hydrogen production, membrane technology for the HI_x decomposition and screening tests on corrosion resistant materials. The thermal efficiency of the bench scale test, however, was less than 10% due to large heat losses in the HI section [252].

The next step, starting in 2005, was the design and construction of a pilot plant with a production rate of 31 Nm^3/h of H_2. The pilot plant will be operated under the simulated conditions of a nuclear reactor [48] using an existing helium gas circuit to provide helium of 880°C at a system pressure of 2 MPa. A schematic of the test facility is shown in Fig. 85 [253].

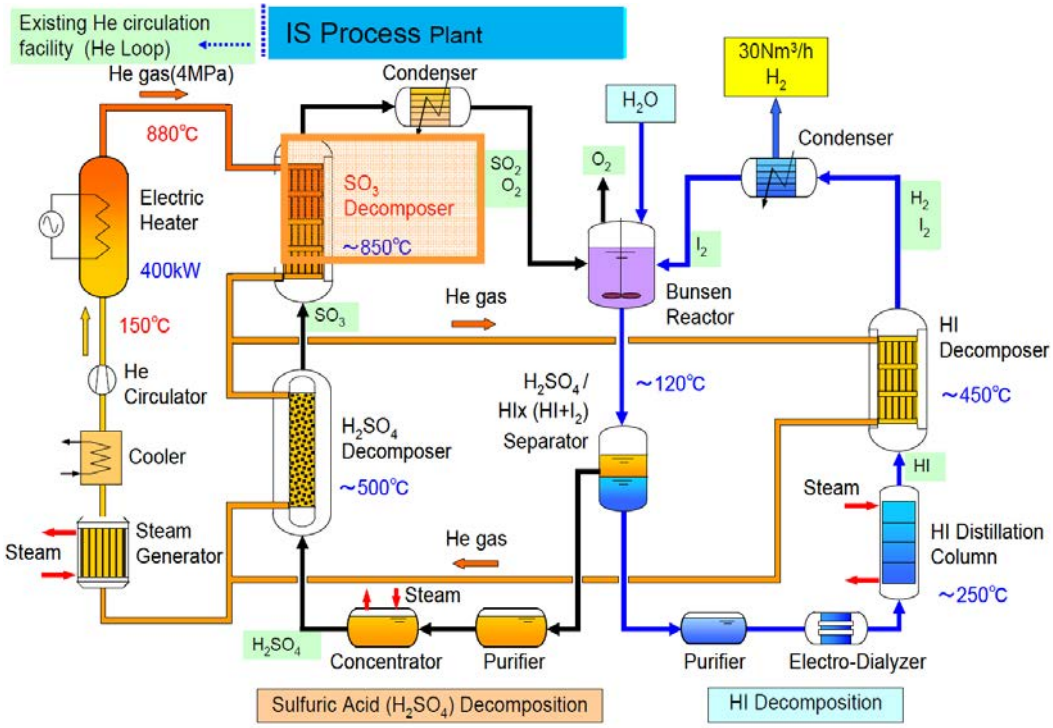

FIG. 85. JAEA hydrogen production test plant [253].

To ensure component integrity in the S–I process, JAEA has initiated a three year construction plan for an S–I process engineering test facility. The facility is to be made of practical materials such as ceramics and glass-lined metals, and will be operated under high pressure up to 1 MPa. All components of the three sections — the Bunsen reaction, the sulphuric acid decomposition and the hydrogen iodide decomposition — are to be verified for their integrity independently by the end of fiscal year 2012. After component verification, the sections will be connected to produce hydrogen at a rate of 0.1 Nm^3/h. The experimental data obtained through these tests will be used to design a nuclear hydrogen demonstration plant for coupling to the existing HTTR plant at JAEA, Oarai.

Precise control of the composition of the reaction product solution is essential for the Bunsen reaction, since deviations from the nominal values may result in, for example, a breakdown of the liquid–liquid separation process or an iodine precipitation. JAEA has developed an on-line monitoring system for composition measurement and control of the reactant feed rates [254].

A survey of other Bunsen reaction routes to overcome excess iodine and water in the cycle is also being undertaken. The electrochemical route, vigorously being pursued at JAEA and ENEA is considered to be an attractive option [255–257]. This route combines reaction and product separation steps and vastly reduces the iodine load of the cycle. However, membranes of required properties have to be developed to generate concentrated product solutions without cross-contamination by eliminating permeation, electro–osmotic drag, etc.

The sulphuric acid decomposer concept for the pilot plant at JAEA is shown in Fig. 86, and some characteristic parameters are listed in Table 20 [258]. The decomposer consists of two vertically stacked multihole heat exchanger blocks made of Si–SiC ceramics with a total height of 1.5 m. The helium gas flows through the inside channels. Test fabrication of the SiC blocks was successfully completed by Toshiba. Helium leak tests verified the seal performance. Other tests were also conducted, such as in a SO_3 decomposer test loop or a H_2SO_4 flow test loop. The dimensions of the SO_3 decomposer component for the pilot plant are a diameter of ~0.7 m and a total height of 3.1 m.

For the HTTR-IS plant, this H_2SO_4 vaporizer component would presumably have a diameter of several metres and a height of ~10 m. Limitation in size also limits the hydrogen production, making a modular concept for this component more practicable. Current investigations are dedicated to single aspects of the S–I cycle. Tests were conducted with a H_2SO_4 purifier to remove the impurities HI, I_2 and H_2O. In leak tests, a helium leakage rate of 1.5×10^{-8} $(Pa \cdot m^3)/s$ at the connection of the SiC blocks was measured [259].

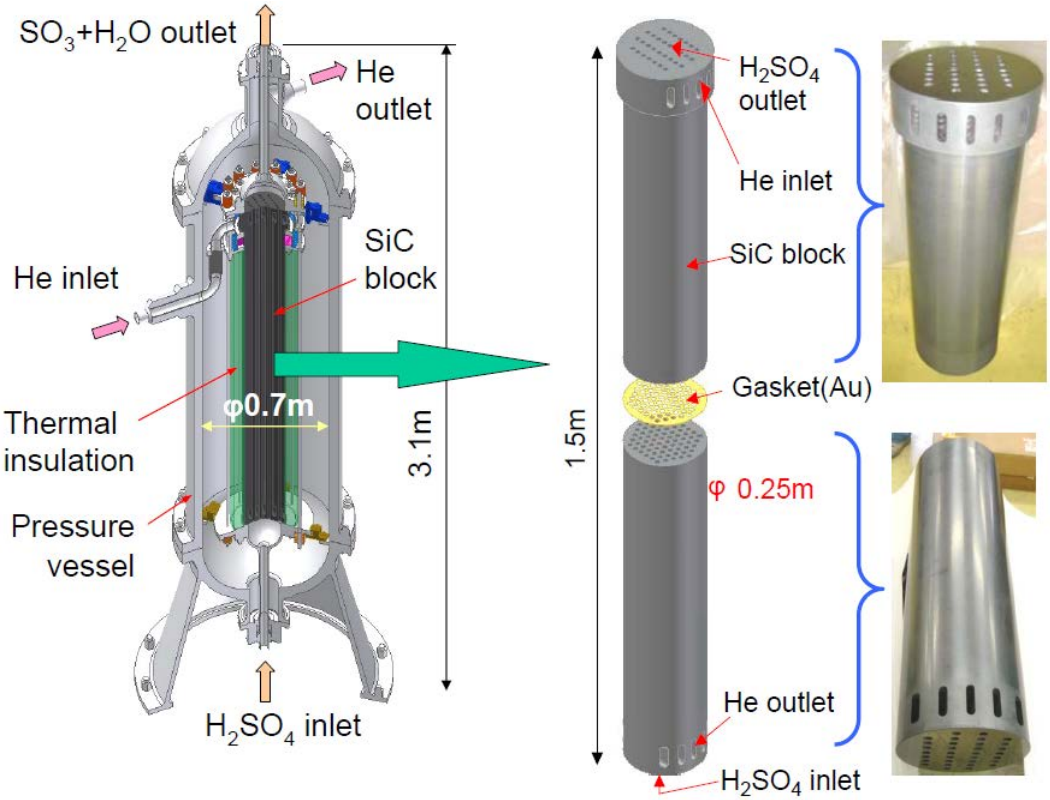

FIG. 86. JAEA prototype heat exchanger for sulphuric acid vaporization [258].

TABLE 20. CHARACTERISTICS OF THE JAEA H_2SO_4 DECOMPOSER FOR THE PILOT PLANT [258]

Primary side	
Inlet/outlet temperature	710/535°C
Pressure	4 MPa
Helium flow rate	330 kg/s
Secondary side	
Inlet/outlet temperature	460/435°C
Pressure (MPa)	2 MPa
Sulphuric acid flow rate	240 kg/s
Sulphuric acid concentration	90 wt%
Quantity of exchange heat	82.7 kW
Maximum heat flux	80 kW/m^2
Number of heat transfer channels	32 (H_2SO_4), 38 (He)
Heat transfer channel inner diameter/length	1.5/148 m

For the SO_3 decomposition step in the pilot plant, a shell and tube type heat exchanger has been selected, as shown in Fig. 87. The decomposition reaction progresses in the SiC tube filled with a catalyst. In order to prevent corrosion and to enhance heat exchange, SiC was adopted as material for the tube. Some important parameters of the SO_3 decomposer are given in Table 21 [259].

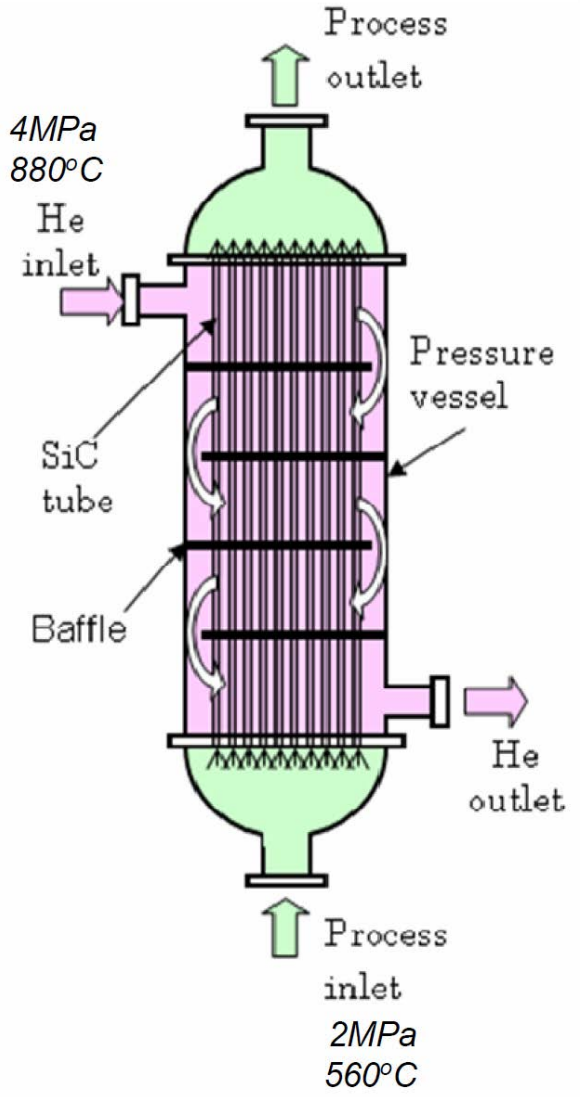

FIG. 87. JAEA shell-and-tube type SO_3 decomposer [253].

TABLE 21. CHARACTERISTICS OF THE SO_3 DECOMPOSER

Heat duty	72 kW
Helium coolant flow rate	0.113 kg/s
Inlet temperature	880°C
Pressure	4.0 MPa
Process gas inlet flow rate	566 mol/h
Inlet composition	90 wt%-H_2SO_4
Process gas inlet/outlet temperature	560/850°C
Pressure	1.5 MPa
Tube inside/outside diameter	30/40 mm
Tube length	2 m
Number of tubes	100
Heat transfer area	18.6 m^2
Overall heat transfer coefficient K	0.656 W/(m·K)
Volume to fill catalyst	0.139 m^3

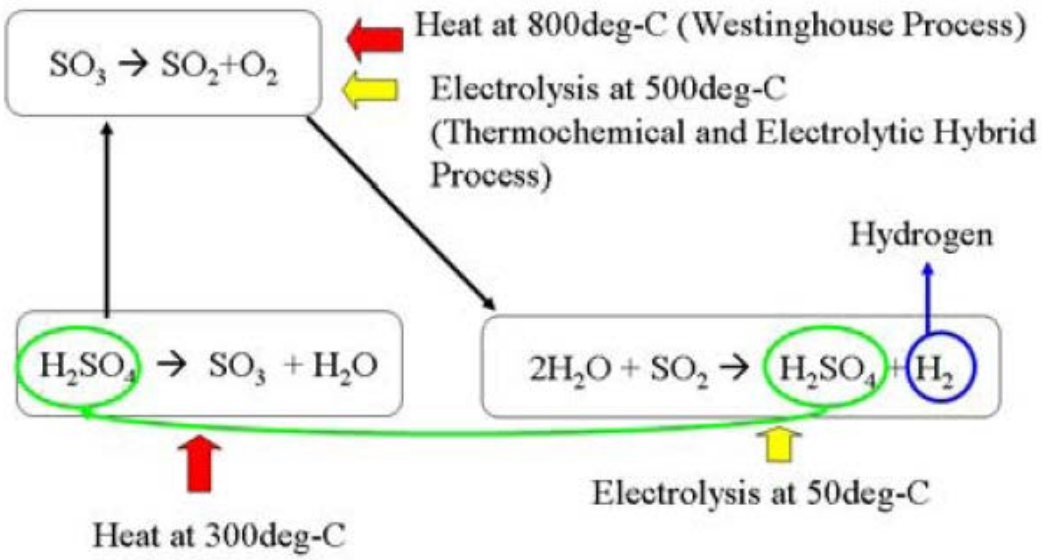

FIG. 88. The JNC cycle as modification of Westinghouse cycle [59].

Since only efficient control of the composition in the HI section guarantees stable hydrogen production, in situ composition measurement techniques are being studied. One option is the employment of radiation (gamma, neutron) probes to measure transmittance through a multicomponent solution [260].

Studying the improvement of the HI section, Japan is concentrating on EED to increase the HI concentration in the azeotropic HI_x mixture solution by applying membrane technology [161]. Its technical challenges arise from the fact that EED demands much electrical energy (thus decreasing cycle efficiency) and that the low mechanical strength of the required membranes causes difficulties for scaling up the facility to a larger plant. Experimental data so far have shown a concentration increase from 10 to 15 mol of HI per kg of H_2O. Also the HI conversion ratio could be increased from 22 to 61% at 450°C using special silica permselective membranes to separate the slightest amount of H_2 produced through catalytic activation in the reactor in order to shift the equilibrium toward the decomposition of HI. Unreacted HI, remaining H_2 and I_2 is then cooled down, resulting in partial condensation of I_2. The liquid I_2 is then separated and returned to the Bunsen section, while the rest is recycled to the hydrogen permselective membrane reactor [252].

4.6.7.2. HyS cycle with fast breeder reactor

In Japan, the former JNC (now JAEA) suggested a modified Westinghouse cycle. It is a thermochemical and electrolytic Hybrid Hydrogen Process in the Lower Temperature Range (HHLT), also called the JNC process, to be connected to a sodium cooled fast breeder reactor (FBR) [261]. At a coolant outlet temperature of 500°C, typical of an FBR, the decomposition fraction of SO_3 is not more than ~8%, which, however, can be raised significantly if electrolysis by ionic oxygen conductive solid electrolyte is applied (Fig. 88). The reaction equations are:

(1) $2\ H_2O + SO_2 \rightarrow H_2SO_4 + H_2$ (>100°C, E = 0.55 V)

(2) $H_2SO_4 \rightarrow H_2O + SO_3$ (>450°C)

(3) $SO_3 \rightarrow SO_2 + 0.5\ O_2$ (>500°C, E = 0.13 V)

where the required voltage for the SO_3 splitting reaction is expected to be less than 0.2 V (0.13 V theoretical) at 500°C.

For the conceptual design of an FBR providing 395 MW(th) and 82 MW(e), hydrogen could be produced at a rate of 47 000 Nm^3/h assuming an overall efficiency of 42% [262]. A drawback of this cycle, however, and adding to the investment cost, is the use of two electrolysers, one in a high concentration acid at lower temperatures and one in a corrosive atmosphere at higher temperatures.

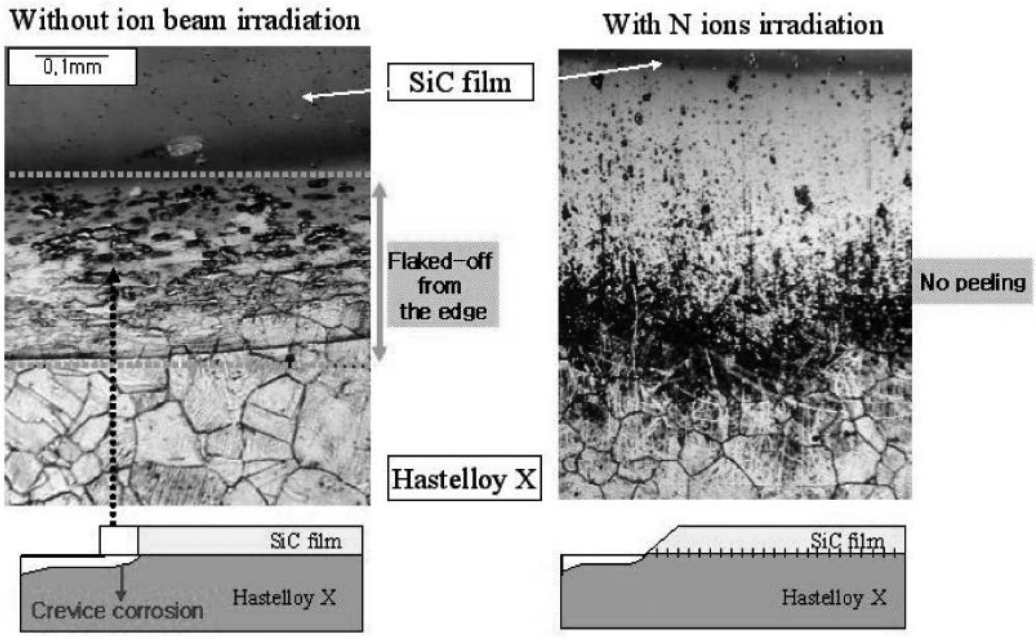

FIG. 89. Effect of ion beam mixing on corrosion resistance [266].

4.6.8. Experimental activities in the Republic of Korea

The Republic of Korea began investigation of the S–I cycle in 2004 with the construction and operation of a small scale process loop made of glass components for a hydrogen production rate of 40–100 Nm^3/h. A simple process for HI_x decomposition based on EED and using a Korea Institute of Energy Research (KIER) silica based catalyst was demonstrated in 2008 in three tests, each of 5 h continuous operation at atmospheric pressure and at a hydrogen production rate of 3.5 L/h including iodine recycling. The next step will be a 200 L/h laboratory scale facility to be operated under pressure [63, 263]. More experimental data are needed to fully understand the HI process and to develop and validate thermophysical models. To avoid corrosion problems for HI components, the materials selected are SiC and Hastelloy C.

The process heat exchanger for H_2SO_4 decomposition currently under investigation in the Republic of Korea is composed of helium channels and sulphuric oxide gas channels. Due to the highly corrosive environment, a composite material with a high temperature superalloy was chosen, where the surfaces in contact with the sulphuric oxide gas are coated with a corrosion resistant, silicon carbide ceramic material. To avoid possible delamination along the interface caused by different material properties between the basis material and the coating, the ion beam mixing technology has been developed to smooth the change of material properties (Figs 89 and 90). This is a process where, in a vacuum, the surface is treated with a beam of high energy ions to pass through the thin SiC film and cause intermixing of the atoms in the surface area, forming a new solid phase different from the substrate or film. Regarding the channels, a hybrid concept is being considered. The helium channels on the primary side have a compact semicircular shape similar to PCHX. The sulphuric acid gas channels on the secondary side are of a plate fin shape, providing sufficient space to install and replace the catalyst for the SO_3 decomposition [264].

An H_2SO_4 decomposition unit was constructed and operated at 900°C and 1.5 MPa using a non-noble catalyst ($Cu/Fe/Al_2O_3$) and ionic SO_2 absorber. The O_2 production rate was greater than 150 L/h [265]. The demonstration of a pressurized S–I cycle is planned as the next step in 2009–2011, with H_2SO_4 decomposition at 1.7 MPa.

At KAERI, a 10 kW process heat exchanger test facility has been erected to study the component lifetime (Fig. 91). It consists of a gas circulator, heaters, hot gas duct, PHX, air cooler and gas supply system. It is operated on the primary side with nitrogen of temperatures up to 1000°C at 4–6 MPa at flow rates of 2 kg/min. On the secondary side, the working fluid is SO_3 gas of 950°C at 1 MPa and a rate of 1 kg/min, which is decomposed in the PHX to SO_2 and O_2. The larger gas channels also take the catalyst. The material is SiC coated Hastelloy, with an ion beam (N_2) treatment applied to fix the ~1 μm SiC layer onto the substrate. So far the PHX has been tested over 88 h with 250°C sulphuric acid [267].

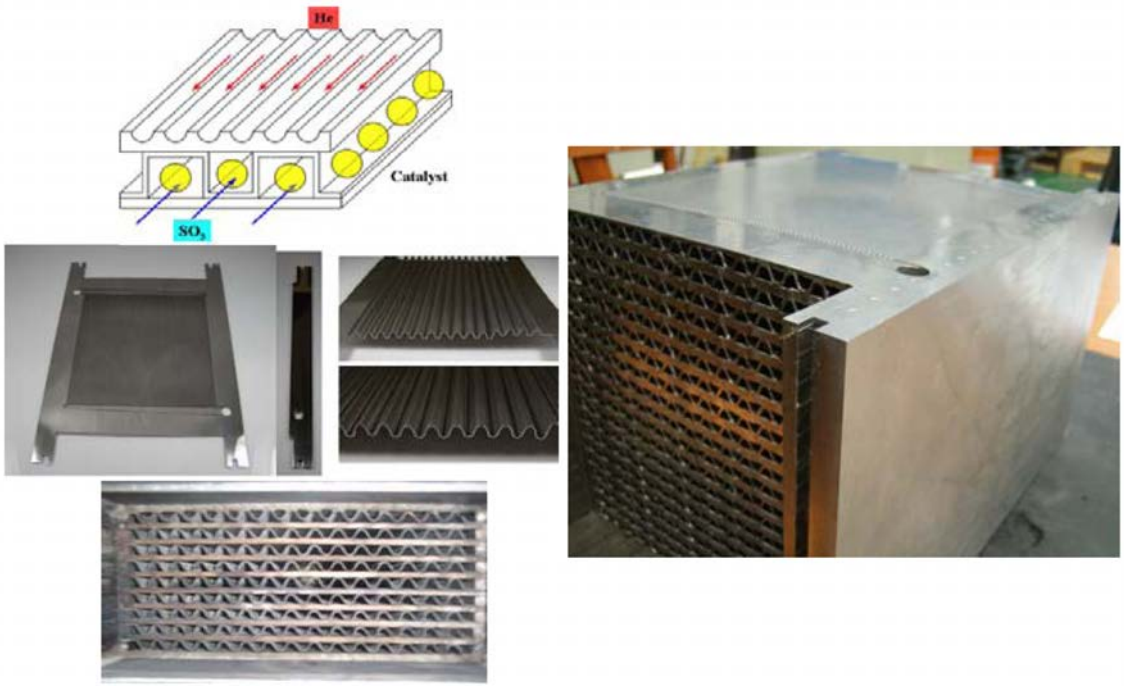

FIG. 90. Mock-up for process heat exchanger investigations in the Republic of Korea [266].

CFD analysis has been applied to develop the concept of a direct heat exchanger for SO_3 decomposition, as shown in Fig. 92. It is based on a ceramic hollow fibre membrane module where the SO_3 mixture (with SO_2, O_2, H_2SO_4 and H_2O) at 450°C is mixed with 920°C hot helium and catalytically (Al_2O_3) decomposed. This requires, however, the successful development of a properly working ceramic membrane for separation of the He–SO_2 mixture [268].

Since the equilibrium conversion yield of hydrogen iodide is very low, to obtain a high decomposition rate the Republic of Korea has suggested the employment of a tank-in-series model for the HI decomposer (Fig. 93). This consists of multiple cascade reactors where each is connected to a selective membrane in a helium chamber, in order to maintain non-equilibrium conditions and thus enhance the decomposition rate [269].

4.6.9. Experimental activities in the United States of America

4.6.9.1. Sulphur–iodine cycle

As part of NERI and in collaboration with General Atomics, CEA and Sandia National Laboratories (SNL), an integrated laboratory scale (ILS) loop for the S–I process has been designed, constructed and operated. A S–I cycle ILS test loop at prototypical pressure and temperature conditions has been constructed by General Atomics in collaboration with SNL and CEA-Saclay (Fig. 94) [270, 271]. CEA designed and tested the Bunsen reaction section, while General Atomics took care of the HI decomposition section and SNL took care of the H_2SO_4 decomposition section. Construction and test operation of all sections was completed in 2008.

In the first phase, the ILS sections were operated in an open loop arrangement under design conditions, i.e. at temperatures between 120 and 850°C and at pressures up to 2 MPa. The new countercurrent flow design of the Bunsen reactor by CEA laid out for H_2 production at a rate of ~110 NL/h was described in Section 4.6.3. For the sulphuric acid decomposition, a bayonet type reactor was selected composed of an outer and inner SiC tube and heated by an electric heater. HI decomposition was based on extractive distillation taking HI_x feed with a 2:8:10 molar ratio of HI:H_2O:I and using phosphoric acid for I removal.

The second phase dealt with initial integrated shakedown operations, control verification, transient response tests and further process improvements. The system achieved a production rate of up to 75 standard litres of H_2 per hour. A flowsheet optimization made by France based on the reference model has shown efficiencies of around

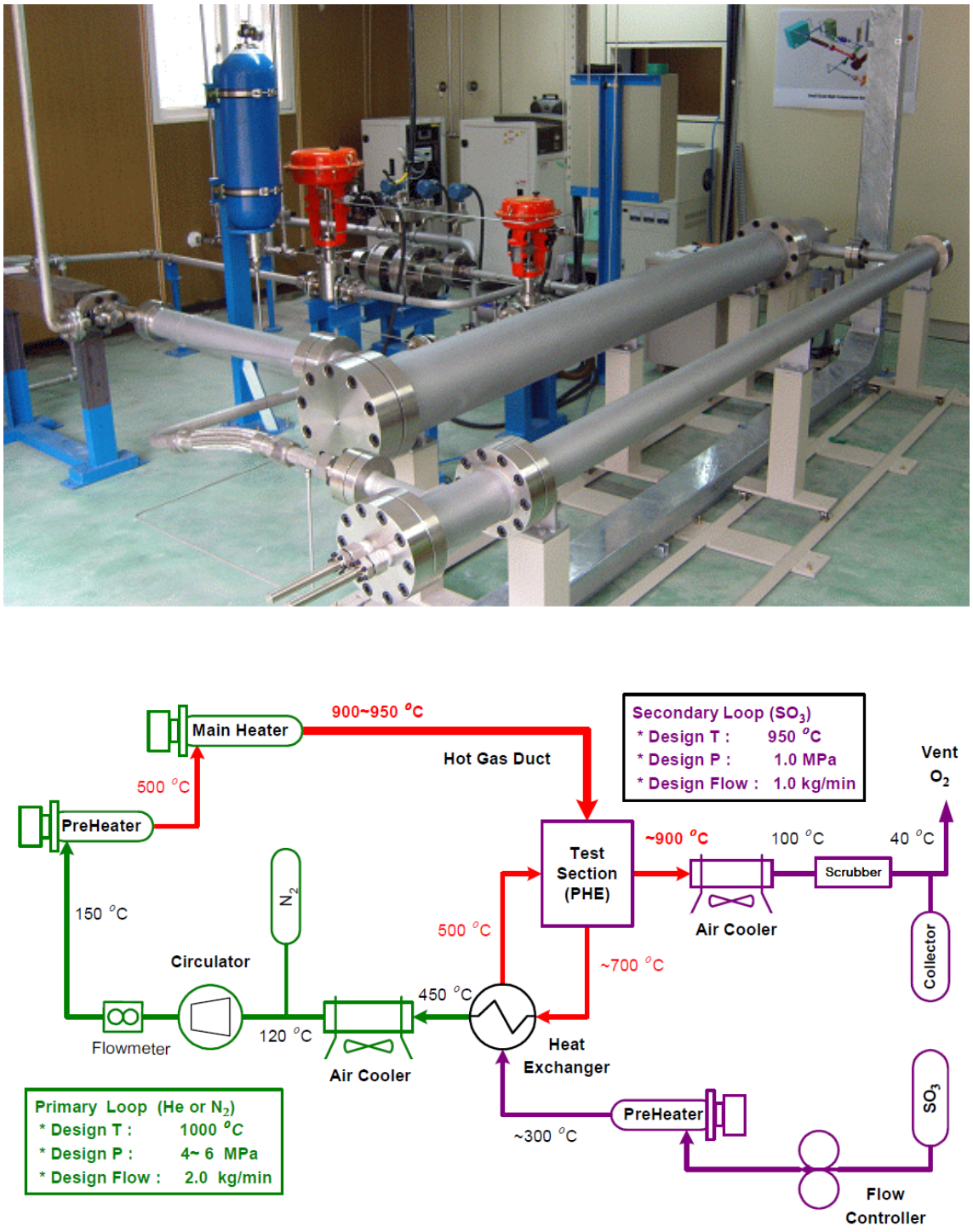

FIG. 91. Photograph and schematic of the 10 kW gas loop for process heat exchanger testing at KAERI [265, 267].

40%. Recent results on HI_x thermodynamic properties will probably lead to a lower efficiency. After successful demonstration of closed loop operation at General Atomics, the project was concluded in April 2009 [271].

At SNL, as part of the NHI programme, a bayonet type heat exchanger and silicon carbide integrated catalytic decomposer (SID) combining the functions of a boiler, superheater, decomposer and recuperator in a single unit has been developed, as shown in Fig. 95 [272, 273]. The bayonet type decomposition reactor features internal recuperation and allows all of the connections to be made at relatively low temperatures. While the materials Teflon, Viton or steel are used in the low temperature regions (<200°C), SiC is used in the high temperature region.

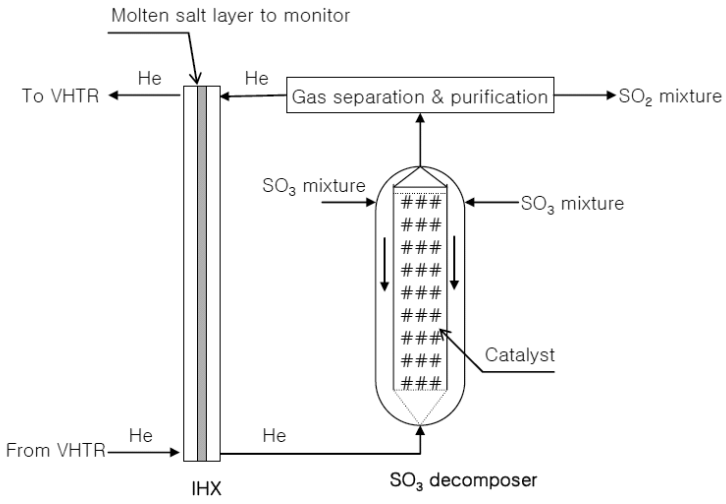

FIG. 92. Concept of a directly heated SO_3 decomposer system [268].

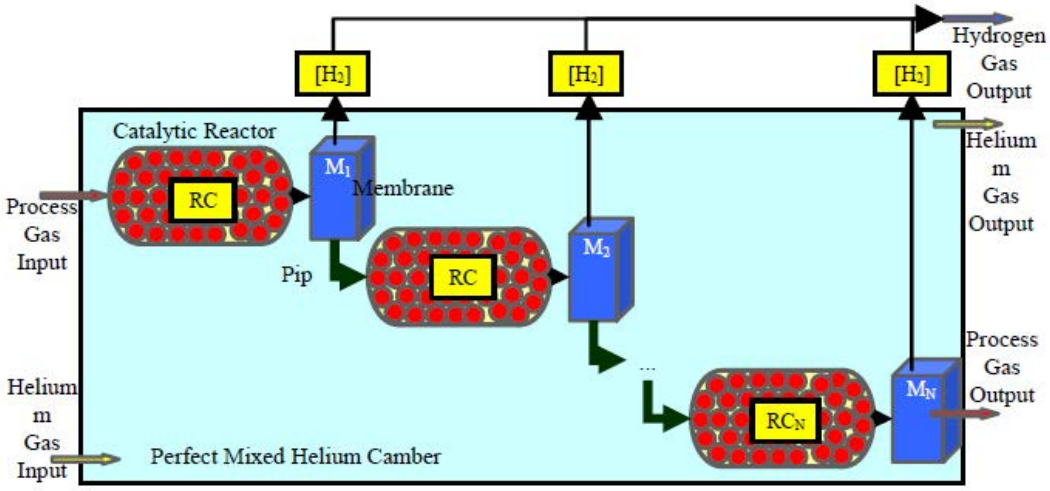

FIG. 93 . Tank-in-series model for a hydrogen iodide decomposer [269].

The components have non-wetting metal surfaces to avoid severe corrosion problems in contact with the hot acid. The continuous recuperation of the exiting gas heating up the incoming acid gases provides an increase in efficiency.

The bayonet decomposer consists of one closed-end tube coaxially aligned with an open-end tube to form two concentric flow paths. A flow of concentrated sulphuric acid enters the SID and flows upwards through the outer annulus of 2.7 mm width, is heated up in the boiler and superheater sections (total length: 622 mm) to ~700°C and gasified into the components SO_3 and H_2O before reaching the catalytic region. Further heating to the maximum operating temperature decomposes the acid vapours to SO_2 and O_2, which then flow downwards through an inner annulus between the central quartz wall and the inner SiC tube of 0.56 mm width. The porous medium catalytic region with a height of 229 mm is filled with spherical pellets, 4 mm in diameter, made of silicon with 1% Pt. Two types of tests were conducted with SID, the first with variation of catalyst temperature and flow rate at atmospheric pressure, and the second with variation of the pressure at constant flow rate.

Theoretical studies have been conducted with the CFD code FLUENT for the numerical simulation of the SID unit, including the aspects of fluid flow, heat transfer and chemical reactions in the decomposer region. Different shapes of catalyst pellets were examined as well as the effects of variation of flow rates, showing that numerical results were consistent with the experimental results [273].

FIG. 94. ILS loop demonstration of S–I process at General Atomics [270].

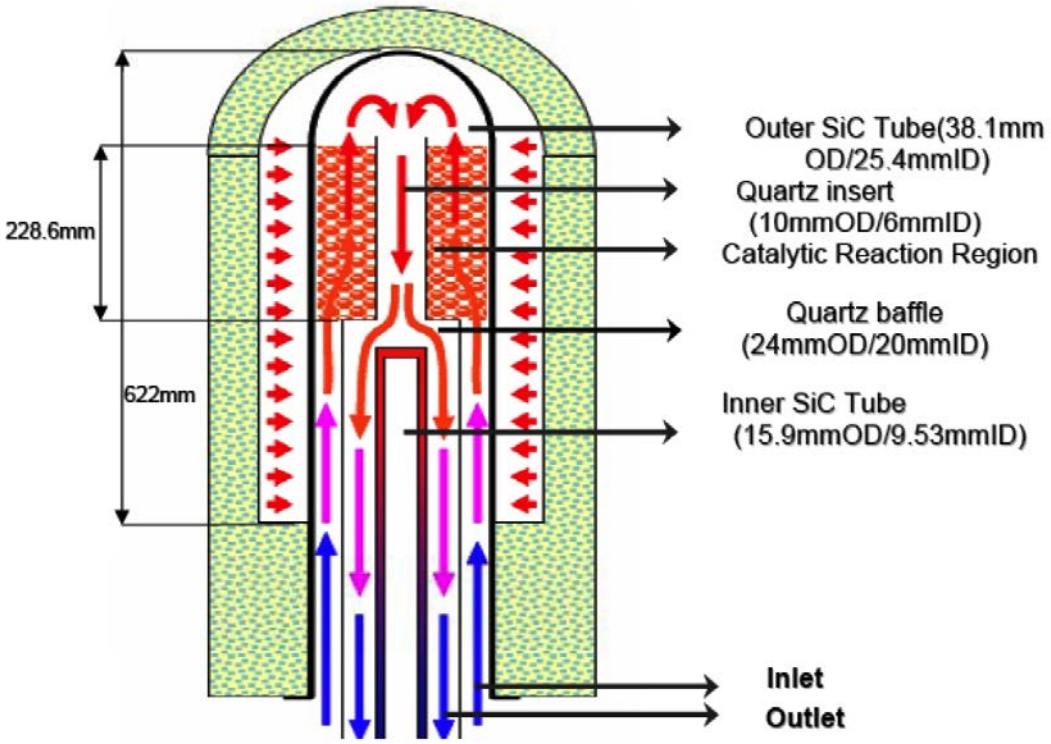

FIG. 95. Schematic of the SNL silicon carbide integrated catalytic decomposer SID [272].

The bayonet acid decomposer approach was also used as the basis of the HyS process design in the related study (see Section 3.4.3). The next steps will include testing of the multitube bayonet decomposer and the design, construction and testing of a pilot scale plant with demonstration of a helium heated decomposer [274].

General Atomics proposed an extractive distillation technique that uses phosphoric acid (H_3PO_4) as a medium to concentrate the HI solution by separating the iodine from HI/H_2O and breaking the HI/H_2O azeotrope [275].

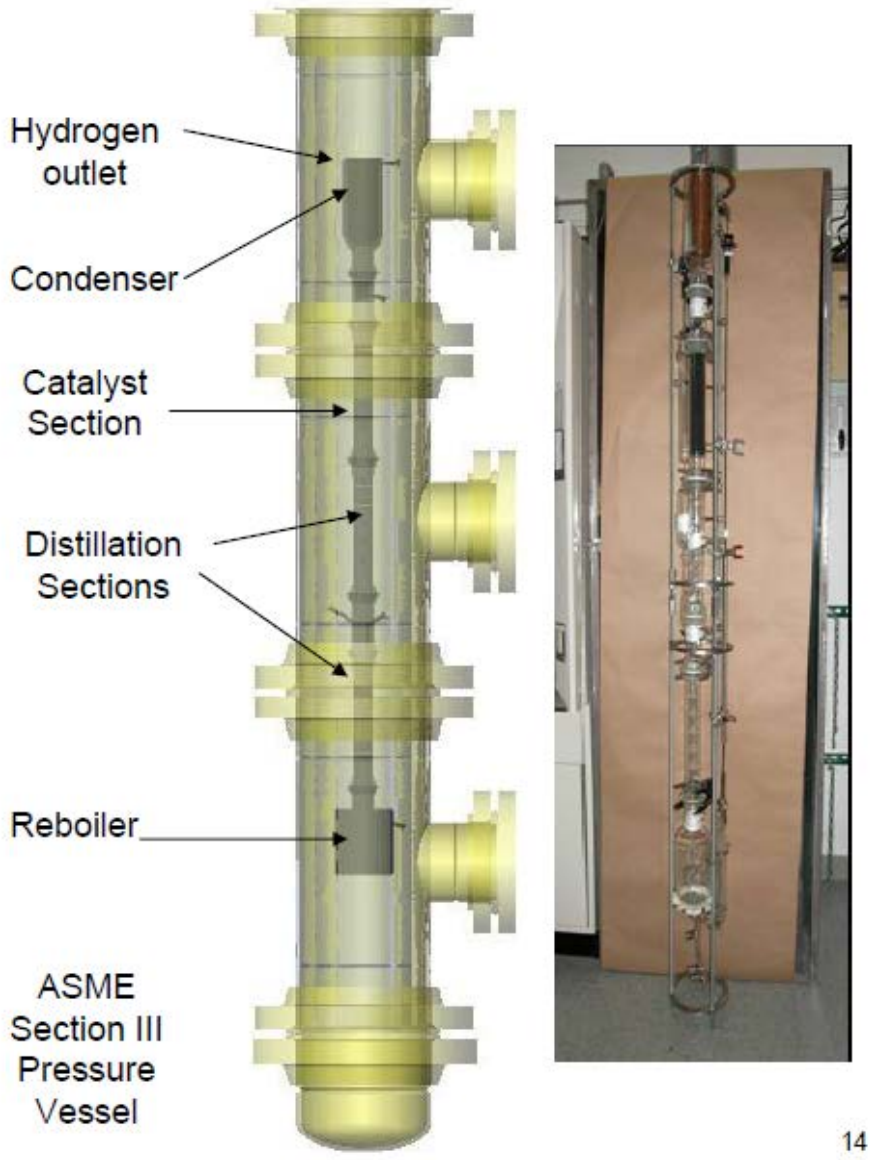

FIG. 96. Glass–metal system for initial experiments in reactive distillation column [276].

However, the need for a third compound (phosphoric acid) in extractive distillation unfavourably complicates the cycle. The phosphoric acid itself should be recovered through a separate cycle consuming a large amount of energy, which reduces the efficiency. Due to the extreme corrosiveness of boiling phosphoric acid, the choice of materials is essential. Ta alloys and Ag appear to have acceptable corrosion resistance.

In the USA, initial reactive distillation experiments have been conducted in a glass–metal system (Fig. 96) at temperatures of 250–300°C and pressures of 2–4 MPa. Hydrogen generation could be measured continuously [276].

Catalysts applied to this reaction are platinum, palladium and ruthenium, but also others such as ceria (CeO_2), nickel and carbon. A theoretical analysis with reactive distillation has shown that the overall conversion will be enhanced by 10–15% if the decomposing gas is replenished with much higher moles of liquid. This reflux liquid also improves the reactive distillation column performance by taking iodine away from the reacting system. The assessment of the energy consumption in this section of the S–I cycle, however, is still uncertain. Efforts have been put into the development and validation of a reliable simulation with the Aspen Plus tool. The model developed has been demonstrated to fairly describe phase equilibria of the HI–H_2O–I_2 ternary system, and it can be effectively applied for mass and heat balance assessment [156].

FIG. 97. Electrolyser installed in SRNL test facility [163].

4.6.9.2. The hybrid sulphur cycle

Starting in 1976 with experimental activities, Westinghouse has proven the feasibility of all basic chemical steps. By 1978, Westinghouse had demonstrated in a closed loop a 120 NL/h production on a laboratory scale. FZJ in cooperation with JRC Ispra successfully realized the operation of a three-compartment electrolysis cell at 80°C and 1.5 MPa in a 600 h run. The H_2 production rate was 10 NL/h. FZJ also verified the heat consuming step of sulphuric acid splitting on bench scale under HTGR conditions at 4 MPa and with 950°C heat from an electrical furnace [277].

SRNL has based its work on the use of PEM technology which promises high electrochemical efficiency and competitiveness of capital costs. SRNL completed a 100 h test on a single-cell SO_2 depolarized electrolyser (SDE) for use in the HyS cycle, and started testing of a multicell electrolyser (Fig. 97). Recent work at SNL also resulted in further process improvements. A flowsheet study using the process analyser software Aspen Plus resulted in a net efficiency for hydrogen production by the HyS hybrid cycle connected to a helium cooled reactor of 48.8% (HHV) [278]. This assessment is based on a nuclear heat input at 900°C, an SDE operation at 100°C and 2 MPa, an H_2SO_4 concentration of 65% and a cell voltage of 0.525 V [163].

The next steps will be the scaling up of the electrolyser active cell area to 400 cm^2, and later 1000 cm^2, the demonstration of a full scale single tube decomposer, the operation of a 300 kW pilot plant, and eventually the engineering scale demonstration of the HyS cycle [274].

5. NUCLEAR REACTOR FOR HYDROGEN PRODUCTION

5.1. REQUIREMENTS OF A NUCLEAR HYDROGEN PRODUCTION SYSTEM

5.1.1. New generation nuclear reactors

The next generation of nuclear reactors (Generation IV) is expected to be introduced in about 20–30 years from now. The concepts of such reactors, however, are being developed today based on requirements leading to further progress of the nuclear technology by addressing the areas of safety and reliability, proliferation resistance and physical protection, economics, and sustainability [279].

5.1.1.1. Safety and reliability

In the future, nuclear power will require a further enhancement of the safety standards. Safer operation of nuclear reactors can be obtained by designs with a very low probability and degree of core damage, minimal consequences even after severe accidents and limitation of the consequences to the plant site. The accident management will be further improved such that the public will not be affected and off-site emergency response will be almost unnecessary. This can be achieved through a robust design, a high level of inherent safety and transparent safety features, and by sharing experience on an international basis. In order to be competitive, reliability and performance must be at a very high level that is achievable by considering both technical improvements and the improvement of individual and organizational performance.

5.1.1.2. Proliferation resistance and physical protection

International safeguards must be strengthened against misuse of fissile material by diversion of weapons-usable material during enrichment and reprocessing activities. Controlling and securing nuclear material can be provided for by modified design features or other innovative measures and international policies to make potential diversion or theft or a sabotage act unattractive, and to make dispersion of material more difficult. A robust design is also a means to protect against actions related to war or terrorism.

5.1.1.3. Sustainability

Sustainability as the ability to meet the needs of both the present and future generations is mainly looked at in terms of nuclear fuel supply over a long period of time and spent fuel management with the requirement of meeting environmental objectives. The fuel resources available are essential, as is and reactor deployment for each potential fuel cycle such as the once-through approach, modified open cycle or fuel reprocessing. Prolonged availability of resources can be achieved by breeding new fissile material or by recycling used fuel. Future radioactive waste management must include processes leading to significantly reduced quantities of waste to be safely stored, transported and disposed of. Furthermore, a considerable reduction in toxicity and a lifetime not significantly longer than its natural limits will simplify the requirements of a safe operation of the repositories.

5.1.1.4. Economics

The development toward a simpler reactor design, economical plant sizes and life cycles, and improvement of the plant's efficiency will help in achieving costs competitive with those of other energy options. The economic risk can be reduced by employing modular reactor designs and using improved or innovative construction techniques. Future nuclear reactors must also be flexible in meeting the need for energy products other than electricity. The penetration of non-electricity markets by supplying process heat/steam for district heating, seawater desalination or hydrogen generation will enhance efficiencies and thus competitiveness.

5.1.2. The Generation IV International Forum initiative

The Generation IV International Forum (GIF) was founded in 2000 as a joint initiative of nine countries (Argentina, Brazil, Canada, France, Japan, Republic of Korea, South Africa, United Kingdom, USA), later joined by Switzerland (2002), Euratom (2003), China and the Russian Federation (both in 2006). The main objective is the development of the fourth generation of nuclear reactors between 2030 and 2040; apart from being safer, more reliable, more economically viable and more proliferation-resistant, these reactors are also expected to penetrate non-electrical markets such as the supply of process heat (e.g. for hydrogen production) on a large scale.

After the evaluation of some 100 potential Generation IV designs that had been suggested, the GIF agreed in 2002 to continue studies on six selected nuclear reactor designs that were deemed to meet the above requirements and to be deployable in due time [279]:

— Gas cooled fast reactor (GFR) system;
— Lead cooled fast reactor (LFR) system;
— Molten salt cooled reactor (MSR) system;
— Sodium cooled fast reactor (SFR);
— Supercritical water cooled reactor (SCWR) system;
— Very high temperature reactor (VHTR).

The Generation IV concepts are designed for higher coolant temperatures than most of today's nuclear reactors. This will enable future reactors to generate electricity at a higher efficiency as well as heat or steam, which can be transferred to various processes depending on the temperature level provided. All proposed Generation IV systems are able to supply heat for lower temperature industrial processes (< ~500°C).

All systems are intended to have a long service lifetime of 60 years. Except for the VHTR and one of the two types of SCWR with a once-through cycle, all systems are designed for a closed cycle allowing an actinide management by generating fissile material and using recycled fuel, thus alleviating the radioactive waste issue. The three fast reactor designs offer the possibility of burning all actinides to further reduce waste. All six reactor concepts could produce hydrogen.

In expectation of significantly increased demand for hydrogen in the future, mass production of hydrogen is a major goal for Generation IV systems. Due to the need for high temperature heat, the systems of interest in this context will be basically the helium cooled reactors GFR and VHTR, the MSR and also one of the LFR designs appropriate to be linked with a H_2 production system. The principal methods of future nuclear hydrogen generation considered are the water splitting processes of thermochemical cycles and high temperature steam electrolysis.

The overall advancement in the development of individual road maps for all Generation IV nuclear reactor systems will be made based on long term R&D in three distinct phases:

— The viability phase to investigate whether the basic concepts and key technologies and processes are feasible under the given conditions;
— The performance phase to verify and optimize processes, phenomena and material capabilities at an engineering level;
— The demonstration phase to licence, construct and operate a prototype plant.

5.1.2.1. Gas cooled fast reactor

The GFR system (Fig. 98) features a fast spectrum helium cooled reactor and closed fuel cycle. The high outlet temperature of the helium coolant of 850°C makes it possible to deliver electricity and process heat with high conversion efficiency. The GFR uses a direct Brayton cycle helium turbine for electricity and can provide process heat for the production of hydrogen. Through the combination of a fast neutron spectrum and full recycling of actinides, GFRs minimize the production of long lived radioactive waste isotopes.

The active core is composed of prismatic blocks. A potential fuel design is composite ceramic–ceramic fuel (cercer) with closely packed, coated (U,Pu)C kernels or fibres, or, alternatively, ceramic clad, solid solution metal (cermet) fuels. The reference fuel design currently being considered is a ceramic plate matrix with a honeycomb inner structure containing small fuel cylinders. The need for a high density of heavy nuclei in the fuel leads to

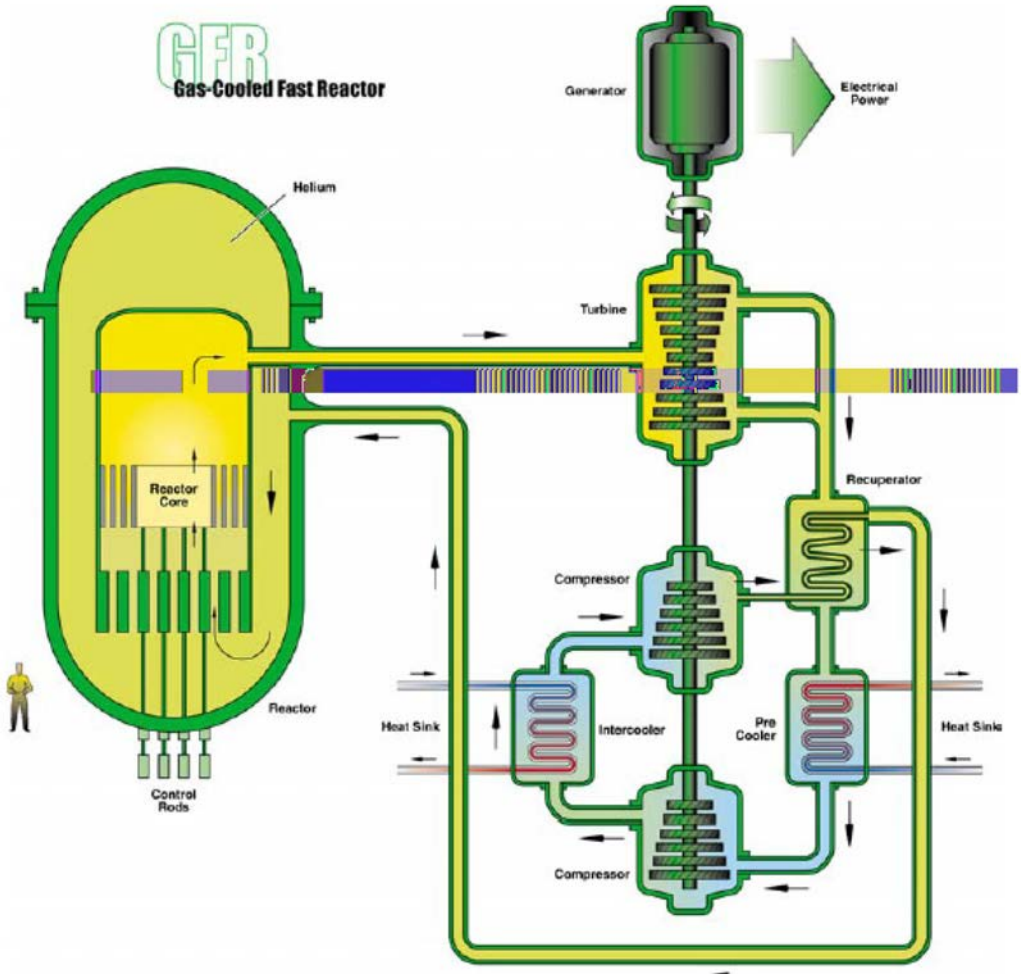

FIG. 98. Generation IV gas cooled fast reactor system [279].

actinide–carbides (mixed Pu–U carbides) as the reference fuel and actinide–nitrides. The matrix material is silicon carbide. The reference power size is 600 MW(th)/275 MW(e) to be utilized for electricity production, hydrogen production and cogeneration.

5.1.2.2. Lead cooled fast reactor

LFR systems are Pb or Pb–Bi alloy cooled reactors with a fast neutron spectrum and closed fuel cycle for efficient conversion of fertile fuel and actinide management. The favourable neutronics of Pb and Pb–Bi coolants enable low power density, natural circulation cooled reactors with fissile self-sufficient core designs that hold their reactivity over their very long refuelling interval. The plant sizes considered are small (50-150 MW(e)), medium (300-400 MW(e)) and large (1200 MW(e)). The small battery option operates on a very long refuelling interval (15–20 a), with a cassette core for electricity production on small grids contributing to proliferation resistance. On the other hand, this concept has the largest R&D needs and longest development time.

The LFR is cooled by natural convection with a reactor outlet temperature of 550°C. The longer term option seeks to further exploit the inherent safety features and controllability advantages of a heat transport circuit with large thermal inertia and a coolant that remains at ambient pressure. The coolant outlet temperature should be raised sufficiently to enter markets for hydrogen and process heat, possibly as merchant plants. LFRs hold potential for advances compared with state of the art liquid metal fast reactors in the following areas.

The nearer term options use metal alloy fuel or nitride fuel if available, containing fertile U and transuranics. Metal alloy fuel pin performance at 550ºC and U/TRU/Zr metal alloy recycling and remote refabrication

technologies are already substantially developed in sodium cooled systems. Mixed nitride fuel is also possible for the 550ºC options; however, it is clearly required for the higher temperature option.

Low pressures in the primary system allow a decrease of thickness of the vessel walls. The favourable properties of Pb coolant and nitride fuel, combined with high temperature structural materials, can extend the reactor coolant outlet temperature into the 750–800ºC range in the long term. In this option, the Bi alloying agent is eliminated, and the less corrosive properties of Pb help to enable the use of new high temperature materials. The required R&D is more extensive than that required for the 550ºC options because of the new structural materials and nitride fuel to be developed.

A safety relevant drawback of Pb and Pb–Bi coolants (unlike Na) is the tendency of erosion and corrosion of steels. Therefore, it has to be ensured that steel surfaces are always covered with a protective oxide layer. Furthermore, fast reactor structural materials are exposed to a much stronger neutron flux and a harder neutron spectrum than the structural materials of thermal reactors [280].

5.1.2.3. Molten salt reactor

MSRs are being considered for a reference electric output of 1000 MW(e) and can be used for electricity production, hydrogen production and cogeneration. Furthermore, they can be used for transmutation (almost to completion). MSRs are fuelled with uranium or plutonium dissolved in a mixture of molten fluorides, with Na and Zr fluorides as the primary option. This molten salt fuel flows through graphite core channels and creates an epithermal neutron spectrum. The coolant with an outlet temperature of ~700°C transfers the heat via intermediate heat exchangers to a secondary and then to a tertiary circuit before arriving at the power conversion system. MSRs have the following unique characteristics, which may afford advances:

— Good neutron economy, opening alternatives for actinide burning and/or high conversion;
— Low fissile inventory, increasing resistance to proliferation;
— Inherent safety afforded by fail-safe drainage, passive cooling and a low inventory of volatile fission products in the fuel;
— Refuelling, processing and fission product removal that can be performed on-line, potentially yielding high availability;
— Actinide feeds of widely varying composition to the homogenous salt solution without the blending and fabrication needed by solid fuel reactors.

Fluoride salts with higher solubility for actinides such as NaF/ZrF_4, but also for thorium, are preferred for this option. Salts with lower potential for tritium production would be preferred if hydrogen production were the objective. Lithium and beryllium fluorides would be preferred if high conversion were the objective. The reactor may be started using LEU, but can also use ^{238}U or ^{232}Th as a fertile fuel dissolved as fluorides in the molten salts. Operating temperatures of MSRs range from the melting point of eutectic fluorine salts (about 450°C) to below the chemical compatibility temperature of nickel based alloys (about 800°C). The high melting point of the coolant implies the requirement of external heating devices and the need to prevent freeze-up during operation.

The main objective of the fuel characterization research is to determine the optimum process for separating fission products, including lanthanides, without removal of minor actinides. The fuel salt has to meet requirements that include neutronic properties (low neutron cross-section for the solvent components, radiation stability, negative temperature coefficient), thermal and transport properties (low melting point, thermal stability, low vapour pressure, adequate heat transfer and viscosity), chemical properties (high solubility of fuel components, compatibility with container and moderator materials, ease of fuel reprocessing), compatibility with waste forms, and low fuel and processing costs.

(A) Experience with MSRs

An extensive database on molten salt reactors was built up in the 1950–1970s in the USA (ORNL) and the then Union of Soviet Socialist Republics. In the USA, MSR systems were tested in two experimental reactors. Molten salt reactors were first proposed in 1943 for a nuclear powered aircraft. In the ‘Aircraft Reactor Experiment’ of 1954 with 2.5 MW(th) power, which operated for several days with a fluoride molten salt (NaF/ZrF_4) system, peak temperatures up to 880°C were achieved [281].

In order to be used as a breeder, the MSR must have a low fission product inventory, i.e. it must be purified frequently by liquid extraction methods. In the two-fluid breeder version, U and Th were kept in different fluids separated by graphite walls. An 8 MW(th) MSR experiment (MSRE) with a thermal neutron spectrum and a thorium fuel cycle was constructed and was operated from 1965 until 1969. It demonstrated safe operation with a Li/Be fluoride salt as well as flexibility and ease in handling of the ^{233}U fuel. The problems encountered were radiation hardening of the Hastelloy N material and tritium production from the lithium. The early MSR programme was eventually discontinued, since it was in competition with the more supported fast breeder programme [281].

(B) Aqueous homogeneous reactor (AHR)

The so-called AHR was originally designed in Los Alamos [197]. Its characteristic feature is the fuel, which is uranium sulphate or uranium nitrate dissolved in either light or heavy water and acting as a coolant and moderator, and circulating continuously between the reactor core and a processing plant where unwanted radioactivity was removed. Due to its self-controlling features, it is considered a very safe reactor. The first homogeneous liquid fuel reactors, operated since 1944, were mainly used for nuclear experiments, benefiting from the high neutron fluxes that at the same time caused the problem of metal corrosion. AHRs, however, never developed to the commercial stage. As of 2006, only five AHRs were being operated, mainly for the production of medical isotopes, which can be easily extracted directly from the nitric acid base fuel solution. One example is the 20 kW(th) ARGUS reactor in operation at the Kurchatov Institute in Moscow since 1981.

These reactors were originally given the name ‘water boiler’ due to the observed bubbling of the liquid fuel. The bubbles are hydrogen and oxygen gas formed by radiolytic dissociation of the water from ionizing irradiation of fission products or, accounting for a small percentage, of neutron and gamma radiation. Based on this phenomenon, hydrogen production by diverting thermal neutrons into an aqueous blanket was considered, but never matured. The principal problems of AHRs were the corrosive nature of the fuel, the retention of radioactivity, the continuous fission product removal and the explosive nature of the radiolysis products.

5.1.2.4. Sodium cooled fast reactor

The interest in SFRs is principally guided by their ability in terms of management of uranium resources, high level wastes, and particularly plutonium and other actinides. Fast reactors with a fully closed cycle promise a reduction in uranium demand and transuranium (TRU) waste by two orders of magnitude compared with conventional LWRs. SFRs also offer, of course, the option of electricity production, which may be extended later to hydrogen production and cogeneration, although interest in process heat applications with liquid metal cooled reactors is relatively new. Plant sizes range from modular systems of a few hundred MW(e) to large monolithic reactors of ~1500 MW(e). The sodium coolant allows efficient heat transfer and ensures high fuel power rates with core outlet temperatures of typically 530–550ºC. Fuel options for the SFR are MOX and mixed U–Pu–Zr metal alloy. Further studies will investigate the behaviour of the fuel containing minor actinides, processes for their recycling and refabrication into new fuel, and decay heat removal from the core under accident conditions.

Another major safety feature is that the primary system operates at essentially atmospheric pressure, pressurized only to the extent needed to move the fluid. Potential hazards are given due to its chemical reaction with air and water, and due to boiling if accident temperatures exceed 900°C. To improve safety, a secondary sodium system acts as a buffer between the radioactive sodium in the primary system and the steam or water that is contained in the conventional Rankine cycle power plant. A large margin to coolant boiling could be achieved by design.

Sodium cooled liquid metal reactors are technologically well developed. Demonstration plants in several countries ranged from 1.1 MW(th) (EBR-I in 1951) to 1200 MW(e) (Superphénix in 1985). Today, SFRs are operating in Japan, France and the Russian Federation. In 1988, the European fast reactor (EFR) collaboration was founded aiming at the design of a large scale, MOX fuelled monolithic SFR. But there is also interest in smaller modular type units, and even battery type (< 100 MW(e)) units. Most of the experience available is from Russian submarine reactors and the former US Integrated Fast Reactor programme [280].

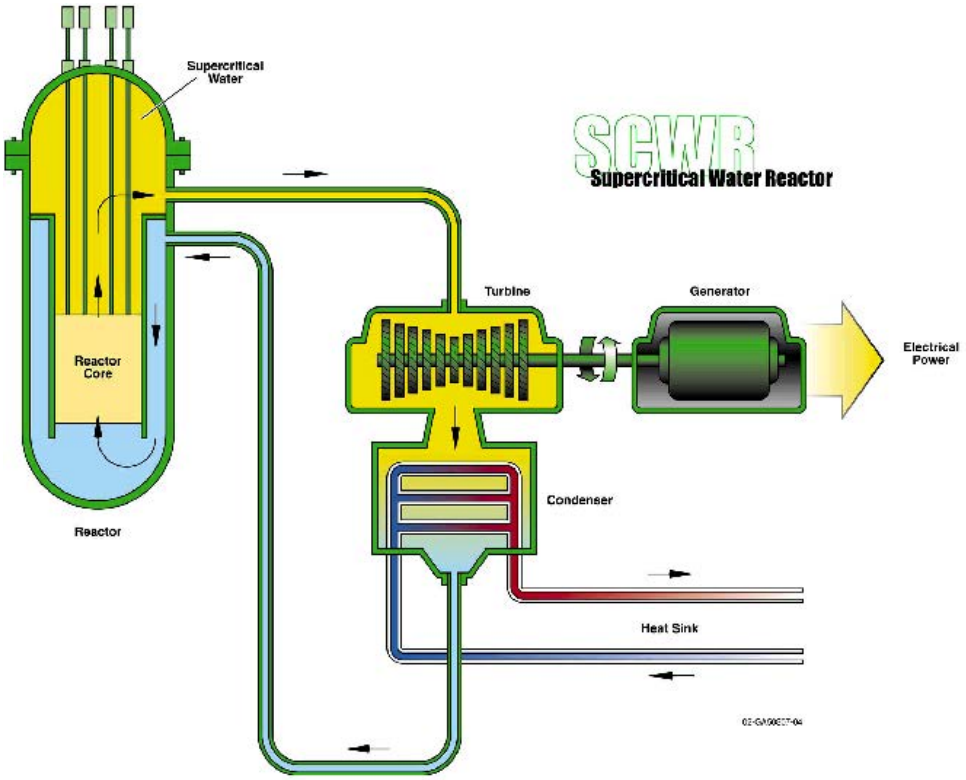

FIG. 99. Generation IV supercritical water cooled reactor system [279].

5.1.2.5. Supercritical water cooled reactor

The supercritical water cooled reactor (SCWR), originally proposed by the University of Tokyo in 1989, is a high temperature, high pressure water cooled reactor with no flow recirculation system and a direct cycle primary system (Fig. 99), and can be seen as the evolutionary development of today's conventional LWRs. SCWRs are operating above the thermodynamic critical point of water (374°C, 22.1 MPa). These systems have an epithermal neutron spectrum, but depending on the core design, may have a thermal or fast neutron spectrum. Reference power size is an output of 1700 MW(e). High pressure coolant of 25 MPa is heated from 280°C to about 510°C and delivered to a power conversion cycle. SCWRs have unique features that may offer advantages compared to state of the art LWRs, including:

— Excellent economy with high thermal efficiencies of up to 44%;
— Lower coolant mass flow rate per unit thermal power, offering a reduction in pumping power and reactor equipment;
— No risk of boiling crisis (i.e. dry-out) owing to the absence of a second phase in the reactor, thereby avoiding discontinuous heat transfer regimes during normal operation;
— Simpler design, since steam dryers, steam separators, recirculation pumps and steam generators are eliminated;
— Extension to hydrogen production and cogeneration at a later stage.

A number of SCWRs are currently under development. The two main lines being followed are a large reactor pressure vessel with ~0.5 m wall thickness to contain the core, and reactor designs that use distributed pressure tubes analogous to the CANDU reactors. Operating pressures are about 25 MPa with coolant outlet temperatures of 625°C, which facilitates process heat applications. Direct supercritical water cycles with the turbine technology are already available [282].

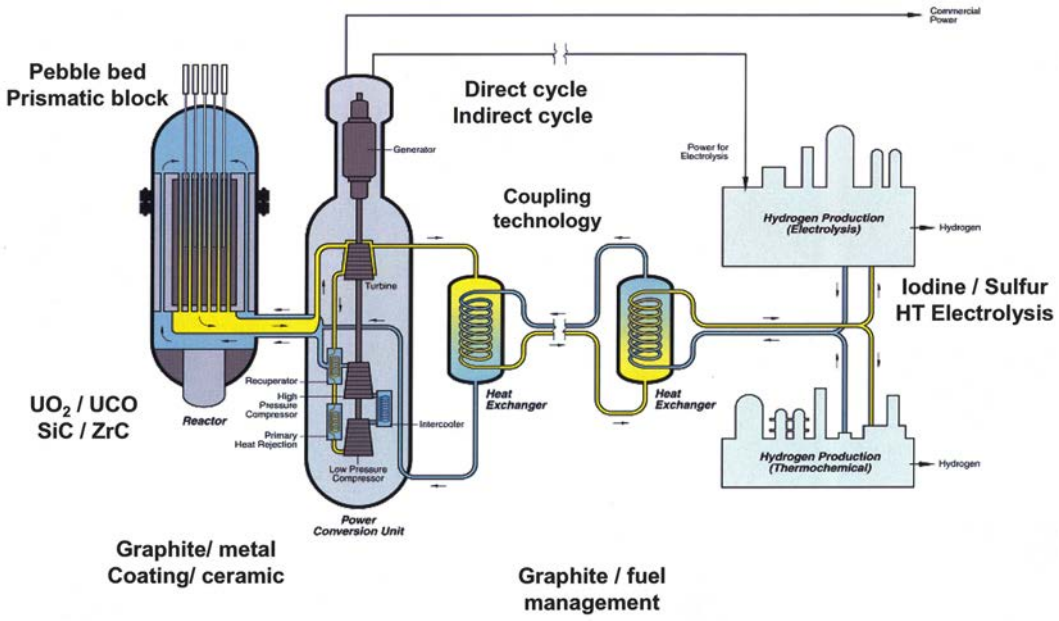

FIG. 100. Generation IV very high temperature reactor plus hydrogen production system [279].

State of the art supercritical steam cycles in conventional power plants are mostly designed with a single steam reheat and regenerative feedwater heating reaching efficiencies of up to 54%. In principle, each steam reheat process increases the thermal efficiency of the cycle. It also reduces the amount of moisture in the last stages of the turbine that must be removed. A single steam reheat raises the efficiency by about 3–4% compared with no-reheat. However, more than two reheat processes are not practicable, since equipment cost would increase with each reheat stage. Therefore, using the high temperature heat from an SCWR to heat water in the hydrogen production loop is a viable option. Recuperator type heat exchangers have to be used [283].

5.1.2.6. Very high temperature gas reactor

A highly promising Generation IV reactor concept is the VHTR (Fig. 100). Its characteristic features are a helium cooled, graphite moderated, graphite reflected, thermal neutron spectrum reactor core with a reference thermal power production of 600 MW(th) and an electricity output of 275 MW(e). The reactor core type of the VHTR can be a prismatic block core or a pebble bed core. Coolant outlet temperatures of 900–1000°C are ideally suited for a whole spectrum of high temperature process heat applications. For electricity generation, the helium gas turbine system can be directly set in the primary coolant loop. The employment of a direct cycle gas turbine allows for a high efficiency of more than 50%. The basic technology for the VHTR has been well established in former HTGR plants and in the broad experience from research projects (see also Section 5.3.1).

The safety basis for all VHTR concepts is to design the reactor to a very high degree of passive safety to avoid release of fission products under all conditions of normal operation and accidents, including beyond design basis events. The VHTR system is a nuclear reactor concept with an easily understood safety basis that permits substantially reduced emergency planning requirements and improved siting flexibility compared with other nuclear technologies. Still, further R&D efforts are necessary, including on the performance of graphite and fuel. The proliferation resistance feature of the VHTR is mainly given by the fuel itself. To obtain a significant quantity of either uranium or plutonium from the LEU fuel requires large quantities of ^{14}C-contaminated carbon to be removed and further efforts by grind–leach, burn–leach or electrolysis in nitric acid to obtain a small amount of nuclear material from the TRISO coated particles. For irradiated LEU fuel, the high burnup of spent fuel provides highly radioactive fuel with poor plutonium isotopic composition for weapons usage.

The VHTR system is considered the prime candidate for large scale hydrogen production. Furthermore, cogeneration of heat and power makes the VHTR an attractive heat source for large industrial complexes. The

VHTR could be deployed in refineries and petrochemical industries to substitute large amounts of process heat at different temperatures, including hydrogen generation for upgrading heavy and sour crude oil. Core outlet temperatures of 1000°C and higher would expand nuclear heat applications to such processes as steel, aluminium oxide and aluminium production. Heat application processes are generally coupled with the reactor through an intermediate heat exchanger.

5.1.2.7. Generation IV reactor summary

The principal characteristic features of the above Generation IV nuclear reactor systems are summarized in Table 22.

5.1.3. The INPRO initiative

An international initiative complementary to GIF started in 2000 by the IAEA, called the International Project on Innovative Nuclear Reactors and Fuel Cycles (INPRO). As of 2009, 30 Member States plus the European Commission were participating in INPRO. Both the IAEA and OECD/NEA are participating as observers to GIF.

While the GIF is serving essentially as a designers' initiative, INPRO also includes other countries and has a longer time horizon. It incorporates IAEA safeguard considerations more directly, encompassing both designers and end users and their requirements. Nuclear energy is considered in the broader perspective of future energy needs, and problems are addressed from the point of view of potential users — especially those in developing countries, for example, with small grids and/or those interested in desalination and nuclear cogeneration of heat and power — by identifying their specific needs. A methodology for the assessment of innovative nuclear reactors and fuel cycles has been developed [284], which is currently being applied on a national basis by Argentina, India, the Republic of Korea and the Russian Federation.

5.2. REQUIREMENTS OF NUCLEAR ENERGY IN INDUSTRIAL APPLICATIONS

Most industries need to rely on a secure and affordable supply of energy to guarantee continuous and reliable operation of their process units. Ensuring supply security by diversifying the primary energy carriers and, at the same time, limiting the effects of energy consumption on the environment will become more important goals in the future.

The industrial requirement of full availability and reliability must be realized by an additional plant. Having a large scale plant and a second large one as a backup system might be an unreasonably high investment. Backup units could, of course, also be provided by fossil fired boilers. While gas fired boiler fuel costs are high, the capital costs are low compared to those of extra nuclear capacity. Also, the ramp-up time for a gas fired boiler idling at temperature and pressure is very short [285]. A modular arrangement of 2–6 nuclear units, depending on the industrial plant size, will be necessary for redundancy, reliability and reserve capacity, all reasons that again reduce the power size per modular unit. The arrangement could comprise multiple identical reactor modules or multiple reactor modules of differing ratings and configurations. Smaller power sizes allow for simplicity and robustness by higher safety margins, even at higher operational temperatures. One of the reactors would be typically operated for electricity generation, but could easily and quickly be switched to process heat supply if necessary [286]. The facility power plants may dispatch electrical power to the grid or take power from the grid depending on the price of electricity from the grid and the cost of facility generation. Power is also taken from the grid to augment the facility power supplies if necessary to meet facility demand. The demands for steam, electricity and high temperature gas will vary within certain ranges. Further design capabilities are [287]:

— Acceptance of a full load rejection from either steam, electrical or high temperature gas demand;
— Acceptance of zero steam flow demand, zero power demand and/or zero high temperature gas demand;
— Accommodation of coincident steam, electrical and high temperature gas demand.

A pebble bed reactor design would further enhance availability because of its on-line refuelling capability, which eliminates the requirement for periodic refuelling outages. The small power size of modular HTGRs is also favourable for operation in less developed electrical grids.

TABLE 22. MAIN FEATURES OF THE SIX GENERATION IV NUCLEAR REACTOR CONCEPTS

	GFR	LFR	MSR	SFR	SCWR	VHTR
Reference thermal power (MW)	600	125–400 3600	2250	1000–3800	3900	600
Power density (MW/m^3)	100	~70	22	350	100	6–10
Reference electric power (MW(e))	275	50 1200	1000	150 1500	1700	275
Efficiency (%)	48	33–40	44–50	39	41–44	>50
Neutron spectrum	Fast	Fast	Epithermal-thermal	Fast	(a) Thermal (b) Fast	Thermal
Fuel cycle	Closed	Closed	Closed	Closed	(a) Open (b) Closed	Open
Conversion ratio	Self-sufficient	1.0		0.5–1.3		
Coolant	Helium	Lead, lead-bismuth	Fluoride UF salt	Sodium	Water	Helium
Coolant inlet/ outlet temp. (°C)	490/850	/550 /750–800	565/700–850	/530–550	280/510	640/1000
Pressure (MPa)	9	0.1		~0.1	25	
Fuel	^{238}U and 20% Pu in composite ceramics	Metal alloy or nitride with ^{238}U and TRU	Liquid mixture of Na-, Zr-, U-fluorides	MOX, minor actinides, Zr oxide or metal alloy	UO_2, MOX stainless steel or Ni alloy cladding	UO_2 ZrC-TRISO coated particles in pebble or prism
Main purpose	Electricity, actinide management	Electricity, actinide management	Electricity, actinide management	Electricity, actinide management	Electricity, actinide management	H_2 production, electricity, actinide management

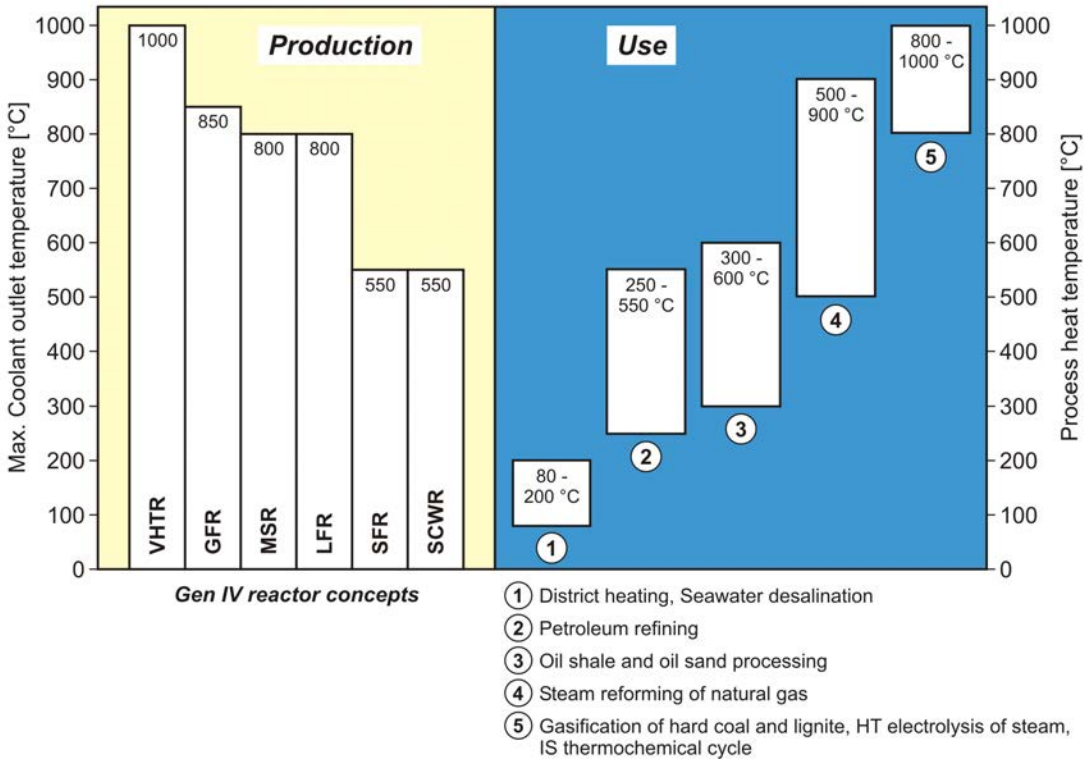

FIG. 101. Temperature ranges in production and use for Generation IV reactor systems [289].

In industrial applications of nuclear process heat, the hot coolant will transfer its heat to the chemical process via an intermediate heat exchanger. The main purpose of the intermediate circuit is to clearly isolate the chemical from the nuclear island. In this way, the direct access of primary coolant to the chemical plant and, in the reverse direction, of product gases to the reactor building can be prevented. Thus it is possible to design the chemical side as a purely conventional facility and to have possible repair works being conducted under non-nuclear conditions. The operation of the nuclear and the industrial facilities will be taken care of by separate companies, with each being liable for its own activities and meeting the respective regulations. On the chemical side, there are certainly many companies operating different chemical facilities.

The reactor coolant and its maximum temperature are essential criteria for determining which nuclear concepts are appropriate for coupling with hydrogen production processes. Figure 101 shows coolant outlet temperatures of the Generation IV concepts ranging between 550 and 1000°C compared with the process heat temperature ranges needed for various chemical processes. Coolant exit temperatures of the reactor at full load must be maintained at all levels of partial load. The coolant outlet temperature needed for the chemical processes should be about 50°C above the bulk process temperature [288]. As far as the maximum helium temperature is concerned, a value of 900°C is already suited for steam reforming applications. A value of 950°C, however, would significantly reduce the heat transfer area and improve efficiency, which is a potential for the future. The maximum coolant exit temperature of 1000°C remains a challenge to both reactor fuel and metallic materials (reactor pressure vessel, thermal barriers, etc.).

In contrast to electricity generation, the needs and requirements of industrial end users for process heat applications are much more versatile in terms of power, temperature, transient capability, availability, reliability and flexibility. The nuclear plant should be able to be switched between the operation modes of heat production only or electricity production only. Furthermore, a variation of the nuclear power output should be possible within a reasonable range. The transient capabilities of the reactor under normal or accident conditions have to match with the transient loads imposed by the industrial processes, requiring a common control strategy for both islands. Buffer capacities need to be provided. The difference in lifetime requirements should also be considered, which is in the range of 60 years for a nuclear plant and about 20 years for processing plants.

Of particular significance is the consideration of conceivable operation disturbances or accidents in such combined nuclear and chemical facilities. Apart from their own specific categories of accidents, a qualitatively new

class of events, characterized by interacting influences, will have to be taken into account. The problems that need to be addressed by an appropriate overall safety concept are the question of the safety of the nuclear plant in the case of an explosion of a flammable gas on the chemical side, or vice versa, the question of what influence an accident-induced release of radioactivity will have on the continuation of operation of the chemical plant. But there are also the more frequently expected cases of thermodynamic feedback in the case of a loss of heat source (nuclear) or heat sink (chemical).

The main safety concern in oil refineries is fire and explosion. For this reason, nuclear plants should be located in separate zones, away from hazardous areas, and should be operated independent of the conventional refinery side. Other constraints on the choice of location of the nuclear plant will be given by the need to be close to the industrial site, i.e. feedstocks, fuel, transportation or other resources [81]. Due to the limitation of the consequences to the plant site, as is expected from a Generation IV nuclear reactor, the typically defined evacuation area will not overlap with the industrial site.

5.3. PROCESS HEAT HIGH TEMPERATURE REACTOR DESIGN

5.3.1. Experience with HTGRs

Graphite moderated, gas cooled reactors (GCRs) have been in operation since the 1950s, with unit sizes of up to 670 MW(e). The first commercial plant was Chinon in France, a CO_2 cooled Magnox type reactor with 70 MW(e) starting in 1957. The next generation of GCRs was the advanced gas cooled reactor (AGR) operating with CO_2 as the coolant at higher outlet temperatures (~650°C) and a pressure of 4.3 MPa, and with higher efficiencies. The first commercial plant, Dungeness B in the United Kingdom with 1110 MW(e) in two units, was started in 1983. The final stage of GCR development is represented by the HTGR. GCRs have accumulated more than 600 operation years so far. A comprehensive outline of the historical development of GCRs in the world is given in Ref. [290].

HTGRs are characterized by an all-ceramic core, a core structure made of graphite as a moderator and reflector, helium gas as a single phase inert coolant, coated particle fuel and a low power density core. The use of refractory core materials combined with a helium coolant allows high coolant temperatures up to 950°C or even higher, and a high thermal efficiency results in a number of significant advantages. The low power density and large heat capacity of the graphitic core, the absence of coolant phase changes and the prompt negative temperature coefficient represent inherent safety advantages.

Direct experience with HTGR plants up to now has been gathered in the United Kingdom, Germany, the USA, Japan and China. A total of seven units have been constructed. Their main characteristic features are given in Table 23. Experience with HTGR plants started in the 1960s with the construction of experimental reactors — the 20 MW(th) Dragon in Winfrith, UK, which was a joint project of the OECD countries, the 46 MW(th) AVR reactor in Jülich, Germany, and the 115 MW(th) Peach Bottom power plant in the USA. All three mainly served as research instruments and were operated with high availability. In addition, the plants in Germany and the USA were also able to generate a significant amount of electricity. There was also an experimental GCR in the USA designed for a very high coolant outlet temperature of 1320°C. The 3 MW(th) He cooled Ultra High Temperature Reactor Experiment (UHTREX) built at the Los Alamos Scientific Laboratory in the late 1960s was mainly used for high enriched uranium (HEU) UC_2 fuel testing.

Two HTGR prototype plants have been developed as a follow-on step: the 330 MW(e) Fort St. Vrain (FSV) reactor in the USA and the 300 MW(e) Thorium High Temperature Reactor (THTR-300) in Germany. The former used a prismatic core, while the latter used a pebble bed core, both being connected to a conventional steam cycle. These demonstration units, however, were not very successful during their several years of operation, mainly suffering from technological problems (which could be solved), and they eventually lacked the political and financial support at a time where the severe accidents of Three Mile Island in the USA and, in particular, of Chernobyl in the former Soviet Union strongly influenced worldwide public acceptance of nuclear energy. But both plants proved the feasibility of larger sized HTGRs and the operation of related system components, and provided experience from an additional 17 years of operation, which is beneficial for future designs. None of the five HTGRs is currently in operation. The only HTGRs currently in operation are the test reactors in Japan and China.

The Japanese High Temperature Engineering Test Reactor (HTTR) is a 30 MW(th) experimental reactor which became critical in 1998. The active core, with 2.9 m of total height and 2.3 m in diameter, is composed of 150 hexagonal fuel assemblies. The average outlet temperature of the helium coolant is 850–950°C. The heat is removed by a water cooler only or, in a parallel operation mode, 20 MW(th) by water cooler and 10 MW(th) via an IHX to a secondary helium circuit. The latter is for testing process heat application conditions. JAEA demonstrated the feasibility of reaching an outlet temperature of up to 950°C, with ~900°C heat transferred through the IHX to the secondary circuit that could be coupled to a heat utilization process.

The Chinese HTR-10 with a pebble bed core producing a power of 10 MW(th) was built at the Institute for Nuclear and New Energy Technology (INET) of the Tsinghua University and is also basically a research tool. First criticality was achieved in 2000. The active core consists of some 27 000 fuel spheres with low enriched (17%) UO_2 TRISO particles. Coolant outlet temperatures are 700 and 900°C. The reactor core and steam generator are housed in two steel pressure vessels in a side-by-side arrangement. Operational experience has been acquired with regard to system and component performance. Experiments have been conducted to demonstrate the safety features of modular HTGR designs. Experience has been obtained in the design, construction, operation and licensing of modular HTGRs. In addition, active R&D programmes are being carried out on helium turbine technology (HTR-10GT). By the end of 2007, the HTR-10 had been in operation for 569 d and had accumulated 2503.4 MW·d. A modernization of the HTR-10 is planned in terms of more instrumentation. The experimental working programme includes long term operation of the reactor, fuel irradiation and more steam cycle investigations.

The experience achieved with HTGR operation so far has shown a steady improvement of components and fuel. Safety tests in the AVR and more recently in the HTTR and HTR-10 confirmed the predicted excellent physical behaviour of the core under abnormal operating conditions.

5.3.2. General design of a process heat HTGR

The trend toward large sized plants, originally following the size of commercial LWRs, was gradually abandoned in the 1980s in favour of small modular type HTGRs which have been used since in many variants for future reactors. Although lacking the advantage of economies of scale, modular type HTGRs are attractive because of the simplicity of design, lower capital costs and the fact that they serve the lower-power market, with a number of appropriate candidates in deregulated industrial countries or developing countries. In particular, the tall and slim core geometry allows for the inherent temperature limitation of the fuel temperature due to a self-acting decay heat removal which works on the physical processes of heat conduction, radiation and free convection such that the maximum fuel temperature under loss of forced convection (LOFC) accident conditions remains below 1600°C, a level that can be sustained by the fuel without further damage.

The production of high quality steam at 530°C and 15 MPa in an HTGR allows the operation of a steam turbine prior to the ‘normal’ steam application system for electricity production. The operation of such a process heat HTGR is flexible in the choice of the coolant temperature at steam generator inlet such that the product steam could be adjusted to the needs of the chemical industrial plant. The efficiencies possible are 40–43% for the electricity generating system with steam turbine, up to 48% with a closed cycle gas turbine and even up to 50% with a combination of both. In the CHP mode, the efficiencies are estimated in the range of 80–90%.

The traditional power conversion cycle is the Rankine steam cycle, where temperatures of ~550°C are achieved. An advanced feature introduced for various HTGR concepts is the direct Brayton power cycle technology, where high temperature heat is directly converted to electricity, with efficiencies of over 50% achievable, depending on the temperature.

There are two main parameters in the regulation concept for the nuclear process heat production system:

— The life steam temperature at the steam generator outlet, which can be regulated with helium flow rate (blower), which is sufficiently flexible;
— In the case of larger changes, the helium temperature at the reactor outlet, which can be regulated with a change of thermal power production (position of control rods).

Also in the case of accidents, a reactor core designed for a 950°C gas outlet temperature will operate at higher fuel element temperatures than an identical reactor designed for only a 700°C gas outlet temperature.

TABLE 23. MAIN FEATURES OF HTGRs WHICH WERE OR ARE BEING OPERATED

	Dragon (OECD)	AVR (Germany)	Peach Bottom (USA)	Ft. St. Vrain (USA)	THTR-300 (Germany)	HTTR (Japan)	HTR-10 (China)
Reactor type	Experimental	Experimental	Experimental	Prototype	Prototype	Experimental	Experimental
First criticality	1964	1966	1967	1974	1983	1998	2000
Out operation (status)	1975 (safe encl.)	1988 (defuelled)	1974 (safe encl.)	1988 (defuelled)	1988 (safe encl.)	— (operation)	— (operation)
Thermal power (MW)	20	46	115	842	750	30	10
Electric power (MW)	—	15	40	330	300	—	—
Power density (MW(th)/m^3)	14	2.6	8.3	6.3	6	2.5	2
He inlet/outlet temp. (°C)	350/750	270/850, 950	377/750	405/784	270/750	385/850, 950	250, 350/700
He pressure (MPa)	2.06	1.1	2.5	4.9	3.9	4.0	3.0
Fuel element type	Pin	Spherical	Pin	Prismatic	Spherical	Pin-in-block	Spherical
Fuel	Oxide	Carbide/Oxide	Carbide	Carbide	Oxide	Oxide	Oxide
Enrichment	HEU, LEU	HEU, LEU	HEU	HEU	HEU	LEU	LEU
Coating		BISO, TRISO		TRISO	BISO	TRISO	TRISO
Pressure vessel	Steel	Steel	Steel	PCRV	PCRV	Steel	Steel

In the OTTO (once through then out) loading scheme of a pebble bed reactor, the power production is such that high power densities are obtained in the upper, cold part of the core, while small power production is given in the lower, hot part. Temperature differences between fuel and coolant are proportional to the power density and therefore small in the lower part of the core. This allows higher coolant outlet temperatures to be achieved at reduced maximum fuel temperatures. Other advantages are the increased efficiency of control rods in the upper part of the core due to the higher neutron flux and the avoidance of a burnup measurement system which reduces the complexity of the fuel loading system. The OTTO scheme, however, is only good for a core height of 4–6 m. For larger core heights, as encountered in small modular reactor concepts, the multipass scheme for the fuel pebbles is preferred. Therefore, due to higher temperatures in the lower part of the core, power density is reduced for the process heat HTR-Modul.

Some adjustments are required with regard to maximum temperature and pressure levels in the primary circuit of a process heat plant, because the chemical processes are mainly expected to be operated at a lower pressure than would be the case, for example, in the direct gas turbine design. Another general difference is the fact that the cold gas temperature in the process heat applications is generally much lower (250–300°C) than in gas turbine applications (450–550°C), having a beneficial feedback on the pressure vessel design and material choices. Fuel temperatures during normal operation should stay below 1200°C to avoid an impact on the fuel performance and larger release rates of fission products.

In comparison with the electricity generating nuclear plant, several modifications are necessary for the process heat variant:

— Reduced power density to compensate for the higher core outlet temperature level;
— Reduced system pressure as compromise between a high pressure desired for its favourable effect on operating and accident conditions of the nuclear reactor and a low pressure desired for chemical process reasons in the secondary and tertiary circuits;
— Two-fuel zones in the pebble bed to minimize the occurrence of hot/cold gas strains in the core to achieve a radial temperature profile that is as uniform as possible;
— Ceramic (graphite) liner to replace the metallic liner because of the higher temperatures.

A part of the safety concept is the employment of a non-integrated arrangement with separate vessels for the generation and conversion of heat, and a containment to enclose the total primary circuit. Placement of the nuclear unit underground ensures enhanced protection against atmospheric explosions of gas clouds, fire or aircraft crash. For the German PR-500 process heat reactor concept, an underground construction of at least 6 m was foreseen.

All new modular HTGR concepts use steel vessels as the primary enclosure with water or air cooled reactor cavity cooling systems. The reactor building as protection against outer impacts is designed as a filtered confinement, which is not necessarily gas-tight (unlike a containment). This is a controversial issue, since the containment is ‘traditionally’ recognized as a necessary safety barrier. This concept makes the fuel element an eminently important component as the principal containment for radionuclides.

5.3.3. Fuel and fuel cycles

The key areas of known strength in the VHTR concept at this time are its robust fuel, high burnup and the use of the once-through LEU fuel cycle. The basic fuel-containing unit is given in the form of a tiny coated particle with a fuel kernel containing LEU or plutonium. The kernel is surrounded by a TRISO coating which consists of a porous buffer layer plus an interlayer of SiC between two layers of high-density isotropic PyC. The coating represents the primary barrier to the release of fission products, which are generated in the kernel during operation. A reactor core for 400–600 MW(th) will contain between 10^9 and 10^{10} individual fuel particles. The particles are embedded in a graphite matrix to form the fuel elements. The type of fuel element has developed in two directions:

(1) The pebble bed concept pursued in Germany, the Russian Federation, China and South Africa consists of a 60 mm diameter sphere composed of a 50 mm diameter fuel zone with some 10^4 coated particles (or 1 g of ^{235}U) uniformly dispersed in a graphitic matrix, surrounded by a fuel free carbon outer zone. Hundreds of thousands of pebbles are required to fuel a nuclear plant. They can be continuously given to and withdrawn from the reactor. The uranium concentration in the fuel is an order of magnitude less than in traditional nuclear fuels.

(2) The prismatic core concept pursued in the United Kingdom, the USA, Japan and the Russian Federation is based on a hexagonal graphite block with boreholes which are, in the US design, either coolant channels or loaded with fuel compacts containing the coated particles. In the Japanese block core design, the boreholes of a fuel assembly are filled with fuel rods ('pin in block') to contain the compacts (with the coated particles), and the coolant flows through the annular gap between rod and inner surface of the borehole. Burnable poison zoning is applied for power flattening. Neutron burnable poison is needed in the prismatic reactor core with the fissile material where distribution is tailored such that maximum power density is toward the top of the core where the cooling gas has the lowest temperatures, and power density is minimal in the core bottom where the coolant temperatures are highest, and peak fuel temperatures are below the design limit for normal operation (1250ºC).

Plant configuration and operating conditions are such that fuel temperatures during both normal operations and accident conditions are limited to preclude radionuclide release. High burnups of up to 60–70% FIMA may be achievable with a single-pass, multicycle irradiation in VHTR. Spent fuel from such a 'deep-burn' design could be either given to a final disposal or reprocessed to fast reactor fuel. Current concepts, however, are based on an initial once-through irradiation without recycling. But technologies to reprocess and recycle TRISO fuel are also under consideration. The ongoing R&D and the past experience provide a good basis to be able to close the VHTR fuel cycle in the future, if needed.

One of the attractive features of the HTGR is its flexibility in the use of fuel cycles. While the baseline fuel cycle is the once-through LEU fuel cycle, other fuel cycle options are possible and have been successfully tested in both prototype HTGRs and materials test reactors.

The fuel is fissile material, which may be ^{235}U, ^{233}U or plutonium, and fertile material, which may be ^{238}U or ^{232}Th. Combinations lead to possible fuel cycles with:

— LEU with or without Unat fertile particles;
— Plutonium/thorium or plutonium/uranium in mixed oxide (MOX);
— Plutonium-only fuel particles;
— Thorium based fertile particles and uranium based fuel particles;
— TRU and/or minor actinide (MA) fuel particles.

The LEU cycle uses uranium with a minimum enrichment of 5–6%, rising to up to 19% depending on the reactor type. All current commercial HTGR projects are based on this fuel.

A thorium–plutonium (Th–Pu) cycle with Pu to replace the HEU was considered at a very early stage, with initial studies conducted in the UK in the early 1960s. Similar to PWRs, the use of a mixed plutonium/depleted uranium fuel can also be envisioned. The mixture could be in the form of an oxide (MOX), carbide or nitride. The solution of 'plutonium-only' cores, a unique feature of HTGRs, was investigated by the USA and the Russian Federation as part of a programme to examine consumption of excess weapons-grade plutonium.

Thorium based cycles are the HEU/Th cycle with or without ^{233}U recycling where the thorium generates ^{233}U representing the best fissile isotope for thermal spectrum reactors. The main advantage of this fuel cycle, which has been extensively studied for HTGRs, is the considerably reduced natural uranium consumption when operated in a closed cycle at very high conversion factors. For the above reasons, the HEU cycle was considered as the reference cycle from the beginning of HTGR development in both the USA and Germany. Studies of the medium enriched uranium (MEU)/thorium cycle began in the USA in the late 1970s as a result of efforts to minimize the proliferation risks.

5.3.4. Hot gas duct

The primary hot gas duct is a horizontal pressure vessel to provide the connection between reactor pressure vessel and IHX, i.e. between core and heat sink. It has the task of transporting the hot helium from the reactor to the heat exchanger. Design options for hot gas ducts are based on either coaxial ducts or separate tubes. In the coaxial double-tube design, the hot helium flows through the inner heat-insulated tube, and cold helium flows back to the core through the annular space between inner and outer tube (Fig. 102). The pressure tube is water cooled and insulated by metal foils, the hot gas tube has carbon insulation.

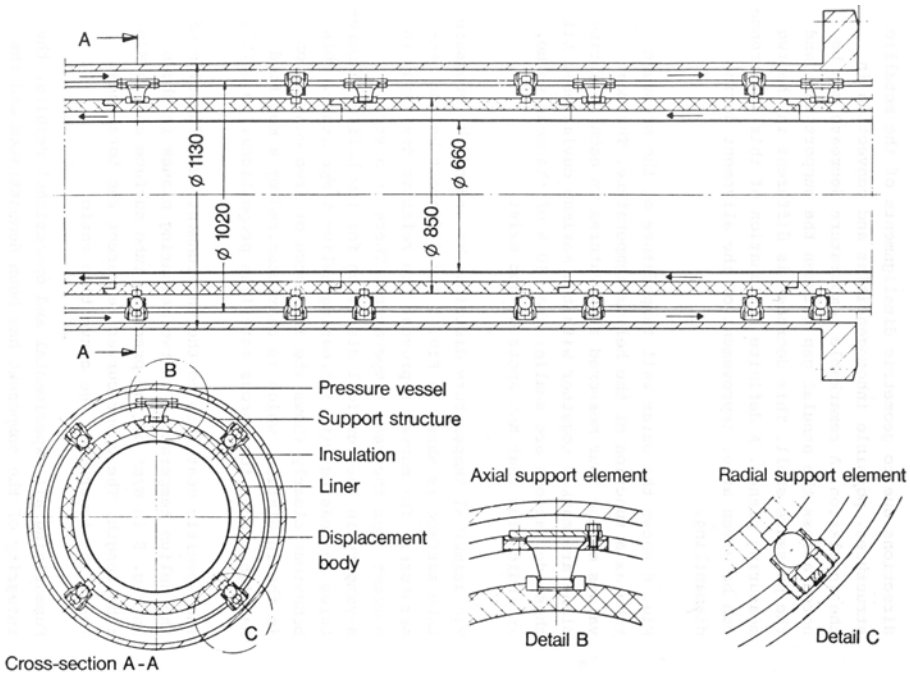

FIG. 102. Hot gas duct in the German KVK loop test facility [291, 292].

In the design with separate tubes, coolant circulates along two separate heat-insulated tubes. The coaxial design is the most widely applied, which ensures higher mechanical stiffness, better compactness and lower heat losses to the environment. However, this design is more complicated and has lower reparability. Intermediate (secondary) circuits, as well as other circuits with lower temperatures may utilize the simpler design with separate tubes.

The coaxial ducts are designed as pressure vessels according to the leak-before-break principle, where the early detection of a leakage would allow immediate plant shutdown. Furthermore, the inside pipe containing the hot

helium is also designed for a pressure of 4 MPa, although the pressure difference to the annular space around containing the returning cold helium is not more than 100 kPa during normal operation. The nominal lifetime of the hot gas duct component should be the entire reactor operation period of ~60 years. Correspondingly, there is a secondary hot gas duct in the secondary circuit between IHX and the process heat exchanger.

The hot gas duct for the PNP reactor was designed for 950°C and 4 MPa with a helium mass flow of 37 kg/s (flow velocity of ~60 m/s) [291]. Inner insulation was given in the form of either metallic foils or solid fibres, or carbon ceramics. A number of investigations regarding fracture mechanics of the duct were carried out. The leak-before-break criterion was met, even at room temperature. Testing of this component was conducted with air and helium in the high pressure helium component test loop facility KVK (see also Section 6.3.2).

For the coaxial ducts connecting nuclear and chemical reactors, design data were 900°C maximum temperature at a pressure of 4.2 MPa and a mass flow of 37 kg/s. Dynamic effects of an LOFC accident can be mitigated by so-called burst diminishers installed inside and outside the ducts. This is the idea of having a tube inside a pressure tube, which is capable of taking up the blast pressure to allow the depressurization to proceed more gently, e.g. due to many small boreholes in the walls [293].

Intermediate heat exchangers and other issues of coupling are described in detail in Section 6.

5.3.5. Helium coolant

Under normal circumstances, helium is a highly pure coolant with impurities in the ppm range. At higher temperatures, however, these impurities, typically O_2, H_2O, CO_2, N_2, H_2 and CH_4, may lead to enhanced corrosive interactions with graphitic and metallic materials in the primary circuit. The essential reactions are those with the oxygen containing impurities and the graphite, resulting in dust formation. CO and CH_4 may decompose under certain conditions, with the carbon dust depositing and releasing the 'original' impurities, which could start a new corrosion cycle, thus leading to a carbon transport with the helium through the primary circuit. Depending on how much of the helium is routed through the purification system, a certain part of the coolant activity is also directly being removed from the circuit. Under steady state normal operating conditions, the activity in the coolant is low.

With an increasing temperature level in the core during normal operation, the coolant chemistry will change as well. Due to the higher temperatures at the metallic heat exchanger surfaces in process heat plants, there will be enhanced reactions of gaseous impurities resulting in corrosion, carburization and decarburization. The type of process depends on the temperature, the gas composition and the metal used. PNP-helium is a standardized testing gas that was defined as indicated in Table 24.

Maximum allowable change rates for the reactor coolant temperature under normal operation depend on the temperatures of the reactor coolant and the metal structures in contact with the coolant. An acceptable stress is limited to the lower level at higher temperatures due to creep damage on the structures. For the example of the HTTR, based on a parametric analysis of the structural integrity of the IHX hot header and reducer, the maximum allowable change rate for the coolant temperature is limited to 15°C/h at temperatures of 650°C or above.

5.3.6. Examples of process heat HTGR concepts

A variety of conceptual designs for follow-up HTGRs have been developed, differing mainly in their core type (pebble/block) and power conversion system (direct cycle/steam cycle/intermediate heat exchanger), but also in their application target (electricity/CHP/process heat/district heating), and with thermal powers ranging between 10 and 1600 MW.

The following subsections provide descriptions of examples of future nuclear reactor concepts dedicated to the (co-)production of hydrogen, or — in an initial demonstration project — to electricity production and modified in follow-on projects to additional industrial applications. These concepts have been elaborated by different countries within their national research programmes and presented in detail in papers and at conferences.

TABLE 24. COMPOSITION OF PNP-HELIUM

Composition	H_2	CH_4	CO	H_2O
Partial pressure in 4 MPa PNP-helium (Pa)	50	2	1.5	0.15

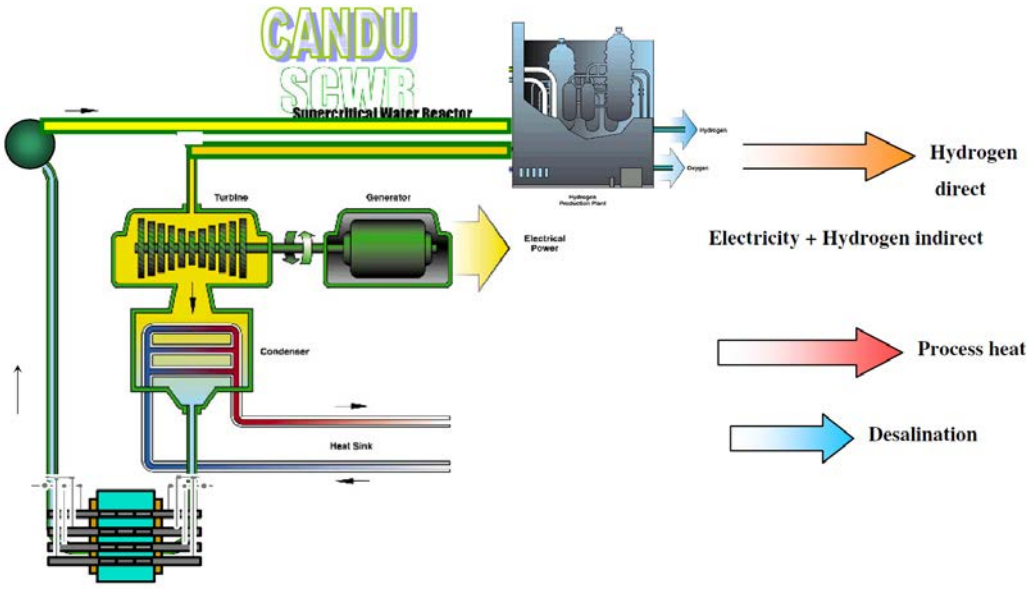

FIG. 103. Temperature ranges in production and use of nuclear energy [282].

5.3.6.1. Canada

The Generation IV concept pursued in Canada is the CANDU-SCWR (Fig. 103). According to preliminary specifications [282, 294], the CANDU-SCWR will produce a thermal power of 2540 MW and an electric power of 1220 MW, corresponding to an overall efficiency of 48%. The moderator is heavy water, while the coolant is light water. The UO_2/Th fuel has a ^{235}U enrichment of 4%. Coolant inlet/outlet temperatures are 350/625°C at a pressure of 25 MPa. There is also the idea of a CANDU-X superheat version which would have additional steam superheat channels capable of further heating up the coolant to 750°C or higher [294].

The Canadian ACR-700 is a pressurized light water cooled, heavy water moderated reactor with a thermal power of ~2000 MW. Similar to CANDU reactors, the ACR design is based on the use of modular horizontal fuel channels surrounded by a D_2O moderator. Major differences are the use of light water coolant and slightly enriched uranium fuel (2.1 wt% ^{235}U), which results in a more compact reactor design. The design also features A higher coolant pressure of 13 MPa at the inlet and a higher outlet temperature of 326°C. Pressure tube reactors are more flexible with regard to flow, flux and density changes; flow rate adjustment and fuel reloading can be handled more easily. The more recent Canadian design is the ACR-1000, similar to the ACR-700 in the use of D_2O moderator and H_2O heat transport and other general features, but a 1200 MW(e) system.

5.3.6.2. China

Based on the experience with the HTR-10, an industrial scale modular HTGR demonstration plant (Fig. 104), the Shidaowang nuclear power plant, HTR-PM, featuring 2 × 250 MW(th) pebble bed reactor units driving one Rankine steam cycle turbine–generator set of 200 MW(e), is being projected as one of the key national technological projects [295]. Corresponding design and R&D work started in 2004. Site preparation and construction permit licencing are currently under way. Manufacturing of long lead components is under contracting. The plant will serve as a starting point to further develop and deploy advanced nuclear technology for the purpose of process heat application, including for hydrogen production.

The design of the HTR-PM demonstration plant is characterized by a ‘two reactors with one generator’ scheme. Two standardized reactors with a total thermal power production of 500 MW collocating one steam turbine generator set have an electric power output of 200 MW. The average thermal power density is about 3.2 MW/m^3 with a maximum value of 6.4 MW/m^3 in the equilibrium core. The average helium coolant outlet temperature is 750°C and the average inlet temperature is 250°C. The rated mass flow rate of the coolant in the primary circuit is

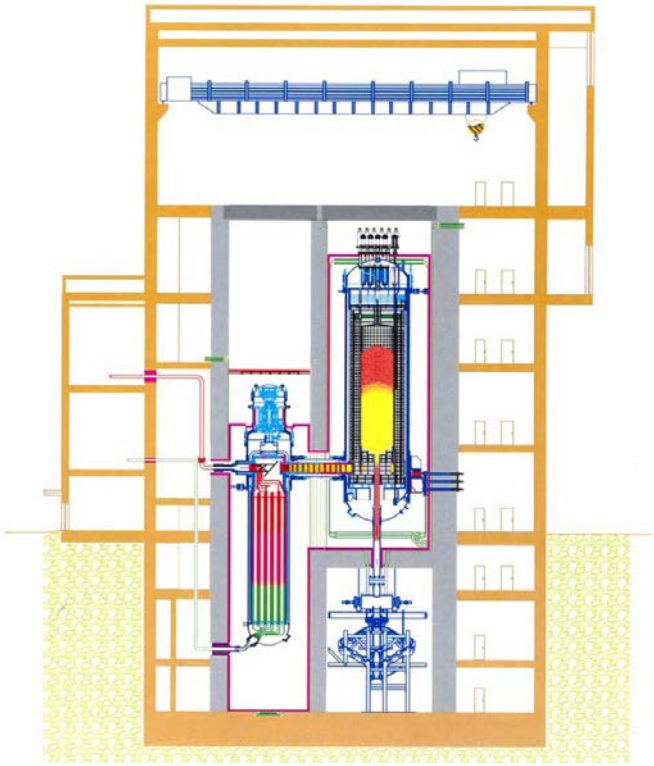

FIG. 104. Schematic of the 250 MW(th) HTR-PM reactor building with steam generator [295].

TABLE 25. HTR-PM MAIN CORE DESIGN PARAMETERS

Thermal power of two units	500 MW(th)
Electric power	200 MW(e)
Average/maximum thermal power density	3.2/6.6 MW(th)/m^3
Reactor coolant inlet/outlet temperature	250/750°C
Core upper plenum inlet pressure	7.0 MPa
Core pressure drop	0.058 MPa
Helium mass flow rate per unit	96 kg/s
Active core height/diameter	11/3.0 m
Reshuffling scheme	Multi-pass, 15 cycles
Average/maximum burnup	90/100 GW·d/t
Reactor pressure vessel inner diameter/height	5.7/24.9 m
Power conversion efficiency	42%
Steam outlet temperature/pressure	566°C/13.2 MPa
Superheated steam flow rate per unit	96 kg/s

96 kg/s, with about 6% flowing as bypass through the control rod channels and gaps between the graphite segments. The rated system pressure is 7.0 MPa. Table 25 gives some key design parameters of the HTR-PM.

The primary pressure boundary is composed of the reactor pressure vessel, the steam generator pressure vessel in a side by side concept, and the hot gas duct pressure vessel, which connects the other two vessels. The helium circulator is a vertical compressor installed on top of the steam generator. A feature of the HTR-PM design is the novel steam generator, which does not consist of a series of nestled helical coil tubes within the steam

generator shell, but rather a number of individual, small helical tube bundles connected at the top and bottom. Designed for 250 MW of thermal power, the steam generator is vertically seated and consists of 19 helical type heat transfer assemblies in a countercurrent flow arrangement. The secondary feedwater is heated and live steam of 538°C at 13.5 MPa is generated to drive the turbine–generator system. In the side reflector, eight control rod units are arranged as the primary shutdown system, which allows the quick hot shutdown of the reactor. The side reflector also includes the 22 small absorber ball units as the second independent and diversified shutdown system.

The primary confinement contains all the equipment of the reactor primary circuit. It includes columnar cavities for both the reactor pressure vessel and the steam generator connected by the hot gas duct. Total volume of the confinement is 3700 m^3. The design pressure in the confinement is 0.13 MPa.

5.3.6.3. France

Based on principles of the HTR-Modul concept and evolving from the US GT-MHR concept, AREVA-NP has been developing the conceptual design of ANTARES, a flexible, modular concept for high, medium and low temperature heat applications and power. In the VHTR concept for electricity generation in a combined cycle power conversion system, the block type core generates a power of 600 MW(th) with a helium outlet temperature of 850°C at a pressure of 5.5 MPa (Fig. 105) [35]. ANTARES uses an annular core consisting of 102 columns with 10 fuel blocks each. This reference configuration, however, may be subject to future changes depending on further optimization studies on the feasibility of a larger fuel block size. ANTARES employs an indirect cycle power conversion system which can be adapted to different cogeneration schemes.

The reference design for the IHX is a plate type heat exchanger for a heat load of 635 MW(th) with inlet/outlet temperatures for the primary helium of 850/390°C at a flow rate of 240 kg/s. The secondary coolant is a nitrogen–helium mixture with inlet/outlet temperatures of 300/900°C at a rate of 614 kg/s. Maximum pressure loss should not exceed 0.1 MPa on the primary and 0.2 MPa on the secondary side. The feasibility of the components has either been proven already or has been deemed achievable at a low technological risk [296]. The general arrangement is based on a single IHX. In contrast, the tubular IHX considered as a fall-back solution would require at least a two loop configuration due to its reduced heat transfer capability compared with a compact plate heat exchanger.

Based on the ANTARES concept, AREVA has developed the preconceptual design of an HTGR for hydrogen production within the USDOE NGNP programme. From that, a modified NGNP version for near term realization was created. The plant has two primary loops, each coupled to a steam generator via a hot gas duct. The lower coolant outlet temperature of 750°C allows an increase in thermal power to 625 MW(th). The steam cycle concept is flexible in that, in addition to electricity production, cogenerated high temperature steam can serve a wide range of process heat facilities. The key parameters of the plant are listed in Table 26 [37].

5.3.6.4. Germany

The use of the basic reactor design for both electricity and process heat generation was a fundamental request in former German industrial HTR development programmes. This applies to the past projects on direct gas turbine cycles (e.g. HHT Nuclear Plant with High Temperature Reactor and Helium Turbine of Large Power), steam cycles (THTR-300, HTR-500) and the related nuclear process heat projects (Prototype Nuclear Process Heat (PNP), NFE) which only required some adjustments with regard to the maximum temperatures and pressure levels of the primary circuit, because the chemical processes are mainly operated at lower pressures than is the case, for example, in the direct gas turbine design. Another general difference is the fact that the cold gas temperatures in the process heat applications are generally much lower (~250–300°C) than those in the gas turbine application (450–550°C), having a beneficial feedback on the pressure vessel design and material choices.

A wide variety of nuclear process heat HTGR concepts were proposed in Germany between the 1970s and 1990s, initially of larger size and later of smaller size. Among them were the modified version of the HTR-500, the 170 MW(th) HTR-Modul concept and the AVR-50. All were characterized by a supply of energy at high temperature levels in the order of 950°C, which allows the achievement of high chemical reaction rates. Of special importance was the 45 MW(th) AVR test reactor in Jülich, which was operated between 1967 and 1988. It became the world's first pebble bed reactor to successfully achieve a coolant outlet temperature of 950°C, proving the feasibility of the pebble bed HTGR concept under high temperature process heat conditions with a high availability.

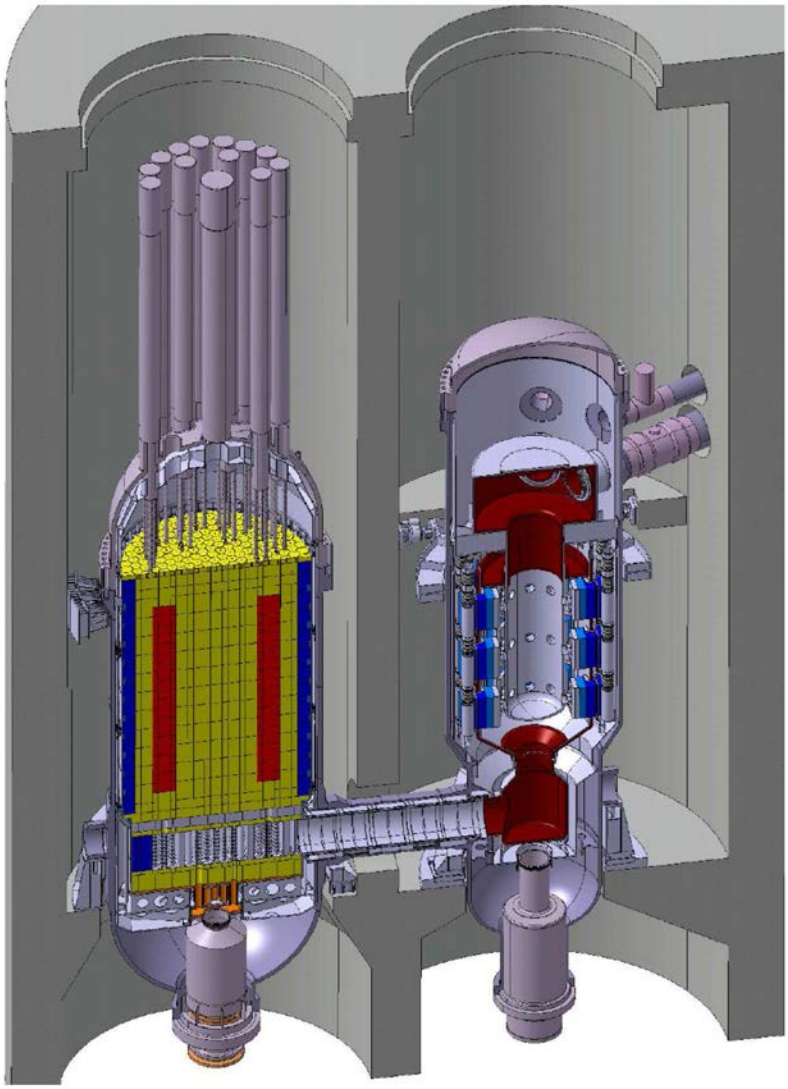

FIG. 105. AREVA-NP's VHTR nuclear heat source ANTARES primary circuit with reactor pressure vessel (left) and plate type IHX (right) [297].

TABLE 26. MAIN CHARACTERISTICS OF THE AREVA NEAR TERM NGNP CONCEPT FOR STEAM PRODUCTION

Prismatic core	102 columns × 10 blocks
Thermal power	625 MW(th)
Helium inlet/outlet temperature	325/750°C
Helium pressure	6 MPa
Secondary coolant	water/steam
Steam temperature	566°C
Steam pressure	16.7 MPa

(A) Prototype nuclear process heat (PNP) reactor

Within the German PNP project, a significant part of the effort was dedicated to the design and demonstration of the ability of HTGRs to be used for process heat applications. The concept for a nuclear process heat plant with

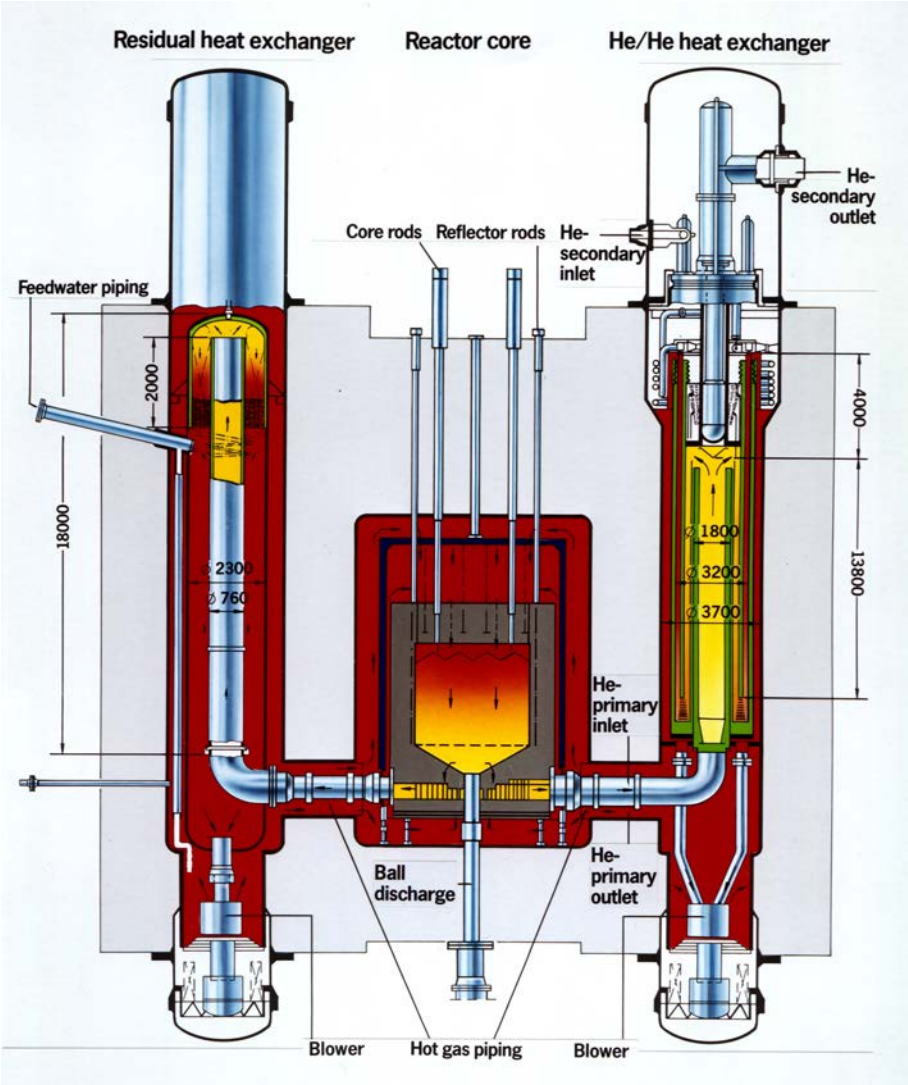

FIG. 106. Schematic of the prototype nuclear process heat plant PR-500 for hydrogasification of lignite (left) and steam gasification of hard coal (right) [293].

a pebble bed high temperature reactor was originally based on thermal power sizes of 500 MW (PR-500) and 3000 MW (PNP-3000). The PR-500 pebble bed reactor, closely corresponding to the THTR-300, was designed to produce 523 t/h of steam at a temperature of 265°C and a pressure of 2 MPa, plus an electric power of 55 MW. The coolant helium is heated up from 265 to 865°C. The hot gas plenum is designed such that maximum gas temperature differences should be not higher than 60 K. The reactor was placed in a pre-stressed concrete pressure vessel (also similar to the THTR-300) surrounded by three units, each containing a heat exchanger and blower in an external arrangement [298].

The PR-500 demonstration reactor was designed for both types of coal gasification (Fig. 106) employing an IHX for steam–coal gasification or a steam–methane reformer for the nuclear hydrogasification of coal. The operation of this nuclear system was designed to yield 41 000 m^3 of SNG for steam gasification of 50 t/h of hard coal and 26 500 m^3 of SNG and 18.4 t/h of charcoal for hydrogasification of 166 t/h of lignite.

Part of the safety concept is the employment of a non-integrated arrangement with separate vessels for the generation and the conversion of heat, and a containment to enclose the total primary circuit. Placement of the nuclear unit at least 6 m underground provides enhanced protection against external impacts.

For adaptation of the reactor design to the chemical process, the reactor pressure had been fixed in the PNP project to 4 MPa, well below the pressure for electricity generating plants (~7 MPa). The choice of the pressure is also important to reduce the loads on the high temperature barriers in case of depressurization accidents either in the primary or in the secondary circuit. Other important aspects of reactor design are the amount of cogenerated

electricity, high availability and optimization toward significant simplification of the nuclear island. Heat transfer under varying operational load conditions, hot gas mixing in the core bottom and the lifetime of the hot gas thermal insulation have been comprehensively investigated in experiments. When starting up the fully cold plant, the steam–coal gasification plant will reach full operation after ~50 h and the hydrogasification plant after about 60 h [293].

The large size reactor concept of the PNP-3000 with a thermal power of 3000 MW was foreseen to be connected to steam reforming with 1071 MW of heat input to six main loops with each containing either a steam reformer plus steam generator or an intermediate heat exchanger, and electricity cogeneration with 540°C/19.5 MPa turbine steam. In the pebble bed with an OTTO loading scheme, the coolant was heated up from 300 to 950°C. Additional systems required were four active decay heat removal systems. All components were positioned in a pre-stressed concrete pressure vessel. The key parameters of both PNP plants are listed in Table 27.

(B) Process heat HTR-Modul

The baseline concept in this development was the electricity producing 200 MW(th) HTR-Modul pebble bed reactor designed by Siemens-Interatom with a tall (9.4 m) and slim (3 m diameter) core. An arrangement of the active core in an annular geometry permits the thermal power output to be raised from 200 to 600 MW without changing the basic philosophy of the 1600°C limit.

A variant of the HTR-Modul for process heat production has been designed for a thermal power of 170 MW to deliver helium at temperatures of 950°C. The key parameters of the plant are also given in Table 27. In comparison with the electricity generating nuclear plant, several modifications are necessary for the process heat variant:

— Reduced power and power density to compensate for the higher core outlet temperature level due to the requirement of self-acting decay heat removal from the core, i.e. for the maximum fuel temperature to stay below 1600°C in the case of an LOFC accident (for the process heat HTR-Modul: 3 → 2.55 MW(th)/m^3, 200 → 170 MW(th)).
— Reduced system pressure as a compromise between a high pressure desired for its favourable effect on operating and accident conditions of the nuclear reactor and a low pressure desired for chemical process reasons in the secondary and tertiary circuit. The pressures in the different circuits should be in the same range, slightly increasing toward the outside (for the process heat HTR-Modul, 7 → 5 MPa; with IHX, 4 MPa).
— Two fuel zones in the pebble bed to minimize the occurrence of hot/cold gas strains in the core to achieve a radial temperature profile as uniform as possible, in order to avoid additional loads on the high temperature heat exchanging components operating under extreme conditions.
— Ceramic (graphite) liner to replace the metallic liner because of the higher temperatures.

TABLE 27. MAIN CORE DESIGN PARAMETERS OF GERMAN PROCESS HEAT REACTOR CONCEPTS

	PR-500	PNP-3000	HTR-Modul
Pebble bed core (# fuel spheres)	550 000	3 360 000	260 000
Thermal power (MW(th))	500	3000	170
Thermal power density (MW(th)/m^3)	5	5	2.55
Helium inlet/outlet temp. (°C)	265/865	250/950	300/950
Helium pressure (MPa)	4	4	5 (with IHX: 4)
Helium mass flow rate (kg/s)	159	820	50
Active core height/diameter (m)	5/5	6/11.3	9.4/3
Reshuffling scheme	OTTO	OTTO	Multipass
Steam outlet temperature (°C)/ pressure (MPa)	265/2	540/19.5	540/11.5
Steam flow rate per unit (kg/s)	145	150	38

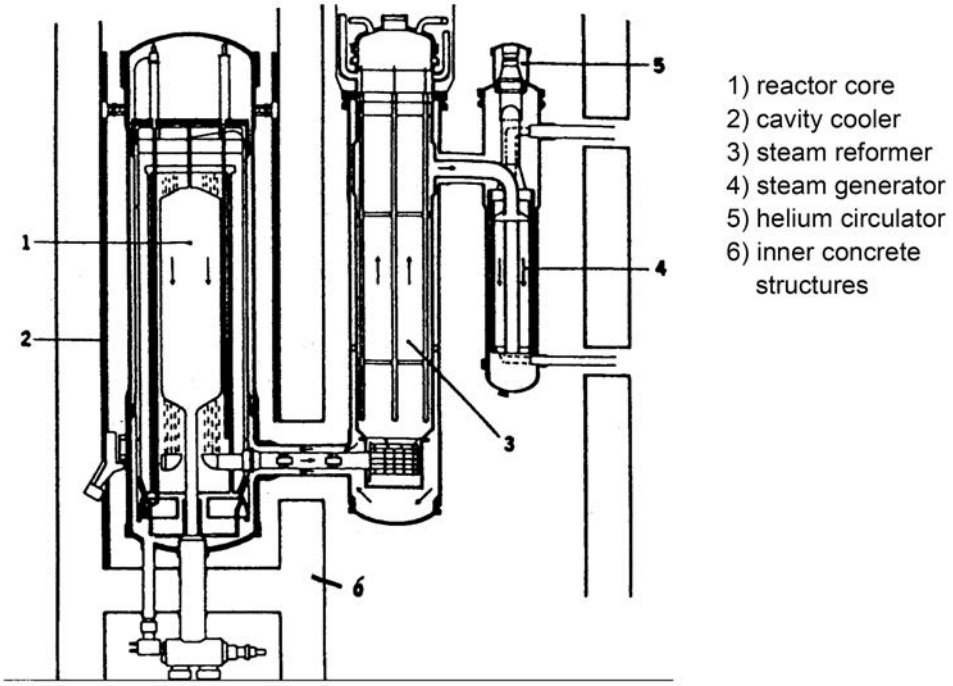

FIG. 107. Arrangement of modular HTR with a steam reformer/steam generator loop.

For nuclear process heat plants connected to steam–methane reforming (Fig. 107), the primary helium coolant is directly fed to the steam reformer, which consumes 71 MW, and to the steam generator, which is operated with 99 MW. The reduction of the helium temperature will be conducted at a slow rate (~1 K/min) to avoid thermal stresses of the heat consuming components. Partial load conditions of the steam reforming process can be regulated by changing the feedgas flow. A requirement, however, is that product gas quality, i.e. composition, should remain constant, which can be accomplished by keeping the reforming temperature constant.

5.3.6.5. India

Under the high temperature reactor programme, BARC is currently developing a compact high temperature reactor (CHTR) as a technology demonstrator for associated technologies [299]. The CHTR is a small-sized, molten heavy metal (Pb–Bi) cooled, beryllium oxide-moderated reactor for the production of a thermal power of 100 kW and a core outlet temperature of 1000°C (Fig. 108). It may therefore serve as a compact power pack in remote areas not connected to the electrical grid, but also be connected to high temperature process heat applications such as water splitting hydrogen production. The reactor is characterized by several advanced passive safety features [300].

The core of the CHTR is composed of 19 prismatic BeO moderator blocks. Each of these blocks has a centrally located graphite fuel tube which contains the fuel in the form of compacts in nine boreholes arranged around the coolant channel in the centre, as can be seen from the cross-section of the CHTR core shown in Fig. 109. Fuel tubes are made of high density, isotropic, nuclear grade carbon–carbon composite or graphite and protected with oxidation resistant coatings. The moderator blocks are surrounded by 12 movable and 6 fixed blocks of BeO reflector, which again are surrounded by graphite reflector blocks. The core is contained in a reactor shell made of a material resistant to corrosion against the Pb–Bi coolant and suitable for high temperature applications.

Top and bottom closure plates of similar high temperature and corrosion resistant material close this reactor shell. Above the top cover plate and below the bottom cover plate, cylindrical vessels called coolant plenums are provided for coolant exit and entry into the core. The upper plenum has a graphite block for guiding coolant flow between the fuel tube and the downcomer tube provided for return of the cold coolant to the lower plenum. The reactor shell is surrounded by two gas gaps that act as insulators during normal reactor operation and reduce heat loss in the radial direction. These gas gaps help in dissipating neutronically limited power to an external sink, in

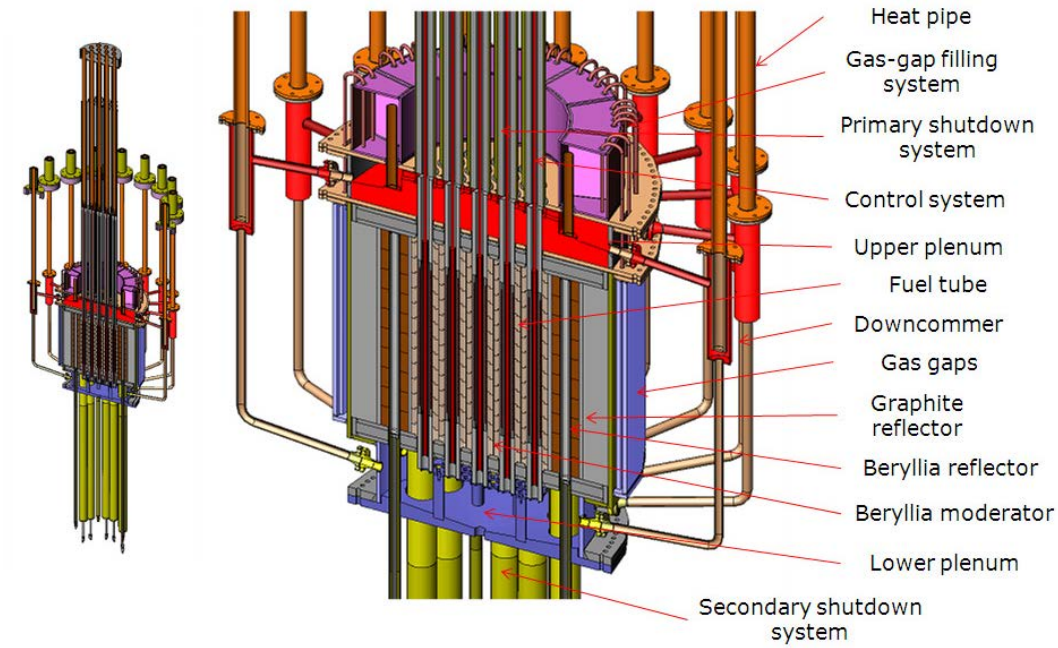

FIG. 108. Schematic of the Indian CHTR [299].

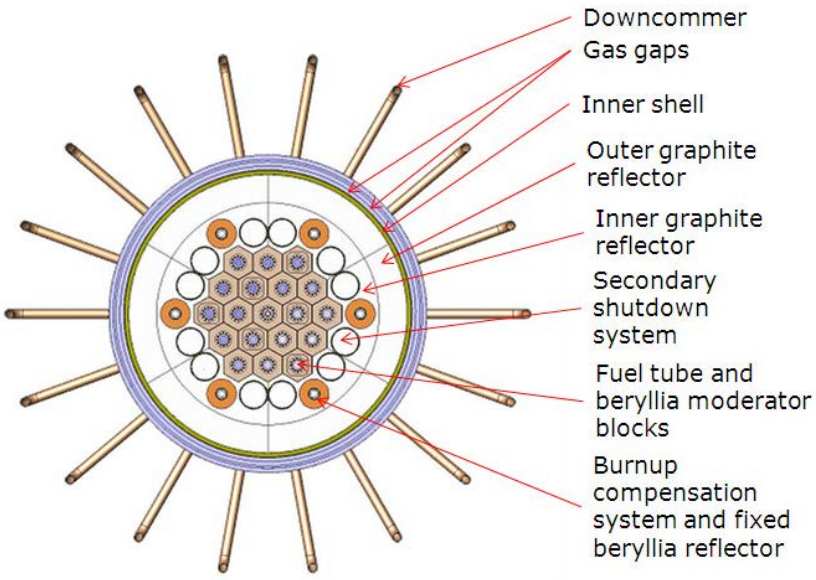

FIG. 109. Cross-section of the CHTR core [299].

case of a postulated accident. A passive system has been provided to fill these gas gaps with molten metal in case of an abnormal rise in coolant channel outlet temperature. Nuclear heat from the reactor core is removed passively by natural circulation based flow of coolant between the two plenums, upward through the fuel tubes and returning through the downcomer tubes.

On top of the upper plenum, the reactor has heat utilization vessels to provide an interface to systems for high temperature process heat applications. A set of sodium heat pipes passively transfers heat from the coolant to these heat utilization vessels. To shut down the reactor, a set of seven tantalum alloy based shutoff rods has been provided, which fall by gravity in the central seven coolant channels. Twelve control rods of the same material have been provided in the balance fuel tubes. Appropriate instrumentation like neutron detectors, fission/ion chambers

and sensors, and auxiliary systems such as cover gas system, purification systems, etc., are being incorporated into the design.

The fuel concept is based on compacts with TRISO coated particles containing a (^{233}U–Th) mixed carbide kernel. The fuel is designed to operate up to 1000°C during normal operation. The expected core lifetime is 15 years. The heat is removed by molten Pb–Bi eutectic alloy coolant which circulates through the core by natural convection, flowing upwards through the coolant channels in the moderator blocks into the upper plenum, where it is heated up from 900 to 1000°C. Downward flow is through the downcomer tubes in the graphite reflector blocks into the lower plenum. Both plenums have graphite flow guiding blocks.

Heat utilization vessels are located on top of the upper plenum; heat from the hot coolant is passively transferred to the vessels by means of 12 sodium heat pipes. Heat pipes are also activated under accident conditions to transfers heat to the atmosphere. The reactor is shut down by 18 floating annular B_4C elements as the primary system and by seven shutoff rods made of tungsten, which fall by gravity in the central seven coolant channels as the secondary system. The major characteristic design and operating parameters of the CHTR are listed in Table 28.

At present, a detailed design of the CHTR has been established after completing the conceptual design of the reactor and associated systems. Experimental facilities are at various stages of development to carry out a wide array of studies related to liquid metals, passive safety and heat removal systems. The manufacturing capabilities for BeO, carbon components and TRISO coating based particle fuel have been successfully achieved. Subsequent to the manufacture of fuel, materials and other systems, a critical facility for the CHTR will be set up.

The principal objective of the CHTR is the demonstration of the various innovative technologies such as fuels, materials and various passive safety features applied in this concept.

In order to generate hydrogen on a large scale using high temperature thermochemical processes (>850°C), a follow-up nuclear plant, called the Indian High Temperature Reactor for Hydrogen Production (IHTR-H), is currently being designed for a thermal power output of 600 MW(th). The design is based on a pebble bed type fuel configuration using a molten salt based coolant with several inherent and passive safety features. The main goal is the supply of heat at ~1000°C for large scale hydrogen production at a rate of 80 000 Nm^3/h, 18 MW(e) of electricity generation, plus the production of desalinated water at a rate of 375 m^3/h [299].

TABLE 28. CHARACTERISTIC PARAMETERS OF THE CHTR [299]

Thermal power	100 kW(th)
Core configuration	Prismatic block type
Core diameter/length	1.27/1.0 m
Loop height	1.5 m
Moderator	BeO
Reflector	BeO, graphite
Coolant	Pb–Bi eutectic alloy (44.5% Pb and 55.5% Bi)
Inlet/outlet temperature	900/1000°C
Flow rate	6.78 kg/s
Fuel tubes	19 (one per moderator block)
Inner/outer diameter	35/70 mm
Tube length	1.4 m
Compact diameter/length	10/35 mm
Fuel	(^{233}U,Th)C_2 TRISO coated particles
Enrichment	33.75%
Heavy metal contents	^{233}U: 2.7; Th: 5.3 kg
Burnup	~68 GW·d/t
Lifetime	5500 equivalent full power days

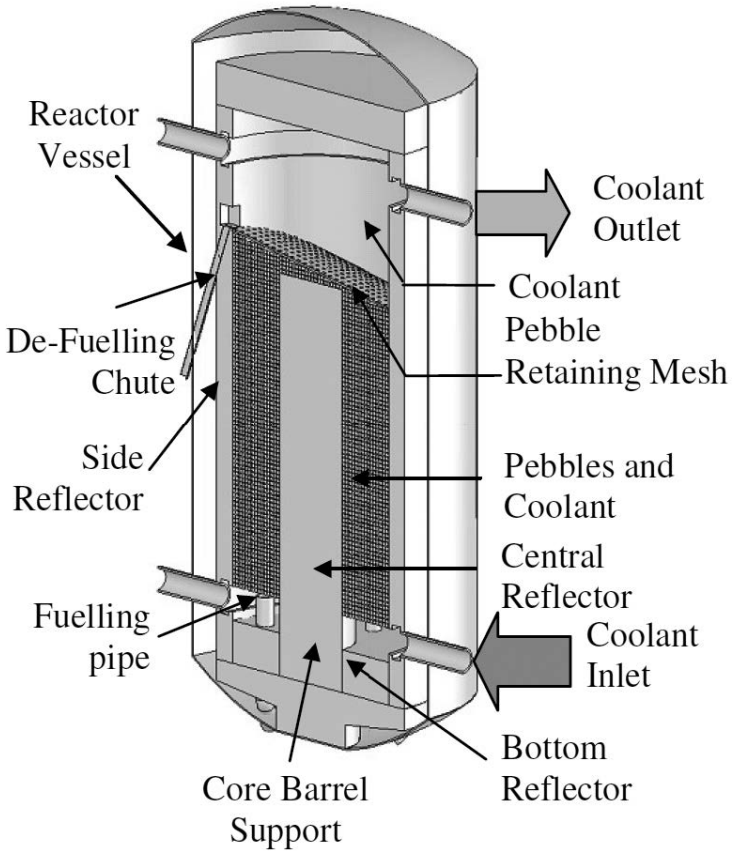

FIG. 110. Core configuration of the Indian 600 MW(th) IHTR [300].

For this reactor various design options for fuel configurations, such as a prismatic bed and pebble bed, were considered for thermal hydraulics and temperature distribution analysis. Coolant options such as molten lead, molten salt and a gaseous medium like helium were analysed. Furthermore, other criteria such as ease of component handling, irradiation related material and fuel degradation, better fuel utilization and passive options for coolant flow, etc., were also considered. Initial studies carried out led to the selection of a pebble bed reactor core with a molten salt based coolant. Figure 110 shows a schematic of the IHTR reactor.

5.3.6.6. Japan

(A) Commercial nuclear hydrogen production with GTHTR300C

In the GTHTR300C (C for cogeneration), the reactor is operated with an outlet temperature of 950°C. A thermal power of 170 MW is transferred from the primary to the secondary helium in the IHX. The secondary helium can be heated up to 900°C. The helically coiled He–He intermediate heat exchanger is installed between the reactor pressure vessel and gas turbine system. The outlet helium gas of 135°C from the compressor is used to cool the reactor pressure vessel so that the vessel can be made of LWR steel. The recuperator recovers turbine exhaust heat. The efficiency of the recuperator affects the electricity cost significantly. Compact and high efficient plate heat exchangers operating in high pressure helium gas are employed.

Helium heat in the secondary circuit is then passed via a compact process heat exchanger to a third loop of hydrogen production. The hydrogen production system will be designed according to existing non-nuclear industrial standards [55]. The reactor will be connected to an S–I thermochemical water splitting process. The requirement from utilities for the GTHTR300C is two year continuous operation. The reactor design specifications of the GTHTR300 and the GTHTR300C are the same except for the reactor outlet and inlet helium temperature and the helium flow rate. Major design specifications of the GTHTR300 and the GTHTR300C are listed in Table 29.

TABLE 29. MAJOR DESIGN SPECIFICATIONS OF THE GTHTR300 AND GTHTR300C

	GTHTR300	GTHTR300C
Reactor thermal power (MW(th))	600	
Thermal power density (MW(th)/m^3)	5.8, maximum 13–15	
Core coolant flow (kg/s)	439	322
Core inlet/outlet temperature (°C)	587/850	594/950
Gas turbine inlet temperature (°C)	850	
Core coolant pressure (MPa)	6.9	5.1
Average/maximum fuel burnup (GW·d/t)	112/140	
Electricity generation (MW(e))	274	202
Intermediate heat exchanger (MW(th))	—	170

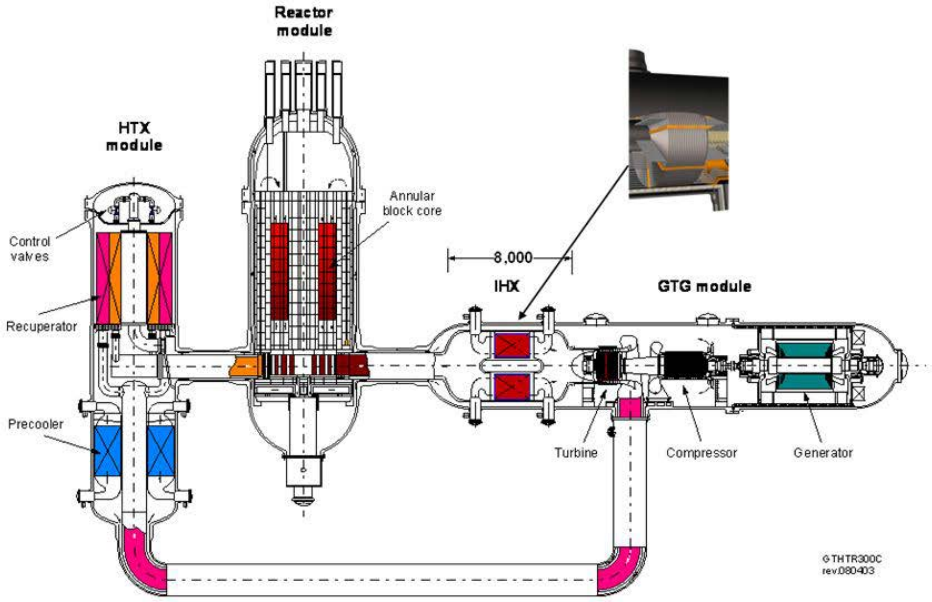

FIG. 111. Design of Japan's VHTR system GTHTR300C for hydrogen production with S–I cycle [54].

Figure 111 shows the system layout of the GTHTR300C. It consists of four system modules: a reactor module, a gas turbine module, a heat exchanger module and an intermediate heat exchanger module.

JAEA has conducted a compressor development programme to investigate helium compressor aerodynamics compared with air compressors. For the magnetic bearing development, a test rig has been constructed which is a one third scale mock-up for the generator rotor [55]. The secondary helium pipes in the heat transfer loop penetrate the reactor confinement building. Failure of heat transfer tubes in the IHX and the secondary helium pipe outside the reactor building can create a flow path to release helium coolant to the environment and to flow air into the reactor. However, multiple isolation valves are installed on the secondary helium piping near the penetration of the reactor building to mitigate the consequences of beyond design basis events.

Assuming a hydrogen conversion efficiency of 50% and an availability of 90%, the average amount of hydrogen is 24 000 Nm^3/h, corresponding to the supply of some 100 refuelling stations (assuming ~6000 Nm^3/d per station) to keep a total of about 160 000 FCVs (~3.6 Nm^3/d) operating [301].

The hydrogen production system coupled to the HTGR should be a non-nuclear-grade chemical plant to reduce construction and maintenance costs, because hydrogen produced by the cogeneration HTGR system must be economically competitive with hydrogen produced by the conventional fossil system. Figure 112 shows the design classification of the GTHTR300C [55].

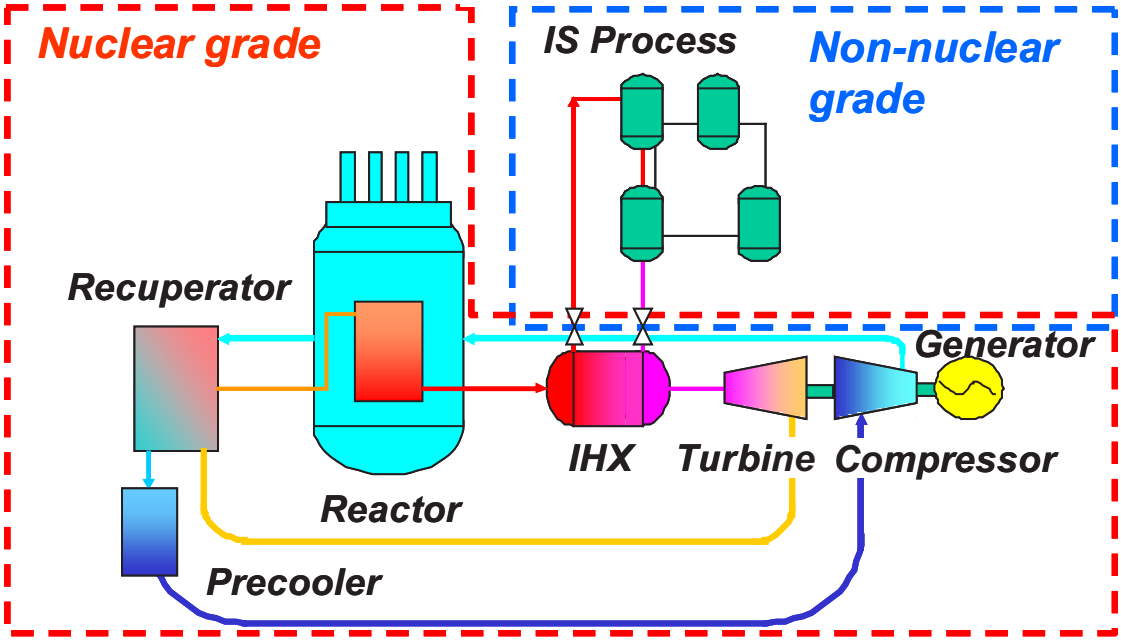

FIG. 112. Design classes of the VHTR-IS system GTHTR300C [302].

(B) Hydrogen production with fast reactor

The so-called 'FR-MR' concept has been suggested [105, 303] for performing methane–steam reforming at much lower temperatures, ~550°C, by employing membrane reformer technology. Thus it would be possible to utilize the nuclear heat of sodium or lead cooled FBRs or of supercritical water cooled reactors. The FR-MR is designed to be a sodium cooled fast reactor with a thermal power of 240 MW(th) and coolant inlet/outlet temperatures of 500/580°C and, at an advanced stage, 450/600°C. Heat is transferred via an IHX to the membrane reformer at temperatures of 565 and 580°C. H_2 production is assessed to be 200 000 Nm^3/h using a feedstock (CH_4) input of 50 000 Nm^3/h. Membrane reforming heated by nuclear energy can also be applied in the refining industries, helping to save hydrocarbon feedstock. Furthermore, it would allow coal gasification at reduced temperatures [105].

5.3.6.7. Republic of Korea

The reference concept of a nuclear process heat reactor currently planned in the Republic of Korea is a VHTR with a thermal power of 200 MW(th) and a coolant outlet temperature of 950°C at 7 MPa. It will be an underground reactor with an intermediate heat exchanger and a process heat exchanger to be connected to a five train S–I thermochemical plant (see Fig. 15 in Section 2.7.2). A limiting factor for the power level is the size of the reactor pressure vessel, which should not have longitudinal welding and is to be fabricated by domestic suppliers. Four different core designs are currently being discussed for the demonstration plant, two based on a pebble bed and two on a block core design. The power size is 200 MW(th), making it the proper size to be connected to an oil refinery plant or a hydrogen production plant [266].

Based on the German HTR-Modul concept, a pre-conceptual design of a 200 MW(th) pebble bed reactor for process heat applications, NHDD-PBR200, has been developed at KAERI. Coolant inlet and outlet temperatures are 490°C and 950°C, respectively. Two-zone fuel reloading and the placement of a neutron absorber material in the upper part of the side reflector have been proposed to flatten the axial power profile and lower the fuel temperatures.

Unlike in the concepts of other countries, the Republic of Korea is pursuing the NHDD project as a hydrogen dedicated nuclear plant. The hydrogen production methods actively being investigated are the S–I cycle, high

temperature steam electrolysis and the hybrid-sulphur cycle [266]. The previously pursued methane–methanol–iodomethane thermochemical cycle [304] has been discontinued.

The chemical plant is expected to need more scheduled shutdowns due to replacement of components (valves, seals, etc.) or catalyst. Therefore, the hydrogen section is divided into five trains to allow for a continuous operation of the VHTR reactor. This concept requires a manifold of hot gas ducts to distribute heat from the reactor to the trains [266].

5.3.6.8. Russian Federation

(A) MHR-100GT concept as process heat reactor

The reference design for a nuclear process heat complex is the so-called MHR-T energy-technological complex composed of 4 × 600 MW(th) reactor modules and designed for the production of electricity and hydrogen through steam reforming of methane or high temperature steam electrolysis [305]. Some important parameters are listed in Table 30.

Also other preconceptual studies for various process heat applications have been conducted based on the small modular MHR-100 high temperature reactor (Fig. 113), which again is based on the well developed, joint US–Russian GT-MHR concept [69]. The MHR 100GT reactor is designed for a thermal power capacity of 215 MW with a helium outlet temperature of 850°C and employs a direct Brayton cycle for electricity production at a 46.1% efficiency.

The process heat options being investigated are:

— Heat and power cogeneration (MHR-100GT);
— Hydrogen production by means of SMR (MHR-100SMR);
— Hydrogen production by means of HTSE (MHR-100SE);
— High temperature heat supply to crude oil refinery (MHR-100OR).

The MHR-100GT reactor is designed for a thermal power capacity of 215 MW and employs a direct Brayton cycle for electricity production with an estimated 46.1% efficiency. Helium inlet and outlet temperatures are 558 and 850°C, respectively. In the heat and power cogeneration plant, additionally water is delivered at a temperature of 145°C [69].

(B) Metal cooled fast reactor for steam reforming of methane

Another technology has been developed in the Russian State Scientific Centre Institute for Physics and Power Engineering in the frame of activity on non-electricity applications of advanced liquid metal cooled fast reactors realized since 1990 [72]. One of the proposed applications is hydrogen production by methane thermal disintegration through direct contact heat transfer from the liquid metal coolant Pb–Bi to a hydrogen containing gaseous raw material such as methane. In direct contact heat exchangers, heat transfer takes place between two immiscible fluids coming into direct contact.

TABLE 30. CHARACTERISTIC PARAMETERS OF THE MHR-T

Thermal power	600 MW(th)
Helium outlet temperature	950°C
Power for hydrogen production	
Electric	205.5 MW(e)
Thermal	160 MW(th)
Hydrogen output	54 050 t/a
Lifetime	60 a

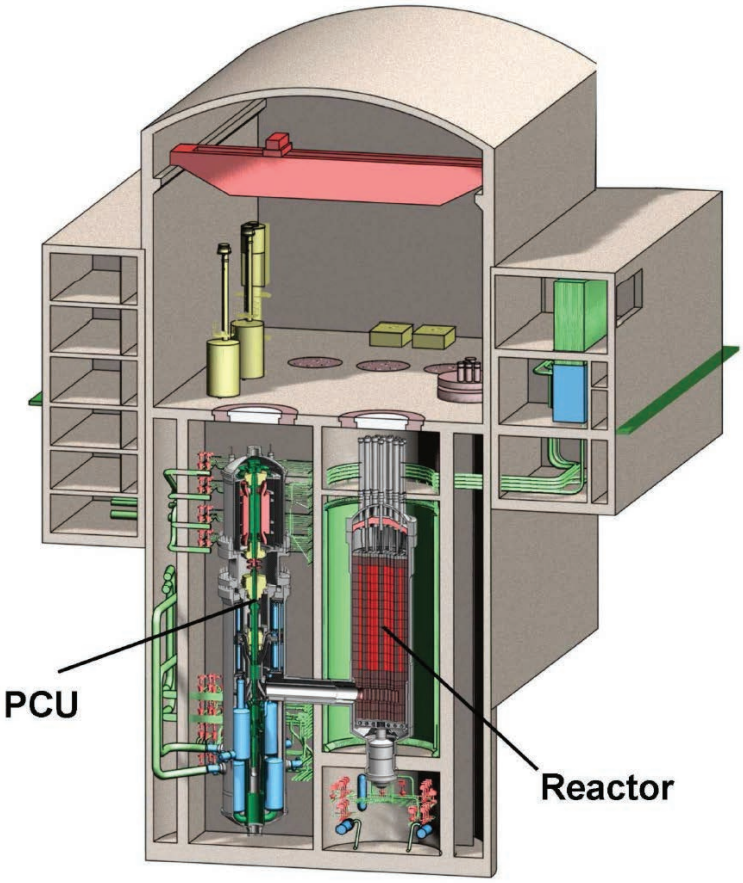

FIG. 113. Schematic of MHR-100GT [69].

As is shown in the schematic in Fig. 114, the Pb–Bi (secondary) coolant is heated up from the primary reactor coolant (Pb–Bi, Pb, or Na) in a metal–metal IHX and circulates through a reactor vessel. Methane is given into the lower part of the vessel, where it bubbles through the hot coolant and is partially decomposed (pyrolysis). A separation device then separates the hydrogen from the solid carbon and still un-decomposed methane. The method foresees the use of a liquid metal heated by reactor coolant up to 700°C and methane under atmospheric pressure. The assumed yield of hydrogen in this process is up to 95%.

In a similar process, instead of pure methane, a mixture of methane and water vapour enters the reactor vessel. In this case, hydrogen is generated via the reforming reaction while bubbling through the hot secondary liquid metal coolant. At 700°C, a methane partial pressure of 0.05 MPa and a steam to methane ratio of 2, the hydrogen yield was estimated to be ~85%.

5.3.6.9. South Africa

The demonstration power plant proposed by the PBMR company is a 400 MW(th) pebble bed modular reactor (PBMR) in a filtered confinement with a direct cycle gas turbine to convert the heat into 175 MW of electric power (Fig. 115) [306]. Its pebble bed core is to be annular with a solid inner reflector column of prismatic graphite reflector elements. The PBMR uses the closed Brayton cycle with a recuperator and intercooler arranged in a non-integrated design with the reactor and the power conversion unit in two different vessels side by side in a filtered confinement. The PBMR turbine plant is of a horizontal, single shaft design. Coolant inlet and outlet temperatures are 500°C and 900°C, respectively, at a pressure of 9 MPa. Operation targets are a 40 year nominal lifetime and 95% availability.

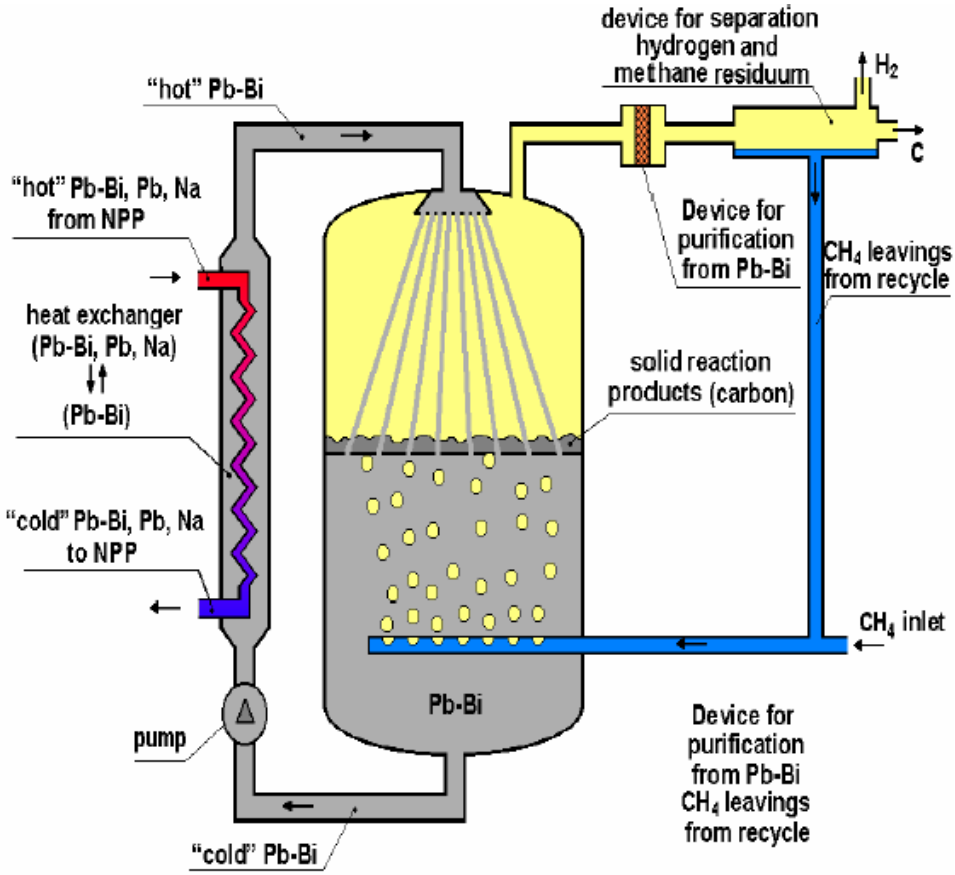

FIG. 114. Hydrogen production by methane thermal disintegration in the reactor coolant [72].

A later change in the market strategy has led to a modified PBMR plant concept, NPP200 for cogeneration (Fig. 116), with lower technological risk and more credit taken from existing HTGR technologies, in particular, the extensive pebble bed experience from Germany. The power size has been lowered to 200 MW(th) in a core of about 3 m diameter and about 10 m height in order to better meet the needs of process heat/steam customers and to compete with smaller scale energy plants.

5.3.6.10.United States of America

The GT-MHR (Fig. 117) consists of a set of four 600 MW(th) MHR modules with each unit coupled to an IHX to transfer the heat to a secondary helium loop. The heat is then transferred to the S–I based hydrogen production system. The IHX design is based on the PCHX (see Section 6.2.2.1). The IHX design consists of 40 modules and associated manifolds within an insulated steel vessel, with each module transferring about 15 MW(th) [158].

In the S–I cycle based H2-MHR, each of the four modules is coupled to an IHX, through which heat is provided to the thermochemical cycle at temperatures above 800°C, whereas the remaining heat is used for electricity production to operate pumps and compressors on the H_2 production side. The primary helium loop and H_2SO_4 decomposition unit will be operated at a 7 MPa system pressure, the secondary helium loop at a slightly higher pressure. Nominal peak process temperature for the H_2 production is 900°C. Assuming a H_2 production efficiency of 45% and a plant capacity factor of 90%, the annual H_2 production rate will be 3.68×10^5 t delivered at a pressure of 4.0 MPa. Several different concepts for coupling the H2-MHR to the S–I process are being evaluated. The option to run the H_2SO_4 and HI decomposition reactions in series, as shown in Fig. 118, is favoured over the option of parallel operation. The reason is that the design conditions are more optimized with respect to heat utilization and heat exchanger pinch points, and because the power topping cycle used with the parallel

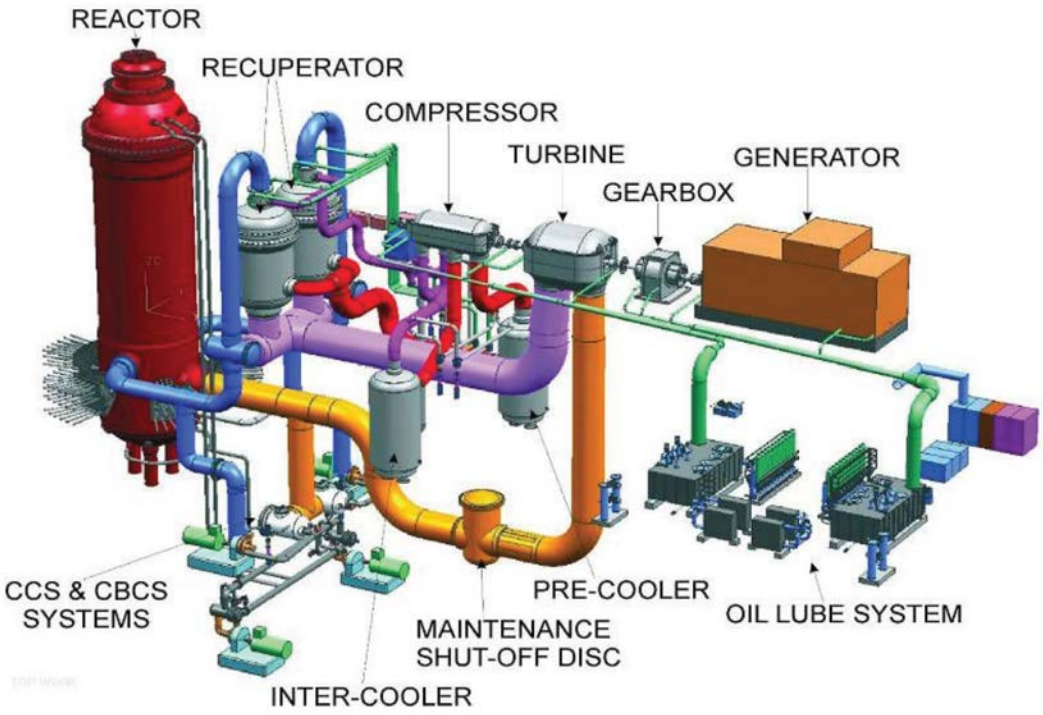

FIG. 115. Schematic of the 400 MW(th) PBMR [307].

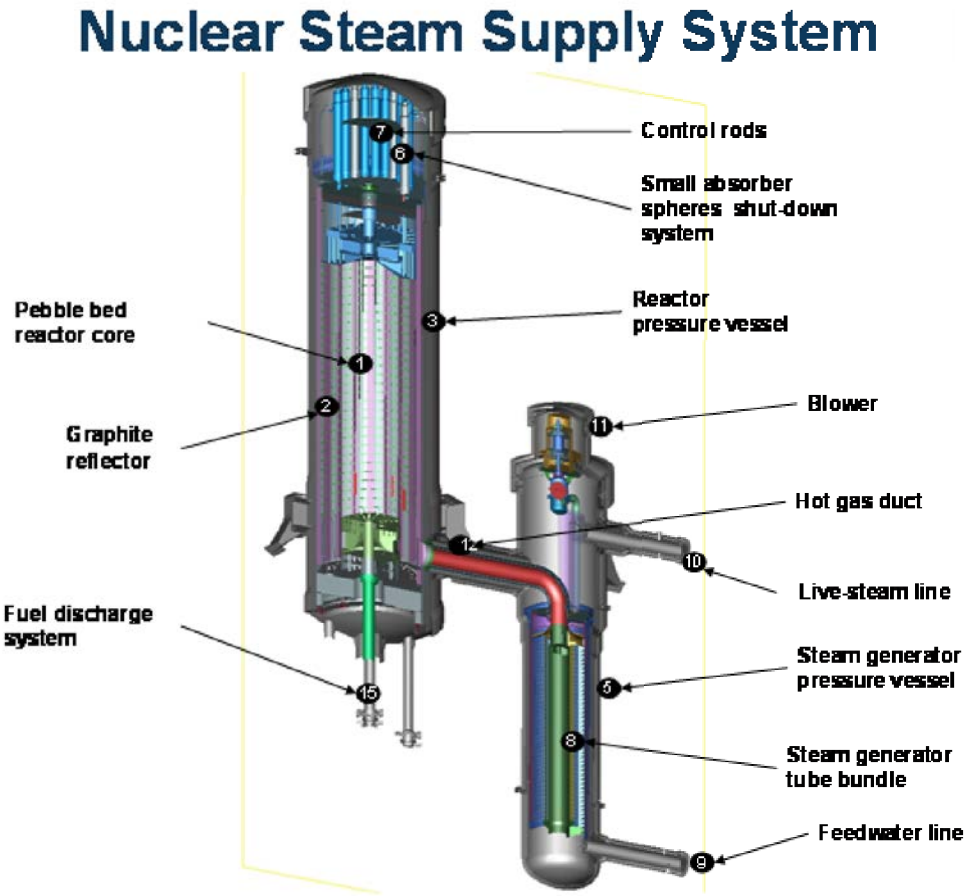

FIG. 116. NPP200 concept with nuclear steam supply system [75].

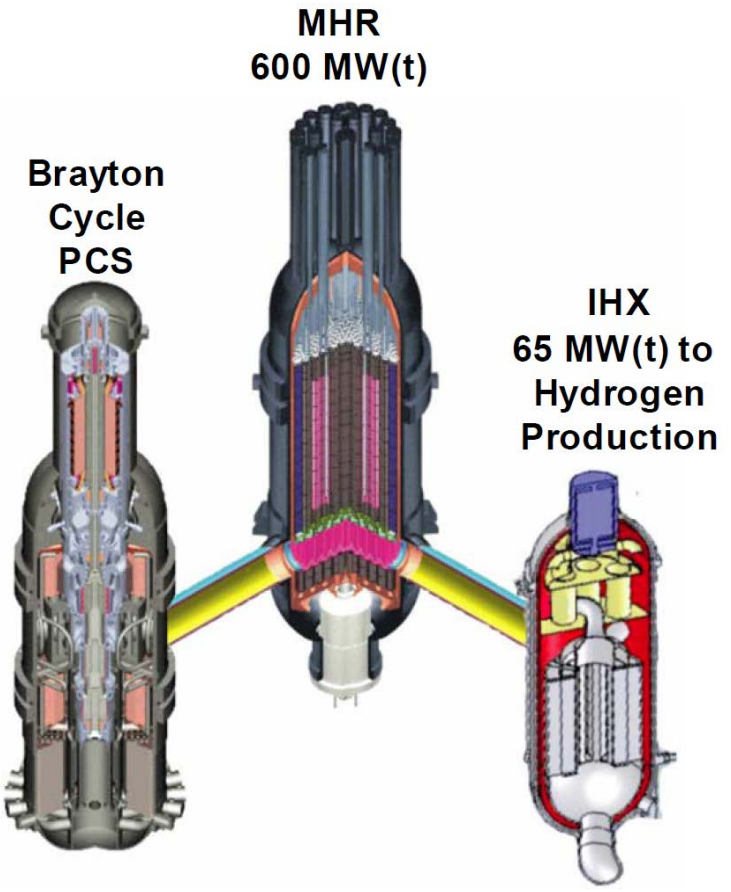

FIG. 117. NGNP preconceptual design based on the GT-MHR [270].

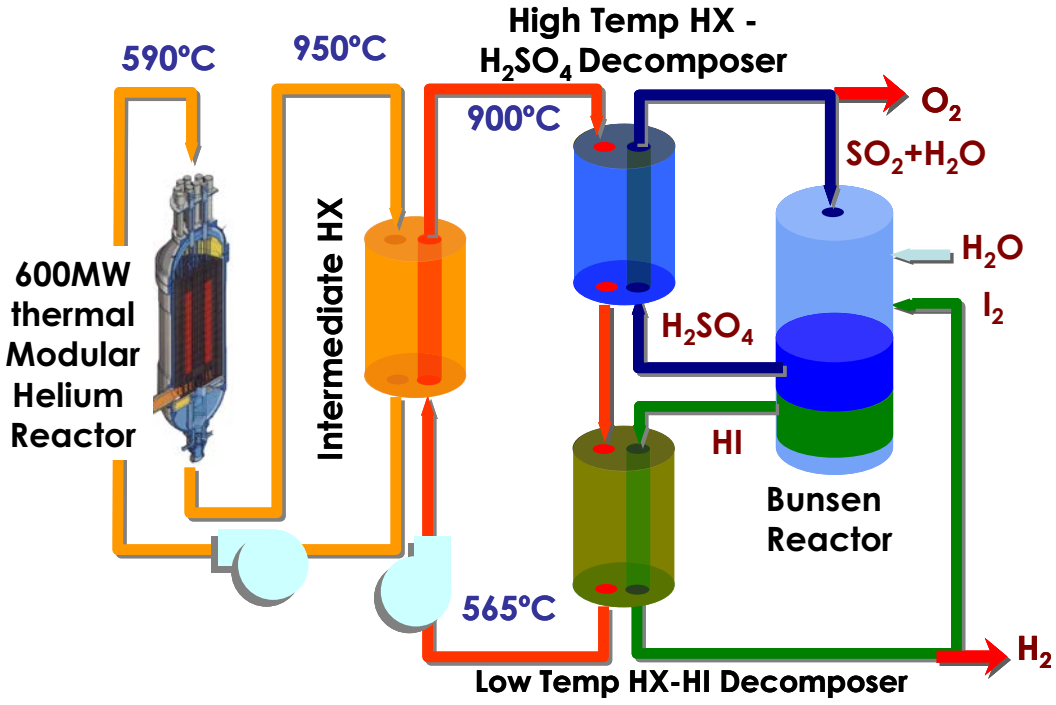

FIG. 118. Concept of the US H2-MHR coupled with the S–I cycle [158].

configuration adds complexity without significant improvements in the overall efficiency [149]. Overall efficiency is expected to be 45%.

In the HTSE-based H2-MHR (see Fig. 23), 68 MW of heat is transferred through a printed circuit IHX to produce superheated steam, while the remaining power is taken for electricity production. The concept of the HTSE section is to have 12.5 kW(e) 500-cell stacks with 100 mm × 100 mm cells. The efficiency of the HTSE system coupled to an advanced reactor has been estimated by INL to be 45–50%. An electrolysis module would contain 40 of the 500-cell stacks consuming 0.5 MW(e). Eight such modules could be installed in a structure that could be mounted on a typical truck trailer, with 292 trailer loads required for a full scale plant consisting of four 600 MW(th) MHR plants [308]. About 90% of the nuclear heat generated is used to produce electricity. The remainder of the heat is transferred through an IHX to a steam generator. Both electricity and steam are supplied to the electrolytic cell. The steam generator supplies very superheated steam to the cells at a temperature of 750–950°C, and a pressure of 1–5 MPa [309]. Design parameters for the HTSE cells are given in Table 31 [310].

The reference design (Fig. 119) [311] considers a large size cylindrical core of 2400 MW(th) with a power density of 10.0 MW/m^3 made of 265 fuel columns with ten blocks each. This design differs from an earlier design which had an annular fuel arrangement. The fuel is 15% enriched UCO for a maximum burnup of 156 GW·d/t. The active core inside a 9.2 m diameter reactor vessel is cooled by a liquid fluoride salt (2LiF–BeF_2) at near atmospheric pressure. The large power size, which can be selected up to 4000 MW(th), represents the main difference from a gas cooled reactor whose decay heat removal capability limits its size to ~600 MW(th). The closed primary loop immersed in a tank contains a separate buffer salt to be used as a heat sink for various transients [312].

The safety goals of the AHTR are identical to those of an MHTGR. In an LOFC scenario, the liquid salt will develop a significant natural convection, through which a much larger quantity of heat can be transported to the reactor vessel compared with a gaseous coolant. This limits the maximum fuel temperature to an estimated 1160°C in such a case. Another difference is the small difference in the coolant between core inlet and outlet of approximately 100°C. Reactor inlet and outlet temperatures of the primary FLiBe coolant are 600ºC and 704ºC, respectively. Operation of the LS-VHTR is at near atmospheric pressure. The coolant inventory of a 1000 MW(e) plant is ~280 m^3 [312].

During normal power operation, when the primary loop operates in forced circulation, heat is transferred to four intermediate liquid salt loops using a modular, compact IHX, before it is utilized for electricity or hydrogen generation. Upstream of the IHX modules are the four primary pumps. The primary loop including the reactor

TABLE 31. ELECTROLYSIS CELL CHARACTERISTIC DESIGN OF CONCEPTUAL HTSE PLANT

Active cell area	100 cm^2
Electrolyte	Scandia-stabilized zirconia of 10 μm thickness
O_2 electrode	Strontium-doped lanthanum–manganite of 1500 μm thickness
H_2 electrode	Nickel–zirconia cermet of 50 μm thickness
Bipolar plate	Nickel–aluminium of 2500 μm thickness
Total cell height	4.06 mm
Number of cells per stack	500
Stack height	2.03 m
Total number of cells	12×10^6
Total active area	120 000 m^2
Total hot volume	$26 \times 15 \times 5$ m^3
Cell operating conditions	850°C, 5 MPa, 0.2 A/cm2, 1.1 V
Water consumption	22.3 kg/s
Hydrogen production (LHV)	2.5 kg/s or 238 t/d at 50% overall efficiency

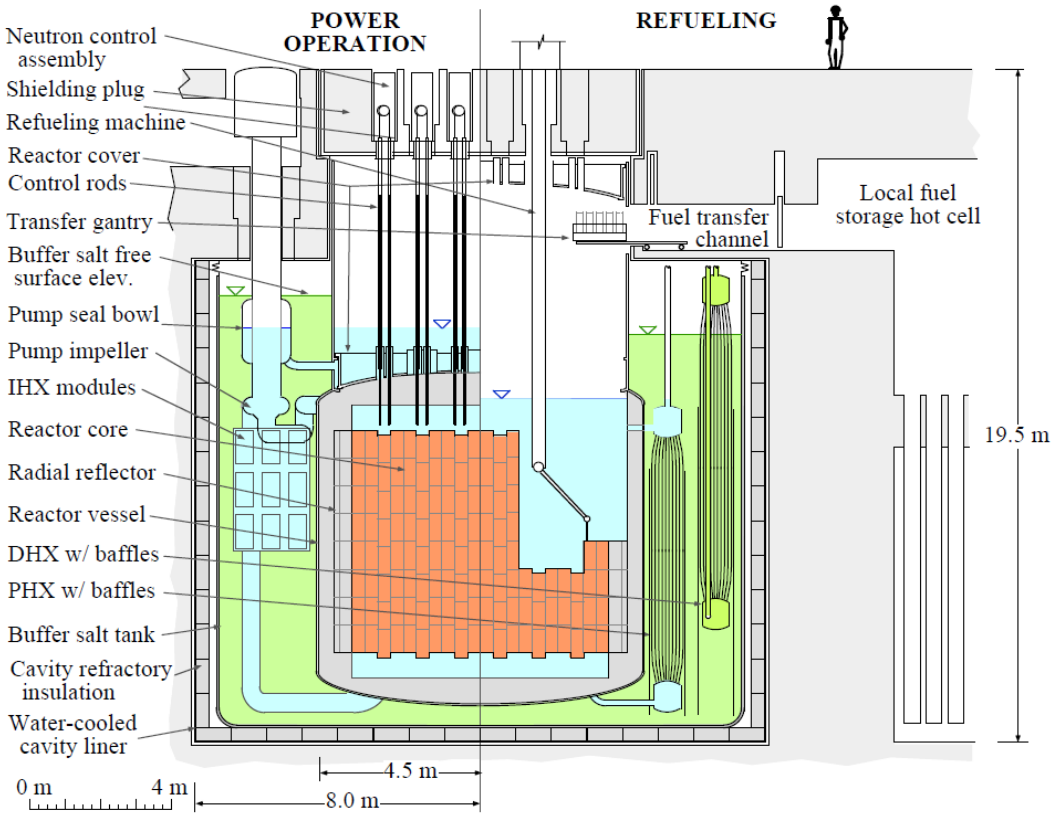

FIG. 119. Cross-section of the 2400 MW(th) LS-VHTR [311].

vessel, IHX, pumps, and connecting pipes, is immersed in buffer salt ($NaF–NaBF_4$) with an average temperature of 500ºC. Electrical efficiencies are expected to be near 50%. Further R&D activities are seen in areas such as the development of a more detailed reactor design and of a refuelling concept, qualification of a coolant that does not contain the toxic beryllium and study of coolant properties at temperatures above 1000°C [313].

Also a pebble bed version of a molten salt cooled advanced high temperature reactor (PB-AHTR) with 900 MW(th) and 410 MW(e) has been designed and analysed [314]. It is characterized by a power density of 20–30 MW(th)/m^3, much higher than the 4.8–6.0 MW(th)/m^3 typical of modular helium reactors, and thus has a much smaller size. The core delivers a low outlet temperature of 704°C, with an average temperature of 652°C. In the proposed PB-AHTR fuel design, the spheres have (only) a 30 mm diameter, with a 2.5 mm thick outer graphite shell and a low density graphite kernel at the centre of the pebble.

The pebbles move through channels located inside seven hexagonal so-called pebble channel assemblies (Fig. 120). The primary coolant is FLiBe ($7Li_2BeF_4$) flowing at an average speed of 0.38 m/s through the core to heat up from 600 to 704°C. The intermediate coolant selected is FLiNaK (LiF–NaF–KF).

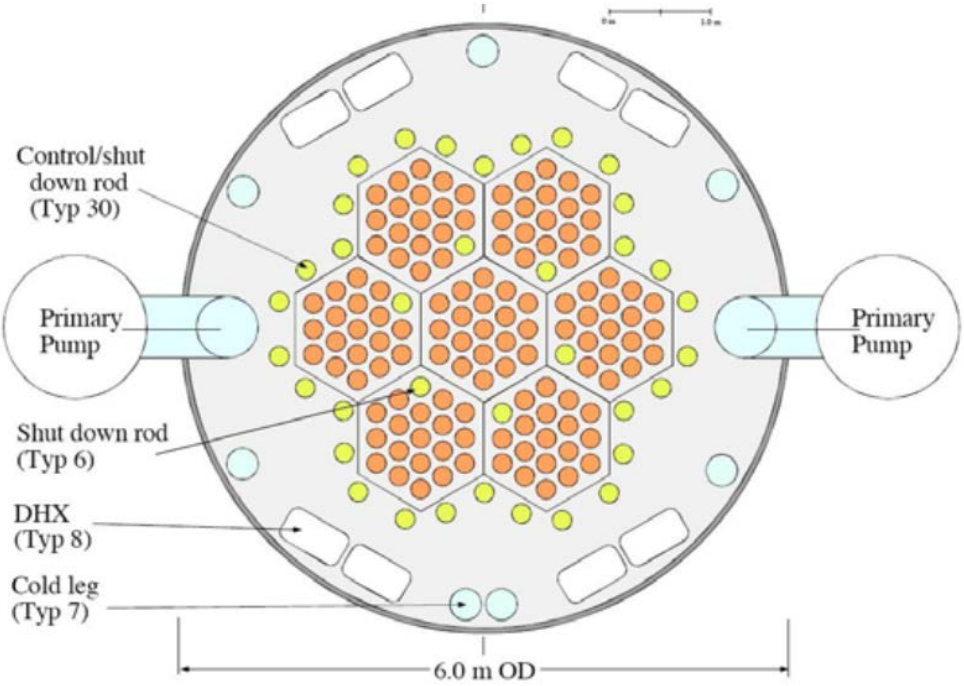

FIG. 120. Plan view of the modular PB-AHTR at the pebble-channel elevation [314].

6. ISSUES OF COUPLING

Coupling of a nuclear heat source to various hydrogen production processes or other process heat applications can basically be done in two ways, with heat transfer:

— Via an intermediate helium circuit from the reactor to the process heat plant;
— Directly to the high temperature heat exchanger in the primary circuit.

In HTGR plants such as Fort St. Vrain (USA) or THTR-300 (Germany), but also in a number of former concepts, the heat of the primary circuit helium was transferred directly to the steam generator for steam production. Within the German PNP project, the nuclear steam reforming concept was based on direct heat transfer to the process gas in the reformer tubes. Most new concepts of nuclear hydrogen production, however, particularly those using thermochemical cycles, are based on the concept of an intermediate circuit, in which heat from the secondary helium is transferred in a process heat exchanger to the application process.

6.1. CONCEPT OF A NUCLEAR HEAT EXCHANGER

Heat exchangers play an important role in the cycles, since they connect reactors and pipelines to transport reactants and allow for heat input or recovery. Any combination of an HTGR with chemical processes will most probably need an IHX for a decoupling between the primary circuit and the heat utilization system for the following reasons:

— Separation of the nuclear island for safety reasons, reducing the risk of interaction with the chemical plant;
— Limitation/exclusion of radioactive contamination of the product (e.g. tritium);

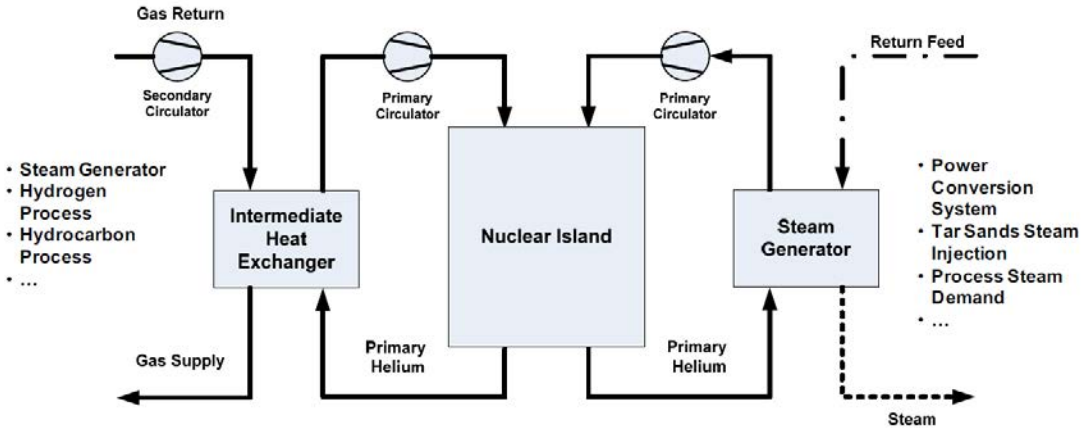

FIG. 121. Generic reference configuration for NGNP [90].

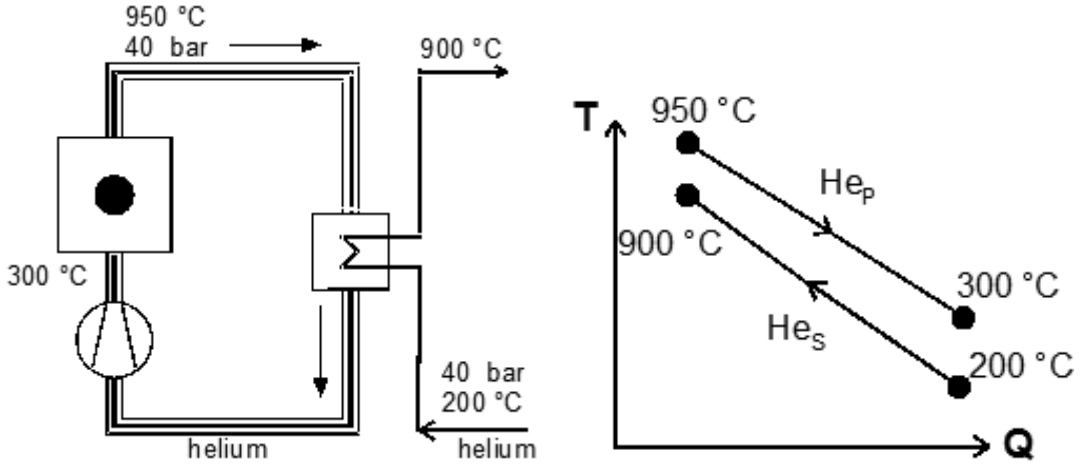

FIG. 122. Primary circuit of a modular HTGR with IHX principle flow diagram (left); T–Q diagram for use of nuclear heat (right).

— Exclusion of ingress of corrosive process media into the primary circuit;
— Near-conventional design of heat utilization system with ease of maintenance and repair;
— Flexibility in system design, e.g. in the choice of coolants for intermediate circuit.

The clear physical separation allows for the heat application facility to be conventionally designed and for repair work to be conducted under non-nuclear conditions. Also, an intermediate circuit which separates the nuclear reactor helium coolant from the power conversion system is attractive, since it gives flexibility in the design and allows the use of CO_2 as a fluid in the secondary circuit [315]. The flow diagram of the combination of a primary and a secondary circuit is shown in Fig. 121.

The employment of an indirect cycle, however, is connected with some disadvantages:

— Requirement of an IHX as an additional component, which increases capital costs;
— Decrease of temperature potential of heat transferred to production facilities due to additional heat losses, which reduces plant efficiency.

The concept of an indirect cycle HTGR with IHX is illustrated in Fig. 122, showing the flow diagram of the combination of a primary and secondary circuit together with the respective T-Q diagram.

The IHX has to work under the harsh conditions of high temperatures and temperature differences, and also of high pressures and pressure differences putting stringent requirements to the materials selection.

Heat exchanging components in the temperature range of 700–1000°C have long been state of the art in conventional technologies of the process industries. Also, pressure conditions in the heat exchangers and heat transport lines can go up to high values. Their limitations are principally dictated by the available materials, whereas the optimal choice is defined by economics. Particular to nuclear applications in an HTGR are the aspects of helium as a coolant, similar pressures on the primary and secondary sides, operating times of more than 100 000 h, the assumption of abnormal operational or accident states, the presence of process gases and the limitation of activation of product gases.

As a result of analysis of design experience and operating heat exchangers [316–318], the following general recommendations on optimization of IHX designs can be formulated:

— The IHX parameters at 100% power strongly depend on the application process and process circuit. The IHX design must be simple, compact, and easy to install and operate, with a possibility of detecting and eliminating damage. Unit power sizes up to 300 MW appear to be convenient.
— The IHX design must have the required strength characteristics, including long term strength, and a lifetime of up to 100 000 h.
— The design of the IHX and its elements must have high reliability and meet all safety requirements to ensure operability in all reactor plant operating modes. The simultaneous impact of maximum temperatures and maximum pressure differences on heat exchanger elements should be avoided.
— The IHX structure forming the boundary between primary and secondary helium must withstand a creep buckling load as the result of an accidental pipe rupture within the secondary helium piping system. This accident is considered the severest to these structures.
— At helium temperatures up to 950°C, the IHX heat exchange surface can be made of proven metallic nickel based alloys. At temperatures of 1000°C and above, it is necessary to use ceramics (SiC based materials).
— In order to reduce thermal stresses, IHX large load bearing elements must be shielded against the impact of high temperature gas flows.
— Connections between IHX elements must be leaktight to prevent intercircuit and bypass leaks and must ensure compensation of thermal structural deformations.
— Inhomogeneous temperature distribution in the heat exchanger cross-section, temperature pulsations in elements, and element vibrations induced by high velocity gas flows must be eliminated or minimized.
— The principal designs of the IHX must be validated by both theoretical and experimental analyses.

Much work has been dedicated to the development of a design philosophy for components at VHTR temperatures. No present technology can actually meet the anticipated requirements in terms of long life performance, pressure drop and mechanical resistance. Additional work for nuclear applications and qualification of these methods is needed. The final choice will be made according to criteria such as local stress/strain conditions, corrosion, dust susceptibility, in-service inspection, qualification and, of course, cost [274]. For those to be applied to future nuclear systems, i.e. for high temperatures and pressures, appropriate material selection will be essential [319]. The main difficulties in IHX development are seen in the proper choice of structural materials that can be operated over longer times at temperatures up to 1000°C (see Section 6.6).

The IHX in an HTGR represents the pressure boundary of the primary circuit, which sets stringent requirements on the boundary integrity and must be provided through implementation of prerequisites and conditions eliminating brittle fracture of this component. In the case of possible primary circuit leaks, radioactive fluid will therefore be retained in a leaktight reinforced concrete containment. Coolant leakage from the primary circuit into the secondary circuit is typically prevented by a pressure gradient, with the higher pressure on the secondary side to keep radioactivity in the primary system. A further coolant leakage beyond the containment will be limited by closing quick-response shutoff valves.

Table 32 lists the primary and secondary system pressures for various IHX designs of nuclear process heat reactor concepts, with all having the higher pressure on the secondary side, except for the ANTARES concept (which corresponds to the European concept developed within the EU project RAPHAEL (see Section 2.3.3.2)). The decision for the opposite pressure gradient in the ANTARES/RAPHAEL IHX design is based on the choice of a plate type heat exchanger, for which potential pressure transients on the secondary side are particularly challenging. The choice can also be defended with a safety argument, namely the advantage of quickly and easily detecting an IHX failure by radioactivity measurements in the secondary circuit.

TABLE 32. PRESSURE DIFFERENCES FOR SELECTED HTGR CONCEPTS

Concept	Primary pressure (MPa)	Secondary pressure (MPa)
HTTR	3.91	4.02
HTTR-IS	4.0	4.1
GTHTR300	5.00	6.15
GTHTR300C	5.1	5.13
KVK	3.99	4.19/4.35
HTR-Modul process heat plant	3.99	4.38
PNP-500	4.0	4.2
H2-MHR (S–I)	7.0	7.1
VG-400	4.9	5.4
MHR-100SMR	5.0	5.3
NGNP-GA	6.23	6.23
ANTARES (PHP)	5.5	5.0

6.2. TYPES OF INTERMEDIATE HEAT EXCHANGER

Various technologies for heat exchanging components designated for nuclear applications have been developed in the past. Different heat exchanging configurations are currently being pursued. Apart from the classic design of shell and tube (U-tube, helical) representing the more established technology, there are also plate, plate fin, and printed circuit or plate-machined type heat exchangers (PMHX). But two-stage heat exchangers are also possible, employing separate sections with different configurations and materials, and designed for different lifetimes. Potential fluid flow configurations are single-stream, parallel-flow, counter-flow, cross-flow, serpentine-flow or multistreaming. The proper selection will be the result of optimization, apart from the necessary operating conditions, e.g. in terms of volume, weight or cost. A strong incentive for a compact IHX, i.e. heat exchangers with large surface area densities of greater than 700 m^2 per m^3 of heat exchanger volume and specially designed heat transfer surface geometries, favours these novel designs [320].

6.2.1. Shell and tube

The characteristic feature of a shell and tube heat exchanger is the convective heat transfer through the tube walls. The helix type IHX (Fig. 123) consists of a bundle of helical tubes arranged around a central return gas duct for the hot secondary helium. Coiled tubes enlarge the heat transfer area and allow thermal expansion. The support system for the tubes consists of support cylinders with star shaped, welded-on support plates serving to take the weight of the bundle. A segmental design of the support structure limits the axial relative expansion caused by the operation temperature. In the upper cold area, the mechanical loads are carried by the vessel cover. This ensures access to the secondary system for in-service inspection and repairs without the need to open the primary circuit.

In the helical IHX, primary hot helium (950°C) entering the heat exchanger flows via a mixing and deflecting device at the bottom of the component upwards through the bundle and is cooled up to 300°C. The cooled primary helium flows back into the gap between the wall of the reactor pressure vessel and the gas shroud of the heat exchanger to the blower at the bottom of the component. The secondary helium enters the component at the top. After entering into a ring conduit, the helium with a temperature of 200 °C is uniformly distributed over the tube bundle and heated up to 900°C in counterflow. The cycle is closed by the hot header which is insulated on the inside. The hot helium leaves the IHX at the top of the component. The maximum wall temperatures in the tubes in normal operation are 920°C; the maximum pressure difference between the primary and secondary sides is 0.2 MPa under operational conditions. In depressurization accidents, they have to withstand the full pressure difference in a limited time period.

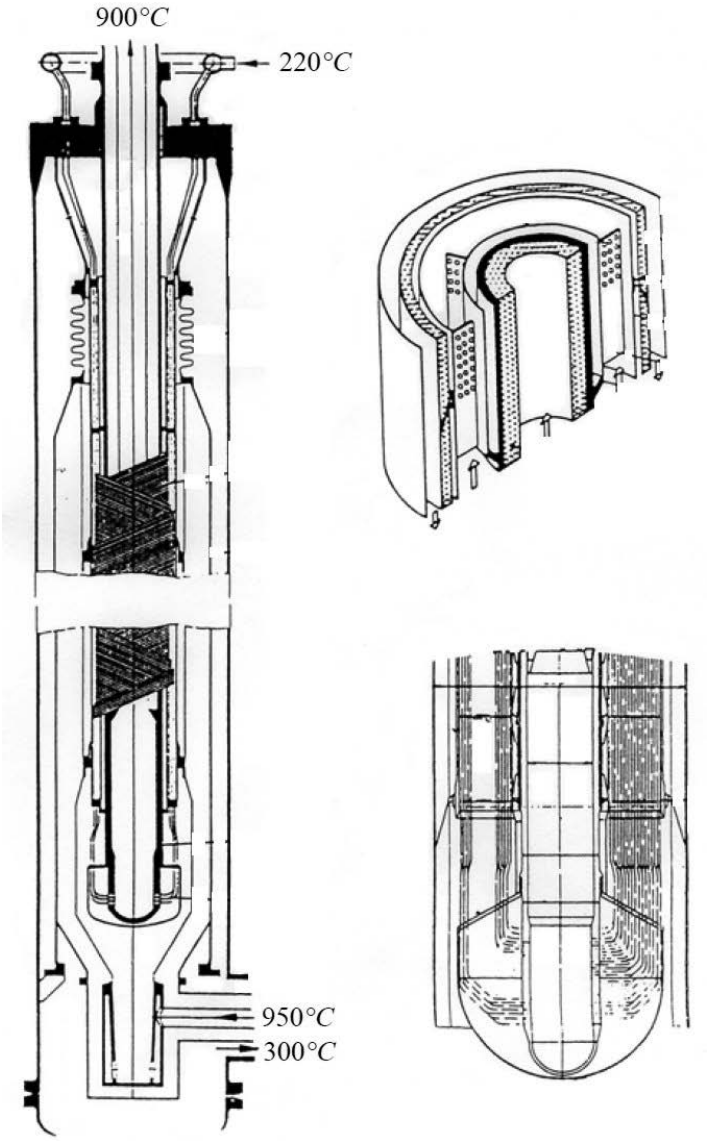

FIG. 123. Intermediate heat exchanger for nuclear applications [198]. Helical tube bundle (left); details of hot gas collector tube and support structures (right).

The advantages of the shell and tube IHX are that repair works can be done relatively easily and its thick walls will result in a larger corrosion resistance, and thus a longer lifetime. The major drawbacks of tubular heat exchangers are the large size of the component connected with higher costs, and the relatively low heat transfer density. The technology has been proven in the VHTR temperature range in the operational experience gained within the German PNP project (see Section 6.3.2) and as a real nuclear component in the HTTR (see Section 6.3.3).

6.2.2. Plate heat exchanger

Plate type IHX concepts representing the more advanced technology are promising because of their small, compact design and their high integration possibilities; the large variety of geometric configurations and complexity; and their high heat transfer density, and therefore their high efficiency. The IHX is composed of elementary modules in the power range of, for example, 1–5 MW each. A module consists of a stack of plates. The flow of primary and secondary fluids is in channels between the plates. The primary surface of the plate heat exchanger consists of corrugated plates formed by shock waves. The hydraulic diameter of the flow channels is in the range of 2–10 mm, but

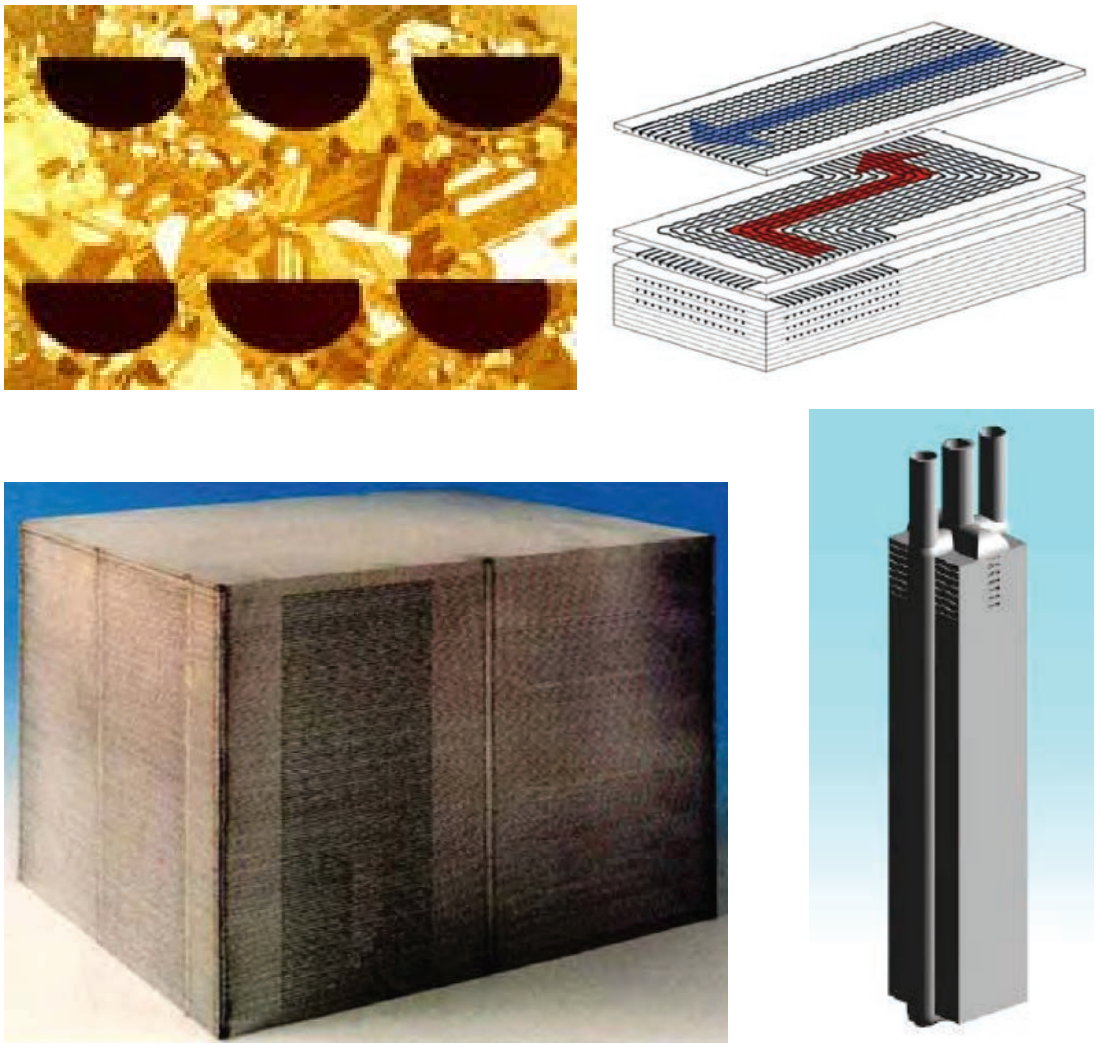

FIG. 124. Printed circuit heat exchanger (PCHX) [321].

wide gap plates for viscous fluids are also manufactured. Experience exists with the manufacture of large plates with a width of up to 2 m and a length of up to 12 m. A plate IHX can be operated at pressures of up to 50 MPa. Operating conditions achievable so far are temperatures up to 200°C and pressures up to 2.5 MPa.

The development of a plate design IHX is challenging since it should meet the criteria of compactness, high thermomechanical resistance, high thermal efficiency (95%), low pressure drop, no leakage, inspectability, long lifetime and cost effectiveness. Thin walls may cause a corrosion problem, leading to a potentially shorter component lifetime. The available experience with plate IHX modules is, unfortunately, not under the conditions or at the size required for an HTGR. Final qualification must be made in larger scale (MW range) test facilities under representative operation conditions [38]. Compared with the shell and tube type, plate IHX modules are less easily repaired. Rather than inspection of individual coolant passages, only integral leak tests can be conducted, with IHX modules isolated from the system when leaking.

6.2.2.1. Printed circuit heat exchanger

A printed circuit heat exchanger (PCHX) module is composed of machined metal plate layers of ~1 mm thickness containing coolant channels for the primary fluid alternating with those for the secondary fluid (Fig. 124), flowing, for example, counter to each other (top right). The flow channels with a semicircular profile (top left) are electrochemically edged into the plates using a technique similar to that for printing electrical circuits.

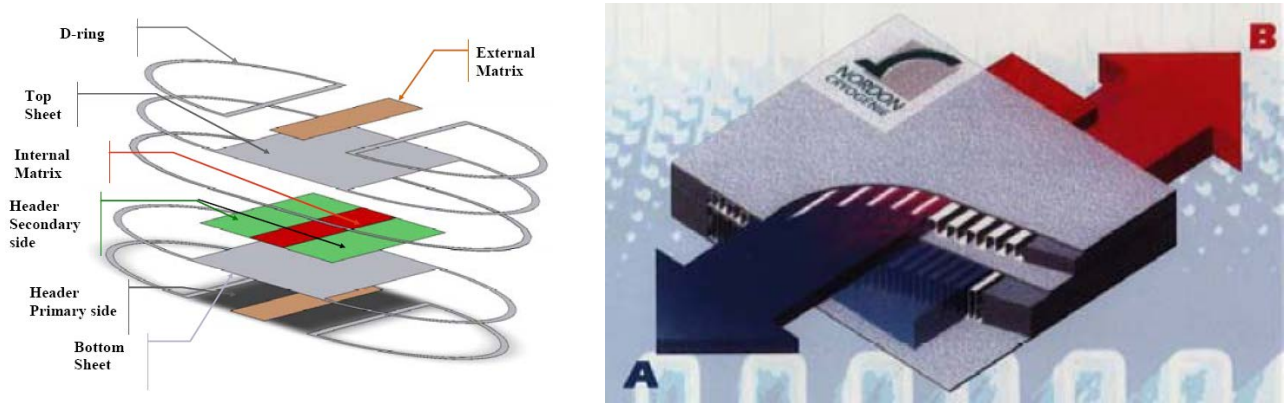

FIG. 125. Two variants of plate fin IHX [36] with Brayton Energy design (left); Nordon design (right).

This manufacturing technique makes complex streams possible. Channels may be straight or wavy and can have hydraulic diameters as small as 0.7 mm, leading to laminar flow on both sides. The metal plates are stacked (top right) and then diffusion bonded. The bond between the metal surfaces is formed by applying heat and pressure, promoting a grain growth across the boundary between the plates, thus becoming a solid all-metal core (bottom left) [320].

PCHX designs have been developed that are highly robust and have high thermal efficiencies, allowing pressures of 50 MPa and temperatures of 900°C. The ability to etch very small channels leads to a highly compact component. Surface area densities may be as high as 2500 m^2/m^3. So far, PCHX modules have been made of stainless steel and nickel alloy. The basic modules can be taken to construct heat exchangers to any desired scale. Extensive experience with PCHX exists in gas processing in the petrochemical industries.

6.2.2.2. Plate fin heat exchanger

In the plate fin heat exchanger (PFHX), the fins are corrugated sheets separated by the plane plates (Fig. 125). Fins have the tasks of extending the surface for heat transfer given by convection and conduction, and providing channels for the coolant flow. Different fin forms are possible, such as straight or wavy fins, or offset strip fins. The latter tend to enhance flow turbulence and thus improve heat transfer. A concern with regard to corrosion is given with the small fin thickness, which may be 0.2 mm or even less, and may limit the lifetime at high temperatures. Testing has been done under steady state and transient conditions. Plate fin heat exchangers appear more economical, but less robust than PCHX modules, representing a low technological risk if used at temperatures below 500°C [296].

Two variants are pursued for the plate fin IHX. The one proposed by Brayton Energy has wavy or straight fins on a flat support plate. The independent cells (Fig. 125, left) allow an arrangement for the IHX module which is flexible under thermal loads. Using flow channels with 0.3 mm hydraulic diameter and a high fin density, a high compactness (~10 m^3) could be achieved. The second variant, from Nordon (Fig. 125, right), employs a different type of fins, serrated offset strip fins, on a support plate.

6.2.2.3. Hybrid plate heat exchanger

Hybrids of different plate heat exchanger concepts are also possible and can be chosen if attributes of different concepts are to be combined. An area of application of such hybrid heat exchangers (H2X) is heat transfer between two very different fluids. An example is a sodium–CO_2 IHX, with low pressure, large heat transfer, and the requirement for larger channels to avoid plugging on the sodium side, and with poor heat transfer and therefore high pressure favouring smaller channels on the CO_2 side [322].

6.2.3. Spiral heat exchanger

Spiral heat exchangers of the ACTE design have a cylindrical shape where the fluids circulate in a countercurrent flow in spirals around the longitudinal axis. Flow is highly turbulent, which enhances the heat transfer. Also, the heat transfer area is very high at 1600 m^2/m^3.

6.2.4. Direct contact exchanger

In advanced fast reactor designs, direct contact heat exchange from a liquid metal to water is currently being considered for steam generation in power production, and could economically eliminate the need for the intermediate loop in a liquid metal reactor design. The vigorous agitation of the two fluids, the direct liquid–liquid contact and the resultant interfacial heat transfer area give rise to large volumetric heat transfer coefficients and rapid steam generation. Further R&D is needed to optimize heat transfer and flow stability and to minimize aerosols for direct contact heat exchange systems.

6.3. INTERNATIONAL R&D ON IHX CONCEPTS FOR HTGRS

6.3.1. France

For the IHX of France's ANTARES indirect cycle concept by AREVA NP, several novel technologies have been reviewed and tested [36, 323]. The technologies identified for compact IHX currently under investigation are [36]:

— Plate machined, stamped or chemically etched heat exchanger and assembled by diffusion bonding;
— Plate fin heat exchanger;
— Corrugated plate heat exchanger;
— Spiral heat exchanger.

The plate IHX modules are located in a pressure vessel. Due to the limited possibility for in-service inspection, leaktightness of the plate IHX is not strictly required. Instead, closure valves will be implemented on the secondary inlet and outlet piping. Leak detection can be done at a very low mass flow rate by measuring fission gas activity in the secondary He–N_2 coolant, which is at lower pressure than the primary helium. The plate IHX modules must be easily removable. The lifetime is planned for 20 years, compared with 60 years for the plant [297]. Figure 126 shows a potential design of an IHX vessel for ANTARES containing, in a symmetrical arrangement, eight plate type IHX modules with 75 MW(th) each.

A PCHX or plate type IHX is also being considered for the recuperator component in a Brayton (direct) cycle HTGR. This IHX is used to transfer the remaining heat in the coolant at the turbine outlet to heat up the high pressure gas at the compressor outlet [296]. Since the modules are relatively stiff, their active height is limited to the order of 1 m. The total volume required for ANTARES is about 25 m^3. The AREVA specifications for the recuperator heat exchanger component of ANTARES are listed in Table 33.

Within the French programme, PCHX tests were conducted in the air test loop CLAIRE where the Reynolds similarity was used to simulate helium. The thermal and mechanical performance of PCHX modules was investigated under steady state and transient working conditions. The main difficulty is to obtain a homogeneous flow pattern in the channels. The heat transfer density achieved was 26 MW/m^3. Other results of the plate IHX investigations were high efficiencies of greater than 95% and the potential for further design optimizations. The assessment of lifetimes, however, appears to be difficult owing to lack of creep and creep-fatigue test data [324].

Carburization and decarburization reactions may be critical to the thin heat transfer walls in the plate type IHX regarding the particular environment with the helium–nitrogen mixture as the coolant on the secondary side [38]. The preferred material for the hot section of the IHX is Alloy 617, with alternatives being Alloy 230 and Hastelloy XR. A large materials programme includes experimental studies to qualify materials at high temperatures and to define the acceptable impurity contents in the coolant (to be controlled by the helium purification systems). Dedicated helium loops are, for example, the CORINTH loop at CEA, Saclay, or are still under development at CEA, Electricité de France (EdF) and AREVA [297]:

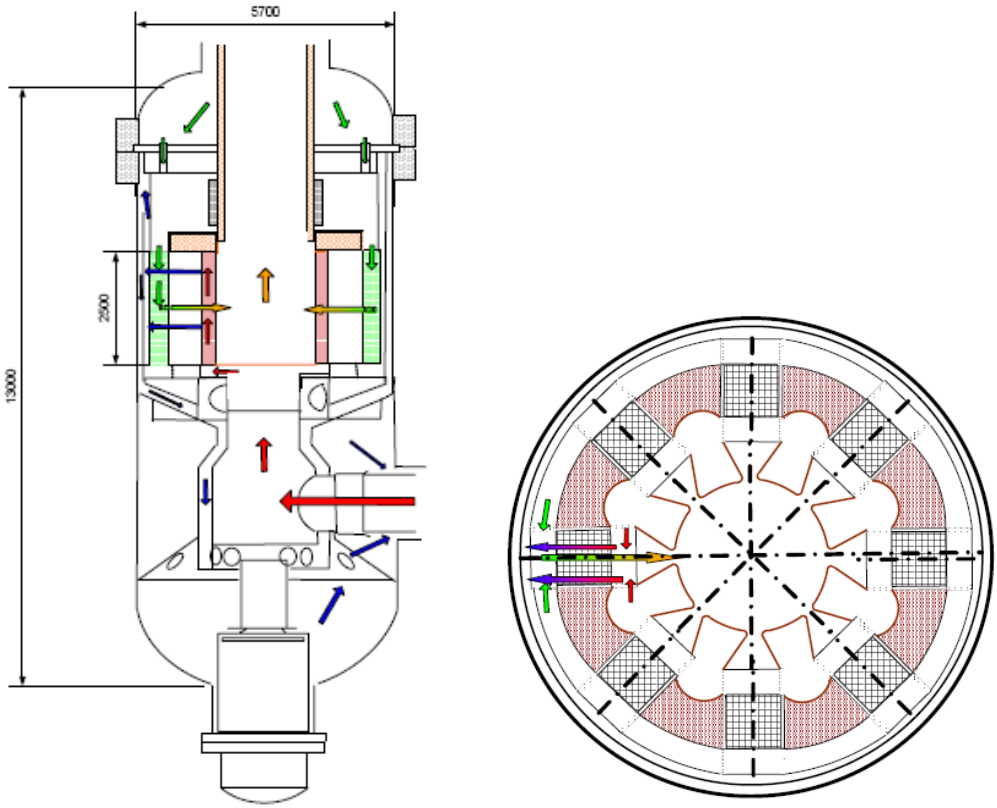

FIG. 126. ANTARES IHX vessel with integrated plate IHX modules [36].

TABLE 33. PRECONCEPTUAL DESIGN SPECIFICATIONS OF THE PLATE TYPE INTERMEDIATE HEAT EXCHANGER FOR THE FRENCH ANTARES CONCEPT [296]

	IHX in ANTARES
Thermal capacity	635 MW(th)
Thermal efficiency	95%
Material	Alloy 230, Alloy 617
Size of vessel	
PMHX	25 m^3
PFHX (Brayton Energy)	10 m^3
PFHX (Nordon)	30 m^3
Primary helium	
Inlet temperature	850°C
Outlet temperature	390°C
Design pressure	5.5 MPa
Design pressure drop	<0.1 kPa
Flow rate	240 kg/s
Secondary helium/nitrogen mixture	
Inlet temperature	300°C
Outlet temperature	900°C
Design pressure	~5.5 MPa
Design pressure drop	<0.2 kPa
Flow rate	614 kg/s

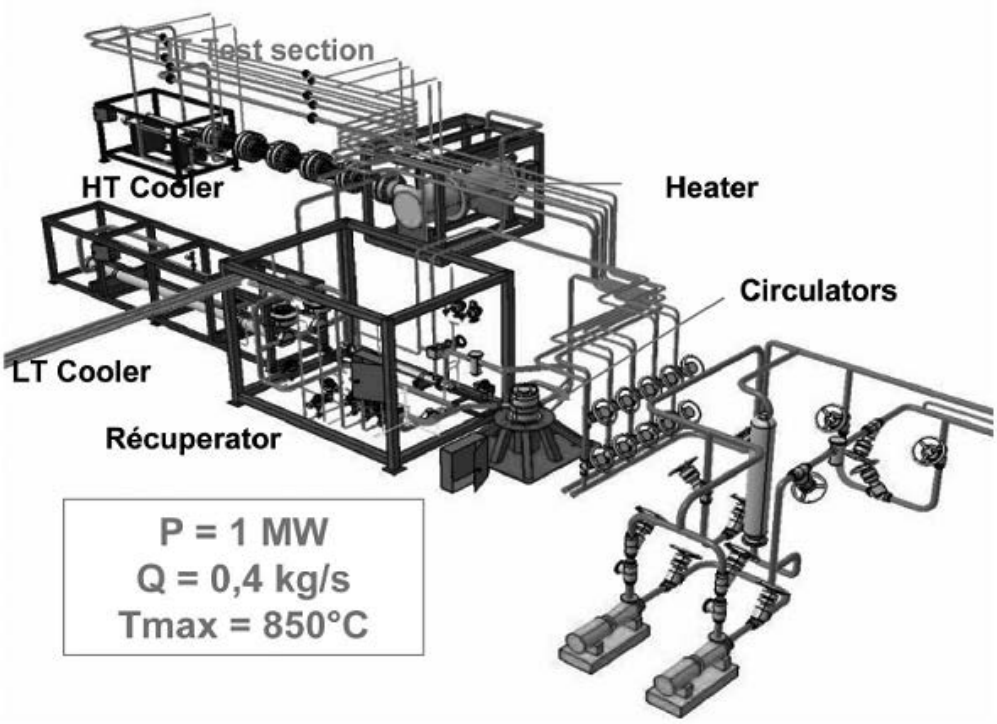

FIG. 127. Planned HELITE loop for the ANTARES IHX investigation [38].

— The CLAIRE air loop at CEA, Grenoble, with a low flow rate on either side of ≤0.2 kg/s, high temperatures up to ~950°C at a maximum inlet pressure of 0.8 MPa for thermohydraulic component testing and mechanical fatigue testing;
— The PAT air loop at EdF, Chatou, with a large flow rate and low temperature;
— The HEFUS helium loop at ENEA, Brasimone, with low flow and medium temperature;
— The HELIOKA loop currently under development at FZK, Karlsruhe;
— The 1 MW HELITE helium loop (Fig. 127) to be built at CEA, Cadarache, to provide 850°C helium to a high temperature test section and 500°C helium to another, medium temperature test section;
— A helium loop of at least 10 MW for final qualification.

While the plate type IHX has been selected as the reference concept for ANTARES, the multiloop tubular type IHX is considered as a backup solution [36]. The preliminary design proposed for the tubular type IHX (Fig. 128) consists of four 152.5 MW(th) units located around the reactor vessel. A total of 2411 helically wound tubes made of Inconel 617 and with an active length of 28.2 m, an inner diameter of 16.6 mm and a tube wall thickness of 2.2 mm will be employed in the four modules. The secondary fluid is 80% nitrogen based (‘air’), to allow use of components derived from existing CCGT technology, and 20% helium, to enhance the IHX thermal performances.

6.3.2. Germany

The example given in Fig. 129 represents the German reference design of a process heat HTR-Modul in a side by side arrangement of nuclear reactor and IHX vessel for each modular unit.

The thermal power of the nuclear reactor and of the IHX is 170 MW, the limitation of power is given by the requirement of self-acting decay heat removal in accidents with a total loss of active cooling. If larger thermal powers were needed, an annular core would be required. The limitation in this case is caused by the dimensions and type of reactor pressure vessel.

The employment of an IHX was also suggested within the PNP project with regard to the steam gasification of hard coal, for which the main characteristic data are given in Table 34 for comparison. A facility for large

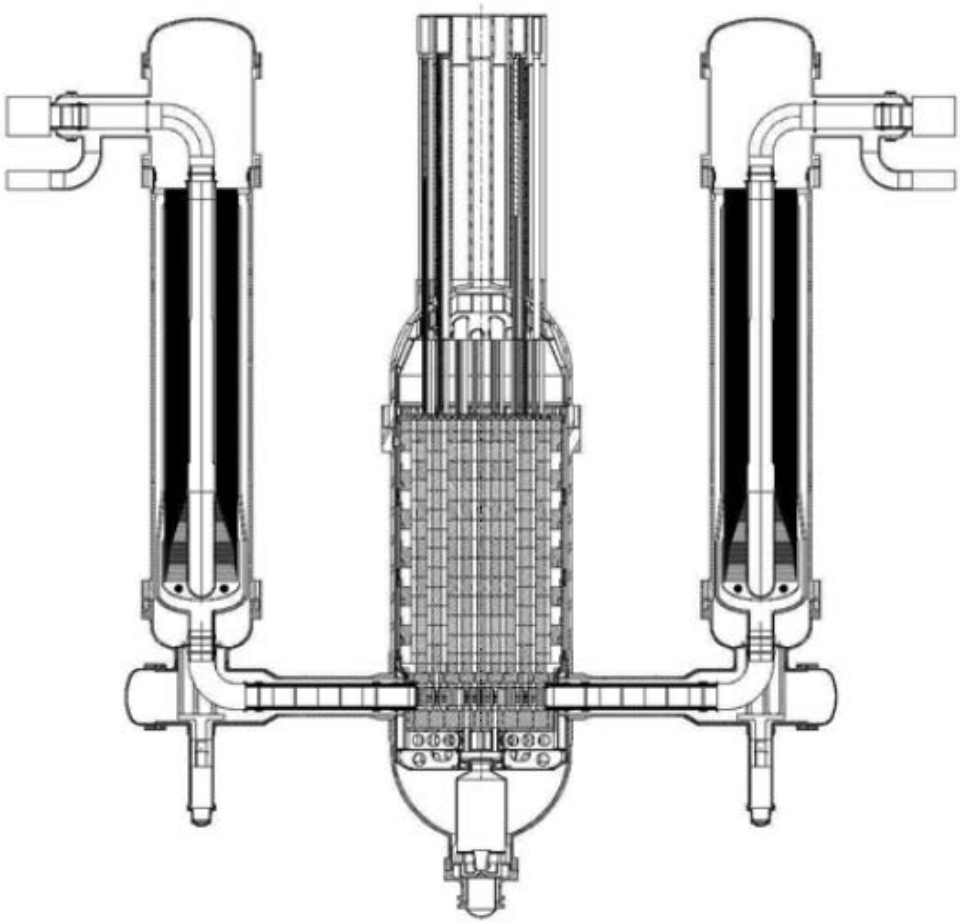

FIG. 128. ANTARES tube type heat exchanger as a backup solution [36].

TABLE 34. OPERATIONAL DATA OF THE COMPONENT TEST LOOP KVK

Thermal power	10, maximum 12.8 MW(th)
Temperature	950, maximum 1000°C
Pressure	4, maximum 4.6 MPa
Helium flow rate	3, maximum 4.3 kg/s
Helium velocity	60 m/s
Temperature transient	± 200 K/min
Presssure transient	0.5 MPa/s

component testing (KVK) was constructed and successfully operated by Interatom within the PNP project [326]. In a heating system consisting of a heater with steam, a natural gas burner and an electrical heater with a total thermal power of 10 MW, helium was heated up to 950°C at 4.0 MPa (Figs 130 and 131). Some operational parameters are listed in Table 34.

Two IHX components were constructed and tested in the KVK loop, one with a helical tube bundle by the company Steinmüller and another one with U-tubes manufactured by the company Balcke–Dürr (now, Babcock AG). Figure 132 shows schematics of both components, and Fig. 133 shows both IHX components under construction. The KVK plant also allowed testing of large diameter hot gas ducts, a steam generator, valves for hot helium and other components like the hot header, or auxiliary plants as for gas purification.

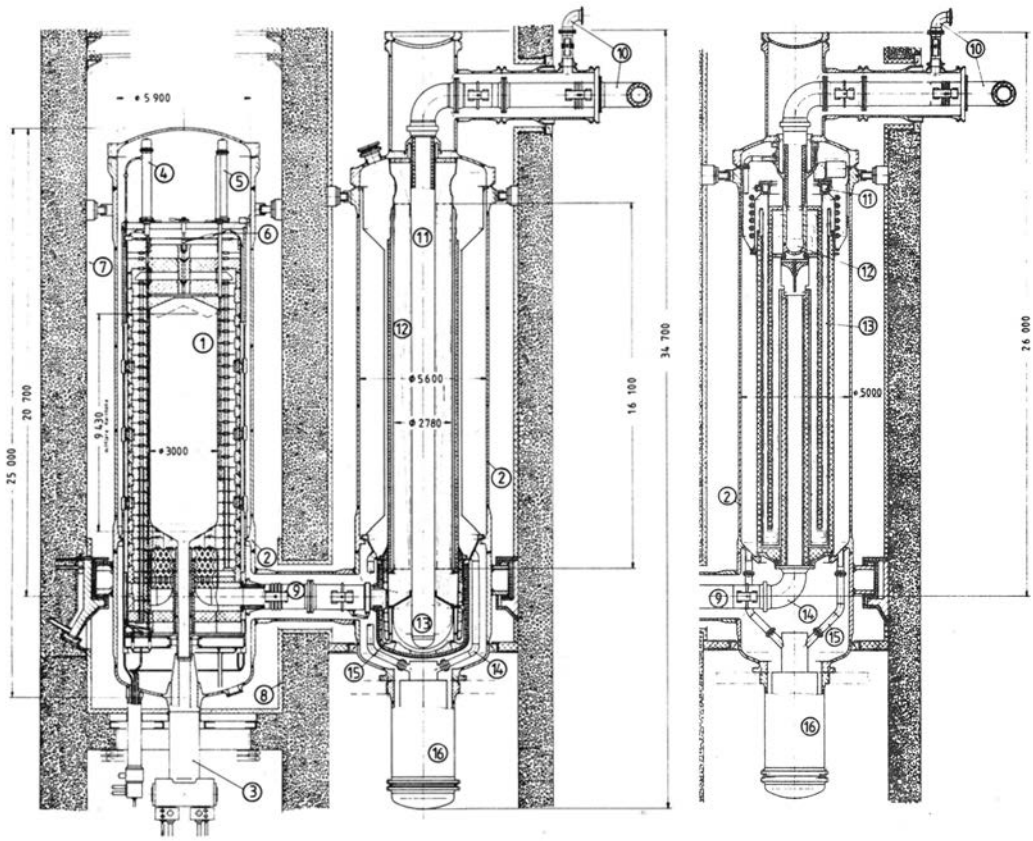

FIG. 129. Arrangement of HTR-Modul (left) with Helix-IHX (middle) or U-tube-IHX (right) [325].

The relevant data of the IHX test components are listed in Table 35 compared with the data of an IHX component to be connected to the two German concepts of a process heat nuclear reactor. Each component had a thermal power of 10 MW. The most critical part in the design of a helical tube concept with regard to temperature loads, the hot header for the secondary helium, was tested in the 10 MW component in a 1:1 scale related to the large component. The tube systems had the same dimension in the test and for the nuclear application. The materials for the tubes, headers, supporting structures and gas ducting on the primary side were the same as planned for the nuclear application. A uniform flow distribution through the helix tube bundle necessary to minimize relative movements between the tubes is achieved by an integrated flow distributor. The connection to the secondary helium circuit is identical for both IHX types [327].

Both heat exchanger components were operated over several thousands of hours without any difficulty. The table shows that the specific data of the test components were very similar to those planned for the nuclear application. Gas temperatures, pressures and material temperatures in the KVK facility were even identical to those of the nuclear design.

According to the BBC/HRB strategy, the IHX for a nuclear heat supply system based on the concept of the medium-sized HTR-500 was designed as a tandem type He–He heat exchanger separated into a high temperature and a low temperature section. This arrangement offers the chance of separate replacement of the high temperature part if necessary, and the use of less expensive materials for the low temperature part. The materials of choice, at that time, were Inconel 617 for the high temperatures and Incoloy 800 for the low temperatures. Selecting a split-up temperature of ~700°C, the low temperature range would be covered by conventional material technology.

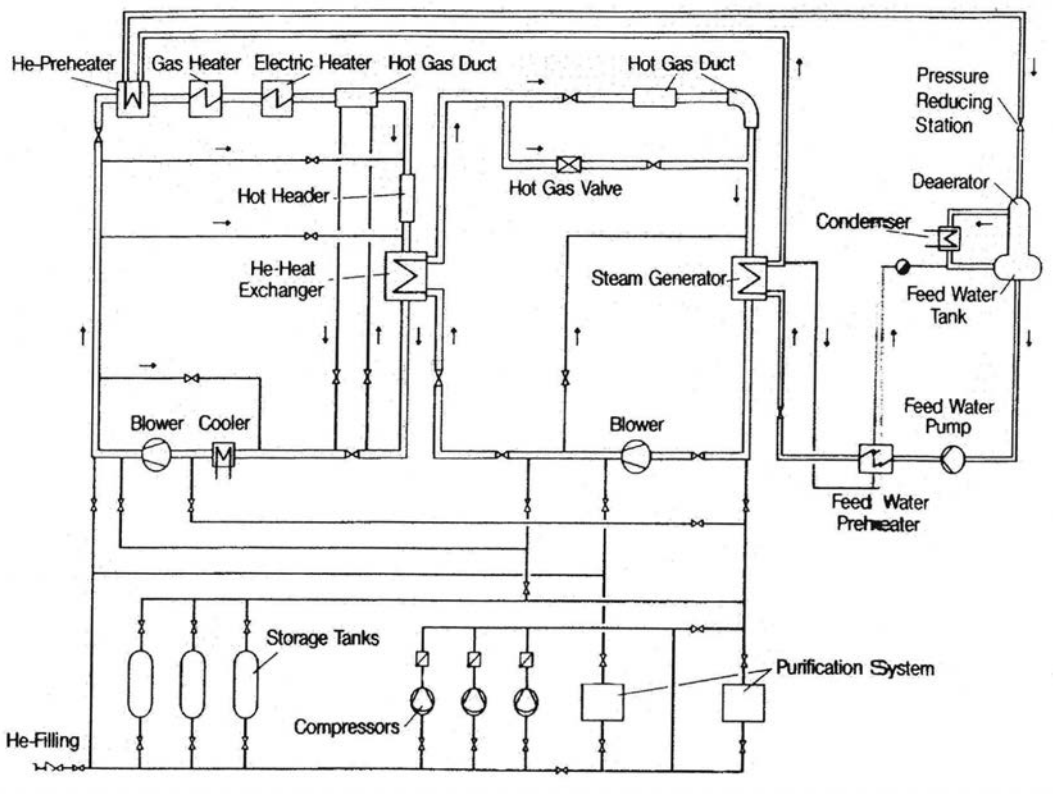

FIG. 130. Flowsheet of 10 MW KVK facility for testing nuclear process heat components [326].

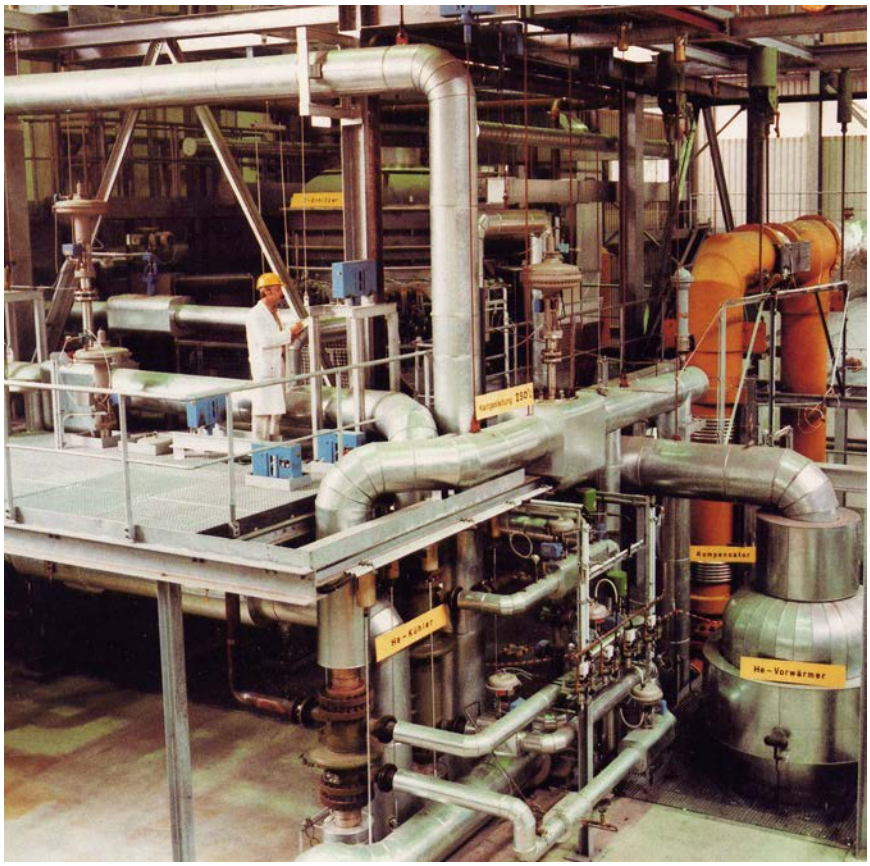

FIG. 131. 10 MW KVK facility for testing nuclear process heat components [292].

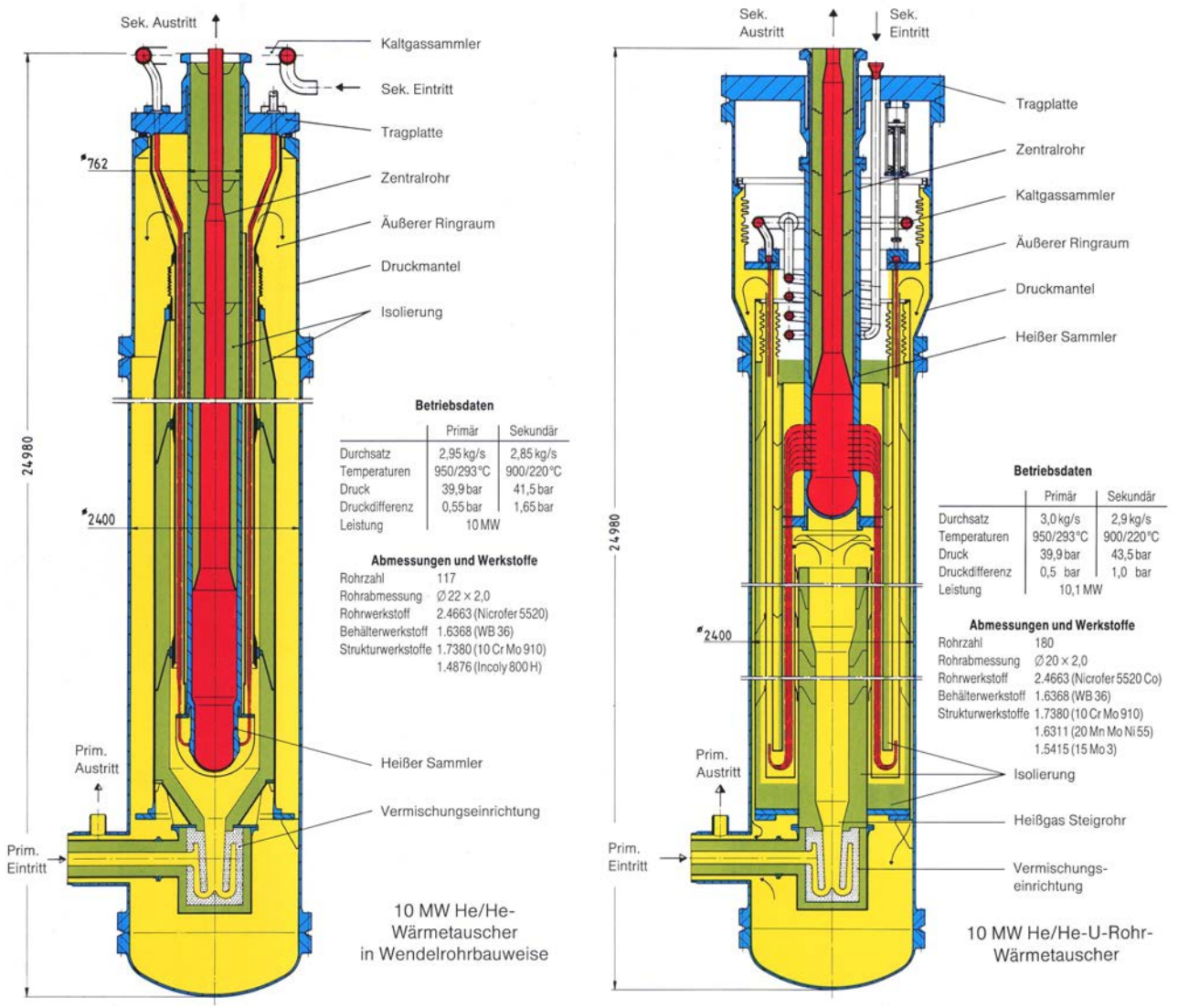

FIG. 132. Two IHX components tested in KVK with helical tube bundle by Steinmüller company (left) [328]; U-tube bundle by Balcke–Dürr company (right) [329].

A combination with the steam–coal gasification was also considered possible, further optimizing the system and increasing its efficiency. While in a first step hydrogasification would degasify the coal, the steam gasification could then completely gasify the remaining coke.

Apart from the KVK plant, experimental work was also conducted in the high temperature helium test facility (Hochtemperatur-Helium-Versuchsanlage (HHV)), the EVO (Energieversorgung Oberhausen) plant, insulation test facilities and other specific facilities (Table 36) to test, for example, friction, fretting, wear, materials and depressurization. On the basis of the broad experimental programme, the following statements can be made with respect to the feasibility of the shell-and-tube type IHX:

— Two helium heated IHX have been successfully tested on the 10 MW power level and at maximum helium heating temperatures of 950°C (primary) and 900°C (secondary). So far, the process parameters have been tested under real conditions of the nuclear application. The operating time of the helical tube bundle was more than 5000 h and that of the U-tube bundle was more than 4000 h. Overall it was stated that an IHX following one of the two designs investigated (helical tubes and U-tubes) can be designed for a power of 170 MW and can be operated for 100 000 h on the basis of the available experience.

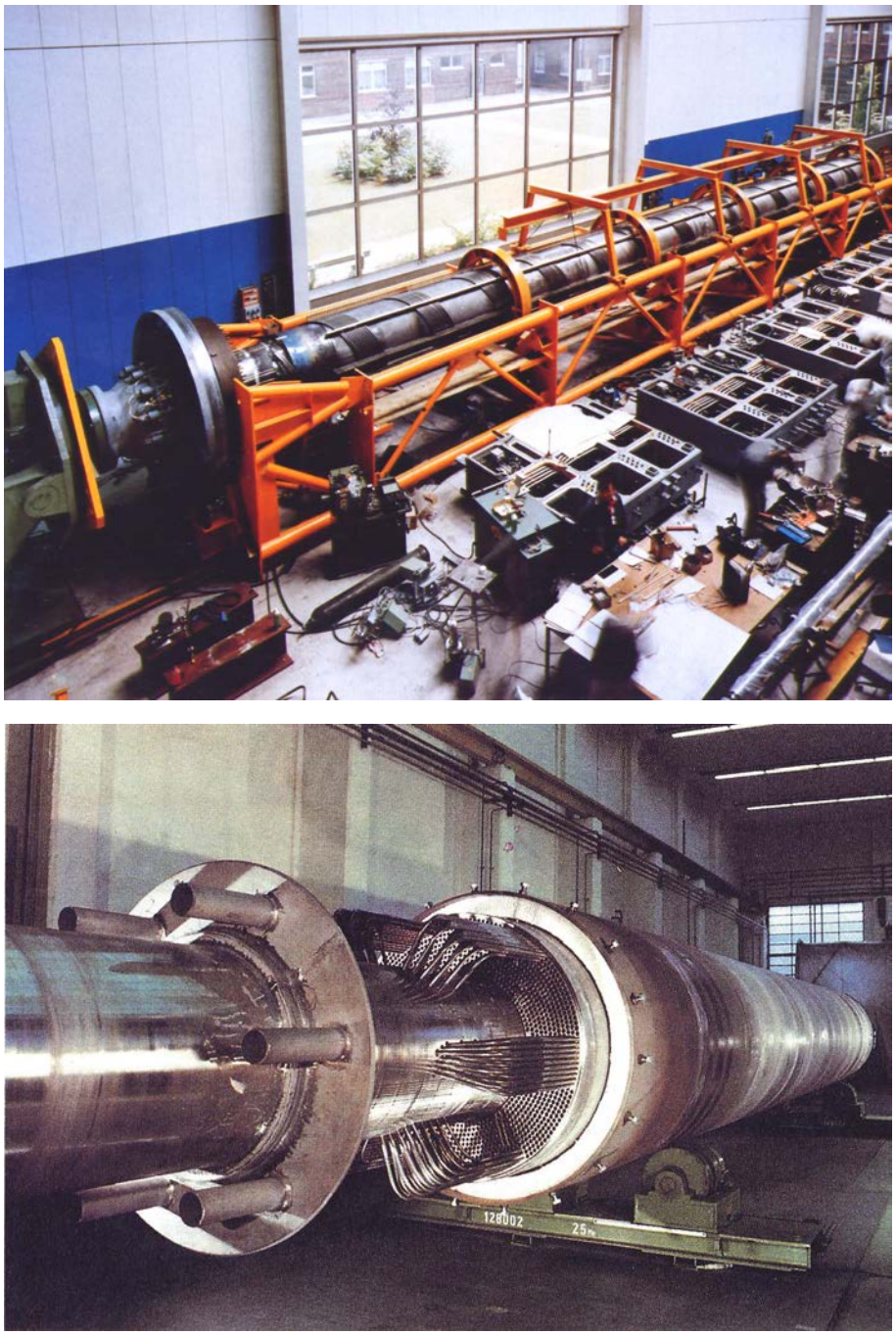

FIG. 133. IHX component with helical tube bundle (Steinmüller) (left); U-tube bundle (Balcke-Dürr) (right) [292].

— Parallel to the integral testing of the components, additional testing in KVK was carried out for a hot gas header of the helical tube bundle, hot gas ducts (including bends and expansion bellows), hot gas valves and a steam generator.
— The thermodynamic data of the heat exchanger designs have been confirmed by the experiments. Average heat fluxes of ~40 kW/m² can be realized at reasonable pressure drops.
— The components were tested in steady state operation and under transient conditions. Transients of ±7 K/min were tolerated by the components without failure.
— The measured vibrations did not result in serious loads to the heat exchanger tubes.
— The bearing forces for the load transfer system of the cold header and the bundle were within the range of calculated values.

TABLE 35. COMPARISON OF DATA OF IHX TESTED IN KVK FACILITY WITH DATA OF IHX FOR NUCLEAR APPLICATION

IHX in	KVK		170 MW(th) HTR-Modul [325]		500 MW(th) PNP [330]	
	Helical	U-Tube	Helical	U-Tube	Helical	U-Tube
Heat capacity (MW)	10	10.1	171.7	171.7	125	125
Material						
Tube	Nicrofer 5520	Nicrofer 5520	Alloy 617	Alloy 617		
Size						
Bundle outer diameter (m)	1.5	2.0	2.78	1.512	2.52	2.098 (hot) /2.815 (cold)
Tube outer diameter (mm)	22	20	22	20	22	20
Tube wall thickness (mm)	2	2	2	2	2.2	2
Tube length (m)			38.2	30.0	40.7	32.7
Number of tubes	117	180	1612	2470	1444	1900
Primary helium						
Inlet temperature (°C)	950	950	950	950	950	950
Outlet temperature (°C)	293	300	292	292	293	293
Inlet pressure (MPa)	3.99	3.99	3.99	4.05	4.0	3.99
Outlet pressure (MPa)	3.935	3.94	3.97	3.99		
Flow rate (kg/s)	2.95	3.0	50.3	50.3	36.9	36.9
Secondary helium						
Inlet temperature (°C)	220	220	200	200	220	220
Outlet temperature (°C)	900	900	900	900	900	900
Inlet pressure (MPa)	4.19	4.35	4.38	4.35	4.2	4.35
Outlet pressure (MPa)	4.025	4.25	4.19	4.19		
Flow rate (t/h)	2.85	2.9	47.3	47.3	35.6	35.6
Heat transfer area (m^2)		3500	4254	4700	4000	3900
Lifetime (h)	—	—	140 000	140 000	140 000	140 000

TABLE 36. LARGE HELIUM TEST FACILITIES

	Facilities			
	EVO	HHV	EVA II	KVK
Purpose	Test of total power plant	Test of gas turbine and large components	Test of steam reformer bundle	Test of IHX components
Location	Oberhausen	Jülich	Jülich	Bensberg
Electric power (MW)	50	45	10	10
Thermal power (MW)	150	45	—	—
Heating device	Fossil burner	Compressor	Electric heater	Electric heater
Maximum helium temperature (°C)	750	850	950	950
Helium pressure (MPa)	2.87	5	4	4
Helium mass flow (kg/s)		200	3.8	3
Operation time (h)	50 000	1000	10 000	10 000

— Ultrasonic inspection of IHX tubes after 4700 h of operation did not reveal any deviations.
— As many as 656 cycles from 950°C to 710°C and the reverse with a transient of ± 40 K/min did not cause any damage to the header.
— Tests with a pressure difference of 4.3 MPa between the primary and secondary sides of the hot gas header at 970°C were carried out over a time period of 455 h to simulate a depressurization accident. No damaging influence was identified.
— Insulation and gas ducting structures inside the tube bundles did not show any damage.

6.3.3. Japan

6.3.3.1. Testing of the Japanese IHX in the HTTR

The IHX used in the HTTR is a vertical, helically coiled counterflow type heat exchanger, as shown in Fig. 134. The primary helium enters the IHX through the inner pipe of the primary concentric hot gas duct attached to the bottom of the IHX. It flows upwards outside the tubes, transferring the nuclear heat of 10 MW to the secondary helium cooling system, and flows back through the annular space between the inner and outer shells. The secondary helium flows downwards inside the heat transfer tubes and flows upwards in the central hot gas pipe through the hot header.

A double-walled shell with a thermal insulation attached on the inside surface of the inner shell provides reliable separation of heat resisting and pressure retaining functions. Cold helium flowing through the annulus brings uniform temperature distribution throughout the outer shell, which has a pressure retaining function. Insulation inside and outside the central hot gas pipe keeps the heat transfer low to obtain a high efficiency.

To minimize constraints of axial and radial thermal expansion of the helically coiled heat transfer tubes, a floating hot header combined with the central hot gas duct and passing through the central space inside the helix bundle is adopted. A tube support allows free thermal expansion of a helix in radial direction. The differential pressure of 0.1 MPa only acts on the heat transfer tubes to reduce mechanical loads to ≤1 MPa. An innovative type of tube support and a coaxial double-wall shell are applied to reduce thermal loads to ≤40 MPa. Table 37 shows the major design specifications of the IHX as operated in the HTTR [331] and as projected for the combined cycle version of the GTHTR300C [56].

6.3.3.2. IHX concept for the GTHTR300C

The IHX of the GTHTR300C (Fig. 135) has been designed for a thermal power of 170 MW(th) on the basis of the proven concept of the shell and tube type IHX of the HTTR operated at 950°C and 4 MPa. Pressure in the

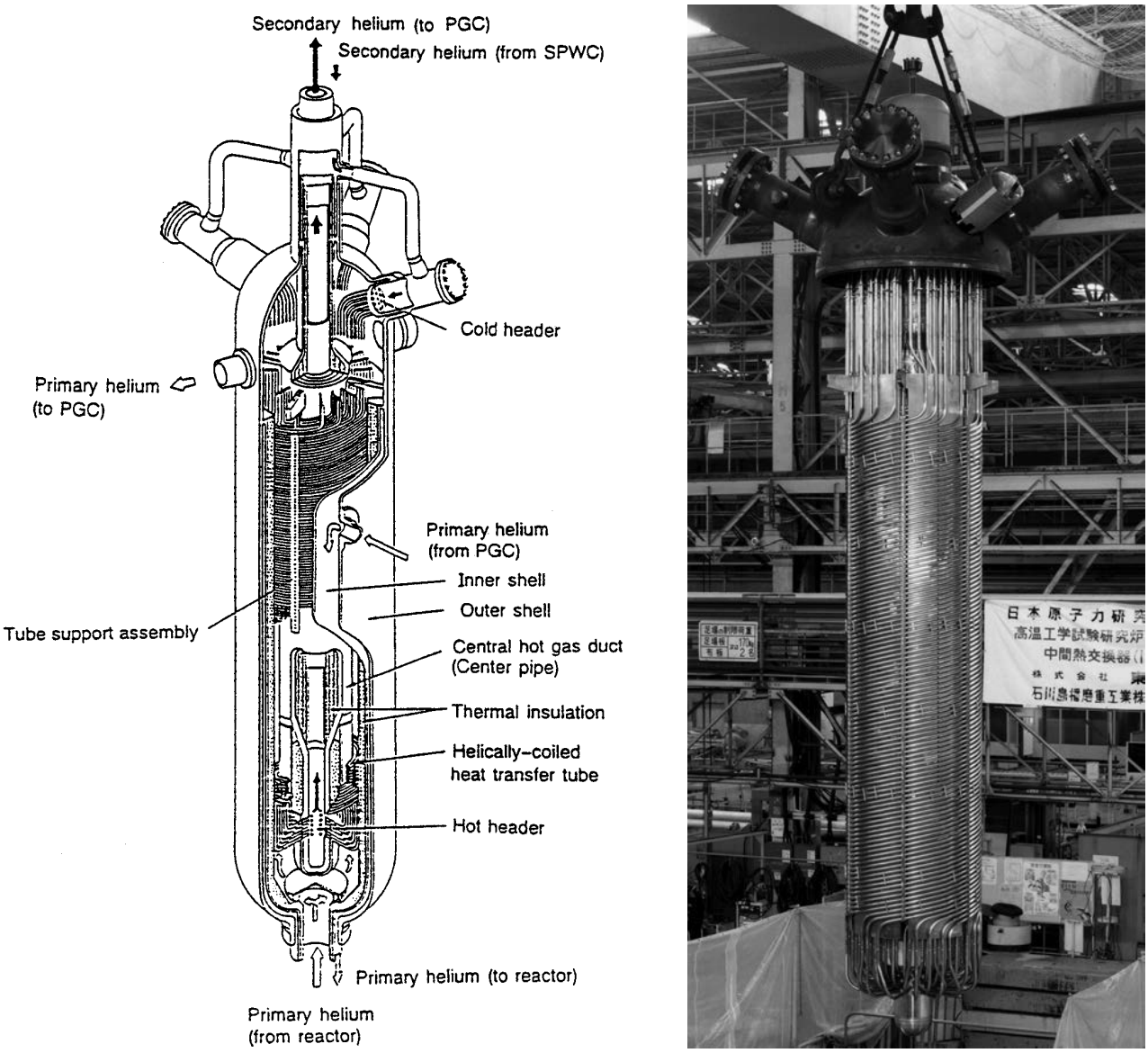

FIG. 134. Schematic and photograph of the He–He intermediate heat exchanger in the HTTR [331].

secondary loop is slightly higher (5.13 MPa) than in the primary loop (5.1 MPa). The logarithmic mean temperature difference (LMTD) is 154°C (HTTR: 113°C), which is inversely proportional to the heat transfer surface area required. In the IHX the pressure difference is kept lower than 0.15 MPa by a differential pressure control system to limit the creep damage. The lifetime is planned to be 20 years [55].

6.3.4. Russian Federation

An intermediate helium circuit will also be used in the Russian Federation's HTGR designs VG-400 and VGM [332]. Two IHX designs were developed and tested. The first design is based on straight-tube shroudless cassettes; the second features cassettes with helical tubes [332, 333]. Pressure in the secondary circuit is higher than in the primary circuit. The main characteristics and structural layouts of the IHX designs are given in Table 38 and Fig. 136 [332].

The straight-tube IHX consists of cassettes inside a profiled shroud, and an equilateral triangle arrangement of tubes in the cassettes in two rows around the central tube. Cassettes are arranged at two levels in order to reduce pressure losses at the heat exchange surface inlet and outlet and to improve helium flow formation at the shell side

TABLE 37. DESIGN SPECIFICATIONS OF THE He–He INTERMEDIATE HEAT EXCHANGER IN THE HTTR

	IHX in HTTR	IHX in GTHTR300C
Type	Shell-and-tube, helical	Shell-and-tube, helical
Heat capacity (MW)	9.94	170
Shell material	2.25Cr–1Mo steel	SA 533 (Mn–Mo)
Tube material	Hastelloy XR	Hastelloy XR
Size		
Inner/outer shell diameter (m)	1.352/2.0	
Shell height (m)	11.0	
Inner/outer bundle diameter (m)	0.84/1.31	1.84/4.57
Effective tube bundle height (m)	4.87	2.94
Tube outer diameter (mm)	31.8	45.0
Tube wall thickness (mm)	3.5	5.0
Tube length (m)	22	14.2
Number of tubes	96	724
Heat transfer area (m^2)	244	1448
Maximum temperature		
Shell (°C)	430	<350
Tube (°C)	955	955
Maximum pressure (MPa)		
Shell	4.81	6.0
Tube (differential pressure)	0.29	0.29
Primary helium (shell side)		
Inlet temperature (°C)	850–950	950
Outlet temperature (°C)	389	850
Inlet pressure (MPa)	4.06	5.00
Pressure drop (kPa)	1	31
Flow rate (kg/s)	3.4	324.2
Secondary helium (tube side)		
Inlet temperature (°C)	273	491
Outlet temperature (°C)	775–860	900
Inlet pressure (MPa)	4.21	5.15
Pressure drop (kPa)	20	58
Flow rate (kg/s)	3.0	80.3
Design lifetime (a)	20	20

inlet. In the helical-tube design, the heat exchange surface consists of 19 cassettes arranged in a triangle inside a hexahedral shroud. Tubes are wound around the central load-bearing tube and form four coils with a diameter ranging between 232 and 406 mm.

The IHX in the MHR-T plant is used to transfer heat at temperatures of up to 1000°C to the hydrogen production application and is separated into two heat exchangers due to limitations on the heat exchanger casing size. The heat exchanger is vertically arranged, pressurized and modular, with the possibility of constructing separate modules. One IHX contains 121 modules. In order to reduce wall temperatures, the inner surface of the casing is fitted with thermal insulation and an air cooling system at the outer surface. Candidate materials for the IHX removable internals are the steels 12Cr18Ni10Ti, 08Cr18Ni9, 08Cr16Ni11Mo3, and high nickel alloy CrNi55MoWZr.

For the GT-MHR plant, which uses an indirect (in the intermediate circuit) gas turbine cycle, an IHX was developed based on the design with helical tubes wound in one coil. The IHX is inserted into the heat transfer unit casing where the primary circuit helium blower is located. Internal metal structures shape the circulation path between the IHX and the gas blower. This IHX design is more compact than the modular one. However, with the IHX power equal to the GT-MHR power, the IHX tube bundle does not fit into a casing of acceptable size and weight; this is why the IHX is divided into two parts. Moreover, in the helical-tube IHX, hydraulic resistance in the secondary circuit (on the tube side) is 3–5 times higher than in the primary circuit (on the shell side).

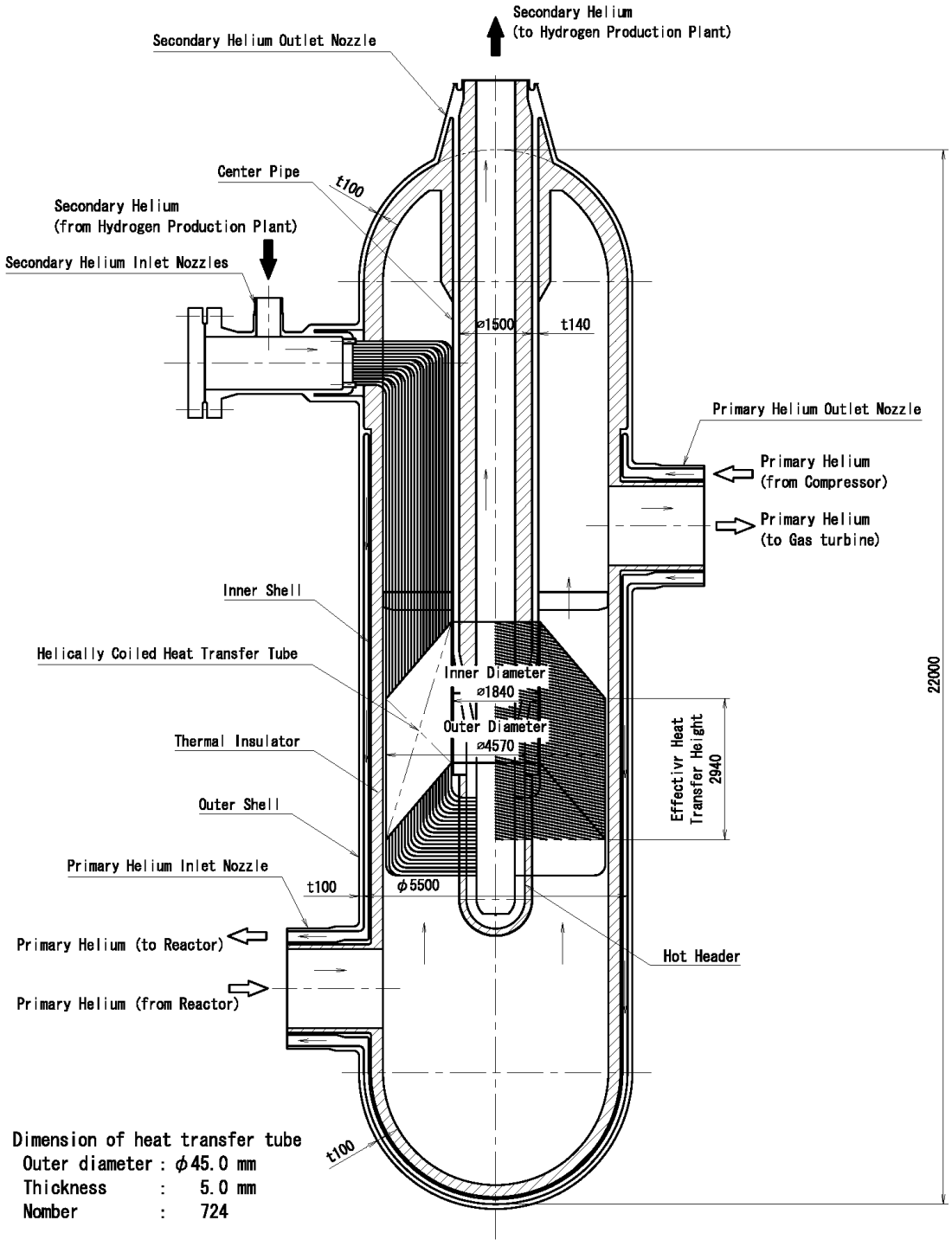

FIG. 135. Conceptual drawing of the IHX for GTHTR300C [55].

TABLE 38. MAIN PARAMETERS OF THE IHX DESIGN OF THE RUSSIAN FEDERATION'S REACTOR CONCEPTS [332]

Parameter	VG-400	VG-400, VGM	MHR-T	GT-MHR
Power (MW)	110.5	76.9	105.5	302.5
Mean LTD (°C)	154	171	136	34.5
Primary Circuit				
Coolant	Helium	Helium	Helium	Helium
Flow rate (kg/s)	85	59.1	135.5	159.3
Inlet/outlet temperature (°C)	950/700	950/700	1000/850	849/484
Inlet pressure (MPa)	4.9	5.0	6.42	7
Pressure loss (kPa)	23	12.8	33.4	16.2
Secondary Circuit				
Coolant	Helium	Helium	Helium	Helium
Flow rate (kg/s)	38.6	24.2	38.65	171.4
Inlet/outlet temperature (°C)	350/900	290/900	450/975	460.8/800
Inlet pressure (MPa)	5.4	5.2	6.92	7.46
Pressure loss (kPa)	46	18.6	45	210
Geometrical Characteristics				
Type of heat exchanger and tubes	Modular, straight-tube	Modular, helical	Modular	Coiled, helical
Size of tubes				
OD × δ (mm)	14 × 2	21 × 2.5	4	30 × 4
length (m)	5.38	10.9		49
Number of tubes	163 × 42	19 × 132	252 × 121	2300
Tube material	CrNi55Mo WZr	CrNi55Mo WZr	SiC-based ceramics	CrNi55Mo WZr
Bundle OD/ID (m)		0.435/0.20	3.35	4.88/1.544
Bundle height (m)		10.1	2	10.0
Casing OD (m)		2.3	5.7	~6

LTD = Log temperature difference δ = wall thickness
OD = outer diameter ID = inner diameter

6.3.5. United States of America

6.3.5.1. Conceptual design of IHX for the US H2-MHR

In the USA, the reference design for a next generation HTGR is the 600 MW(th) modular helium reactor (MHR). For the purpose of hydrogen generation, the concept of an H2-MHR has been developed, which is to be coupled to a hydrogen production technology based on either an S–I thermochemical cycle or high temperature electrolysis. The IHX for this facility is based on the PCHX design [334]. The characteristic data of the IHX design for the H2-MHR are listed in Table 39.

For the S–I cycle based H2-MHR, the IHX as currently planned will consist of 40 modules of PCHX with each module transferring 15 MW(th). All modules plus associated manifolds will be placed into an insulated steel vessel of a size similar to that of the MHR vessel. For the HTSE-based H2-MHR, the IHX component would be much smaller due to the small amount of heat being transferred. The IHX could be either composed of PCHX units or follow the more conventional helical coil design [335].

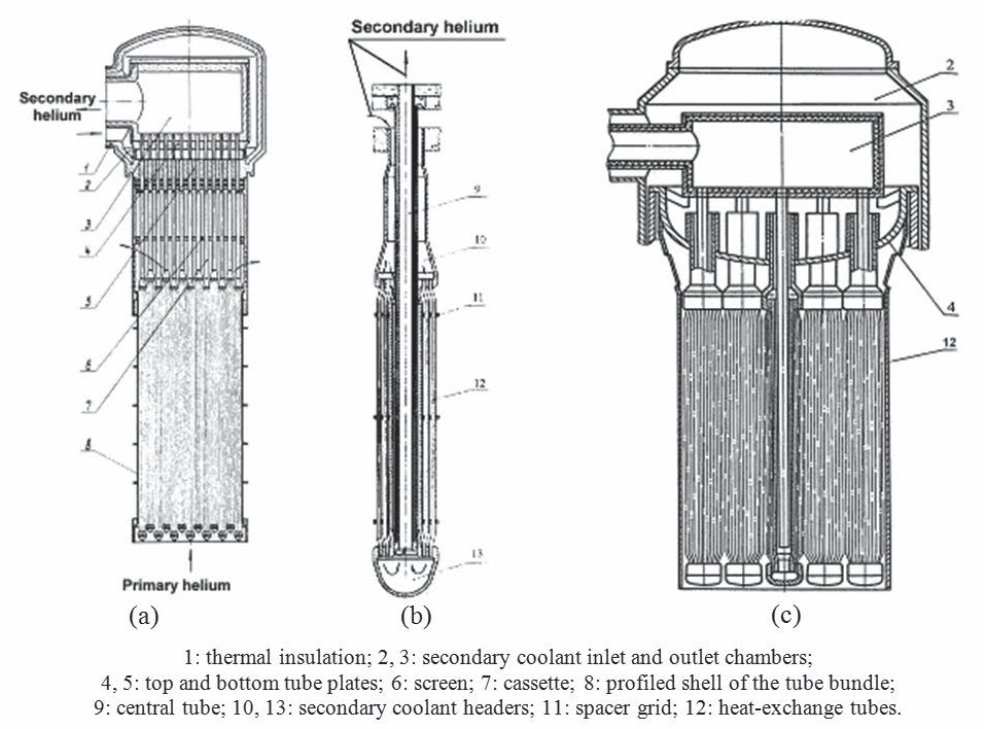

FIG. 136. Structural diagram of the straight-tube IHX design for the VG-400 [332]: (a) VGM power plants; (b) straight-tube cassette; (c) helical-tube IHX.

TABLE 39. DESIGN SPECIFICATIONS OF THE He–He IHX FOR THE H2-MHR CONCEPT [335]

	IHX in H2-MHR
Type	Printed circuit heat exchanger
Heat capacity	600 MW(th)
Material	Alloy 800H materials
Size of vessel	
Diameter	6.9 m
Active heat transfer height	8 m
Wall thickness	2 mm
Size of module	
Length	0.6 m
Width	0.65 m
Height	1.5 m
Number of modules	40
Primary helium	
Inlet temperature	950°C
Outlet temperature	590°C
Design pressure	7.0 MPa
Design pressure drop	40.7 kPa
Flow rate	320 kg/s
Secondary helium	
Inlet temperature	450°C
Outlet temperature	975°C
Design pressure	7.1 MPa
Design pressure drop	13.1 kPa
Flow rate	222 kg/s
Heat transfer area	5230 m^2

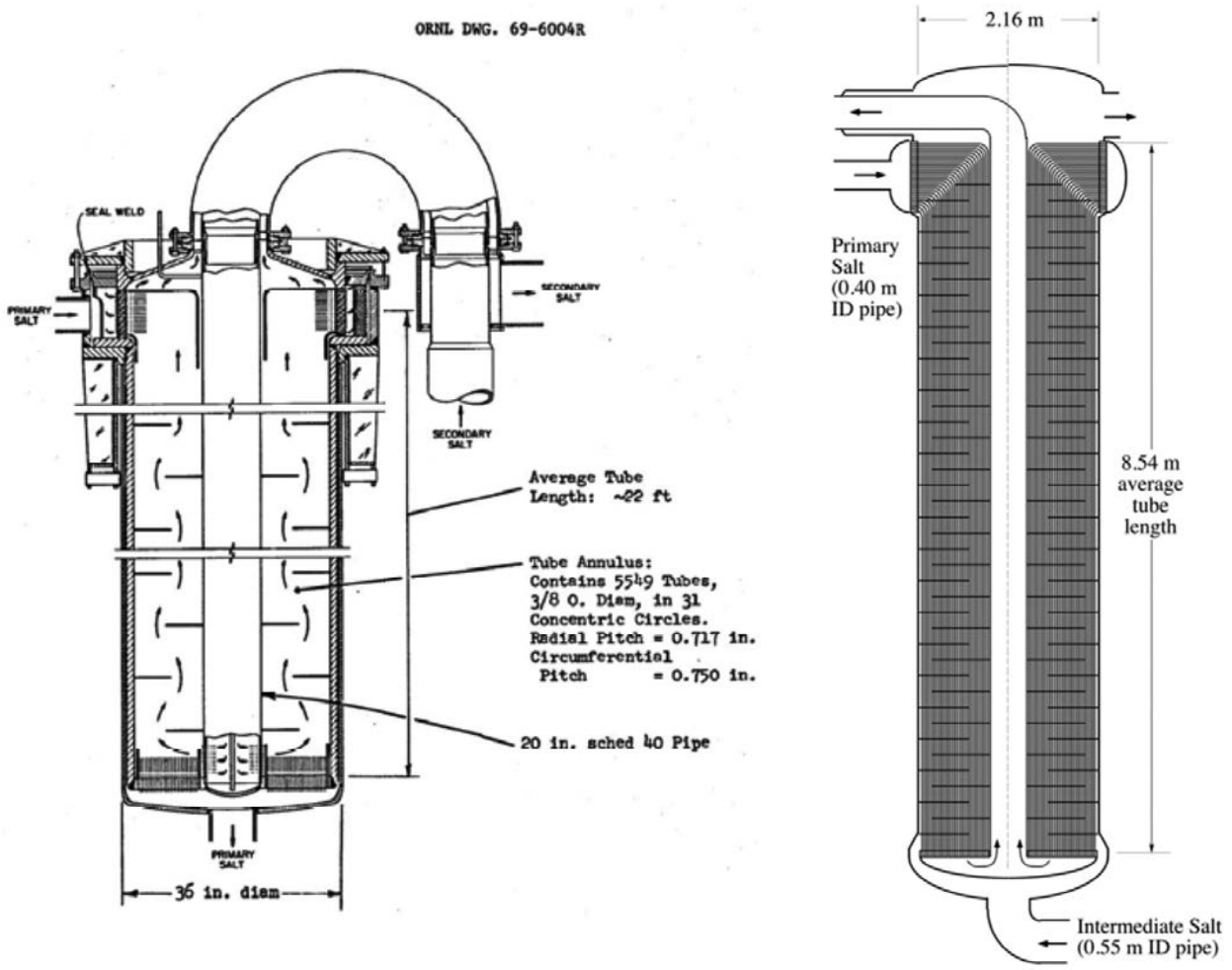

FIG. 137. Salt–salt IHX design developed for the former MSBR project (left) [336] and for the PB-AHTR (right) [337].

6.3.5.2. Conceptual design of IHX for the US AHTR

The salt–salt intermediate heat exchanger design for the modular 900 MW(th) PB-AHTR has been adopted from a former development within the molten salt breeder reactor (MSBR) programme at ORNL [314, 336]. In the MSBR, the heat exchanger was designed as a 563 MW(th) shell and tube IHX (Fig. 137, left), in order to facilitate in-service inspection and reliability. Each IHX in the MSBR had 5900 tubes with a length of 6.6 m and an outer diameter of 9.5 mm. To minimize the salt inventory, knurled tubing was proposed to enhance heat transfer. The velocity of the salt fluid was maintained at 3.0 m/s in the tubes and 2.3 m/s in the shell. A large LMTD of 95°C was used, resulting in a high power density of 120 MW/m^3. For the PB-AHTR, a lower LMTD is desired, to increase the power conversion efficiency, and thus a significantly larger surface area will be used [314]. The PB-AHTR [337] will have four IHX modules with 225 MW(th) each and two primary pumps in the intermediate loop (Fig. 137, right).

The IHX is a one-pass vertical exchanger with disk-and-doughnut baffles to hold the L-shaped tubes, to control cross-flow and to minimize the flow-induced vibration. The tubes have a helically knurled surface to improve heat transfer and to minimize salt volume. The primary salt on the tube side flows downwards, while the intermediate coolant flows upwards on the shell side. The tube material may be a high temperature structural alloy sandwiched between thin layers of a corrosion resistant cladding material. Some characteristic data of the IHX are listed in Table 40.

TABLE 40. DESIGN SPECIFICATIONS OF THE SALT–SALT IHX FOR THE PB-AHTR CONCEPT [337]

	IHX in PB-AHTR
Type	Shell-and-tube one-pass vertical heat exchanger
Heat capacity	225 MW(th)
Material	Alloy 800H/Hastelloy N
Size of shell	
Diameter	2.16 m
Height	7.98 m
Wall thickness	12.7 mm
Size of tubes	
Length	8.54 m
Outer diameter	9.525 mm
Wall thickness	1.335 mm
Number of tubes	9465
Central tube (upcomer) diameter	0.55 m
Primary salt	FLiBe (Li_2BeF_4)
Inlet temperature	704°C
Outlet temperature	600°C
Design pressure drop	139 kPa
Flow rate	905.87 kg/s
Secondary salt	Finak (LiF–NaF–KF)
Inlet temperature	545°C
Outlet temperature	690°C
Design pressure drop	143 kPa
Flow rate	823.60 kg/s
Heat transfer area	2418.99 m^2

The aircraft and other industries have developed compact heat exchangers with buffer gas zones to separate different fluids that may react explosively, such as hot gases vaporizing fuels in aircraft. The same technologies enable trapping of tritium from the primary system in the heat exchanger of an MSR for hydrogen production [338].

6.4. PROCESS HEAT EXCHANGER CONCEPTS

The development and qualification of a compact IHX is challenging; even more challenging is the IHX on the process side, where heat is decoupled in specially designed heat exchangers to be directly transferred into the chemical process feedstock. The process heat exchanger (PHX) is a component working under conditions of high temperatures, large pressure differences and a corrosive environment on the secondary side. PHX developments in various countries are described in Section 4.6. For process steam production, typically a tertiary cycle will be employed, with heat transfer via a steam-to-steam heat exchanger providing an additional barrier against tritium migration to the process system.

6.5. COOLANTS FOR INTERMEDIATE CIRCUITS

6.5.1. Candidates

The coupling of a nuclear process heat plant to any process requires the economic, safe and reliable transport of high temperature heat from the primary heat source to the process. The choice for the appropriate secondary

TABLE 41. PROPERTIES OF SOME NUCLEAR REACTOR COOLANTS [311]

Coolant	T_{melt} (°C)	T_{boil} (°C)	Density (kg/m^3)	Capacity (kJ/(kg·K))	Conduct. (W/(m·K))	Viscosity (10^{-6} m^2/s)
Helium [a]		–269	3.8	5.2	0.29	11.0
Water [a]	0	290	732	5.5	0.56	0.13
Sodium	97.8	883	820	1.27	62	0.12
Lead [b]	327	1740	10 540	0.16	16	0.13
Bismuth [c]	271	1564	9 467	0.1645	15.6	0.083
Pb–Bi [b]	124	1670	10 530	0.151	~9.5	0.30
FLiBe [d]	459	1430	1 940	2.42	1.0	2.9
FLiNaK [d]	454	1570	2 020	1.886	0.92	1.43

[a] at 7.5 MPa
[b] at melting point
[c] at 760°C
[d] at 700°C and 0.1 MPa

coolant will be made depending on its thermophysical properties (melting point, vapour pressure, density, heat capacity, viscosity, thermal conductivity), as well as on its availability, material compatibilities, cost, nuclear performance, toxicity, purification capability (e.g. tritium removal), piping/valving complexity, recovery after primary system depressurization and ingress of large quantities of coolant into the reactor, maturity of development, and last but not least, safety concerns. Candidates for secondary coolants are steam, inert gases like He, He/N_2, molten/liquid salts, or liquid metals. Table 41 summarizes relevant properties for a number of coolants [311].

The industrial process heat market in the lower and medium temperature range is very large. At temperatures below 600°C, the demand is mainly in the form of steam. It is inexpensive, and the large latent heat of vaporization of water is advantageous for many applications. In addition, steam is often used as a reactant and to supply mechanical work like driving pumps. As process applications use higher temperatures, steam and water become less appropriate as a heat exchange medium, since they are highly corrosive at this level, and other heat carriers such as gases, liquid salts, or liquid metals will be used [311].

Attractive materials for heat exchange and coolants at higher temperatures have low circulation costs and are non-chemically reactive. Materials with high temperature and pressure are unattractive because of the high containment material costs and pressurization equipment. The chemical industry uses molten fluoride salt for heat transfer because of its high boiling point and positive reaction properties with water and air [339]. Another parameter influencing the choice of a heat transport fluid is distance. Over longer distances, liquid salts and steam are expected to have lower heat transport costs. A general problem of intermediate circuit coolants, which are different from the primary coolant, is the possibility of ingress of an external medium into the primary system (like a water ingress accident in an HTGR). In the event of a heat exchanger leak, chemical ingress into the primary system is dependent on the chemical composition and pressure gradient between the primary and secondary system fluid. The ingress of He or a $He–N_2$ gas mixture will not cause a problem to the fuel. Higher pressures will enhance heat transfer, but a limitation may be required with regard to the strength of materials exposed to a corrosive environment. The rate of heat transfer through the PHX determines chemical reaction rates and sizing of the chemical reactor.

6.5.2. Gaseous coolants

Gaseous coolants include fluids such as helium, carbon dioxide, nitrogen and air. Helium is a well understood fluid and considered the fluid of choice in the secondary circuit for many HTGR concepts. It has a high specific heat and provides optimal performance due to the absence of neutron moderation and absorption. Unlike sodium that violently reacts with water and air, helium, as an inert medium, does not exhibit chemical interaction. The low thermal conductivity of helium results in poor heat transfer even at high coolant velocities. Helium purification and contamination detection on the primary coolant are essential systems for the identification of leaks and mitigation

or prevention of chemical attack. A helium intermediate circuit is characterized by high costs for large sized coolant circulators and other process equipment. Heat losses are higher than those for the liquids due to the larger pipe diameter leading to a larger heat exchange surface. The larger diameter also results in greater pipe wall thicknesses. Helium pumping requirements and heat loss have been found to increase more with separation distance than is the case with liquid salts (and liquid metals) [340]. But the He as an intermediate circuit coolant has minimum mass and the lowest cost compared with other options, although the capital costs of the inventory storage required are rather high. Gases require high pressures and may cause problems in the case of leakage, with potential transportation of radioactivity to the outside and loss of the ability to effectively remove decay heat by natural circulation.

Another suggestion for a working fluid is a mixture of 80% nitrogen and 20% helium, which has a density near those working fluids that are used in current turbine designs [315]. An N_2–He mixture has been suggested as a working fluid in the secondary circuit for the French ANTARES concept. The mixture with nitrogen eases the selection of the turbine, but is at the expense of a higher risk of nitridation of the metal surfaces at high temperatures.

Experience with the coolant CO_2 has been gathered to a large extent within the British advanced gas cooled reactor programme. The higher density of CO_2 compared with helium is of advantage because it allows smaller velocities for the same pressure drop. Under accident conditions, CO_2 efficiently transports heat by a stronger natural convection compared with helium. The CO_2 circuit components can be designed to be smaller and are therefore less expensive. Also, leakage rates are smaller than those of helium. The main issues are seen in the CO_2 radiolysis under normal operating conditions and the control of coolant chemistry due to the presence of the large amounts of graphite structures [341].

For short separation distances between the nuclear plant and the process plant, a near term solution would be helium as transfer coolant [340].

6.5.3. Liquid/molten salt coolants

The use of liquid and molten salts in nuclear systems has been subjected to extensive R&D. Liquid salt means a clean salt, whereas a molten salt refers to a primary coolant in nuclear applications where the fissile material and the fission products are contained in the salt, which involves a much higher challenge to materials with regard to corrosion.

6.5.3.1. Molten salts

Molten fluoride salts have a wide solubility range for U and Th, are thermodynamically stable, do not undergo radiolytic decomposition, have a low vapour pressure, do not attack nickel based alloys, have a higher heat capacity than sodium (allowing for smaller components) and have a low heat conductivity (slow temperature changes) [281].

Molten salt candidates that meet basic criteria such as sufficient chemical and radiation stability and compatibility with graphite and high temperature alloys (e.g. Hastelloy N) can be categorized into alkali fluorides or mixtures of these with either BeF_2 or ZrF_4. Mixtures of two or sometimes three compounds are required to achieve a sufficiently low melting point. The need for materials with low vapour pressure limits the share of BeF_2 or ZrF_4 to less than 40–45% [312].

Molten fluorite salts have the advantage of great stability with respect to both high temperatures and radiation. Activation levels of molten salts appear to be acceptable. Coolant disposal after 60 years of operation should be possible as low level waste. Neutronic performance of the liquid salt is strongly dependent on the isotopic and elemental composition. The disadvantage is that molten salts (also molten metals) carry the risk of corrosion of structural core materials, which proceeds at high rates with increasing temperature. All salts except for LiF–BeF_2 exhibit a positive coolant density coefficient and coolant void ratio [312].

6.5.3.2. Liquid salts

At lower temperatures, nitride salts have been widely used in the chemical industries. The coolants demonstrated in high temperature systems are helium and liquid fluoride salts, which have shown chemical stability and relatively non-corrosive behaviour. The heat transfer properties are similar to those of water. Experience with fluoride salts has long existed in the alumina production industries, where aluminium oxide is dissolved in a

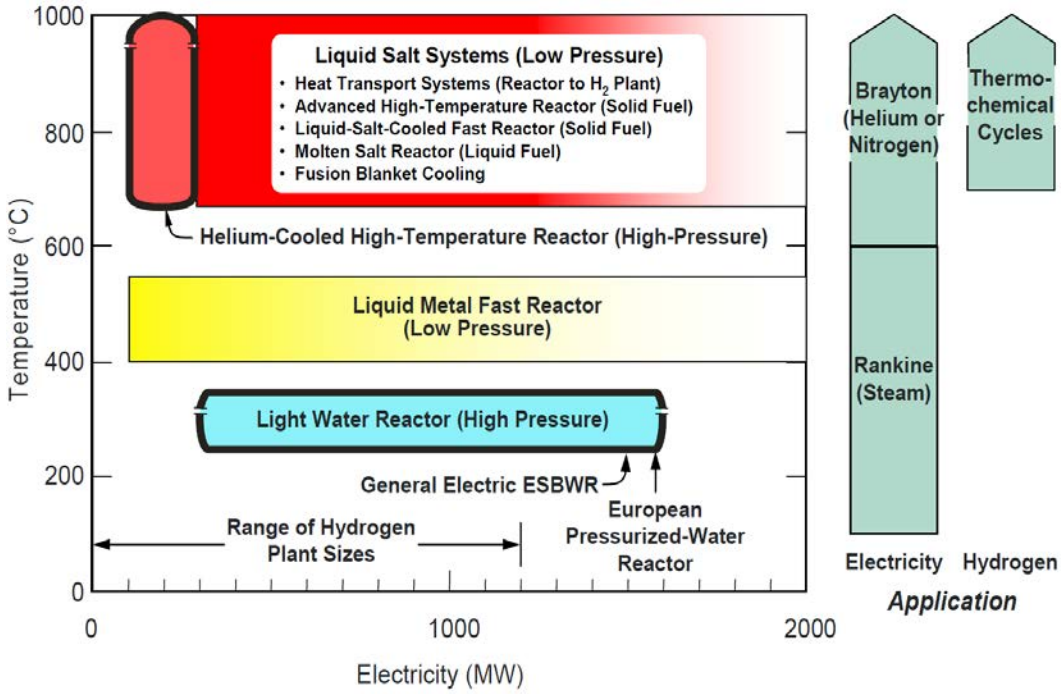

FIG. 138. Coolants for different reactor types [338].

mixture of sodium and aluminium liquid fluoride salts (cryolite: $3NaF{\cdot}AlF_3$) at ~1000°C. In high temperature reactors, both helium and liquid fluoride salt coolants have been applied. Liquid fluoride salt coolants are economically strong because of their enormous heat transport capability compared with gases, therefore allowing a minimization of equipment. The liquid salt is at atmospheric pressure, whereas the helium is at high pressure (Fig. 138) [342]. Compared with sodium coolant, liquid and molten salts have an advantage because of their much larger heat capacity.

A salt cooled loop can operate at any desired pressure by installation of a pressurizer with an inert gas. The salts are essentially incompressible; thus the gas pressure in the pressurizer, which determines the system pressure, could be easily adjusted to the needs of the potentially connected chemical factory. Liquid fluoride salt coolants have good material compatibility and low corrosion rates with high nickel alloys, when proper chemistry control is used. As a baseline concept, the so-called FLiBe has been selected and is being suggested for use in the US concept STARH2. FLiBe is a mixture of lithium fluoride (LiF) and beryllium fluoride (BeF_2) in a molar concentration ration of 67 to 33: $^7Li_2BeF_4$. It is expensive because of the high cost of Be and the enriched Li (isotopic concentration >99.995% of ^7Li). Another candidate, Flinak, (LiF–NaF–KF), is a well characterized, inexpensive mixture with excellent heat transport properties, but with a high melting point of 454°C [340].

Beryllium salts are less attractive due to high costs and toxicity concerns, requiring industrial safety standards. A $NaF–BeF_2$ or $LiF–NaF–BeF_2$ salt has excellent heat transfer characteristics, but it would be neither economically viable nor practical. Chloride salts, e.g. LiCl–KCl, have an advantage due to their low cost and low melting points, but the thermodynamic properties of chloride salts in contact with metallic alloys are not as favourable as those of fluoride salts [340]. Furthermore, chloride salts need isotopically separated chlorine to avoid nuclides with high cross-sections. The highly mobile activation product ^{36}Cl causes a problem for waste management.

The salts are mixtures of different fluorides to optimize their physical properties. All lithium salts use (almost) pure ^7Li because of its low nuclear cross-section. The salts have melting points between 300 and 500°C and atmospheric boiling points typically above 1200°C. In order to avoid freezing of the molten fuel salt and the liquid salt coolants in the intermediate circuit, they must stay at a sufficiently high temperature [338]. A startup from atmospheric temperature needs a preheater to melt the salt before circulation can start. This preheating would require the design and installation of a centralized handling and storage unit in order to facilitate the melting and

introduction of the salt to the loop. A loss of circulator power may cause the liquid salt to freeze. A major concern with using compact heat exchangers in combination with these fluids is plugging of the flow channels [340].

In emergency cases, the liquid fuel is dumped to passively cooled critically safe tanks. The liquid fuel allows on-line refuelling and a wide choice of fuel cycle options. Fission products can be removed on-line. For actinide burning, the advantage is that there is no fuel fabrication step. Proper materials may have upper temperature limits of <750°C.

The coolant for the LS-VHTR (or AHTR) is a mixture of fluoride salts that does not contain fuel. A salt coolant is also considered an option for the intermediate circuit in sodium fast reactors and with a supercritical CO_2 power cycle. Besides a reduction in equipment size, a major advantage is that there are no chemical reactions between the three different coolants.

For long separation distances between the nuclear plant and the process plant, there might be an advantage for liquid salts compared with helium in terms of cost and efficiency.

6.5.4. Liquid metal coolants

Liquid metal coolants (Na, NaK, Pb, Pb–Bi) are generally considered for fast reactor systems (also N_2O_4 has been studied in the Russian Federation) because of their high thermal conductivity, indifference to radiation and useful temperature range at low pressure. All have a high boiling point compared with water and therefore do not need to be pressurized at higher temperatures as water, leading to less stringent requirements on vessels and piping.

Sodium coolant is easy to handle, has favourable thermophysical properties and is practically not corrosive to metals. But it is not inert and explodes violently in contact with water. The main advantage is the excellent heat transfer. A drawback is the formation of ^{24}Na, requiring radiation shielding against its intense neutron radiation for the primary loop.

Lead and lead–bismuth (Pb–Bi) eutectic alloy are chemically inert heavy liquid metal coolants, but they require higher pumping power. Lead does not react with water, nor does it burn in air. Due to its relatively high melting point, the use of pure lead generally requires operation at higher temperatures to reduce the risk of the lead freezing and also to avoid excessive embrittlement of structural material subjected to fast neutron flux at low temperatures. as lead exhibits an excellent resistance to corrosion, it was one of the first metals used as a material in chemical engineering. Channels with oxide protective coatings are unwettable by lead. Favourable characteristics are the very low vapour pressure and the very high boiling point of 1740°C precluding accidents with coolant boiling. Lead has good heat transfer characteristics. Corrosive attack on ferritic–martensitic and stainless steels remains negligible up to 400°C owing to the low solubility of impurities. Lead provides excellent radiation shielding against gamma radiation and allows high temperatures. Any leaked lead would solidify without significant chemical reactions. While helium is favoured for large plants, lead is advantageous for smaller plants [280].

A lead–bismuth eutectic (LBE) mixture has a reduced melting point, but corrosion rates are enhanced, which limits the maximum coolant temperatures (to ~550°C) and coolant velocity. For exposure times up to 7000 h, austenitic steels can be employed in an LBE with the appropriate oxygen activity up to a temperature of 500°C. Martensitic steels can probably be used in this environment up to 550°C, but for a limited time because of the high oxidation rate. Another major concern is a certain radiation problem that arises from the bismuth. The activation of ^{209}Bi to the volatile gamma emitter ^{210}Po becomes a radiological hazard, which can be alleviated by the employment of an intermediate circuit [280]. The mass and cost of the Pb–Bi coolant are higher than with other coolants, but the necessary heat exchanging surface is smaller.

Unlike with lead, a major disadvantage could be the limitation of bismuth resources, supposing there is a significant deployment of LFRs in the future. One SVBR-75/100 reactor system as suggested in Ref. [343] would require a specific mass of bismuth of ~1100 t/GW. World resources of Bi are currently estimated to be ~5 million t. The estimated annual world mine production of bismuth is ~5600 t (as of 2006) with the main producer countries being China, Mexico and Peru.

Experience with lead based coolants is mainly from the Russian Federation, where these coolants were used in the reactors of eight nuclear submarines, each powered by a compact, Pb–Bi cooled 155 MW(th) reactor, and in two prototype nuclear power plants with an accumulated experience of 80 reactor-years (quoting a reference of 1999) [343].

6.6. MATERIALS FOR HIGH TEMPERATURE HEAT EXCHANGERS

6.6.1. Requirements

Structural materials for both in-core and out-of-core components in Generation IV reactors experience higher temperatures, higher neutron doses and a much more corrosive environment than do those for existing reactors. Of the utmost importance is the choice of suitable heat exchanger materials in order to guarantee good heat transfer and safe and reliable reactor performance. Materials undergo degradation if exposed to high temperatures, neutron irradiation or corrosive environments. Therefore good resistance to oxidation, corrosion, fouling, creep, thermal shocks and thermal fatigue, but also adequate mechanical properties such as strength and toughness, are required. Other important issues are availability, workability and cost of materials.

Materials should be resistant against thermal stresses during repeated heating and cooling cycles and have good structural stability to avoid graphitization, grain growth or phase changes. Creep–fatigue interaction and creep rupture strength of base metals and weldments causing unacceptable dimensional changes and distortions as well as final rupture are the most important factors determining the integrity and structural lifetime of components at elevated temperatures. Other R&D is concentrating on primary helium coolant chemistry and acceptable ranges of impurities. Considering the protective effect of oxide layers on metal surfaces, a slightly oxidizing chemistry may result in an extended component lifetime. Also, the development of less brittle ceramic materials is being pursued. At the high temperatures of a VHTR, even small amounts of impurities such as H_2O and CO_2 in the primary coolant will cause degradation in the mechanical strength of the metal as a result of chemical reactions with these impurities.

The basic requirements of Generation IV reactor materials are [344]:

— Geometric stability against thermal and irradiation creep, void swelling;
— Favourable mechanical properties such as strength, ductility, creep rupture, fatigue and creep–fatigue interactions;
— Resistance to irradiation damage (hardening, embrittlement) at high neutron doses;
— Chemical compatibility between materials and coolant and fuel, respectively;
— Good workability and weldability;
— Low cost.

The safe operation of components requires methods that can predict materials degradation. Their development is necessary to allow extrapolation to operational parameter ranges outside the ones covered by experiments, and to better understand the physical mechanisms responsible for the observed behaviour. Higher confidence in lifetime assessments of VHTR materials requires an understanding of related microscopic and macroscopic physical phenomena. Long term performance is determined by the complex operational conditions. Up to now, rather simple damage rules in connection with large safety margins have been applied, ideally to already well known materials. This methodology, however, is insufficient when new materials or modified service conditions are considered. Materials modelling can provide physically based input and valuable contributions to design rules and code cases for damage interactions. Multiscale (length, time), multicode simulations and corresponding multidimensional validation experiments were undertaken to understand the mechanical properties of the materials. States of stress in the material, actual environment, local microstructure, stress–strain temperature history and exposure time are important aspects to be studied [345].

6.6.2. Damage mechanisms

Various mechanisms for materials damage exist in a VHTR environment (Table 42). The problem is related to the fact that the thermal stability of the HTGR graphite core is higher than that of the IHX structural materials. Wide data distribution requires a large number of tests for qualification. At lower irradiation temperatures, the dominant mechanism is irradiation creep due to point defects. At higher temperatures above 650°C, it is thermal creep. Local mechanical properties can be determined with microhardness, nano-indentation and nano-pillar-compression tests. Structural, electronic and magnetic analysis of the material can be undertaken using synchrotron radiation with a powerful X ray source. Near surface areas can be analysed without damaging the material [345].

TABLE 42. DAMAGE MECHANISMS IN A VHTR ENVIRONMENT [345]

Type of exposure	Expected type of damage
Temperature	Phase reactions (precipitations, particle dissolution, segregation)
Neutron irradiation	Displacement damage (point defect clusters like black dots, loops and voids leading to swelling, hardening, embrittlement) Helium damage (bubble formation at particle–matrix interfaces or grain boundaries) Radiation induced segregation and ion beam mixing (local alloying)
Environment (He + CO/CO_2, H_2, H_2O, O_2, impurities)	Oxide layer (eventual softening of matrix, weakening of grain boundaries) Carburization (hardening and embrittlement due to carbide formation) Hydrogen embrittlement Degradation of fibre–matrix interface
Mechanical load	Creep damage (irradiation and/or diffusion controlled dislocation movement, void formation along different types of boundaries) leading to plastic deformation, fibre pull-out, and rupture

Constant load creep tests at different load levels and test temperatures provide the basic data for deriving the time dependent allowable stresses considering creep rupture and creep strain limitations, including specified safety margins such as extended operating time or increased temperature. Creep laws and design values are normally derived from creep rupture tests on uni-axially loaded specimens and applying certain hypotheses to calculate equivalent stresses or strains.

For the lifetime and wall thicknesses of real components, multi-axial loading situations must also be considered. A multi-axial stress state is often characterized by an effective stress, which represents a measure of the material stressing. Important for the failure is also the deformation behaviour and the orientation of the principal stresses, which determine the pattern of the cracks formed at the outer surface [346]. Cyclic stresses of components are simulated by strain-controlled fatigue tests at constant temperature in both helium and air environments. For components exposed to multi-axial loadings, lifetime is the essential parameter determined in tests with pressure, tension or torsion loads.

In oxidizing environments and at high temperatures, metals are prone to oxidation processes; also hot corrosion, carburization, sulphidation and nitridation may be possible. If carburization occurs, the ductility will decrease; if decarburization occurs, the strength will decrease; and if internal oxidation occurs, the potential for crack initiation increases with the associated decrease in ductility and toughness. As a result of oxidation, a non-metallic oxide layer is formed on the metal surface, while reducing the amount of certain alloying elements in the material that react with the oxygen, connected with a loss of material thickness. Alloying elements in the metal are, for example, chromium, aluminium and silicon. Improvements can be made by modifying the alloy compositions by adding reactive elements such as Y, Ce and La, in order to enhance adhesion of the oxide layer, particularly under thermal cyclic conditions. For many commonly used metals (such as iron, nickel and cobalt), sulphur is a highly aggressive oxidant. Reaction rates are orders of magnitude faster than those in oxygen [347].

An oxide layer on the surface can be an advantage if it protects from further oxidation and corrosion by not allowing constituents such as C, N and S to permeate, which are made responsible for internal corrosion. It may, however, not be stable under all conditions due to mechanical loadings or thermal cycling. The oxidation resistance of most high temperature metallic materials, such as stainless steels and superalloys, is based on a protective chromium oxide (Cr_2O_3) layer, which is thermodynamically stable even at elevated temperatures and resists sulphidation. However, in environments with an unbalanced carbon activity versus the oxidation potential, the oxide scale is reduced by reacting with the carbon from the alloy.

At temperatures above 600°C, the material structure changes, e.g. carbides are deposited. Carburization attack taking place in conditions with low oxygen partial pressures generally causes the formation of internal carbides, leading to alloy embrittlement and degradation of mechanical properties. The only acceptable corrosion mode appears to be passive oxidation, characterized by the slow and sustainable growth of an external oxide scale which can protect the alloy from direct interaction with the gas environment. This, however, requires that the primary coolant chemistry be controlled by a purification system to adjust the impurity contents in the helium [348]. Graphite deposition has destructive effects due to the growth of graphite in the cracks and pores of the oxide layer,

leading to spalling of the oxides. Dense oxide scales of alumina, chromia and — most effectively — SiO_2 can generally protect from internal carburization [347].

Chromium, which is an essential constituent of the alloy, has been identified as an essential element in the various chemical processes [349]. In the presence of water molecules, chromium reacts to yield the oxide, while chromium carbides ($Cr_{23}C_6$) are decarburized to yield Cr and CO. A carburization reaction of Cr occurs in the presence of CO to yield chromium carbide and chromium oxide, with the latter acting as a stable protective layer. Therefore, a certain CO partial pressure in the helium would be important. For bright metal surfaces, chromium carbides can be formed at temperatures below 850°C. For high CO concentrations, carbon deposition is possible at temperatures below 650°C. Another important alloying element is aluminium, which improves the high temperature performance of steels. Silicon improves the high temperature corrosion resistance of high alloy steels, especially in carburizing conditions.

During long term service at high temperatures, metallic materials inevitably undergo ageing processes which result in microstructural evolution and changes in mechanical properties, such as ductility. Experimental programmes are conducted to characterize the ageing capacity, corrosion resistance, and mechanical behaviour before and after irradiation. Different ageing treatments are tested with regard to their influence on the microstructure.

Fouling is the deposition of unwanted species or layers from flue gases on component surfaces. It is often accompanied by corrosion and erosion, whose products may decrease heat transfer efficiency.

6.6.3. Materials for intermediate heat exchangers and nuclear steam reformers

6.6.3.1. Candidate materials

There are various types of materials under consideration [347].

(A) Ferritic–martensitic steels

Advances in the development of ferritic–martensitic (F–M) materials by alloy and microstructural modifications have made these materials appropriate for applications at elevated temperatures in power generation and the chemical industry, and possibly also in some Generation IV designs. Their maximum service temperatures depend on the steel type, alloying and surface stability. However, ferritic stainless steels lose their strength at temperatures above 650°C. The advantages are good void swelling resistance and creep resistance. Oxidation resistance of ferritic stainless steels is superior to that of Cr–Mo steels. Martensitic and ferritic stainless steels have better thermal conductivity and lower coefficients of thermal expansion than do austenitic grades. Therefore, they are more suitable to be used under thermal cycling conditions. They also exhibit a reduced activation, meaning a rapid radioactive decay of activation products. The drawbacks are the low long term creep rupture strength at higher temperatures and irradiation embrittlement at temperatures up to 400°C.

(B) Austenitic stainless steels

Nickel alloying transforms the ferrite crystal structure to the austenite structure. Cr–Ni steels have relatively low cost, good mechanical properties and moderate oxidation resistance. Therefore they are commonly used in low performance high temperature applications. Austenitic stainless steels show good creep resistance up to the higher temperature range and reasonable resistance to corrosion. Stainless steels can be used up to 800–900°C. Above that temperature, the protective Cr_2O_3 layer starts to decompose. Corrosion resistance is improved in so-called superaustenitic grades by alloying with a sufficient amount of molybdenum, nitrogen or nickel [347]. The drawback is void swelling at already moderate neutron doses, which is much higher than in F–M materials. Knowledge on irradiation behaviour is still poor for many metals.

(C) Nickel based superalloys

Nickel based alloys are predestined for high temperature applications up to 1050°C. New developments have excellent creep rupture properties and high temperature strength, in addition to good oxidation resistance and

surface stability. Nickel based superalloys can be strengthened by alloying them with Al and Ti. These oxide particles stabilize the protective oxide layer and reduce creep at high temperatures. The major problems are radiation embrittlement, swelling and phase instability, which make them rather the material of choice for out-of-core applications such as heat exchangers. Furthermore, high-nickel alloys are particularly susceptible to sulphidation attack.

(D) Oxide dispersion strengthened alloys

Oxide dispersion strengthened (ODS) steels are made through a mechanical alloying process. They have good high temperature properties and show resistance to swelling and radiation embrittlement. Mechanical properties of ferritic and martensitic steels at elevated temperatures can be improved by dispersion hardening with oxide particles (e.g. Y_2O_3 or TiO_2). For example, with yttrium alloyed ODS steels, creep resistance of ferritic ODS steels is good up to 1100°C [347]. Compared with conventional superalloys, ODS steels have a higher resistance to cyclic oxidation and scale spallation. There is concern about the long term microstructural stability. The advantageous properties still need to be confirmed for the higher dose range.

(E) Intermetallics

Intermetallics, a new class of materials between metals and ceramics, are compounds which are chemically bonded together and form a solid phase that significantly differs from the single elements in terms of crystal structure, and chemical, mechanical and electrical properties. Titanium aluminides belong to the promising compounds in high temperature and structural applications. They are characterized by a low density, high specific yield strength, high specific stiffness, good oxidation resistance and good creep resistance at high temperatures up to 700°C, and even higher temperatures with coating. The limitations are the low ductility and fracture resistance. Intermetallics have strong potential for replacing superalloys and stainless steels in moderate and high temperature structural applications.

(F) Refractory alloys

Refractory alloys such as niobium, molybdenum, tungsten and tantalum characterized by melting temperatures above 2000°C are appropriate for high temperature applications up to 1400°C with good creep and swelling resistance and no phase transformations below the melting point. They show, however, poor corrosion resistance, a lack of low temperature ductility, very weak oxidation resistance and radiation embrittlement at lower temperatures. Their use at high temperatures is limited to reducing environments or vacuum. In addition, high cost and difficult manufacturing processes make them inappropriate for Generation IV reactors.

(G) Ceramics

Due to their high melting point and modulus of elasticity, structural ceramics, such as silicon nitride silicon carbide zirconia (ZrO_2) and alumina (Al_2O_3), are superior to metals in that they exhibit high resistance to oxidation, corrosion, abrasion and creep. The disadvantages are poor thermal conductivity (with the exception of SiC) and toughness. SiC based ceramics are suitable for high temperature heat exchangers due their relatively low cost, developed manufacturing technology, good thermal conductivity and high thermal shock resistance. SiC and Si_3N_4 have a good oxidation resistance because of a protective SiO_2 layer that forms in oxidizing environments. Deposits and gaseous species can react with the SiO_2 layer and restrict utilization of SiC. Otherwise, SiC can be used up to 1400°C in air and up to 1650°C in inert environments. Their resistance to high temperature attack by molten salts and slags must be ensured.

(H) Composites

Composite materials, metal–matrix or ceramic matrix materials (CMCs), combine the desired properties of different types of materials. Metal–matrix composites typically have a light metal matrix of Al, Mg or Ti. Because of the sufficiently high melting point, only Ti–matrix composites are potential materials for elevated temperatures.

A continuous SiC fibre reinforced Ti-alloy has been developed for temperatures up to 800°C. Ceramic matrix composites consist of a ceramic matrix reinforced with ceramic fibres. There application range is at high temperatures of 1000–1500°C due to their good thermal stability and high melting points. The advantage of using composites instead of monolithic ceramics is the improved toughness. On the other hand, composite materials are inhomogeneous and anisotropic. Examples for such 'thermostructural materials' are Al_2O_3 matrix SiC particle reinforced CMCs developed for high temperature heat exchangers having a maximum service temperature of 1500°C. Although all constituents are intrinsically brittle, they can exhibit non-brittle mechanical behaviour. Since CMC materials always have a certain degree of porosity (~10%), if used as a heat exchanger material, they exhibit leakage rates (for helium) which might become unacceptable, a problem that can be overcome by impervious SiC protective coatings.

6.6.3.2. International research efforts

No industrially developed material is currently available for sustained operation at very high temperatures [324]. Nickel based alloys such as Haynes 230 (Alloy 230), Inconel 617 (Alloy 617) and Hastelloy XR are the principal candidate materials for high temperature components in the primary system (IHX, turbine blades) of a VHTR. The IHX is a component outside the reactor, and therefore irradiation effects on materials performance are less significant. The material choice for a nickel based alloy for long operation periods of the IHX implies a maximum operating temperature in the range of 400–450°C for the core inlet and about 850°C for the core outlet, including potential transients. Regarding the definition of the main materials, Table 43 summarizes the chemical composition of the main candidate materials.

(A) France

Within the French materials programme, IHX candidate materials have been selected on the basis of mechanical properties, corrosion properties in impure He, and welding and forming ability. Candidate IHX materials in the 850–1000°C temperature range are nickel based alloys (Alloy 617, Alloy 230), ODS, and SiC Alloys 617 and 230.

The IHX reference materials selected for the French ANTARES reactor concept are Alloy 230 and Alloy 617, which are currently undergoing comprehensive characterization studies [36]. Figure 139 shows experimental data on the key parameter — creep resistance — for both candidates.

Corrosion tests with Alloy 230, Alloy 617 and Hastelloy X conducted in the CORALLINE facility with a duration of up to 800 h have shown that at 750°C, Alloy 230 oxidized less than the other two materials, whereas Alloy 617 oxidized most, exhibiting internal and intergranular oxidation. Creep strength for Alloys 230 and 617 was about the same, and both were higher that of Hastelloy X [350]. Fatigue relaxation tests must be conducted under vacuum and impure helium. Especially the extensive wall material testing for high temperature alloys at a temperature of 950°C showed that this component can be applied in connection with process heat HTGRs.

With regard to the long term oxidation resistance of Alloy 617 at 950°C under oxidizing helium representative of a chemically controlled VHTR environment, corrosion tests performed at 950°C up to 5000 h showed that Alloy 617 oxidized with the growth of a surface chromium oxide scale that included titanium and with internal oxidation of aluminium. Corrosion also induced formation of a carbide-depleted zone below the surface [348].

(B) Germany

With the development of HTGR concepts in the 1980s producing heat at temperatures of up to 1000°C, comprehensive research programmes were conducted at FZJ on IHX candidate materials. For the steam cycle HTGR, the iron base Alloy 800H was qualified up to 750°C; for the steam generator, nickel based alloys with higher creep rupture strength are required for the high temperature components in process heat nuclear systems. Within the frame of the PNP project, the corrosion resistance of materials to PNP-typical helium (see Section 5.3.5) was investigated with the goal being to predict material behaviour for a 40 year operation period. The expected types of corrosion were oxidation and (de-)carburization.

TABLE 43. CHEMICAL COMPOSITION OF MAIN CANDIDATE MATERIALS
(average wt%)

	Al	B	C	Co	Cr	Cu	Fe	La	Mn	Mo	Ni	P	S	Si	Ti	W
Alloy 617	1.12	0.002	0.08	11.58	22.16	0.08	1.49		0.11	9.80	Bal.	0.003	≤0.002	0.06	0.35	
Alloy 800	0.54		0.074	0.27	20.65	0.13	Bal.		0.94	0.17	30.55	0.34	0.0004	0.40	0.53	
Alloy 800H	0.15 –0.60		0.05 –0.10		19.0 –23.0		Bal.		≤1.5		30.0 –35.0		≤0.015	≤1.0	0.15 –0.60	
Alloy 230	0.38	0.002	0.11	0.30	22.38	0.08	0.77	0.014	0.49	1.28	Bal.	0.005	≤0.002	0.39	≤0.01	14.07
Hastelloy X	≤0.5	≤0.01	0.05 –0.15	0.5 –2.5	20.5 –23.0	≤0.50	17.0 –20.0		≤1.0	8.0 –10.0	Bal.	≤0.04	≤0.03	≤1.0	≤0.15	0.2 –1.0
Hastelloy XR	≤0.05	≤0.01	0.05 –0.15	≤2.5	20.5 –23.0	≤0.50	17.0 –20.0		0.75 –1.0	8.0 –10.0	Bal.	≤0.04	≤0.03	0.50 –0.25	≤0.03	0.2 –1.0

Note: Bal. — balance.

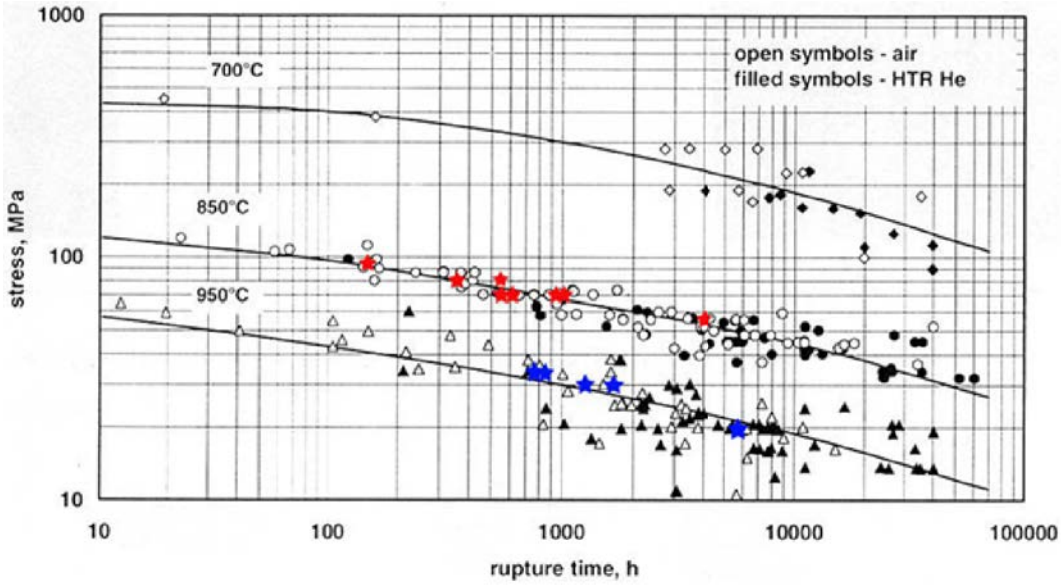

FIG. 139. CEA experimental data with Alloy 230 (red symbols) and Alloy 617 (blue symbols) [36].

No deleterious high temperature gas corrosion effects have been found at temperatures up to 750°C. At higher temperatures, compositions of the impurities with excessively high or very low carbon activities may cause carburization or decarburization, respectively. By keeping the CO partial pressure of the cooling gas helium in a well defined range, unacceptable carburization/decarburization reactions can be avoided. The impurity concentrations in the primary circuit helium are expected to lie within this range without the need for conditioning [351], and no negative influence on mechanical properties is expected.

The most extensively investigated high temperature materials in the German PNP material programme were Alloy 800 (or Incoloy 800: X10NiCrAlTi3220), Alloy 800H and Alloy 617 (or Inconel 617: NiCr22Co12Mo). With regard to materials for splitting tubes, the experimental work was concentrated on the four iron based alloys Incoloy 800H, Incoloy 802, Alloy IN519 and Manaurite 36X. Also considered were the nickel based wrought alloys Inconel 617, Nimonic 86, Hastelloy X and Hastelloy S. Alloy 617 already has a very large database of numerous mechanical properties and creep data measured in air and a helium atmosphere [324].

For the purpose of measuring creep resistance and the 1% time elongation limit of all materials, long term tests were done over 10 000 h in air and HTGR helium, and over 5000 h in product gas of the methane reforming process (Figs 140 and 141). The longest test durations were 34 000 h for Incoloy 800H, ~70 000 h for Alloy 617 and ~100 000 h for Alloy 800. The creep resistance for Alloy 800H after 30 000 h at 850°C was measured to be 16.5 N/mm^2 with an expected value of 11 N/mm^2 after 100 000 h. The respective data for Alloy 617 after 30 000 h at 950°C were 13 and 7 N/mm^2.

Of the investigated candidate materials, Alloy 617 exhibited the highest level of creep strength. There is no influence of the simulated HTGR helium on the 1% creep strain limit or on the creep rupture strength for this material up to about 20 000 h. This observation is valid for all alloys investigated. The rupture elongation of specimens in the simulated HTGR helium atmosphere was in the scatter band of values obtained in air [352]. In the PNP environment, however, Alloy 617 corrodes actively above ~920°C.

An increase of the temperature from 800 to 900°C will result in a reduction of the 100 000 h creep rupture strength by 40–50%. The conceivable use of ceramics-made splitting tubes was, in those days, not deemed feasible due to inappropriate material properties (strength, brittleness, porosity) and the manufacturing and connecting technologies, but was considered an option for the future.

As a result of the PNP materials programme, materials information, design data and analysis methods for the metallic structural components needed in process heat HTGRs have been made available, and the recommendation was given that the heat exchanger tubes of helix type IHX modules could be operated for up to 100 000 h at 950°C.

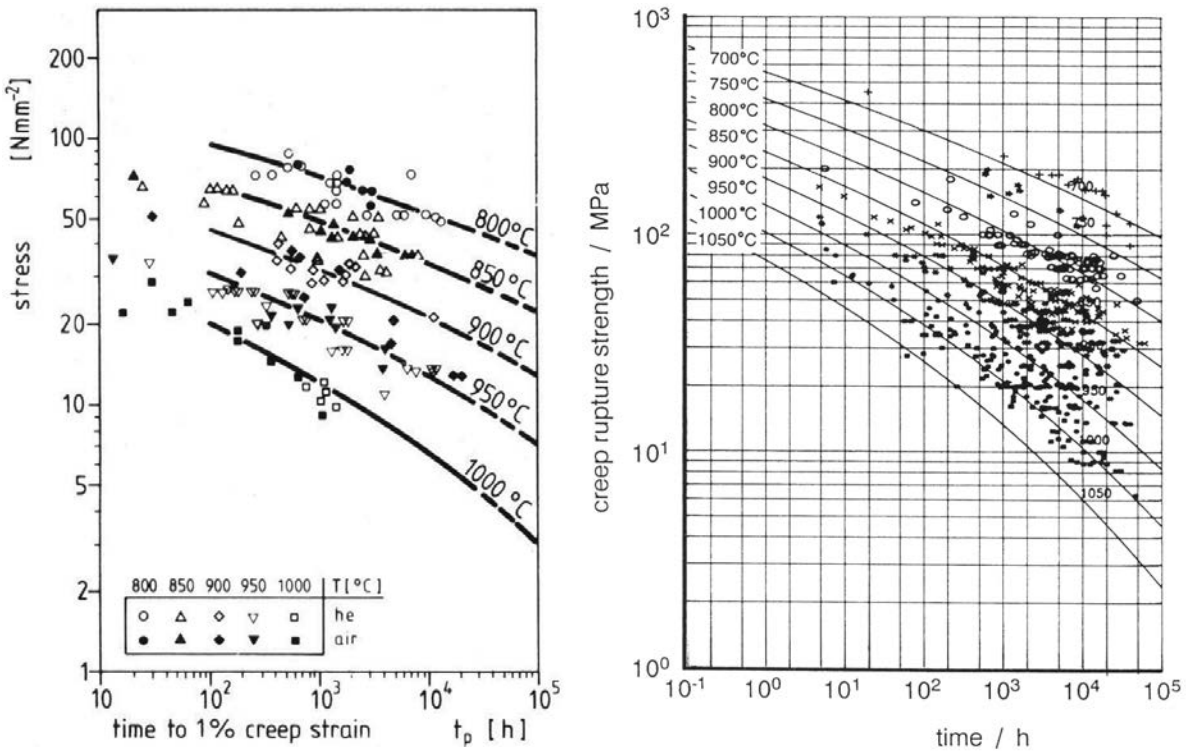

FIG. 140. Creep properties of Inconel 617 [352, 353].

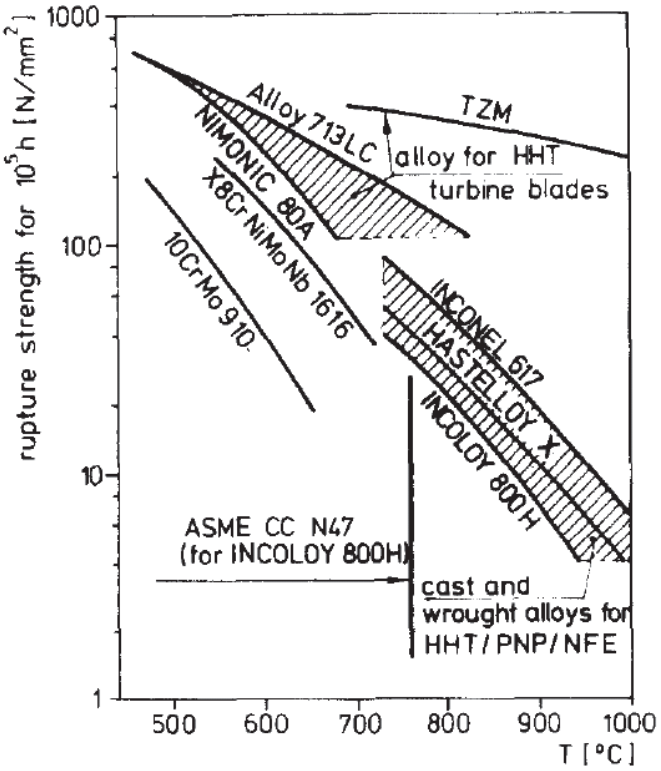

FIG. 141. Creep rupture strength versus temperature for materials under consideration for advanced HTGRs [352].

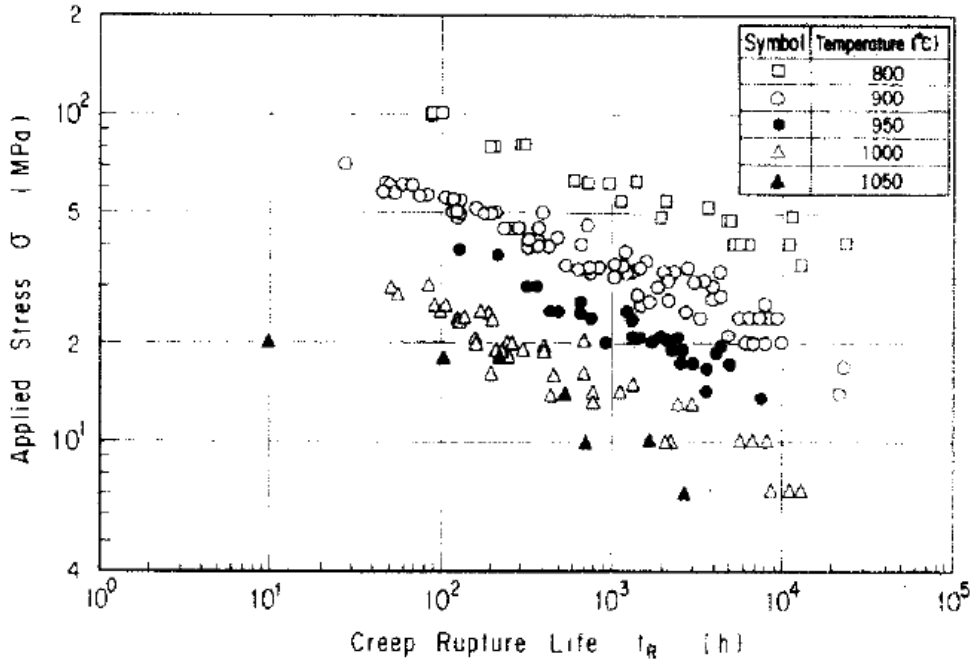

FIG. 142. Creep rupture life for Hastelloy XR [354].

(C) Japan

In the HTTR, a nickel based, heat resistant superalloy, Hastelloy XR, was selected for the IHX, a further development from the nickel based Cr–Mo–Fe superalloy Hastelloy X, which is used for the heat transfer tubes and hot header in the IHX [354]. The difference is an improved compatibility attained by:

— Optimizing the manganese and silicon contents to promote the formation of a stable and adherent $MnCr_2O_4$ layer;
— Lowering the aluminium and titanium contents to minimize internal oxidation and intergranular attack;
— Lowering the cobalt content to reduce radioactive contamination in the primary coolant;
— Optimizing the boron content to improve creep strength.

Figure 142 shows measurements of creep rupture strength at different temperatures, revealing that trends in stress dependence and data scattering are quite similar at 1000°C and at lower temperatures. Therefore Hastelloy XR appears to be stable at or below 1000°C. Hastelloy XR suffers no degradation in creep rupture strength, except in a decarburizing environment [354]. Hastelloy XR exhibits very good stability in a VHTR environment, but it is not so good in terms of creep resistance.

Hastelloy XR-II represents a further refinement on Hastelloy XR, with increased creep rupture strength [355]. Boron, having a significant effect on the creep rupture lifetime of Hastelloy XR, was found to be optimal at contents of 0.004–0.007%. Above this limit, however, the chance of weld cracking became unacceptable.

(D) Republic of Korea

For most metallic internal structures, Alloy 800H or Hastelloy X materials have been verified for higher temperatures. For very high temperatures, ceramics or carbon fibre reinforced carbon composites are considered. The technical problems with those materials are the low machinability due to low toughness, insufficient bonding methodology, the lack of an internationally accepted design code, and the lack of long term and high temperature irradiation data [266].

Westinghouse's Advanced Energy Systems Division performed a screening test to select a structural material for the SO_3 decomposer, and they recommended SiC and some other alloys from the viewpoint of their absolute

weight change. One of the recommended alloys is RA330 which is an austenitic heat and corrosion resisting alloy. According to their experimental results, RA330 has good corrosion resistant properties below 800°C [268].

(E) United States of America

In the USA, technology development has been started to qualify a material for the IHX that can be used as a heat transfer and structural material at 850–950°C and that can sustain a lifetime of up to 60 years in a helium environment. For the NGNP, the prime candidate materials considered are the nickel based Alloy 617 and Alloy 230. Current tests are dedicated to the measurement of creep and creep/fatigue life, the effects of impurities in NGNP helium on alloy microstructure and performance, and the development of a database necessary for the ASTM International/American Society of Mechanical Engineers (ASME) code qualification. The goal of the measurements is to determine differences in alloys for ultimate use in materials selection and establishment of safety margins [356].

From reviews of the existing Alloy 617 data collection, it was found that many of the datasets are incomplete, missing important information such as the material pedigree and original test data curves necessary for studies and modelling [356]. Picking up on the German 100 000 h results for Alloy 617, it was judged that these data, if extrapolated to the nominal 60 year lifetime of a VHTR and including a safety factor, would result in a too low a stress to rupture value. Another major drawback was seen in the wide scatter of the mechanical properties data, probably due to the relatively broad ranges specified by ASTM/ASME for the chemical elements Al, Ti, Co, Mo and others, and due to the differences in the steelmaking techniques and procedures employed by the various manufacturers. For the development of a nuclear grade Alloy 617, a refinement of the manufacturing process and the alloy chemistry within the current specified limits was recommended [357].

Compared with Alloy 617, Alloy 230 is a relatively new alloy with partially improved properties (e.g. yield strength, tensile strength). Although Haynes has provided ORNL with a large number of raw creep curves for Alloy 230 for use in ASME codification requirements, a comprehensive established database is still lacking at present [356].

Ageing experiments were conducted to investigate the dynamic process of microstructure evolution to predict material degradation for long term reactor operation. The ageing tests were undertaken in laboratory air at temperatures of 900 and 1000ºC for up to 3000 h. The ageing tests performed on Alloy 617 and Alloy 230 were aimed at examining the influence on hardness and tensile strength after different ageing periods up to 3000 h. It was observed that hardness increased during the early stages of ageing, but softened after extended ageing times. From corrosion studies at 900 and 1000ºC, it was concluded that Alloy 230 exhibited better corrosion resistance at elevated temperatures than Alloy 617. Penetration of Al_2O_3 causing internal oxidation was found to be more severe in Alloy 617 [358].

6.6.4. Materials for process heat exchangers

6.6.4.1. Materials research

A severe problem is the extreme corrosiveness of the materials in contact with the acids at high temperatures and pressures. Screening tests have been conducted in various institutions for corrosion resistant materials in environments typical of the operation conditions of the S–I cycle. Ceramic and quartz have excellent corrosion resistance, but exhibit manufacturing problems due to their brittleness, particularly if exposed to thermal stress. Quartz cannot be used at pressure above 0.3 MPa due to its fragile characteristics. Also, ceramics can only be applied in a limited pressure range of 0.1–2 MPa [264].

6.6.4.2. International research efforts

(A) European Union

For the concept of a European VHTR coupled to an S–I cycle, as was proposed by the HYTHEC project (see Section 2.3.4.2), a tube and shell type H_2SO_4 decomposer has been suggested. Incoloy was the selected material for the tubes and shell, while SiC was chosen for the high temperature heat exchanging tubes. SiC will also be used for

the heat exchanger tubes in the HI section. The material assumed for the pressure vessels and heat exchanger shells is carbon steel with acid brick liners for the internal shielding [359].

(B) Germany

For the gas generator of a nuclear steam–coal gasification plant, the heat exchanger walls are exposed to hot helium, with its unavoidable corrosive impurities, on the primary side, and to an oxidizing atmosphere (due to steam surplus) with the hot fluidized bed including different gases and carbon ash components on the process side. An additional effect to be considered is erosion by fluidizing carbon particles. Resulting from numerous long term tests with a large number of alloys in a laboratory scale fluidized bed (50–100 g/h of coal throughput) conducted by the Mannesmann Research Institute (MRI), the material AC66 was found to show a favourable corrosion resistance in the presence of the sulphur containing process gas in coal gasification, whereas a corrosion rate of 0.2 mm in 3000 h due to grain boundary oxidation was observed in Alloy 800, too high for an economic lifetime of the immersion heat exchanger [360]. AC66 (X5NiCrCeNb 32 27), a new development by the MRI, is an alloy with high chromium content and additions of cerium and niobium, but no aluminium or titanium.

(C) Japan

The candidate materials for the sulphuric acid decomposition are, for example, Alloy 800 and Hastelloy. Other materials considered are SiSiC, SiC and SX (Fe–Cr–Si). For the hydroiodic acid decomposition section, Hastelloy is foreseen, and for the Bunsen reaction, Ni alloys, ceramics, Zr, Ta and glass lining are favourites.

The severest condition in the HI section is boiling at 400°C and high pressures of 2 MPa, with silicon containing materials showed the highest corrosion resistance.

The main results can be summarized as follows:

— In the gaseous environment of sulphuric acid decomposition, refractory alloys that have been used in conventional chemical plants show good corrosion resistance.
— In the gaseous environment of HI decomposition, a Ni–Cr–Mo–Ta alloy presents good corrosion resistance.
— In the case of the Bunsen reaction section, glass-lining materials show suitable corrosion behaviour.
— In the environment of HI_x distillation, tantalum shows excellent corrosion resistance.
— For the severest environmental condition — the boiling of concentrated H_2SO_4 under high pressure, e.g. 2 MPa — ceramic materials containing silicon as SiSiC, SiC or Si_3N_4 are the only materials that show good corrosion resistance [361].

The decomposition of H_2SO_4 at high temperatures results in a very aggressive chemical environment. The class of candidate materials for the decomposer is based on SiC.

(D) Republic of Korea

For heating of the sulphuric acid preceding the decomposition step, a two stage heating device has been designed, as shown in Fig. 143. A combination of Teflon lined parts, SiC tubes and a Hastelloy C276 outlet plenum are being used to enable a good corrosion resistance to the SO_3 environment [264].

Resulting from immersion coupon corrosion tests with corrosion resistant materials (refractory metal, reactive metal, superalloys and ceramics), only Ta and Nb based refractory metals and ceramic mullite were found to withstand the extremely corrosive environment in the HI section [362]. Severe pitting and dissolution was observed in reactive metal zirconium alloys and in the nickel based superalloy C-276.

(E) United States of America

Regarding the S–I thermochemical cycle, corrosion testing of metals exposed to HI, I_2 and water resulted in the selection of Hastelloys B and C to be suitable for vapour phase exposure to HI and steam, while Ta, Ta–2.5W and Ta–10W should be used for HI_x liquid solutions. Figure 144 shows the material selection for the H_2SO_4 decomposition section [276]. Corrosion testing of ceramic materials exposed to H_2SO_4, SO_2 and water vapour at

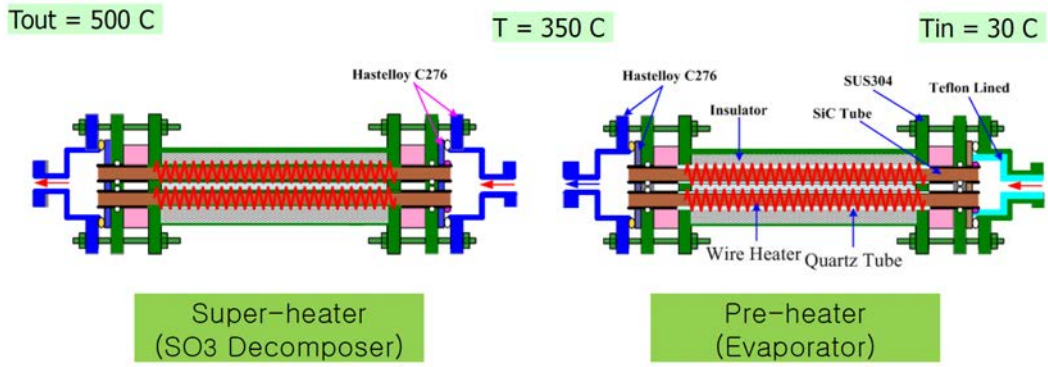

FIG. 143. Two-stage device for heating sulphuric acid [264].

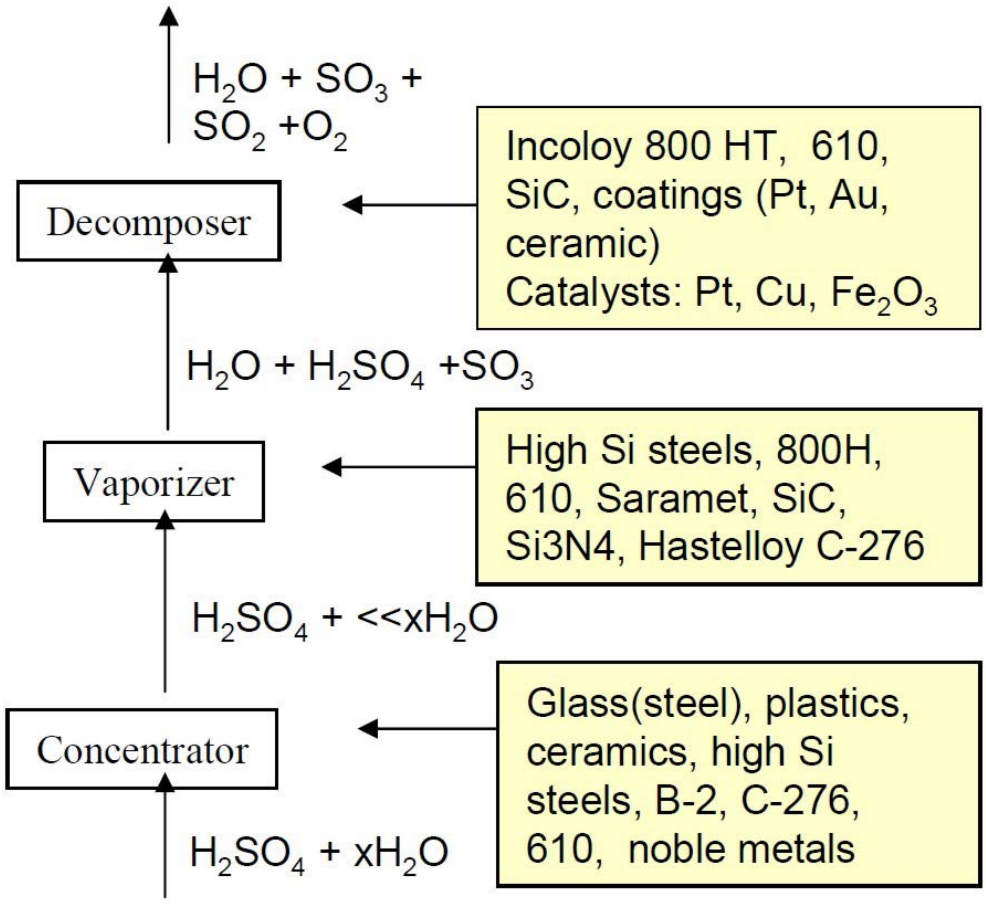

FIG. 144. Material candidates for components in the H_2SO_4 decomposition section.

800ºC showed that SiC, Si_3N_4 and Al_2O_3 all have excellent corrosion resistance to these chemicals. Exposure of metallic samples to FLiNaK molten salt at 800ºC showed that nickel coated Incoloy 800H and pure nickel resisted corrosion.

Multiple heat exchanger designs for a high temperature sulphuric acid decomposer were analysed using thermohydraulic codes and finite element analysis, including the Sandia bayonet design, the Ceramatec ceramic compact decomposer design and a traditional tubular reactor design [363].

7. SAFETY OF NUCLEAR HYDROGEN PRODUCTION

7.1. INTEGRATION OF NUCLEAR–CHEMICAL PLANTS

The principal requirement of a nuclear plant is that radioactivity is completely retained inside the plant, even in extreme accidents, with no severe consequences outside the fence. Following the severe nuclear accidents at Three Mile Island (partial core melt) and Chernobyl (completely destroyed plant), the search for new solutions in nuclear technology began. Potential solutions can be approached from different directions. Concepts pursued include those where a core melt is not necessarily excluded, but its probability is reduced with improved decay heat removal systems. Others try to limit the consequences to the reactor building by means of a core catcher and cooling device. Finally, there are concepts where melting of the core is excluded by nature, characterized by low power densities and passive decay heat removal in connection with the preservation of the barriers against fission product release.

Fulfilling certain principles implies concrete safety related requirements, from which general safety concepts can be derived (Fig. 145). The development of an acceptable level of safety, however, is a dynamic process. Its further and steady improvement should be a top priority of research efforts at any time [364].

For nuclear process heat plants, which are typically linked with a chemical factory, e.g. for hydrogen production, the safety concept has to comprise the particular aspects given by the close connection of the two plants and their potential interactions. It will consider general features such as a non-integrated design (i.e. heat generation and heat conversion in separate vessels), underground placement of the nuclear island and inertion of the containment/confinement. But it will also include special features such as filters and shutdown and isolation/separation systems to disconnect the chemical from the nuclear plant in the case of major operation problems on the nuclear or chemical side. The IHX component is one of the principal barriers which will be exposed to different temperature and stress levels under normal operation and accident conditions. Reducing the stress level can be achieved by keeping pressure differences between the primary and secondary circuits small. Secondary ducts within the boundary of the reactor building will be enclosed by additional guide pipes.

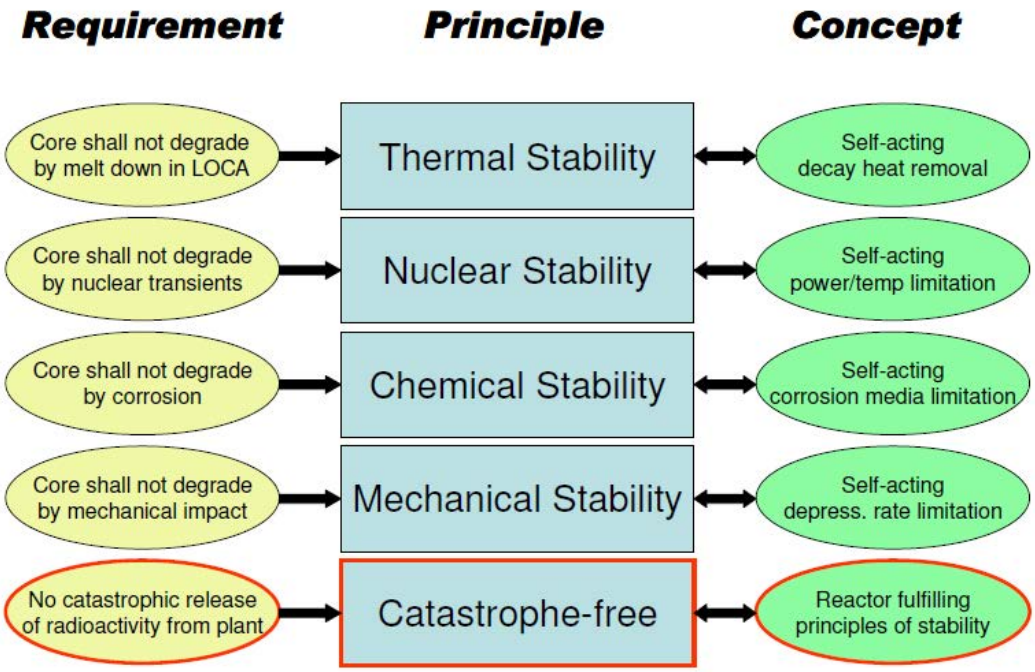

FIG. 145. General safety requirements [364].

A first phenomena identification and ranking table (PIRT) study has been recently conducted in the USA [311] to address the safety challenges of a coupled HTGR and hydrogen production facility and to evaluate the importance of effects on equipment or people as primary consequences, with a focus on the nuclear plant. A fundamental difference in the safety design philosophy is seen between chemical and nuclear plants, which is given by the nature of the hazardous materials (radioactive, toxic, combustible) in the plant. While nuclear reactors are designed to contain fuel and generated radioactive materials inside the reactor building under all circumstances, most chemical plants, which handle combustibles, are built without a containment structure, in order to prevent the accumulation of explosive concentrations [365].

7.2. BASIC CONSIDERATIONS FOR A HYDROGEN SYSTEM SAFETY

7.2.1. Safe design of the nuclear reactor for process heat applications

The primary goal is the safe use of hydrogen and the control of the risks associated with its use. Inherent in all hydrogen designs are:

— Consideration of the conditions in which the system is operated;
— Fail-safe operation that accounts for the potential modes of failure;
— Long term plans that cover the operational life of the system.

The potential hazards from the hydrogen plant are determined by the input and output of the chemical plant and by the process chemistry [365]. Processes always include the handling of hydrogen. Depending on the production method, oxygen as a by-product is also involved. Steam reforming of methane requires the handling of large inventories of natural gas feedstock and synthesis gas product. In thermochemical cycles, hazardous chemicals are used internally and recycled within the process. Under accident conditions these chemicals may be released to the environment. Depending upon the temperature and pressure, each of these chemicals can be a liquid, a mist or a gas. The primary hazards associated with hydrogen systems are combustion, pressure, low temperature, hydrogen embrittlement and exposure. Quantities greater than 7500 m^3 under standard conditions are usually located outside or in specially designed structures. Storage vessels that contain liquid hydrogen use special insulation or vacuum jacketing.

The most common mechanical components for controlling the flow of hydrogen are valves, check valves and regulators. These may be manual or remotely controlled using electric or pneumatic actuators, which must be of an explosion proof design. Check valves are used to prevent unwanted backflow. Regulators control the system pressure. Controls also include fluid sensors such as pressure gauges, flow meters, liquid level indicators and the control system.

Vessels and piping that confine or may confine hydrogen should be protected against over-pressurization with a pressure relief system. The relief system typically consists of relief valves and rupture disks, usually used in parallel as a fail-safe path to direct overly pressurized hydrogen to the vent system. Emergency venting at rates sufficiently high for gas cloud formation can be placed such that ignition can be excluded. Outside the hydrogen containing system, the control system may monitor for gas or fire. Hydrogen detectors are typically placed above a likely leak point where hydrogen may accumulate, and at the intake of ventilation ducts. Infrared cameras can image heat over a wide field of view. Ultraviolet detection is used to specifically detect hydrogen flame. Hydrogen systems may also use catalytic converters and getters to remove unwanted or excess hydrogen. Filters may be used to remove impurities from hydrogen in the system.

In a risk assessment, a systematic approach is made to identify risk factors and potential hazards, to determine frequencies of abnormal event scenarios, to quantify consequences and to evaluate mitigation measures to control or minimize the risk. Risk management measures include efficient leak/fire detection, isolation and shutdown systems, efficient natural ventilation, grounding, safety distances and fire walls.

7.2.2. Identification of hazard sources

Safety items can be categorized into several classes. The items associated with the accidental release of radioactive materials and core damage from thermal turbulence are categorized into the class with the largest hazards. In relation to these items, the system must be designed with high reliability and redundancy to avoid the loss of safety functions. On the other hand, the items associated with continuous normal operation are categorized into the class with lowest hazards, for which such a high level of reliability and redundancy is not required.

The hydrogen production system connected to a nuclear plant will most probably not be designed as a nuclear grade system. Therefore, particular safety items other than the 'conventional' safety features will not be provided in the chemical part of the combined system. There are three areas of concern associated with combined nuclear–chemical plants:

— The hydrogen production system is the final heat sink for the nuclear reactor.
— Flammable substances are present in the system.
— The product hydrogen is handled outside the nuclear plant.

The potential hazardous events in connection with the hydrogen production system are:

— Tritium transportation from the core to the product hydrogen and methanol;
— Thermal turbulence induced by problems in the chemical system;
— Fire and explosion of flammable mixtures with the process gases;
— Release of toxic material.

A safety related issue is the operability of the production process system during a nuclear reactor scram. According to the actual safety regulations, the ultimate heat sink of a nuclear power plant is limited to water and/or air, and cannot be electricity or chemical energy as the result of a conversion process. Therefore the production process system is not designed to take over safety functions for the nuclear system; these are exclusively left to the reactor cooling system.

In case of a scram of the HTTR, the power output immediately falls to such a low level that the reactor safely shuts down and remains in a sub-critical state. Concerning the steam reforming system, the abrupt cut in heat input is usually followed by an instantaneous disconnection of the feedstock supply and filling of the steam reforming loop with nitrogen to prevent carbon deposition on the catalyst. Also, the large heat capacity of the catalyst allows for a reduced rate of temperature decrease [207].

7.2.3. Hazards in electrolysers

The risks of (alkali) electrolysis plants are given by [366]:

— A potential explosion of the hydrogen contained in the system;
— A leakage of electrolyte following overpressure;
— A failure of the cooling water system possibly connected with a mixing of H_2 and O_2;
— Corrosion of parts of components with potential release and mixing of H_2 and O_2 and/or electrolyte liquid;
— Mud formation in the gas piping and subsequent change of operational behaviour (e.g. increased operation temperature leading to enhanced corrosion, sudden pressure changes, abnormal heat exchanges, blockage of circuits);
— Damaging of hydrogen containing pipelines.

Initiating events are typically given by, for example, component failure due to corrosion, a sudden disconnection from electricity supply where downstream components may not be shut down right in time, or human error (supply faults, confusion of cell polarity, etc.).

7.2.4. Hazards in thermochemical cycles

The hazardous potential in thermochemical cycles is given by the H_2 and O_2 produced and by the presence of hazardous chemical compounds in the cycle processes. Process intermediates include large amounts of sulphur dioxide, sulphur trioxide and sulphuric acid. Sodium hydroxide (NaOH) is used as a scrubbing agent. All chemicals, interim products and products resulting from side reactions or improper conditions are mainly characterized by their corrosiveness and toxicity. Corrosiveness is particularly enhanced by the given high operation temperatures and pressures. Accumulation of impurities will affect the heat release process in the reactor components and may lead to overheating or overpressurization of the reactor with exothermic reactions [19]. Also, in the O_2 production section, the high operating temperature of 450–530°C is an important safety issue [367]. To ensure the safety and health of workers and to protect the environment, a safety concept must concentrate on minimizing the quantities released in the case of inadvertent pipe ruptures, system spills or leaks.

Multiple step thermochemical cycles produce hydrogen and oxygen in separate reactions, which can be realized at different locations, thus isolating the H_2 containing systems and reducing the chance for explosions. Lower temperature thermochemical cycles operate at temperatures lower than the auto-ignition temperature of hydrogen. In the case of an air ingress, no clean operation can be achieved. In the case of loss of integrity of either hydrogen storage or any other hydrogen handling subsystem, the hydrogen generation reactor must be shut down immediately. This will have an influence on all parts of the whole system.

Probabilistic risk assessment (PRA) methods are able to analyse plant designs and identify weaknesses of the system. Qualitative analyses try to find event sequences which can cause system failure, while quantitative analyses calculate the probabilities of a system failure. Facilities with nuclear hydrogen production will need specific approaches and detailed analysis.

The consequences of accident scenarios can be investigated in more detail if precise information on the process streams and energy flows is available. Due to the different chemical processes applicable, the involved quantities of the hazardous materials may vary. Chemical dispersion events are difficult to contain.

Since the hydrogen handling section does not need the high process temperature, it can be located at the farther end of the chemical plant, away from the nuclear plant. Subsequent handling of the H_2 such as compression, storage or, if appropriate, liquefaction, can be easily done at sufficient safety distances.

HyS is a process in which 50 wt% of sulphuric acid from the electrolysers, which contains dissolved SO_2, is stripped of the sulphur dioxide, and further concentrates the sulphuric acid to 75 wt%. The sulphuric acid is then decomposed to steam, oxygen and sulphur dioxide at high pressure and high temperature. The product and stripped SO_2 is dissolved in water and sent as an anolyte to the electrolyser. Water is supplied to the cathode where it is separated into hydrogen and oxygen ions, converting the SO_2 water solution into sulphuric acid.

The HyS process involves many hazardous chemicals that are commonly used in chemical processing and manufacturing, and the process products are either explosive or are oxidizers. The hazards to be considered are:

— Loss of containment of highly corrosive acid;
— Loss of containment of toxic gas;
— Loss of containment of flammable gas;
— Enhanced flammability of materials in pure oxygen;
— Loss of containment of high pressure helium.

7.2.5. Hazardous materials in the chemical plant

Depending on the accident scenario, a chemical plant may release flammable or corrosive or toxic species. Gaseous species may form heavier than air gas clouds in the environment, enhancing the risk of damage to people and equipment. The physical and chemical properties of hydrogen and its potential hazards are described in detail in the Appendix.

7.2.5.1. Oxygen

The hazards associated with the presence of pure oxygen are considered even more serious than those when handling hydrogen. Oxygen is colourless, odourless and tasteless. Unlike air, compressed air, nitrogen and other

inert gases, oxygen is very reactive. Many materials that are usually considered non-combustible (such as carbon and stainless steels, cast iron, aluminium, zinc and Teflon) can burn in the presence of pure oxygen. Also, oxygen makes normal fuels burn much more quickly and easily, potentially causing fires to burn out of control and risk severe injury to personnel and total system loss. Organic materials may even react explosively with oxygen. Furthermore, oxygen accelerates degradation of most materials. Oxygen is an effective oxidant and will form oxides with all other elements except helium, neon, argon and krypton. The risk of ignition and sustained combustion within oxygen systems is considered to be an inherent hazard. The presence of an oxygen enriched atmosphere cannot be easily detected by the human senses.

Future large scale production of H_2 from water splitting processes will require the handling of huge masses of oxygen, for which there is still a lack of experience [365]. Standard methods for oxygen system design, materials selection, oxygen cleaning, and oxygen compatibility testing of materials and components need to be further developed. Oxygen pipelines require extreme cleanliness of the wall surfaces to avoid oxygen fire.

There is a concern about the possible impacts of long term locally elevated levels of oxygen from the continuous release of oxygen from the hydrogen production facility. Oxygen, like other gases in the atmosphere, can be considered as a pollutant if the concentrations are significantly different from normal atmospheric levels. Oxygen permeates many materials, and increases in the oxygen content of materials could significantly change their characteristics in a fire and some of their other properties. There are no regulatory or industrial standards for the continuous release of large quantities of oxygen, because there never has been a need for such a standard.

7.2.5.2. Carbon monoxide

Carbon monoxide is a colourless, tasteless, odourless, but highly toxic and flammable gas and requires special precautions in handling and storage. Its toxicity in humans and animals is caused by the extraordinary affinity for haemoglobin (210–240 times greater than that of oxygen), which is responsible for the O_2 transport in blood. If inhaled for a sufficient period of time, it results in unconsciousness and death at higher levels. An atmosphere containing 0.2% CO is lethal after about two hours. It is a chemical asphyxiant with a recommended threshold limit of 0.01 % in air.

CO is not corrosive and not an irritant; it is rapidly oxidized to form CO_2. CO is slightly lighter than air at ambient conditions. CO is an unwanted by-product of all oxygen-undersaturated combustion processes involving carbon. At high pressures, CO reacts with steel to produce small quantities of iron carbonyl.

A pure (dry) CO–air mixture does not burn at standard temperature and pressure, but in the presence of small amounts of H_2O or H_2, it can significantly enhance the rate of CO oxidation reactions. CO burns in air with a non-luminous, bluish flame. The flammability range is 12.5–74 vol% in air and 15–94 vol% in oxygen; it widens with increasing temperatures. A CO mixture with air does not detonate. In a mixture with oxygen, the detonation range is 38–90 vol%. The maximum detonation velocity in oxygen is around 2800 m/s.

7.2.5.3. Carbon dioxide

Carbon dioxide is an inert, colourless and odourless gas. It is non-toxic at physiological concentrations, becomes narcotic above 5% and results in unconsciousness at levels of 7–10% after a few minutes; the recommended threshold limit for an eight hour day is 0.5%. CO_2 is universally present in fires. It is also present at an approximately 5% concentration in exhaled air. CO_2 is heavier than air and therefore tends to flow into low lying areas.

7.2.5.4. Sulphur dioxide

Sulphur dioxide (SO_2) is very toxic and may be fatal if inhaled. Vapours are corrosive and cause extreme irritation. Fire will produce irritating, corrosive and/or toxic gases. The gas may burn, but will not ignite readily. It may react violently with water. Containers may explode when heated (ruptured cylinders may rocket). Vapours from liquefied gas are initially heavier than air and spread along the ground.

7.2.5.5. Sulphuric acid

Sulphuric acid, H_2SO_4, is a non-combustible, strong mineral acid. Pure sulphuric acid is an oily clear liquid which does not burn but which may decompose upon heating to produce corrosive and/or toxic fumes. It has a high electrical conductivity. In spite of the viscosity of the acid, the effective conductivities of the $H_3SO_4^+$ and HSO_4^- ions are high, making sulphuric acid a good conductor. It is also an excellent solvent for many reactions. Sulphuric acid is soluble in water at all concentrations. Its hydration reaction is highly exothermic. Containers may explode when heated or if contaminated with water. The H_2SO_4 vapours are toxic by inhalation, ingestion or contact and may cause severe injury, burns or death. Burns from sulphuric acid are potentially more serious, as there is additional tissue damage due to dehydration and release from the reaction with water. The dispersal of acid aerosols and gaseous sulphur dioxide is an additional hazard of fires involving sulphuric acid.

Sulphuric acid reacts with most metals via a single displacement reaction to produce hydrogen gas and the metal sulphate. Contact of sulphuric acid with metal drums may cause the release of flammable and explosive hydrogen gas. Hot concentrated acid reacts with tin, zinc and copper to produce a salt, water and sulphur dioxide, whereas the dilute acid reacts with metals high in the reactivity series (such as Zn) to produce a salt and hydrogen. Therefore storage drums should be coated with acid resistant material. Lead and tungsten are resistant to sulphuric acid. Also, explosion-proof electrical equipment and fittings should be used wherever sulphuric acid is handled or stored.

In a number of hydrogen production processes, sulphuric acid is a gas at high temperature and pressure and presents a significant risk of becoming a major potential accident source term where its release would form a plume or fine aerosol.

7.2.5.6. Hydroiodic acid

Hydroiodic acid or hydrogen iodide is a clear to yellow liquid with a characteristic pungent sulphide-like odour. The boiling point is 127°C. It is a non-combustible substance that does not burn but that may decompose upon heating to produce corrosive and/or toxic fumes (they are toxic by inhalation, ingestion or skin contact, likely to cause severe injury or death). Contact with most common metals may liberate hydrogen gas. Containers may explode when heated.

7.3. TRITIUM CONTAMINATION

Tritium balancing is an important aspect of the planning, operation and decommissioning of any nuclear plant. Tritium is a weak beta emitter (18 keV) with a half-life of 12.3 years and is generally present in the form of tritiated water (HTO). It is radiologically relevant by incorporation with a biological half-life of 12 d for ‘free’ tritium and up to 400 d for T in organic compounds. Less radiologically relevant is the gas HT or tritiated methane (CH_3T).

For HTGRs, what is most important is the capability of tritium to pass through metallic walls, penetrating the water/steam and/or product gas cycle. Its extreme mobility requires effective retention mechanisms in a process heat plant. Specific concerns refer to the:

— Tritium permeation into the secondary circuit for product contamination;
— Accumulation of tritium in the purification system for waste removal issue;
(a) Tritium inventory of spent fuel for disposal issue.

7.3.1. Tritium sources in the primary circuit

There are various sources of tritium in the reactor core of an HTGR during normal operation:

— Ternary fission product [^{235}U (n,f) T] with a fission yield of 1.2×10^{-4} (UO_2 fuel) and, to a lesser extent, from the ternary fission product ^6He (fission yield ~3×10^{-5}) which decays immediately to ^6Li. Ternary fission accounts for ~50% of total tritium production.

— Activation reactions of traces of lithium [^{6}Li (n,α) T] and boron [^{10}B (n,2α) T] in the graphite components and control rods (and burnable poison) and from other reactions [^{10}B (n,α) ^{7}Li] → [^{7}Li (n,nα) T], [^{12}C (n,α) ^{9}Be] → [^{9}Be (n,α) ^{6}He]. These reactions account for ~35% of the total tritium production.
— Activation of the ^{3}He fraction in the helium coolant (share of 1.38×10^{-6} in natural composition produced from air) and the ^{3}He as the decay product of tritium [^{3}He (n,p) T]. A permanent source of ^{3}He is given by the introduction of make-up helium to compensate for the coolant leakage ,estimated to be ~0.1%/d (for the THTR-300). Helium-3 activation accounts for ~15% of the total tritium production.

The tritium produced in a fission process in the HTGR will be completely retained within intact TRISO coated fuel particles. Only a small fraction originating from fuel particles with a broken coating or from uranium contamination of the core graphite is expected to escape into the coolant. On the other hand, tritium originating from boron is usually assumed to be completely released into the coolant. Tritium produced from lithium impurities in the graphite can rapidly diffuse through the graphite components into the coolant. The expected value of lithium concentration in the fuel element matrix A3-3 (used for the THTR-300 fuel) was found to be 10 wt-ppb; for A3-27, it was even down to less than 1 ppb, much lower than the design value fixed at 50 ppb to cover uncertainties and different graphite grades.

Tritium production in the first year of operation of an HTGR is higher by 70% compared with the equilibrium value due to the not yet burned up ^{6}Li in the graphite and ^{3}He in the coolant, as was estimated for a 2250 MW(th) plant [368]. In the equilibrium core, there will be no further contribution from the lithium in reflector graphite. Lithium from the fuel element matrix will only come from the fresh fuel. The amounts of tritium from ^{3}He depend on the helium leakage rate and the supply of new coolant.

The principal forms in which tritium exists in the primary circuit are HT, CH_3T and HTO due to isotope exchange reactions. Each hydrogen atom in a potential final product could act as an exchange partner for a tritium atom. The specific tritium activity is therefore proportional to the number of H atoms per molecule and inversely proportional to the molecular weight. HT is the dominant part and mainly created by the reaction of water impurities with graphite. From AVR experience with 950°C operation, an H_2:CH_4 ratio of about 100:1 can be expected. At lower outlet temperatures, the ratio will become smaller (~10:1 for 750°C).

In a nuclear heat exchanger (steam reformer, steam generator), tritium can migrate through tube walls directly into product gas, and vice versa, H_2 from the secondary side to the core. Furthermore, the steam generated on the secondary side and used in the reforming process contains tritiated water (HTO) that may find its way to the product gas. In the case of an indirect cycle plant where process steam would be delivered through a steam converter, another effective barrier against tritium transfer is given.

In connection with an HTSE process, gaseous HTO may escape the system with the H_2 product gas, while the remaining liquid HTO accumulates in the circuit and partially leaves the system with the drain water. In H_2 production plants based on thermochemical cycles, tritium that permeates the tertiary circuit can react with hydrogen containing process chemicals by isotopic exchange reactions to form, e.g. in the S–I cycle, tritiated compounds like $HTSO_4$ and TI.

Before hydrogen or any other product from a nuclear process will be usable as a normal commodity, it must have a tritium contamination below the tolerated limits specified by the national legislation. Therefore one safety requirement is to correspondingly reduce tritium penetration of the products. In this case, the required safety items are not directly related to reactor safety and thus can be classified at the lowest safety level.

7.3.2. Tritium removal

7.3.2.1. Radioactive decay

The decay product of tritium is ^{3}He, which will result in the production of new tritium. Therefore this sink term is often conservatively neglected in the modelling of tritium behaviour.

7.3.2.2. Helium purification system

Most impurities in the helium coolant, including tritium, are effectively removed from the primary system by the gas purification system, through which a partial stream of the coolant is routed. The degree of removal depends

on how much of the coolant is bypassed through the purification system. The system is characterized by a gas purification constant:

$$\alpha_{ps} = \frac{\dot{m}_{ps}}{m_{He}}$$

where α can reach a value of 0.05 h^{-1}.

With regard to tritium, purification is practically 100%. It is done in two steps:

— Oxidation bypassing a CuO-based catalyst bed (in AVR: Pt; in Peach Bottom: gettering by Ti) where HT reacts at 180–240°C to HTO which is captured in a molecular sieve (higher temperatures up to 800°C are needed to efficiently burn the methane);
— Low temperature absorption at 20–30°C.

The captured tritium will go to the waste disposal.

7.3.2.3. Adsorption

An important sink for tritium in the HTGR is the graphite structures where the tritium is bound by adsorption, chemisorption and eventually diffusion into the inside of the graphite. The tritium might later, with decreasing production, be desorbed again. Complex processes are taking place in the adsorption of tritium on graphite and its influence by the presence of hydrogen. Experimental evidence of this sorption effect was given by measurements of tritium in the Peach Bottom reflector, where the tritium contents exceeded the amount expected to be generated in the reflector by a factor of four.

The sorption effect is increased with increasing neutron fluence. From the graphite, it can be released again by desorption at higher temperatures (>800°C) or by exchange reaction with non-radioactive hydrogen. Essential for the buffer effect of the graphite for tritium is its solubility in the graphite lattice as a result of the high excess H_2 versus HT in the coolant, whose concentrations are directly linked. For the AVR, the partial pressure ratio was estimated to be ~10^5.

The equilibrium was experimentally found to be reached within several hours, which is a short period of time compared with the reactor operating time. It can be described by a Langmuir isotherm [369]:

$$A = A_m \frac{bp}{1 - bp}$$

where

A is the number of adsorbed tritium molecules per gram of graphite;
A_m is the saturation coverage of graphite surface, = 2.8×10^{18} T molecules per gram of graphite at 1000°C;
b is the adsorption coefficient, = 7.53 $mbar^{-1}$ at 1000°C;
p is the T partial pressure (mbar).

An intermediate circuit purified by a sweep gas flow serves as an additional boundary between the primary and secondary circuits. If oxygen or steam is added to the sweep gas, part of the tritium could be bound as HTO, which does not permeate according to the exchange reaction:

$$H_2O + HT \rightarrow HTO + H_2$$

But the effectiveness of the conversion to tritiated water in helium at low concentrations still needs to be proven [370].

7.3.2.4. Leakage

Another possible path for a transition of radionuclides into the product gas is by leakage in the heat exchangers. A leakage of radioactivity from the primary to the secondary circuit requires a pressure drop from the primary toward the secondary loop, in contrast to the plant's condition during normal operation. A measure to prevent a major risk is the installation of gas supervising systems to trigger the disconnection of the product gas lines from the grid.

7.3.3. Tritium/hydrogen permeation

7.3.3.1. Transport mechanisms

Under the operating conditions of a process heat HTGR with its high coolant exit temperatures, hydrogen and tritium are highly mobile, resulting in permeation through the walls of heat exchanging components. Tritium can be transported from the primary side through the metal walls of heat exchanger tubes to the process side by permeation, and can eventually contaminate the products hydrogen or methanol.

The permeation process through a metallic wall is thermally activated. It begins with the dissociation of the diatomic gases H_2, HT at T_2 at the surface. Transport through the wall is as atoms until recombination takes place at the exit side. All single processes (adsorption, penetration, diffusion, desorption) strongly depend on material and surface effects as well as on temperature and pressure conditions. The permeation rate Φ for tritium through a metal can be described by a combination of Fick's diffusion law $\Phi = D(c_1 - c_2)/d$) and Sieverts' solubility law $c = L\sqrt{p}$ [371]:

$$\Phi_{T2} = K_{T2} \times \frac{F}{d} \times \left[\sqrt{p_{T2}(1)} - \sqrt{p_{T2}(2)}\right]$$

$$= K_{T2} \times \frac{F}{d} \times \sqrt{p_{T2}(1)} \quad \text{for} \quad p(2) << P(1)$$

where K = D·L is the permeation coefficient:

$$K = D_0 L_0 \times \exp\left\{-\left(Q_D + Q_L\right)/\left(RT\right)\right\} = K_0 \times \exp\left\{-Q/\left(RT\right)\right\}$$

where

D is the diffusion coefficient;
L is the solubility;
F is the permeation surface;
d is the (effective) wall thickness of the permeation barrier;
p(1) is the partial pressure at entrance side;
p(2) is the partial pressure at exit.

The above equation is valid for concentration equilibrium between the gas phase and surface, and shows that the driving force for the permeation process is the partial pressure difference between the two gas spaces. Measurements reveal a relationship of

$\Phi \sim p^n$ with $0.5 \leq n \leq 1$ for $p \leq 0.1$ MPa, and $n = 1$ for $p > 0.1$ MPa.

In the opposite direction, hydrogen on the process side can permeate through the tube walls into the primary circuit, causing corrosion reaction with the graphite structures. Additionally, by transport of carbon in helium circuits, carbon deposition surfaces of high temperature alloys could result in changes of material properties. Therefore measurements of hydrogen permeation rates have been carried out depending on wall temperature, type

of material, wall thickness and partial pressure of hydrogen. The influence of steam is especially important, because a layer of oxide is formed on the surfaces of the metallic walls on the process side.

For hydrogen permeation from the process side, there will always be the linear dependency due to $p_{H2} > 0.1$ MPa. Countercurrent permeation of tritium (to the outside) and of hydrogen (to the inside) was observed to have no influence upon each other.

Considering the reaction $0.5\ T_2 + 0.5\ H_2 \leftrightarrow HT$ and the law of mass action:

$$k_{eq}^2 = \frac{p_{T2} \times p_{H2}}{p_{HT}^2}$$

the permeation of tritium through a tube wall is given by [368]:

$$\Phi_{T2} = K_{T2} \times \frac{F}{d} \times k_{eq} \times \left[\frac{p_{HT}(1)}{\sqrt{p_{H2}(1)}} - \frac{p_{HT}(2)}{\sqrt{p_{H2}(2)}} \right]$$

where k_{eq} is the equilibrium constant, its value is ≈ 0.5 in the primary circuit.

Assuming that excess hydrogen is available in the primary circuit and there is a negligible amount of tritium on the secondary side, the total permeation rate is proportional to the square root of the hydrogen partial pressure, and the permeation rate related to tritium is correspondingly reduced according to the partial pressure ratio p_{HT}:p_{H2} [368]. Since the permeation rate is inversely proportional to the square root of the atomic mass, the permeation of tritium will be lower by a factor of $3^{-1/2}$ compared with hydrogen.

7.3.3.2. Growth of protective oxide layers

In nuclear process heat plants, gas composition at the heat exchanger walls is such that the metals typically react with the in situ formation of an oxide layer. While permeability is high for bright surfaces, oxide layers on the heat exchanger surfaces were found to significantly reduce the tritium (and hydrogen) permeation rates through the metal walls in the temperature range of interest (T >600°C). The barrier effect depends on a variety of parameters, among which are process gas compositions, pressure, temperature and material. Oxide layer thickness, growth rate, quality and behaviour under changing loads can only be investigated in experiments.

Chromium oxide (Cr_2O_3) is responsible for the oxide formation on austenitic and nickel based metals, while magnetite (Fe_3O_4) is responsible for the oxide formation on ferritic steels. The protective layer formation takes place mainly on the process side in the highly oxidizing atmosphere, while on the helium side, the forming layer may remain porous and instable. Rather than the layer thickness, what is important for large reduction factors is dense and homogeneous coverage. Under steam reforming conditions, an oxide layer will rapidly develop on the tube surface. A drawback of protective oxide layers is their poor stability against temperature cycling. The controlled addition of water vapour may enhance the formation or repair of oxide layers. Pre-oxidation of the metals could also be an option.

The permeation rates of tritium through the walls of high temperature heat exchangers have been measured as a function of temperature, the type of materials and the process conditions of the steam reformer, steam generator and IHX. Selective filter systems to take up tritium from helium circuits have been developed, consisting of hydride forming materials such as Ti, Ce or Zr, or cerium mixed metals.

A protective coating could also help reduce permeation of tritium. Figure 146 presents the permeability of various metals to tritium in the 400–700°C temperature range. The metal coating as a permeation barrier can principally be applied to the outside or the inside of a tube. Such a coating solution, however, still needs to be developed and validated in terms of the coating material and the coating process, with an emphasis on ensuring the homogeneity of the coating. Furthermore, coating integrity must be ensured over the IHX lifetime and after exposure to thermomechanical cyclic loadings. Candidate coating materials are SiC or Y-stabilized ZrO_2. Potential coating processes are the ion beam mixing technology and the atmospheric plasma thermal spray technology.

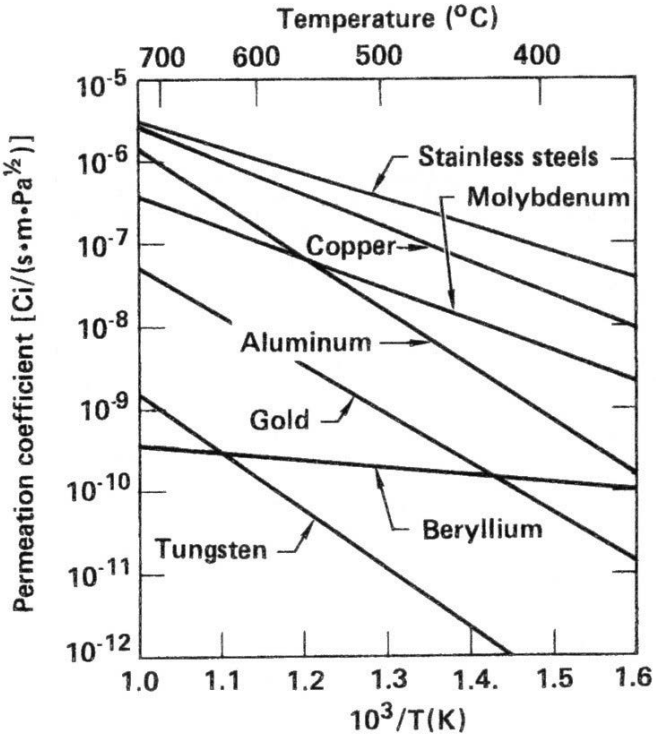

FIG. 146. Permeability of various metals to tritium [370].

7.3.4. Tritium studies in Germany

7.3.4.1. Permeation of hydrogen through metal walls

At the Research Centre Jülich, the first permeation experiments were conducted at the beginning of the 1970s focusing on steam generator materials and operation conditions of a two cycle HTGR. With regard to a layout of the purification system, carbon deposition on the gas (primary) side, corrosion reactions on both the gas side and the steam side, and the permeation of hydrogen generated on the steam side by metal corrosion were studied. Decreasing hydrogen permeation rates were observed starting at a high initial value and later reaching an equilibrium value about two orders of magnitude lower. The transient behaviour was explained with the oxide layer formation on the ferritic steel surfaces. Peaks and other anomalies observed in the permeation profile are presumably the result of an oxide layer not completely free of cracks and pores [372].

For process heat plants studied within the PNP project in Germany, experimental investigations were made on the hydrogen permeation process through reformer tube walls made of high temperature alloys. The experimental device AUWARM (Facility for the Investigation of Hydrogen Permeation through Reformer Materials) (Fig. 147) was operated from 1976 and allowed long term (1000–3000 h) testing at temperatures up to 1000°C and pressures up to 3.2 MPa. Short term analyses were used for pre-selection of materials. Permeation rates were measured as a function of various parameters such as wall temperature, gas composition, material, oxide layer and transient temperatures [373].

Results have shown that in situ oxide layers show a large inhibition of permeation at temperatures above 650°C. Decreasing permeation rates following temperature increases demonstrated the accelerated growth of the oxide layer. In particular, the behaviour of Cr_2O_3 was identified as being decisive for the permeation resistance [374]. Still, the uncertainty is relatively large at lower temperatures, also when looking at measurements from operated HTGRs.

In Fig. 148, a typical permeation test run in AUWARM under nuclear coal gasification conditions is given where the time dependent hydrogen permeation flux was measured on two tube specimens made of Incoloy 800H [375]. The temperature curve and the times where the specimen was exposed to the process gas are also given in the figure. The experiment was made in the pressure range from 0.5 to l MPa and the temperature range from 450 to 950°C. The strong reduction in the permeation rate is due to the growth of the protective oxide layer. Furthermore,

FIG. 147. Test facility AUWARM of FZJ for measurements of hydrogen permeation.

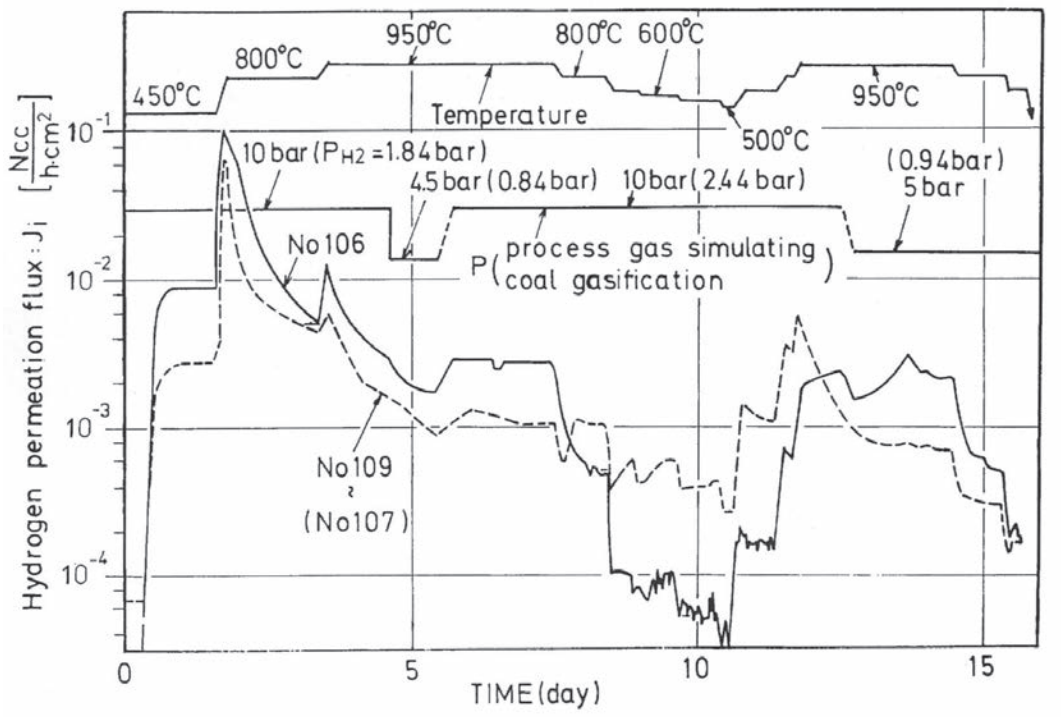

FIG. 148. Hydrogen permeation flux measurements for two Incoloy 800H samples [375]. Testing gas composition — representing that for steam–coal gasification — was: 8.8–13% CO, 4.3–6.5% CO_2, 0.9–1.05% CH_4, 18–27% H_2, and 53–69% H_2O.

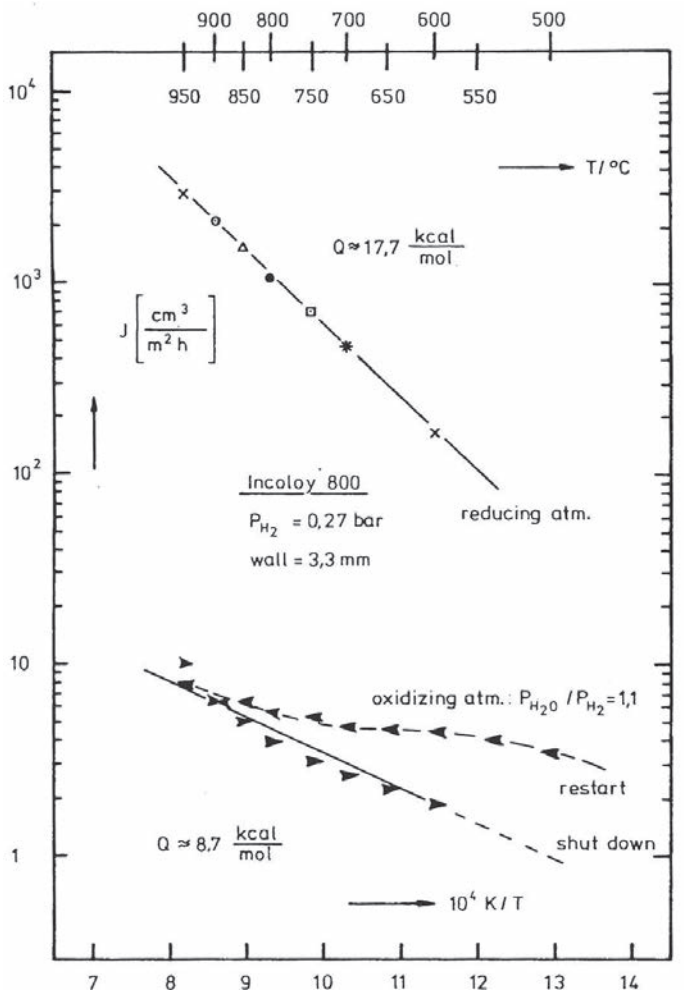

FIG. 149. Arrhenius diagram of H_2 permeation for clean and oxidized Alloy 800 surfaces [378].

impairment of this protection layer can be observed, concluded from the increasing permeation flux following the decrease of temperature, and also its healing behaviour. In contrast, temperature peaks of ±50°C were observed not to have a significant effect on the oxide layer [374]. The effects of temperature and partial pressure on hydrogen permeation through Incoloy 800 have been examined experimentally, confirming the expected tendency of increasing permeation rates with increasing H_2 partial pressures and temperatures [376].

Defining an inhibition factor, H, as the ratio of permeation flow through a bright material over that of an oxidized material, factors of around 2000 were measured for high temperature alloys at 900°C (Fig. 149). Particularly good results were achieved for Hastelloy X, where the development of a homogeneous, dense chromium oxide layer with a chromium–manganese spinel coating was observed. Factors are lower (~100) for ferritic steels [371]. For the nuclear steam–coal gasification semi-technical plant (see Section 4.2), a reduction factor of up to 520 was measured [377]. From experience with the AVR steam generator made of ferritic steel, a factor of ~50 was derived. This value could be raised to 600 by doping the feedwater with oxygen. This process, however, may have a deteriorating effect on austenitic materials. The lower limit of 20 was eventually fixed as a design value for ferritic steels [371].

For the hydrogen transportation process, permeation coefficients have been derived from the experiments as a function of temperature for a number of metals. With regard to the PNP reactor design, the Arrhenius relationship of K_{H2} for high temperature alloys was set with the constants [371]:

Lower limit: $K_{o,H2} = 3.2\times10^{-2}$ (cm^3 H_2/(cm·s·$bar^{1/2}$)) Q = 74.1 kJ/mol

Upper limit: $K_{o,H2} = 7.0\times10^{-2}$ (cm^3 H_2/(cm·s·$bar^{1/2}$)) Q = 66.2 kJ/mol

and with the experimentally confirmed relationship

$$\frac{K_{o,T2}}{K_{o,H2}} = \frac{1}{\sqrt{3}}$$

As a typical result, around 50 mL/(m^2·h) of hydrogen was measured at 900°C for typical steam reformer applications. These quantities of hydrogen could be easily removed by the gas purification plant. The stability of oxide layers during transients and other loads have to be considered and may influence the data. The above measurements are conservatively covered by the relationships to be used in design calculations [371].

7.3.4.2. Permeation of tritium through metal walls

Prediction of tritium permeation rates remained difficult due to the extreme difference of the respective partial pressures, with ~1.5 MPa for hydrogen on the secondary side and ~10^{-4} Pa of tritium in the primary coolant. Therefore the experimental facility TRIPERM was designed within the PNP tritium investigation programme to conduct continuous measurements of tritium permeation and, at the same time, hydrogen permeation. Due to licensing problems with the handling of tritium, deuterium was used instead as a model gas in the experimental programme. The facility was constructed such that two separate gas circuits were formed, representing the primary and secondary circuits. The atmospheres in both circuits could be independently analysed and checked for concentration changes. Permeation coefficients derived from the experimental data are given in Fig. 150 for hydrogen and deuterium through Incoloy 802. They are compared with the calculated tritium permeation coefficient concluded from these measurements [379]. A comparison of tritium permeation coefficients for different metals with different surface conditions is shown in Fig. 151 [371].

7.3.4.3. Experience with tritium in AVR and THTR-300

After the water ingress incident in 1978, 290 000 GBq (7900 Ci) of tritium was found in the AVR reactor, corresponding to the release from a ten year operation period. Furthermore, injection tests in the AVR have shown that T concentrations in the coolant were observed to be decreasing five times faster than would have been expected from simple operation of the purification system [368].

In order to investigate the effect of chemisorption on fuel element matrix graphite surfaces, an A3 graphite sphere was exposed to a helium atmosphere containing tritium at a concentration of 0.56 GBq/m^3 and heated at 600°C over 100 h. The resulting tritium concentration profile inside the sphere was measured in a range between ~10^5 Bq/g (sphere surface) and ~4×10^4 Bq/g (sphere centre) [376].

Much higher concentration levels will be reached after longer reactor operation. The level was found to be two orders of magnitude higher in an AVR sphere after approximately six years at full power [380].

Initial operation of the THTR-300 has shown that tritium content in the coolant was less than in the AVR, but was not yet in an equilibrium state. Load changes during reactor operation are expected to result in increased tritium in the steam turbine cycle due to damage to the protecting oxide layer following the mechanical impact. Tritium measurements in the THTR primary coolant are shown in Fig. 152 revealing the direct correlation with the hydrogen containing impurities (H_2, H_2O, CH_4, NH_3) in the helium [381].

Tritium concentrations in the steam circuit were generally observed to be low. The measured concentrations in the steam circuits of AVR and THTR-300 were in the range of 10^4–10^5 Bq/kg.

7.3.4.4. Modelling of tritium behaviour

Analogous to the US code TRITCO (see Section 7.3.8.3), the computer model TRIK was developed to calculate tritium behaviour in a pebble bed reactor. The physical mechanisms considered in the model can be seen in Fig. 153, which also shows the mass flows across the boundary of the helium coolant system. The integral tritium behaviour during reactor operation can be assessed, if the complex fuel sphere flow with multiple core passages is taken into account to provide the burnup state and thus tritium production rates. The coupled process of pebble flow and burnup was assumed to be temporally decoupled [369].

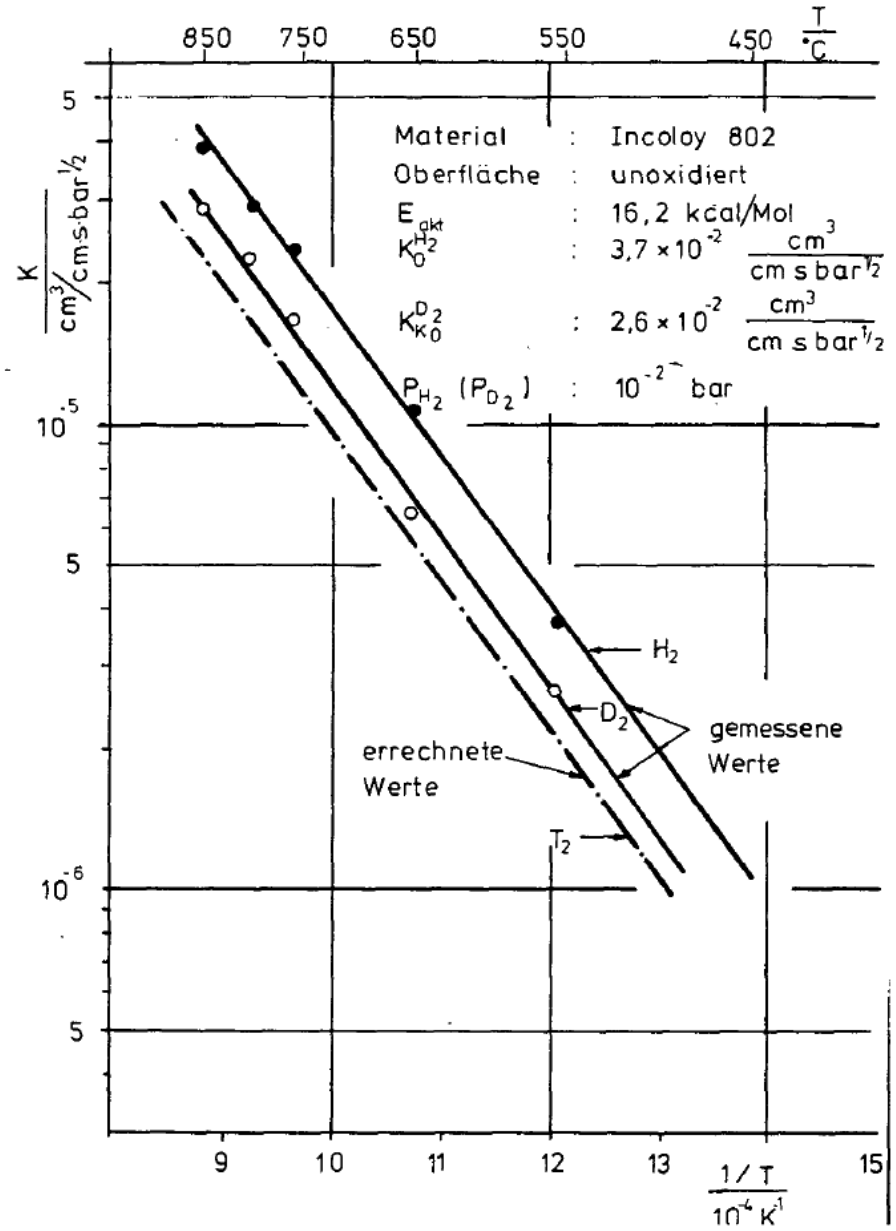

FIG. 150. Arrhenius diagram for the permeation coefficients of H_2, D_2 (both measured), and T_2 (calculated) through bright Incoloy 802 [379].

Calculation results [369] for the conditions and status of AVR as of mid-1975 have shown that the input for lithium impurities in the graphite is a highly sensitive parameter. Tritium contribution from boron is relatively small (compared with the US block type reactors), since excess reactivity which has to be compensated by absorber spheres is low. More uncertainties are introduced due to the complex transport and release behaviour of tritium in graphite, which require further efforts for verification and validation of the corresponding modelling approach (Table 44).

For the example of the 170 MW(th) process heat HTR-Modul, the reactor internal tritium production and release into the helium coolant was assessed in a conservative way, as is summarized in Table 45 [382].

A certain tritium load in the products steam or fuel gas is already given, independent of the nuclear operation. Feedwater contamination (originating from former atomic weapons testing) contributes up to 26 Bq/kg to the process steam and up to 56 Bq/kg to the product gases. Using fossil feedstock adds another 37 Bq/kg of natural T contamination. For nuclear coal gasification, the tritium load of the product gas was estimated to be 185 Bq/kg for

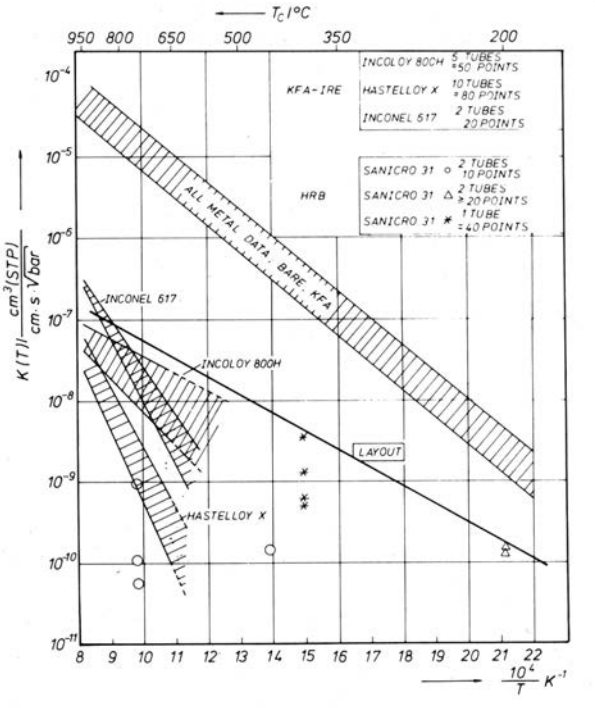

FIG. 151. Arrhenius diagram of effective tritium permeation for clean and oxidized surfaces [371].

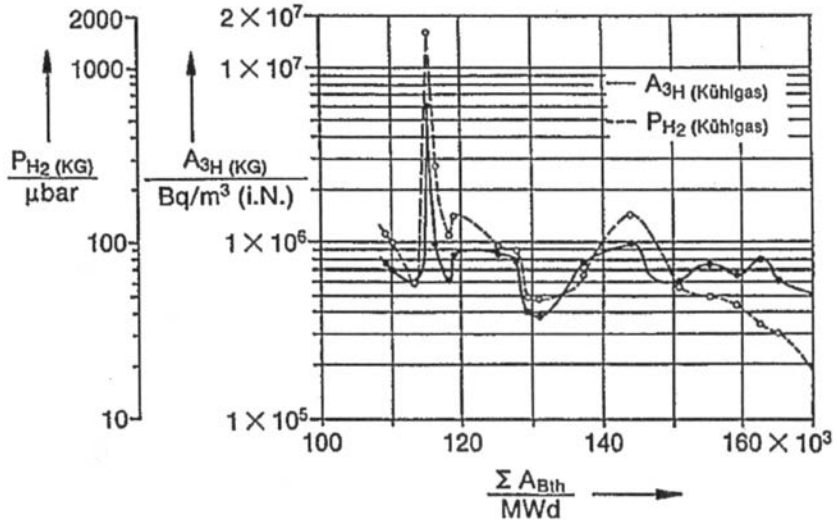

FIG. 152. Correlation between tritium and hydrogen containing impurities in THTR-300 coolant [381].

hydrogasification and 444 Bq/kg for steam–coal gasification. Under the pessimistic assumption of no protective oxide layer, these figures increase to 1850 and 2590 Bq/kg, respectively, but with further potential for reduction given by operational measures. All of the above figures apply to SNG and H_2, but not steam [377].

According to the German Preventive Radiation Protection Ordinance, neither licensing nor announcement is required for the use of fossil products refined by nuclear process heat whose tritium content does not exceed 5000 Bq/kg. This special case is the exception to the rule where for any fabricated product the specific radioactivity limit is lower by a factor of ten compared with the above figure (i.e. 500 Bq/kg) [383]. The background for this special rule resulting from discussions in the context of the PNP project is the fact that, depending on the origin of

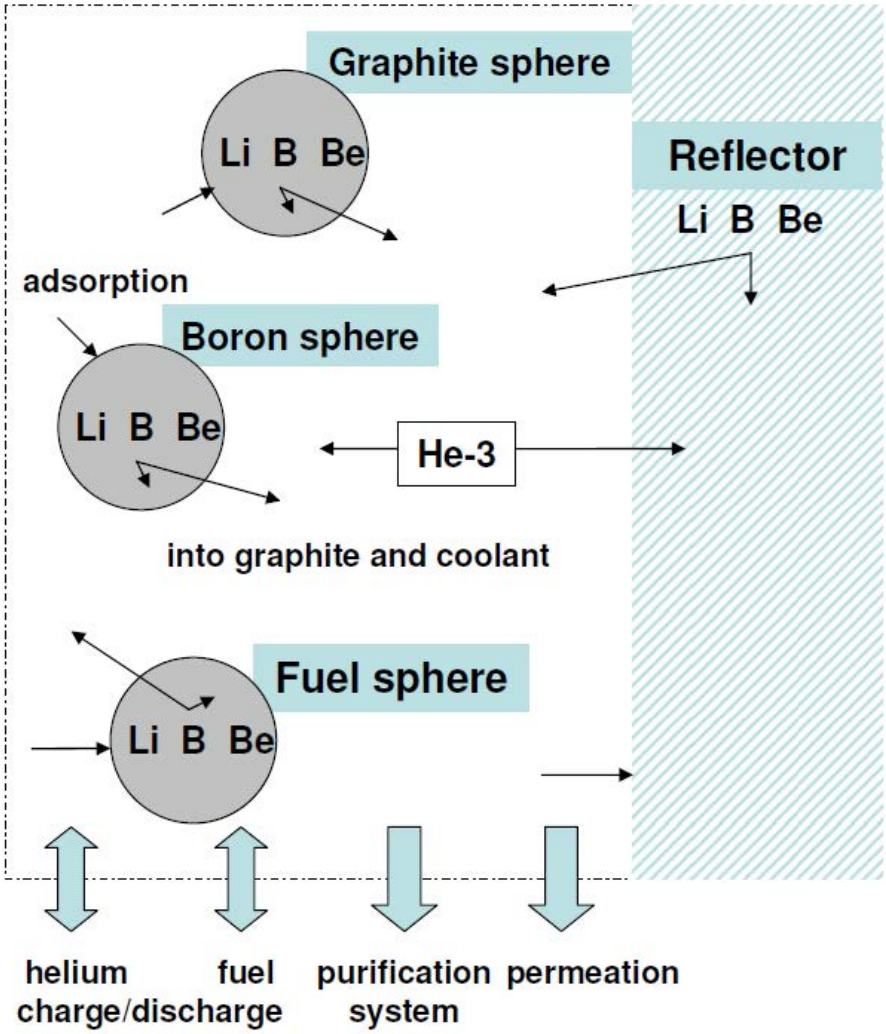

FIG. 153. Physical mechanisms of tritium behavior considered in the TRIC code [369].

TABLE 44. CALCULATED AND MEASURED SPECIFIC TRITIUM ACTIVITIES IN THE AVR IN 1975 [369]

Tritium in:	Calculated	Measured
Graphite spheres (Bq/g)	7 500 000	6 600 000–7 400 000
Helium coolant (Bq/cm^3)	10	4–400
Life steam (Bq/g)	160	150–260

the feed natural gas, the natural activity content would often have already reached the free limits given by the law. In the new German Preventive Radiation Protection Ordinance issued in 2001, the free limit for tritium has been raised to an activity of 1 TBq or, alternatively, a specific activity of 1 GBq/g [384].

As a result of the PNP-project, it was found that hydrogen permeation for steam reformer application represents a problem that can be solved. For processes using an IHX the permeated quantities of hydrogen can be reduced even more. As long as the heat exchangers remain intact, even under conservative assumptions, the

TABLE 45. TRITIUM PRODUCTION AND RELEASE FOR THE 170 MW(th) PROCESS HEAT HTR-MODUL [382]

Tritium source	Tritium production rate (10^3 Bq/s) (%)		Tritium release rate into coolant (10^3 Bq/s) (%)	
	Initial phase	Equilibrium	Initial phase	Equilibrium
Fission, direct	895 (14)	1057 (43)	89 (4)	126 (12)
Fission, ^{6}He	0 (0)	184 (8)		
^{6}Li, particle	838 (14)	313 (13)		
^{6}Li, matrix	1256 (20)	449 (18)	1341 (63)	481 (47)
^{6}Li, reflector	2613 (42)	81 (31)	68 (3)	47 (5)
^{10}B, absorber	6 (0)	6 (0)	6 (0)	6 (0)
^{3}He primary	626 (10)	366 (15)	626 (30)	366 (36)
Total	6234 (100)	2456 (100)	2130 (100)	1025 (100)

expected radioactivity on the secondary side remains small compared with the tritium concentration by permeation. Results were assumed to be tolerable in the PNP project in comparison with other allowed levels of radioactive contamination. With regard to the 5 Bq/g limit (according to the former Radiation Act of 1989), it would not be exceeded in any of the operational states in the PNP-500 [330].

7.3.5. Tritium studies in Japan

7.3.5.1. Permeation of tritium through metal walls

For hydrogen produced with nuclear energy in Japan, the target value of tritium contents is 11.8 Bq/g of H_2. This upper limit value would lead to an exposure rate of <10 mSv/a for the consumer, which is lower than the exposure rate by natural radioactivity by a factor of 100 [385].

For the case of the HTTR in combination with a steam reforming system, the flow paths of the tritium (HT) and hydrogen (H_2) have been identified as shown in Fig. 154. Tritium removal from the helium coolant is only partially effective, since in the HTTR, the purification systems are installed in the bypass loop and their flow rates are selected based on the concentrations of other impurities.

Preliminary calculations were performed to determine tritium concentration at steady state for the HTTR steam reforming system. These results indicate that the combination of the self-grown oxide layer effect and a reasonable flow rate through the helium purification systems is sufficiently effective to restrict the tritium concentration in the product gas to an acceptable level.

The permeability of IHX materials was investigated at JAEA in a component test facility using hydrogen and deuterium (instead of tritium). Results have been acquired in a small scale apparatus using test pipes made of the high temperature alloys Hastelloy X and Hastelloy XR, the designated materials for IHX heat exchanger tubes and steam reformer pipes. Test tube dimensions were 1000 mm in length, 31.8 mm outer diameter, and 3.5 mm wall thickness. Test conditions were tube temperatures of 600–850°C and H_2 partial pressures of 0.1–4 kPa in helium gas. The flow rate was 0.1 NL/min of the mixture gas. The test series also confirmed the phenomenon of oxide layer formation, which reduces the permeation rates [387].

In another experimental series, the effect of counter-permeation of deuterium (to simulate tritium) and hydrogen, i.e. the influence on permeation if hydrogen is present at the outside, was investigated. The test tube here consisted of Inconel 600 with an inner diameter of 7 mm and a thickness of 1.2 mm. Mixtures of argon with hydrogen and deuterium were flowed at constant rate and constant pressure through the test pipe and the outer so-called measurement tube (inner diameter: 50 mm). With deuterium flowing inside and hydrogen outside the test tube, it was found that for low partial pressures of deuterium <100 Pa, its permeation rate to the outside is decreasing if the hydrogen partial pressure is >10 kPa. This is due to the fact that the dissolved H atoms are saturated on the surface. For the real system of HTTR combined with steam–methane reforming, hydrogen partial

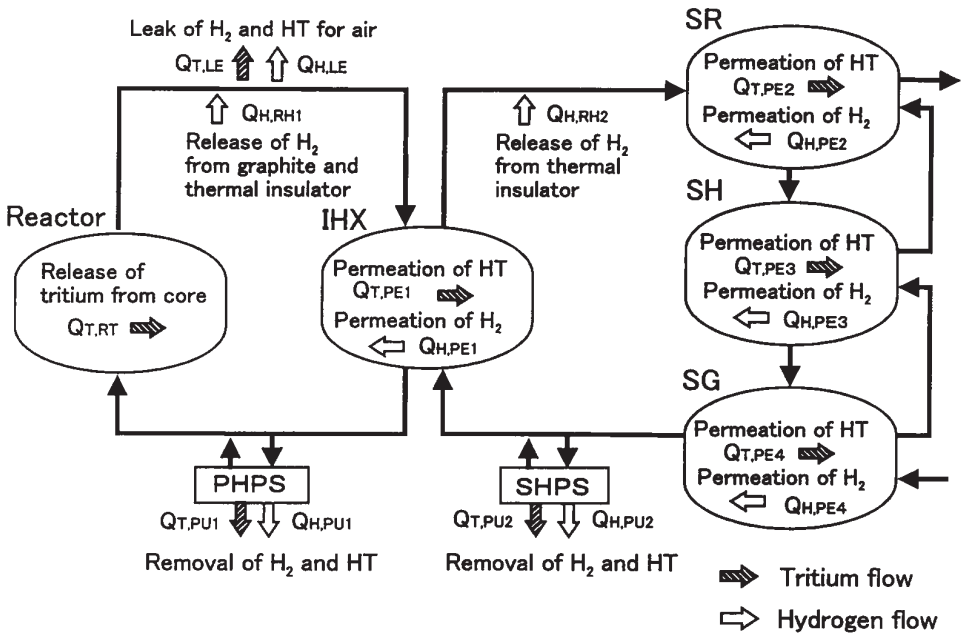

FIG. 154. Tritium (HT) and hydrogen balance in HTGR hydrogen production system [386].

pressures in the catalyst pipes will be about 2 MPa. Therefore a comparatively low amount of tritium is expected to be transferred from the primary circuit to the hydrogen production system [388].

The reduction of permeability at the presence of an oxide film layer was again confirmed, with the observed factor of 100–1000 enhancing with time. The ratio of hydrogen to deuterium permeability was measured to be 1.32 at 670°C; it decreases with increasing temperatures.

In another Japanese study, the oxidation effect of Alloy 800 and Alloy 617 on hydrogen permeation was investigated. A reduction of the permeation rates by two orders of magnitude with hardly changed activation energy was measured when using an oxidizing H_2–CO gas mixture [390].

Assuming an Arrhenius type relationship for the permeability and taking the data of activation energy and pre-exponential factor for high temperature alloys from the literature, the hydrogen permeability through Hastelloy XR was assessed as shown in Fig. 155. The new data indicate a somewhat lower permeability compared with previous work, presumably due to formation of an oxide layer on the IHX tube surfaces [389].

7.3.5.2. Experience from HTTR

First experience has been gained from the HTTR operation at 950°C with regard to hydrogen behaviour in the core [389]. In this case, the sources of hydrogen are, in the primary circuit, the oxidation processes of moisture in the graphitic core and, in the secondary circuit, water liberated from insulation material. Since the latter produced a higher water concentration, the H_2 transport was actually from the secondary to the primary circuit. Figure 156 shows the H_2 and H_2O behaviour during the first 950°C operation period of the HTTR.

One of the objectives of the 50 d high temperature operation test at the HTTR conducted in 2010 was to analyse the tritium behaviour. Results are not yet available. Figure 157 shows a schematic of the device to measure tritium activity in coolant samples at the HTTR.

7.3.5.3. Modelling of tritium behaviour

For the GTHTR-300C reactor, any tritium not captured in the secondary loop purification system will permeate through the process heat exchanger walls of the SO_3 decomposer or HI decomposer and mix with the hydrogen containing chemical compounds of the S–I process and may accumulate up to a certain equilibrium, while the tritium bound in the product hydrogen will be removed from the system [302].

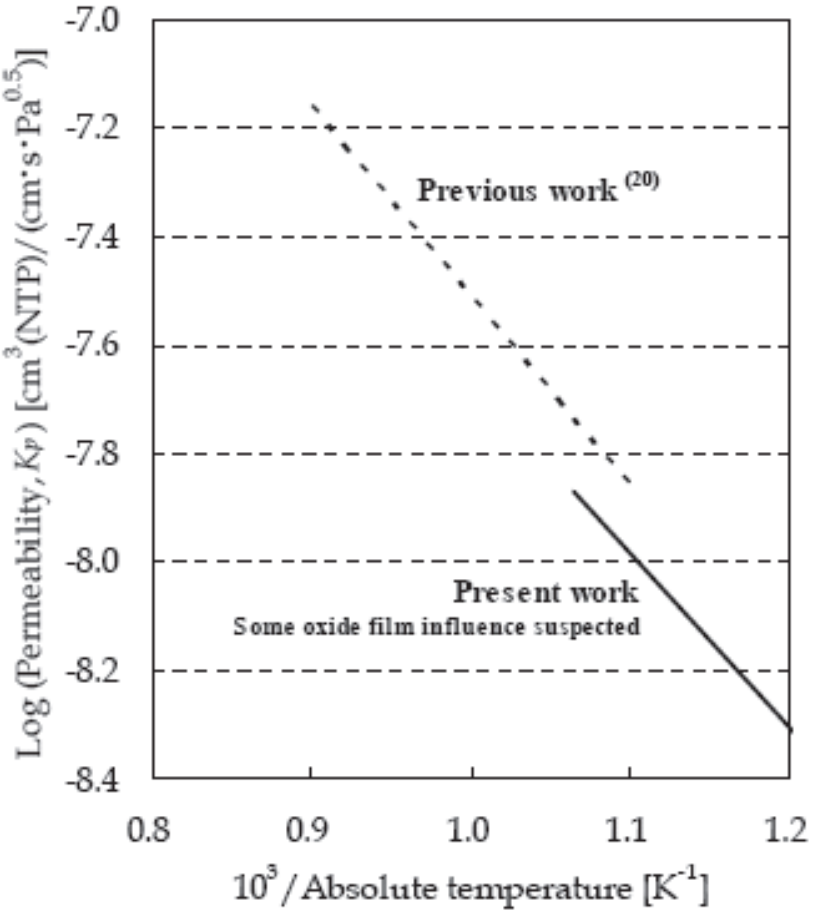

FIG. 155. Previous work [387] on hydrogen permeation in Hastelloy XR compared with newer results [389].

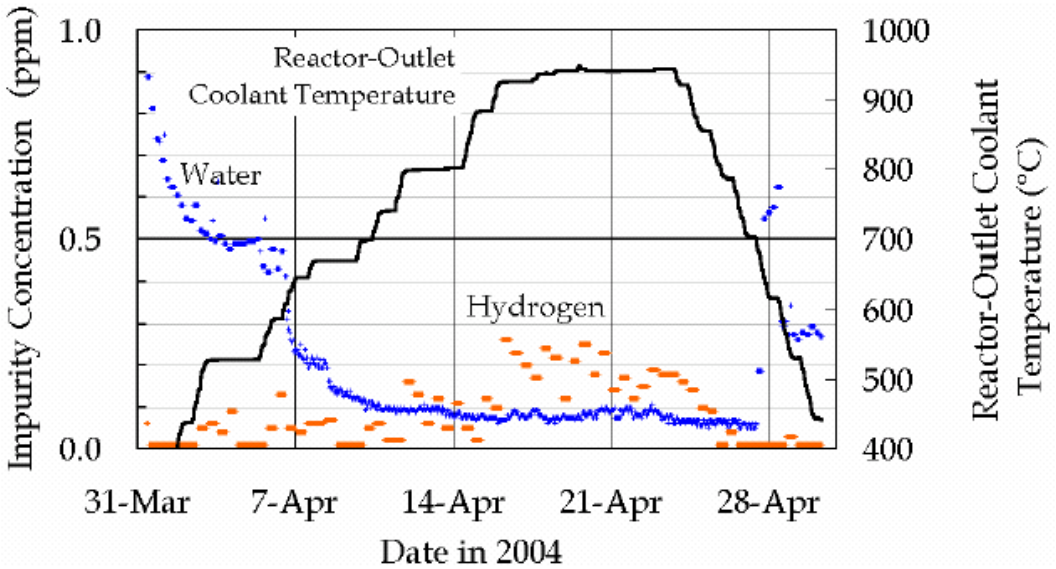

FIG. 156. Hydrogen and water behaviour in the primary cooling system during the first operation of HTTR at 950°C [389].

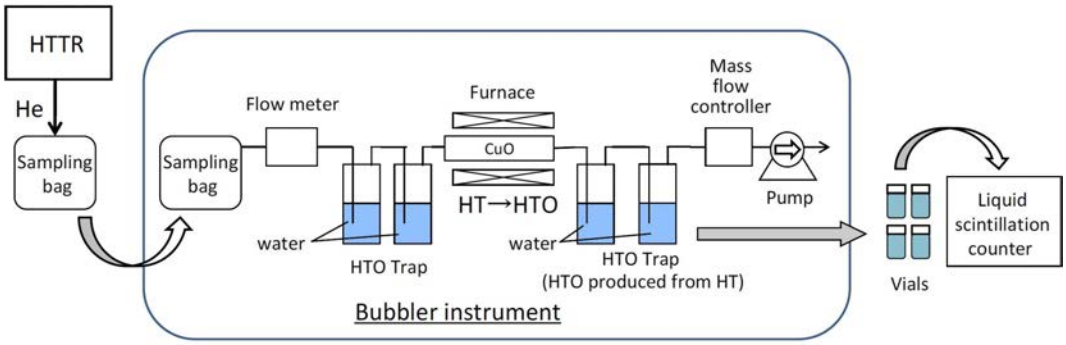

FIG. 157. Tritium measurement at HTTR, from [391].

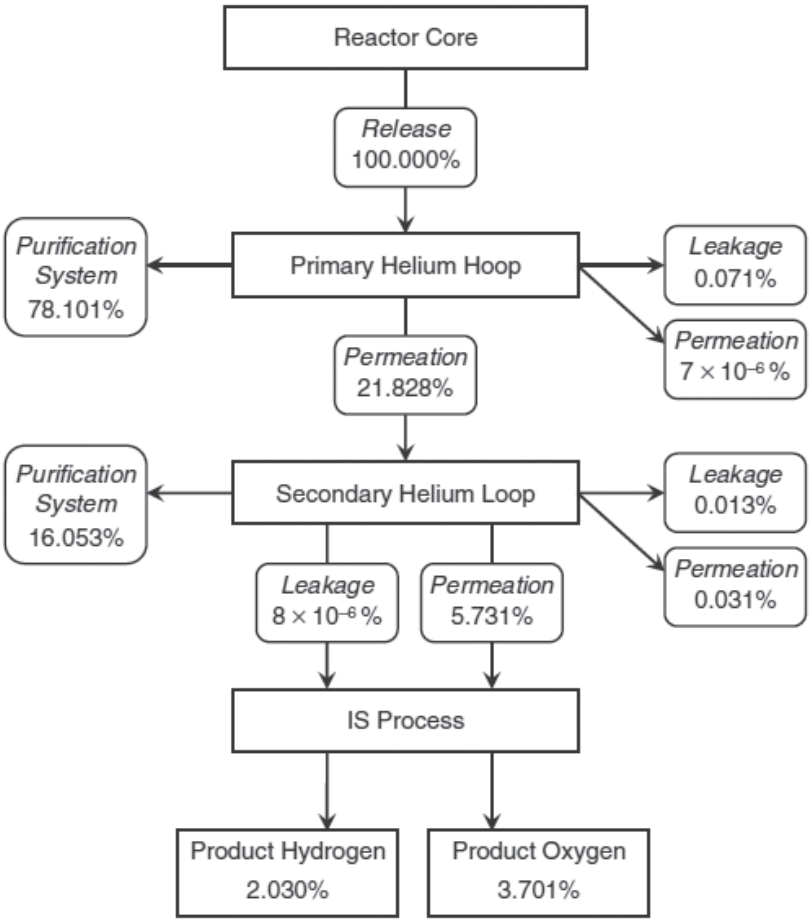

FIG. 158. Assessment of tritium release for the GTHTR300C with S–I cycle based on conservative assumptions [302].

THYTAN, a dynamic simulation model, has been developed at JAEA to calculate tritium mass balance for the GTHTR300C with S–I cycle, taking into account the different tritium birth, transport and release/removal processes [302]. Figure 158 shows the results of the assessment under conservative conditions, which means application of permeation rates valid for the metallic materials without protective oxide layer.

7.3.6. Tritium studies in the Republic of Korea

At KAERI, an improved version of the TRITGO code was used, which also included tritium transport via the process heat exchanger into the S–I cycle. Based on a 600 MW(th) VHTR system, the tritium contamination level was predicted to be 0.055 Bq/g of hydrogen product, which is three orders of magnitude lower than the respective regulation value of 56 Bq/g of H_2 in Japan [392].

7.3.7. Tritium studies in the Russian Federation

In accordance with Russian Radiation Safety Norms (NRB-99) [393], it is necessary to obey the limits of personnel exposure to tritium shown in Table 46 [332].

In ongoing nuclear power plant projects, the annual exposure doses to the public in normal operating conditions are limited to 10 μSv for aerosols and 10 μSv for liquid wastes [394].

Taking into account the experience of prototype HTGR operation in the USA and in Germany, and the experience of Russian MHR-T reactor design, an HTGR with a thermal power of 600 MW can be reasonably expected to release about 9250–11 100 GBq/a (250–300 Ci/a) of tritium into the primary circuit.

In the case of (the already existing) utilization for nuclear process heat for residential heat supply, Russian regulations prescribe at least three protective barriers against penetration of radioactive substances from the primary circuit to the heat supply network. Two of the above mentioned protective barriers should represent tight heat-transmitting surfaces (a material barrier), separating working environments of adjacent circuits of coolant. In addition, at least for one of the material barriers, the pressure of the heated up medium should be above the pressure of the heating medium (a pressure barrier) with the difference being not less than 0.1 MPa, taking into account errors of used monitoring systems [70].

7.3.8. Tritium studies in the USA

7.3.8.1. Experience with tritium in Peach Bottom and Fort St. Vrain

A mass balance for tritium in the Peach Bottom reactor was estimated based on calculations and observations during reactor operation. The assumptions used were a fission yield of 1×10^{-4}, a ^3He:^4He ratio of 2×10^{-7}, and a lithium impurity level of 0.05 ppm in the core and reflector graphite. Essentially all of the tritium that was contained in the primary coolant was trapped in the purification system, which was based on the getter effect of the titanium. The advantages of such a system are the easy capture of other gases (H_2O, O_2, N_2), the avoidance of expensive heating and cooling sections, and the possibility of regeneration of the Ti bed with a separation effect between hydrogen and tritium.

Table 47 summarizes the tritium source estimates at the end of life of the fuel after four years [395]. The largest source resulted, as expected, from fission in the fuel (~55%). Post-testing examination of fuel compacts has shown that hot fuel released a significant portion of its tritium whereas colder compacts retained most of their inventory. A surprisingly large source was given with the ^{10}B reactions in the control rod and poison material. Some concentration measurements, however, indicate that tritium from that origin did not migrate into the coolant. The estimate of the tritium from ^3He bound in the graphite structures is based on the assumption that half the porosity in the graphite is assumed to be open porosity and therefore accessible to helium penetration. The tritium from lithium impurities was estimated from measured lithium levels ranging between 1 and 10 ppb.

TABLE 46. LIMITS OF PERSONNEL EXPOSURE TO TRITIUM [393]

Nuclide	Half-life (a)	Compound type, inhalation	Maximum yearly intake (Bq/a)	Allowable yearly average volumetric activity (Bq/m^3)
^3H	12.3	G1 (tritiated water steam)	1.1×10^9	4.4×10^5
		G2 (gaseous tritium)	1.1×10^{13}	4.4×10^9
		G3 (tritiated methane)	1.1×10^{11}	4.4×10^7

TABLE 47. TRITIUM SOURCES IN THE PEACH BOTTOM HTGR [395]

Tritium origin	Amount of tritium at end of life (after four years) (GBq)
In fuel from ternary fission	44 850
In graphite from ^{3}He reactions	1 590
In graphite from ^{6}Li impurities	2 680
From ^{10}B reactions	32 400
Σ	~81 520

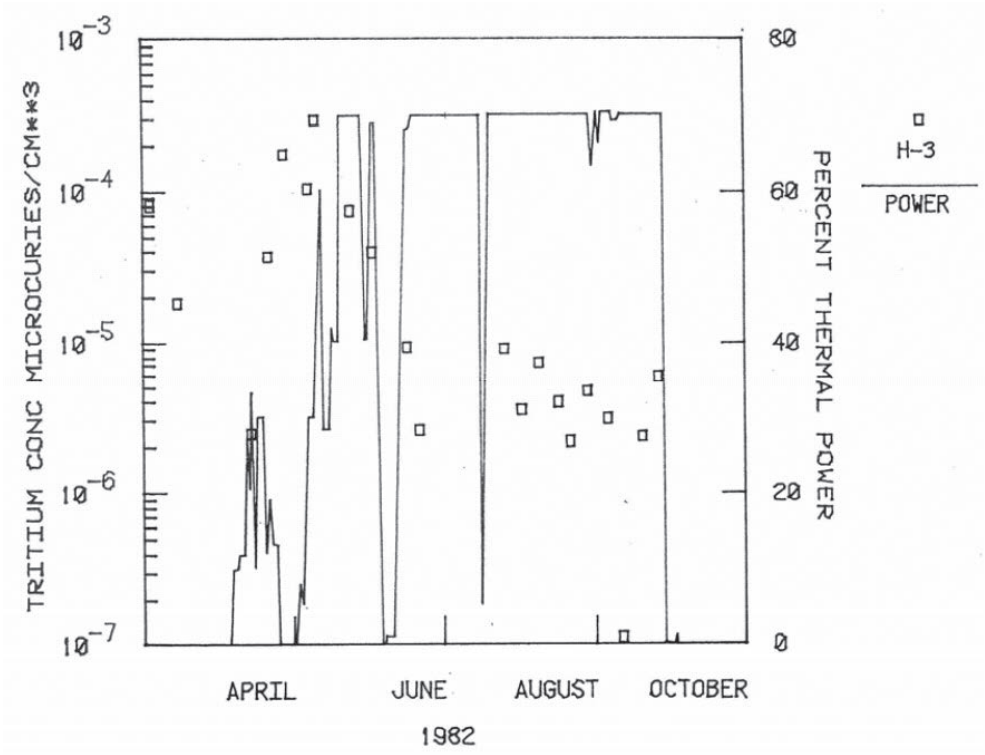

FIG. 159. Tritium concentration in the primary coolant versus thermal power of Fort St. Vrain [334].

The observed tritium level in the helium coolant was found to be close to the level of tritium production from ^{3}He, indicating that most of the tritium produced in reactor core materials was retained there and did not migrate to the primary coolant helium. This implies that essentially only tritium in the coolant contributes to release to the environment [395]. The total amount of tritium produced in the Peach Bottom core 2 during 897 equivalent full power days was about 70 300 GBq (1900 Ci). The total amount released to the primary coolant during three years of operation was about 22 200 GBq (600 Ci), for an overall release fraction of 0.32 [396]. Removal of tritium from the core was mainly given by the fission product trapping system, through which the fuel element purge flow passed. Leakage identified was by off-gas through the stack, discharge with liquid waste or a leak to the chemical cleanup system from steam generator purge. A small portion of around 40 GBq (1.1 Ci) per year was also estimated to permeate from the primary coolant helium through the steam generator tube walls into the secondary coolant water with a further release to the environment by secondary coolant water losses.

Also in the Fort St. Vrain HTGR, tritium activities have been measured by grab samples and continuous monitor devices (Fig. 159). The measurements of tritium concentration in the primary coolant revealed low values at the level of ~0.0004 GBq/m^{3}, demonstrating an effective removal mechanism by adsorption on the core graphite surfaces [334]. A total of ~11 400 GBq (307 Ci) of tritium as HTO was removed from Fort St. Vrain by the purification system after

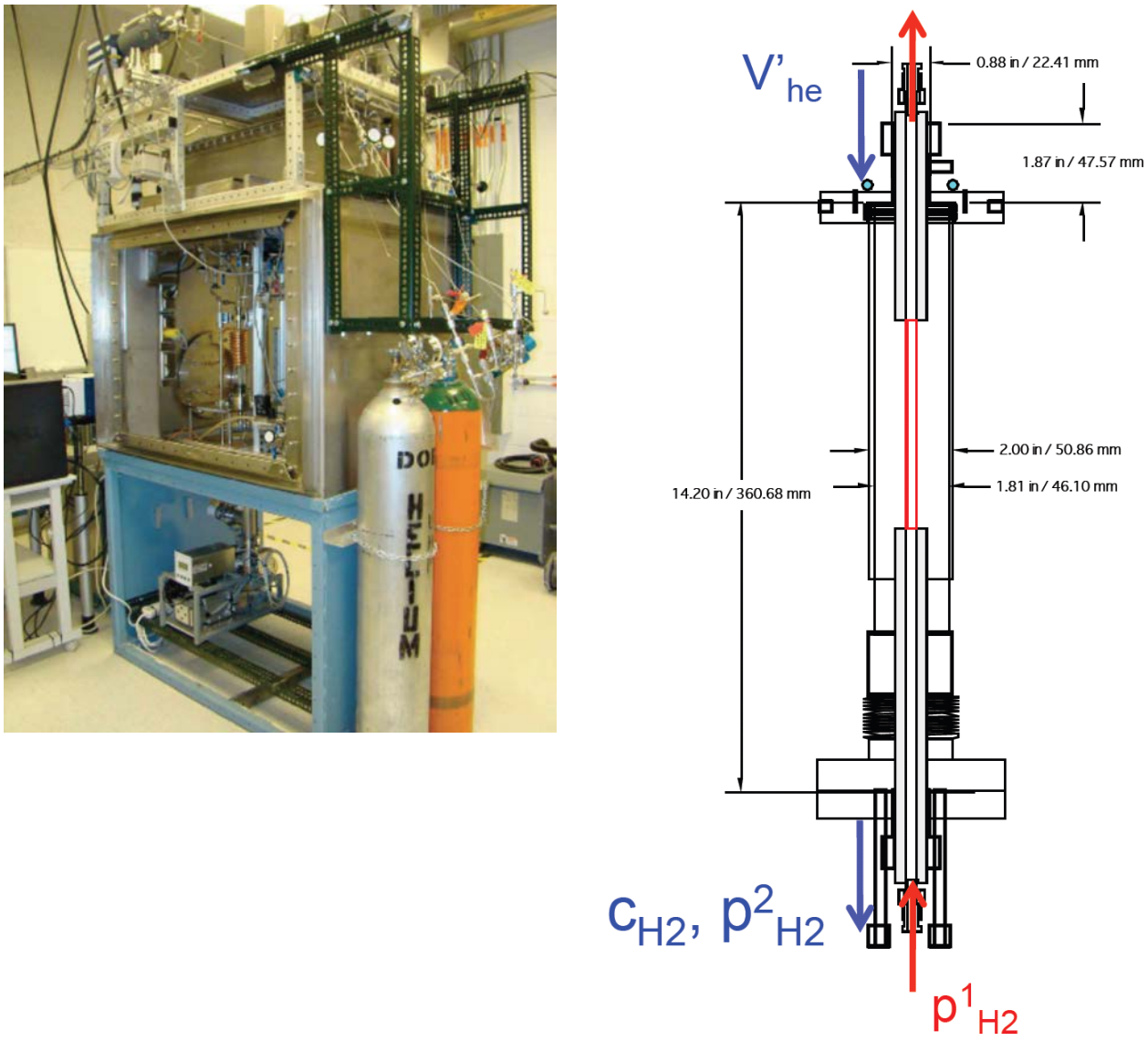

FIG. 160. Schematic and photograph of the INL Safety and Tritium Applied Research facility [397].

101 equivalent full power days. Another unknown amount was removed by the titanium getters, which operated sporadically. During this initial period, most of the tritium was in the form of HTO because of the low H_2:H_2O ratio. The HTO activity removed is roughly equal to the amount produced by ^{3}He activation [396].

7.3.8.2. Permeation of hydrogen and tritium through metal

As part of the USDOE NGNP programme, INL recently constructed the Safety and Tritium Applied Research (STAR) facility for the measurement of hydrogen and tritium permeation through structural materials (Fig. 160) [397]. It is planned to investigate the three high temperature material candidates Alloy 617, Alloy 800H and Alloy 230 at temperatures up to 1000°C. The test section consists of a heated tubular sample which separates two independent counter-flowing helium gas flows, representing the hydrogen/tritium-loaded primary helium flowing through the inside of the sample and the secondary helium flowing on the sample outside. In the case of hydrogen, the concentration range examined is greater than 1000 ppm, whereas tritium radiation counters are able to trace much lower concentrations. First test results confirmed existing literature data for alloys 617 and 800H.

7.3.8.3. Modelling of tritium behaviour

The TRITGO computer model was developed in 1974 at ORNL for calculating tritium transport and distribution behaviour from its origin in the core to the product hydrogen [398]. Sources considered are the ^{3}He in the coolant, lithium and boron impurities in the graphite, and ternary fission. Removal mechanisms are radioactive decay, helium purification and sorption on graphite.

For the tritium generated by fission in the fuel particles, rapid diffusion/permeation is assumed in kernel, buffer and PyC layers, whereas in SiC, the recommended diffusion coefficient is temperature dependent with a pre-exponential factor of $D_o = 4.7 \times 10^{-15}$ m^2/s and an activation energy of Q = 76.5 kJ/mol [399]. These data are based on measurements for particles with different kernel materials irradiated at up to 1575°C to burnups up to 75% FIMA and PIE-annealed between 900°C and 1400°C [400].

The assessment of tritium contamination was made for the HEATRIC type IHX as part of the H2-MHR concept. The calculation of tritium flux from the primary to secondary helium was based on a semi-empirical correlation for Incoloy 800:

$$\Phi = 61.02 \times C_t \times \sqrt{\frac{p}{C_{H2}}} \times \frac{\exp\{-6250/T\}}{t}$$

where

Φ is the flux, μCi/(m^2·h)
C_t is the tritium concentration in the primary coolant, referenced to standard temperature and pressure, μCi/m^3
P is the total primary-side pressure, atm
C_{H2} is the hydrogen impurity concentration in the primary coolant, vol-ppm
T is the IHX wall temperature, K
t is the IHX wall thickness, mm.

Assuming a linear temperature profile from 1000°C to 636°C of the IHX wall and a tritium concentration of 3.7×10^5 Bq/m^3 (10 μCi/m^3) in the primary coolant, the tritium permeation rate was calculated to be approximately 11×10^5 Bq/s (40 μCi/s). Assuming further that all tritium transferred goes into the product H_2, the contamination of the H_2 gas would amount to 0.8×10^5 Bq/Nm^3 (or ~890 Bq/g), which is about one order of magnitude higher than the maximum limit specified in the US regulations. A more thorough analysis will be conducted when a more detailed design of the total plant is available [334].

In a cooperative effort between INL and JAEA, the Japanese THYTAN code has been applied to the Peach Bottom reactor for the purpose of validating the various submodels (sources in core, permeation, leakage, purification) to be compared with the existing measurements and corresponding US calculations. The results in Fig. 161 show the comparison of the published data [395] with the THYTAN results (blue dashed lines), demonstrating that the observed maximum value in the experiments matches the new calculations. It can be concluded that the computed solution from THYTAN is slightly conservative, but THYTAN has shown itself to be capable of matching at least some of the experimental data. Others such as tritium concentration in the secondary coolant (i.e. HTO in steam generator) could not be precisely estimated due to lack of data for the Peach Bottom HTGR [401].

The THYTAN code has also been applied to predict tritium release behaviour for the NGNP plant connected to either HTSE or S–I cycle based hydrogen production [401]. Due to existing major uncertainties with regard to permeability through heat exchanger walls or equilibrium constants of the isotope exchange reactions on the one side, and various possibilities for measures to further reduce tritium release on the other side, overall tritium release is expected to be sufficiently low to meet all regulatory requirements.

INL has developed the Tritium Permeation Analysis Code (TPAC), which is based on a MATLAB/SIMULINK software package [402]. First verification and validation efforts have been conducted by comparison of the separate code modules with analytical solutions. Considering the total system model, results were found to closely agree with Peach Bottom second core data, where measurements were conducted during startup, full power and after shutdown (Fig. 161). A comparison is also planned with HTTR data acquired during operation at 950°C

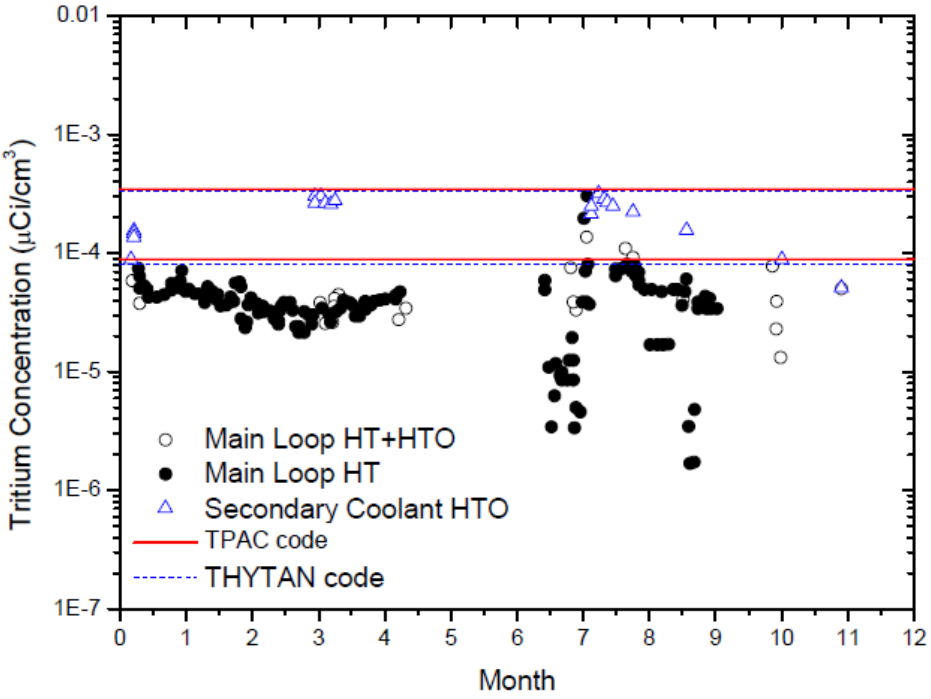

FIG. 161. Comparison of tritium concentration in the Peach Bottom reactor, between the observed concentrations [395], THYTAN calculations [401] and TPAC calculations [402].

gas outlet temperature. In addition to the various tritium sources, sinks, leakage and models for permeation through pipes, vessels and heat exchangers, the model includes also electrolyser and isotope exchange models for analysing hydrogen production systems including HTSE and S–I processes. Due to the presence of water and hydrogen in the steam electrolysis section, HTO and HT are formed, a part of which may escape from the system with the drain water or the hydrogen product. The other part may be recirculated into the system. In the S–I cycle, the present hydrogen containing compounds may transform into the tritiated species HTO, $HTSO_4$, and TI, and circulate and accumulate in the process. Preliminary predictions have been made for a VHTR [402].

In contrast to HTGRs, the tritium in a molten salt reactor is highly mobile in the salt and tends to diffuse through the high temperature heat exchangers into the working fluid of the power cycle. Its entering the steam cycle will result in tritiated water. Isotopic separation of tritiated water from non-tritiated water in the steam cycle is difficult and expensive. The potential option to use a fluoroborate coolant salt in the secondary heat transfer system to trap the tritium appears feasible, but complex and expensive. In the liquid salt cooled AHTR, tritium production is dominated by the $^{6}Li(n,\alpha)^{3}H$ reaction and the $^{9}Be(n,\alpha)^{6}He$ with subsequent decay to ^{6}Li. For the 900 MW(th) plant, the tritium production rate has been estimated to be ~7030 GBq/d [403].

7.4. EXPLOSION HAZARDS

7.4.1. Phenomena and modelling

7.4.1.1. Combustion modes

Essential to the consideration of accidental consequences is the estimation of hazards and hazard levels, e.g. overpressures, thermal radiation, the throw of debris or missiles, and the damage level or the vulnerability of the receiving objects. In chemical explosions, which are usually exothermal oxidation reactions, a great portion of the combustion energy is carried by the developing blast wave uniformly distributed in all directions. Depending on the various types of combustion process (slow deflagration, fast turbulent combustion, detonation), the pressure history characterized by peak overpressure and increase/decay rate will be different. Deflagration and detonation differ in

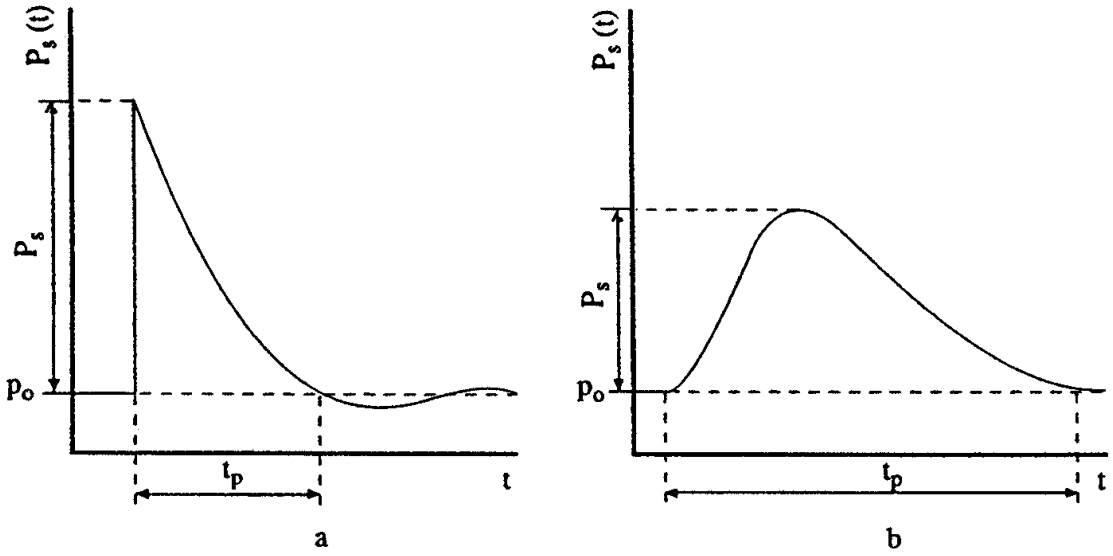

P_o: initial pressure; P_s: peak side-on overpressure; t_p: duration of positive phase

FIG. 162. Pressure–time function for detonation shock wave (left) and deflagration pressure wave (right) [404].

peak overpressure, in the duration of the impulse (time-integrated pressure), in the steepness of the wave front and in the decrease of overpressure with propagation distance. The different pressure transients for the two combustion modes are shown in Fig. 162.

(A) Deflagration

In a confined deflagration with flame speeds of 1–10 m/s, the volume expansion of the gas acts like a piston displacing the unburned gas. The deflagration pressure wave is characterized by a slow increase of pressure and fluid velocity in the region preceding the flame front. Pressure buildup will take place even at low flame speeds and remain at the obtained level, since the gas cannot expand beyond the confinement. The pressure inside is independent of the location and mainly determined by the fraction of burned gas.

The static pressure loading in slow deflagration processes is described by the so-called adiabatic, isochoric, complete combustion (AICC) pressure representing an upper bound in a confined space. Mitigation is given by incomplete combustion, venting, radiation/conduction heat losses, or the addition of diluents. Therefore the maximum static pressure will be generally lower than the AICC pressure. On the other hand, initial turbulence increases the degree of combustion and thus the pressure. The pressure buildup depends on the flame propagation and the degree of confinement. Particularly hazardous configurations are those which are heavily confined, like tubes, pipes or channels where — if long enough — even in insensitive methane–air mixtures, high flame speeds and pressures can be reached. Venting can reduce the pressure.

The combustion of a hydrogen–air mixture in an unconfined vapour cloud explosion (UVCE) typically liberates only a fraction of 0.1–10% of its thermal energy content, in most cases less than 1% [405]. Depending on the combustion mode, the explosion is connected with a more or less destructive pressure shock wave. The overpressure to be expected in the deflagration of an unconfined hydrogen–air vapour cloud is in the order of 10 kPa.

(B) Fast deflagration

In the intermediate stage of a fast deflagration with the flame front still travelling at subsonic speed, a preceding shock wave is developing in the still unburned mixture. The peak overpressure is lower; however, the pressure drop takes place over a longer period of time. This means that the impulse, i.e. the integral of pressure over time, which is a measure for the load upon a structure, is about the same in both cases. The peak overpressure increases with increasing flame speed. Transient pressures can be locally higher than the AICC pressure. Inhomogeneity can result in local detonations decaying to deflagrations. In the long distance range, the pressure

wave for both deflagration and detonation exhibits about the same shape decaying with 1/r. Local explosions like from jet flames result in locally high pressures and can also lead to high flame speeds in less confined areas and even trigger a detonation wave.

(C) Detonation

In contrast to a deflagration, the detonation is a combustion mode with the flame travelling at supersonic speed in the order of 2000 m/s. The flame front proceeds by shock wave compression of the unburned gas. It is characterized by a distinct pressure spike and a subsequent almost exponential decrease. The shock wave, which is at the same time the flame front, is followed by the reaction zone, in which a pressure discontinuity is observed where the pressure even drops to values lower than atmospheric pressure. Peak overpressures in the near field are typically in the range of 1.5–2 MPa. The pressure wave gradually decays and eventually turns into an acoustic wave.

In geometries which allow the transition from deflagration to detonation, pressures near the location where detonation takes place may be much higher than the so-called Chapman–Jouguet (CJ) pressure of a stabilized (and idealized) detonation wave which is due to a precompression effect by the propagating shock wave [406]. In confined spaces, peak pressures can range between 'normal' deflagration peak pressure and very high pressures following deflagration–detonation transition (DDT). The transfer of a detonation wave into adjacent mixtures is possible and has been observed for planar clouds, whereas in spherical clouds, fast deflagrations are more likely to occur.

(D) Real gas cloud

In reality, a gas cloud shows the typically expected features of a non-premixed, inhomogeneous concentration distribution, air entrainment at the boundaries and stratification. The explosion of a real gas cloud will lead to non-ideal blast waves. Deviations from the ideal situation are able to either enhance or to attenuate the pressure buildup. Non-stoichiometry as well as ignition at the cloud edge will certainly have a damping effect on the pressure buildup. The flame spreading in a non-spherical cloud is spherical until it reaches the cloud edge at some point; then it continues in the direction where still gas can be found. The pressure decreases immediately behind the flame front because of the upward expansion of the combustion products. Near the ground, long, flat. stretched clouds of heavier than air gases may experience multipoint ignition connected with a sequence of pressure peaks, and more turbulence generating terrain roughness or obstacles in the flow path.

Unlike a heavy gas cloud, which would be of a pancake form, a hydrogen vapour cloud would soon cover an area which is taller than that of a hemispherical cloud with the same explosive inventory. Only in the case of just vaporized LH_2 after a large scale spill would the cold gas cloud travel and stretch near the ground, until sufficient air had entrained from the outside to make the gas positively buoyant, causing it to develop into a vertically stretched cloud shape.

7.4.1.2. Blast pressure waves

The propagation of a pressure wave in a compressible medium can be described by the Rankine–Hugoniot equations based on the conservation equations for mass, momentum and energy. From this relationship, it can be derived that the density ratio of air, if assumed to be an ideal gas, behind and in front of the shock front is limited to about six. For air as a real gas, however, assuming to dissociate or ionize at high temperatures, this ratio can be significantly higher.

Accurate empirical and theoretical models exist for detonation waves. According to the Chapman–Jouguet (CJ) theory, detonation represents a linear discontinuity, transforming the reactants completely to products at an infinite reaction rate. Detonation velocity and pressure can be calculated from equilibrium chemistry as a function of the gas mixture only. The data for hydrogen at NTP in an unsupported detonation are:

CJ velocity:	1968 m/s
CJ detonation pressure:	1.58 MPa

The CJ theory predicts the thermodynamic state immediately behind the detonation wave, but cannot describe the structure of the wave. Processes inside the detonation front are extremely complex, involving multidimensional

shock interactions in an intensive turbulent reacting medium. Still, the simple, one dimensional CJ model prediction of velocity and overpressure is quite close to what is observed, within a few per cent for velocity and with a 10–15% difference for the pressure measurements [407]. CJ (and AICC) pressures of a fixed gas mixture increase linearly with the initial pressure at constant initial temperature, and are inversely proportional to the initial temperature at constant initial pressure. However, the CJ theory is not capable of determining the dynamic detonation parameters such as detonatability limits, initial energy or critical tube diameter. No theory exists so far that provides estimates of these parameters. CJ parameters of a gas or gas mixtures can be calculated with the code STANJAN developed at the Stanford University.

In the ZND (Zel'dovich–von Neumann–Doering) theory, the detonation wave is described as a 2-D, dome shaped shock wave where at its front both temperature and pressure rise. It is followed by a reaction zone, whose thickness is determined by the reaction rate. Here the detonable substance reacts at high pressure and temperature until everything is transformed into product gases. The chemical reaction causes a rapid fall in pressure (the 'von Neumann spike'). The reaction zone remains unchanged (steady) when moving through the substance. A variable ranging between 0 and 1 describes the respective state and the progress of the chemical reaction. Detonation velocities and pressures are less than for a plane shock front.

A very simple way of modelling blast effects is the 'TNT equivalent' method derived from the decay of shock waves from high explosive or nuclear explosions in the atmosphere. This is an estimation of the mass of TNT per unit mass of fuel whose detonation would result in the same blast wave at the same distance. One kg of TNT translates into the energy of 4520 kg, meaning that 1 Nm^3 of hydrogen gas corresponds to 2.22 kg of TNT. The weakness of the TNT equivalent model, if applied to a vapour cloud explosion, is that it ignores the pressure–time characteristic differences between a gas cloud and a detonative TNT explosion. It is deemed to overestimate near-field and underestimate far-field effects. Furthermore, the model does not consider the influence of turbulence and confinement.

Numerous explosion experiments have been evaluated to derive blast charts. Commonly known and accepted are the Baker–Strehlow blast curves for vapour cloud explosion in the open atmosphere and the TNO blast waves for hemispherical explosions. These are good engineering tools, finding there limits when real gas clouds rather than idealized gas clouds are considered. An improvement toward a more realistic modelling was made with a new set of blast curves, called the Baker–Strehlow–Tang curves, by considering more precise blast pressure decay behaviour. The result is a considerable reduction at long distances. The curves were validated in all combustion regimes [408].

The TNO multienergy method is based on the multi-energy concept, which consists in the feature of gas deflagration that overpressure and blast develop only under appropriate boundary conditions, i.e. only where the flammable mixture is partially confined and/or obstructed [409–411]. This assumption can be made provided that transition to DDT does not take place. For hydrogen, this requirement is not as easily fulfilled as it is for most hydrocarbons. Based on the multi-energy concept, a vapour cloud explosion is modelled as a series of hemispherical model charges. Each model charge is characterized by a charge size and strength. The charge size is related to the heat of combustion present in the source, while the charge strength is related to the explosion overpressure. Based on these characterizations, scaled blast parameters (peak overpressure, positive phase duration) as a function of scaled distance have been calculated (Fig. 163) [411].

The strength of the blast wave is expressed as a number between one and ten representing categories of 'insignificant' to 'detonative'. Calculation results suggest that damaging explosions can occur only when flame acceleration takes place within a plant structure [410, 411]. The charge strength can be determined either by numerical calculation with CFD codes or by using experimentally based correlations between overpressure and details of obstacle configurations [412]. The charge size is influenced by the so-called 'critical separation distance', which is the distance between two obstructed regions above which a vapour cloud explosion can be modelled as two separate sources of blast. Guidance has been obtained in experimental research projects [413]. It was found that the critical separation distance between a 'donor' and an 'acceptor' increases with the explosion overpressure up to a maximum of half the donor dimension.

The Research Centre Karlsruhe has developed the calculation models DET1D and DET3D to determine the characteristic detonation parameters within the reaction zone and outside in the unburned mixture. These models have been mainly applied to assess the load on a nuclear containment upon confined combustion of homogeneous mixtures of H_2, O_2, N_2 and H_2O. Code validation was made against the Russian RUT experiments and balloon tests conducted by the German Fraunhofer Institute for Chemical Technology (FH-ICT). Parameter calculations of a

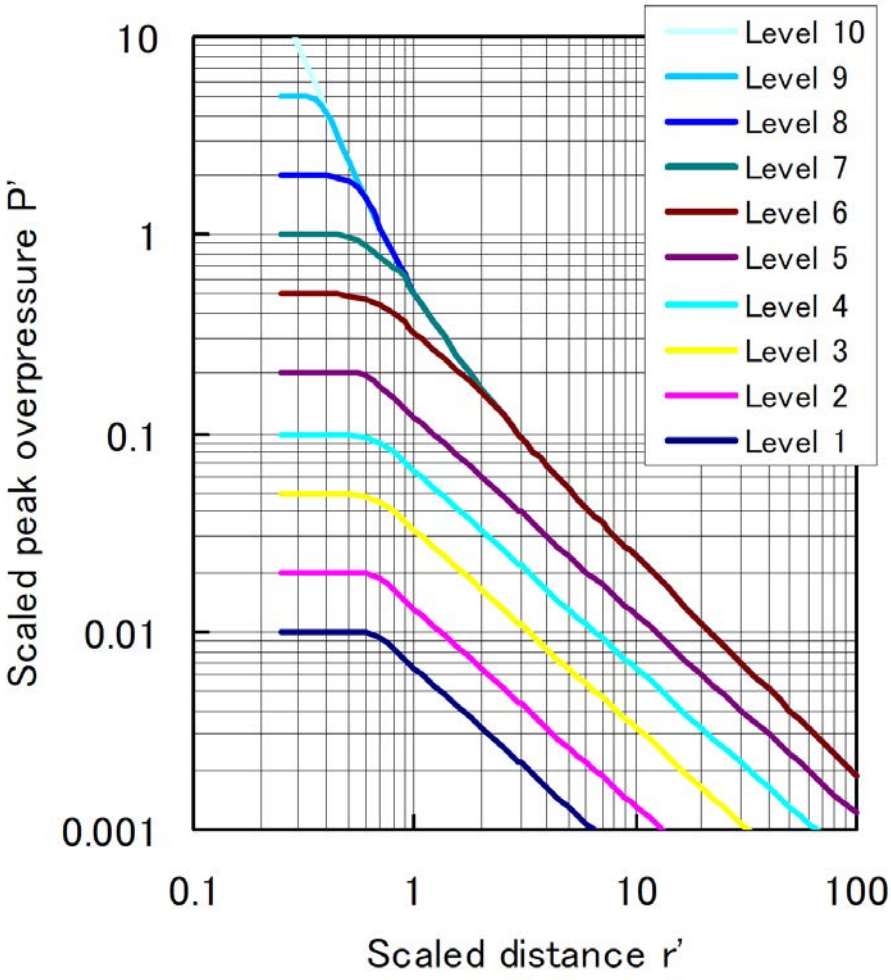

FIG. 163. Blast overpressure versus scaled distance for different explosion strengths according to the multi-energy method [411].

3-D detonation have shown that the 3-D structure is not important for the pressure load and that a relatively coarse grid provides sufficient accuracy [414].

The state of the art approach to modelling of combustion phenomena are 3-D CFD codes, which need to be adapted to the spatial and temporal lengths characteristic of chemical reactions. Typical time steps for hydrodynamic flow calculations are in the order of 10^{-6} s, and 10^{-10} s for the H_2–O_2 reaction mechanism [414]. Many approaches are based on the assumption of incompressible flows and are restricted to slow deflagrations or to pure detonations. For fast deflagrations with Mach numbers greater than 0.3, incompressibility can no longer be assumed, since pressure waves are not negligible. Examples of CFD codes applied to combustion are AIXCO (RWTH Aachen, Germany), AUTOREAGAS (TNO & ANSYS Century Dynamics, the Netherlands), CFX (Harwell, UK), FLACS (CMI, Norway), FLUENT (Fluent, USA), GASFLOW (FZK, Germany), PHOENICS (CHAM, UK). The application of the computer models should be limited to cases or ranges for which the codes were validated.

7.4.1.3. Interaction of blast wave with structure and structural response

The effects of an explosion which have an impact on structures are pressure changes (blast wave) and air movement (explosion wind), as well as thermal radiation and flying missiles. Only a third of the chemical explosion energy is involved in the generation of the detonation blast wave; the other two thirds are released at a much slower rate during the subsequent mixing and burning of the detonation products with the air [415]. In general, structural responses are highly dynamic, highly inelastic and highly interactive. The dynamic interaction of a blast wave with

the structure depends on the pressure–time history, i.e. rise time and duration of positive phase and peak pressure or the impulse (which is the time integral of the pressure).

In a confined or partially obstructed area, an explosion will create a structure loading where two phases can be distinguished, the reflected blast loading phase followed by the gas loading phase. When the pressure wave hits the (rigid) wall, gases are brought to a rest and the wave is reflected. At normal incidence, the reflected shock wave further compresses the burned gases, increasing the pressure by about a factor of 2.3. The mixture of reflected pressure waves and deflected airflows is the result of reverberation of the initial high pressure, short duration reflected wave, with the amplitude decaying with each reflection until eventually pressure levels out at gas pressure loading. The less venting there is available, the longer the latter phase lasts. The more complex the structure, the more difficult is the prediction of the critical conditions for mechanical failure for a given load history.

Forces acting on a structure will lead to a deformation the extent of which depends on the material properties and structure composition. For a static or quasi-static load, i.e. a constant or slowly changing load like from a simple deflagration, it will be in equilibrium with the internal forces resulting in a deformation of the structure. For a dynamic load, i.e. a fast load transient, however, a 'dynamic' contribution from inertia forces will add to the equilibrium, which can show positive or negative acceleration, i.e. the mass and stiffness of the structure will play a major role. The load from a gas explosion is considered a dynamic load due to its short overpressure duration, which is typically in the range of 100–200 ms. Detonations tend to excite the high natural frequencies of a building, whereas deflagrations are more effective for the lower frequencies. It appears to be technically more difficult to design a building against both explosion modes rather than only one.

Methods used to determine structural response and resistance are either empirical in nature, widely applied in risk assessment and mainly based on pressure peak values or pressure–impulse (P-I) diagrams, or analytical and numerical methods. An empirical and very global approach of determining the strength of structures is to relate overpressures to the degree of observed damage. This very useful and easy handling method is widely used. The relationship between pressure and damage, which is derived from TNT explosions, cannot satisfactorily be transferred to vapour cloud explosions. The pressure decay from a TNT explosion is much faster than that from a vapour cloud explosion. The high impulse and the suction effect due to the below atmospheric pressure phase will certainly result in a different damage pattern. Thus damage criteria such as those derived by Schardin from TNT explosions are not directly applicable [416].

Another global approach couples pressure peak with impulse. The impulse, i.e. the pressure — negative and positive — integrated over time, is a measure of the explosion energy, which also varies in time and space over the exposed structure surface. Damage to the structure resulting from a blast wave may be subdivided into direct effects and what is called 'progressive collapse', a kind of secondary failure following the change of the load pattern on a structure due to the direct effects. Features of a P–I diagram are the asymptotes in P and I direction and the monotonic relationship between P and I, which suggests a subdivision into three regimes: impulse controlled, peak load controlled and an intermediate dynamic stage [417]. P–I diagrams are being widely used in damage assessments not only for structural damage, but also for predicting blast induced human injuries. They are providing useful information on the vulnerability of targets.

An example of a P–I diagram is given in Fig. 164 showing the experimental results for the observed damage in per cent, after different types of houses were exposed to a certain explosion (pressure/impulse) load [404, 410]. Only the impulse is important for the damage effect of a short term load (= shock wave), whereas it is the maximum overpressure that is important for the longer-term load (= pressure wave). The solid lines in the figure indicate the lower boundaries for light damage, for severe damage and for collapsing structures of the houses investigated.

A comparison of detonations of explosives and blast waves resulting from nuclear weapon explosions, characterized by quasi-static pressure due to a longer impulse time, shows that, assuming the same damage, the detonation pressure or the pressure resistance of an object is much higher than the resistance against a blast wave from nuclear tests [418].

7.4.1.4. Heat radiation

Thermal radiation is a primary mode of heat transfer. Radiation is the dominant mechanism of heat transfer in large fires involving hydrocarbons, producing intermediate unstable radicals (O, H, OH, N, etc.) and stable non-luminous gaseous combustion products (CO_2, CO, H_2O, NO_x, etc.) and soot particulates.

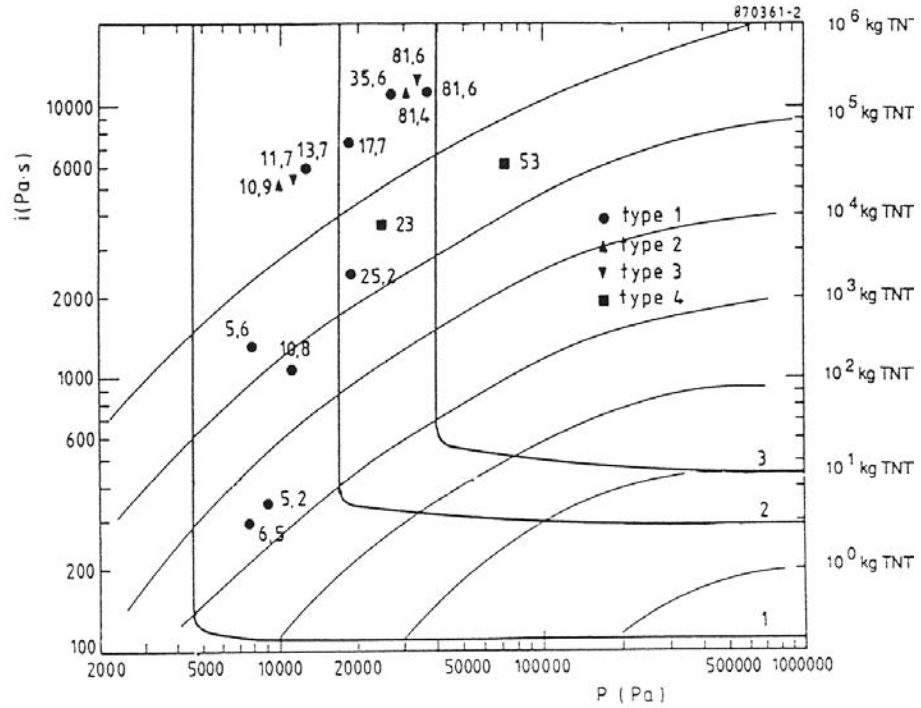

FIG. 164. Pressure–impulse diagram with experimental damage values for different house types [410].

The contribution to the radiative transfer in flames can be regarded as being due to luminous and non-luminous radiation. The gaseous species present, such as CO_2, H_2O and CO, do not scatter radiation significantly, but they are strong selective absorbers and emitters of radiant energy. The actual quantity and distribution of combustion products and/or soot produced in fires depend on the type and configuration of fuel and local supply of oxygen. In contrast to hydrocarbon fuels, the hydrogen burns more cleanly in air, producing a non-luminous, almost invisible, pale blue flame due to spectral water vapour bands.

7.4.2. Release of flammable gases into the nuclear containment building

The production of hydrogen and its handling requires understanding of the fire and explosion hazards which may result from the leakage of flammable materials that are used in the chemical processes applied, such as methane, hydrogen and carbon monoxide. Since deflagration or even detonation have the potential of causing significant damage to safety components, these components should be designed against fire and explosion according to the highest safety level.

The addition of CO to an H_2–air mixture increases the detonation sensitivity of the mixture. The lean limit of H_2 decreases if the CO concentration increases. The addition of 1.2 vol% CO to an H_2–air mixture means a reduction of the lower flammability limit (LFL) from 4 to 3.6 vol%; the addition of 6% CO requires only 2% H_2 to become flammable. A mixture of CO and H_2 will have a flammability limit lower than that of either fuel. Not much information is available on the auto-ignition behaviour of CO–H_2 mixtures. The auto-ignition temperature of CO drastically decreases with the addition of small amounts of H_2 or moisture. Also, few data exist on burning velocities for both H_2–CO and H_2–CO–steam mixtures in air [419].

Figure 165 shows flame speed measurements for a hydrogen–methane–air mixture in an explosion vessel. Gas mixtures varied over a wide range of hydrogen contents, from pure methane–air to pure hydrogen–air fuel compositions [420]. The flammability range of the fuel mixture was found to be widened, as expected, with increasing hydrogen content.

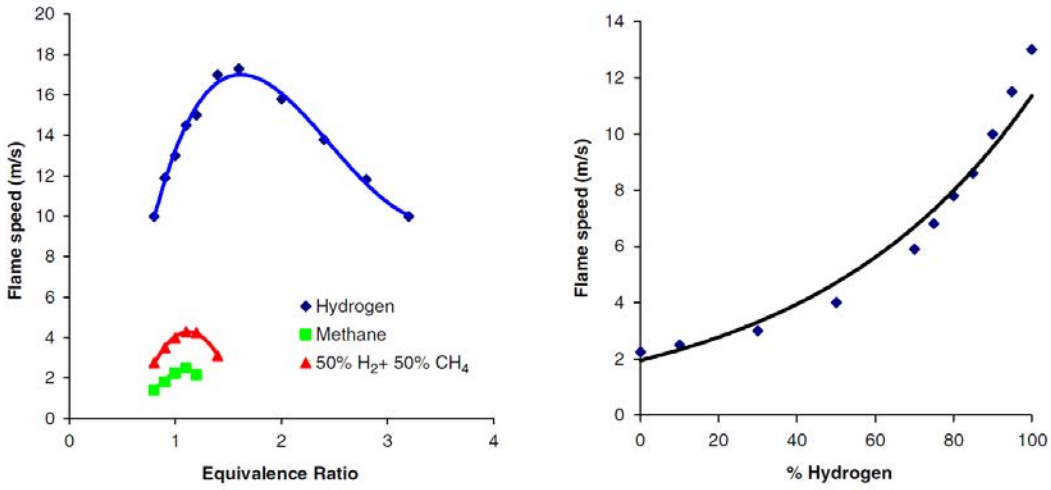

FIG. 165. Measured flame speeds versus H_2 concentration in hydrogen–methane–air mixtures [420].

In the case of accidents, the process gases are mostly light and hot, tend to rise immediately and do not form free explosive gas clouds. However, they may increase turbulence in the containment atmosphere. Various inert components in the gas mixture strongly reduce the chance of an ignition or reduce flame speed and overpressure.

An undesired reaction within the reforming process is the decomposition of carbon monoxide with the formation of carbon which is enhanced with decreasing temperatures:

$$2\,CO \rightarrow C + CO_2$$

7.4.2.1. Germany

(A) Safety of PNP plant

The safety concept is based on the postulated double-ended fracture of a single heating tube of the heat exchanger. Ingress of process gas into the reactor building, however, is only possible after the simultaneous failure of an IHX tube and a secondary duct of the intermediate circuit. This should be practically excluded by design measures such as an appropriate closing valve arrangement in the secondary circuit and a double-pipe construction, i.e. an arrangement of two concentric pipes with both the inner and outer pipes designed to withstand the process gas pressure and with the annular gap filled with inert gas and monitored. Also, in design according to the 'leak before break' criterion, a complete pipe failure should not occur. Safety measures on the primary side are the shutdown of the reactor and of the primary circulator and the closing of the isolator valves. The leak before fracture criterion commonly used in the nuclear field still needs to be proven for the conditions of a process gas pipe. Flow restrictors ensure that the pressure loss time of the primary system is sufficiently long to avoid destructive dynamic forces in the primary system [293].

In the case of the immersion heat exchanger of the steam–coal gasifier, process gas release is assumed to take place at sonic speed through a 13 cm^2 opening. Considering leak detection within 15 s results in about 80 kg of gas mixture (process gas plus steam) entering the primary cell. Process gas mixtures of coal gasification plants are usually composed of the fuel components CH_4, CO, H_2 and C_2H_6, and the inert gas components CO_2, N_2 and water vapour under certain pressure and temperature conditions.

In the case of steam reforming with the reformer as a primary component, a pipe rupture will cause an ingress of process gases into the core, where corrosion of the fuel element matrix and other graphite structures could take place and generate further flammable gases. Prevention measures here are the limitation of the process gas quantity by quickly reacting automatic valves, a dumping system to empty the steam reformer via a relief valve and a primary gas purification system to limit graphite corrosion. The fracture of a steam reformer tube will lead to a leak size of 80 cm^2. Assuming the closure of the isolation valves in the process gas duct after 8 s, the quantity of gas mixture entering the core will be about 600 kg [421].

Information on flammability ranges of mixtures of CO, water gas, inert gas (He, H_2, H_2O) and air as a function of pressure and temperature, as well as on the maximum allowable fuel content and the maximum inert gas content, has been gained from experiments within the PNP safety programme. The flame extinguishing effect was observed to be in the order $H_2O > He > N_2$. The mixture relation according to the Le Chatelier Rule was found to be in good agreement with experimental data and can therefore be used for calculating flammability ranges of any mixture [419]. The effect of an addition of H_2O on the flammability limits has not been verified so far, but it presumably will not be significantly different from CO_2 or N_2. The influence of graphite dust on the flammability range still needs to be examined.

(B) Hydrogen–carbon monoxide mixture explosion studies

The Research Centre Karlsruhe (FZK) conducted experiments in an explosion tube to investigate the turbulent combustion of H_2–CO–air mixtures in fully confined, partially obstructed geometry and, in particular, to examine the influence of the CO component on flame acceleration [422]. To this end the tube was equipped with an array of obstacles of a blockage ratio (BR) of 45% and a distance of 0.5 m. Mixture composition and initial pressure are the parameters the test series.

Tests were performed with 11 and 18% fuel gas concentration; the results are presented in the velocity–distance diagrams shown in Fig. 166. The curves with the circles in the two diagrams represent the case where the fuel is pure hydrogen. Replacing half the H_2 with CO (5.5% H_2 + 5.5% CO = 11% fuel gas) (Fig. 166, top) results in a subsonic flame (<200 m/s), with no acceleration, in contrast to the combustion of pure hydrogen in air where the regime of a choked flame (500–700 m/s flame speed) is reached after an acceleration phase. Some influence of the initial pressure can also be observed.

Analogous experiments with 18% fuel gas concentration (Fig. 166, bottom) reveal a different picture. The combustion of pure hydrogen causes rapid flame acceleration up to the quasi-detonation regime, while more moderate and longer lasting acceleration up to detonation speed is the outcome of the experiments with 9% H_2 and 9% CO.

The results clearly demonstrate a damping effect of CO on the turbulent combustion speed of H_2–CO–air mixtures when compared with turbulent combustion in pure H_2–air mixtures. This effect is probably caused by the relatively long induction and reaction time of the complicated oxidation mechanism of CO. This process requires as an initiating component OH-radicals, which have to be provided in a sufficient amount by the H_2 oxidation. The resulting time delay between hydrogen and CO oxidation was detected in the H_2–CO–air experiments with the installed photodiodes, which showed two spatially separated flame zones moving along the tube.

With respect to safety analysis of nuclear steam reforming systems, the mitigation effect of CO additions on the observed flame speed and the resulting pressure loads should be taken into account. Treating CO simply as H_2 in the analysis would lead to overly conservative load estimates.

7.4.2.2. Japan

Fire and explosion events inside the reactor building may cause severe damage to nuclear safety systems. It is therefore required that the possibility of a flammable gas leak inside the reactor building should be low enough to avoid any fire and/or explosion at this location. The potential sequence of flammable gas ingress into the reactor building is the simultaneous failure of a secondary helium pipe inside the containment and a reformer tube in the hydrogen production plant outside the containment (Fig. 167). To minimize explosion hazards inside, the helium piping and chemical reactor should be designed according to the highest level of reliability and laid out against extreme (design) earthquakes. Furthermore, a combination of the containment vessel isolation valve installed in the helium piping and the emergency shutoff valve in the process feed line is planned.

Since the steam reforming system will be laid out as a non-nuclear facility, it is basically not equipped with additional safety systems. In the case of an explosion event in the vicinity of the reactor building, the thermal load and blast overpressure may be strong enough to cause some damage to the containment. Therefore it is required to prevent significant leakage of flammable gases in the vicinity of the reactor building. A double tube was foreseen in the HTTR steam reforming system to prevent leakage of flammable gas, which would allow for the location of the H_2 system near the reactor. Emergency shut-off valves are also provided to isolate the failure location of the pipe and thereby limit the amount of leakage.

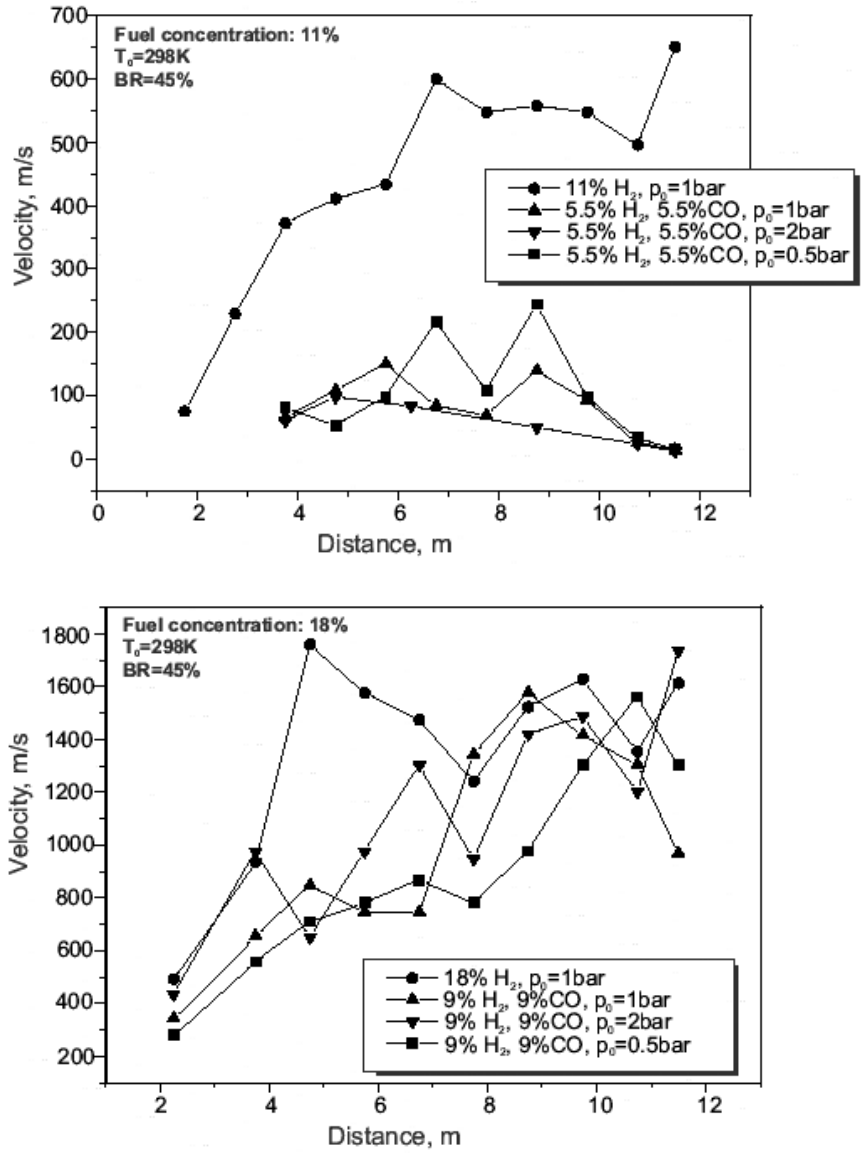

FIG. 166. Flame velocities of H_2–CO–air mixtures measured in FZK detonation tube tests [422].

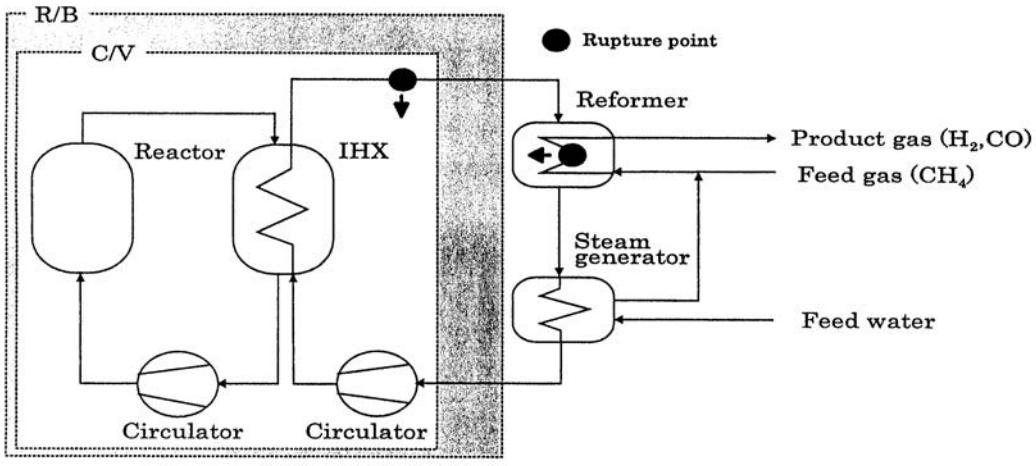

FIG. 167. Ingress of flammable gases into the reactor containment for the HTTR-SMR [386].

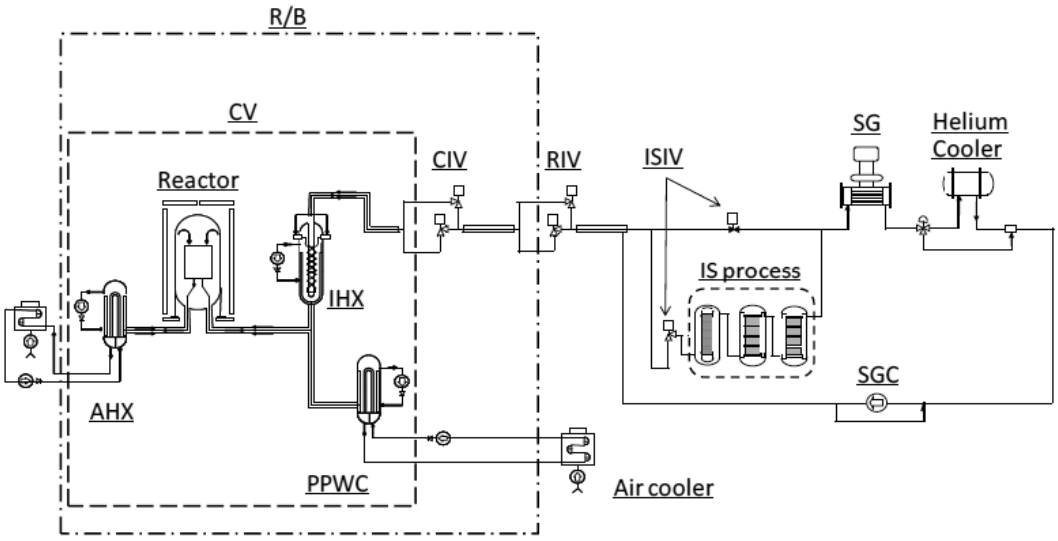

FIG. 168. Isolation valves in the HTTR-IS system for containment (CIV), reactor building (RIV), and S–I process (ISIV) [423].

In the HTTR steam reforming system, the HTTR containment building does not have the capacity to withstand severe radiation heat and blast overpressure. Therefore it is necessary to minimize the risk of a huge fire or explosion event. One possibility is the separation of the accident source and the HTTR, which may be given by a safety distance or a fire-proof separation wall.

On the nuclear reactor side, the key component is the high temperature isolation valve. Its purpose is to prevent the release of any radioactivity with the coolant to the chemical system; it also represents a barrier to the ingress of combustible gases into the nuclear building. The isolation valve is to be designed for helium temperatures of 900°C or above [385].

The containment isolation valves (CIVs) and the reactor building isolation valves (RIVs) are installed in the secondary helium cooling system, acting as a barrier to prevent radioactive release from accidental rupture of the IHX tubing and, on the hand, to prevent chemicals or combustible gas from passing to the primary system following an accidental failure of hydrogen plant equipment. In addition, the S–I process isolation valves (ISIVs) are installed to isolate the chemical process from the secondary helium cooling system in the case of abnormal events of the S–I process (Fig. 168) [423].

Tests have been conducted at JAEA with a scaled down isolation valve of 3 m height (Fig. 169). It is an angle valve with inner glass wool insulation and a flat valve seat made of Hastelloy X. In order to sustain the temperatures of more than 900°C on the hot leg, the valve must be designed against unacceptable thermal deformation. Its functionality at 905°C and 4 MPa with helium flow rates of 2.5 kg/s, and its leaktightness (leakage rates measured were less than 0.1 cm^3/s, target value was 4.4 cm^3/s) in both open and closed cycles confirmed the basic structural integrity and maintainability. In the lower part of the figure, an electric heater unit can be seen, which was installed to heat the helium gas and the inner structure up to 900°C. The isolation valve component needs further improvement with regard to valve seat durability [385].

As a countermeasure against explosion, the design of a coaxial pipe for combustible gases with a reduced rupture probability has been developed. A schematic of the pipe is shown in Fig. 170. It is composed of an inner pipe, in which the combustible gas flows, and an outer pipe filled with nitrogen to prevent leaking of combustible gas to the atmosphere in the case of a rupture of the inner pipe. A failure of the outer pipe can be detected by a nitrogen pressure drop, upon which hydrogen production could be stopped safely [385].

Helium gas can transfer to the process side only if the primary pressure is greater than the secondary pressure until equilibrium. A quick activation of the shutoff or separation system is necessary to prevent radioactivity release from leakage. In the case of repair/maintenance of the chemical reactor, the removal of possibly contaminated process gas is done via stack by a system of catalytic burner, cooler and filter. Rupture of the reformer tube may cause release of catalyst into the primary system, transported downwards by gravity into a catalyst capturing device.

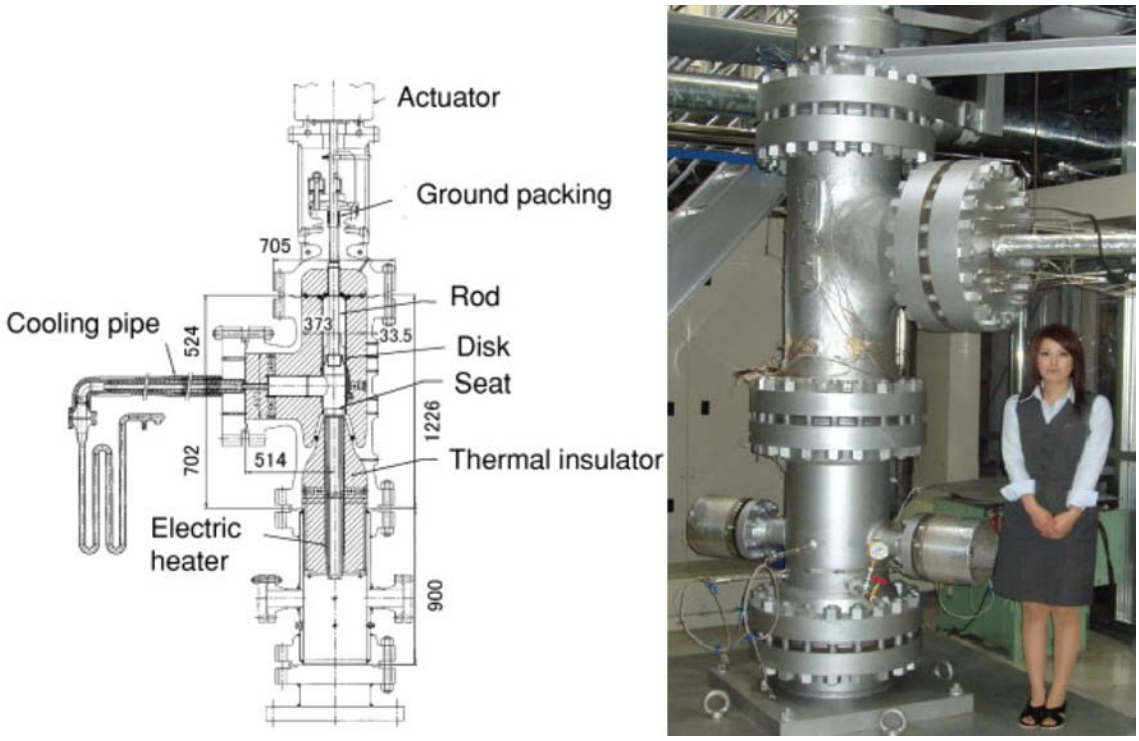

FIG. 169. Schematic of JAEA high temperature isolation valve concept (left), half scale model (right) [385].

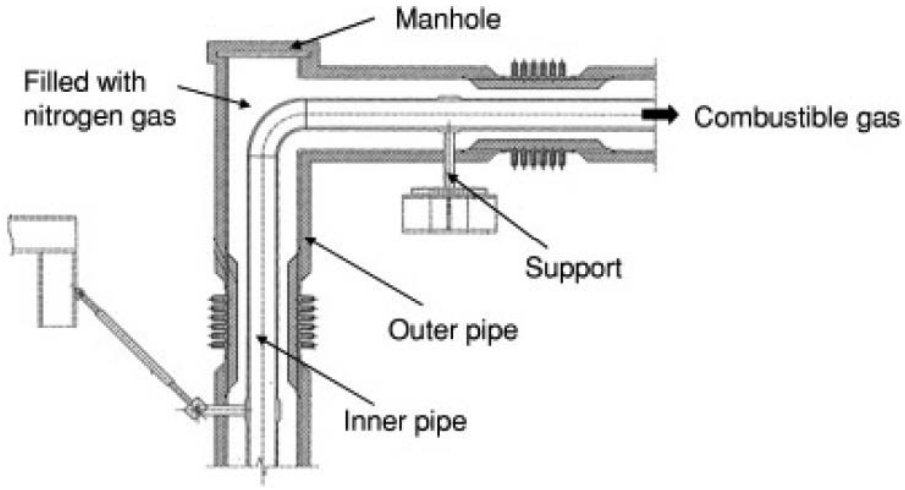

FIG. 170. Schematic of coaxial pipe for combustible gases [385].

7.4.3. Release of flammable gases outside the containment building

Due to its low probability, the scenario of an explosion wave hitting the nuclear plant from the outside is generally assumed to belong to the residual risk, but it may gain importance for the case of nuclear process heat plants in connection with the production and handling of flammable gases in the vicinity.

The danger of possible detonations or deflagrations of explosive gas clouds that could be released from tank ships or trucks, or from nearby chemical plants, and that might travel toward a reactor building has been the subject of substantial theoretical and experimental investigation. This kind of threat is strongly dependent on the local environment and the future development plans for that area. Individual characteristics of the site and the layout of reactor buildings will be relevant. Basic aspects to consider would be to avoid large flat surfaces; to surround the reactor building with auxiliary equipment buildings; to use underground construction for the reactor systems, the

spent fuel storage systems and important connecting conduits; and to provide for sufficient hardening of the above ground portions.

From the different types of release, the catastrophic failure of a pressure tank is the case where — for a short time — the largest fraction of released mass would be within the flammability limits. The most likely release type, however, is a high momentum stationary (jet) release, in which case the fraction of mass within the flammability limits would be smallest.

7.4.3.1. Definition of safety distance

There is a wide variety of possibilities for the definition of 'safety distance' and it is largely dependent on the country or document in question [424]. As commonly understood, a safety distance is the required minimum separation distance between a potential hazard source, e.g. the location of a flammable gas leakage, and the vulnerable object to be protected from an external impact. But apart from the difficulty in providing a precise definition, another problem arises with the necessity to select the appropriate method for quantifying a separation distance. Fixing of numerical values could be done by estimations assuming severe accident conditions or the application of probabilistic risk assessment methods taking account of mitigation measures such as fire walls. And last but not least, there is a need for harmonization of the various approaches of quantification among the countries.

The separation distance is usually determined as a function of the quantity of hydrogen involved ('quantity–distance relationship'). It may be fixed on the basis of credible events, taking account of — if referring to hydrogen — the evolving flammable atmosphere as well as of the heat and pressure wave resulting from a possible ignition. The separation distance can then be defined according to physically defined criteria, e.g. the dose of thermal radiation or the peak overpressure, to have reached a certain threshold value. A particular aspect is the risk of projectiles which may be thrown much further away than the blast pressure based safety distance. A basic prerequisite is the knowledge of the source term, which is dependent on leak size and the thermal dynamic conditions of the leaking substance. Small, hardly quantifiable leakage, e.g. from cracks in welding seams, will be a safety issue.

It should be noted that during transportation of high temperature fluids, it is vital that the distance between the nuclear power source and the hydrogen production site be as short as possible. This is conditioned by the need to preserve the high temperature potential and to reduce the coolant pumping requirement and capital costs. However, from the viewpoint of safety assurance, the hydrogen storage, hydrogen production plant and reactor plant should be located at a distance from one another. Consequently, it is necessary to find a reasonable compromise when analysing the economic effectiveness and safe arrangement of the mentioned objects.

7.4.3.2. France

According to Ref. [425], the recommended safety distance from nuclear buildings is 500 m to cover the risk of a hydrogen–air vapour cloud explosion in the H_2 production plant. For the assumed released mass of M = 1500 kg of H_2 (flammable quantity accumulating during a 30 min production period), this translates into a k-factor of about 44, which appears to be very conservative if compared with the German (k=8) or US approach (k=18). Also assuming the full TNT equivalent of the H_2 mass for a non-uniform hydrogen vapour cloud with a vertically long-stretched shape may lead to a very conservative estimation.

7.4.3.3. Germany

(A) Experimental work on vapour cloud explosion

Apart from the experience obtained by observations and lessons learned from explosion accidents, numerous experiments have been performed worldwide to investigate the transient behaviour of overpressures following the explosive combustion of fuel–air mixtures. Tests were conducted under various conditions such as confined, partially confined or unconfined, larger scale or smaller scale geometry, fuel type and constitution, with the main goal of development of or comparison with simulation approaches. As expected, the most dangerous configurations were found to be those with a major obstruction, even for less sensitive fuel gases such as methane.

Among the numerous experimental activities worldwide was the PNP gas cloud programme as part of the nuclear power plant safety programme. The FH-ICT conducted various series of tests using mixtures of propane, ethylene, methane and hydrogen with air to investigate detonation and DDT in spherical, hemispherical and tube geometries. Unconfined hemispherically shaped hydrogen–air mixtures at volumes between 7.5 and 2100 m^3 were ignited measuring a maximum overpressure of 6.3 kPa, which corresponds to a flame velocity of 84 m/s [426–429]. Balloon tests were conducted with hemispherically shaped hydrogen–air mixtures with a volume of 50 m^3 and concentrations of 20 and 29.6 vol%. Ignition occurred at the centre on the ground by means of an explosive to trigger detonation. Pressures were measured at various positions inside and outside the balloon. Visually measured flame speeds agreed well the theoretical values [414]. The influence of partial confinement on the combustion behaviour of H_2–air mixtures was examined in further ICT tests employing a 10 m × 3 m × 3 m lane with parallel walls [430–432], which resulted in one case in a DDT event [433].

The extensive experimental research programmes on gas explosions within the EU projects MERGE and EMERGE [434] have shown that overpressures are mainly determined by the fuel type, geometric scale, and arrangement and number of obstacles which are passed by the propagating flame.

(B) BMI guidelines for protection of nuclear power plants

A formula for the safety distance is generally acknowledged to have the form:

$$R = k \times M^{1/3}$$

where

R is the safety distance, m;
M is the mass of the flammable substance, kg.

The relation may be modified by damping parameters if some sort of protective measure is applied (e.g. wall or earth coverage). The k-factor depends on the building to be protected (from German recommendations: 2.5–8 for a working building, 22 for a residential building, 200 for no damage) and on the type of substance.

The guidelines for the Protection of Nuclear Power Stations from Shock Waves Arising from Chemical Explosions drafted by the German Federal Ministry of the Interior (BMI) in 1976 [435] has defined for nuclear power plants a k-factor of 8 in the safety distance relation (lower curve in Fig. 171), meaning that the detonation of a mass M results in a maximum overpressure of 30 kPa in a distance of R. The mass M is either unsaturated hydrocarbons or compressed gas, assuming a premixed stoichiometric mixture of hemispherical shape and central ignition. If the flammable mass is a pressurized liquid, k is reduced to 6.3 (or 50% of the mass). For cryogenic liquids or hydrocarbons under standard conditions, k is 3.7 $m/kg^{1/3}$ (or 10% of the mass).

With respect to the HTTR with steam reforming system, the k-factor becomes 3.7 (for LNG). If applied to the foreseen 400 m^3 LNG tank, the result according to the above equation is a required safety distance of 205 m. Such a safety distance would actually be fulfilled if the planned distance between reactor building and the LNG tank of at least 300 m were realized. What is not considered here is the flammable content of the steam reformer, which is sited in the immediate vicinity of the reactor building and thus is not in compliance with the BMI guidelines, which require a minimum safety distance of 100 m.

The guidelines are valid for nuclear power plants of present design. It is explicitly mentioned that “no statement can be given at present concerning its application to future nuclear process heat plants”. They were excluded due to uncertainties in the knowledge of gas cloud explosion scenarios. It is supposed to be a concomitant effort with the development of nuclear process heat plants to solve the problem of external vapour cloud explosions.

(C) Underground siting of the nuclear plant as an enhanced safety feature

The different nuclear components such as fuel elements, primary circuit and containment act as barriers to retain the radioactivity inside the plant. The integrity and interdependence of these barriers is a key requirement of reactor safety. Depending on conditions of normal operation and accidents, these barriers are efficient in different ways. In normal operation, the function of the first barrier, the fuel element, is sufficiently good to retain nearly all

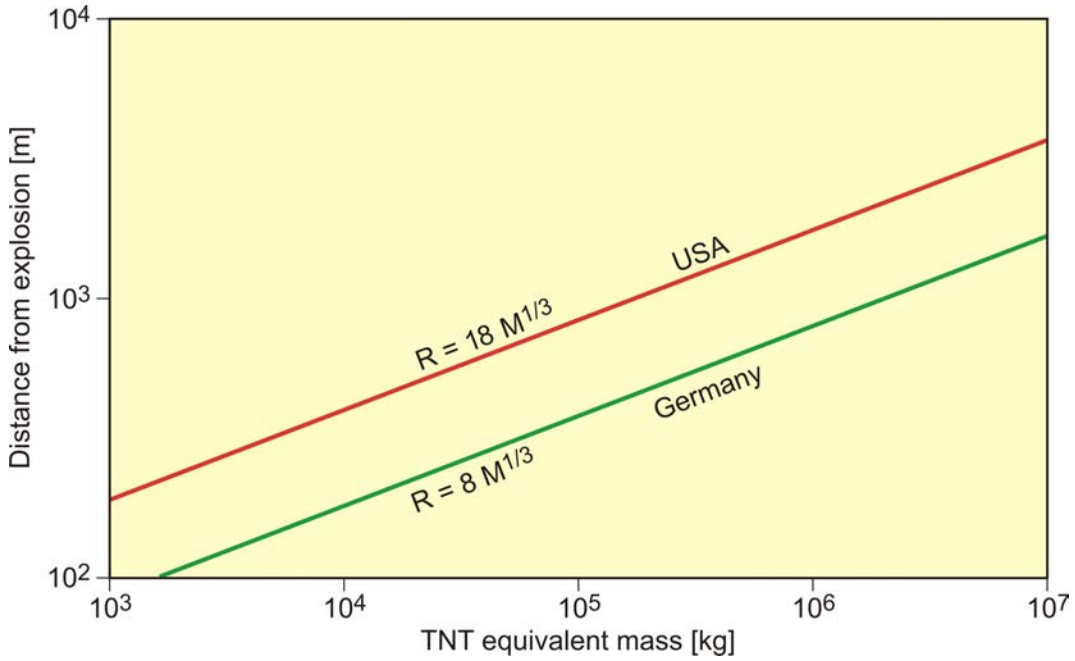

FIG. 171. Safety distance as a function of the quantity of released liquefied gas according to the BMI guidelines and US Regulatory Guide 1.91.

fission products. The retention of the radioactivity inside the reactor has to be efficient enough to limit the releases to the environment, in the case of an incident, to an amount less than a fraction of 10^{-5} of the overall inventory.

A further global expansion of the use of nuclear power and its public acceptance require the prevention of catastrophic releases of radioactivity in the case of severe accidents [436]. A series of protection systems for a nuclear power plant characterized by a complete below-ground construction and earth coverage is shown in Fig. 172.

The total primary system enclosure is pre-stressed with radial and axial tendons to prevent bursting of the vessel. The primary system is enclosed in an inner primary concrete cell, placed inside a reactor building to protect the reactor against impacts from the outside. Underground siting even prevents dangerous consequences of terrorist attacks on the plant. These new safety characteristics of the plants to be assigned to all other activities such as installations of fuel supply and disposal in the nuclear energy economy have to be proven.

7.4.3.4. Japan

In Japan, the High Pressure Gas Safety Law, which applies also to hydrogen, defines safety distances for chemical plants containing < 10 000 kg of flammable materials — which would apply to the combined system of HTTR plus S–I process — as follows:

17.0 m to public buildings;
11.3 m to residential buildings;
8.0 m to facilities which are operating burners.

(A) Safety concept for HTTR combined with SMR or S–I process against fire and explosion

Figure 173 shows for the example of the HTTR plus a steam reforming system the potential fire and explosion hazards which may have an impact on the reactor containment. A safety distance can be selected to mitigate the effects of thermal load from fire and blast overpressure from explosion. Comparing these effects, the explosion pressure wave causes greater damage than does the fire itself. The explosion event is taken into account to estimate adequate safety distances.

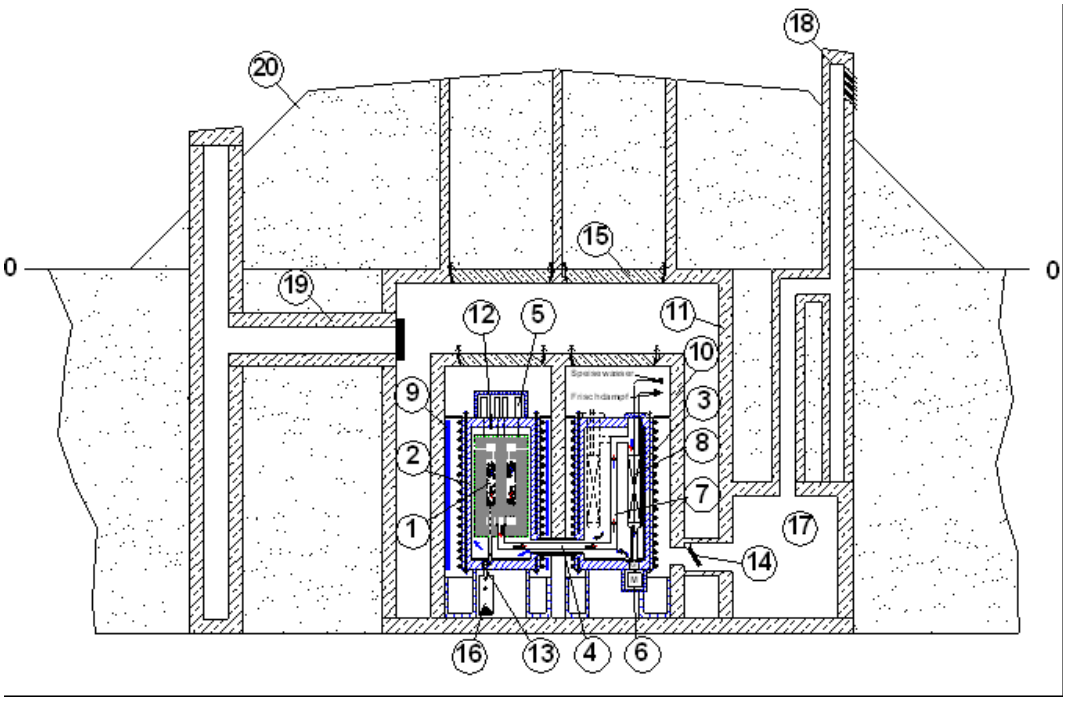

1: reactor core (here: 300 MW(th) with annular design and RPV inner diameter of 6 m), 2: prestressed reactor vessel, 3: prestressed vessel for steam generator, 4: prestressed connecting vessel, 5: control- and shut off system, 6: helium circulator, 7: hot gas duct, 8: steam generator, 9: cell cooler, 10: inner concrete cell, 11: outer reactor building against extreme impacts, 12: fuel loading device, 13: fuel discharge device, 14: flap, 15: concrete closure, (16) storage vessel for spent fuel elements, 17: sedimentation area + filter, 18: stack with filters, 19: transport channel, 20: cover of reactor building

FIG. 172. Concept of underground siting against extreme impacts from outside [436].

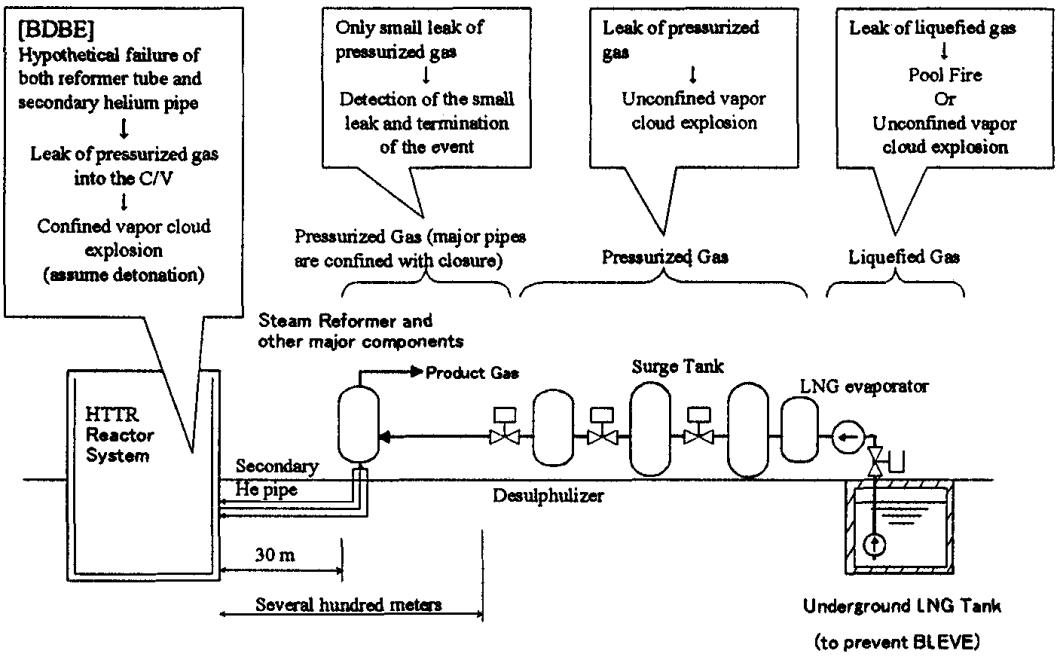

FIG. 173. Possible effects of fire/explosion accidents outside the reactor containment for the HTTR-SMR [386].

The basic safety concept as proposed by JAEA is to provide some safety barriers between the HTTR and the steam reforming system so as to prevent the anticipated operational occurrences for anticipated design basis events related to the steam reforming system. Design basis events related to the HTTR system have already been considered. It is therefore important to discuss additional anticipated design basis events that could originate due to the connection of the steam reforming system with the HTTR. Additional safety design requirements and corresponding countermeasures for the hydrogen production system are given in Table 48 for the different operational conditions of the HTTR.

Adequate measures for the occurrence of an event or its propagation are provided: pressure resistance design, combustible gas leak detection system, fire extinguishing system and emergency shutoff system. Incidents with small or medium amounts of leakage appear to represent no hazard to the nuclear system. In terms of mitigation, safety distance and alternatively an explosion-proof/fire-proof wall are considered to allow shorter distances.

Concerning the concrete of the building, it is expected to exhibit no significant change of its mechanical properties over 24 h at 175°C, and is designed to not exceed a wall-averaged limit of 175°C from radiation heat, in order to maintain the structural strength of the concrete. Overpressure of the incidental blast wave is limited to 10 kPa (USA: 7 kPa, Germany: 30 kPa) to ensure no failure of the reinforced concrete and the steel frame components.

The computer code system P2A was developed at JAEA to analyse fire and explosion accidents for the HTTR steam reforming system [437]. It consists of the commercially available programmes PHOENICS for leakage, pool fire and atmospheric dispersion simulation; AUTOREAGAS for deflagration and blast wave effects; and AUTODYN for detonation and impact on structures. The three single codes are coupled by interface programmes. Calculations have been made considering leakage of LNG from the storage tank or a pipeline with a subsequent large scale pool fire changing the local atmospheric wind flow pattern, or the formation of a methane vapour cloud, its ignition and explosion with a pressure wave hitting the HTTR building.

Assuming a leak position 200 m from the reactor building and a leakage rate of 34 kg/s over 44 s (corresponding to a total volume released of about 3.5 m^3 of LNG) did not show a spreading of the vapour cloud toward the reactor building at significant concentrations. The cloud volume within the flammability limits was estimated to be around 2300 m^3 after 69 s. The ignition of the cloud near the leak position resulted in a maximum overpressure of 0.3 kPa, which decayed to a level as low as 0.01 kPa in front of the reactor building [437].

(B) Dispersion and explosion analysis for the GTHTR300C

A preliminary analysis to estimate the separation distance was performed by JAEA for the GTHTR300C in the case of a hydrogen explosion [438, 439]. The 3-D computational fluid dynamics code STAR-CD was used for the assessment of hydrogen dispersion and its transient concentration distribution in the open atmosphere applying the standard k–ε turbulence model.

TABLE 48. SAFETY DESIGN REQUIREMENTS FOR THE HTTR HYDROGEN PRODUCTION SYSTEM

Operational condition	Event	Safety requirement	Countermeasure
Normal operation	Tritium transport from core to product gas H_2	Reduction of tritium radiation level in product gas	Restriction of permeation through tube walls Removal of tritium in the coolant by purification system
Anticipated operational occurrence	Thermal turbulence	Prevention of thermal turbulence to propagate to primary He loop	Mitigation of vibration of secondary helium temperature by steam generator installed downstream
Accident	Fire/explosion from leakage of flammable gases	Prevention of leakage inside and in the vicinity of reactor building Mitigation of accident consequences	Upgrade design category of helium piping, reforming tubes Double-walled tubes Inerting of the compartment Safety distance

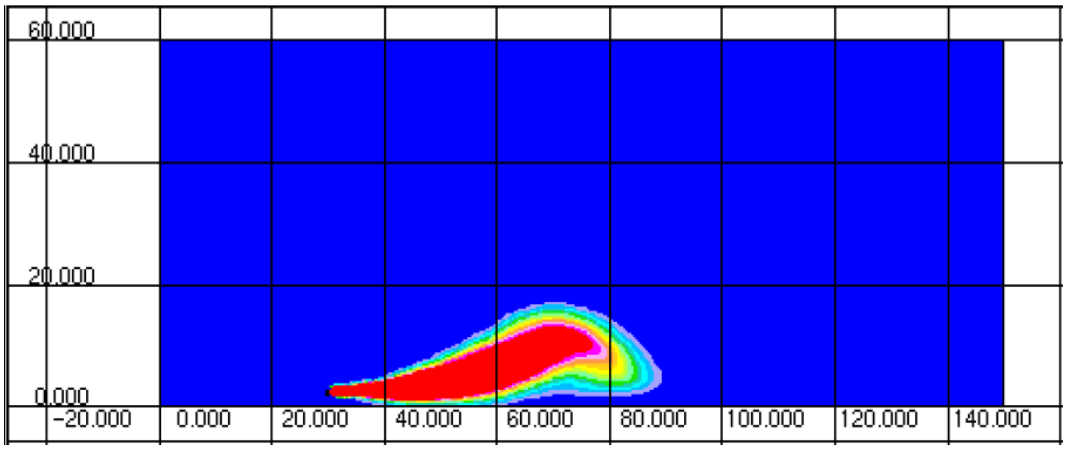

FIG. 174. H_2 concentration contours after 10 s with the flammable portion of the cloud (≥ 4 vol% in red) [438].

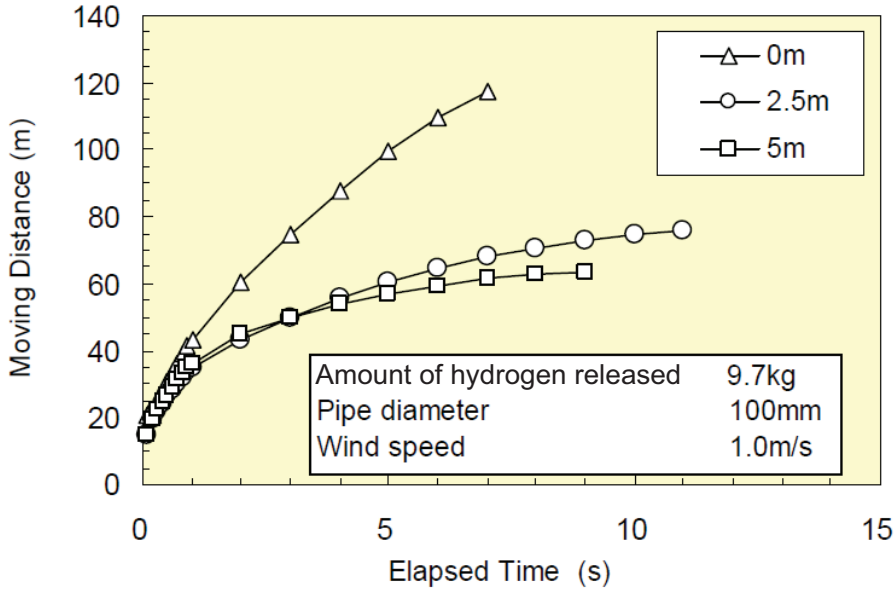

FIG. 175. Downwind distance as a function of the H_2 quantity released [438].

In the scenario analysed, the assumption was a rupture of the H_2 pipeline with the release of a pressurized hydrogen gas jet at critical speed. The mass flow rate was assumed to be constant. The release phase was followed by a dispersion phase in the open field until the H_2 gas cloud was dissipated below the LFL. Further assumptions were a released H_2 quantity of 9.3 kg at a rate of 0.77 kg/s over 12 s, a pipe diameter of 20 mm, a release height of 2.5 m and a wind speed of 1 m/s. The maximum downwind distance of the explosive gas cloud before dissipation after 16 s was calculated to be 44 m (Fig. 174).

Increasing the quantity of hydrogen released leads to an increased downwind distance. A variation of the release height has shown that ground release leads to the longest downwind distance, while there is no significant difference for the cases with 2.5 and 5 m of release height (Fig. 175). Also, a larger pipe diameter with correspondingly shorter release time results in longer downwind distances.

Hydrogen jet flames resulting from ignition of unintended releases can be extensive in length and pose significant radiation and impingement hazards. Depending on the leak diameter and source pressure, the resulting separation distances might become unacceptably large. The employment of barrier walls around H_2 containing systems is an option to reduce hazards. Vertical barriers, however, may deflect jet fires down or back toward the hydrogen facility. Therefore tilting the barrier at some angle could help reduce this effect.

A physical barrier is also an effective means to reduce the travel distance of the hydrogen cloud. In the JAEA study, the effect of a wall assuming a height of 7 m at a distance of 5 m to the release point, which itself is at a height of 5 m, is shown in Fig. 176. For a horizontal jet (Fig. 176 (top)), the H_2 cloud hitting the wall is split into two parts, resulting in a drastic decrease of the travel distance. If the jet is inclined upwards at an angle of 22.5° (Fig. 176 (bottom)), the wall is only partly touched by the gas cloud, and there is no effect for angles over 45°. But the wall effect of the over 45 degrees of the jet angle disappears because a hydrogen cloud goes over a wall in this case. The calculations have shown the positive effect of a protection wall which can be designed such that travel distances will be limited to values below 100 m.

A second step in the analysis is the estimation of a safe distance beyond which the overpressure following the explosion of the H_2 gas cloud has decayed to an acceptable level. This level was assumed in the JAEA analysis to be 10 kPa, similar to the NRC value of 1 psi (~7 kPa). The explosion overpressure is strongly dependent on the time elapsed after the beginning of the release. Figure 177 shows the calculation results for the separation distance as a function of time in the case of a release of 97 kg of hydrogen from a 100 mm diameter pipe. The separation distance is defined by a sum of travel distance of the cloud and the distance of the peak overpressure of 10 kPa. The figure exhibits the tremendous importance of consideration of the cloud travel distance (yellow part of the bars).

It was concluded from the analysis that a relatively short distance between the reactor plant and the hydrogen production plant should not pose any risk to the overall safety, especially if the reactor and the process plant are separated with an earth mound or any other type of wall. The employment of a blast-proof protection wall rising 2 m above hydrogen pipelines that significantly reduces the travel distance of the flammable cloud might be sufficient to limit the safety distance between the nuclear plant and the hydrogen production-site to 100 m or less [438]. Further studies will be conducted at JAEA to confirm the sufficiently conservative approach.

(C) Safety of fuel cell vehicles

A study to investigate the risk associated with a refuelling station based on high pressure gaseous hydrogen and to examine accident scenarios and the relevant safety requirements has been initiated by the Japan Petroleum Energy Centre. As a major result, the analysis has shown that, except for highly unlikely events, a minimum safety distance of 6 m should be sufficient. It is intended to propose a revision of the existing High Pressure Gas Safety Law, which currently requires a clearance distance of 11.3 m [440].

To investigate the safety of FCVs and then be able to establish a set of codes and standards, the Hydrogen and Fuel Cell Vehicle Safety Evaluation Facility, Hy-SEF was constructed. It includes a fire and explosion resistant, contained area for testing hydrogen vessels and vehicles under accident conditions [42]. The investigation of the flammable region of a hydrogen vapour cloud released from a pressure vessel was done in a wind tunnel test series in 2001. If stored at 35 MPa and applying a 0.8 mm diameter pinhole, concentrations of >4% were observed up to a distance of 2–3 m. If large amounts of hydrogen were released within a short period of time, the flammable cloud sections extended to about 20 m [441]. Also explosion test series have been conducted with premixed H_2–air at different concentrations in 5, 37 or 300 m^3 volumes. Measurements were made for the flame speeds and overpressures at various distances studying the influences of ignition mode, obstruction and a barrier wall [442].

7.4.3.5. Russian Federation

According to the safety requirements for nuclear plants connected with a hydrogen production plant, technical measures have to be taken against blast pressure waves from vapour cloud explosions. The measures include explosion source removal or screening, building structure reinforcement (increased stiffness and inertia of cross-sections) or other technical solutions aimed at decreasing the energy potential of explosive process units [443].

If there are (or are supposed to be) any external explosion sources at a distance of up to 5 km from nuclear plant structures of category I (Table 49), this pressure is calculated or assumed to be equal to 30 kPa [444].

The energy potential, Q_v, of the process units intended for hydrogen production through water electrolysis are to be calculated on the basis of design solutions ensuring $Q_v < 27$ (explosion hazard category III). The permanent presence of the servicing personnel in the electrolysis compartment is not recommended. Continuous monitoring of the progress of technological processes is performed by the operator from the control panel room. Automated shutdown takes place if emergency protection thresholds are reached.

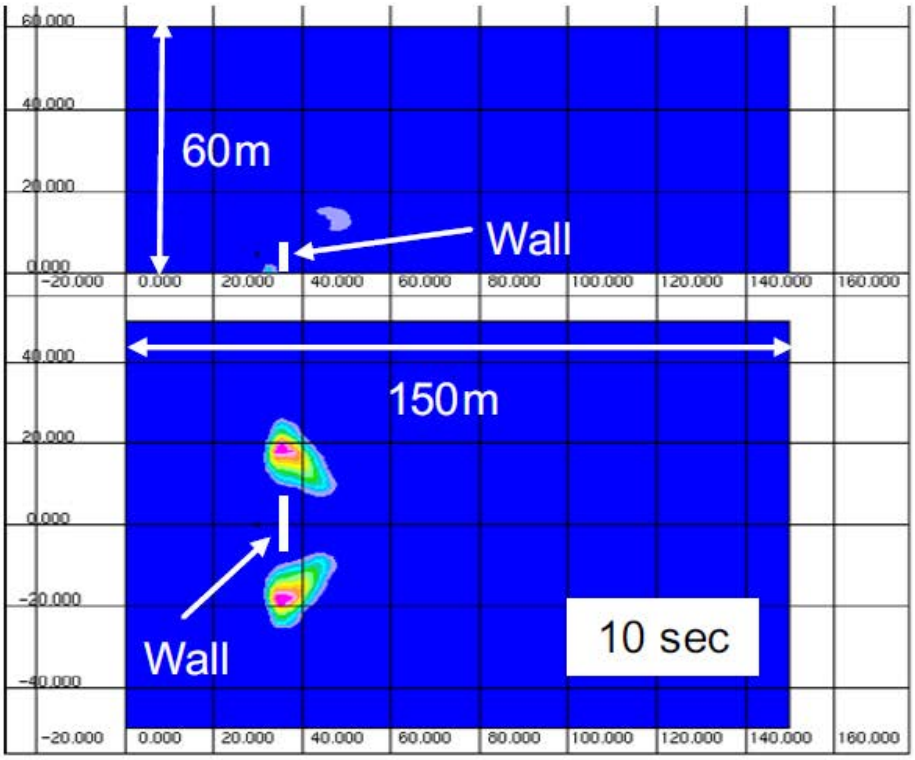

(a) Horizontal jet

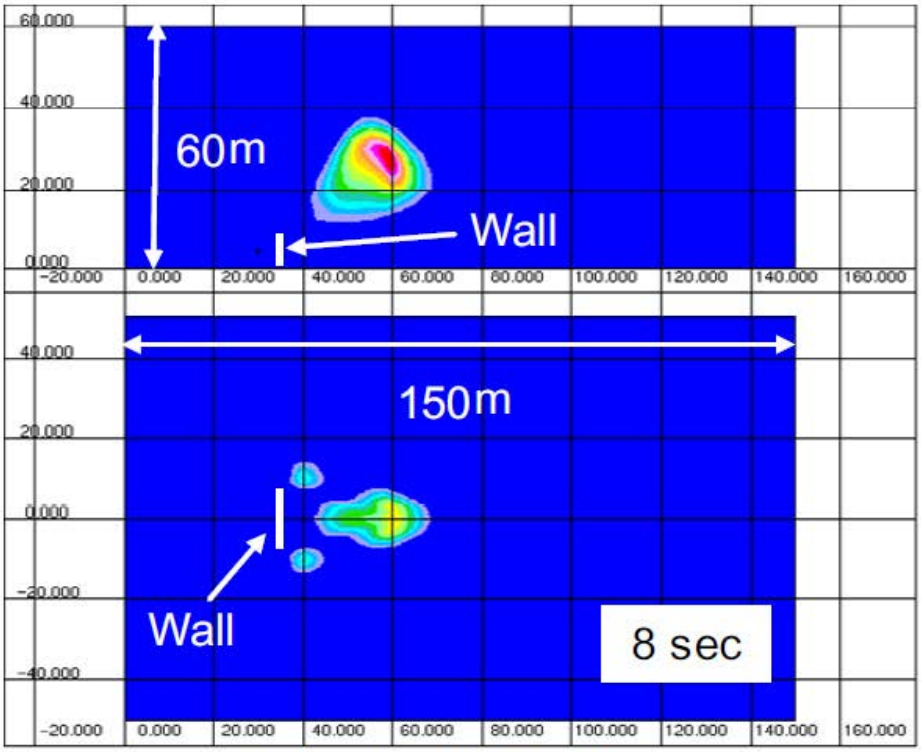

(b) Angle of 22.5 degree

FIG. 176. Hydrogen concentration contours in the presence of a barrier wall [438].

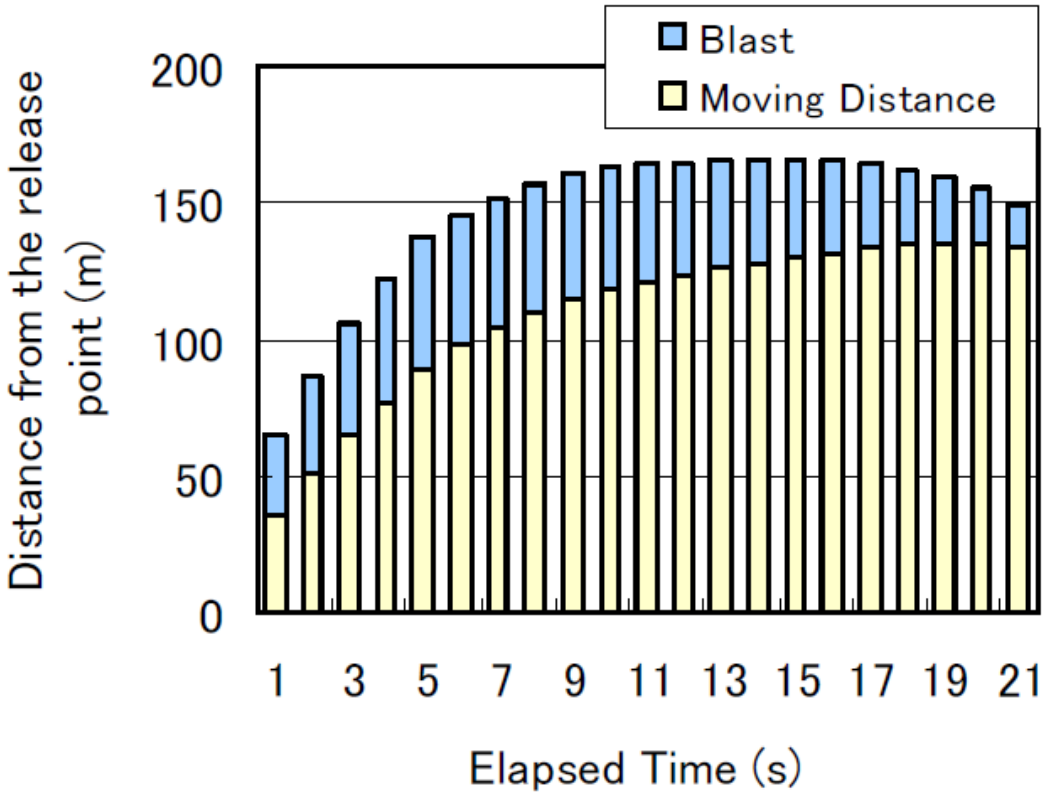

FIG. 177. Distance from the release point with an overpressure of 10 kPa [438].

TABLE 49. EXPLOSION HAZARD CATEGORIES OF PROCESS UNITS [445]

Explosion hazard category	Relative energy potential of released gas cloud, Q_v	Mass of released gas cloud (kg)
I	>37	>5000
II	27–37	2000–5000
III	<27	<2000

For nuclear power plants, pressure in the shock wave front should be assumed to be equal to 10 kPa taking account of on-site explosion sources. If there are (or are supposed to be) any external explosion sources (oil refineries, basic storehouses of fuel and lubricants or explosives, gas lines, etc.) at a distance of less than 5 km from a nuclear plant structure of category I, the pressure in the shock wave front is to be calculated or assumed to be equal to 30 kPa. Designed explosion and fire hazardous facilities are to meet the following requirements [445]:

— Buildings accommodating control rooms (operator rooms) should be constructed outside the destruction area or be capable of withstanding shock wave impact; in the latter case, they should be equipped with independent means to support normal systems operation and personnel activity in emergencies.
— Permanently attended administrative and other buildings should be constructed outside the destruction area.
— Plant-shared facilities (power, steam and water supply, etc.) should be constructed outside the destruction area or be capable of withstanding shock wave impacts.
— For each object containing process units of any explosion hazard category, it is necessary to calculate zones in which the concentration of fuel in the vapour cloud that forms in the emergency remains below the explosion limit. The emergency response plan shall specify actions to be taken by the personnel in case of emergency to prevent ignition of the vapour cloud sources within the calculated zones.

In accordance with the safety rules to be observed in the production of hydrogen by water electrolysis, hydrogen storage should be located at a distance of at least 15–30 m from the storehouses and production buildings, and a minimum of 100 m from administrative buildings [446]. The mass flow during the release of hydrogen or other explosive gases located in close proximity to the reactor pressure can be reduced owing to the modular equipment design, optimal number of fast-response isolation valves sealing off the leaking sections, and reduced cross-sections of pipelines and overall size of equipment that may contain explosive fluids.

If possible, the reactor building should be buried relative to the process plant. In another variant, it is necessary to arrange screening with an earth mound, a reinforced wall or (what is less costly) a rising wall in the place of possible hydrogen leak from the pipeline. Therefore, it appears to be possible to arrange the hydrogen process plant and the reactor building at an acceptable distance from each other (not exceeding 100 m), observing all technical measures ensuring the safety of such arrangement.

According to the analysis of the MHR-T based SMR process, high concentrations of water steam in the steam gas mixture transport area, even in the case of leaks, prevents the formation of explosive mixtures in any initiating events or meteorological conditions. Detonative mixtures can form only in chemical plant compartments not connected to the reactor plant, and therefore these compartments can be removed to the required safe distance from the nuclear power plant main building. The modular equipment design and interfaces between the four-module nuclear plant and the chemical plant should prevent failures that may disable more than one MHR-T module. Therefore, an accident in one reactor module would not affect the safety of the remaining modules, and an uninterrupted operation of the entire power complex, in turn, would support a high availability factor.

7.4.3.6. USA

In the USA, it is judged according to the NRC Regulatory Guide 1.91 [447] that structures, systems and components important to safety and designed for high wind loads are also capable of withstanding pressure peaks of at least 7 kPa resulting from explosions. No additional measures need to be taken if the equation

$$R = 18 \times W^{1/3}$$

is met where

R is the safety distance, m, from an exploding charge;
W is the mass of TNT (equivalent), kg, of the exploding material (upper curve in Fig. 177).

For the LNG storage tank of the HTTR SMR system, the 400 m^3 of LNG correspond to a TNT equivalent of 1859 t, which then translates into a safety distance of as long as 2.2 km. This approach appears to be unrealistic for the HTTR SMR system considering the fact that much larger stationary LNG tanks up to 200 000 m^3 ($\rightarrow R \approx 18$ km) have been established worldwide. NRC Guide 1.91, however, offers additional options such as risk analysis for further reduction of the safety distance. Other countermeasures considered are a fire wall, berm (separating hill) as shown in Fig. 178 for the US H2-MHR concept and in Fig. 179 for the US STAR-H2 reactor concept, where the reactor modules are located in underground silos while the primary helium circulator, the IHX, the intermediate helium loop circulator and respective piping are located in an adjacent silo. The below-grade positioning of the reactor core has further safety related advantages in that it is more resistant to sabotage and to damage from seismic events; also decay heat can be dissipated to earth if necessary.

A key issue for safety and licensing of the H2-MHR is the collocation of the MHR modules with the hydrogen production plant. From the technical point of view, the distance of high temperature heat transfer should be minimized.

In a recent study to evaluate the separation requirements, INL applied methods of probabilistic risk assessment using the risk analysis code SAPHIRE to assess safety distances between an NGNP and a hydrogen production plant. Calculations have shown that a distance below 110 m would result in the need to consider regulatory issues demanding mitigation measures. Passive barriers such as an earthen wall result in a significant reduction of the core damage frequency. The recommendation given is a safety distance between 60 and 120 m plus a mitigation barrier against explosion events. All on-site quantities of hydrogen should be minimized to less than 100 kg. Additionally, it is recommended to transport the hydrogen gas in a coaxial pipeline with an inert atmosphere (nitrogen) in the annular space [449].

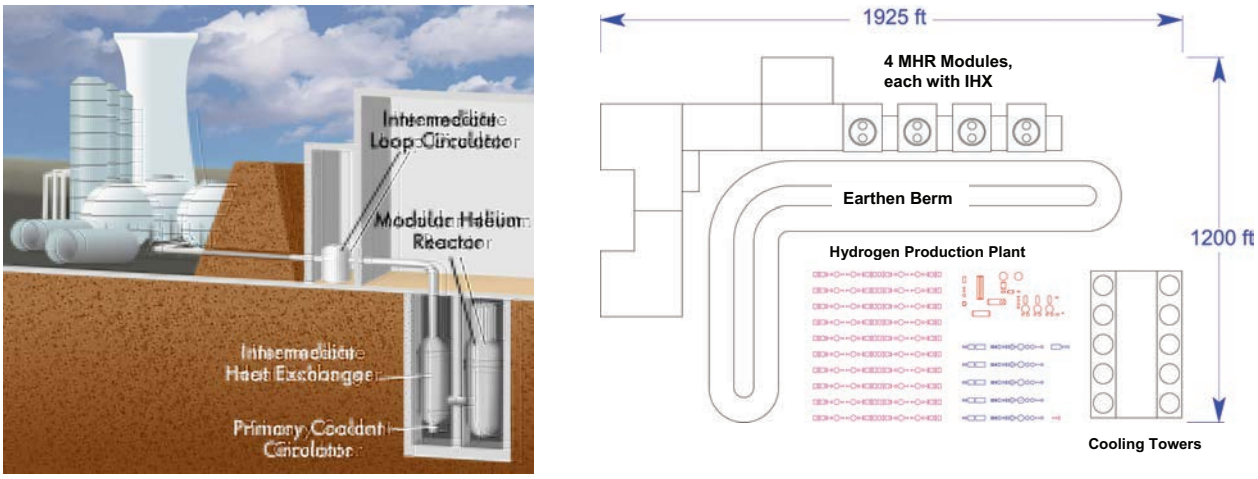

FIG. 178. Safe separation of nuclear and chemical section by earthen berm [93].

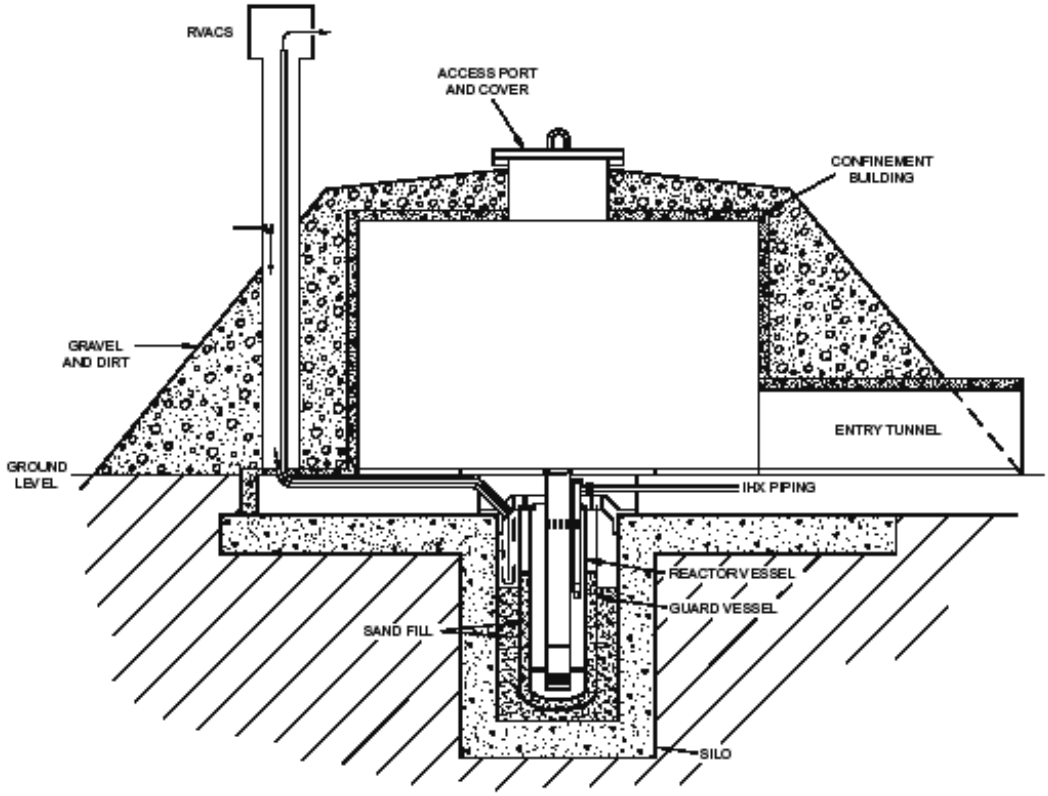

FIG. 179. Underground nuclear reactor STAR-H2 [448].

Other recommendations from the INL study include a 100 kg on-site limit for hydrogen storage, a quick pipe-out after production and the use of double-walled pipes for hydrogen transport. Also, the nuclear plant control room should be located outside the dispersion zone for chemical release.

7.4.4. Hazard from liquid hydrogen storage

For economic reasons in terms of storage and transportation, it makes sense to transform the product gas hydrogen into its liquid state. Also, for the concept of the HTTR combined with steam reforming, the feedstock methane was planned to be delivered in liquid form as LNG. In these situations, the storage vessel represents the

largest risk for the adjacent nuclear plant if the content is inadvertently released. The instantaneous release resulting from a catastrophic failure of the vessel can be excluded if the vessel arrangement is underground. The conceivable accident scenario here is the vessel opened at the top with the cryogenic liquid vaporizing into the atmosphere.

According to the IAEA recommended cryogenic pool vaporization rates, 10% of the liquid flash-vaporizes, while for the remainder, the rates are set at 10 mm during the first minute and 0.5 mm/min afterwards. Experimental data, however, with liquid hydrogen (LH_2) in a dewar (i.e. no major heat input from walls or bottom) were found to be much higher, in the range of 30–66 mm/min [450]. Regression rates of burning LH_2 pools can even be enhanced up to 1000 mm/min if solid oxygen formed at the surface to the open atmosphere reacts with the hydrogen in violent, unstable burning. Assuming an underground storage vessel to contain about 100 t of hydrogen as LH_2, it could have the approximate dimensions of 15 m diameter and 10 m height. For the above given range of regression rates, the contents of such a vessel if open at the top would vaporize completely within 2–5 h. This is an extremely long time in terms of the atmospheric dispersion process for hydrogen, particularly with regard to its extremely strong positive buoyancy, meaning that it will be impossible to have all hydrogen available involved in a potential vapour cloud explosion.

An important result from earlier experiments with the release of LH_2 and subsequent ignition conducted in the late 1950s was that neither detonation nor the tendency toward a detonation was observed. Detonation hazards from an open LH_2 pool appeared relatively slight when in contact with solid air, and were the most severe if oxygen was accumulating. Ignition of the vapour above the pool (depth: 50–300 mm) was by either spark or flame source in the range of up to 8 s after spillage. The later the ignition, the larger was the developing fire ball. The hydrogen flames principally remained limited to the pool size, but were largely extended, up to 50 m, vertically. They were even able to ignite separated flammable gas pockets creating a new fire ball. The radiation heat after ignition did not significantly change the pool regression rate. In the case of delayed ignition, observed explosions were presumably due to condensed air reacting with the pool [451].

Partial obstruction near the pool was found to lead to higher pressure pulses, making it advisable not to have any barricading structures around LH_2 storage vessels. A detonation in a free hydrogen–air mixture, however, seems to be highly unlikely. Only when using strong igniters or by the initiation of a shock wave was it possible to detonate the hydrogen–air mixture following the spillage of small amounts of LH_2 [452].

In Japan, experimental work with LH_2 release and subsequent ignition has led to similar results. Burning rates expressed as liquid level regression were measured to be 24 mm/min, which was six times that for gasoline. Both ‘normal’ and the much more violent ‘abnormal’ burning with very high flames was observed, when the burning LH_2 came into contact with solidified oxygen from the air [453].

7.5. INTERACTION BETWEEN NUCLEAR AND CHEMICAL SYSTEM

A system with an endothermic chemical reactor connected to an HTGR exhibits thermal dynamics which differ significantly from those of the nuclear reactor itself.

In the Japanese HTTR core, the coolant temperature is primarily controlled by the reactor power, not by the coolant flow rate. Nuclear heat is transferred to the helium gas with the result of a linear relationship between reactor power and helium temperature. On the other hand, in the chemical reactor where endothermic reactions take place, the heat input necessary to cause the reaction increases tremendously with increasing reaction temperature due to the Arrhenius type temperature dependence of the reaction rate. Temperature fluctuations are transferred to the nuclear plant and might affect its operation. A temperature change of more than 15°C compared to ‘normal’ will shut down the reactor. Therefore the development of an adequate control technology is required in order to balance the difference in the thermal dynamics between the nuclear and chemical reactor. For the HTTR, the selected design and arrangement of the steam generator with a maximum allowable temperature change of 10°C at the outlet is expected to fulfil this control function.

A higher probability of malfunction or failure is expected on the process side rather than on the power generation side. Safety measures are required to mitigate potential disturbances resulting from a malfunction or failure in the hydrogen production system to allow for a continuous reactor operation without reactor scram.

The safety design of the nuclear plant is based on the defence in depth concept. Therefore, in the case of a reactor scram, the propagation of thermal turbulences should be stopped in the secondary loop. The safety requirement for this event is to limit the secondary helium temperature variation within ±15 K at the inlet of the IHX to prevent a reactor scram.

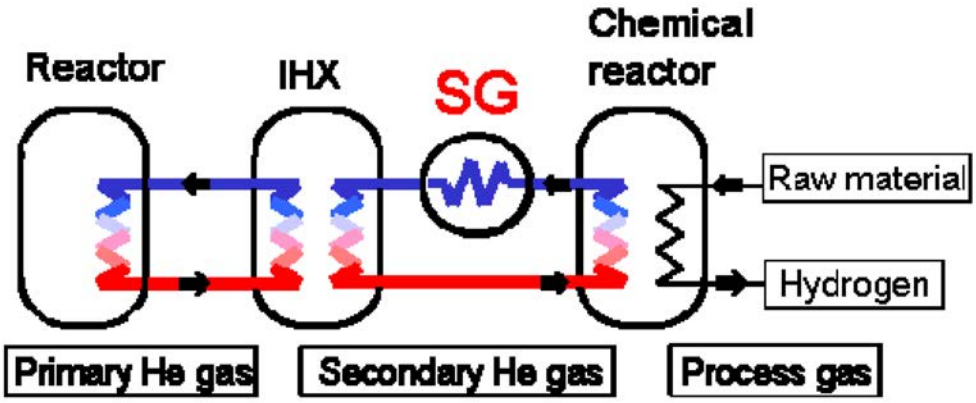

FIG. 180. Arrangement of steam generator in HTTR circuits [454].

7.5.1. Analysis of HTTR with steam–methane reforming system

The operating procedures for startup and shutdown are similar, but reversed. Before startup, nitrogen is supplied at a pressure of 2.2 MPa. The HTTR is then started. When the secondary helium gas is heated to above 500°C and the steam generator is controlled at the rated pressure of 5.0 MPa, steam is gradually supplied to the system and nitrogen is released into the environment with this steam by switching the flow line. With the steam flow rate constant at rated conditions and the helium gas temperature at the inlet of the steam reformer increased to 700°C, methane feedgas is supplied to the system. Even during low startup system operation, a stepwise increase in the feed flow rate by 10% (as it is difficult to control the feedgas at low flow rate levels), results in a stable helium gas temperature level at the inlet of the IHX due to the influence of the steam generator. After 60 h, the helium gas temperature reaches 950°C and the entire system can be operated automatically.

If the methane supply system is shut down due to a loss of electric power or a malfunction of the control system, the helium gas temperature at the steam reformer outlet will increase. The steam generator installed downstream of the steam reformer in the secondary loop (Fig. 180) can cool the hot helium gas down to the saturation temperature of the steam, thus providing a stable controllability for any disturbance at the steam reformer due to the large heat sink capacity and preventing a reactor scram. However, if the feedwater supply is interrupted, the steam generator cannot continue to operate. It is therefore proposed to re-use the generated steam as feedwater after condensation in the radiator.

The steam reforming system is a ternary cooling system. A change of the flow rate of either the feedgas or the water to the steam reformer induces a thermal disturbance of the helium outlet temperature on the reformer due to the change of the amount of heat input for the reforming reaction. If the temperature of the helium returning to the IHX exceeds the allowable limit, the reactor will scram.

In order to prevent a scram of the HTTR due to a loss of feedwater, the hot helium gas is cooled by the steam generator and the generated steam from the steam generator flows into a natural ventilation type radiator connected to the steam generator. The condensed water is then supplied to the steam generator as feedwater. The steam generator can keep its water contents for normal operation. The total heat capacity is about 8.8 MW, representing the heat capacity of the steam reformer, super heater and steam generator. Furthermore, if a pressure drop is detected in the cooling system due to pipe failure or valve malfunction, and the water level in the steam generator is low due to interruption of the feedwater flow, the valve in the steam line closes, while that in the radiator steam supply line opens passively through an automatic air supply system. Generated steam is supplied to the natural convection type radiator and is cooled down. Condensed water is recycled to the steam generator as feedwater. This system does not require electric power or feedwater.

Static calculations of the cooling ability of the steam generator have been carried out, showing that a reduction of the feedgas changes the outlet temperature of the reformer correspondingly. But the steam generator mitigates the temperature variation within 5°C. The continuous cooling of the hot helium gas by the steam generator allows the HTTR steam reforming system to continue at normal operation. A transient analysis assuming a stepwise decrease in process gas flow rate by 20% indicated that increased heat input to the steam generator due

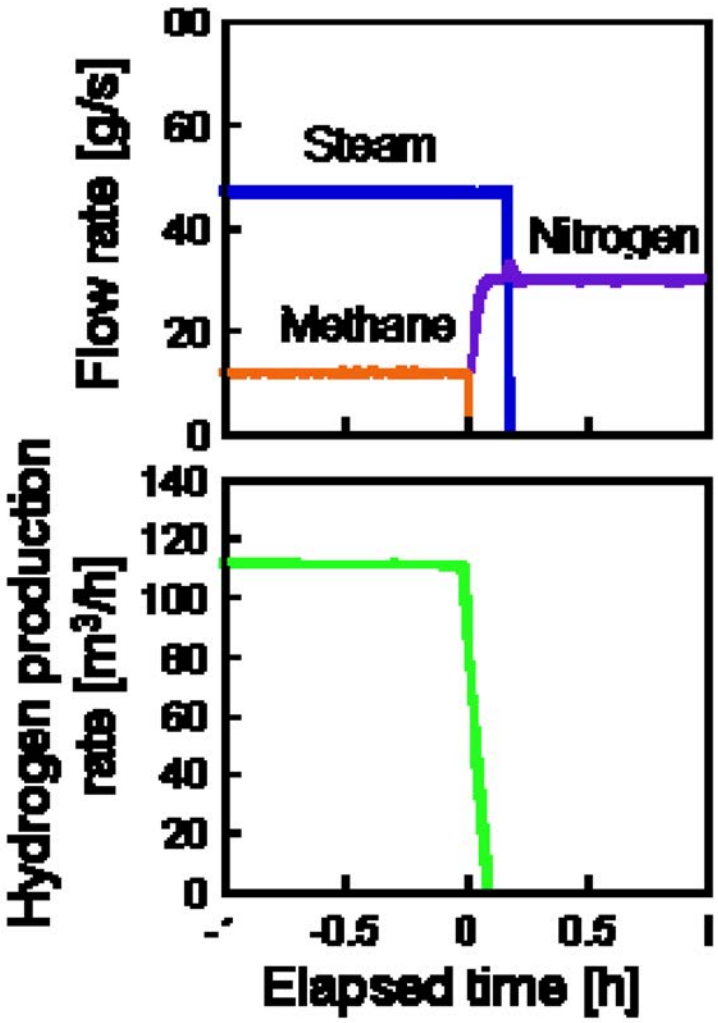

FIG. 181. Flow rates of methane, steam, nitrogen, and production rate of hydrogen during the system controllability test [454].

to increasing helium inlet temperature only results in an increase in steam quality at saturation temperature due to boiling, but not in an increase of the steam temperature.

Performance tests were conducted in 2001–2002 in a mock-up test plant to check the ability of hydrogen production and controllability of the experimental facility. The test of system controllability was made by simulating the accident scenario of a loss of chemical reaction, i.e. the disconnection from the methane feed, representing the worst case with regard to temperature fluctuations transferred to the secondary helium, and examining the transient behaviour of the H_2 production system and temperature fluctuations at the steam generator. In parallel, the experimental data were used for dynamic analysis code validation [210].

The mock-up plant included all key components described in Section 4.1.3.3. As illustrated in Fig. 181, nominal flow rates in the test were 12 g/s of methane and 47 g/s of steam, when — at time 0 — methane feed, and thus hydrogen production, was shut off. The helium temperature at the steam reformer outlet increased from 632 to 837°C after 1.2 h. At the same time, the temperature at the inlet was raised from 531 to 762°C. Helium temperatures at the steam generator outlet (nominal: 263°C) were observed to fluctuate not more than within the range of –5.5 to +4.0 K, which is within the specified range of –10 to +10 K required for HTTR-SMR operation. The test demonstrated that the steam generator in the HTTR-SMR system can effectively be used as a thermal absorber to mitigate temperature fluctuations created by the chemical side.

7.5.2. Analysis of HTTR with sulphur–iodine process

The S–I process is classified as a non-nuclear-grade system. Safety function for continuous operation is kept by the backup nuclear-grade equipment during S–I process abnormal conditions. The thermal load disturbance absorption system, the steam generator, is one of the backup equipment. The S–I process does not need any safety function for continuing reactor operation [455]. In addition, a method for preventing tritium permeation has been proposed which allows the S–I process to be released from radioactivity control area. The only remaining abnormal events which need to be evaluated as part of a reactor safety assessment would be the fire and explosion hazards caused by combustible gas leakage from the S–I process and toxic gas leakage that may jeopardize the operator room [423]. The anticipated operational occurrences (AOOs) and accident scenarios identified for the HTTR-IS are listed in Table 50.

7.5.3. Analysis of GTHTR300C with sulphur–iodine cycle system

For the Japanese VHTR design, GTHTR300C, it is planned to have three control valves installed in the primary circuit in order to mitigate the turbulence of inlet helium temperature of the gas turbine and keep the rotation speed of the generator constant. In the case of pressure loss in the secondary circuit, the hydrogen production system is disconnected from the IHX by an isolation valve. The helium pressure between the IHX and isolation valve is recovered by the helium supply system to continue power generation operation [55].

TABLE 50. ANTICIPATED OPERATIONAL OCCURRENCES AND ACCIDENT SCENARIOS IN HTTR-IS SYSTEM [423]

AOO-1:	Increase in IHX PGC revolution The coupling of the IS process would change the operating conditions at the secondary side of the IHX from the original HTTR safety review. Hence, the quantitative value of the evaluation items would change.
AOO-2, 3:	Closing and opening of air cooler bypass flow control valve The HTTR modification decreases the mass flow rate of the pressurized water in the primary pressurized water cooler since the secondary pressurized water cooler would be replaced by other components, e.g. IS process, SG, etc. Hence, the quantitative value of the evaluation items would change.
AOO-4:	Opening of exhaust valve in secondary helium storage and supply system The HTTR modification would change the inventory of the secondary helium cooling system and would require a flow capacity increase of the exhaust valve. Hence, the quantitative value of the evaluation items would change.
AOO-5:	Closing of isolation valve in secondary helium cooling system The event was newly identified because of the installation of isolation valves in the secondary helium cooling system.
ACD-1:	Rupture of inner tube in co-axial hot gas duct in secondary helium cooling system The IS process coupling decreases secondary helium cooling system flow rate from the original HTTR safety review. Hence, the quantitative value of the evaluation items would change.
ACD-2:	Rupture of piping in secondary helium cooling system The HTTR modification requires the design change of the secondary helium cooling system in order to provide heat to the IS process. Hence, the quantitative value of the evaluation items would change.
ACD-3:	Rupture of IHX heat transfer tube The HTTR modification requires installation of the isolation valves in the secondary helium cooling system since the secondary helium cooling system will be modified to penetrate the CV and R/B in order to provide heat to the S–I process. Hence, the progression of the scenario would change.
ACD-4:	Rupture of S–I process boundary The rupture of the S–I process boundary would cause a leakage of combustible and toxic gases and result in an explosion and operator poisoning. The event should be evaluated as an external event by using appropriate design parameters.

The hydrogen production system is coupled with the HTGR via a heat transfer loop. The safety requirements for all types of reactor system are to protect people and the environment from harmful effects of ionizing radiation. The exposure of the public remains as low as reasonably achievable (ALARA) in operational states, and radiological risk is acceptably low in accident states. The defence in depth concept is employed to prevent accidental release of radioactive materials.

The hydrogen production system coupled with the HTGR should be a non-nuclear grade chemical plant to reduce construction and maintenance costs, because hydrogen produced by the cogeneration HTGR system must economically competitive with hydrogen produced by the conventional fossil system. With the following requirements, a non-nuclear grade hydrogen production system in a cogeneration HTGR is achievable:

— The HTGR can continue safe operation independent of operational conditions of the hydrogen production system;
— The heat transfer loop, which provides hot helium gas from the IHX to the hydrogen production system, is not required to perform any nuclear safety function to prevent AOOs and accidents;
— Events originating in the hydrogen production plant do not affect the safe operation of the HTGR.

The functions of the heat transfer loop are primary helium cooling, pressure load control on the IHX heat exchanger tubes and impurity concentration control during normal operation. Thermal load degradation of the hydrogen production system can be detected as a temperature increase at the turbine inlet. Actuation of these control valves decreases the helium flow in the core. The reactivity control system reduces the reactor power to keep the reactor outlet helium temperature at the rated operating condition of 950°C.

7.6. RELEASE OF TOXIC MATERIALS

Similar to the nuclear site, the mandatory safety demonstration for the industrial site is based on risk evaluation and analysis of the risk reducing measures taken by the operator. A risk analysis leads to the ‘determination’ of major accident scenarios in terms of potential impact outside the site limits.

The classic scenario involves a loss of the containment for the hazardous material by, e.g. leakage, pipe rupture or the catastrophic failure of a tank, and may lead to:

— Pool formation with evaporation/vaporization;
— Jet or pool fire;
— Explosion as vapour cloud explosion (VCE) or boiling liquid expanding vapour explosion (BLEVE) connected with pressure effects and missiles;
— Toxic dispersion with effects on human health.

The orifice through which the material escapes can vary over different shapes and sizes. The leaking fluid can flow into different geometries. And finally it is the thermodynamic conditions of the fluid which determine its release behaviour.

In the case where there is no early ignition, the vapour cloud shape is further determined by density differences, atmospheric conditions and topography. Several phases of a gas cloud formation can be distinguished. In the early phase, the gas cloud is still unmixed and usually heavier than the ambient air. Heavier-than-air substances result in near-ground, flat clouds. The following phase is characterized by a gradual entrainment of air from outside into the gas cloud, enlarging its volume and changing its temperature and concentration. In the final phase, due to atmospheric dispersion, density differences between the cloud and ambient air will be levelled out. The jet release of a substance under pressure is usually connected with the formation of aerosols characterized by an inhomogeneous concentration distribution.

The spreading of a gas cloud in the atmosphere is strongly influenced by the wind conditions, which change with height. Vertical wind profiles can be determined as a function of the so-called stability categories depending on the temperature conditions. As an example, Pasquill suggested the categories A, B and C for unstable, D for neutral, and E and F for stable conditions. The spreading mechanism of a gas in the atmosphere is mainly by mixing with the ambient air.

For large amounts released, the evolving gas cloud can itself influence the atmospheric wind conditions changing wind and diffusion profiles in the atmosphere. This so-called vapour blanket effect can be observed particularly at low wind velocities, where the atmospheric wind field is lifted by the gas cloud and the wind velocity inside the cloud drops to practically zero. For low wind speeds, additional effects such as further heating of the gas cloud due to energy supply from diffusion, convection or absorption of solar radiation, as well as radiation from the ground will play a certain role, since they reduce gas density and enhance positive buoyancy.

The turbulence structure of the atmosphere is composed of large scale turbulence described by the large scale wind field, and of isotropic turbulence, which is a rapid variable superimposed on the medium wind field. While larger eddies are responsible for the cloud meandering, the small eddies eventually determine the spreading of the gas cloud. Further factors influencing the turbulence structure within a gas cloud are velocity gradient (sheer forces), current created by buoyancy forces and heat transfer from/to the ground. The topography also has a strong influence on the atmospheric wind field and thus on the spreading of the gas cloud. Obstacles such as buildings or other barriers may deflect clouds and increase the degree of turbulence.

Chan [456] performed calculations for the numerical simulation of LNG vapour dispersion from a fenced storage area and found that a vapour fence can significantly reduce the downwind distance and hazardous area of the flammable vapour clouds. However, a vapour fence could also prolong the cloud persistence time in the source area, thus increasing the potential for ignition and combustion within the vapour fence and the area nearby. In the presence of buildings or other obstacles, the wind direction is also expected to play an important role for the cloud dispersion, due to the shielding effects of these obstacles. The obstacle effect is twofold: in one way it inhibits gas convection, but on the other hand it creates turbulence, thereby increasing gas dilution, extending the flammable region and even accelerating flames.

Since the S–I process generates toxic gases such as SO_2, SO_3 and HI, toxic gas inflow into the reactor control room must be prevented. Layout and design of systems such as the ventilation and air-conditioning system and gas-sensing system will be performed and evaluated. Toxic gas diffusion and risk analysis are taken into consideration in order to evaluate the toxic gas effect in the HTTR-IS system design [455].

7.7. INTERNATIONAL REGULATIONS FOR HANDLING HAZARDOUS MATERIALS

7.7.1. IAEA Safety Guides

Apart from the need to meet the criteria specified in the Codes of Practice on siting and design, the plant designer has to assess the hazardous potential from external human induced events. For this purpose, the respective IAEA Safety Guides discuss information and design criteria required for the various categories of events with respect to siting [457] and design [458].

Fires due to human induced events may have safety significance. Adequate precautionary measures are the reduction of the amount of combustibles in the vicinity of the nuclear plant and the installation or strengthening of protection barriers. Additional design features may be the redundancy of safety systems, physical separation by distance, separate fire compartments, and fire detection and extinguishing systems. Load-bearing concrete structures are recommended to have a minimum thickness of 0.15 m to withstand a 3 h standard fire. The allowable temperature for reinforced bars and structural steel is 500°C for short term fires of less than 6 h.

In the case of gas cloud explosions, the capacity of the plant structures to resist blast overpressures has to be assessed. Potential secondary effects to be considered are fire, loss of off-site power, smoke and heated gases, ground motion and missiles. The pressure–distance relationship developed for TNT can be utilized for solid substances. Structures with reinforced concrete walls with a thickness of at least 0.5 m will normally be capable of withstanding substantial overpressures.

Protection measures are similar to those for fire. In addition, ventilation systems should be designed such that an ingress of flammable gases is prevented. Also, vapour accumulation in confined external areas should be prevented by avoiding long alleys and inner courtyards or providing adequate openings. Categories of events related to fire and explosion from flammable fluids are given in Table 51. These possible events resulting from activities nearby the nuclear plant are strictly characteristic to the region. Therefore, both the actual facilities/activities and those anticipated during the expected plant lifetime must be taken into account. The initial events given in the above table may trigger follow-on events with serious impacts on the nuclear plant, as described in Table 52.

TABLE 51. IDENTIFICATION OF SOURCES AND ASSOCIATED INITIAL EVENTS [457]

Facilities and transportation systems	Relevant features of the facilities and traffic	Initial event
Oil refinery Chemical plant Storage depot Pipelines Other nuclear facilities	Quantity and nature of substances Flowsheet of process in which hazardous materials are involved Meteorological and topographical features of the region Existing protective measures in installation	Explosion Fire Release of explosive, flammable, corrosive, toxic or radioactive clouds Ground collapse, subsidence
Railway train, wagon Road vehicle Ship, barge	Frequency of passage Type and quantity of hazardous material associated with each movement Features of the vehicle (incl. protective measures) Meteorological and topographical features of the region	Explosion Fire Release of explosive, flammable, corrosive or toxic clouds

TABLE 52. IMPACT ON NUCLEAR POWER PLANTS AND ITS CONSEQUENCES [457]

Impact on the plant	Parameters	Consequences of impact
Pressure wave	Overpressure at the plant as a function of time	Collapse of parts of structure or disruption of systems and components
Missile	Mass Velocity Shape Size Kind of material Structural features Impact angle	Penetration, perforation or spalling of structures, or disruption of systems and components Collapse of parts of structure or disruption of systems and components
Heat	Flux	Disruption of systems or components Ignition of fire combustibles
Smoke and dust	Composition Concentration and quantity as a function of time	Blockage intake filters Habitability of control room and other important plant rooms and affected areas
Flammable and explosive gas	Concentration and quantity as a function of time	Permeation of the plant and fire or explosion inside plant Explosion or fire on-site
Corrosive, toxic, radioactive gas, aerosols	Concentration and quantity as a function of time Corrosive, toxic limits	Permeation of the plant Habitability of control room and affected plant areas Corrosion and disruption of systems or components
Ground shaking	Response spectrum	Mechanical damage
Flooding	Level of water Velocity of impacting water	Damage to structures, systems, and components
Subsidence	Settlement, differential displacement, settlement rate	Collapse of structures or disruption of systems and components

The evaluation of all available information should be carried out such that in a first step, a screening procedure is carried out. This can be done by using a screening distance value (SDV) for certain sources, beyond which these sources become insignificant, or a screening probability level (SPL) as limiting values; or it can be a pragmatic approach based on expert judgement. The SDV and SPL must be chosen conservatively small to keep the risk resulting from such human induced hazards at an acceptably low level. Some Member States use an SDV in the range of 5–10 km for explosions, and a value in the range of 1–2 km for fires.

Sources can be stationary or mobile. If an industrial area is considered, those can be process units, storage tanks, pipelines or on the other side tank trucks, cargo ships. Further compulsory information deals with the nature and quantity of the hazardous materials, flowsheets of the processes, dimensions of the facilities, pipeline characteristics, operating conditions, traffic facilities (harbours, railways, roads), meteorology of the region and its topography. If practicable, a full quantitative risk analysis should be conducted to identify accident scenarios and the magnitude of the associated radiological consequences.

All potential sources of explosions not eliminated by the screening process should be evaluated in further detail. Usually it is sufficient to limit considerations to the dominant sources only. A design basis explosion should be established. The evaluation should be based on the pessimistic assumption that the maximum amount of explosive material is involved in the explosion (unless there are very good reasons not to do so). For mobile sources, the analysis should include the frequency of shipments increasing the probability of a hazard.

For the establishment of a design basis explosion, the TNT equivalent is usually taken to define the relation between the weight of the explosive material and the safety distance, unless this relationship has been directly developed from experiments for certain chemicals. Then the parameters of pressure waves and ground shock can be estimated. Hazards arising from flammable liquids should be evaluated in terms of the:

— Location and quantities for each facility;
— Probability of a vessel rupture or a leak;
— Maximum quantities released and respective release probabilities;
— Probability of release from a mobile source in transit;
— Places nearest to the nuclear power plant where hazardous pools may collect.

For the design basis event, the location and size of a pool of the flammable liquid and potential flow paths should be assessed, as well as the related danger to the nuclear plant. Liquefied gases vaporize after release and form a vapour cloud that may drift towards the nuclear plant, with the potential effects of either an external explosion or a penetration of the building to endanger personnel or safety systems. The behaviour of the vapour cloud strongly depends on the meteorological conditions. Therefore, source positions with predominant wind direction away from the nuclear plant would reduce the probability of an event. The detailed evaluation includes the assessment of the:

— Probability of occurrence of an event;
— Quantity released;
— Probability of a vapour cloud drifting to the nuclear plant;
— Dilution due to atmospheric dispersion;
— Probability of ignition of the flammable vapour cloud inside or outside the plant.

For sub-cooled liquefied or pressurized gases, particular care has to be given to the release behaviour in terms of their transient vaporization rates.

The application of Gaussian type dispersion models to simulate cloud drifting is also mentioned; however, this finds its limits if density differences between cloud and ambient air cannot be neglected, and if topography or any obstruction might influence the dispersion behaviour. In this field, modern calculation tools are available such as advanced box models or 3-D CFD codes, which might be applied for comparison purposes or for detailed analyses of partial aspects.

Boundary conditions for the case of sub-cooled liquefied gases as recommended in the Guide are the assumptions that:

— For small amounts of leakage, all liquid is immediately vaporized;
— For large amounts of leakage, the liquid covers all the surface area of the pool and a fraction of 10% is assumed to vaporize spontaneously in an initial gaseous puff, followed by vaporization or regression rates of 10 mm in the first minute and 0.5 mm thereafter.

7.7.2. European directives

7.7.2.1. Seveso I

As a consequence of the Seveso accident in 1976, where a highly toxic vapour cloud of dioxin was released into the atmosphere by a chemical plant, Member States of the then European Economic Community (EEC) decided to reinforce regulation on industrial activities. The so-called Seveso Directive (82/501/EEC) [459] was adopted in 1982 aimed at the prevention and control of similar accidents in the future. Its scope was later extended to the storage of dangerous substances, and was subsequently reviewed in close cooperation between the European Commission and the European Process Safety Centre (EPSC), an international, industry based organization dealing with process safety and safety management systems.

7.7.2.2. Seveso II

In 1996, the Seveso II Directive or Council Directive 96/82/EC [460] was adopted, replacing the old one and including new requirements related to safety management systems, emergency planning and other areas; the Seveso II Directive was also in harmony with the IPPC Directive 96/61/EC concerning integrated pollution prevention and control. After a certain transition period for adjustment of national laws to comply with the new directive, the directive became mandatory in 1999 for both industry and public authorities. The main objective of Seveso II, which also applies to non-commercial establishments, is the prevention of major accidents with the release of dangerous substances or mitigation of the consequences to humans and the environment. The directive distinguishes between lower tier and upper tier establishments, characterized by exceeding or not exceeding specified threshold quantities for certain substances. Concerning hydrogen, in the directive the lower threshold was fixed at 5 t and the higher threshold at 50 t. However, the Member States are free in adopting stricter measures than those of the directive.

The new directive defines the general obligations of the establishment operator as well as the general duties of the ‘competent authorities’ (CAs) of the Member States. It recognizes and accommodates a wide range of management systems. Operators have to demonstrate in a hierarchy of written documents that technical and organizational measures for a safe operation are being taken. The CAs have to examine these documents prior to the start of construction or operation. The level of detail and specificity of the documentation is increasing through the levels from a written Major-Accident Prevention Policy (MAPP) via a Safety Management System (SMS) and Internal Emergency Plan to Working Documents. The background of the requirement of an SMS is the fact that in 90% of known major accidents, management failure such as poor organization or inadequate training was identified.

7.7.2.3. Explosion protection

The European directive 94/9/EC [461] on Equipment and Protective Systems Intended for Use in Potentially Explosive Atmospheres, also known as ATEX 100a, went into force in 1996. It refers to the safety of both electrical and non-electrical equipment, protective systems, components, or safety controlling or regulating devices which are being put on the market and taken into operation in potentially hazardous locations. It applies to all industrial, explosion-endangered areas and mining areas where flammable gases, vapours, mists or dusts in mixtures with air under atmospheric conditions (temperature range from –20 to 40°C, absolute pressure range from 0.08 to 0.11 MPa) can be present. This directive divides equipment and protective systems into groups and categories.

Another European directive of the European Parliament and of the Council, named 1999/92/EC or ATEX 118a, on Minimum Requirements for Improving the Safety and Health Protection of Workers Potentially at Risk from Explosive Atmospheres [462] was adopted in December 1999. This directive provides for a classification into zones of the places where explosive atmospheres may occur. Hazardous locations are divided into two groups:

Group I: Mining with firedamp (= flammable gases contained in coal) or coal dust;
Group II: All other areas with potentially explosive atmospheres formed by flammable gases, liquids, combustible dusts.

TABLE 53. AREA CLASSIFICATION OF GROUP II WITH POTENTIALLY EXPLOSIVE ATMOSPHERES FOR EUROPEAN HAZARDOUS LOCATIONS

Gases	Dusts	Frequency of explosive atmosphere	Equipment to be used
Zone 0 Category 1G	Zone 20 Category 1D	Continuously or long periods or frequently	Protection level very high, two independent means of protection
Zone 1 Category 2G or 1G	Zone 21 Category 2-D or 1D	Occasionally	Protection level high, suitable for normal operation and frequent occurrence of disturbances, faults are expected
Zone 2 Category 3G or 2G or 1G	Zone 22 Category 3-D or 2-D or 1D	Unlikely in normal operation, but if it occurs then only for short periods	Protection level normal, suitable for normal operation

Potentially explosive areas are subdivided into zones (1999/92/EC) or categories (94/9/EC) to describe the potential frequency of the occurrence of an explosive atmosphere (Table 53).

For ignition by sparks or flames, flammable gases or vapours are classified into four groups:

—Group I: firedamp in mines (methane);
—Group IIA: least readily ignited gases (e.g. propane, benzene);
—Group IIB: more readily ignited gases (e.g. ethylene);
—Group IIC: most readily ignited gases (e.g. hydrogen, acetylene).

8. USES OF HYDROGEN

8.1. CURRENT USES OF HYDROGEN

The first industrial applications of hydrogen were in the early 19th century as a fuel gas for lighting and heating. The hydrogen was mainly produced from the anaerobic reaction of hot coal and water vapour. It was used for many years in commercial and residential applications until it was eventually replaced with natural gas.

Of the annual production of 8 EJ or ~190 Mtoe of hydrogen, most is in the form of ‘captive’ hydrogen (consumed at the producer’s place) (Fig. 182). Only an estimated 5% of the total hydrogen production is supplied as ‘merchant’ hydrogen (produced centrally und transported to the consumer), requiring the appropriate infrastructure for transportation and distribution. Other market types are by-product and stranded hydrogen produced in the chemical industries and either used internally as a raw material or fuel, or simply vented or flared if no marketing infrastructure is available. Only 1% of current hydrogen production is used for direct energy purposes. The hydrogen market in Europe is 64% captive hydrogen, 27% by-product hydrogen and 9% merchant hydrogen [463].

There is a wide variety of industrial customers for hydrogen which require, depending on the application area, different quantities and purities of hydrogen. The largest consumer of hydrogen is the chemical industry, with a demand for hydrogen growing at an annual rate of 7–10% [465]. As is shown in Fig. 182, about half the total hydrogen is used for producing ammonia (fertilizer), 35% is used in petroleum refining processes (tendency increasing due to heavier crude oils), 8% is used in methanol production, 1% is used as a fuel in space programmes, and the residual amount is used for other purposes [464]. The most important processes for producing hydrogen in refineries are steam reforming of natural gas (59%) followed by off-gas purification (35%) [107]. The merchant suppliers may operate a hydrogen plant or a hydrogen supply pipeline. Figure 183 shows the specific demand for hydrogen in refineries in the USA over the past 25 years, revealing a strong increase in recent years due to the increased processing of lower quality, heavy crude oils and other unconventional fossil resources. For a present throughput of 20 Mbbl/d, this translates into a hydrogen demand of 28 000 t/d [144].

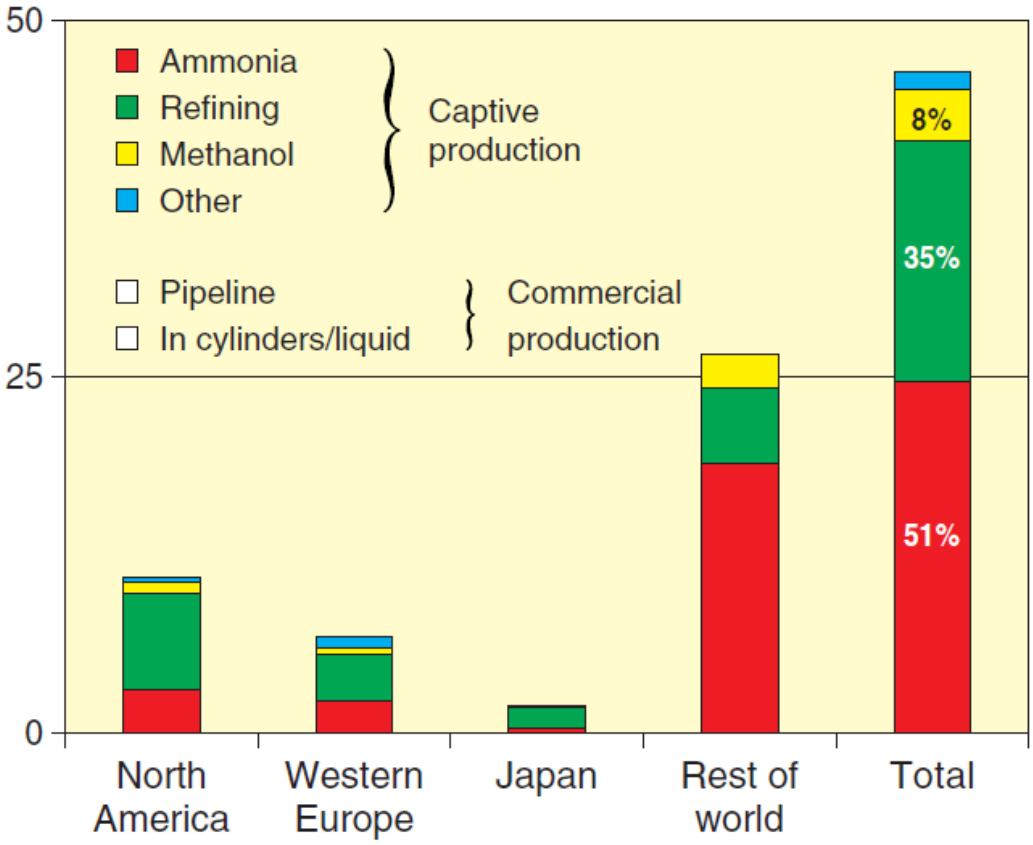

FIG. 182. Global hydrogen production and use (in million t) [464].

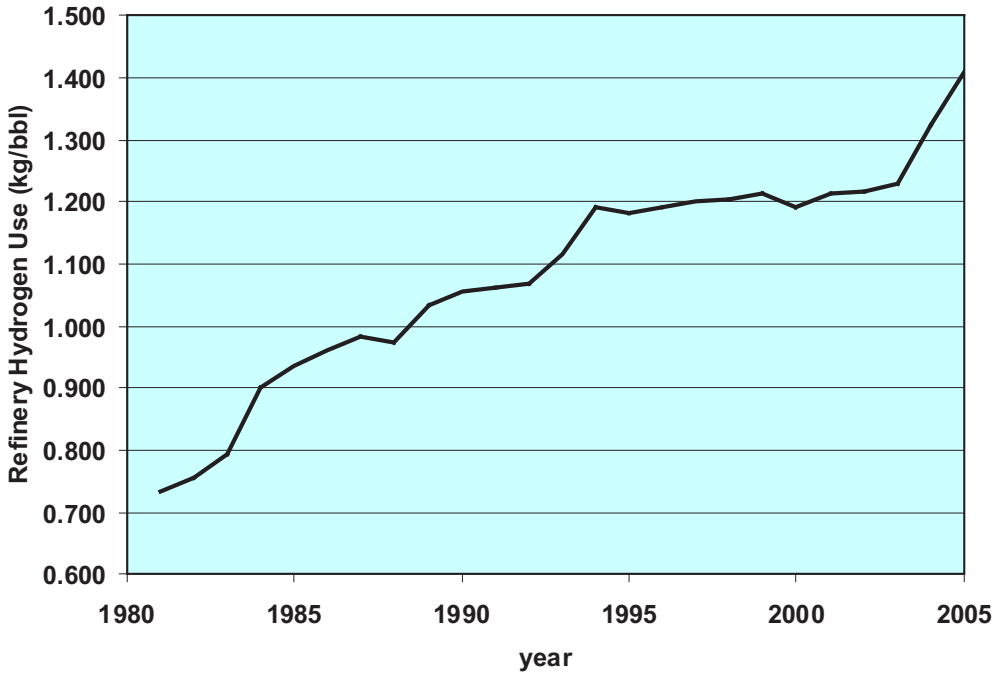

FIG. 183. Hydrogen consumption in the US refineries between 1985 and 2005 [144].

8.1.1. Non-energetic and indirect energetic use

Indirect energetic use of hydrogen occurs in refineries where the H_2 is used in catalytic cracking operations or hydro-treating to upgrade heavy and unsaturated compounds into lighter and more stable species. It is also used in the production of synthetic fuels via Fischer–Tropsch synthesis, of methanol, or of SNG. Furthermore, it is used in the hydrogenation of coal and heavy crude oil. Hydrogen is also used to remove sulphur from crude oil and gasoline, and to purify gases, e.g. by capture of oxygen traces in argon. Other H_2 consuming processes are welding and glass production. In the glass production process, the hydrogen is used as an oxygen scavenging atmosphere (~6% H_2 and ~94% N_2), and to prevent oxidation of the large tin bath in the float glass process. Polishing and melting of high quality optical glass is done by means of a soot free hydrogen flame. In the food industry, the properties of fats and oils are changed through hydrogenation of organic intermediate products like amines and fatty acids, making food less susceptible to oxidation and spoilage.

Specific applications for liquid hydrogen [466] are in the metal industries, where LH_2 is used in the metal production process directly (e.g. tungsten, tungsten carbide, molybdenum metal powder), and, if mixed with inert gases, in secondary processes to act as a reducing atmosphere in heat treating, sintering and copper brazing. In the electronics industry, highly pure hydrogen is mainly needed as a carrier gas for active elements such as arsine and phosphine in the manufacture of integrated circuits, polycrystalline silicon for semiconductors, optical fibres for communication, or fused quartz. The pure water vapour required is generated from mixing oxygen with vaporized LH_2. The hydrogen is either used as atmosphere or as a clean burning fuel. In power plants, LH_2 can be used for the cooling of large electric turbogenerators and to protect piping in nuclear reactors.

The following is a list of non-energy and indirect energy applications of hydrogen:

— Heavy oil hydrogenation for the production of preprocessed crude oil;
— Hydro-cracking of heavy distillates, which are difficult to reform, by using hydrogen and catalysts to convert into lighter fractions (kerosene, light and heavy gas oil, fuel oil (‘naphtha’); cracking by heating or catalytic reforming to obtain various fuel qualities;
— Hydro-treating, i.e. a process that reduces sulphur or nitrogen content of the feed;
— Hydro-processing, i.e. a process used for desulphurization and substantial removal of most other impurities (nitrogen, oxygen, heavy metals) from the products of distillation processes; for example, desulphurization of heating oil grade S by 80% requires approximately 146 Nm^3 of H_2 per toe;
— Fischer–Tropsch synthesis for the production of synthetic liquid fuels;
— Methanol synthesis, also for the production of base materials for plastics;
— Coal hydrogenation for the production of synthetic oil;
— Methanation for SNG production;
— Chemical processing to manufacture chlorine, caustic soda, and hydrogenated non-edible oils for soaps, insulation, plastics, ointments and other chemicals;
— Hydrogenation of organic interim products for the production of polyamides, cyclohexane, fat alcohols, fat hardening;
— Synthesis of ammonia (NH_3) for the production of fertilizer and synthetic materials (acrylic fibres);
— Oxo-synthesis for alcohol production;
— Pharmaceuticals to produce sorbitol, which is used in cosmetics, adhesives, surfactants and vitamins;
— Direct reduction of iron ore for sponge iron production, raw iron in the metal industries;
— Metallurgy to use pure hydrogen/oxygen flames in cutting, welding, brazing, annealing;
— Food processing to hydrogenate plant fats and oils, such as soybean, fish, cottonseed, and corn oil, for hardening;
— Electronics to create a special atmosphere for the production of semiconductor circuits;
— Reduction gas, protection gas in high temperature operations, such as glass manufacturing to use high-purity flames for cutting and welding, artificial gemstone/diamond production, to create high-purity atmospheres in furnaces or protective atmospheres for float glass production, sintering processes, silicon chemistry;
— Generator cooling in power industry.

8.1.2. Direct use as a fuel

Hydrogen was first used at a large scale in balloons and large airships (Zeppelin) toward the end of the 19th century, although here the hydrogen was not used directly as a fuel, but rather as a lighter-than-air gas to provide positive buoyancy. The idea of using liquefied hydrogen as aircraft and rocket fuel was considered as early as 1918, stressing that hydrogen had a larger heat content than any other fuel. A strong increase in the demand for hydrogen was given with the developing space aviation programme in the USA. The first systematic experimental investigations in the USA to investigate its use as a fuel for aircraft and to study the properties of LH_2 and the low temperature impact on materials started in the 1940s. But it was not until the 1950s that the attractiveness of LH_2 gradually became evident, despite its low availability and handling hazards. This was due to incentives for the development of airplanes for use at very high altitudes, advances in LH_2 technology, and experiments indicating that hydrogen could combust readily at low pressures. The first (of three) successful in-flight tests of an experimental hydrogen-propelled aircraft were made in the USA in 1957 with the 'Project Bee', a B-57B twin-engine aircraft. The one engine operated on hydrogen fuel for about 20 min at a speed of Mach 0.72 before the fuel tank ran empty [467].

In 1958–1959, it was decided in the USA to use LH_2 and LOX in the rocket engines of the upper stages of Centaur and Saturn, successful programmes of unmanned space missions and manned moon voyages, respectively, marking the first time that this high energy propellant combination was used in practical applications. The subsequent NASA programmes Apollo and Space Shuttle then applied LH_2 at a large scale. A total of 12 000 m^3 of LH_2 was necessary to fill up the tanks of the Saturn V carrier rockets. For a space shuttle launch, the required quantity of LH_2 is 2380 m^3, of which 1454 m^3 is for loading the external tank, with the remainder mainly used for pre-chilling of fuel lines or lost as boiloff [468].

Some 40 years ago, almost all produced LH_2 was consumed in the various space programmes. Although this share has decreased to about 25% today, the space industry still is one of the main customers for liquid hydrogen. Numerous examples for the application of LH_2 are described in more detail in Ref. [469].

8.2. USES OF HYDROGEN AS A RAW MATERIAL

8.2.1. Petrochemical industries

The refining of crude oil is a well established technology. The type of crude oil discovered and produced, however, is changing, with the average crude oil becoming gradually heavier connected with higher CO_2 emissions from the processing, a tendency which is expected to continue [470]. Industrial processes such as oil refining, shale oil production and tertiary oil recovery require massive quantities of hydrogen and high temperature heat/steam. Temperatures required for petroleum refining processes are mainly in the range of 500–600°C, but may sometimes reach 950°C.

From a typical refinery capacity of 180 000 bbl/d or 10.55 million t/a, approximately 10 million t/a of refinery products are being generated. This corresponds to an energy consumption of about 5.5% of the energy content of the oil processed mainly in the form of high temperature heat for distillation columns and thermal crackers for distillation, desulphurization and many other processes. The corresponding CO_2 emissions amount to about 1.73 million t/a [471]. The product spectrum of the world's refinery production in 2005 is shown in Fig. 184.

A refinery consists of a complex system of units with highly optimized energy and mass flow structures. The heat and power demand of a refinery depends on its size, but also on its distillation capacity and the type and amount of downstream processing, as well as on the product balance. Table 54 gives an overview of the energy demand for an average refinery in North America and various refinery processes, respectively, as was estimated for the year 2005 [81].

Similar information for a somewhat different list of refinery processes for a plant capacity of 6 million t of crude oil throughput [472] is given in Table 55 showing a typical need of about 350 MW of thermal power. For comparison, in the Lurgi study of 1988 [473], the total process heat demand for a refinery of the same size was estimated to be ~450 MW(th).

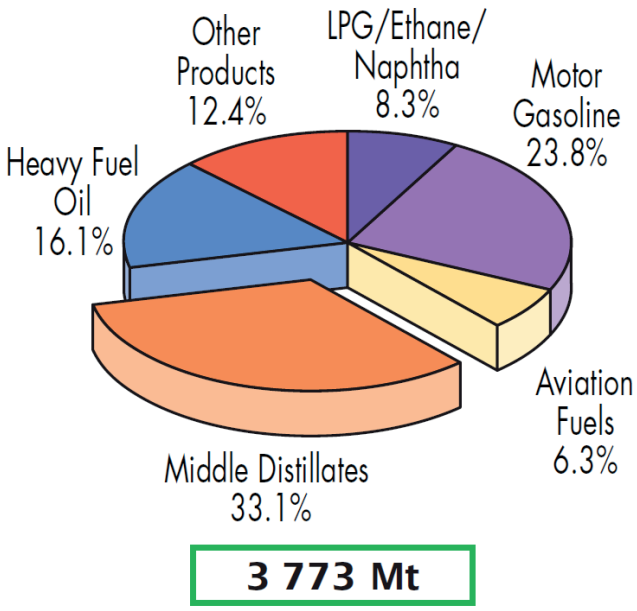

FIG. 184. World refinery production 2005 [7].

TABLE 54. AVERAGE ENERGY DEMAND FOR NORTH AMERICAN REFINERIES [81]

Process	Energy demand per refinery (MW(th))			
	Steam	Electricity	Fuel	Total
Atmospheric distillation	19	14	78	111
Vacuum distillation	8	2	21	31
Coking	9	3	38	50
Catalytic cracking	–18	30	50	62
Catalytic hydro-cracking	12	17	26	55
Hydro-treating	11	35	171	217
Catalytic reforming	11	10	94	115
Total:	52	111	478	641

Petroleum refineries convert petroleum from its natural state to a range of commercial products. About 90% of petroleum products are fuels such as gasoline, aviation fuel, distillate and residual oil (diesel oil, heating oils, industrial oils), liquefied petroleum gas, coke and kerosene. The remaining 10% goes to non-fuel products such as ethylene, propylene and benzene.

Most industrial heat is consumed in the 400–600°C temperature range. The energy is typically supplied by firing produced process gases. Additional natural gas firing is needed for high temperature processes. Standard practice is to use steam in equipment considered ‘critical units’ such as turbo-machines. Non-critical equipment usually relies on off-site electricity supply, with redundant equipment powered by steam in the case of maintenance or accidental shutdowns. To become totally independent of external energy providers, refineries are operating cogeneration plants which provide ‘secure’ electricity for their own needs, the surplus electricity being consumed in other facilities or sold to the grid.

TABLE 55. HEAT DEMAND OF A REFINERY WITH 6 MILLION t/a OF CRUDE OIL THROUGHPUT [472]

Unit	Thermal power (MW)	Product temperature (°C) in/out
Atmospheric distillation feed	105.0	270/390
Vacuum flasher feed	38.5	270/390
Gasoline desulphurization		
feed	5.7	320/370
reboiler stabilzation	10.1	230/240
Reformer 1		
feed	9.7	475/543
intermediate	13.8	446/543
intermediate	9.2	479/543
reformer 1	5.8	503/543
reboiler stabilization	11.7	230/250
Reformer 2		
feed	9.5	450/540
intermediate	7.1	475/540
intermediate	5.3	480/540
reformer 2	3.7	485/540
reboiler stabilization	6.5	230/250
Middle dist. Desulphurization feed	6.9	340/380
Hydrocracker		
recycle reactor 1	14.4	214/407
recycle reactor 2	1.7	340/485
reboiler debutanizer	28.7	290/370
reboiler fractionating column	21.1	260/330
reboiler vacuum fractionating	8.4	320/360
VCC plant		
hydrogen	5.5	220/490
product	5.7	380/435
reboiler debutanizer	9.1	330/350
reboiler fractionating column	6.0	300/330
Total net process heat:	~350	

8.2.2. Ammonia synthesis

More than 80% of the world's production of ammonia and ammonium compound derivatives is used as fertilizer. Of the remaining 20%, 5% is used in chemical manufacturing (explosives, fibres and plastics, pharmaceuticals), and the remainder is used for refrigerants and in the pulp and paper industry. The total demand of hydrogen is currently 250×10^9 Nm^3 per year or about 50% of the world H_2 production. Demand in the EU is 33×10^9 Nm^3/a or ~55% of the European production. The synthesis reaction runs as an exothermic catalytic reaction according to the Haber–Bosch process which was developed between 1905 and 1913:

$$N_2 + 3\,H_2 \quad \leftrightarrow \quad 2\,NH_3 \qquad +104\ kJ/mol$$

Operating conditions are low temperatures (~400–500°C) and high pressures (up to ~50 MPa) to favour the equilibrium toward ammonia. The catalyst is a mixture of iron oxide and aluminium oxide. Still, not more than 15% of the feedstock is converted to ammonia, while the remaining unconverted gases are recycled. The most energy consuming part of an ammonia plant is the air liquefaction process and the compression steps. With high operation temperatures and atmospheric pressure, the above reaction is shifted toward ammonia decomposition. The separation step requires ~3.5 MJ of heat per Nm^3 of H_2.

The ammonia compound can also easily be utilized as a chemical energy carrier for long distance energy transportation. The big advantage is the densification factor for the hydrogen of 1333. Ammonia is liquid at ambient temperature and easily transportable in pipes and storable in containers.

8.2.3. Direct reduction of iron ore

Among the largest consumers of hydrogen is the steel industry, where the hydrogen is used to upgrade raw iron to steel. The direct reduction iron (DRI) process is applied for the production of iron and steel from iron ore. DRI is performed with either coal or synthesis gas in fixed or fluidized beds of iron ore to reduce the ore to sponge iron, which can be smelted directly to steel in an electric arc furnace. The major chemical reaction is:

$$Fe_2O_3 + 3\ CO \quad \leftrightarrow \quad 2\ Fe + 3\ CO_2 \qquad +39\ kJ/mol$$

The chemical reduction process can also be conducted with hydrogen to replace the coal, thus reducing CO_2 emissions, assuming the H_2 is from a nuclear or renewable source:

$$Fe_2O_3 + 3\ H_2 \quad \leftrightarrow \quad 2\ Fe + 3\ H_2O \qquad -73\ kJ/mol$$

While the latter process takes place at ~500°C and 3–4 MPa, the former process operates at 800°C and 0.3 MPa.

Steel production has risen sharply from 200 million t in the 1950s to about 1300 million t in 2007 [474] and is responsible for the release of 2106 million t of CO_2 into the air. The traditional primary blast furnace is a countercurrent gas–solid reactor where the iron oxide is reduced with coke and limestone. With a typical input of 80% ore and 20% scrap metal plus fossil energy, the iron is melted and the liquid metal separated from the slag and converted into steel by oxidation of impurities and controlled addition of alloying elements.

According to the World Steel Association, the estimated energy consumption is in the order of ~30 GJ/t of steel for primary steel production methods and ~11 GJ/t for secondary steel production (recycling) [474]. Assuming a nuclear assisted process with cogeneration of hydrogen and electricity, and based on a 1000 t/d production rate, the feed required for the production of 1 million t of steel has been estimated to be about 1.43 million t of Fe_2O_3 plus ~65 800 t of hydrogen to obtain the iron at 900°C, plus ~8.4 MW(e) to heat the iron up to 1600°C [475].

A large blast furnace plant at a power level of ~1600 MW(th) produces a tonne of iron every 10 seconds. The overall iron yield is very high at ~99.5%. Blast furnaces are used for about 65% of all steel making, but account for 90% of worldwide steel industry emissions. Purified iron is needed for the production of high quality steels with electric arc furnaces, which are more environmentally benign than the traditional blast furnaces. The heat needed to melt the metal is produced by electricity. This process requires inexpensive sources of hydrogen if the old production methods are to be replaced with electric arc furnaces [476].

8.2.4. Coal liquefaction

8.2.4.1. Direct process

Coal liquefaction processes were developed in the first half of the 20th century. Coal has the potential to provide almost every product that can be produced from oil. Bergius or Pott/Broche used a direct method to convert coal by a hydrogenation process. The conversion to a liquid is done in a single step by dissolution in a solvent at elevated temperatures and pressures followed by hydro-cracking with hydrogen:

$$C + H_2 \quad \leftrightarrow \quad –CH_2– \qquad –308\ kJ/mol$$

$$CH + 0.5\ H_2 \quad \leftrightarrow \quad –CH_2– \qquad +209\ kJ/mol$$

As shown in Fig. 185, pulverized coal is mixed with oil and catalyst to produce an oily, medium sized interim slurry which is either reprocessed to a coal oil or, in a subsequent step, after mixing with hydrogen, passes through a series of hydrogenation reactors at 450–490°C and 20 MPa, and in the presence of an iron oxide powder as

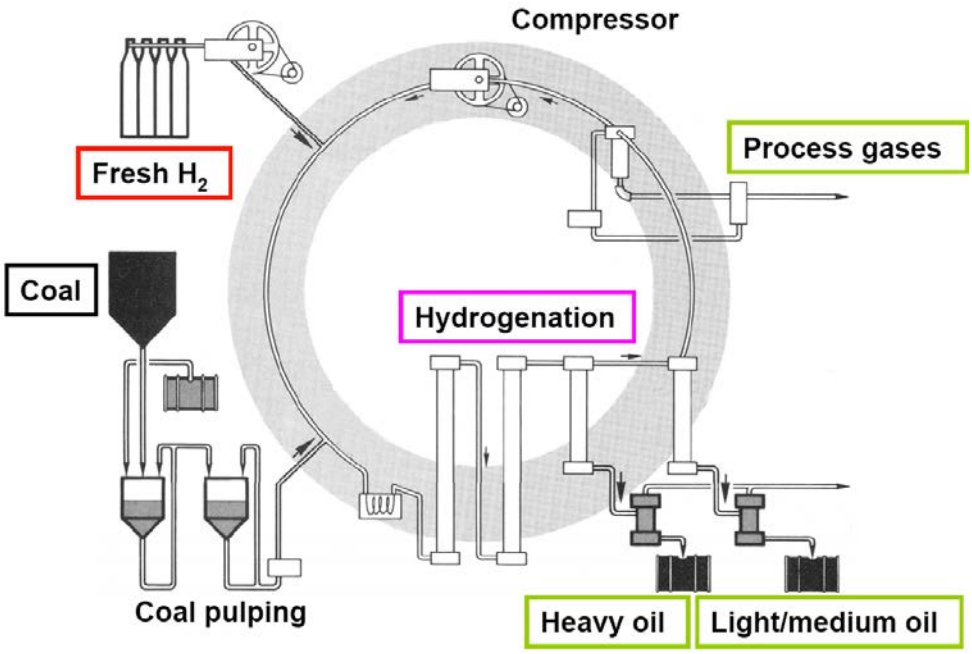

FIG. 185. The direct way from coal to oil [217].

catalyst to a coal oil. Here the coal having a molecular weight of over 5000 splits into smaller pieces with the concomitant accretion of hydrogen. Thermodynamic conditions determine the quantity and type of products, and they can be adjusted to the feedstock. Coal to liquids (CTL) processes require about 5–8 kg of H_2 per bbl to produce transportation fuels. The coal demand for 1 t of 'coal oil' is 1.25 t to be hydrogenated plus 1.36 t for the hydrogen plus 1 t for the process heat.

Overall thermal efficiencies for the direct method are generally in the range of 60–70% in modern processes. Different kinds of pyrolysis (high temperature, mild, rapid) with different liquid yields have been developed and tested in pilot plants, however, no demonstration plant has been operated so far.

Direct coal liquefaction puts stringent requirements on the type and quality of the coal, and its products need further upgrading before being used as transportation fuel. On the other hand, it achieves favourable efficiencies. Brought to large technical maturity by Pier, Germany operated 12 coal hydrogenation plants from 1940 to 1944 to produce 4 million t/a of coal gasoline [117, 118]. British Coal developed a two stage direct coal liquefaction process called 'liquid solvent extraction' where two reactors in series are applied. Coal dissolution with little or no catalyst is done in the first stage, while hydro-treatment of the heavy coal liquids takes place in the second stage. The thermal efficiency for a conceptual coal liquefaction plant based on this process was estimated to be >60% [477].

8.2.4.2. Indirect process

In contrast to the direct process, Fischer and Tropsch started from synthesis gas. In their indirect liquefaction process, developed between 1922 and 1926, coal is gasified in a first step to synthesis gas followed by a catalytic hydrogenation of the CO where synthesis gas is reacted at relatively low temperatures and pressures (220–340°C, 2–2.5 MPa) to high quality clean fuels:

$$2n\ H_2 + n\ CO \leftrightarrow (-CH_2^-)_n + n\ H_2O + \text{heat}$$

or, if the production of long carbon chain alkanes is favoured:

$$(n/2 + m)\ H_2 + m\ CO \leftrightarrow C_mH_n + m\ H_2O + \text{heat}$$

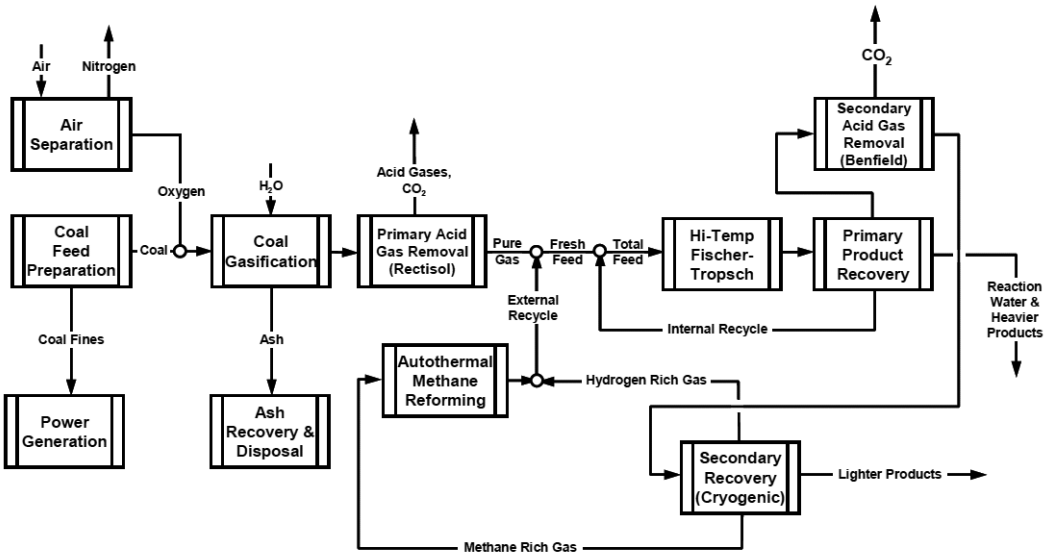

FIG. 186. Schematic of conventional CTL process, from [479].

After the volatiles have been cleaned out of the gas stream, the water gas shift reaction is applied in order to adjust the H_2:CO ratio and match requirements for the hydrocarbon synthesis and produce CO_2 as the main by-product. In CTL processes, more than 40% of the synthesis gas is shifted to make the required hydrogen. Catalysts are selected depending on the product spectrum requirements. Special catalysts are used to rebuild the molecules into liquid hydrocarbons and remove by-products.

The product spectrum depends on the operating conditions applied with the higher temperatures/pressures to yield synthetic gasoline and chemicals, whereas the low temperature process leads to the production of synthetic naphtha, kerosene or high quality diesel fuel. Gasifier product gases with a H_2:CO ratio of around 0.5 to 0.7 are recommended as a feed to the Fischer–Tropsch process when using an iron catalyst. A high H_2, low CO_2, low CH_4 content is required for chemical and fuel production. In general, liquid products are of lower quality compared with those from direct liquefaction processes [477].

The generation of 1 kg of Fischer–Tropsch product requires an input of 4.5 kg of coal and 7.2 kg of water, and it produces 9.3 kg of CO_2 plus 0.4 kg of solid waste [478]. The tremendous CO_2 emissions of CTL fuels made from coal are a major disadvantage, being more than double of those for crude oil derived fuels.

The Fischer–Tropsch process is a preferred liquefaction process because it has a large experience basis and yields high quality fuel (diesel) containing only very little sulphur. The drawback is that coal liquefaction is comparatively expensive, particularly at the front end where all contaminants have to be removed before processing to a gas or liquid. The indirect process is superior to the direct one because of the lower operational pressures necessary and thus a higher reliability of the plant, and a higher grade product spectrum. Efficiencies are around 40%, being lower than for the direct process, and in modern plants up to about 55%. Economics demand large scale plants with a massive demand for hydrogen and oxygen. Figure 186 shows a schematic of the conventional CTL process.

Technical plants use solid bed (Arge process) or flue stream reactors (Synthol process). In the Arge process, apart from gasoline, preferably solid paraffins are produced, whereas gaseous hydrocarbons are produced in the Synthol process. The Fischer–Tropsch synthesis yields a gasoline with low octane number, but a higher value diesel fuel compared with coal hydrogenation.

A major disadvantage is the significant quantity of CO_2 that is emitted during the synthesis gas production. If an independent source of H_2 and O_2 were available, e.g. from a water splitting process by nuclear or renewable energies, processes like air separation, steam generation and shift reaction would no longer be required and process related CO_2 release would be significantly reduced [480].

8.2.4.3. International CTL industrial applications

Starting as early as around 1840, both direct and indirect methods of coal liquefaction were developed in Germany to industrial maturity in the 1940s applying brown coal and stone coal. Coal liquefaction in Germany, however, eventually became uneconomic and was later abandoned. Significant R&D work was initiated during the oil crisis in the 1970s in the USA, the UK, Japan, and other countries. Activities in Germany resulted in the operation of a pilot plant with a production rate of 200 kg/d. Since then, only a few joint international projects, e.g. with South Africa, have remained, the only country to apply this technology still today at a large scale.

Recent trends have revived interest in coal liquefaction technologies as an alternative means of generating transportation fuels and other oil products used in a number of countries as insurance against crude oil supply problems [477]. Primarily, high oil prices, increasing demand from China and India, US refining capacity limitations, and increasing reserve replacement costs as well as a growing desire for energy independence from foreign sources create the political will to explore more domestic energy resources. Lignite is considered an ideal feedstock for coal liquefaction because of its low relative cost and high hydrogen content. Newer processes convert the syngas to methanol before transforming it to other liquid fuels. An alternative option is use of outside (allothermal) production of hydrogen and oxygen, like from a (nuclear) water splitting process. Engineering studies are required to optimize the modified flowsheets for a nuclear assisted hydrogen coal liquefaction plant and to assess the economics [481].

The Mobil Oil process is principally based on a new catalyst which allows easy production of liquid fuels from methanol. Gas to liquid (GTL) capacity, however, is expected to grow slowly due to the huge and risky investment. By 2050, an estimated 5–10% of the transportation fuel demand may be covered by GTL fuels [470].

China, with its abundant coal reserves, is experiencing a strong growth in coal liquefaction. Fischer–Tropsch fuels are considered feasible and practical options to replace petroleum based fuels in China in both the short and medium terms [22], and thus reduce its dependence on oil imports. Commercial scale plants are already in the design and construction phase. A coal liquefaction plant has been constructed in Shenhua, China, with a throughput of 9.7 million t/a of coal to be converted into 5 million t of gasoline, kerosene, diesel and other fuels. For the next few years, China is planning the construction of 27 coal liquefaction plants. More liquefaction plants based on the direct process are planned, with a total capacity of 60 million t/a of oil. China will soon become the worldwide volume leader in CTL fuel production. In cooperation with SASOL, China is currently involved in two plants planned for Inner Mongolia to deliver an annual capacity of 60 Mt of oil. The first plant, with a 1 million t/a capacity, is expected to produce gasoline and diesel by 2007. Also a plant able to produce 50 000 bbl of ethanol per day is planned. Further coal to chemicals (CTC) plants are planned in regions with proven coal reserves for ammonia and methanol production.

In Japan, the liquefaction of bituminous coal was promoted under the Sunshine project which started in 1974. The so-called ‘NEDOL’ liquefaction technology (Fig. 187) has been developed where the three processes of direct hydrogenation, solvent extraction and solvolysis were merged to one. The result is a light-distillate rich oil produced under mild reaction conditions. But also the liquefaction of low-rank coal is being investigated in Japan. The so-called brown coal liquefaction (BCL) technology is currently being tested on pilot scale in a 50 t/d plant in Australia [128].

A 150 t/d pilot plant for bituminous coal was operated between 1996 and 1998 and provided engineering data for a commercial plant to follow. Japan is currently the only country active in large scale process development.

The South African corporation SASOL Limited is a fuels and chemicals manufacturing company and the largest gasification centre in the world. Since 1955, SASOL has been producing higher value oil products from low grade coal, today at an output of 150 000 bbl/d of fuels and petrochemicals, supplying about 40% of the domestic demand for liquid fuels [124]. The SASOL complex in South Africa consists of three facilities at two sites. Sasol Two and Sasol Three located in Sasolburg comprise the world’s two largest gasification facilities.

Within the USDOE’s Clean Coal Technology Demonstration Program, a liquefaction plant with a capacity of 1000 t/d was commissioned based on the ‘mild pyrolysis’ process. North Dakota has received recent attention regarding coal liquefaction with the proposal of a 10 000 bbl/d facility with expansion opportunities to 50 000 bbl/d. If diesel is included in the fuel mix at the proposed coal liquefaction plant, coal based diesel could be blended with biodiesel. Also, the KIER in the Republic of Korea is currently testing CTL in a 15 bbl./d pilot plant.

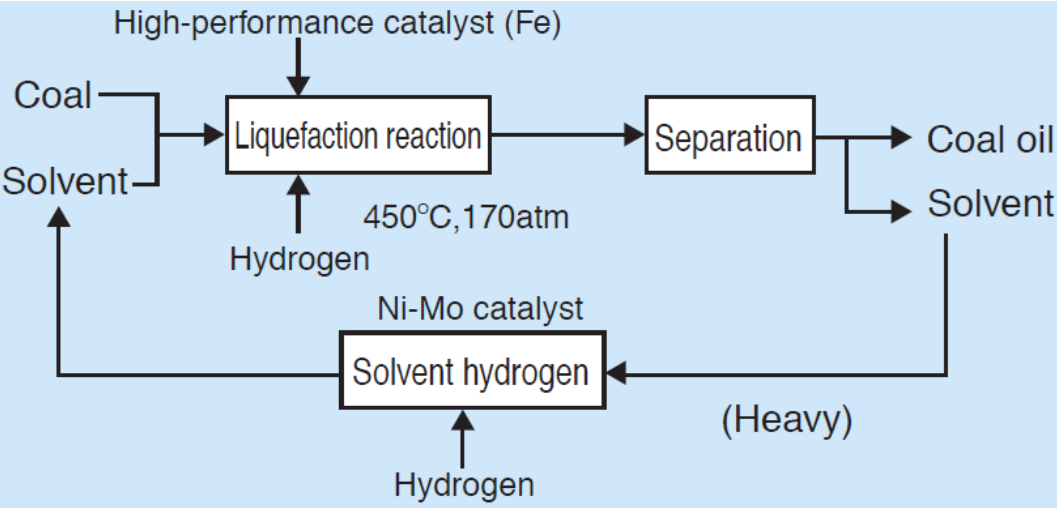

FIG. 187. Schematic of the Japanese NEDOL bituminous coal liquefaction process [128].

8.2.5. Methanol synthesis

The methanol industry is the third most important user of hydrogen. Methanol is a high octane alcohol, a colourless liquid with a boiling point of 65°C that is easily ignitable, with a flammability range between 6.7 and 36.5 vol% in air. Commercial methanol synthesis involves reacting CO, H_2 and steam over a copper–zinc oxide catalyst in the presence of a small amount of CO_2. Methanol is produced, e.g. through synthesis gas from coal by clean coal technologies with CO_2 from the reverse water shift reaction and the hydrogenation of carbon dioxide at 250–300°C and 5–20 MPa by:

$$CO_2 + 3\ H_2 \quad \leftrightarrow \quad CH_3OH + H_2O \qquad +50\ kJ/mol$$

Other feedstocks like natural gas or heavy oils are also possible. The product gas from coal gasification is not appropriate for methanol production owing to its high fraction of CO_2 and methane. The preceding POX step could reduce the methane fraction. To best use the raw product syngas in methanol synthesis and limit the extent of further syngas treatment and steam reforming, it is essential to maintain the following conditions:

— A H_2:CO ratio of at least 2;
— A CO_2:CO ratio of about 0.6 to prevent catalyst deactivation and keep the catalyst in an active reduced state;
— Low concentrations of N_2, CH_4, C_2^+, etc., to prevent the buildup of inert gases within the methanol synthesis loop;
— Low concentrations of CH_4 and C_2^+ to limit the need for further steam reforming.

Alternative methanol production occurs via direct hydrogenation of carbon monoxide:

$$CO + 2\ H_2 \quad \leftrightarrow \quad CH_3OH \qquad +91\ kJ/mol$$

This second reaction demands more energy, is slow and incomplete. Therefore the product gas should contain only small amounts of CO_2 and have an H_2:CO ratio of ~2.2. The methanol synthesis reaction is equilibrium controlled, and excess reactants (CO and H_2) must be recycled to obtain economic yields.

Methanol is a classic basic material for chemical production chains, e.g. the production of chemicals such as propylene, poly-propylene, phenol or acetone. The methanol to gasoline (MTG) process is an effective route for CTL processing where methanol is directly converted to gasoline:

$$n\ CH_3OH \quad \leftrightarrow \quad (-CH_2^-)_n + H_2O$$

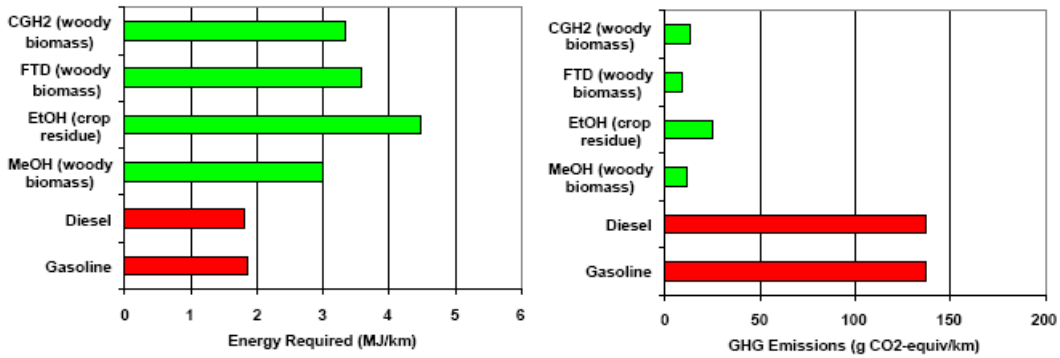

FIG. 188. Comparison of today's petroleum fuels with alternative non-fossil derived fuels [482].

The process is simple and robust in design and operation and promises high plant availabilities. It was demonstrated in New Zealand, but has not been conducted so far at a large scale. Still, MTG plants are currently foreseen in China and the USA [118]. A new MTG plant with coal based methanol production in Jincheng, China, started operation in 2009. It has a 100 000 t/a of gasoline capacity which may be extended to 1 million t/a later. Commercial application of methanol as a fuel, however, is limited due to its high toxicity and relatively low energy density (~65% of that of gasoline).

Methanol can be used in direct methanol fuel cells and also in higher temperature fuel cells for electricity production or even in PEFC after a reforming stage. Methanol is also used for the production of alternative automotive fuels such as DME (see Section 3.2.3.3). A route to transport fuels is hydro-treating/hydro-cracking to a naphtha-like product with upgrading to diesel. But the high pressure and high hydrogen requirement of hydro-treating routes makes this route much too expensive. A major issue is the catalyst stability and lifetime. The co-production of chemicals and fuels undoubtedly offers the most interesting opportunities.

The world market for methanol was 40 million t/a in 2007 which is expected to increase to 80 million t/a by 2020. Most methanol is currently produced from coal and natural gas. It is used as feedstock for fuel addition and chemical materials such as formaldehyde and acetic acid. Emerging markets are seen in the transportation sector. At present, the largest plants with a capacity of ~5500 t/d are operational in the Islamic Republic of Iran and Trinidad.

8.2.6. Alternative transportation fuels

The transportation sector and stationary power applications are widely viewed as the two critical sectors where there may be an opportunity to greatly expand the future use of hydrogen. Most of today's transportation fuels are being generated from refining crude petroleum oil. Petroleum fuels which are well qualified for widespread use and offer a number of benefits which make it likely that they will continue to dominate the overall fuel mix:

— High energy density;
— Strong demand from the current stock of vehicles and a widely established infrastructure for delivery to users;
— Relatively low cost;
— Easy, low-cost handling and transport at atmospheric temperature and pressure;
— Extensive experience and knowledge of fuel systems, coupled with considerable progress in optimization;
— Ease of long term storage.

But petroleum fuels also have at least two major drawbacks: potential supply limitations, including significant geopolitical dependencies for many countries, and high CO_2 emissions. For both of these reasons, there are strong incentives to develop and secure acceptable substitutes [470]. Figure 188 and Table 56 list various transportation fuels for both ICE and FCVs, and some of their characteristics.

Not only is hydrogen considered a transport fuel which may be applied in the future on a large scale, it is also a basic building block with increasing significance (and market potential) for the production of conventional liquid fuels, but also — partially — for other alternative fuels or synthetic fuels. Diversification of fuel supply is the

TABLE 56. COMPARISON OF TRANSPORTATION FUELS

Fuel	Main source	Molecular weight	Density (kg/m^3)	HHV (MJ/kg)	Energy per volume (GJ/m^3)
Hydrogen	NG, oil, coal, water, methanol	2.02	0.08988	141.9	2.6 at 20 MPa 10.3 at 80 MPa
LH_2	hydrogen	2.02	70.8	141.9	9.9
Natural gas (methane)	fossil resource	16.04	0.7175	55.5	8.1 at 20 MPa 32.1 at 80 MPa
LNG	NG	16.04	422.6	55.5	~20.5
LPG (propane)	refining of petroleum, NG	44.1	581	50.4	25.2 ~23.4
Methanol	NG, coal, biomass	32.04	793	22.7	18.0
Ethanol	biomass, grain, corn	46.07	794	29.9	23.5 ~22.3
Gasoline	crude oil	100–105	745	47.4	30.4–34.8
Diesel	crude oil	~200	832	45.8	35.7–36.2
Biodiesel	biological oil, animal fats	120–320	830–850	39.8	32.6–33.4
DME	NG, coal, organic material	46	670	31.7	21.1
MTBE	isobutylene	88.15	741	7.8	28.1
Toluene	crude oil, tolu tree	112	862	42.5	26.9
Ammonia	NG, heavy oil	17	771	22.5	17.4
Jet A	crude oil	144–226	775–830	46.5	34.2

NG = natural gas; MTBE = Methyl T-butyl ether

driving force to move away from crude oil and gradually displace conventional petroleum products, meeting the challenges of air pollution, CO_2 emissions and supply security. If captured CO_2 is used for their production, they would even represent CO_2 neutral alternatives.

Production of synthetic liquid fuels requires the input of carbon, hydrogen and energy. All three can be taken from fossil fuels or biomass. An IEA analysis suggests that the least expensive alternative to oil based fuels is large CTL plants, which are cost effective at oil prices above US$60/bbl. GTL and hydrogen produced from natural gas are strongly influencing fuel production cost. Biomass to liquid (BTL) fuel is cost competitive only if low cost biomass is available [470].

8.2.6.1. Substitute natural gas synthesis

SNG is the starting point for many industrial chemical processes. The exothermic methanation reactions are:

$$CO + 3\,H_2 \leftrightarrow CH_4 + H_2O \qquad +205\ kJ/mol$$

$$CO_2 + 4\,H_2 \leftrightarrow CH_4 + 2\,H_2O \qquad +165\ kJ/mol\ of\ CO_2$$

The second reaction (Sabatier reaction) is slow and incomplete. Therefore, the product gas should contain only small amounts of CO_2 and have an H_2 to CO ratio of ~3.2, conditions that are achievable in non-catalytic steam–coal gasification, but under stringent operating conditions not possible for the catalytic process. The use of coal gasification raw gas is less economic for on-purpose methanol or hydrogen production compared with the gas from autothermal processes. The conversion of coal to SNG offers the option of transporting the energy content of coal via pipeline.

8.2.6.2. Synthetic fuel production with atmospheric CO_2

Besides storage, there is also the option of using CO_2 as a raw material, i.e. taking it directly as a C1 building block to be used as reaction partner in chemical and biotechnological processes and built into products. Storage time would correspond to the product's lifetime, ranging between decades for long lived polymers and practically zero for synthetic fuels.

As of 2005, the worldwide anthropogenic CO_2 emissions from using fossil fuels amounted to 28 Gt/a. The main (large, stationary) sources are the energy sector with 10.5 Gt or 46%, the transportation sector with 5.6 Gt or 24%, steel production with 1.5 Gt or 6%, refineries and the chemical industry with 1.2 Gt or 5%, and others. The CO_2 sources in the transportation sector are small and numerous and therefore not appropriate for sequestration and further use. The same holds for the firing of fossil fuels for heating purposes [118].

Different from the storage option where CO_2 is taken out of the CO_2 cycle, no CO_2 is usually saved in the case of using it as a carbon source. It would only be saved if the energy required for the reduction of CO_2 as the reverse process of combustion is from a CO_2 emission free energy source. CO_2 as a raw material is obviously available in large amounts, but only a small quantity can be utilized and only in a few industrial processes. The industry uses approximately 120 million t of CO_2 per year. Although most of it will be consumed again (urea synthesis), at least 10 million t/a would be available for chemical conversions. Other applications are in the beverage industry, for enhanced oil recovery, and in its supercritical state as a technological fluid. As an inert and safe gas, it is also used as a protective gas and in its solid state for refrigeration [10].

For products of the chemical industries, the estimated substitution potential amounts to 178 million t of CO_2 per year, which is not more than 0.6% of the total annual anthropogenic CO_2 emissions worldwide. The use of carbon for synthetic fuel production would increase the potential by a factor of 10, but it would not change the atmospheric CO_2 concentrations, since subsequent combustion of the fuels will immediately recycle the CO_2 back to the atmosphere. The purity of CO_2 is an important prerequisite that eliminates the CO_2 emitted from fossil power plants as source candidates. Their use would require an extensive purification as a preceding step. Exceptions are the emissions from IGCC plants.

The most common method of recovering atmospheric CO_2 is by absorption using aqueous potassium carbonate. The external energy source to be used (mainly for hydrogen production) can be, for example, in the form of electricity. The use of nuclear primary energy would provide the option of unlimited liquid fuel production without any greenhouse impact [476].

The CO_2 or dry reforming process can be applied for the production of synthesis gas, which is then converted by means of Fischer–Tropsch synthesis to gasoline or diesel fuels. In GTL technologies, atmospheric CO_2 can be used as a carbon source for the conversion with hydrogen to synthetic liquid fuels, such as methanol or its derivates methyl T-butyl ether (MTBE), dimethylcarbonate, or dimethylether. Furthermore, it allows the direct production of DME from CO_2 and H_2 [483]. Methanol and dimethyl-carbonate (DMC) are considered alternatives to the currently used gasoline; DME may replace diesel fuel. The above processes, however, are only reasonable if there is a source of (inexpensive and) 'clean' hydrogen feedstock. Technological challenges for the development of energetically efficient processes are seen in the areas of catalysis and reaction kinetics.

KIST developed and demonstrated a direct methanol production process using hydrogen and captured CO_2 (CAMERE-I process) with an integrated steam reformer for hydrogen production (CAMERE-II process). The concept of nuclear methanol is now to introduce nuclear energy into the steam reforming process using an advanced HTGR (Fig. 189). A 450 MW(th) plant would be able to produce 1 million t/a of methanol and recycle at the same time 0.35 million t/a of CO_2 [61].

8.2.6.3. Hythane

Hythane is a blend of natural gas and hydrogen with a fraction of 8–30% of hydrogen. Since methane emits NO_x and has a relatively narrow flammability range that limits the fuel efficiency, the addition of a small amount of hydrogen extends the lean flammability range significantly. Hythane is more buoyant and more diffusive than methane. Methane has a slow flame speed, especially in lean air–fuel mixtures, while hydrogen has a flame speed about eight times faster and is much more easily ignited.

Hydrogen is a powerful combustion stimulant for accelerating the methane combustion within an engine, and it is also a powerful reducing agent for efficient catalysis at lower exhaust temperatures. In the case of explosive

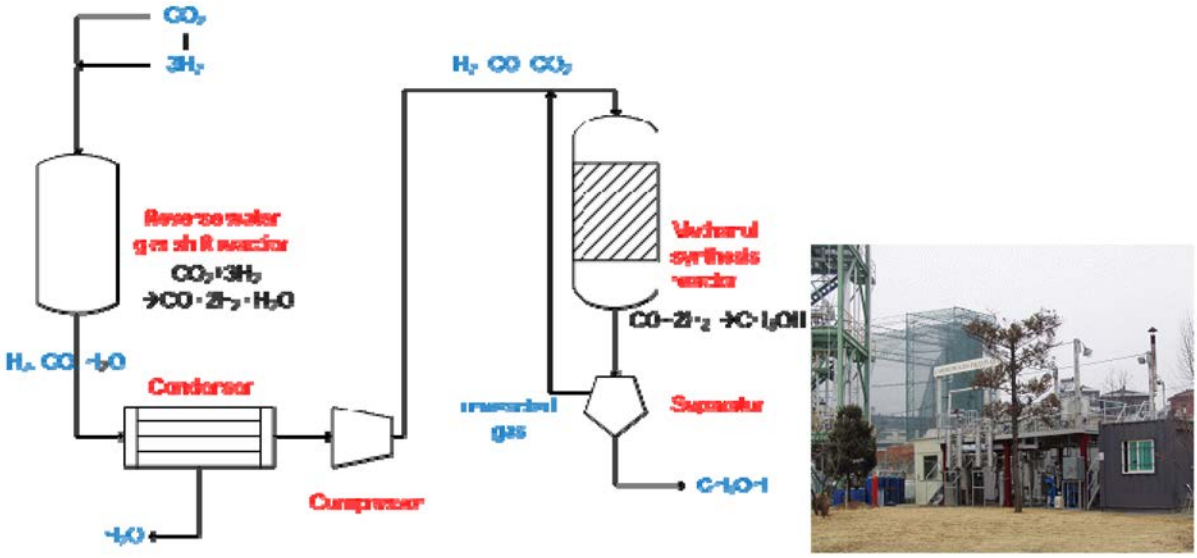

FIG. 189. Methanol synthesis flow scheme (left) and 80 kg/d capacity pilot plant operated by KIST (right) [67].

combustion, a hythane explosion is expected to be stronger than a methane explosion, but exhibits significantly lower pressures than do pure hydrogen explosions [484].

Hythane could represent an interim step on the way to a hydrogen based economy. A big advantage is the fact that hythane can benefit from the existing infrastructure for natural gas without major changes. The same holds for hythane combustion in a natural gas driven internal combustion engine. Test vehicles in public transportation running on hythane are being operated at various places in the world.

8.3. PROSPECTS FOR USE OF HYDROGEN

For future large scale applications of hydrogen, it should be kept in mind that electricity and hydrogen can form a symbiosis, allowing an optimization of electricity generating systems with regard to the substitution of fossil energy carriers currently being used for load following and peak demands. This is due to the fact that electricity and hydrogen are principally interchangeable, i.e. the production of hydrogen (e.g. via electrolysis) and the re-conversion of hydrogen into electricity (and heat) (e.g. by fuel cells). This fundamental interconnection is being addressed as ‘hydricity’ [279].

With increasing production of electricity from renewable energies instead of fossil fuels, novel energy storage systems are needed to compensate for the strong variations of supply and demand. Hydrogen may here play an important role as a storage element for energy that can easily be retrieved upon demand [11]. In addition to the industrial hydrogen demand as a chemical product, commercial growth of hydrogen production is expected, most probably starting in the coming decades in road transport and in the residential and service sector to expand the application as a fuel in fuel cell vehicles and stationary power generation.

Niche market applications such as hydrogen powered consumer electronics may play a role, specifically in the area of public acceptance, in the introduction of hydrogen in the energy system [28]. All these potential applications may contribute in the medium term to an increased need for clean hydrogen production routes. The further future beyond 2030 may see a significant increase in hydrogen consumption due to cost reductions in the production technologies and a stronger demand from the transport sector.

8.3.1. Near term demand for tertiary oil recovery

Crude oil is a finite resource. Conventional oil production will peak at some point and then gradually decline, increasing the share for unconventional oil production. Therefore, there will be an increasing demand for more capacity to refine heavier grades of oil, including other non-conventional liquids such as condensates, natural gas

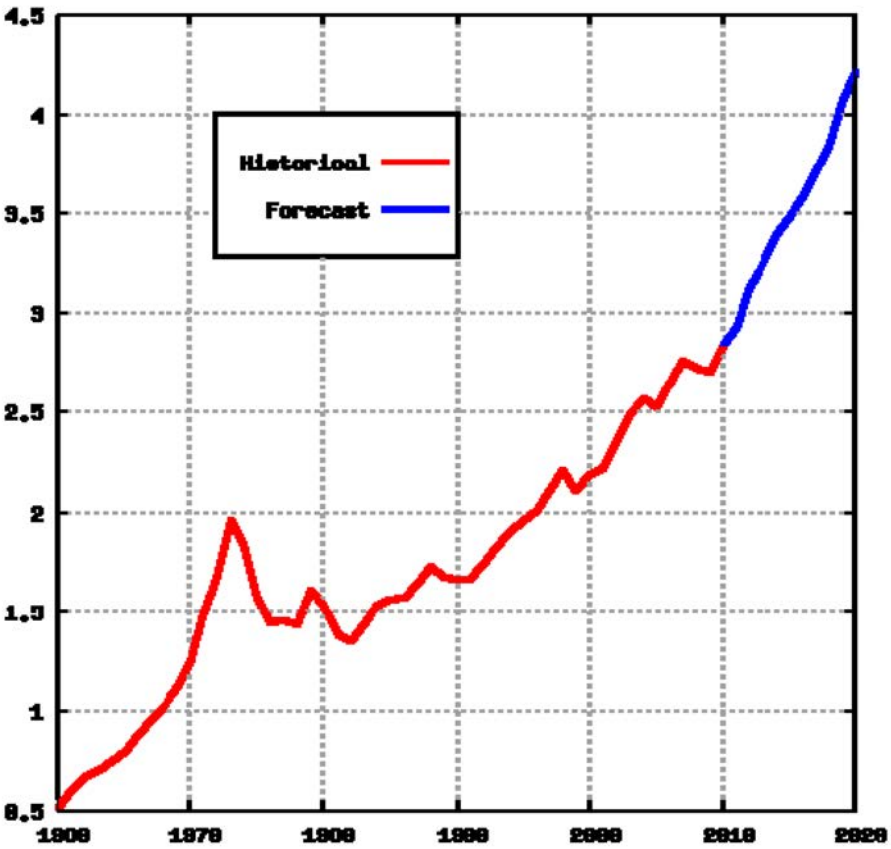

FIG. 190. Canadian oil production (David Moe, 2008).

liquids, tar sands, bitumen, extra heavy oil and oil shales, but also synthetic fuels from anything to liquid (XTL) processes to contribute to global petroleum supply. While the economics of heavy oil might be promising, the harnessing of non-conventional resources is handicapped by high development costs, consumption of large quantities of water and natural gas, and severe environmental impacts.

Heavy oil is a dense and viscous kind of oil with high contents of sulphur and metals. Extra-heavy oil resources are mainly located in Venezuela. Large reserves of oil exist in the form of highly viscous crude oils inaccessible by methods available at present. It is expected that the considerable oil reserves in Canada (Fig. 190) could be recovered by improved methods. Thermal methods are the most developed technology, where steam injection plays the overwhelming role. The type of steam required depends on, e.g. the depth of the resources, porosity of the rock matrix or oil viscosity. For improved recovery methods, high pressures of 12 MPa and more are necessary. Oil yield increases significantly with the steam temperature and pressure. Oil recovery steam generators currently on the markets are in the power range of 1.5–15 MW(th), providing steam at pressures up to 17 MPa and temperatures up to 350°C, and at rates of up to 110 t/h (250 000 lb/h) [81]. Dry saturated steam of high temperature to be injected into deep oil wells could be produced by an HTGR.

But besides steam, large quantities of hydrogen will also be required for tertiary oil recovery (upgrading to synthetic crude), which requires a significant increase of the present power capacity to allow for efficient large scale hydrogen production in the future.

8.3.1.1. Shale-oil recovery

Most of the world's oil shale resources (estimated at 75%) are located in the Green River Formation in the USA, with estimated resources of 1.5–1.8 trillion bbl of oil [81]. The largest oil shale producer and consumer country, however, is Estonia, with peak production of 31 million t in 1980 (today ~15 million t/a) [485]. Shale is a

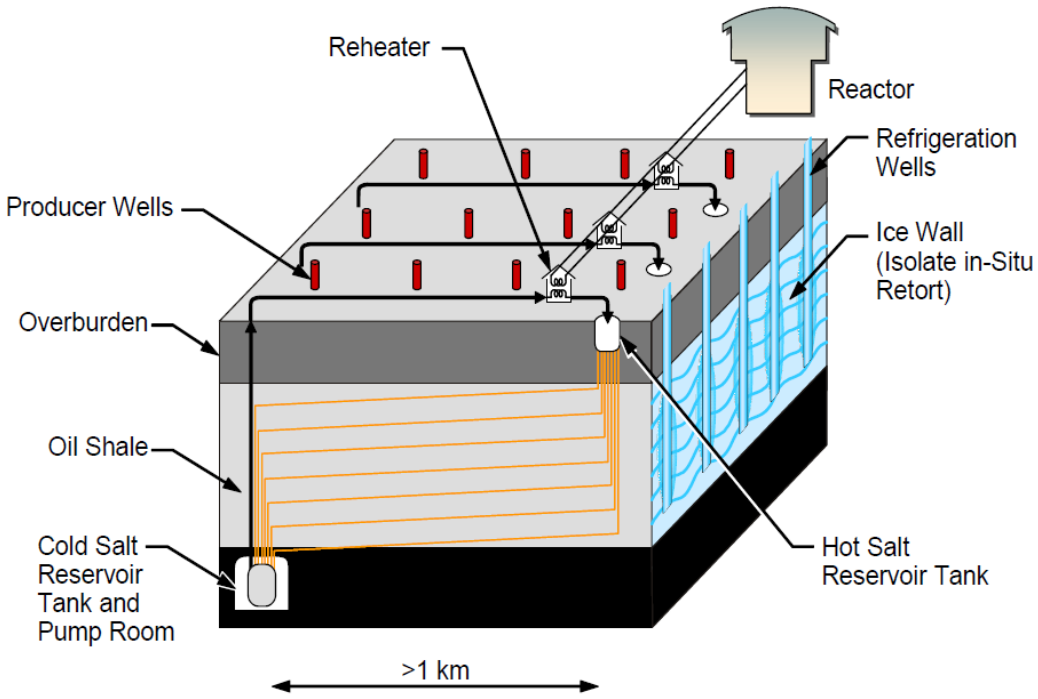

FIG. 191. Example for underground heating of oil shale with nuclear heat [311].

fine-grained rock of sedimentary origin containing, but varying widely in content and composition (quality) of, high-molecular organic substances (kerogen) embedded in its inorganic matrix. Criteria of oil shale reserves are energy rating, location, depth and thickness of seams, mining technology, world price and transportation costs compared to alternatives, and protection of the environment.

Oil and gas can be extracted by destructive distillation. Only some of these organic compounds (the natural bitumen) are soluble. Depending on the site, the rock contains an average of 10–20% insoluble organic matter and bitumen — in some cases the organic content can be as high as 60%. At temperatures of 350–400°C, the yield can be 20–200 L of oil per tonne of shale. The negative aspects are the immense toxic waste which is left by the oil shale chemical industry, the large CO_2 emissions from oil shale power stations and the deterioration of water quality [485].

The high temperature heat required to heat the oil shale could be provided by nuclear energy. Figure 191 shows a schematic of a nuclear based system where the heat transfer is made by liquid metal or liquid salt heat transport loops. The direct use of high temperature heat avoids the conversion of electricity to heat. Another advantage of the nuclear system is a significant reduction of CO_2 compared with other methods of synthetic crude oil production. The distances from reactor to well are sufficiently short that heat transport is practicable. About 12 GW(th) of high temperature heat would be required to produce a million barrels of oil per day. In practice, the required temperatures would be near 700°C [311].

8.3.1.2. Tar sands oil recovery

Tar sands are a mixture of sand, clay, water and bitumen (viscous heavy oil), from which the bitumen is extracted. They represent a major energy resource that increases in importance as world supplies of crude oil become limited; on the other hand, they are the dirtiest fuel on Earth. The hydrogen to carbon ratio of tar sand is ~1, which must be raised to 1.5–2 for conversion to gasoline. Oil sands are mainly located in Canada in the state of Alberta, the regions of Athabasca, Cold Lake River and Peace River, with proven reserves of 174 billion bbl of oil, representing about 80% of the world's technically recoverable resources [470] and 95% of Canadian oil reserves. Oil sands feature an intermediate density and viscosity. The methods involve the in situ steam assisted gravity drainage (SAGD) technology, since ~80% of the deposits in Canada are not accessible for surface mining. The

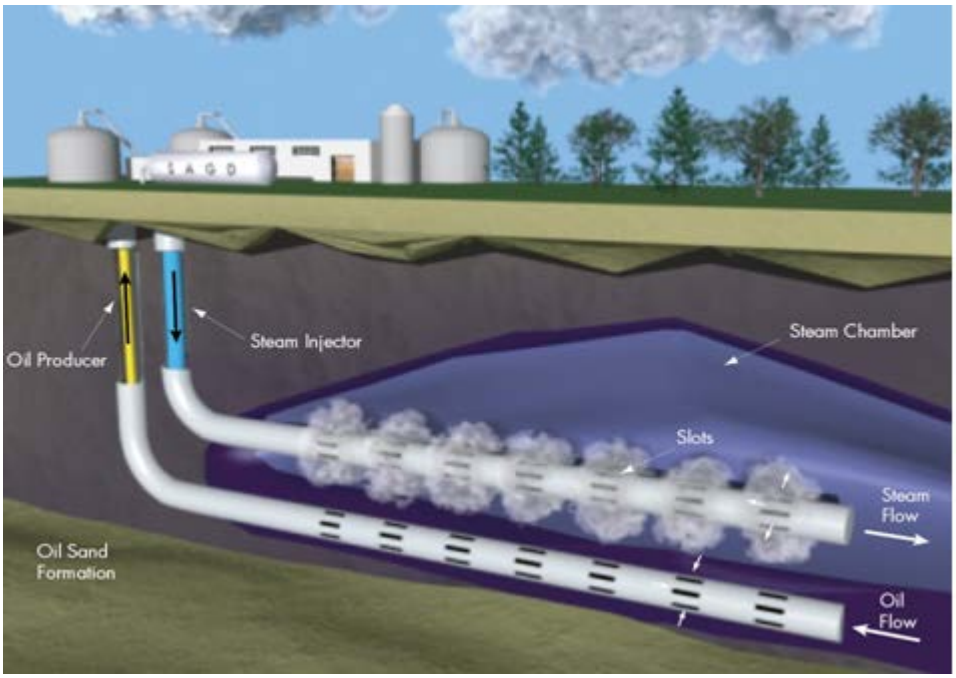

FIG. 192. Schematic of steam assisted gravity drainage (SAGD) [486].

product recovered from the sands is a heavy, sour bitumen. Upgrading with hydrogen is required to transform it into a lighter product (with lower density and viscosity) that can be transported to refineries via pipelines. The products are synthetic crude (refinable by current technology) and petroleum coke. The Athabasca oil sands are estimated to require 3–4 kg of H_2 per barrel as well as steam (14 MPa, 340°C) and electric power for the recovery and upgrading processes. Current production from oil sands amounts to 1300 bbl/d, which is expected to increase to 6 million bbl/d by 2030 [470].

Producing fuels from oil sands requires large amounts of natural gas and water, and produces large quantities of waste material and carbon dioxide. The shale can be distilled autothermically after open pit mining. This method requires hot water of ~70°C and process steam at around 1–2 MPa and has a yield of less than 50% of the organic matter. A second in situ method for high-permeability shales is SAGD, in which two horizontal wells of 0.5–1 km length and at least 50 m below surface are drilled with one about 5 m below the other one (Fig. 192). Steam at high pressure and temperature (10 MPa and 540°C) is continuously injected into the upper well, where the bitumen heats up and flows downwards. The formed emulsion of bitumen, steam and water is drained through the lower well and recovered. A pair of wells is able to recover in the range of 2000 bbl/d of synthetic crude oil.

Other methods are cyclic steam stimulation (CSS) or pressure cyclic steam drive (PCSD) requiring steam of more 300°C and pressures of 8–16 MPa. Novel technologies replace the steam with either solvents, e.g. a liquid salt, or in situ combustion. The possible yield also represents 50% of the in-place reserve. Oil shale contribution is marginal so far, as no industrial scale recovery has yet been envisaged due to the high production costs. Furthermore, the processing is presumed to produce five times more CO_2 emissions than conventional refining. But oil shale would roughly add another 300 billion bbl of oil to the global reserves.

8.3.2. Long term demand for fuel cells for power and heat supply

8.3.2.1. Fuel cell technologies

Various fuel cell types have been developed, usually classified according to the electrolyte used. In Table 57, fuel cell types (Fig. 193) are listed along with their operating temperatures and anode/cathode reactions.

Certain constraints to the fuel cell do apply depending on the type of fuel cell. In low temperature fuel cells, noble metal (Pt) electrodes are necessary to increase the reactivity. Poisoning of electrodes can be minimized by

TABLE 57. OVERVIEW OF DIFFERENT TYPES OF FUEL CELLS

	Electrolyte	Temperature (°C)	Fuel	Oxidant	Efficiency (% LHV)
Low temperature					
AFC	Alkaline	80–200	H_2	O_2	50– 60
PEFC	Polymer	80–100	H_2	O_2, air	40–45
HT-PEFC	Polymer	120–180	H_2, CO	O_2, air	40–50
DMFC	Polymer	80–100	MeOH	O_2, air	25–30
PAFC	Phosphoric acid	200	H_2	O_2, air	40–45
High temperature					
MCFC	Molten carbonate	650	H_2, CO, CO_2, CH_4	O_2, air	50–55
SOFC	Ceramic	750–1000	H_2, CO, CH_4	O_2, air	50–55
LT-SOFC	Ceramic	550–650	H_2, CO, CH_4	O_2, air	50–55

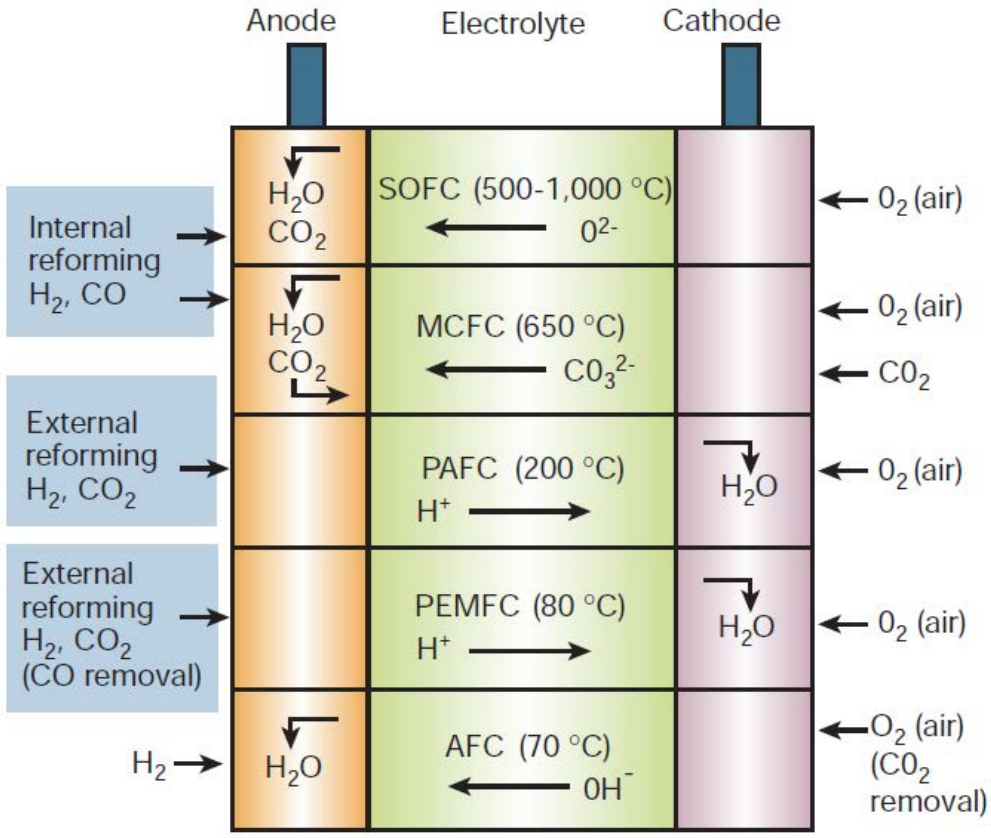

FIG. 193. Different types of fuel cells [487].

purification of the feed stream. Various methods have been developed to remove sulphur, which is a poison to many oxygen electrode catalysts. High temperature fuel cell designs avoid expensive noble metal catalysts. Thermal activation is insensible to pollutants. Drawbacks are performance degradation limiting lifetime and expensive plant components. To avoid dilution of the electrolyte by the product water, it must be removed by evaporation or vaporization. In high temperature fuel cell systems, the water is steamed off anyway.

If carbon containing fuel gases are used instead of pure hydrogen, oxidation must be realized first in a reforming reaction. Internal reforming has the advantage that there is no requirement for hydrogen storage. Incomplete reaction at lower temperatures results in the presence of carbon monoxide, which is a catalyst poison and must be removed, at the expense of efficiency. CO causes no trouble at high operating temperatures since reforming can take place internally. Attempts at a direct conversion of coal or oil in an integrated gasification fuel cell system are currently at an early R&D stage, but they are considered potential primary fuels in the long run.

(A) Alkaline fuel cell

The alkaline fuel cell (AFC) is a highly efficient low temperature fuel cell (<100°C) with a very high power density, and therefore ideally appropriate for mobile applications. The AFC, however, requires a demanding process control that is complicated because of the corrosive liquid electrolyte, a 30% potash lye, and the need for extremely pure fuel (no CO_2), leading to high cost. Efficiencies of 60% and more have been achieved with clean hydrogen and oxygen and noble electrode materials. The AFC was demonstrated to also work with a hydrogen–air system. What remains unsatisfactory is its observed power decrease with operating time.

(B) Polymer electrolyte fuel cell

The polymer electrolyte fuel cell (PEFC), or proton exchange membrane fuel cell (PEM-FC), is an efficient, compact, robust and quiet method of generating electricity. It has a 0.1 mm thick proton conducting foil as a solid electrolyte which is coated on either side with the electrodes representing the so-called membrane electrolyte assembly (MEA). It has the highest power density of all cell types, a relatively low operating temperature and thus long cell lifetime, good load change behaviour and good efficiency at partial load, and good standby performance, thus being appropriate for mobile applications. A problem in PEFCs is the need to keep the polymer electrolyte membrane in a wet state and at higher operating temperatures to prevent a dry-out by means of external wetting [488]. Applicable fuels are hydrogen, reformed methanol or methane with purity requirements of less than 10 ppm of CO, less than 1 ppm of NH_3 and less than 0.1 ppm of H_2S. The development is concentrating on improvement of catalysts and reduction of CO poisoning effects. The electricity output from the fuel cell depends on the availability of oxygen. It is maximal when pure O_2 is used, but can be reduced by a factor of 2–4 in the case of air [489].

The first complete PEM fuel cell system was developed in 1963 and utilized during the Gemini space flights. The 1 kW cell stack employed sulfonated polystyrene membranes as an electrolyte, which was later replaced by the polymer Nafion. Today, PEFCs constitute the main pillar of fuel cell technology in both transport and stationary applications, with an emphasis being placed on system integration and demonstration programmes. The market is generally seen in smaller scale applications, whereas those on a larger scale have mainly disappeared.

(C) Direct methanol fuel cell

Another low temperature fuel cell, the direct methanol fuel cell (DMFC), runs on either liquid or, with better performance but higher system complexity, on gaseous methanol and is normally based on a solid polymer electrolyte. The operating temperature for DMFCs is in the range of 60–130°C, typically around 120°C, producing an efficiency of about 40%. Due to the low temperature conversion of methanol to hydrogen and carbon dioxide, the DMFC system requires a noble metal catalyst. Pt–Ru catalysts were found to produce the best oxidation results at the oxygen electrode. Because of the still ten times higher loading with catalysts compared with PEFCs and the relatively low efficiency and power density due to internal fuel leakage through the membrane, the DMFC is not suitable for large units. Typical areas for DMFCs are in small units from a few Watts up to approximately 2 kW for portable applications. An advantage in mobile applications is the use of the methanol in liquid form at low pressures. But detailed development is still necessary, with major improvements to be seen in a further reduction of degradation rates, simplification and compaction of the system, and further increase of system efficiencies.

(D) Phosphoric acid fuel cell

Most practical experience has been gained in the operation of phosphoric acid fuel cells (PAFCs). Because of the higher operating temperature, PAFCs have a minor CO poisoning problem, plus they offer operation in the CHP

mode providing good quality steam of approximately 200°C. The fuel is hydrogen or reformed methane plus CO converter. The principal poison for the Pt catalyst is sulphur carried in the reformate stream as H_2S. The PAFC has successfully played a pioneering role in the introduction of fuel cell systems. Several hundred ONSI-delivered PAFC stations were tested and have proven technical maturity with 8000 operating hours per year and an availability of more than 90%. Most demonstration tests, however, were terminated after sufficient data were collected. Investment costs are still too high to be competitive [490].

(E) Molten carbonate fuel cell

A molten carbonate fuel cell (MCFC) is being operated in the 500–700°C temperature range with porous Ni catalysts and a molten binary carbonate made of Li_2CO_3/K_2CO_3 or Li_2CO_3/Na_2CO_3 immobilized in a porous matrix of $LiAlO_2$ as an electrolyte. Carbon dioxide yielded at the anode needs to be fed back to the cathode, where it is consumed by conversion to carbonate ions which provide the means of ion transfer. Due to the high operating temperature, there is no need to employ noble metals as a catalyst. A key advantage over low temperature fuel cells is the fuel flexibility. Besides hydrogen, the MCFC can be operated with methanol or methane or coal gas, with external or with partial or full internal reformation; the possibility of internal naphtha reforming is also being examined. In the future, synthesis gas from (internal) coal gasification systems may be linked to MCFC electricity generation, inducing a further increase of coal conversion efficiencies. Recently, the applicability of biomass derived gases has also been investigated.

A number of MCFC installations with the ‘HotModule’ manufactured by the German company MTU are being operated successfully in Germany, Italy and Spain, and have achieved an a accumulated operating time (by 2007) of more than 170 000 h, and the industrial development is expanding [491]. The drawbacks of this fuel cell type are its low current and power densities. A problem often observed in MCFCs is the strong corrosivity of the electrolyte and its leakage through gaskets. Long term experimental operation is still required to demonstrate that ageing of the stack is acceptable. Also, the high serial resistance of the hot carbonate electrolyte limits the efficiency to 40% [492].

(F) Solid oxide fuel cell

The solid oxide fuel cell (SOFC) has a solid ceramic as the electrolyte, e.g. zirconium oxide stabilized with yttrium oxide, in which oxygen ions migrate from the cathode to the anode. Heat and CO_2 are also generated at the anode. The SOFC is attractive because of its very high operating temperature range of 800–1000°C, which allows fast chemical reactions. The high temperatures, on the other hand, imply stringent requirements for materials and construction. Two different stack designs are currently pursued using tubular or flat cell geometry. Typical dimensions of the tubular design are: support (cathode) with an inner diameter of 12–22 mm, 2.2 mm wall thickness, and a length up to 1500 mm, an electrolyte layer of 20–40 μm, and outside the anode with 100 μm thickness. For a flat cell, the typical data are: a gas-tight electrolyte of 150–200 μm thickness, electrodes with 50 μm thickness and 30–50% porosity. Most research efforts are currently conducted on planar SOFCs. With only slight modifications, the SOFC can be operated either in the electrolysis or in the fuel cell mode.

Due to the high operation temperatures, SOFCs convert gaseous hydrocarbons either directly or after internal reforming with a very low emission level. Utilization of the high temperature waste heat raises the overall efficiency to a maximum. Furthermore, the waste gas at the anode, consisting of CO_2, H_2O, CO and residual H_2, could be utilized in other chemical processes. The time needed to heat up or cool down the system limits the use of SOFCs in applications with rapid temperature changes. Heat release during internal reforming, creating sharp temperature gradients, is difficult to control. Also, high temperature corrosion can sometimes be a problem and requires the use of expensive materials and protective layers within the cell. Problems related to sealing have also been observed.

SOFC systems are generally thought to be best suited to the generation of electricity and heat in industrial applications, especially in combination with gas turbines. Recent SOFC development shows potential for high electricity efficiencies of ~60% [228]. The main SOFC applications are seen in larger scale stationary power generation and in smaller scale residential power generation (<10 kW) and auxiliary power units (APUs) for mobile applications. Most of the SOFC power units currently being tested have a power capacity of 1 and 5 kW, respectively. A 100 kW SOFC power plant is being operated in Italy. A 10 kW(e) SOFC stack with 60 planar cells

FIG. 194. A 15 kW class 60-cell SOFC stack constructed and tested at the Research Centre Jülich [493].

(Fig. 194) has been constructed at the Research Centre Jülich and operated for 1500 h. Both hydrogen and methane fuels were tested. The next step will be a 20 kW(e) SOFC system demonstration. Goals of the future development are the reduction of the operating temperature and the extension to larger power units.

8.3.2.2. Hydrogen vehicles

Hydrogen is being considered as a potential energy vector in the transport sector both for internal combustion engine (ICE) and FCV applications, basically with on-board storage of the hydrogen. In recent years, car producers have manufactured a range of prototype ICE and PEM fuel cell passenger cars using hydrogen as the fuel. Numerous demonstration programmes for hydrogen powered vehicles with PEM fuel cell drive trains and — to a lesser extent — with ICE have been initiated, mainly in Europe, Japan and the USA, comprising a broad spectrum of vehicle classes for small and medium range requirements. The development of hydrogen fuelled vehicles is mainly driven by the market, i.e. they have to compete against other technologies such as gasoline–electric hybrid vehicles, which have already achieved a high level of efficiency [82].

For a broad application of hydrogen as a vehicle fuel, however, further R&D work needs to be done, e.g. to develop a hydrogen storage medium allowing hydrogen fuelled PEM fuel cell cars to have range capabilities comparable with those of current baseline gasoline and diesel vehicles. Also, the infrastructure and logistics for distribution and supply must be established, which in turn will be strongly dependent on the demand for hydrogen in the transportation sector. Therefore, before hydrogen is broadly introduced as a fuel in the traffic sector, it may appear in niche applications characterized by special boundary conditions such as a locally high environmental benefit. The main niche markets for the commercial use of hydrogen as transportation fuel are seen in city buses, passenger car fleets and light duty vehicles. Public transportation buses may represent an ideal entry point. Heavy duty trucks may switch to other alternatives such as biofuels.

(A) Internal combustion engine

Hydrogen can be directly used as a fuel in ICEs where the hydrogen burning engine mechanically drives the vehicle. The positive features for such a hydrogen application are the low spark energy requirement, wide flammability range, high auto-ignition temperature and high flame speed. A disadvantage is the low volumetric density which limits the power output of the engine. BMW and Mazda have been the only two mainstream

manufacturers to seriously pursue internal combustion hydrogen technology, with most others preferring to use it to supply a fuel cell and produce electricity. Further advancements to internal combustion hydrogen units appear to be limited in the future.

(B) Fuel cell vehicles (FCVs)

Electricity is expected to play an increasingly important role in the transport sector. PEM fuel cells can be used for on-board supply with electricity (APUs), for uninterrupted electricity supply in decentralized applications, and in light transport systems. The use of pure hydrogen with fuel cells in vehicle propulsion systems offers the benefit that it produces electricity at high efficiency without combustion and, except for water vapour, with zero emissions. It shows reliable startup and can be sized in small and large power packages.

Fuel cell technology has arrived at an advanced technological state. But a gap is apparent between the impressive success of technologies and the development of market opportunities, especially with vehicles. A major market introduction is hampered by the high costs and limited demonstration of reliability and longevity. According to today's fuel cell technology, about 60 g of platinum is necessary for a PEFC for automotive application, whose worth is more than 30% of the current engine costs. Progress is expected from a further development of the membrane electrolyte assembly with higher operation temperatures (>120°C), more freezing tolerance, more impurity tolerance and reduced catalyst need (~0.2 mg/cm^2 of Pt). Resulting from a USDOE field evaluation of fuel cell vehicles from several automobile manufacturers, an average fuel efficiency for future fuel cell car production of 60 miles (~100 km) per kg was deemed a reasonable goal [88]. About 120 fuel cell buses under various demonstration support programmes have been or are currently being tested worldwide, along with more than 1000 prototype, concept and demonstration cars, refuelled at approximately 100 refuelling stations. But costs for FCVs are still far too high. The current cost of a fuel cell bus averages US$1.5 million, and passenger cars cost more than US$100 000. Extrapolating the current development status of a fuel cell stack to the production of 500 000 cars per year, the USDOE reports a value of US$61 per kW and compares this value with the target of US$30 per kW for 2015 [494].

Research is a basis for solving many of the outstanding problems, including lifetime extension to practical levels, cost reduction to acceptable levels in specialized markets, battery replacement, fuel supply and distribution, and advanced fuel conversion technologies (biomass and waste). However, with increasing pressure for higher efficiency and lower emissions, fuel cells can expect a bright future [491].

(C) Hydrogen vehicles with fuel processing

Fuel cell technology has also been considered in connection with a chemical processing unit for the use of widely available liquid hydrocarbons as feedstock to extract the hydrogen by on-board autothermal reforming (ATR) and operate the electric propulsion system of a vehicle. It appears, however, that potential users have moved away from on-board fuel processing and are concentrating instead on on-board storage of hydrogen. This tendency became obvious with the decision of the USDOE in 2004 to discontinue funding of R&D activities. The "no go" decision was based on the expectation that decisive technical criteria such as startup time (less than 1 min at 20°C) and startup energy (less than 2 MJ for a 50 kW fuel processor) would not be met within a reasonable time frame and thus there was no economic advantage over the rapidly emerging gasoline/battery hybrid vehicles [495].

On-board reforming has since been concentrating on small scale fuel processors in combination with a fuel cell for 'power on demand' applications. With the increasing demand for on-board electricity from about 0.8 kW(e) in today's cars to several kW(e) in future vehicles, it is considered to provide this electricity (plus heat) by means of a fuel cell based APU (see also Section 3.2.2.2). Combined with a small fuel cell stack in the order of 5 kW(e), APUs may generate all non-propulsion power in future cars to substitute for the conventional battery. They are advantageous because of their high efficiency and low noise, vibrations and emissions. In addition, they extend the lifetime of the main engine. If sufficiently dynamic and stable to follow all potential states of the system and if reaction by-products and other contaminants can be kept at tolerable levels, APUs may actually represent the first step for fuel cells to penetrate the transportation market at a larger scale, with the prime candidates being energy consuming trucks or recreational vehicles.

Today there are numerous vehicles being tested with electricity supply from PEFC based APUs to gradually substitute for conventional batteries. In cooperation with Delphi Automotive Systems, BMW is

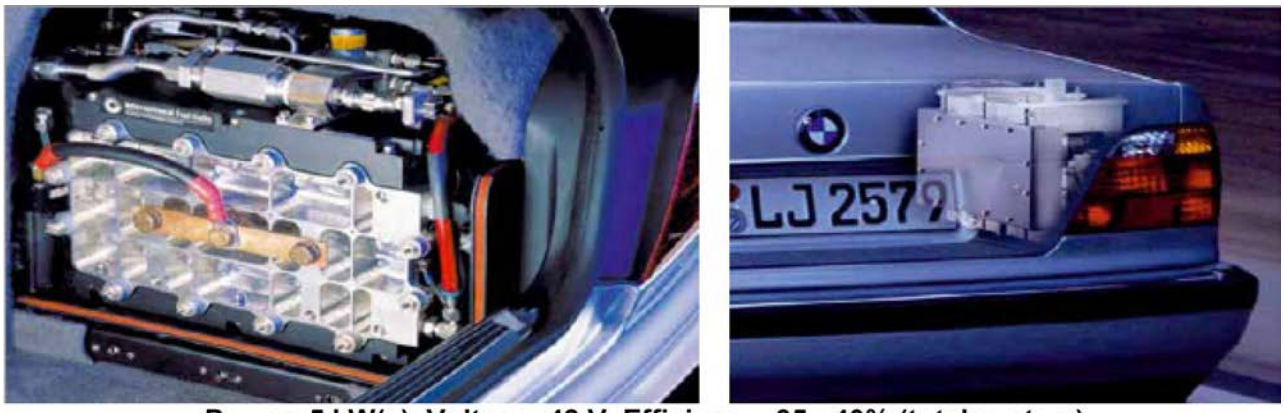

FIG. 195. PEM-FC based APU used in the hydrogen fuelled BMW 750hl [496].

considering an SOFC based APU for their future vehicles. Its feasibility was demonstrated in 2001 with a proof-of-concept unit. BMW has already achieved some experience with low-temperature fuel cell based APUs, where among the 15 hydrogen fuelled vehicles of the fifth generation, a few cars were equipped with a PEM fuel cell (Fig. 195) [496].

8.3.2.3. Marine

Marine transport worldwide currently contributes 14% of the global nitrogen oxide emissions and 7% of sulphur emissions. Therefore fuel cells are also envisaged for use in marine applications if the specific maritime requirements can be fulfilled. Small demonstration projects are testing fuel cells in passenger boats and submarines [497]. An example is the European Fuel Cell Systems for Zero Emission Ships (ZEMSHIPS) project demonstrating a 48 kW(e) fuel cell propulsion system for a ship in Hamburg. Hydrogen fuelled fuel cells may be used in ships that do not need long ranges and can be filled up frequently, whereas ships that need longer ranges would need to use fuel cells based on fuels with higher energy densities, such as liquid natural gas, methanol or ethanol. In particular, the molten carbonate fuel cell (MCFC) with LNG as the fuel currently offers the largest potential as a power system for maritime applications. In the EU's MethAPU project (Validation of a Renewable Methanol Based Auxiliary Power System for Commercial Vessels), methanol fuelled SOFCs in the power range of 250 kW have been investigated, including on-board testing of a 20 kW SOFC. For larger sea-going ships, fuel cell application currently would be limited to auxiliary supply of power in the 500 kW range.

A major driver for using fuel cells in ships is the possibility of reducing emissions drastically. Although, as a rule, gas applications on ships are not permitted, discussions have started on the on-board use of natural gas. The European project FCSHIP (Fuel Cell Technologies for Ships — Environmental Impacts and Costs of Hydrogen, Natural Gas and Conventional Fuels for Fuel Cell Ships) indicates possible future concepts and prepares regulations for the design and operation of fuel cell technology in the marine market [497].

8.3.2.4. Aviation

Aviation is another energy consuming sector growing at a rate of ~5%/a that is required to reduce emissions in the future. Currently contributing a relatively low 2.6% of global CO_2 emissions, this is expected to increase to 3.2% by 2020 [498], since synthetic hydrocarbons or hydrogen may play a significant role in the future.

Aviation fuels are characterized by special technical requirements in terms of energy density, flow characteristics (freeze, viscosity) and thermal stability at higher temperatures (carbon deposition). Alternative products to kerosene, at present the standard aviation fuel, have started either to be blended with or to even substitute for the kerosene. The mixture of traditional Jet A-1 fuel with GTL fuel is in the testing phase. The first commercial flight with a 1:1 mixture was in 2008. A first flight test with a 1:1 mixture of Jet-1 and BTL fuel took

place in 2009. In this regard, hydrogen may play a role in the long term. Another role that H_2 may play in aviation is as a fuel in PEFCs or SOFCs for ground or on-board power supply. The water at a high quality resulting from fuel cell operation could be further used on-board. The preferred storage options are liquid hydrogen for short range missions and JET A-1/ BTL reforming for long range missions [499]. Further development here needs to concentrate on extreme reliability and availability.

The direct use of liquid hydrogen as a substitute for kerosene in an airplane propulsion system was investigated in the CRYOPLANE project. This project was launched in 1990 by a joint German–Russian consortium (DASA as the lead, with the main partners being MBB, MTU, Tupulev and Kuznetsov), and later continued as an EU activity with 35 partners from 11 countries and coordinated by EADS Airbus GmbH. Its objective was to study the feasibility of an aircraft propelled by cryogenic fuels [500]. The aim was to find out whether the use of liquefied natural gas (mainly on the Russian side) or liquid hydrogen (on both sides) as an aircraft fuel was technically possible and reasonable in terms of ecology and economy. Topics covered by the project were scenarios for the transition to an alternative aviation fuel, infrastructure, aircraft design, fuel system layout, engine modifications and ecological issues (e.g. water vapour and NO_x emissions). The transition of short/medium range aircraft serving routes between leading industrial nations was seen as an introduction phase, followed by the development of the appropriate infrastructure and the operation of a demonstrator airplane.

An Airbus A310-300 was selected as the baseline aircraft to be converted to LH_2 propulsion. For the new fuel tank concept, the most favourable design was seen in the top-mounted tank configuration with four tanks, two active ones with 40 m^3 each for either engine, and two passive ones with 80 m^3 each to refill the active tanks. Total fuel weight for the Airbus cryoplane was estimated to be 15.6 t of LH_2 (compared with 27 t of kerosene for the same flight range). Due to the environmental impact on the stratosphere from the formation of long lived ice cloud condensation trails, the typical cruising height of ~12 km would be lowered to ~10 km. The cruising range of the cryoplane was estimated to be 2700 nautical miles (5000 km).

At a later stage in the project, a smaller airplane was chosen to precede the Airbus as the LH_2 demonstrator — a 30 passenger Fairchild-Dornier 328 regional airplane with one of the two engines to be converted to hydrogen fuel. The fuel capacity is 420 kg (6 m^3) of LH_2 stored in two cylindrical tanks underneath the wings (plus 1150 kg of kerosene for the second engine). The advantages of this intermediate step are the availability of the hydrogen engine, the lower investment in infrastructure and the earlier introduction of a series aircraft [501].

A technological development programme for the fuel system components began in 1993, including the selection of materials for tanks and piping, control system and sensors for hydrogen leak detection, fuel pumps, LH_2 gasifier and combustion chamber. The first generation of LH_2 aviation was foreseen to require a fleet of 400–500 aeroplanes and the modification of ~70 European airports. The fuel consumption was assessed to be about 2 million t/a of LH_2 or ~170 t/d for an average size airport.

8.3.3. Stationary hydrogen applications

8.3.3.1. Large scale industrial applications

Stationary applications refer to decentralized power generation by fuel cells, combustion engines or gas turbines, including residential (1–10 kW) and community (5–50 kW) applications, public and commercial buildings, and industrial (50–500 kW) and large scale (1 MW and above) applications. Moreover:

- Large cogeneration (combined heat and power) systems are being manufactured for large commercial buildings or industrial sites that require significant amounts of electricity, water heating, space heating and/or process heat. Fuel cells combined with a heat recovery system can meet some or all of these needs, as well as providing a source of purified water.
- Uninterruptible power supply systems, in which fuel cells are used as backup power supplies if the primary power system fails, are one of the fastest growth areas for stationary fuel cell technologies.
- Niche and power premium applications such as uninterruptible power supply and other backup systems which require short or even instantaneous response, load flexibility, high degree of safety, reliability and availability.

For applications in power and in CHP production, fuel cells have to compete with technologies that have already been established, such as gas and steam turbine plants. Fuel cells promise higher efficiencies at comparable

unit sizes. They offer the chance to reduce the pollution level in urban areas with high population density. Fuel cells also allow for small CHP units for residential use. Many fuel cell power units may be combined to large virtual power plants. In connexion with energy storage, the hydrogen and fuel cell system may compensate for the mismatch between renewable energy sources and energy demand.

The general design of a fuel cell power system forms an assembly of integrated systems including:

— Fuel cell module — assembly of one or more fuel cell stacks and electrical connections;
— Fuel cell stack — assembly of cells, separators, cooling plates, manifolds and supporting structure;
— Fuel and oxidant processing system — to prepare the fuel for utilization by means of catalytic or chemical processing equipment;
— Thermal management system — to provide cooling and heat rejection, and recovery of excess heat, and to assist in heating the power train during startup;
— Water treatment system — to treat and purify recovered or added water;
— Power conditioning system — to adapt the produced electrical energy to the manufacturer's requirements;
— Automatic control system — to maintain the system parameters within the specified limits by means of an assembly of sensors, actuators, valves, switches and logic components;
— Ventilation system — to provide air.

Unlike the use of hydrogen in mobile applications, stationary power applications with hydrogen or natural gas or coal derived gas as a fuel have advanced and have reached market penetration status already. A near term area of demand for H_2 fuel cells includes backup power units, power for remote locations, and distributed generation for hospitals, industrial buildings and small towns.

Stationary fuel cell power systems are currently being tested in field experiments in several countries (e.g. Germany and Norway) to show the feasibility of a combined electrical power and heat supply for households utilizing, for example, PEM fuel cells or SOFCs. They are already commercially viable in remote areas, where they can be installed independent of the grid and where fossil fuel transportation costs are prohibitive. By 2008, the cumulative power capacity had reached 180 MW(e), with an average of 50 units per year installed and an average size of 1 MW [494]. The potential flexibility of SOFCs is what is especially is important for a future strategy of decentralized electrical power supply, as this will help stabilize the demand of electrical power.

8.3.3.2. Small scale combustion installations

The energy used for small scale combustion installations is mainly used for the heating of buildings (residential and corporate), hot water and boilers for small industrial applications, including agriculture. A significant amount of this heat could be replaced with hydrogen or electricity. Both could be provided by nuclear power.

Different types of fuel cell systems are currently being demonstrated and introduced commercially in sizes ranging from a few kW up to MW sizes, often as small, standalone cogeneration systems combining local production of electricity with the use of waste heat for producing hot water and residential heating. For example, 1.2 kW PEM fuel cells are currently being introduced in Japan in limited volume by Ballard Power Systems [502], and the company Vaillant is currently installing a number of PEM fuel cells in Europe. SOFCs can also be made available for small scale CHP in the future [503].

For large generators today's fuel cell systems do not offer higher electrical efficiencies than other technologies that are already on the market such as gas turbines. At the utility scale, hybrid systems integrating fuel cell systems and gas turbines could bring about systems using natural gas with electric efficiencies greater than 65%, and such systems are expected to become cost competitive with competing generating technologies within the next decades [502]. By comparison, current state of the art power plants using combined-cycle technology combining gas turbines and steam turbines have electrical efficiencies of around 55–60% and are currently less expensive (400–500 €/kW) than fuel cell systems (2500–8000 €/kW).

Technologies available for distributed power generation, with electrical capacities of less than 60 MW, include gas turbines, reciprocating engines, microturbines, wind turbines, biomass based generators, solar photovoltaic systems and fuel cells. Some studies foresee that fuel cells might initially emerge as distributed generators in applications where users are willing to pay an extra margin for reliable energy generators. In the USA,

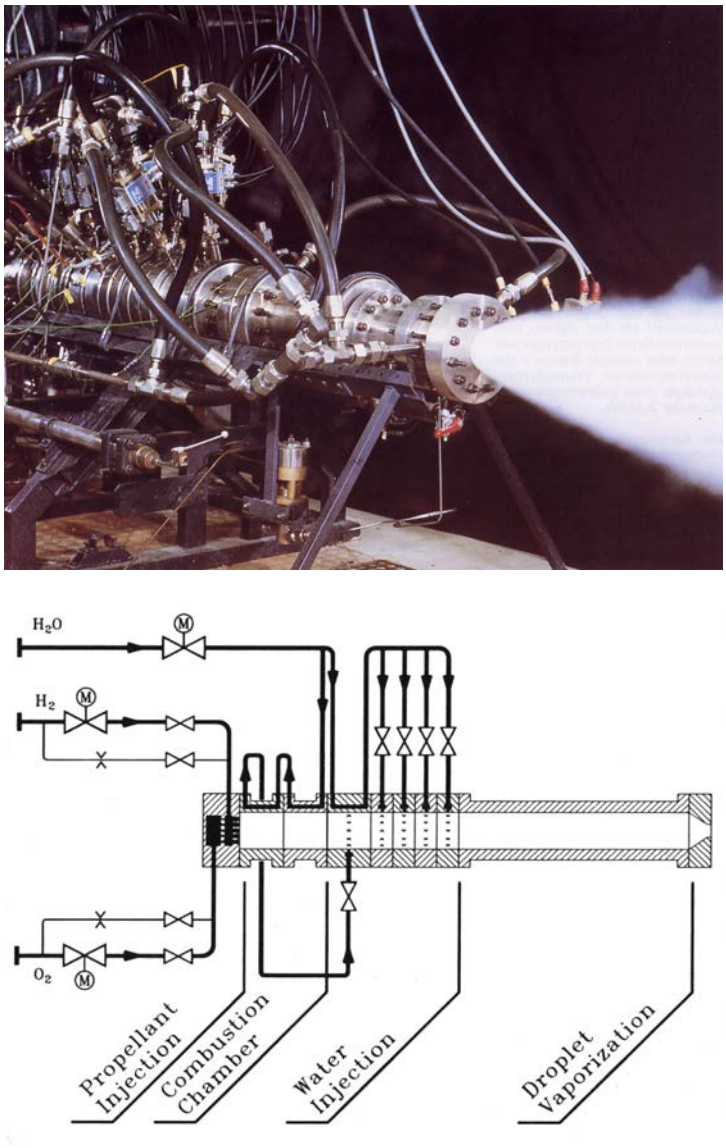

FIG. 196. Photograph and schematic diagram of the DLR LH_2–LOX steam generator [504].

10.7 million distributed generators are in place, of which 99% are small emergency/standby reciprocating engines that are not connected to the grid. The market for distributed generation is typically in the commercial sector in applications where reliable energy is needed or in remote locations where grid power is not available.

8.3.3.3. Peak electricity production using O_2–H_2 steam cycle

The oxy-hydrogen steam cycle represents the direct production of high pressure, high temperature (~1500°C) steam and is applicable for peak electricity production. It is a system with low capital cost promising a high efficiency of ~70% [311].

In a cooperative effort between the DLR (today the Deutsches Zentrum für Luft- und Raumfahrt) and other German companies from 1989 to 1993, the concept of a hydrogen and oxygen fuelled steam generator was developed. This component is actually the re-configuration of an H_2/O_2 rocket engine which allows the instantaneous provision of steam of any desired quality. H_2 and O_2 are compressed and injected into a combustion chamber (see Fig. 196) [504].

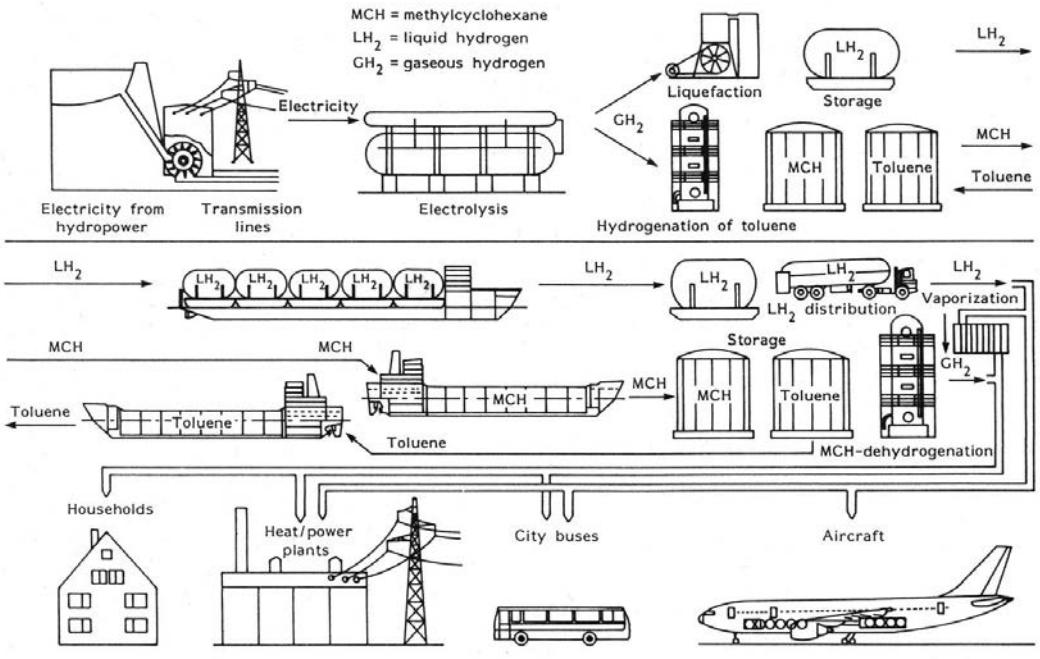

FIG. 197. Concept of the Euro–Quebec Hydro–Hydrogen Pilot Project [507].

A stoichiometric mixture is necessary to generate superheated steam of high quality without any side products. The combustion gas with a temperature of 3000°C can be cooled by adding water to achieve exactly the desired steam condition for injection into the power plant process. The startup time of such a steam generator is in the order of 1–2 s with a combustion efficiency of greater than 99%. The steam generator can act as a backup system for fast power-up of steam generation plants to serve as a cold standby spinning reserve in decentralized power production.

In a first experimental series, a total of 285 combustion tests were conducted in 1991–1992 with a prototype operated in the power output range of between 25 and 70 MW. The second step was the construction of the demonstration facility for H_2/O_2 instant reserve, HYDROSS, consisting of a modified H_2/O_2 steam generator of 2 m length and 0.4 m outer diameter plus a storage and supply system [505]. Full power was obtained after 1 s, and after 3–5 s, there was stable steam production. The experimental version produced steam of 560–950°C at 4–9 MPa. This compact, soot free and low-cost component is largely ready for the market.

8.4. EXAMPLES FOR CONCEPTS OF A LARGE SCALE HYDROGEN ECONOMY

8.4.1. Euro–Quebec Hydro–Hydrogen Pilot Project

In 1987, the concept of a clean energy system based on hydrogen as a transportable medium was presented. It was the result of the cooperation of more than 20 companies and the starting point of the so-called Euro–Quebec Hydro–Hydrogen Pilot Project (EQHHPP) [506]. The idea of this project, as is depicted in Fig. 197, is to use 100 MW of hydroelectric power, of which plenty is available in Canada, for the production of hydrogen via electrolysis. The gaseous hydrogen is then liquefied (requiring another 30 MW(e) input) and transported by barge carrier across the ocean to Europe (Hamburg harbour) for distribution and consumption in various applications. The annual transportation of 14 600 t of LH_2 corresponds to an estimated equivalent power output of 74 MW(e) plus some 7 MW of ‘cold’ energy recovery. The main objective of the EQHHPP was the demonstration of the possibilities of safe transport and distribution of hydrogen, as well as its safe application as a fuel.

For the maritime transportation of the LH_2, concepts of barge carrier ships have been developed with the barge-mounted mobile tanks to also be used for on-shore storage in order to minimize transfer losses (see also Section 9.3.3). The proposed LH_2 terminal in Hamburg’s harbour comprised the port for loading and unloading

operations, a lifting platform to transfer the tanks after being floated out of the barge carrier ship to the shore, and the on-shore storage and distribution devices. The further distribution was planned to be done by tank trucks. Potential uses were seen to be as fuel for the local transportation system, as fuel for aircraft, for residential heating from fuel cell power plants, for gas turbine power plants, or for mixing with natural gas to hythane for introduction into the grid.

The Euro–Quebec project itself-was finally terminated in 1992, but continued to live in the form of various single sub-projects of a hydrogen demonstration programme, such as projects involving city buses, a hydrogen refuelling station in Hamburg, a fuel cell driven boat in Italy, the manufacture and (safety) testing of a 60 m^3 LH_2 model tank for maritime transportation, a 5 MW(e) H_2 fuel cell plant for cogeneration of heat and power in a residential area, and many others.

8.4.2. WE-NET project

One of the most ambitious hydrogen energy research projects pursued in Japan was the International Clean Energy Network Using Hydrogen Conversion, or the World Energy Network (WE-NET) for short. Operating under the wider frame of the New Sunshine project, its main objective was the establishment of a large scale energy system based on hydrogen from renewable energy sources. Starting in 1993, WE-NET was scheduled to run over 28 years in three distinct phases. Phase I (1993–1998) dealt with the survey on key technologies and elemental research and system studies. Phase II (1999–2005) was dedicated to the development of prototype systems in the order of 50 MW. And in Phase III, the hydrogen technologies were to be demonstrated in sub and full systems [508]. The main hydrogen production method was considered to be solid polymer electrolyte water electrolysis. Long distance maritime transportation as LH_2, or as H_2 carrier liquids like methanol or ammonia, was foreseen. On the demand side, the hydrogen was to be used as a fuel in the transportation sector, in fuel cell power plants, in combustion turbines, in households and as chemical feedstock. Originally based on renewable energies, later in Phase II fossil fuels were also considered, to allow the introduction of large amounts of H_2 in the short term.

In Phase I both the conceptual design of the total system and the energy balance and the electricity cost were verified. Phase II was used to continue the development of fundamental technologies and, in particular, to prepare distributed energy technologies. Studies were conducted on stand-alone refuelling stations (steam reforming or electrolysis), metal hydride vehicle tank systems, low temperature fuel cells, and LH_2 (magnetic) liquefaction [509]. Investigation and research in the field of safety was aimed at the establishment of a comprehensive system safety design including a concept of safety measures for the prevention of accidental LH_2 release or the mitigation of accident consequences. These activities included risk analysis of hydrogen subsystems, a collection of data on accidents involving handling of hydrogen, and the review and systematization of existing safety standards. The WE-NET project, originally planned as a long term programme, was eventually discontinued at the end of fiscal year 2002 and replaced with a more specific hydrogen and fuel cell programme to promote commercialization of fuel cells in mobile and stationary applications.

8.5. TRANSITION SCENARIOS

Several transition scenarios for EU25 are described extensively in Refs [510, 511], yet with a focus on the deployment of fuel cell technology. In the 2020 scenarios, fuel cell applications were mentioned with road transport accounting for the largest demand (Table 58).

TABLE 58. PROJECTED MAIN USERS OF HYDROGEN BY 2020 [510]

	Portable FCs for hand-held electronic devices	Portable generators and early markets	Stationary FCs for CHP	Road transport
Cumulative FC sales until 2020 (units)	>>250×10^6	600 000	$4–8 \times 10^5$	$1–5 \times 10^6$
Average power (kW)	0.015	10	20	80
Total power (GW(e))	>>3.75	6	8–16	80–400

TABLE 59. COMPARISON OF ENERGY CONSUMPTION IN MAJOR AREAS

Application	Current annual consumption (10^{18} J/a)	Reference
Energy value of total hydrogen production (world)	7.0	[100]
Energy value of natural gas for ammonia production for fertilizers (world)	2.98	[503]
Energy value of natural gas for hydrogen production for refining crude oils (world)	2.2	[503]
Passenger transport (EU25)	6.05	[512]
Small scale combustion installations (domestic heating, hot water, etc.) (EU25)	12	[513]
Air transport (USA)	3.0	[514]
Air transport (Germany)	0.3	[514]
Air transport (UK)	0.51	[514]
Air transport (Canada)	0.24	[514]
Steel production (world)	11.8	see Section 8.2.3

Table 59 identifies the biggest consumers that currently employ almost 100% fossil resources and that could in principle use nuclear hydrogen or synthetic hydrocarbons instead. All these sectors are linked to both population increase and gross national product.

Figure 198 shows a projection of hydrogen production processes, although no recommendation or prediction is given for the phase-out of fossil based production processes. The HyNet road map [27] predicts that electrolysis from nuclear will be among the first significant sources of hydrogen. The fact that low temperature electrolysis from baseload electricity with intermediate cavern storage of hydrogen makes economic sense was shown in Ref. [223] for the specific case of Canada.

The most immediate possibility for the use of nuclear hydrogen — and one that is overlooked in most strategic documents — is certainly stationary and concerns the fertilizer and petrochemical industries, which not only consume hydrogen but also significant amounts of process heat. This combination is also easiest to implement, as a high demand can be combined with large production and short transport distances, assuming that safety requirements can be met. The combination can possibly be considered economically viable already with low temperature electrolysis, on the condition that the hydrogen is produced from inexpensive baseload electricity with intermediate storage [223]. The combination with refineries would have a twofold positive effect on natural gas and crude oil prices, because it eliminates natural gas consumption in the refinery (the gas could be used more efficiently in other applications) while producing lighter and cleaner liquid fuels from heavy crude oils, oil shales and tar sands that would otherwise be difficult to process.

Due to the complex interaction of the different chemical processes optimized to a very high degree, the potential supply of energy by nuclear power may not be dedicated to a specific process, but rather cover the overall cogeneration of process steam, process heat and electricity. Any substitution of nuclear energy for process heat in large scale industrial productions results in a complicated restructuring of the on-site energy supply system. Processes may also have to be adjusted to reactor operational parameters. However, it promises significant CO_2 reductions and savings of fossil resources with economic competitiveness, which are the dominant challenges for future energy systems. This will include the generation of process steam and sensible heat for a variety of applications beyond dedicated hydrogen production. Quite a number of processes in the different industrial branches were selected and evaluated in Ref. [473] with regard to coupling to a nuclear energy source.

Processes for which helium temperatures of up to 700°C would be sufficient for steam production, and that therefore were deemed to require only minor further development work, include the refining of crude oil and oil production from tar sands and oil shale. A system of nuclear heat transfer into a refinery has been suggested (Fig. 199).

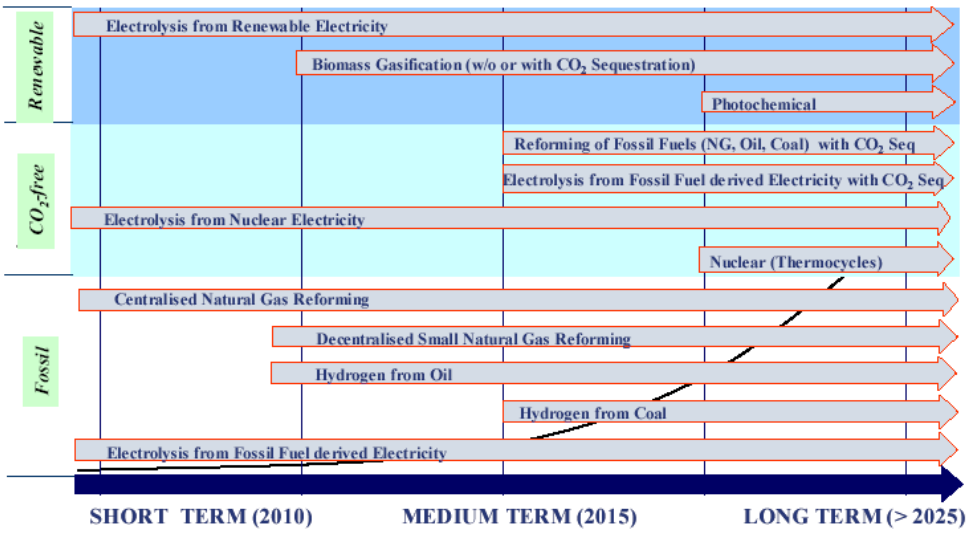

FIG. 198. Maturation of hydrogen production pathways [27].

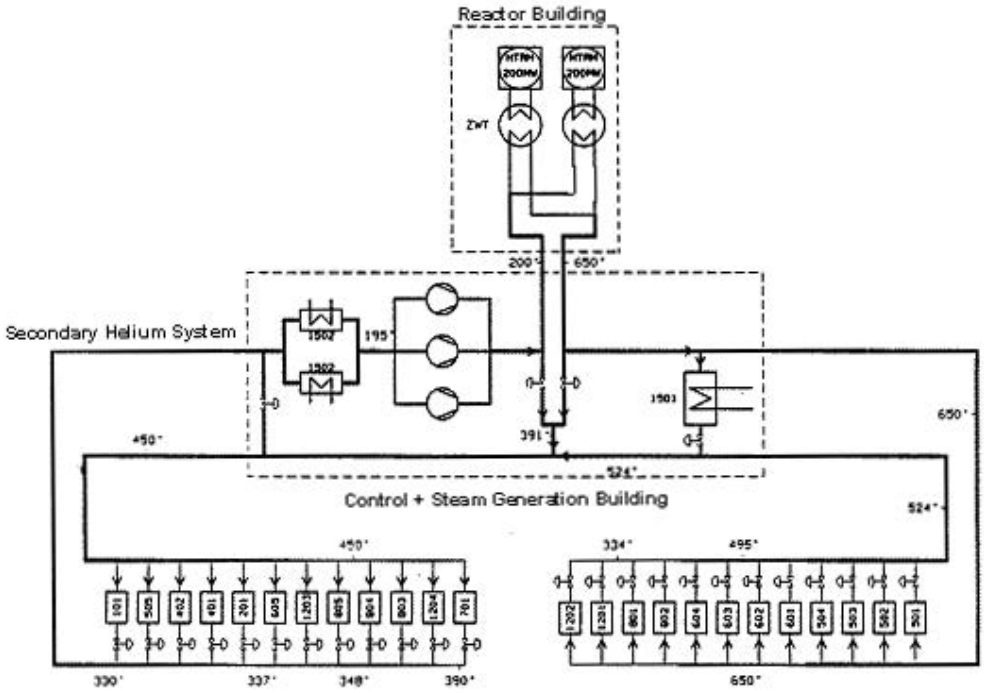

FIG. 199. Heat transfer system: HTR-M refinery [473].

Other processes with operating temperatures of up to 900°C include methanol synthesis with hydrogen production, e.g. from steam–methane reforming or the production or the production of ammonia/fertilizer. A major challenge in most cases is the design of the heat exchanger to transfer heat from the helium into the process. For some processes, heat transfer must take place in narrow temperature/pressure ranges with regard to the desired product spectrum and therefore requires a sophisticated solution with strict conditions. An example is the heat exchanger for the vacuum distillation process where operating temperatures must not exceed the cracking temperature of the feed (see Table 54). The preliminary design of a helium-vacuum distillation feed heat exchanger is shown in Fig. 200 [472].

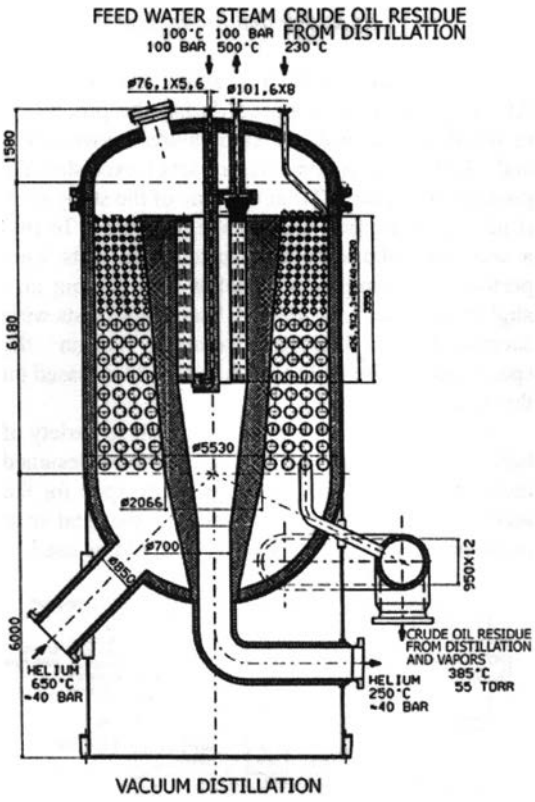

FIG. 200. Preliminary design of a heat exchanger with nuclear-heated helium on the primary and vacuum distillation feed on the secondary side [472].

The so-called hydrogen intermediate and peak electrical system (HIPES) has been suggested [481] as a large scale nuclear and renewable hydrogen production system which includes:

— Hydrogen production by water splitting;
— Hydrogen and oxygen storage in large scale, low cost underground centralized storage facilities;
— Hydrogen to electricity conversion by combustion of the H_2 with O_2 to very high temperature, high pressure steam for a high efficiency steam turbine or, alternatively, in lower cost fuel cells.

Given the huge number of nuclear power plants required for significant nuclear hydrogen or synthetic hydrocarbon production, and given the growth rates of the worldwide primary energy demand, it is clear that an increase in the nuclear contribution can only be gradual. The pressure for building nuclear plants for hydrogen production is a direct function of the volatility of natural gas prices as the main competitor. In conclusion, and independent of any detailed projection of energy demand and mix of energy sources, it seems almost impossible to question the secured long term potential and need for nuclear power to penetrate into the non-electricity market.

The massive demand for heat and electricity will likely rise within the next decades when oil is increasingly extracted from tertiary resources (tar sands, oil shale) whose exploitation requires pumping power and large quantities of steam at above 300°C. The production of synthetic fuels and the upgrading of heavy oils require huge amounts of hydrogen. The industrial demand for heat will be the main driving force for the development of VHTRs, rather than their use as electricity sources [38]. But it is also clear that nuclear alone will be unable to produce the required energy: the capacity for building nuclear plants in the world is too low and the lead-time to construction too long to satisfy the demand, at least in the short and medium terms.

9. HYDROGEN INFRASTRUCTURE

9.1. LIQUEFACTION OF HYDROGEN

9.1.1. Energy requirement

There are different pathways for cooling hydrogen gas down to its boiling point, but all require the same minimum specific exergy. The type of process selected is dependent on different parameters such as the real energy demand determined by the efficiencies of the single compressing and cooling steps, the amounts of irreversible losses, and the availability of the necessary systems and their costs. The minimum specific work (exergy) required for the liquefaction of hydrogen at ambient conditions is composed of [515]:

— The work for cooling the gas to the boiling point determined by the Carnot cycle;
— The work for condensation of the gas;
— Additional work necessary for the temperature dependent ortho–para conversion.

The total minimum (theoretical) energy required for liquefying hydrogen is 3.92 kW·h/kg or 14.1 MJ/kg [516]. The actual technical work required, however, is a minimum of 11.1 kW·h/kg of LH_2, corresponding to 33.3% of the LHV of hydrogen.

9.1.2. Liquefaction process

The first step in the liquefaction process is the precooling of the hydrogen, usually done with liquid nitrogen. This precooling step is necessary, because if a gas is to cool down upon expansion, its temperature must be below the inversion temperature, which is 193 K for hydrogen at ambient pressure. Ortho–para conversion can be done adiabatically simply using a catalyst bed, however, this is at the expense of a temperature increase of the flowing hydrogen. There is also an isothermal method, placing the catalyst into LN_2 or LH_2 at boiling point with the temperature remaining constant [517].

9.1.2.1. Linde–Hampson and Claude processes

Most liquefaction processes in practice use thermodynamic gas cycles with compression, heat exchange and expansion. The Linde–Hampson method is the simplest one, using isenthalpic expansion as a single thermodynamic process. Its efficiency, however, is not very high. Under optimized conditions, the liquefaction energy requirement is 13.12 kW·h/kg of LH_2 plus 6.7 kg of LN_2 per kg of LH_2 for precooling [515]. Hampson applied the process in 1896 for the liquefaction of air, using air at ~20 MPa to be expanded to atmospheric pressure and passing the cooled air through a heat exchanger. A power of 3.7 kW was necessary to produce 1 L/h of liquid air.

A major step in the further improvement of the process was suggested by Georges Claude in 1902 with the use of an expansion engine, a cylinder with a moving piston, i.e. applying ‘external work’, to achieve lower temperatures than the Linde process. Heat is removed as mechanical energy. Later, expansion engines were replaced with expansion turbines, first introduced by Kapitsa in 1936. The Claude process has since become the commonly applied method in large scale liquefaction plants. Refrigeration is conducted in four principal steps (Fig. 201):

(1) Compression of hydrogen gas at ambient temperature, removal of compression heat;
(2) Cooling with liquid nitrogen (~80 K);
(3) Expansion of a part of the hydrogen in an expansion turbine resulting in a further cooling of the residual hydrogen (80 ⟶ ~30 K);
(4) Expansion of residual hydrogen in a Joule–Thomson valve until liquid state is reached.

The final cooling stage from 80 to 30 K represents the most energy intensive step. Possible solutions are either the ‘classic’ cascade refrigeration, with cycles using different coolants (as was demonstrated by Dewar), or the

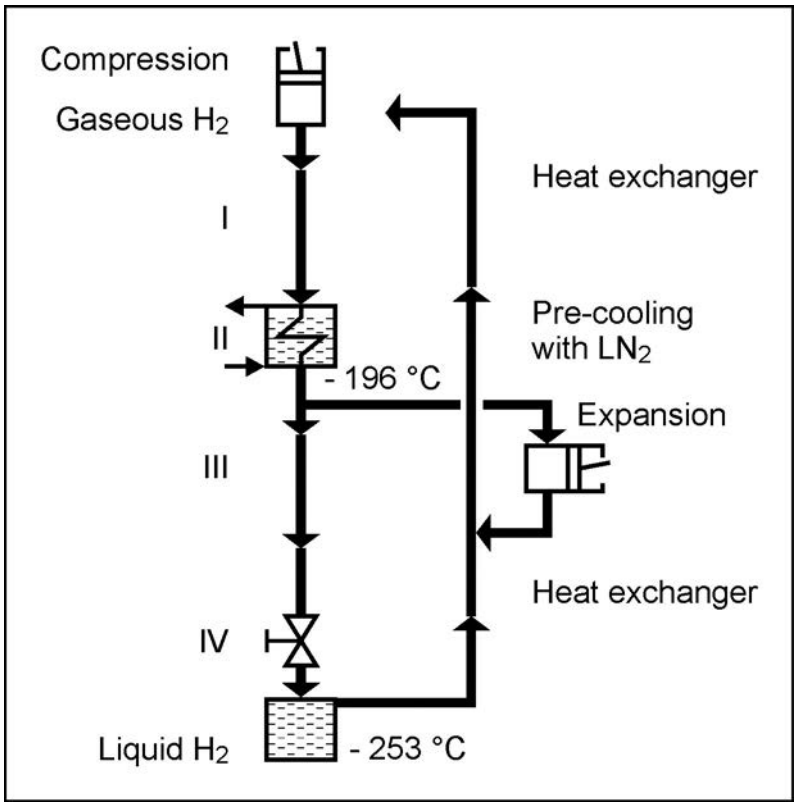

FIG. 201. Schematic of Claude process for hydrogen liquefaction [518].

more economical Brayton cycle, with just one gaseous coolant that is sequentially expanded before it cools down the hydrogen in a countercurrent heat exchanger. Expansion step 3 would already be sufficient for liquefaction. But the Joule–Thomson expansion is applied for the final step to avoid two-phase flow in the expander.

Variations of the dual-pressure Claude process as a large scale liquefaction method have proven to be the optimal solution. The large scale plants of today usually operate with six heat exchanging stages, the first of which is the LN_2 stage. The principle of the heat exchanger is to use the adiabatic expansion with smaller temperature drops per expansion step. The cooled gas is taken to precool the incoming gas, which then starts expansion at a lower temperature level (‘progressive cooling’).

Heat exchangers are typically operated at pressures up to 6 MPa. They are compact to minimize heat input from outside and made of aluminium or chromium alloy steels with sufficiently high thermal conductivity and sufficiently low thermal expansion and that are resistant against hydrogen embrittlement. The ortho–para conversion is also done in several stages at different temperature levels achieving a para fraction of >95%. The maximum impurity level in re-gasified hydrogen is in the order of 1 ppm. Efficiencies are in the range of 60% [519].

9.1.2.2. Magnetic refrigeration process

A magnetic type of cooling was proposed by Debye and Giauque in 1926. The magnetic refrigeration method takes advantage of the magneto–caloric effect, i.e. the adiabatic temperature increase in the presence of a magnetic field in the working material, and a temperature decrease if the magnetic field is removed. The effect benefits from the isentropic demagnetization of a ferromagnetic material as a cooling process. Materials are magnetized slowly at the higher temperature before they are suddenly demagnetized and return to the initial state. The magnetic refrigeration cycle consists of the following steps:

(1) Adiabatic magnetization in an external magnetic field causing alignment of the magnetic dipoles (thus reducing entropy, thus increasing temperature);
(2) Transfer of the heat to a fluid (water, helium) at the same magnetic field strength;
(3) Adiabatic demagnetization with removal of the magnetic field at constant entropy, i.e. decreasing the temperature;
(4) Heat transfer from the gas (to be cooled) to the working material (solid).

The temperature can drop by 10–15 K depending on the strength of the magnetic field. The temperature change is maximal at ± 25 K around the material's Curie point where it changes from ferromagnetic to paramagnetic. Various candidate materials with reversible transition and significant adiabatic temperature change are available covering the total range between 20 and 300 K. The most appropriate materials to show a high magneto–caloric effect are based on gadolinium and some of its alloys, e.g. $Gd_5Si_2Ge_2$ [520].

This method promises a compact cooling system design with a long lifetime, higher efficiencies and lower capital costs, since neither expanders nor compressors are required. The liquefaction work is estimated to be at the level of 7.3 kW·h/kg [521]. Magnetic refrigeration, however, is still at the R&D level. Within the WE-NET project, a 10 kg/d capacity laboratory scale plant was constructed and operated [522].

9.1.3. Liquefaction efficiency

A realistic unit power value for today's large scale liquefaction plants in the USA comprising the whole process of cooling H_2 from ambient temperature to its liquid state at the boiling point, including all thermal and mechanical losses, is in the order of 12.5–15 kW·h/kg [523]. This corresponds to an exergy efficiency of 26–32%. The smaller scale facility in Ingolstadt, Germany, requires an energy input of ~15 kW·h/kg of H_2 or up to about 38% (45%) of the higher (lower) heating value of hydrogen. But even for the most recent liquefaction plants, efficiency has only improved slightly.

Of the costs for a typical hydrogen liquefaction plant, capital costs account for about 63%, mainly due to the compressors and brazed aluminium heat exchanger cold boxes. This is followed by power costs (~30%) and O&M (~7%). Further cost reductions are seen in the development of improved expanders and compressors, lower cost insulation and more efficient refrigeration, but also in the construction of larger scale plants with capacities up to 850 t/d and modular type systems with plant repeatability [523].

9.1.4. Present hydrogen liquefaction capacity in the world

Starting with the Apollo space programme in the USA in the 1960s, hydrogen liquefaction plants have been designed and constructed on a large scale. Their concepts were based on the experience gained from the numerous small scale plants previously developed in laboratories around the world, and on the requirement of economically viable production of LH_2. Also, mobile hydrogen liquefaction stations on a small capacity scale have been constructed to meet the temporary demands, e.g. at testing sites. At present, the total global hydrogen liquefaction capacity amounts to approximately 290 t/d.

In Europe, it was the Ariane space programme that initiated the construction of LH_2 production plants in the 1980s. There are now four plants in Europe with a total capacity of ~25 t/d. In the Russian Federation, two hydrogen liquefaction plants are reported to have been commissioned in the late 1960s at NIICHIMMASH in Serguiev Posad (Zagorsk), north of Moscow, to serve the fuel production for rocket and space systems. The capacities of the plants were 4.3 t/d and 7.2 t/d, respectively, for an annual production of up to 5000 t of LH_2 [524]. The first plant still seems to be in operation. Liquid hydrogen production in China and in India (since 1996) is only temporary and dedicated to their respective space rocket developments. In India, a 1 t/d capacity plant was constructed for the Indian Space Research Organization in Saggonda and a smaller plant for the Liquid Propulsion System Centre in Mahendragiri. One of the first hydrogen liquefaction facilities in Japan has been operating since 1977 at the Noshiro Test Centre (Akita prefecture) a production capacity of ~50 kg/d for rocket propulsion experiments.

Recently, in addition to the existing Japanese space programme, smaller scale production of LH_2 started as part of the current national hydrogen and fuel cell programme. There appears to be a growing market for smaller facilities to serve the needs for LH_2 fuelled vehicles. Table 60 presents an overview of the liquefaction plants around the world.

TABLE 60. OVERVIEW OF WORLDWIDE ON-STREAM HYDROGEN LIQUEFACTION PLANTS

Place	Operator	Capacity (tonnes/d)	Operation since
Sarnia, ON, Canada	Air Products	27	1982
Bécancour, QU, Canada	Air Liquide	11	1988
Magog, QU, Canada	BOC	13.5	1989
Kourou, French Guiana	Air Liquide	2.3	1990
New Orleans, LA, USA	Air Products	32	1963
New Orleans, LA, USA	Air Products	32	1978
Sacramento, CA, USA	Air Products	5.5	1986
Niagara Falls, NY, USA	Praxair	36	1988
Pace, FL, USA	Air Products	27	1994
McIntosh, AL, USA	Praxair	26	1995
East Chicago, IN, USA	Praxair	27	1999
	Total America	238.8	
Waziers, France	Air Liquide	10.5	1987
Ingolstadt, Germany	Linde	4.4	1991
Leuna, Germany	Linde	5.0	2007
Rozenburg, Netherlands	Air Products	5.0	1987
Sergiev Posad, Russian Federation	NIICHIMMASH	4.3	late 1960s
	Total Europe	29.2	
Beijing, China	CALT	0.5	1995
Mahendragiri, India	Asiatic Oxygen Ltd	0.5	1992
Saggonda, India	Indian Space Res. Org.	1.0	2004
Noshiro, Akita, Japan		1.2	1977
Amagasaki, Hyogo, Japan	Iwatani Gas	1.2	1978
Tashiro, Akita, Japan	Mitsubishi Heavy Ind.	0.5	1984
Oita, Japan	Pacific Hydrogen Co.	1.5	1987
Tanegashima, Japan	Japan Liquid Hydrogen Co.	1.2	1987
Kimitsu, Chiba, Japan	Nippon Steel Corp.	0.2	2004
Sakai, Osaka, Japan	Iwatani Gas	10.0	2006
Ichihara, Chiba, Japan	Iwatani Gas	5.0	2009
	Total Asia	22.8	
	Total World	290.8	

9.2. STORAGE

Unlike electricity, hydrogen can be conveniently stored. The major storage options are at high pressures, low temperatures, in porous materials or in the form of (complex) metal hydrides. Due to its low volume related energy density, hydrogen requires a comparatively large volume for storage. While its gravimetric density is three times that of gasoline, the volumetric density is only 25%. What is at first surprising is the fact that even 1 m^3 of liquid hydrogen has, at 71 kg, a lower H_2 mass content than other chemical hydrogen storage media, e.g. gasoline (84 kg), ammonia (136 kg) and even water (111 kg) (Table 61).

TABLE 61. HYDROGEN DENSITIES IN DIFFERENT FORMS OF STORAGE

Fuel	Formula	Density (kg/m^3)	Energy per mass (kJ/kg)	Energy per vol (GJ/m^3)	H_2 density (kg H_2/m^3)
Hydrogen	H_2	0.09	141 890	0.013	0.09
LH_2	H_2	71	141 890	9.9	71
LNG (methane)	CH_4	423	55 530	~20.5	106
LPG (propane)	C_3H_8	581	50 400	25.2	106
Gasoline (octane)	C_8H_{18}	745	47 400	30.4–34.8	118
Methanol	CH_3OH	793	22 700	18.0	99
Ethanol	C_2H_5OH	794	29 900	23.5	104
Methylcyclohexane	C_7H_{14}	862	42 500	26.9	96
Ammonia	NH_3	771	22 500	17.4	136
Water	H_2O	1000	—	—	111

9.2.1. Gaseous storage

9.2.1.1. Pressure vessel storage

A proven technology for storage systems for stationary applications is the steel bottle/tube bundle, based on the use of steel as a structural material and involving gas pressures up to 23 MPa. These systems are essentially used at industrial chemical/metallurgical plants and distribution centres. The storage of compressed hydrogen in high pressure cylinders is bulky and rather expensive compared with the small quantity of hydrogen stored.

A significant amount of energy is needed to compress the gas (e.g. 9% of the stored energy for a 70 MPa tank). The compression process may be isothermal or adiabatic. The difference is the final temperature of the compressed medium remaining constant in the former and rising considerably in the latter case. Multistage compressors with intercoolers operate somewhere in between isothermal and adiabatic compression [27]. In the near term, gaseous hydrogen storage might become possible at a mass fraction of up to 9% [525].

A classification of high pressure tanks for hydrogen storage in vehicles is given in four categories, with Type 1 being the classic heavy, all-metal tanks, Type 2 being metal tanks with a glass fibre wrapping around the cylindrical part, which takes approximately 50% of the pressure load, Type 3 being light-weight tanks made of composite materials (carbon fibre) with a metallic liner inside, and Type 4 being composite tanks with a polymer liner. The weight reduction for Type 3 and 4 tanks is 70% compared with Type 1 tanks.

The principal advantage of composite material is its light weight, reducing total weight by 25–75% compared with a metal tank. For the new generation of pressurized H_2 tanks for vehicle applications designed for 70 MPa, the development of a thermoplastic polymer liner which ensures a maximum loss rate of 1 cm^3 of H_2 per litre of volume per hour and good mechanical strength in the temperature range of –40 to +85°C are important tasks.

Compressed gas in Type III and Type IV tanks is currently the preferred method for on-board vehicular storage. The very high gas storage pressure of 70 MPa will be a practical optimum required to contain a sufficient driving range of fuel, whereas 20–25 MPa is the typical pressure level for stationary hydrogen storage, for instance at a hydrogen refuelling station. Hydrogen vehicle pressure tanks for pressures of 35 MPa have already reached a commercial stage for fleet vehicles [27]. They are relatively expensive, and the high operating pressures give rise to safety concerns in the event of an accident. The targets set by the Strategic Research Agenda are (vehicle range of 500–600 km): 5 kg of storage at 70 MPa (~12 MPa at 20ºC), with hydrogen delivery temperatures between –40ºC and +85ºC and a lifetime of at least 1500 cycles. Vehicle tanks are fitted with various safety and monitoring related components.

9.2.1.2. Underground storage

While short term storage of hydrogen takes place in spherical high pressure tanks, long term underground storage in geological formations may represent a low cost technology in the capacity range of 100 GW·h. Very large quantities of hydrogen can be stored as a compressed gas in salt caverns or deep saline aquifers. Typical parameters are 700 000 m^3 of geometrical volume and a maximum operating pressure of 20 MPa. If the roof of the cavern is at a depth of ~1000 m, the net storage capacity will be around 6000 t with a cushion gas; i.e. the gas contents at minimum pressure ensuring easy recovery, to be around 3000 t hydrogen [526]. Maximum withdrawal rates are about 10% of the storage capacity per day. In a natural storage volume, the ceiling structure must be additionally sealed by water in the capillaries. Natural loss of hydrogen from diffusion through rock and operating loss are estimated to amount to ~5% per cycle. Centralized underground bulk storage facilities favour the use of centralized hydrogen production (such as by nuclear energy) rather than hydrogen transportation from dispersed sources [481].

The safe and economic long term storage of gases, primarily natural gas, in depleted gas fields and natural aquifer formations has been standard engineering practice for many decades [526]. There are two existing underground hydrogen storage sites, including an 8000 t capacity cavern in the USA and another one under construction. In Teesside, UK, three smaller caverns with 200–300 t of H_2 each have been in operation for many years. Other examples are a large aquifer in Beynes, France, with a value of 364×10^6 Nm^3 of town gas with a 56% share of hydrogen, and an exploited natural gas field in Amarillo, TX, which contains 840×10^6 Nm^3 of helium. In addition, the co-storage of hydrogen with natural gas has been proposed. Commercial hydrogen storage technology will be based on natural gas storage technology. There are 417 locations in the USA where natural gas is stored, with a total storage capacity exceeding 2.4×10^{12} Nm^3 [481]. Germany currently has about 170 caverns in use for the storage of natural gas for seasonal load balancing, shutdown and trading reserve [526]. Salt caverns are the ideal and currently the only underground facilities for hydrogen gas storage. Salt rock is highly gastight, does not react with hydrogen (or natural gas), and has low specific construction cost. Research will look at other storage options like aquifers or buried cavern tanks for smaller quantities [527].

9.2.2. Liquid storage

The storage of hydrogen in the liquid phase is highly beneficial due to its high energy storage density and is practicable in many applications. Storage of larger amounts as liquid allows for lower central storage costs and provides greater flexibility. More storage capacity leads to a higher utilization rate of a hydrogen consuming plant [528]. Liquid hydrogen is particularly demanded where the hydrogen is needed at a high purity level and where volume and weight are an issue such as in the transportation sector. The drawbacks are special handling requirements, boiloff losses, the need for control of temperature stability to avoid overpressure, and, most important, the liquefaction energy requirement. LH_2 storage technology is commercially available in a wide range. Vessels are manufactured in sizes from 0.1 to several thousands of cubic metres.

9.2.2.1. Principal tank design

Because of its low temperature, liquid hydrogen must be stored in an effectively insulated container, a dewar or ‘cryostat’. The principal design of a storage tank is a double-walled, vacuum jacketed fluid container (Fig. 202). The outer tank serves as protection for the inner tank against impacts from outside as well as of the neighbourhood if the inner tank fails. The space between the two vessels serves as an insulation layer to minimize heat transfer to the inside. The supporting structure and interconnections have to fix the inner shell, but also ensure that it can freely undergo contraction and expansion due to the numerous temperature cycles (refills) that may occur during the tank’s lifetime. Also, heat transfer from the outside must be minimized. An even more complex structural design is necessary for large vessels. The ideal shape of the vessel is spherical because of the minimum surface to volume ratio and the more uniform distribution of stresses and strains.

A multilayer foil insulation is usually chosen for tank sizes up to 300 m^3 to minimize the transport of radiation heat. It consists of some 60–100 layers of reflective foils fixed on the outside of the inner vessel, with a total thickness of at least 20 mm. (The layered type of insulation is usually called superinsulation.) The remaining void volume of the intermediate space basically serves as vacuum jacket to avoid air condensation on the cold surfaces and heat transport by convection or residual gas conduction [529].

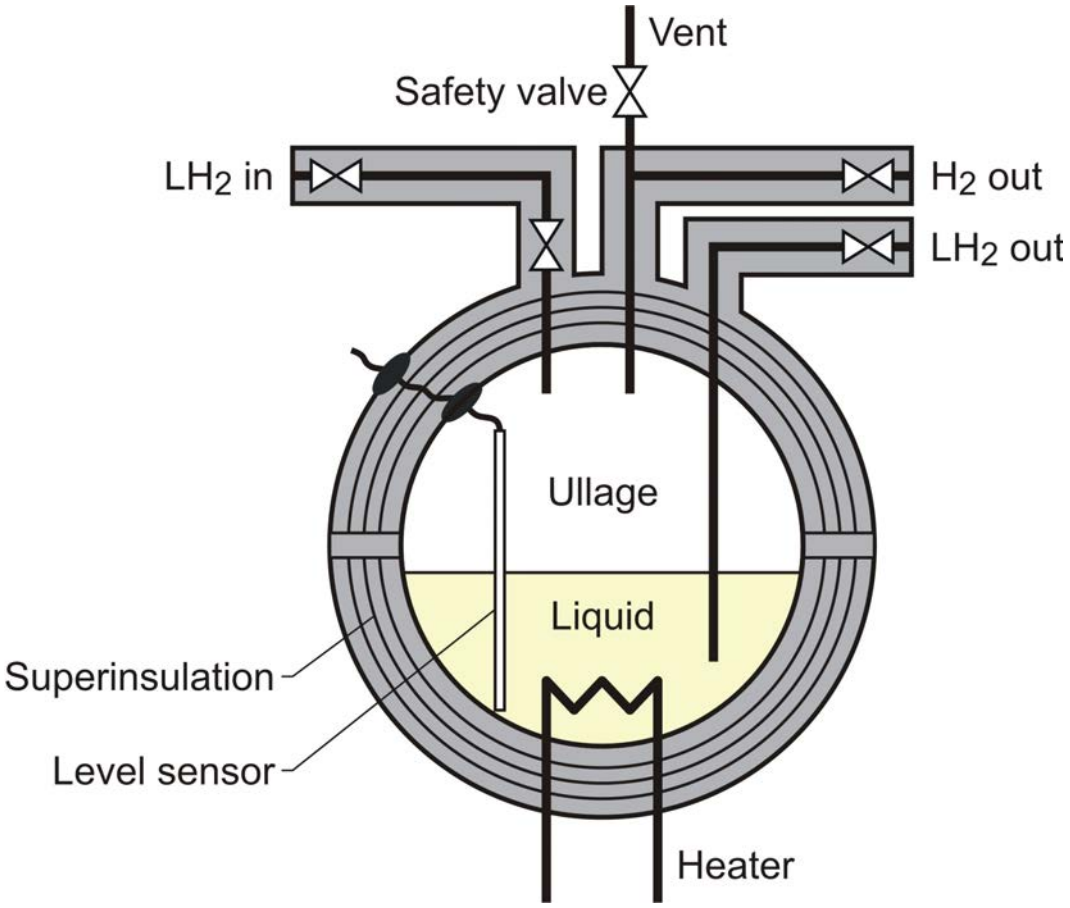

FIG. 202. Principal schematic of LH_2 tank [529].

Maximum and minimum design temperatures are determined by the loss of strength of the storage walls at the higher end and by loss of ductility (embrittlement) at the lower end. A relief valve should be designed to handle abnormal operating conditions such as overfilling. It should open at pressures less than or equal to the design pressure to allow a relief such that the pressure does not rise beyond 110% of the design pressure.

Depending on the insulation quality and the surface to volume ratio, a certain fraction of the stored cryogen is an unavoidable boiloff to keep the rest cold. This amount is in the order of a few per cent per day for a passenger car tank and decreases with increasing volume to 0.4%/d for a 50 m^3 cryogenic tank and an estimated 0.06%/d for a 20 000 m^3 LH_2 tank. Overpressures exceeding specified limits after a certain time, the so-called lock-up time, are relieved via a boiloff valve and a safety valve.

Liquid hydrogen will be expelled from the container by pressurization. This can be done by either a pressurizing gas from an external source or a vaporizer in the form of a heat exchanger which receives liquid from the container by means of a pump or gravity and sends the gas into the ullage space. Some of the liquefaction work can potentially be recovered when the liquid is vaporized, which is a matter of downstream engineering technology. The theoretical maximum is 10% of the energy invested [530]. The autonomy of the storage system, i.e. the time without any loss of the contents, is typically 30 days.

Appropriate materials used for a cryogenic tank are carbon steel for the outer vessel and stainless steel or aluminium for the inner vessel. Tubing from the inner vessel to the outside is generally made of stainless steel with vacuum-sealed transition on the cold side [516]. With regard to further weight reduction, fibre reinforced (composite) materials are being investigated to be used not only for high pressure tanks, but also for cryo-tanks, and with a specific energy storage capacity similar to that of conventional tanks. The advantages would not only be the higher strength compared with steel and the lower weight, but also, due to the lower pressure, the possibility to adjust the shape of the tank to the vehicle structure. On the other hand, composites are prone to enhanced

embrittlement and exhibit an anisotropic thermal expansion, almost none in the fibre direction and a high one perpendicular to the fibre direction.

9.2.2.2. Stationary LH_2 tanks

Large scale LH_2 tanks at the production site typically have a capacity of more than 100 t (~1400 m^3). The ullage gas carries a large refrigeration potential, which is being recovered for the liquefaction process via a vapour return line whenever practical. Tanks at the utilization sites are usually smaller, with capacities from 110 up to 2500 kg for vertical tanks or up to 5300 kg for horizontal tanks. The vessels are usually operated at an overpressure of 1.2 MPa.

Large stationary LH_2 tanks usually have an additional outer wall with the space filled with LN_2. Inner vessel walls are preferably thin due to cost and cooling, whereas the outer walls should be thick for the purpose of stability and stress uptake. Most of the large vessels are of a spherical shape. Lock-up times are in the order of 50 h [519]. Boiloff losses can also be reduced by making sure that most of the LH_2 to be filled is para-hydrogen.

The world's largest LH_2 tank is reported to be located at the Baykonur Cryogenic Centre in the Russian Federation with a total volume of 5600 m^3 [524]. At the NASA Kennedy Space Centre (KSC) in the USA, two identical ball shaped tanks have been constructed which are used within the space shuttle programme. The tanks are 3800 m^3 double-walled, vacuum perlite insulated spherical storage vessels. The outer sphere is made of carbon steel with an inside diameter of 21.34 m, and the inner sphere is made of austenitic stainless steel with an inside diameter of 18.75 m. With nominal maximum LH_2 contents of 3218 m^3, the ullage is about 15%. The tank operated at a pressure of 620 kPa has a boiloff rate of 0.025%/d or about 800 L/d [516].

9.2.3. Solid storage

Other advanced hydrogen storage methods include metallic and chemical hydrides, amides, alanate storage systems and carbon nanotubes. Solid metal and chemical systems offer some unique storage solutions for hydrogen, with the main challenges at the current time being their weight and their slow response time during refuelling. The interstitial storage of hydrogen in carbon nanotubes is another concept with potential for very light weight hydrogen storage, but the R&D is still preliminary. In addition, several other storage systems and mechanisms may be promising, including the use of sponge iron and glass microspheres.

In rechargeable solid state storage, H_2 is absorbed at interstitial sites in intermetallic compounds or stored via phase transitions in complex hydrides. In both cases, the loading with hydrogen is connected with the release of heat (hydrogenation enthalpy) which must be removed. The heat is the enthalpy (heat of formation) of the reaction and is an indication of the strength of the metal–hydrogen bond in the metal hydride phase. When molecular hydrogen from the hydrogen gas comes into contact with the surface of a hydrogen storage metal hydride material, it dissociates into atomic hydrogen and distributes compactly throughout the metal lattice. For refuelling a hydrogen driven vehicle with typically 5 kg within a few minutes, a power in the order of MW is involved [531]. Heat transfer in this order of magnitude requires large, heavy and expensive equipment. Storage materials with acceptable H_2 density are still slower than what is required for rapid refuelling. The hydrogen releasing step takes place in the form of a catalysed hydrolysis reaction which is achieved by means of excess of water. Characteristics to be considered are solubility, excess water, hydration of by-products, reactivity of the catalyst and lifetime.

The advantages of solid state storage are its safety, since low pressures are involved, and its high volumetric storage capacity. The disadvantages are the low gravimetric absorption capacity (of most hydrides) and the high cost. Volumetric and gravimetric capacities are listed in Table 62 for selected hydrides and are compared with gaseous and liquid hydrogen.

Complex hydrides are also considered promising hydrogen storage materials with capacities of up to 5.5 wt% of H_2 (compared with 1.5 wt% of conventional hydrides). These are low density powdery substances consisting of <10 μm particles, but with a high BET surface in the order of several tens of m^2/g. An example is $NaAlH_4$ which was discovered to exhibit enormous hydrogen discharging and recharging ability if doped with Ti as a catalyst. In terms of safety, hydrides have the advantage that heat is consumed in the hydrogen discharge reaction. A safety issue with complex hydrides containing $NaAlH_4$, $LiNH_2$, $Mg(NH_2)_2$, LiH and $LiBH_4$ is that they were found to be flammable, pyrophoric and water reactive. Also, dust cloud explosions may be triggered by spark ignition [532].

TABLE 62. ENERGY CAPACITIES OF HYDROGEN STORAGE TECHNOLOGIES

Material	Volumetric capacity (kW·h/l)	Gravimetric capacity (% of total weight)
MgH_2	3.65	7.6
$FeTiH_2$	3.37	1.89
Mg_2NiH_4	3.31	3.6
$LaNi_5H_6$	3.09	1.37
H_2 liquid at 20 K	2.36	100
H_2 gas at 80 MPa	1.54	100
H_2 gas at 50 MPa	1.11	100

An innovative hydrogen storage system developed by the Austrian Institute of Technology (AIT) uses hollow microspheres for combined high pressure and chemical hydrogen storage. Water carrying the microspheres with a 5–200 μm diameter is injected together with $NaBH_4$ into a reaction chamber where a catalytic reaction takes place to produce hydrogen, $NaBO_2$ and heat. The glass spheres, which are gas-tight at ambient temperature, store the hydrogen at high pressures of 14–70 MPa. Such a system can theoretically reach hydrogen storage capacities of up to 10 wt% [533].

9.3. TRANSPORTATION/DISTRIBUTION OF HYDROGEN

Centrally produced hydrogen must be transported to markets. The development of a large hydrogen transmission and distribution infrastructure is a key challenge. The main transportation modes are water, road, rail and pipelines which form a distribution system for the products to the final consumer. Storage structures are located within the transportation network to accommodate the capacities of different transportation modes. The delivery methods selected are determined chiefly by the production volume and the delivery distance. Small and medium-sized hydrogen consumers use truck, rail and barge transportation modes for hydrogen in either liquid or gaseous form over longer distances. Chemical and petrochemical industries, which produce/consume large quantities of hydrogen, use pipelines and compressors for transportation of the hydrogen gas over short distances [534].

The transportation of hydrogen in the liquid state is considered practicable if it is consumed as a liquid, if the distance is sufficiently long, if large quantities need to be stored, or if high purity hydrogen is required. For liquid hydrogen, the costs of the equipment needed at the customer's site (cryogenic storage tank, vaporizer) and installation are much higher than those for handling gaseous hydrogen. On the other hand, customers that need high pressure hydrogen would need the installation of compression and storage equipment if the hydrogen is delivered as a liquid. Such requirements mainly determine the choice of the more cost effective transportation mode [82].

For sites where no hydrogen production plant is available and only smaller quantities of hydrogen are needed, pipeline delivery methods usually are not competitive. Very small quantities of up to 50 kg of H_2 are mostly sold and distributed via high pressure cylinders. Larger quantities are more likely delivered by tube trailers and liquid tank trucks. A liquid is easier to transport and easier to handle than compressed gas. But compressed gas transportation via tube trailer has lower power requirements and slightly lower capital costs. Distance is the chief deciding factor between liquid and gaseous hydrogen [534].

9.3.1. Pipeline transportation

Most of the hydrogen produced today is transported over short distances only, mainly by pipeline, e.g. on-site in refineries. Pipeline distribution is most effective for large flows and currently amounts to approximately 240 t/d, with pipeline diameters usually ranging between 10 and 300 mm and delivery pressures of up to 10 MPa. Pipelines become competitive when the demand grows to large capacities. The pipeline option may allow carrying much

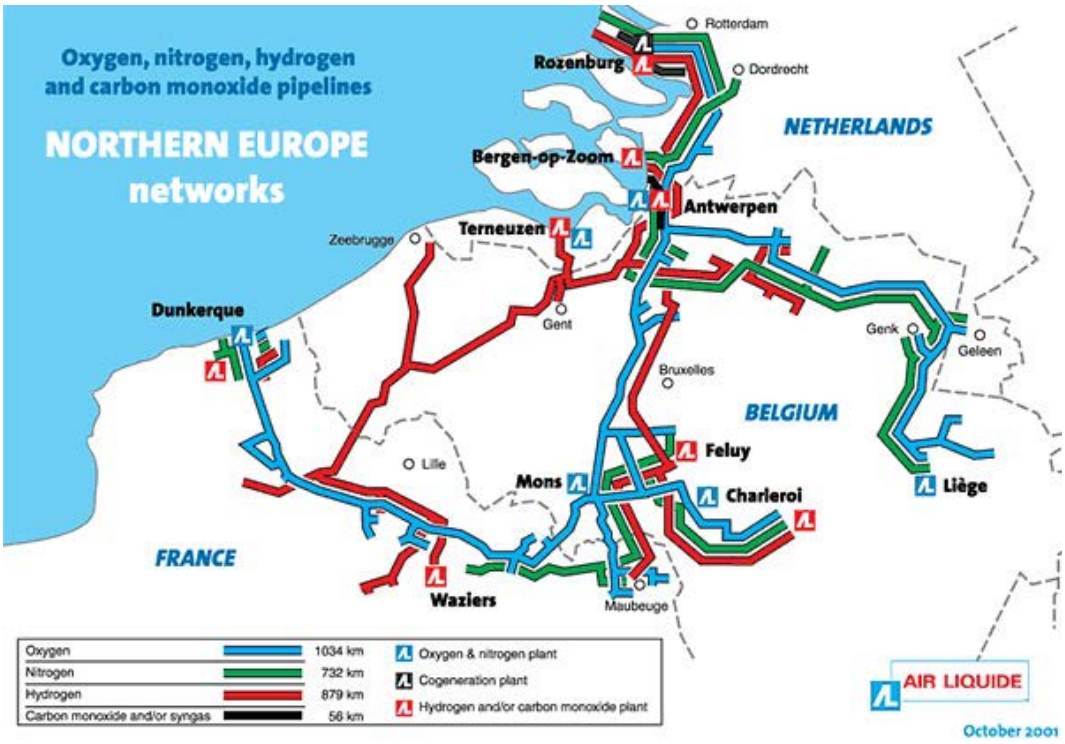

FIG. 203. Pressurized hydrogen supply pipeline system in France, Belgium, the Netherlands and Germany, operated by Air Liquide [535].

higher capacities of hydrogen at no additional cost. Energy loss during transportation is about 4% of the energy content.

Several networks for the commercial transmission and distribution of hydrogen gas have been developed and are being operated by the industrial gas industry with a good safety record. As of 2006, the US hydrogen pipeline network totalled ~2000 km in length, not considered on-site and in-plant hydrogen piping. This, however, is still small compared with about 475 000 km of natural gas transmission lines in the USA or more than 2 million km worldwide. Because of concerns over potential leakage, the hydrogen pipes tend to be much smaller in diameter. Special positive displacement compressors are also required to move hydrogen through the pipelines. The length of hydrogen gas piping tends to be short, because it is usually less expensive to transport the hydrogen feedstock, such as natural gas, through the existing pipeline network than to move the hydrogen itself through new piping systems.

The costs of a centralized hydrogen transmission and distribution system will depend on numerous factors such as distance to the consumer, pipeline diameter, quality and nature of the pipeline materials, operating pressures, rights-of-way, and how the applicable environmental and safety issues in the production, transmission, distribution and dispensing of hydrogen are addressed [7]. Furthermore, pipelines that carry pure hydrogen will require special construction and materials in order to avoid issues of steel embrittlement and leakage. Alternatives to metallic pipelines are polymer and fibre reinforced polymer pipelines.

Larger grids for gaseous hydrogen connecting industrial producers with industrial consumers are being operated in Europe and the USA. The largest agglomeration of chemical and petrochemical industries in Europe is located in the Netherlands and Belgium (Fig. 203) where Air Liquide of France is operating a more than 900 km pipeline grid for hydrogen transportation, currently connecting eight hydrogen units. The Ruhr-H_2 pipeline, also operated by Air Liquide, connects four large scale production plants and six industrial consumers. The capacity of the pipeline is 40 000 Nm^3/h at pressures up to 2.5 MPa. In the USA, most of the approximately 1200 miles (~1930 km) of hydrogen pipelines are concentrated in the states of Texas and Louisiana, where the majority of the US refinery industry is located.

If the use of hydrogen pipelines were to be expanded, possible embrittlement problems for pipes and fittings would have to be considered. The technology is available to prevent embrittlement, but depending on the configuration being considered, distribution costs may be affected.

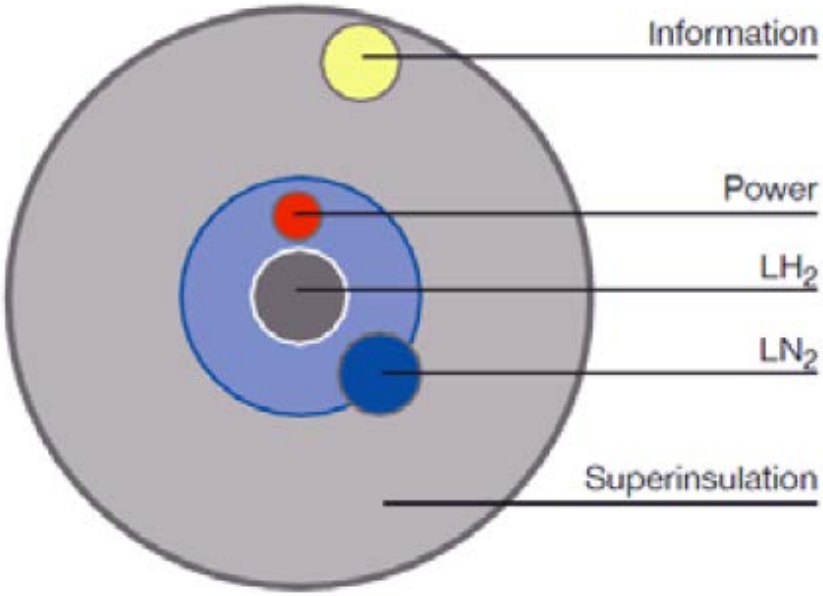

FIG. 204. Schematic of an icefuel cable [538].

Pipeline transportation of liquid hydrogen is realized on a small scale and short range. Similar to LH_2 storage tanks, pipelines are of double-wall design and vacuum jacketed. Because of the high costs increasing linearly with distance, LH_2 pipelines are economically attractive only for short distances. The transfer is done by pressure difference rather than by pumps. Major concerns, apart from heat leakage, are the mechanical stress imposed on the inner line due to contraction/expansion, pressure oscillations upon cooldown and two-phase flow. The Kennedy Space Centre uses a LH_2 (and LOX) pipeline of ~600 m length with an inner pipe diameter of 150 mm. The flow rates are up to 250 m^3/min of LH_2 and 100 m^3/min of LOX [536].

A government funded project in Germany, Integrated Cable Energy for Fuel and Power or icefuel [537], starting in 2006, is aiming at a new, highly efficient infrastructure for transport, storage and conversion of energy. A system for energy storage and the transportation of both chemical and electrical energy as part of a decentralized infrastructure will be developed and tested. The goal is to design a flexible, thermally insulated line for the simultaneous transport of cryogenic liquids (LH_2 or LNG), electricity and data via a high temperature superconducting material (Fig. 204).

Due to the high energy density of LH_2, an energy flux of ~10 MW could be realized through a low viscosity pipeline of less than 20 mm diameter over a 10 km distance. Tests up to now on a laboratory scale have comprised cable samples with 40 mm diameter and lengths up to several tens of metres for a transport capacity of 200–400 kW (LHV). The project also includes the development of infrastructure components such as heat exchangers, junctions, sensors and actuators. In a later stage, it is planned to demonstrate the concept on pilot plant scale [538].

9.3.2. Road transportation of hydrogen

Unlike conventional fuels, the transportation of hydrogen by trucks is limited with regard to volume rather than weight. The amount of gaseous hydrogen transported in pressure tube trailers ranges between 100 kg for short semi-trailers and 300 kg for the larger trailers, equivalent to about 3300 Nm^3. The hydrogen load may even go up to 600 kg with higher volume tubes in carbon fibre composite structures, still light compared to the 40 t gross weight of a tank truck. Distribution of hydrogen as compressed gas is mainly done for shorter distances (200–300 km) and smaller consumers (<250 Nm^3/h) [527].

Today's modern liquid hydrogen trucks can carry up to 3.5–4.2 t, or more than 50 m^3, of LH_2, which is at least ten times more than a tube trailer for gaseous H_2. The typical pressure in superinsulated tanks with an additional LN_2 shield is 0.15–0.2 MPa (maximum pressure: 1.11 MPa). The potential hazard of stratification in the tank does

not really occur in transportation, because the liquid is stirred by the movement and kept in thermal equilibrium. LH_2 trucks will preferably be used to meet the demands of a growing market in the near future. This delivery method is typically limited to small and medium sized quantities and distances of less than 500 km. Replacing conventional gasoline fuel with liquid hydrogen would increase the number of tank truck transports by a factor of three. Design criteria for a LH_2 container used in transportation are essentially the same as for LH_2 storage containers. The differences involve, for example, the degree of insulation required, which is lower in short term transportation compared with long term storage. Also, in general, geometry and weight are limited.

9.3.3. Maritime transportation of hydrogen

Barges carrying liquid hydrogen have been used for fuel supply within the US and French space programmes. Storage containers with a capacity of 947 m^3 of LH_2 have been used on the way from Louisiana to Florida since the NASA Apollo project, today serving the space shuttle. The European Ariane project was supplied with LH_2 by maritime transportation from New Orleans to Kourou, French Guiana, in 20 m^3 storage vessels with vapour or LN_2 cooled multilayer insulation [516]. These transports were discontinued with the beginning of the operation of the 5 t/d capacity, on-site liquefaction plant in 1990.

Various ship designs were developed in the 1990s within the Euro–Quebec project for future maritime transportation. Future LH_2 tank ships are designed for a load capacity of 125 000 m^3 to take up 8150 t of LH_2. The hydrogen gas turbine propulsion system proposed will be fuelled by the LH_2 as well as the boiloff losses. The system allows regaining a part of the technical work that was introduced during the liquefaction process (Enhanced Cryogen Exergy Recovery System (ECERS)).

Flowsheet analysis of the exergy or technically usable energy conducted within the Euro-Quebec project for maritime LH_2 transportation (from Canada to Europe) yielded an estimated overall efficiency of the system of 42%. A fraction of 10.4% of the primary energy input is needed for the hydrogen fuelled propulsion system of the ship. Other major losses are due to the electrolysis step and subsequent liquefaction of the hydrogen gas [539].

Studies of LH_2 maritime transportation were also conducted in Japan based on their broad experience of LNG ship construction. Within the WE-NET project, ships were conceived at a scale to deliver a 10 d supply of LH_2 as fuel to a 1000 MW(e) gas turbine power plant consuming 1200 t of LH_2 per day. With the additional consumption of H_2 for the 6000 sea mile trip (~11 100 km) every 10 days plus estimated losses, one ship transport was to carry some 200 000 m^3 (or ~14 000 t) of LH_2.

9.3.4. Chemical energy transmission systems

Hydrogen also can be transported using hydrogen rich carrier compounds such as ethanol, methanol, gasoline and ammonia. Such carriers offer lower transportation costs, because they are liquids at room temperature and are usually easier to handle than cryogenic hydrogen. But they also require an extra transformation step with costs that must be weighed against the cost savings associated with transporting low pressure liquids.

The key components of a chemical energy transmission system (CETS) or a chemical heat pipe are a primary energy source (fossil, renewable, nuclear) to provide heat to an input catalyst reactor. In this reactor, a mixture of appropriate materials is chosen for the desired endothermic reaction, i.e. for storing energy in the newly created products. After transportation of the product gas mixture at ambient temperatures, the reverse exothermic chemical reaction in an output catalyst converter helps to extract the stored heat for consumption as high grade or low grade heat or in a turbine. In a closed cycle, product materials are then returned to the heat source [540].

Unlike liquid hydrogen, chemical compounds with hydrogen provide an economical method of seasonal storage of energy. The reactions must be reversible, rapid and as complete as possible to avoid unwanted secondary products. They should have a high efficiency and a high reaction enthalpy in order to minimize the masses to be transported, plant and pipe sizes, and operating cost. They must be controllable to allow intermittent storage/retrieval operation. Furthermore, feedstock and products should be inexpensive, non-corrosive, non-toxic, and easy and safe to handle. CETS have to compete against hydrogen pipeline systems or the electricity grid.

Among a wide variety of potential energy carriers, the gas based system ‘synthesis gas/methane’ is one of the most promising and has been the subject of research, development and demonstration considering a connection to both nuclear and solar as the primary source of process heat because of the following advantages:

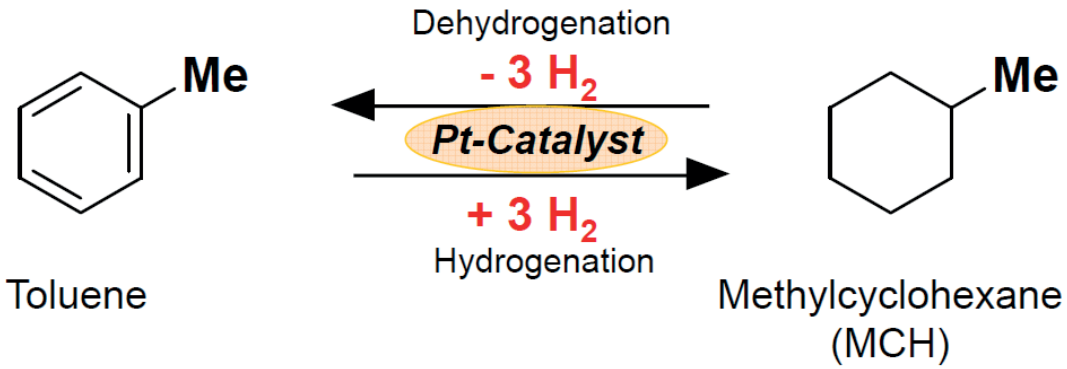

FIG. 205. Methylcyclohexane–toluene CETS [542].

— Chemical reactions proceed in one direction under certain conditions and in the reverse direction under other conditions.
— The reaction is heat consuming in the one direction and heat releasing in the other direction.
— The process takes place only in the presence of a catalyst, otherwise the system remains in a stable status without any reactions.
— All (partial) reaction steps are well known and widely applied in conventional technologies.
— The pipelines required correspond to the former town gas and present natural gas systems.

This methane based CETS became known under the acronym EVA/ADAM with a nuclear energy source and has been demonstrated in Germany, the USA and the Russian Federation (see also Section 4.1.2.3).

The CO_2 reforming process of methane has been studied as a chemical transportation system since 1980 as an alternative, in order to overcome some of the potential difficulties. In contrast to the CH_4–H_2O system, a third pipe is not required since it is not necessary to clean the water. Thus an open cycle system could be adopted. At the Weizmann Institute of Science (WIS) in Rehovot, Israel, a 480 kW solar steam/CO_2 methane reformer was designed, constructed and operated intermittently over two years as a complete solar heat pipe system [541]. The insulated, pentagon shaped reformer box contained eight tubes (length: 6.4 m, diameter: 51 mm) in two rows made of Inconel 617. The 4.5 m long heated section contained the catalyst. In the case of CO_2 reforming, which is thermodynamically more efficient and easier to operate under changing conditions (as in solar), the catalyst was 1% Ru on alumina. The tubes were directly heated by the solar radiation entering through a 600 mm aperture and reflected from the walls of the enclosure. The heat take-up was found to be quite uniform, with no local overheating tendency. The maximum average surface temperature was ~930°C and the heat flux was in the range of 80–84 kW/m^2. The flow rate of the process gas, which could be varied over a wide range of CO_2/H_2O/CH_4 feed mixtures, was limited to ~300 kg/h due to higher than expected pressure drop. It entered the reformer tubes at ~500°C and 1.6–1.8 MPa and left at ~800–830°C.

Another example is the hydrogenation of toluene (C_7H_8) on the supply site and the hydrogen evolution from methylcyclohexane (MCH, C_7H_{14}) on the demand site (Fig. 205). This system offers the advantage of safe and easy transportation at ambient temperatures in chemical tank ships or trucks and mild reaction conditions, with a high yield of toluene in the reforming reaction. The gravimetric storage capacity of MCH for hydrogen is 6.1 wt% or 47 kg of H_2 per m^3 [542].

Many candidates for closed loop reversible chemical energy transportation or seasonal storage systems with varying operating temperature ranges and storage capabilities have been identified, some of which are listed in Table 63. Certain limitations of the long distance heat transport are given by its restricted storage capabilities, by the limited temperature ranges and by the complex distribution systems required.

TABLE 63. ORGANIC SYSTEMS AS CETS CANDIDATES WITH ENERGY CARRIER HYDROGEN

Closed Loop CETS			Temperature range (°C)	Reaction enthalpy (kJ/mol)
$CH_4 + H_2O$	↔	$CO + 3\ H_2$	700–1200	250
$CH_4 + CO_2$	↔	$2\ CO + 2\ H_2$	700–1200	247
$C_2H_2 + H_2O$	↔	CH_3CHO		134
C_2H_6	↔	$C_2H_4 + H_2$		138
C_6H_{12}	↔	$C_6H_6 + 3\ H_2$	500–750	207
C_7H_{14}	↔	$C_7H_8 + 3\ H_2$	450–700	215
C_7H_{16}	↔	$C_7H_8 + 4\ H_2$		252
$C_{10}H_{18}$	↔	$C_{10}H_8 + 5\ H_2$	450–700	359

10. ECONOMIC ANALYSIS OF HYDROGEN PRODUCTION

10.1. EFFICIENCY

Efficiency is a factor that decisively determines the cost of the hydrogen production technology applied. A generally accepted definition for thermal efficiency is the ratio of the HHV of hydrogen (285.9 kJ/mol) over the total thermal energy input required for the decomposition process.

To evaluate the different hydrogen production methods, the basic thermal hydraulic relationships that govern the efficiency of electricity generation are used in combination with electrolysis as well as that of thermochemical processes for hydrogen production. Figure 206 shows the relationships of ΔH and ΔG, respectively, as a function of temperature for electrolytic water splitting (Case A, left) and for a fundamental two-reaction thermochemical method (Case B, right). As a result, the final conversion efficiency is independent of any route of conversion technology, assuming the same conditions for input and output [543].

Both processes — electrolysis and thermochemical cycle — are governed by the same Carnot law depending only on the upper (T_H) and lower (T_L) operational temperature as well as on the dissociation temperature (T_d), which is 4309 K for autothermal water splitting. The efficiency at temperatures at or above 4309 K — i.e. the ultra-high temperature, one-step direct thermal splitting of water — is 100%. At lower temperatures, it can be determined by [543]:

$$\eta = \frac{T_H - T_L}{T_H} \times \frac{T_d}{T_d - T_C}$$

This formula has a direct impact on the choice of technical options:

— The operational temperatures of the heat source and the process should be as high as technically feasible.
— Thermochemical processes or electricity generation at lower temperatures will always be inferior with regard to the thermal efficiency η.
— Since the dissociation temperature is extremely high, water splitting always needs several successive processes to provide the dissociation energy, i.e. electricity generation plus electrolysis (plus heat) or a follow-up of different endothermic and exothermic chemical processes at lower temperatures.

The high temperature processes for the production of hydrogen are at first glance attractive due to the high efficiency perspectives. However, all these processes also require a certain quantity of electrical or mechanical energy. Electricity can be produced either by diverting a fraction of the heat generated from the high temperature source, from another source or from the grid. In all cases, the electricity is produced from a heat source with an efficiency of η_{el}.

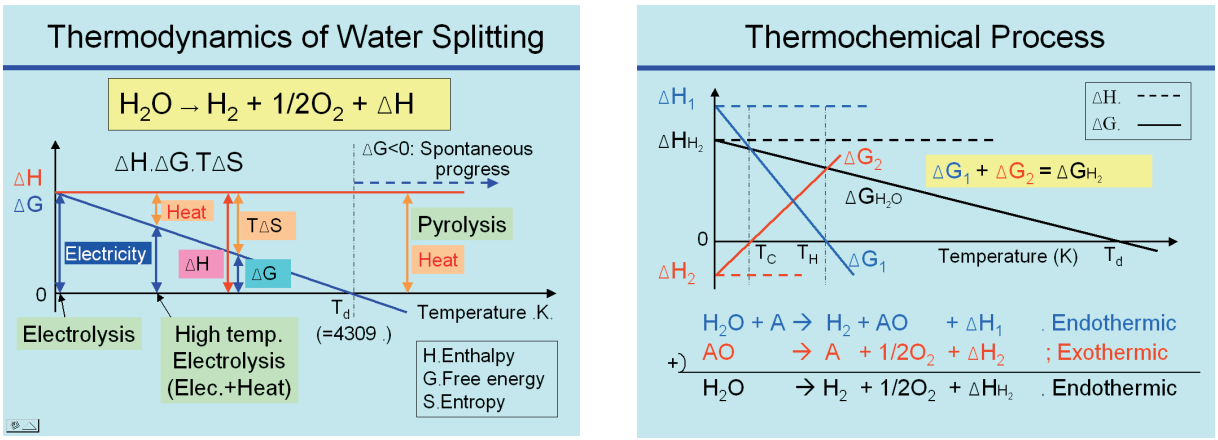

Case A: Electrolysis **Case B: Thermochemical Water Splitting**

FIG. 206. Analysis of hydrogen production by electrolysis and thermochemical processes [543].

An amount of work equal to W needs at least an amount of heat $Q' = W/\eta_{el}$. In each case where the same primary source is used to produce the work and the heat (Q) required for the splitting process, it is necessary to take at least $Q_T = Q + (W/\eta_{el})$ from the heat source. If these quantities are normalized to a unity of produced hydrogen, it is possible to define a global efficiency [151]:

$$\eta_T = \frac{HHV}{Q_T} = \frac{HHV}{Q + (W/\eta_{el})}$$

where HHV is the enthalpy of formation of liquid water at ambient temperature or the higher heating value. Such a global efficiency must be compared with that of the chain:

heat source → electricity → H_2 production by low temperature electrolysis

for which it is easy to estimate a global efficiency:

$$\eta_{T,alkalineelectrolysis} = \eta_{el} * \eta_{electrolyzer}$$

where $\eta_{electrolyser}$ is the electrolyser system efficiency, which can be currently fixed at 0.73.

Enhancing the efficiency for electricity generation and for electrolysis by temperature increase is one option for enhancing hydrogen production. Electrolysis can be done remotely and decentralized or with direct coupling to the reactor by using high temperature steam, the so-called 'hot electrolysis' route.

If the nuclear source is an HTGR, the complexity of the high temperature processes — either thermochemical cycles or high temperature electrolysis — implies that capital and maintenance costs would be higher than for low temperature electrolysis, and the financial risk would certainly be higher, because they are non-proven processes at a commercial scale. The efficiency of the production of electricity (heat to work conversion) can be estimated in the range $0.45 \leq \eta_{el} \leq 0.5$.

Figure 207 shows the results of a comparative study of thermal efficiencies from four different nuclear hydrogen production methods as a function of the temperature supplied to the process [544]. The upper curve, representing a direct cycle advanced gas cooled reactor with supercritical CO_2 as the coolant connected to HTSE, provides the highest efficiencies over the total temperature range. The difference to the lower efficiency of HTSE with the GT-MHR (red curve) is due to the more demanding material requirements and lower reliability. The red curve and the blue curve represent the HTSE and the S–I cycle connected with GT-MHR. For temperatures above 800°C, the predicted efficiencies of the S–I process are similar to those of the HTSE process. The strong decrease

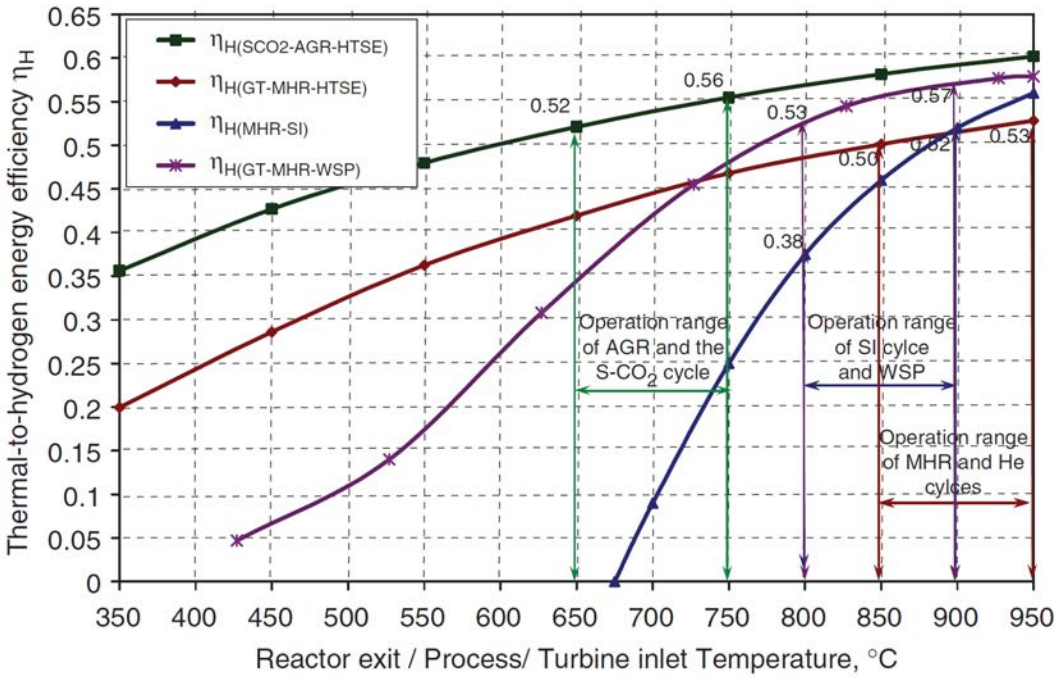

FIG. 207. Thermal efficiencies for hydrogen production with HTSE and S–I cycle [544].

toward lower temperatures for the thermochemical cycle results from the less efficient separation processes connected with larger fluid flows. These curves intersect at ~900°C at an efficiency of slightly above 50%. The possibility of achieving a high efficiency at lower temperatures is a significant advantage in favour of HTSE. The efficiency of the Westinghouse HyS cycle coupled to an MHR reactor is shown in the purple curve. It is higher than the S–I curve due to an arrangement that allows the reduction of heat losses.

The upper bound of the global efficiency of a high temperature process for hydrogen production can be estimated to be 51% [151]. Further refinements of the flowsheet with more realistic values for component efficiencies will lead to a lower overall efficiency. However, it will have to be greater than 33%, and preferably 36.5% or more.

10.2. HYDRICITY

Electricity is generally produced by relatively large, central station plants, although alternative technologies may make distributed production of electricity and cogeneration of heat more feasible. However, no matter what means of production are used, storage of electrical energy is generally costly and not particularly efficient. Much effort has gone into battery technology, superconducting magnets, fly wheels, pumped hydro and other means of ‘storing’ electricity with no clear cost effective winner. Conversely, hydrogen offers flexibility in that it can be stored, although with some challenges. Multiple economic approaches for storing hydrogen may become more feasible. Electricity and hydrogen are also complementary to each other, as electricity must be produced at the time when it is used, whereas hydrogen can be stored for stationary re-conversion into electricity or other use such as transport fuel and mobile re-conversion for driving electric motors. When these complementary characteristics of electricity and hydrogen are coupled with a variety of production strategies, the resulting system is extremely flexible on a macro scale and provides a large number of degrees of freedom in designing a national energy infrastructure by hydricity.

Current power production is normally defined as baseload (8760 h/a) or peak load (< 2000 h/a) with some intermediate load in between. A baseload plant can have high capital costs but lower fuel and operating costs, making nuclear ideal for this role. Alternatively, peak-shaving plants, because they operate intermittently, are characterized by lower capital costs and by higher fuel costs (e.g. natural gas). With hydricity, however, the

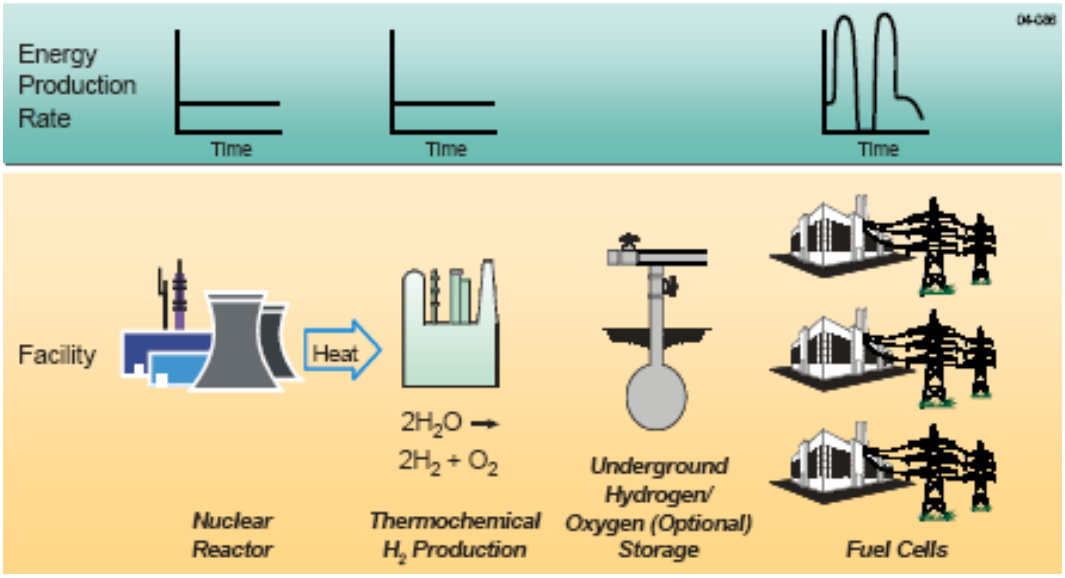

FIG. 208. Baseload cogeneration of hydrogen and power [545].

distinctions between baseload and peak load production will disappear, and the overall system can be optimized using different criteria. The output from a large electricity generating plant may go toward meeting the entire demand during peak periods, but the electrical output can be directed toward generating hydrogen during off-peak periods. Likewise, hydrogen is a potentially attractive form in which to store energy, since the hydrogen output might be distributed or alternatively used to meet peak demand and spinning reserves through fuel cells or being used in combustion engines as long as fuel cells are not yet technically or economically available. The cost of peak power is significantly higher than for electricity during low demand. This fact can favour the introduction of a new system that is predominantly focused on peak/intermediate power production, spinning reserve and load following.

Intermittent, part-time operation of hydrogen production, e.g. by using off-peak power, is economically problematic due to the high investments of the hydrogen production facilities. In this respect, there is a direct analogy to nuclear energy which is predominantly operated in baseload. This will also apply for large scale hydrogen production but will only be feasible in combination with high capacity hydrogen storage to cope with fluctuating hydrogen demands. Thus baseload cogeneration of hydrogen and power (CH2P) might be an economically viable approach in the long term. Figure 208 illustrates the CH2P principle for a nuclear power plant which also delivers heat for high temperature electrolysis or for thermochemical H_2 production, e.g. via very high temperature reactors (VHTRs).

Large scale CH2P technology can easily be introduced into the electricity market for substituting the combustion of oil and natural gas. The establishment of large scale hydrogen production units may help to achieve competitive costs. Inexpensive hydrogen (via economies of scale) will be a precondition for a mass market, but a mass market is also required to create the incentives for investments and the development of new technologies.

Nuclear hydrogen production of the same size as that of the largest existing conventional plants (~8.5 million Nm^3/d) will need about 2400 MW(th) of high temperature heat. This is compatible with a set of 4–6 VHTR modules (400–600 MW(th) each) assuming a conversion efficiency of 50%. With regard to the economies of scale for nuclear hydrogen production, e.g. by the Westinghouse hybrid thermochemical process, a scaling factor of about 0.54 has been estimated. This means that an increase of the power size by a factor of four yields capital costs of only 53% per unit of capacity compared with the smaller plant.

It is obvious that this approach is highly dependent on the availability of large and inexpensive hydrogen storage capabilities. The storage may also include hydrogen generated from regenerative energy sources and thus may even create a symbiosis between nuclear and regenerative energy systems. Moreover, the storage requirements for the use of hydrogen from regenerative sources are very similar to those for the CH2P system. Storage capacity can grow stepwise from the substitution of daily peak demands toward weekly and seasonal compensations.

As long as CO_2 is not a 'rare resource' (e.g. at the site of coal fired power stations), further symbioses can be identified from the conversion of CO_2 and hydrogen into methanol as a liquid transport fuel and storable medium. In the future, methanol storage tanks could play the same role that national oil reserves currently play. It can also be used as an alternative fuel for combustion engines as well as for fuel cells. The double use of the CO_2 exhaust would also contribute to significant reductions in CO_2 emissions, which is the primary goal of a hydrogen economy and not the production of hydrogen, per se.

The economic feasibility of CH2P generation is also dependent on the projected cost and efficiencies of fuel cells. It is expected that the specific capital costs for fuel cells can be reduced to < US$ 100/kW(e) with an efficiency of ~70%. Capital costs would then be much less than for gas-turbine plants (US$ 500/kW(e) and 50% efficiency). The use of oxygen for the fuel cells could further boost their performance. The fuel cells may also be used for traditional CHP applications when using the waste heat for district heating or industrial process heat.

For the production of transportation fuels, there are other advantages of the nuclear generated electricity/hydrogen duality. Currently in petroleum refining, the cost of gasoline is impacted by a variety of factors. These can include foreign production schedules, changes in shipping schedule, spot market prices, weather, international events and many other influences. With hydricity, many of these uncertainties are eliminated. The opportunities will be available to draw upon a stable, reliable, indigenous energy supply unaffected by many factors that currently impact energy prices. The hydrogen and electricity produced from nuclear, also in combination with regenerative energies, may represent an energy system that is characterized by economic stability, enhanced security from international instability and the elimination of massive balance of payment deficits.

10.3. ELECTROLYTIC HYDROGEN PRODUCTION AND GRID CONDITIONS

The main obstacle for abundant production of hydrogen by electrolysis is the high cost of this route compared with petrochemical methods such as steam reforming of natural gas [546, 547]. Due to the high cost share of 80% for electricity in conventional electrolysis, electricity must be made available at a low price level for the sake of competitiveness. The structure of generating units is optimal if the requirements of power balance, reserve capacity, reliability, security and other constraints are fulfilled with minimum total costs. The electricity demand fluctuates on a daily, weekly and seasonal basis, which requires intermediate and peak electricity capacity currently supplied by inexpensive fossil fuels. A less expensive option appears to be the use of electricity from nuclear power at off-peak periods. This operation mode will be analysed in the following from the perspective of grid and plant behaviour and market influence [548].

Off-peak electricity is defined by the demand duration curve of the grid under consideration. Figure 209 shows an example for baseload and partial load percentage with the typical ratio of 1:1. The overall demand is balanced by a park of different power plant types. Nuclear power plants are operated in the baseload mode using the advantage of low fuel cost and distribution of capital cost over continuous operation. Short temporary demand is supplied by plants with low investment/high fuel cost shares such as combined-cycle gas turbine (CCGT) plants. As a result, there is no off-peak situation for nuclear plants for the plant mix shown in the example. Obviously a large share of nuclear power in the plant park is a prerequisite for nuclear off-peak electricity. A decision for deploying nuclear plants for off-peak operation has to compare the cost of nuclear plants versus the flexible fossil-fired plants such as gas turbine or CCGT: As fossil fuels become more expensive, the use of nuclear plants outside the baseload region becomes more attractive.

On the other hand, the optimized selection of plants in the park is also determined by the trade-off between the cost structures of the different plant types. A comparison between CCGT and advanced LWRs is given in Table 64 [549, 550].

Considering a simple splitting of costs into a share for the fuel and another one which is independent of operation, the present values will result in a disadvantage of nuclear power for partial load duration shorter than 80% of the year (Fig. 210). A doubling of the fossil fuel price shifts this limit to 35%, a doubling of both fuels to 40% of the year. From this result, some partial load demand can be delivered by nuclear power plants under economical operation, but there is obviously a need for other than nuclear sources to allow optimized operation of the grid over the full demand range under commercial aspects. This may include the interconnection between different grids.

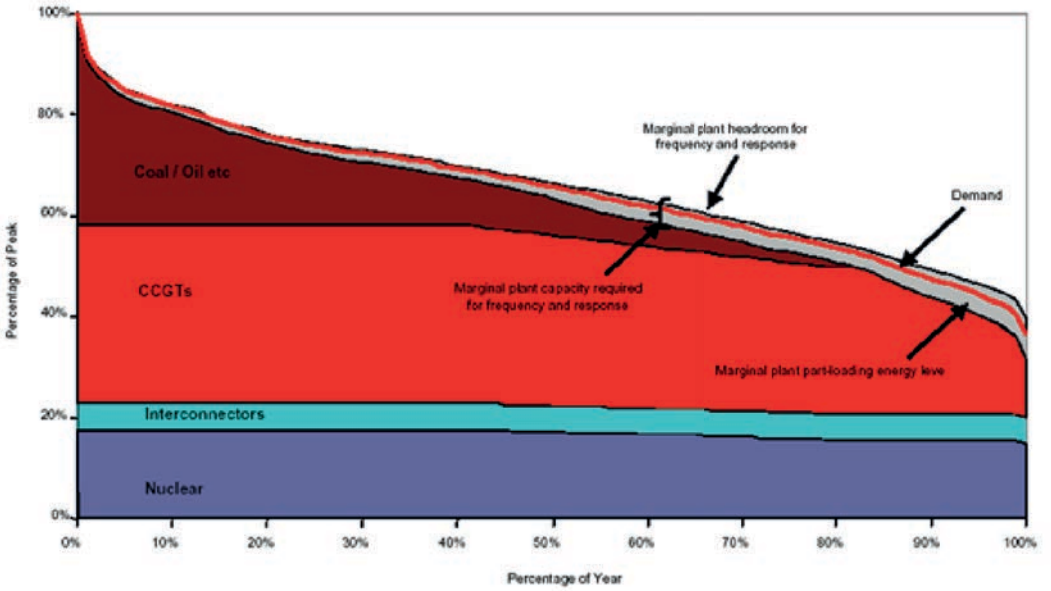

FIG. 209. Example of a demand duration curve for a national grid [551].

TABLE 64. COST STRUCTURES IN DIFFERENT PLANT TYPES (1 € = US $1.20)

	CCGT	Advanced LWR
Capital + O&M (€/MW·h (base load operation))	11	25
Fuel (€/MW·h)	22	4

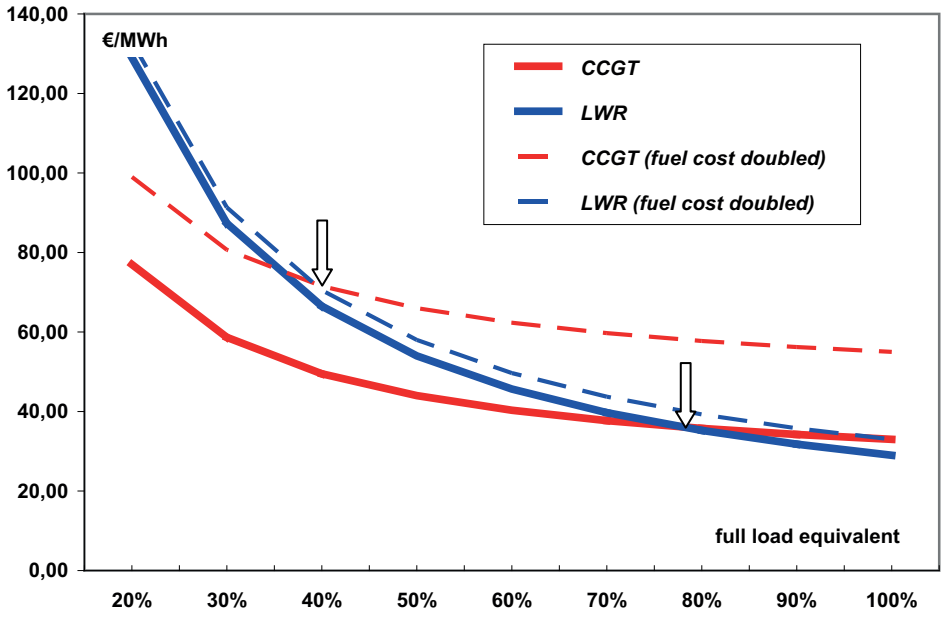

FIG. 210. Cost effect of partial load [548].

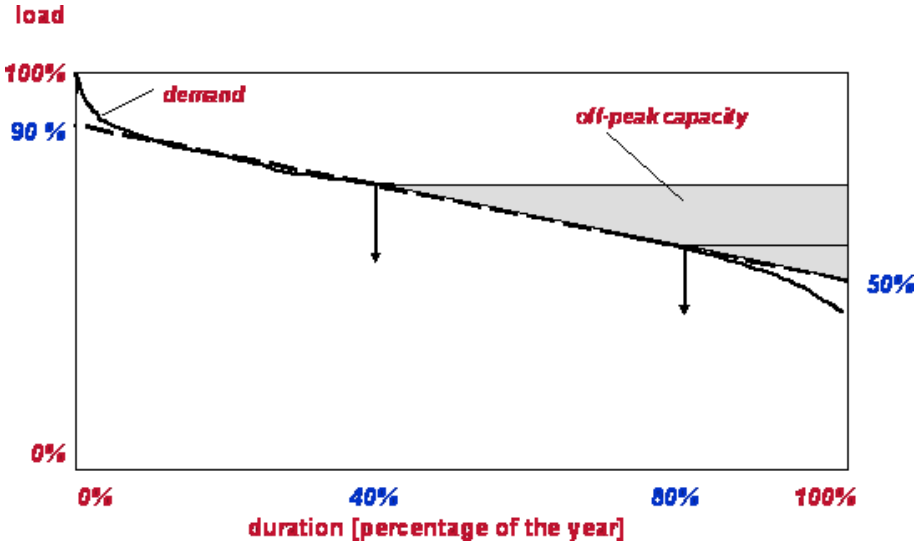

FIG. 211. Approximation of off-peak capacity [548].

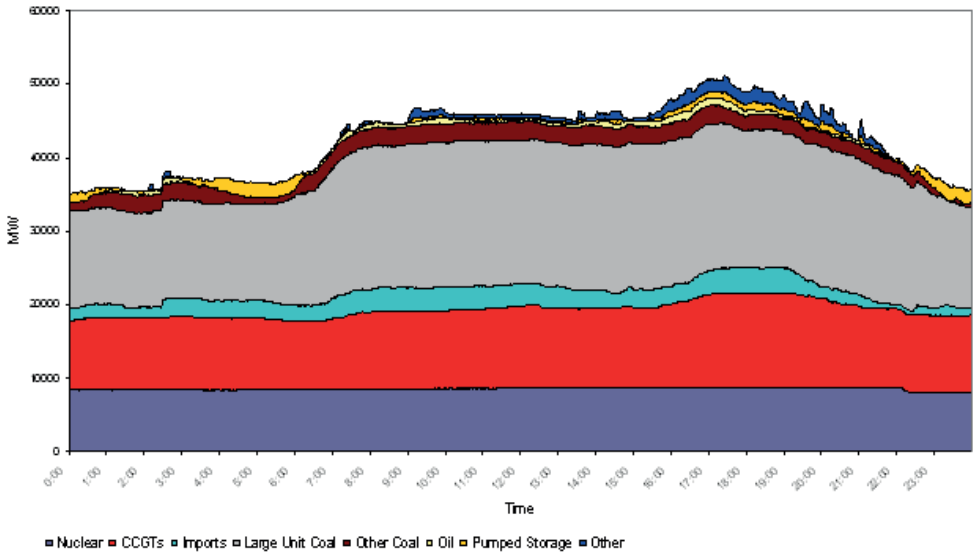

FIG. 212. Example of a daily demand curve for a national grid [551].

The corresponding maximum nuclear off-peak capacity can be estimated from a linear 50% → 90% approximation of the demand duration curve (Fig. 211). The off-peak shares compared with the overall production are 1.1 and 10.3% for the above mentioned limit values 80 and 40%, respectively, i.e. a real off-peak share of nuclear electricity can be expected for the case of increased fossil fuel costs and an adjusted plant park.

Although used so far in this operation mode only occasionally, nuclear power plants are capable of following grid demand by partial load. The characteristic speed for acceptable load changes is up to 10% of full load per minute. The full load range can be crossed in about 1 h. For faster fluctuations, the storage of the steam generators can be used [552]. This should allow following the typical daily grid demand shown by the example in Fig. 212 [551].

The cost of electricity for partial load operation increases for all plant types, but for the range up to the limiting values discussed above, nuclear is the least expensive option. For the following analysis, a simplifying assumption is used, namely that regular grid demand carries the whole constant plant costs, while off-peak

electricity has to cover the costs for the corresponding nuclear fuel demand only, which is not more than 15% of the usual electricity cost as shown in Table 64.

For operation with off-peak electricity, in a first scenario, the reduced duty factor of the electrolysis system has to be taken into account. For a full load equivalent of 40% and the linear approximation discussed above, the hydrogen plant operates on the average at a full capacity equivalent of $\leq 30\%$ only. This results in hydrogen production costs which are more than twice the costs from conventional steam reforming (at present fossil fuel costs). For a feedstock cost share of 75%, the price of feedstock has to triple to reach hydrogen production costs from off-peak nuclear electricity. In this case, the prerequisite for the assumed plant park mix would be fulfilled.

The temporal behaviour of the electrolysis system does not favour partial load operation. It is expected that the heating for high temperature operation has to be maintained over a longer period than the duty time from off-peak electricity. Also there are limits for the exothermic variant of the electrolyser operation [553]. To avoid this, a second scenario assumes continuous operation of the electrolyser plant by temporal use of electricity at the regular price. If there is a 'base demand' large enough for hydrogen from electrolysis at 'full' price, an isolated view on hydrogen production costs during off-peak periods results in a price competitive to that of the conventional petrochemical route. To confirm this possibility, an analysis of — regional — hydrogen markets and applications is required.

Different schemes for using hydrogen stored for levelling source and demand fluctuations have been discussed in connection with deployment of renewables. From the stored hydrogen, electricity can be generated by a gas turbine. For the foreseeable future, electricity from fuel cells will not become less expensive than that from CCGT systems.

As an approximation, the capital costs for electricity production by part time operation of a natural gas turbine plant might be used, although the technical details vary somewhat. For calculating a lower limit for the capital costs, an upper limit for the duty factor of 30% may be assumed. The fuel costs have to be derived for H_2 generated by off-peak electricity and stored. Using the energy content as a basis for comparison, electricity generation costs turn out to be near the generation costs of electricity by photovoltaic systems.

As an overall conclusion, one main obstacle for the storage of electricity by intermediate load hydrogen production is the cost of part time operation of the chain (electrolyser, turbine plant) intended for avoidance of part-time operation of the nuclear plant. The discussion on the development of storage facilities for large volumes of hydrogen has stimulated ideas for optimizing the use of off-peak electricity surplus from nuclear plants and from wind ('NuWind') [223]. Levelling out the fluctuating generation of electricity from wind is a challenge for the grid management when the wind share goes over 20%. The approach of NuWind has been summarized as: "Make H_2 when electricity price is low; sell electricity when high; dispatch electricity when needed, otherwise make H_2…; optimize threshold price for electricity to be sold or converted". Of course, the electrolysis and storage facilities to be provided must handle large amounts of hydrogen: 1 GW of off-peak electrical power results in ~250 000 Nm^3/h of hydrogen to be stored if demand and off-peak electricity phases cannot be synchronized.

10.4. LARGE SCALE VERSUS SMALL SCALE AND CENTRALIZED VERSUS DECENTRALIZED HYDROGEN PRODUCTION

At present, most hydrogen is produced on-site in large scale, commercial SMR units dedicated to the needs of the chemical and petrochemical industries. On-site production means flexible, on-purpose production with low or no transportation costs, a characteristic feature of decentralized hydrogen production. In contrast, centralized hydrogen production refers to large scale systems connected to a hydrogen delivery/distribution network transporting the hydrogen to the point of use in gaseous or liquid state via pipeline or truck. Centralization allows for a secure and stable supply. Centralized large facilities are usually the result of efforts to decrease specific production costs by increasing the unit size (economies of scale) to make the product hydrogen more competitive with other energy vectors.

The use of hydrocarbons in hydrogen production systems will require a carbon sequestration functionality in order to realize the benefits of hydrogen production in general. The sequestration technology still needs to be developed further and verified in the long term. The capture, collection and sequestration of CO_2 from many dispersed small reformer units appears to be prohibitively expensive and practicable only for large scale, centralized fossil fuel handling. Distributed natural gas plants, a low cost option currently, should therefore be replaced by electrolysis plants in the long run.

Also the use of nuclear primary energy as well as hydroelectric power only makes sense for centralized hydrogen production on a large scale. Renewable energy sources (except for hydro) with their low density energy and typically intermittent operation mode will be preferable for a dispersed system of hydrogen generation plants. They can also be used to generate electricity and provide it to the grid at any place. The same applies to hydrogen from biomass plants, which will be limited in size simply because of the transportation of enormous amounts of biomass. Natural gas could be used for both centralized and decentralized production. A swift introduction of hydrogen into the market favours central production [29], which on the other hand will exhibit the problem of increasing the dependency on imports.

The advantage of decentralized distributive generation of hydrogen is the ability to take advantage of the existing and widely available grids for electricity and natural gas. For future applications of hydrogen as part of the energy economy, the installation of a network of small scale production units appears to be a good short term approach for the introduction phase. These could be used to help usher in the hydrogen economy, which will require some infrastructure changes for hydrogen distribution. Market prospects for stationary and mobile fuel cell applications have already led to the development of small scale hydrogen units on the prototype level to either be part of the required infrastructure for fuel cell vehicles or feed local grids for residential stationary fuel cell systems. Small steam reformer or electrolyser units, which are competitors at this scale, are attractive for early low demand stages. They require less absolute capital investment and no transport and delivery infrastructure.

On the other hand, there are drawbacks in terms of the limited efficiency and high cost of hydrogen (both production and primary energy), because these smaller units lack the advantages of the economies of scale factor and of the improved storage efficiency of large plants, assuming large scale demand has built up. For smaller systems, the capital costs become more significant. Furthermore, operation and control of many small units require an inexpensive process control and high safety standards [29]. Also, the hydrogen production plants must meet the purity requirements of fuel cells. If connected to a pipeline grid, a problem may be seen in the mixing of H_2 streams from different sources and thus potentially different degrees of purity.

Small scale reformers, either down sized conventional units or specially designed units, are in the development and demonstration phase and are becoming increasingly powerful and efficient. Whether POX or autothermal reforming is an option will be dependent on economic (innovative) ways of extracting oxygen from air or of separating nitrogen from the product hydrogen. Still at laboratory scale but highly promising is the ion transport membrane (ITM) technology to provide efficient small scale H_2 units. In areas lacking natural gas, reforming of methanol as easily transportable and storable fuel may represent an economical way to produce H_2 locally. In other small scale applications, reforming of methanol may be more cost effective, as may be electrolysis on a very small scale.

The market for very small hydrogen capacities in the range of 50–500 Nm^3/h exists but is limited. Significant technology development has not been observed so far. On-board reforming of methanol is considered an alternative option to hydrogen storage in a fuel cell car which could take advantage of the existing conventional transportation fuel distribution network. Decentralized electrolysers which would be suitable for charging household vehicles exist as a mature technology. Consumer household vehicles can be charged during off-peak house to get less expensive hydrogen from electrolysis. However, this will result in an inefficient ‘well to wheels’ use of energy since it requires that energy be transformed from many forms. This hydrogen will still be very expensive compared with hydrogen produced by steam–methane reforming for which the required heat comes from natural gas. With respect to the planned network of hydrogen refuelling stations, a comparative cost analysis study has shown that up to capacities of 600 Nm^3/h, the delivery of liquid hydrogen by tank truck represents the most economic option [107].

10.5. MARKET INTRODUCTION OF HYDROGEN

The technologies relevant to the hydrogen market are production, storage, transportation and consumption. Of the production technologies to be considered, some have matured for use in economic assessment models like steam reforming and low temperature electrolysis. Other processes such as thermochemical and high temperature electrolytic water splitting still need to be developed. Hydrogen production from biomass or waste is expected to take place but not on a large scale.

The most economical way of producing hydrogen is currently steam–methane reforming. With increasing costs of natural gas, however, this process becomes less competitive, and the generation from coal may be more attractive. The cost of hydrogen production from centralized methane reforming is about the same as for gasoline. It is the distribution costs that make hydrogen expensive. The most expensive production method is electrolysis because of the high electricity cost. This may change with rising hydrocarbon prices and CO_2 taxation in an anyhow largely environmentally regulated market. Distribution costs must be reduced.

An integrated system could supply electricity directly from the reactor. Electricity supply to the process application will result in a revenue loss from the sale of electricity. The revenue loss may not exceed the increase in costs to the process application product due to external electricity purchase.

Additional benefits can be expected if integrating electrolysis and thermochemical hydrogen production due to their unique advantages of decentralized off-peak and centralized baseload production. Thermochemical production is competitive near larger cities, whereas decentralized electrolysis has lower costs farther away from big cities. Thermochemical production also becomes more competitive with increasing capacities. Electrolysis can take advantage of lower off-peak electricity prices as well as of intermittent and decentralized supplies of electricity from renewable sources [224].

Present hydrogen markets are predominantly found for captive hydrogen in the chemical and petrochemical industries. But also the establishment of new markets is on the rise, in the first stage as niche markets, e.g. in the transportation sector, and with a demonstration character. A successful market penetration requires high quality technologies, a corresponding infrastructure, concomitant development of policy regimes and acceptance by consumers. Involving the existing industrial distribution system for hydrogen could lower the barrier for infrastructure buildup and support market introduction.

According to a 2003 IEA analysis, hydrogen may acquire a significant market share only if effective policies for CO_2 mitigation and energy security are in place and if costs are reduced considerably [494]. The objective of the International Partnership for the Hydrogen Economy (IPHE) founded in 2003 is the advancement of policies and common codes and standards that can accelerate the cost effective transition to a global hydrogen economy to enhance energy security and environmental protection. Apart from through policies and regulations, cost competitiveness can be achieved through a combination of further technology development, more efficient supply chain management and the scale effect of large production volumes.

For stationary fuel cell heat and power systems, the most important market segments are small PEFC or SOFC systems for either residential CHP or UPS systems in the range of 1–10 kW, and larger systems in the range of 10–2000 kW, using primarily PAFCs and MCFCs, with applications in commercial buildings and as backup power units. With regard to mobile fuel cell applications, important competitive niche markets are developing. One example is the APU for on-board power supply. The existing road maps and public/private partnerships on both the international and regional levels focus primarily on maturing the technology through research, development and demonstration. The main driver for all these markets is the potential to contribute significantly to CO_2 mitigation and energy security in the medium and long terms [494].

10.6. ECONOMIC ANALYSIS

10.6.1. Economic evaluation

The economics of hydrogen production depend on a wide variety of parameters such as scale and availability of the plant, cost of feedstock, efficiency of the technology employed, state of development (i.e. early stage or mature) and physical distance to end use markets (centralized or distributed production) [534].

A lot of cost analyses can be found in the existing literature, but they are not always comparable. Many aspects of technology costs and performance have not been independently verified, but at least some trends in production cost economics can be observed. Economies of scale clearly apply to large steam–methane reforming plants, with a clear operating cost advantage over smaller units designed for distributed hydrogen production applications. The decisive factor for the centralized SMR production cost is the price of natural gas, which has shown strong variations in recent years. Various uncertainties, idealizations and simplified underlying assumptions were used in the cost analysis, so the results provide more qualitative trends.

The factor ‘efficiency’ is commonly used to compare hydrogen production processes. But it is not the final criterion to select the process. Furthermore, advanced processes often imply high investments, such that energy consumption for the process may not necessarily be the first cost item. Final decisions will be made on production cost grounds, which stresses the importance of reliable estimations. They will provide the basis for directing further R&D studies helping to optimize the system design that could make a given process profitable.

Several comprehensive life cycle analyses have been conducted in recent years to quantify the external costs associated with all forms of energy production and utilization. External costs, although often not considered in traditional economic analyses, are accrued by society in terms of environmental damage and health impacts over the lifetime of the energy system. The European Union project ExternE (External Costs of Energy) [554] was dedicated to the assessment of external costs related to power production and transportation. Among other results, it has been concluded from the studies that nuclear power has the lowest external costs comparison with coal, oil, and natural gas based power [88].

Within the European coordination action INNOHYP, conversion efficiencies for various routes of hydrogen production considering different types of primary energy have been investigated [34]. Results mainly based on a literature evaluation are shown in Table 65. In addition to capital cost disadvantages because of their size, smaller plants tend to have higher feedstock and utility costs, lower conversion efficiencies, and higher per-unit costs for labour and other operations and maintenance costs. Smaller distributed units are likely to have a lower capacity factor. The distributed SMR production cost is ~80% higher than the central SMR production cost. The substantially lower feedstock costs for coal drive the relatively lower overall production cost for coal gasification [534].

In biomass gasification, life cycle CO_2 emissions may be substantially less. The energy density of the biomass feedstock is substantially less than that of coal. And it may not be practical to build a biomass gasification unit with a hydrogen production capacity above a certain size and supply sufficient quantities of biomass to the plant site.

The large scale production of hydrogen from water splitting processes provides a significant synergy in marketing the by-product oxygen. An area of application is, for example, coal gasification to avoid deployment of expensive air separation units.

TABLE 65. ELECTRICAL AND THERMAL EFFICIENCIES OF CONVERSION FOR DIFFERENT HYDROGEN PRODUCTION ROUTES [34]

Conversion route	Conversion efficiency (%)
Wind + electrolysis	70
Tidal + electrolysis	70
Hydroelectric + electrolysis	70
Nuclear heat +SMR+CCS	61
SMR+CCS	58
Thermal cracking	46
Nuclear heat +thermochemical cycles	45
Coal gasification + CCS	32
Nuclear heat + electrolysis	28
Solar PV+electrolysis	10.5
Solar photocatalysis	8
Solar biomass	0.5
Nuclear heat + SMR	76
Solar heat + SMR	61
SMR	76
Coal gasification	59
Solar heat + thermochemical cycles	35

Note: SMR — steam–methane reforming; CCS — carbon capture and storage; PV — photovoltaic.

Production costs for hydrogen are mainly determined by the investment costs. The cost structure is influenced by the production method and the plant size. The share of fuel cost, for example, is in the order of 50–68% in large scale SMRs, whereas it is 28–40% in small reformer units. The cost of electrolytic hydrogen is dominated by the electricity cost (75–80%). In biomass gasification, fuel costs are about 40%. Regarding the development of feedstock prices, the price of natural gas is expected to increase over the next decade, whereas the price of coal is anticipated to remain stable. Electricity costs are strongly dependent on feedstock price fluctuations, in particular fossil fuels.

Table 66 shows advantages and disadvantages of various sources of energy in terms of cost, climate impact, efficiency and availability. Nuclear is one of the least expensive low-carbon energy sources and is less vulnerable to fuel price changes than are the fossil energy sources [555].

Advanced nuclear fuelled thermochemical processes are unproven, but they may provide low per unit production costs in the future. The lower feedstock cost includes the cost of nuclear fuel, net of any co-product benefits from oxygen sales. Operating and maintenance costs include decommissioning costs in addition to the usual labour, taxes, security and other costs.

A future system may work with electrolytic hydrogen generated from nuclear power [489] where the hydrogen is produced when electricity demand is low, stored and then re-converted to electricity in times of peak demand. Steam price increases with increasing natural gas prices; on the other hand, the price of steam produced by nuclear power remains constant as gas prices go up. Even in the more pessimistic case regarding cost production from nuclear, both methods are competitive (at the gas prices at the time of the study, early 2006). As the prices of natural gas go back up, the price of steam production from nuclear production would be even more competitive.

The roundtrip efficiency from electricity to hydrogen and back to electricity strongly depends on the total system. LWRs combined with low temperature electrolysis will achieve a hydrogen production efficiency of not more than ~25%. This figure, however, can be raised both with advanced nuclear plants offering higher thermal-to-electric conversion efficiencies and with changing from low to high temperature electrolysis providing steam at the 800°C. In addition, if HTSE can be operated in the reverse mode as a fuel cell to produce electricity, the same equipment could be used, lowering the capital cost investment. Performance will be maximal if oxygen is used rather than air. In parallel to the fuel cell plants, highly efficient hydrogen–oxygen gas turbines for steam generation could be operated to meet peak demand. For economic reasons, the system requires inexpensive storage of both hydrogen and oxygen.

A candidate for a low cost storage facility is large scale underground storage in geological formations with sufficiently low permeation rates similar to today's storage of natural gas. Oxygen storage might be done in a similar way, but still needs to be demonstrated. Transportation of the hydrogen still appears to be a comparatively expensive part of the chain and could dominate the cost of delivered hydrogen. This can be minimized by focusing on centralized production, storage and use of the hydrogen for peak electricity production. Roundtrip efficiencies of around 60% might be achievable [489].

10.6.2. Cost estimates

The following two tables contain the results of cost estimation studies for two conventional processes of hydrogen production: steam–methane reforming and coal gasification. A comparison is made between state of the art plants and those anticipated for the year 2025.

Characteristic data of hydrogen production by steam reforming are given in Table 67 for two different plant capacities, 1000 and 100 000 Nm^3/h, showing that with increasing plant size, the specific costs of hydrogen are significantly reduced. No major further reduction is anticipated due to the only minor technological progress expected in the future [556].

The characteristic data of hydrogen production in Table 68 are based on an autothermal hard coal gasification plant which also consumes 5% of electrical energy. For the data anticipated for the future, it was assumed that the gasification process can be optimized by lowering the fuel input by 15% and the electricity input by 10%, thus raising the efficiency from 59 to 69% [556].

Exact hydrogen production costs from thermochemical cycles or high temperature electrolysis cannot be given at present, since these methods are still at an early stage of development where uncertainties are still large. Detailed flowsheets are necessary. Investment costs for the production plant strongly depend on the technological solutions applied and the materials selected.

TABLE 66. ENERGY SOURCES FOR ELECTRICITY GENERATION [555]

Energy source	Technology (for cost estimate)	Cost in 2005 (€/MW·h)	Projected cost in 2030 (€/MW·h) [a]	GHG emissions (kg CO_2/MW·h)[a]	Efficiency (%)	Fuel price sensitivity	Proven reserves at annual production
Natural gas	Open-cycle gas turbine	45–70	55–85	440	40	Very high	64 a
	Combined-cycle gas turbine, CCGT	35–45	40–55	400	50	Very high	
Oil	Diesel engine	70–80	80–95	550	30	Very high	42 a
Coal	Pulverized fuel with flue gas desulphurization	30–40	45–60	800	40–45	Medium	155 a
	Fluidized-bed combustion, CFBC	35–45	50–65	800	40–45	Medium	
	IGCC	40–50	55–70	750	48	Medium	
Nuclear	Light water reactor	40–45	40–45	15	33	Low	85 a
Biomass	Biomass generation plant	25–85	25–75	30	30–60	Medium	Renewable
Wind	Onshore	35–175	28–170	30	95–98	Zero	∞
		35–110	28–80				
	Offshore	50–170	50–150	10			
		60–150	40–120				
Hydro	Large plant	25–95	25–90	20		Zero	∞
	Small plant (<10 MW)	45–90	40–80	5	95–98		
Solar	Photovoltaic	140–430	55–260	100	—	Zero	∞

[a] Regarding 2030 costs for fossil fuel based generation, additional costs for CO_2 emissions have been calculated and added, on the basis of €20 and €30/tCO_2, to the current generation costs.

TABLE 67. HYDROGEN PRODUCTION BY STEAM REFORMING AND ITS PROSPECTIVE [556]

	State of the art		Scenario 2025	
Technical data				
Rated power natural gas (kW)	4 500	405 000	4 275	385 000
Hydrogen production (Nm^3/h)	1 000	100 000	1 000	100 000
System pressure (MPa)	1.6	3.0	1.6	3.0
Water demand (m^3/h)	2.1	58	2.1	58
Efficiency (%)	67	74	70	78
Lifetime (a)	20	20	20	20
Utilization (h/a)	8 000	8 000	8 000	8 000
Cost				
Investment (€/kW of H_2)	675	335	675	335
Specific total cost (€ Ct/kW·h of H_2)	3.2	2.3	3.1[a]	2.2[a]

[a] Based on a natural gas prize of 1.4 € Ct/kW·h, not including potential CO_2 taxation or sequestration costs.

TABLE 68. HYDROGEN PRODUCTION BY GASIFICATION OF HARD COAL AND ITS PROSPECTS [556]

	State of the art	Scenario 2025
Technical data		
Rated power hard coal (MW)	486	413
Electricity demand (MW)	25	22
Hydrogen production (Nm^3/h)	100 000	100 000
System pressure (MPa)	5.0	5.0
Water demand (m^3/h)	84	84
Efficiency (%)	59	69
Lifetime (a)	20	20
Utilization (h/a)	8 000	8 000
Cost		
Investment (€/kW of H_2)	1 400	1 400
Specific total cost (€ Ct/kW·h of H_2)	3.8	3.4[a]

[a] Not including potential CO_2 taxation or sequestration costs.

JAEA evaluated the steam reforming process flowsheet and hydrogen production cost from a nuclear and an industrial (conventional) plant [557]. The plants assume similar production rates of hydrogen, as given in Table 69. The PSA for hydrogen purification includes three stages in order to yield a product gas of 99.99% pure hydrogen. The heat energy is provided by combustion of natural gas in the industrial plant and by helium heating in the nuclear plant. The nuclear plant is based on an HTGR sized at 380 MW(th), corresponding to the given hydrogen production rate. Economic parameters assume a cost of natural gas of US$ 0.19.5/Nm^3, a discount rate of 10% and an 8% return on investment. The results of production costs are summarized in Table 70, which indicates that the nuclear plant could have a 15% production cost advantage over the conventional plant.

Preliminary technical and economic estimates [559] of hydrogen production in advanced processes with HTGR heat and electric power demonstrate that SMR can compete with conventional technologies at current gas

TABLE 69. PRODUCTION COST FOR HYDROGEN FROM CONVENTIONAL AND NUCLEAR STEAM REFORMING [558]

	Industrial (conventional) plant	Nuclear HTGR plant
Hydrogen production rate (t/h)	17.9	25.9
Hydrogen product purity (%)	99.99	99.99
Natural gas feed rate (Nm^3/h)	131 118	82 193
Nuclear heat rate (MW(th))	—	380
Nuclear heat temperature (°C)	—	950
Process reforming temperature (°C)	871	871
Process plant construction cost[a] (US$)	305 million	309 million
Hydrogen production cost [a]		
(US$/kg of H_2)	160	137
(US$/$Nm^3$ of H_2)	14.3	12.2

[a] Original estimates were made in Japanese yen, converted at 1 US$ = 110 yen (August 2004).

TABLE 70. PRODUCTION COST AND FINAL COST FOR HYDROGEN FROM DIFFERENT PROCESSES [558]

Process hydrogen from	Production mode	Cost (€/GJ)		
		Feedstock	Production	Final (incl. storage, delivery, dispensing)
Methane reforming	centralized (3 M Nm^3/d)	3	5–8	22–30
Methane reforming	decentralized	4–5	7–12	28–33
Coal gasification	centralized	1.2	13–16	32–37
Biomass gasification	intermediate	2.4	17–22	33–40
Electrolysis	decentralized	14	20–25	35–40
Gasoline	refinery	2.5	6	7

prices even without taking into account the potential taxes for CO_2 emissions. In view of the tendency for further gas price increases, the most economically efficient technology will be thermochemical water decomposition in a S–I cycle. SMR and thermochemical water decomposition can compete with conventional low temperature electrolysis. The advantages of HTSE are not yet clear and will ultimately depend on the capital costs of heat application for electricity production.

Estimates were performed for processes which may be implemented with a helium temperature at the reactor outlet not higher than 950°C. A temperature increase up to 1000°C allows an enhanced efficiency of hydrogen production processes, but increases the cost of creating a safe reactor plant. Therefore a thorough technical–economic analysis is to be performed when selecting the temperature level at the reactor outlet and hydrogen production process pattern.

Based on the above efficiencies given in Table 65, Fig. 213 provides the results on the basis of the energy required to produce 1 kg of H_2. In Fig. 214, the results were translated into estimated hydrogen production costs for the different current and future hydrogen production routes [34].

10.6.3. Cost estimate modelling

In several countries, activities on the projected economic potential of hydrogen production and cost assessments are being performed which help to direct and prioritize research efforts, and to compare and finally

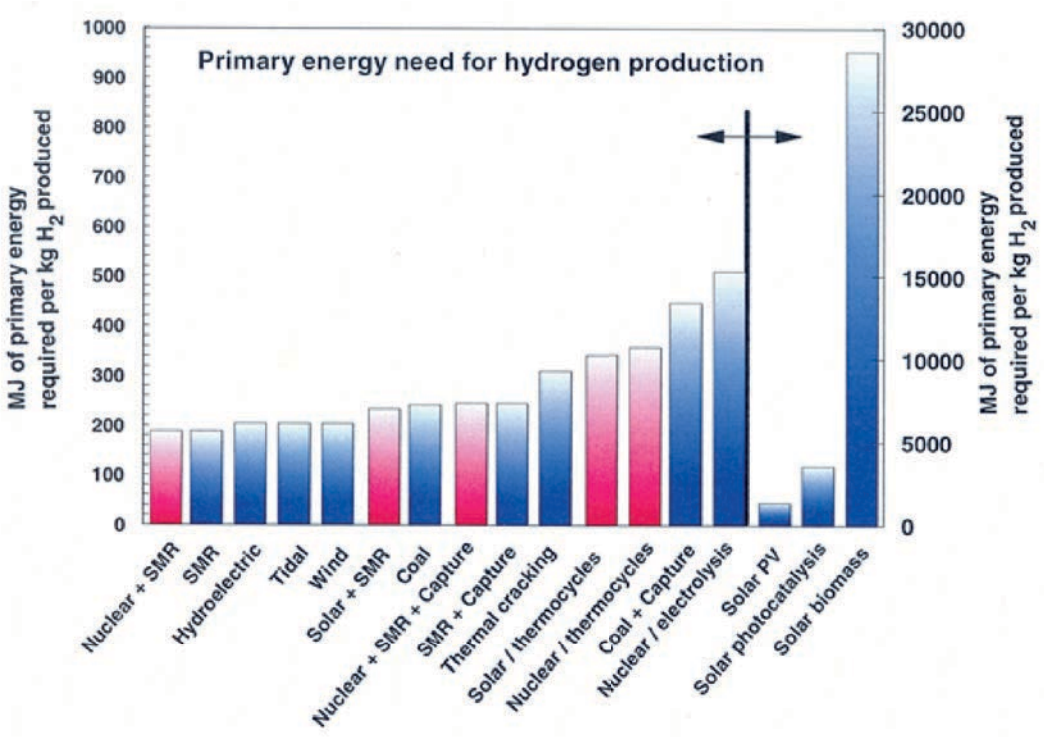

FIG. 213. Primary energy required for hydrogen production based on estimated conversion efficiency values. Methods in red represent future high temperature routes [34].

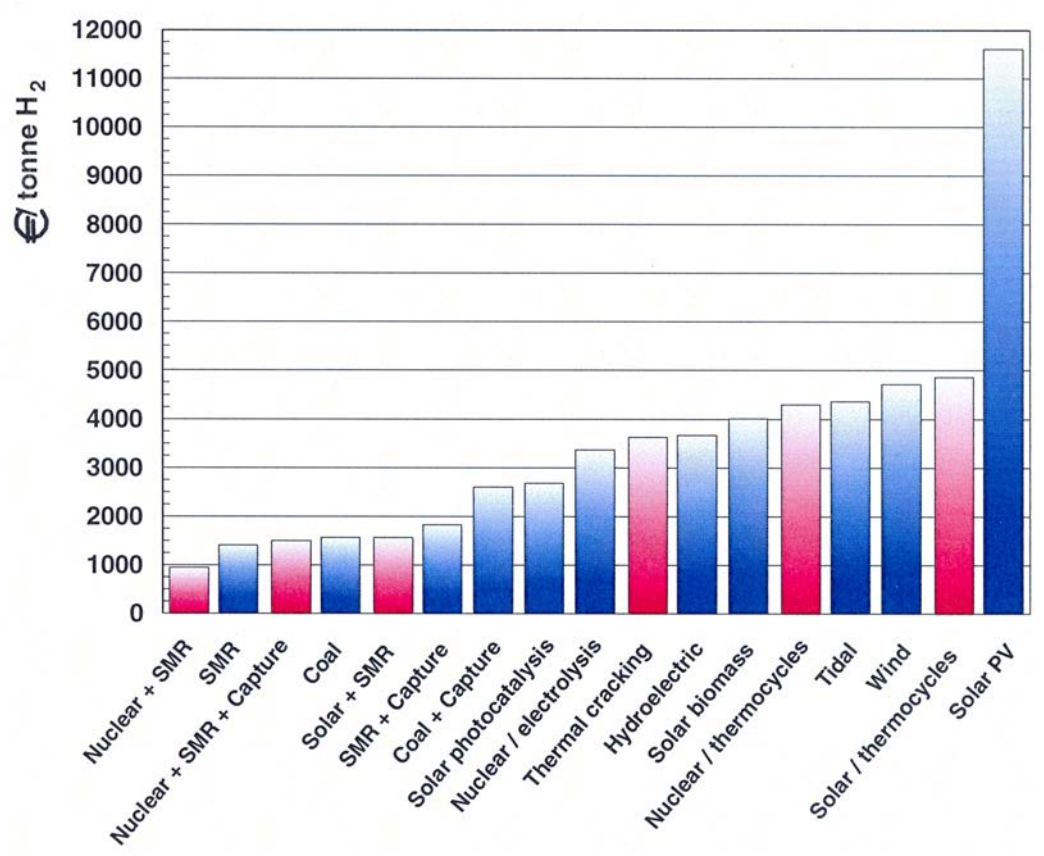

FIG. 214. Estimated hydrogen production costs. Values in red represent future high temperature routes [34].

select the most appropriate processes. Some countries have already developed their own models such as the German–French E3-database, the hydrogen cost analysis model in Canada, and other models in the USA such as the H2A modelling tool developed by the USDOE Office of Energy Efficiency and renewable Energy (EERE). Two international developments are described in some more detail below.

10.6.3.1. GIF G4Econs

Guidelines for estimating costs have been published by the Generation IV Economic Modelling Working Group [560]. Within those guidelines, a methodology also has been established for calculating costs of non-electricity products from nuclear energy. The methodology separates costs into capital costs and annual costs.

The Generation IV Excel Calculation of Nuclear Systems (G4Econs) software is an "integrated nuclear energy economic model" (INEEM) consisting of several nuclear–economic submodels. The modelling effort will be a continuous activity of the GIF Economics Modelling Working Group to develop and further improve and refine a consistent cost estimation methodology for all Generation IV reactor systems [560]. G4Econs comprises models for capital investment/production costs, nuclear fuel cycle, O&M, optimal scale and energy products. Construction costs are integrated into capital costs, which are borrowed, and amortized over a set time period. Operation and maintenance costs are included in the annual costs, which are recurring over the lifetime of the system.

The working group also suggests the use of the 'power credit method' for costs that may be associated with dual-product and electricity generation. This method has been adopted by the IAEA to evaluate the economics of nuclear desalination. The power credit method first calculates total expenses and energy from a single-purpose electricity producing reactor and derives a cost per kilowatt-hour. Then the amount of non-electric product and energy, and the total expenses of the dual-purpose plant are calculated. Electricity production from a dual-purpose reactor is lower than for a single-purpose reactor, but the costs for the dual-purpose plant are higher [561].

10.6.3.2. IAEA HEEP

The IAEA has taken the first step toward the development of a common cost assessment software for nuclear hydrogen called the Hydrogen Economic Evaluation Program (HEEP). Its structure and features are similar to those of the existing DEEP software (for desalination) [562], which is currently being applied in 50 Member States for economic evaluation and screening analyses for country specific nuclear desalination systems. The beta version of the HEEP software was released in January 2010. The IAEA will maintain the software, facilitate its distribution and coordinate further development.

(A) Development of HEEP

HEEP [563] is planned as a common cost assessment tool to consider source of energy to distribution of hydrogen to end user, including its production and storage. HEEP uses a discounted cash flow model that calculates the 'levelized cost of hydrogen'. The HEEP program consists of three modules: (i) the preprocessing module, (ii) the executing module, and (iii) the postprocessing module. The graphical user interface (GUI) provides a user friendly feature to the preprocessing and postprocessing modules of HEEP. It is possible to model and analyse a number of combinations among sources of heat, various processes generating hydrogen, and different methods to store and distribute hydrogen.

A wide range of hydrogen production plants adopting different processes such as electrolysis, high temperature electrolysis, low and high temperature thermochemical, etc., can be considered. It is also possible to carry out economic evaluation of plants operating on conventional processes using fossil fuel. The source heat and/or electricity required by these hydrogen generating processes can be provided by a power plant, which can be a nuclear power plant. The hydrogen generation process plant may be collocated with the power plant or can be isolated from the power plant and receive energy from the commercial grid. In the area of energy source for hydrogen production, HEEP will consider the whole spectrum of nuclear reactors that are appropriate for connection to a hydrogen plant, for instance PWRs and PHWRs for the lower temperature range, FBRs and SCWRs for the medium temperature range, and MSRs and VHTRs for the high temperature range. The current version of HEEP can consider a nuclear power plant delivering thermal energy alone, delivering electricity alone, or

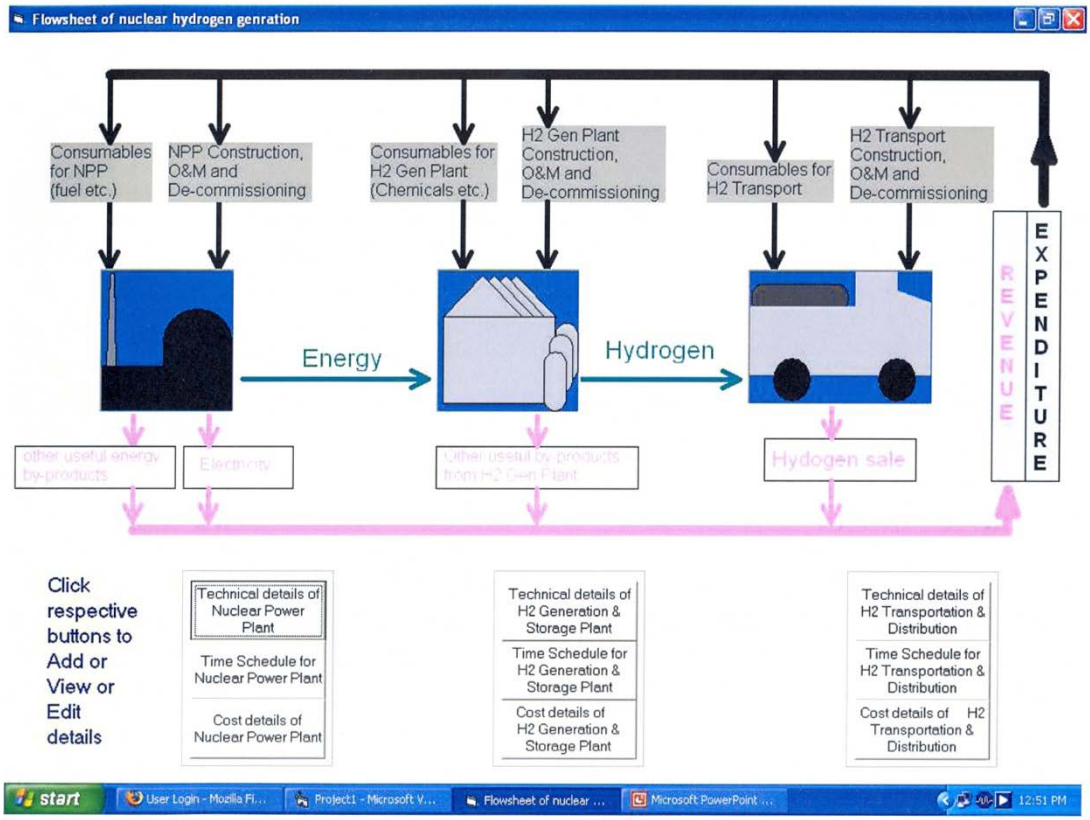

FIG. 215. Example screenshot from HEEP [564].

delivering both thermal energy as well as electricity to a hydrogen generation plant. HEEP can also model various storage conditions and methods of transporting hydrogen to the end user. An example of a screenshot from HEEP in Fig. 215 shows the nuclear hydrogen generation flowsheet.

Communication between the IAEA and the GIF Hydrogen Production Project Management Board is aimed at coordinating their respective efforts.

(B) Preliminary benchmarking of HEEP

Work has been initiated by a number of agencies to estimate the costs of hydrogen production. Results of a life cycle cost analysis of the reference design for a commercial scale HTSE plant driven by a high temperature gas cooled nuclear reactor are provided in a report published by INL [565]. KAERI has published results of a preliminary study on cost estimates for hydrogen generated by the S–I thermochemical process coupled with the modular nuclear reactors generating very high temperature as source of thermal energy [566]. The hydrogen production costs using the information provided in the KAERI publication is re-calculated using HEEP and results are compared with those reported in the publication to carry out benchmarking of the HEEP. This preliminary benchmarking has demonstrated that the elements of hydrogen costs reproduced by HEEP were comparable with the estimates of earlier studies.

(C) Inputs and assumptions for HEEP benchmarking

Input data required for execution of HEEP were prepared based on the information provided in the KAERI report such as technical features of plants, time and cost required for construction and operation of plants, real discount rate assumed, etc. Table 71 provides various technical features, time periods and cost components of different configurations considered for HEEP benchmarking.

TABLE 71. HEEP BENCHMARKING CASE STUDY [566]

Cases	Case I	Case II	Case III	Case IV
Discount rate (%)	5	5	5	5
Nuclear power plant details				
Nuclear power plant configuration	4 × 600 MW(th) PMR	4 × 200 MW(th) PMR	10 × 250 MW(th) PBR	4 × 200 MW(th) PBR
Capacity factor (%)	90	90	90	90
Availability factor (%)	100	100	100	100
Construction period (a)	3	3	3	3
Operating life (a)	60	60	60	60
Cooling before decommissioning (a)	1	1	1	1
Decommissioning period (a)	9	9	9	9
Spent fuel cooling period (a)	2	2	2	2
Waste cooling period (a)	2	2	2	2
Capital cost (M US$)	1835.8	867.58	2944.45	1088.75
Annual fuel cost	120.6	40.2	112.5	36.0
O&M cost (M US$)	38.0	16.8	56.4	19.5
Decommissioning cost (% of total capital cost)	10	10	10	10
Hydrogen generation plant details				
Rated hydrogen generation (t/a)	216 000	72 000	225 000	72 000
Non-process electricity (MW(e))	815	272	849	272
Construction period (a)	3	3	3	3
Operating life (a)	60	60	60	60
Cooling before decommissioning (a)	1	1	1	1
Decommissioning period (a)	9	9	9	9
Capacity factor (%)	90	90	90	90
Availability factor (%)	100	100	100	100
Capital cost (M US$)	1 410	673.33	1 564.75	693.15
O&M cost (M US$)	77	37	77	37

Four different cases resulting from four different configurations of nuclear plants delivering thermal energy to the S–I thermochemical process have been studied. These four configurations of nuclear power plant are (CASE I) four modular units of 600 MW(th) PMR, (CASE II) four modular units of 200 MW(th) PMR, (CASE III) ten modular units of 250 MW(th) PBR and (CASE IV) four modular units of 200 MW(th) PBR.

In this study, it was assumed that a nuclear power plant would generate no electricity and the entire heat produced by a nuclear reactor would be utilized by the thermochemical process generating hydrogen. In the KAERI publication, the availability factor for both plants was not indicated, but for HEEP benchmarking an availability of 100% for the nuclear power plant and hydrogen generating station has been considered.

The S–I thermochemical plant coupled to a 4 × 600 MW(th) nuclear power plant is assumed to be generating 216 000 t of hydrogen annually at an efficiency of 45%. The hydrogen generation capacity of plants coupled to other nuclear power plant configurations is assumed to be directly proportional to the thermal energy generated.

The time periods for cooling before decommissioning (period between end of plant operation to start of decommissioning), spent fuel cooling and decommissioning period indicated in Table 71 are numbers assumed for this exercise, as these time periods were not mentioned in the Korean study.

It is indicated in the KAERI publication that the annual non-process electricity costs of the hydrogen generating plant coupled to a nuclear power plant with four modular units of 600 MW(th) is 428.4 M US$. The non-process electric power given in the above table has been worked out for electricity rates of 0.06 US$/kW·h and a plant capacity factor of 90%, as indicated in the KAERI publication. Since the nuclear power plant is not generating electricity, it is assumed that the electricity required by the hydrogen production plant is bought from the grid at market rate of 0.06 US$/kW·h. The electricity required for hydrogen plants coupled to other configurations is assumed to be directly proportional to the total thermal energy and thus to the annual hydrogen generation.

The KAERI publication gives capital costs for six major sub-systems of both the nuclear power plant and the hydrogen generating plant. The capital costs for the primary and secondary heat transport system are given separately as a common cost component of the nuclear power plant and hydrogen generating plant. The report also gives the costs for supplementary capitalized support and contingency requirements as a common cost for both plants. However, for HEEP benchmarking calculations, primary and secondary heat transport system costs are considered as a component of the capital costs of the nuclear power plant. Seventy-five per cent of the contingency and capitalized supplementary costs has been considered as a component of the nuclear power plant capital costs and the remaining 25% as a component of the capital costs of the hydrogen generating plant. A real discount rate of 5% is assumed, as indicated in KAERI publications.

The HEEP program needs input pertaining to the hydrogen storage facility. However, hydrogen storage was not considered in the Korean study. Hence, when estimating the hydrogen costs in HEEP, the storage period and storage pressure for hydrogen storage system are considered to be zero. Moreover, decommissioning costs are also considered to be zero, as these also were not considered in the Korean study.

The HEEP program is designed to estimate the comprehensive costs of hydrogen from its generation until it is delivered to the end user. This includes hydrogen transportation costs. In this benchmarking study, vehicular transportation of gaseous hydrogen has been considered. The output from HEEP gives the contribution of the nuclear power plant, hydrogen generation, storage costs and hydrogen transportation. For the sake of comparing the results of HEEP with those reported in the Korean publication, the contribution of hydrogen transportation is deducted from the total levelized cost of hydrogen.

Table 72 summarizes technical features, various time periods and cost components of vehicular transportation of hydrogen considered for HEEP benchmarking.

TABLE 72. ASSUMPTIONS FOR GASEOUS HYDROGEN TRANSPORTATION IN HEEP BENCHMARKING [566]

Vehicle capacity	180 kg
Average speed of vehicle	40 km/h
Mileage of vehicle	2.5 km/L
Loading–unloading time per trip	2 h
Procurement period of vehicle	3 a
Life of vehicle	15 a
Refurbishment cost	100%
Number of refurbishments	4
Capital cost per vehicle	100 000 US$
Annual salary of one driver	150 000 US$
Number of drivers per vehicle	3
Price of fuel	0.75 US$/liter
Routine maintenance of vehicle	1% of total cost

TABLE 73. RESULTS OF HEEP BENCHMARKING FOR LEVELIZED COST [566]

Case	Levelized cost of hydrogen (US$/kg)					
	HEEP results					KAERI results
	Total levelized cost of hydrogen	Nuclear power plant component	Hydrogen generation and storage component	Hydrogen transportation cost component	Nuclear power plant + hydrogen generation and storage	
Case I	5.07	1.23	3.02	4.10	4.25	4.06
Case II	5.82	1.62	3.38	4.10	5.00	5.56
Case III	5.36	1.50	3.03	4.10	4.53	4.48
Case IV	6.02	1.79	3.40	4.10	5.19	5.86

Table 73 gives the levelized cost of hydrogen for the four cases described earlier.

The second column of Table 73 gives the total levelized cost of hydrogen. The next three columns indicate the cost of the components of the nuclear power plant, the hydrogen generation plant and the hydrogen storage and transportation facilities. Since in the KAERI study hydrogen transportation was not considered, the sum of the costs in the third and fourth column should be used for comparing results.

10.7. ROLE OF NUCLEAR HYDROGEN IN THE ENERGY MARKET

Nuclear futures will likely include markets beyond baseload electricity. All low carbon options have high capital costs and low operating costs, which is expensive for variable electricity production. There is an enormous existing market potential for nuclear hydrogen, including the savings in CO_2 emissions and other pollutants. As hydrogen from natural gas is the main competitor in this area, it is understood that nuclear has to compete with natural gas.

Nuclear power is less vulnerable to fuel price changes than is coal or gas fired generation, as uranium represents a limited part of the total cost of generating nuclear electricity and is based on sources which are sufficient for many decades and widely distributed around the globe. Nuclear energy is one of the least expensive sources of low carbon energy and also has relatively stable costs. The next generation of nuclear reactors should reduce these costs further.

All the systems related to the Generation IV concepts will need important R&D expenditures; they can be justified only in the context of very large scale hydrogen production, for which the basic economic rules will apply. Solar and wind power are expensive and intermittent but very clean. Coal power is dirty but inexpensive and easy to dispatch. Nuclear power is also distributable on a large scale, relatively inexpensive and carbon free, but radioactive waste storage and proliferation risks are unique challenges that warrant serious consideration. No energy option will be the least expensive and the cleanest and the safest.

Appendix

PROPERTIES OF HYDROGEN

A.1. GENERAL

Hydrogen is the first element in the periodic table with the atomic number 1. It is the lightest and most abundant element in the universe representing 75 mass% or 90 vol% of all matter. On Earth, it is mostly found in compounds with almost every other element. Considering just the compound water, the hydrogen content bound in the total water supply of the world is in the order of 10^{14} t. Hydrogen exists also as a free element in the atmosphere, but only to the extent of less than 1 ppm (by volume). Free ionic hydrogen is more reactive than molecular hydrogen, the non-polar-covalent compound of two hydrogen atoms. In 1776, Henry Cavendish identified hydrogen as a distinct species. It was given the name 'water maker' by Lavoisier seven years later, who proved that water was composed of hydrogen and oxygen.

Hydrogen, with a standard atomic mass of 1.0078225 u, has three naturally occurring isotopes. The most common hydrogen isotope is the stable protium (^{1}H, H) with an abundance in nature of more than 99.98%. The second isotope is the stable deuterium (^{2}H, D) or heavy hydrogen discovered in 1932 by Urey. Deuterium has a natural fraction of 0.014% with physical and chemical properties slightly different from ^{1}H. Nearly all D in natural hydrogen is in combination with hydrogen atoms, the diatomic HD with a fraction of 0.032% in natural hydrogen; the existence of molecular D is highly improbable. The third hydrogen isotope is the radioactive tritium (^{3}H, T) with a half-life of 12.3 a, discovered in 1934 by Rutherford. But also the short lived isotopes ^{4}H, ^{5}H, and ^{7}H have been synthesized in the meantime.

A.2. PHYSICAL PROPERTIES OF HYDROGEN

Hydrogen can be considered an ideal gas over a wide temperature range and even at high pressures (up to ~10 MPa). At standard temperature and pressure conditions, it is a colourless, odourless, tasteless, non-toxic, non-corrosive, non-metallic diatomic gas, which is in principle physiologically not dangerous. One of its most important characteristics is its low density, which makes it necessary for any practical applications to either compress the hydrogen or liquefy it. It is positively buoyant above a temperature of 22 K, i.e. over (almost) the whole temperature range of its gaseous state.

Hydrogen gas is highly diffusive and highly buoyant; it rapidly mixes with the ambient air upon release. The diffusion velocity is proportional to the diffusion coefficient and varies with temperature according to T^{n} with n in the range of 1.72–1.8. Corresponding diffusion rates of hydrogen in air are larger by about a factor of 4 compared to those of air in air. The rising velocity under the influence of positively buoyant forces cannot be determined directly, since they are dependent on the density difference between hydrogen and air as well as on drag and friction forces, shape and size of the rising gas volume, and atmospheric turbulence. The positive buoyancy of hydrogen is a favourable safety effect in unconfined areas, but it can cause a hazardous situation in (partially) confined spaces where the hydrogen can accumulate, e.g. underneath a roof. Both diffusion and buoyancy determine the rate at which the gas mixes with the ambient air. The rapid mixing of hydrogen with the air is a safety concern, since it leads very soon to flammable mixtures, which on the other hand — for the same reason — also will quickly dilute to the non-flammable range.

Because of its small size, its small molecular weight and its low viscosity, hydrogen can cause a problem with respect to the propensity of the gas to leak at a larger molecular flow rate than other gases. Diffusion in small amount is even possible through intact materials, in particular organic materials, which may lead to gas accumulation in confined spaces. Leakage rates are higher by a factor of 50 than those for water and by a factor of 10 compared to nitrogen. The addition of an odorant or colourant would ease the detection of small leaks; however, this is not practicable in most situations, and not feasible for liquefied hydrogen.

Hydrogen gas dissolved in liquids will permeate into adjoining vessel materials. At elevated temperatures and pressures, hydrogen attacks mild steels severely, causing decarburization and embrittlement. This is a serious

concern in any situation involving storage or transfer of hydrogen gas under pressure. Proper material selection, e.g. special alloy steels, and technology is required to prevent embrittlement.

Hydrogen coexists in two different forms, ortho and para hydrogen, whose partition is dependent on the temperature. Normal hydrogen at room temperature is 75% ortho (nuclear spins aligned) and 25% para (spins anti-aligned). In the lower temperature range of less than 80 K, para hydrogen is the more stable form. At 20 K, the thermal equilibrium concentrations are 99.821% para and 0.179% ortho. The transition takes place over a longer period (about 3–4 days), until a new equilibrium state is reached. However, magnetic impurities and also small oxygen concentrations are able to catalyse ortho–para conversions raising the rate by several orders of magnitude (very good: $Fe(OH)_3$) to the order of hours. Any concentration of either spin state can be created at any temperature through the action of catalysts. Most physical properties are differing only slightly between the two spin states. Most important is the large energy difference between the two varieties, which results in major differences for the specific heats and thermal conductivities. The presence of a radiation field results in the generation of free hydrogen atoms and ions, which also act as catalysts before recombining. The recombination on the other hand produces excess ortho hydrogen.

Hydrogen also exhibits a positive Thompson–Joule effect at temperatures above 193 K, the inversion temperature. It means that the temperature of the hydrogen gas increases upon depressurization, which may lead to ignition. For example, the temperature change is six degrees if a sudden pressure drop from 20 MPa to ambient pressure takes place. The chance of a spontaneous ignition just by that effect, however, is small; an explosion is more likely to occur because of electrostatic charging of dust particles during the depressurization or auto-ignition at high temperatures.

Liquid hydrogen (LH_2) has the advantage of extreme purity and under certain conditions the more economic type for storage and distribution (see Section 9), however, at the expense of a significant energy consumption of about one third of its heat of combustion for liquefaction. A drawback is the unavoidable loss by boiloff which is typical to maintain the cold temperature in the tank. The evaporation rate is even enhanced when ortho hydrogen is stored. The heat liberated during the ortho–para conversion at 20 K is huge at 670 kJ/kg compared with a figure of 446 kJ/kg for the latent heat of vaporization at the same temperature. This represents a safety issue requiring a design of the hydrogen loop that is able to remove the heat of conversion in a safe manner.

For open LH_2 pools, it needs to be considered that cold hydrogen gas is less volatile than ambient gas and thus more prone to the formation of a flammable mixture with air. Furthermore, LH_2 quickly contaminates itself due to condensation and solidification of air constituents, which can particularly lead to oxygen enriched zones to form shock-explosive mixtures. In confined areas, an additional hazard is given by the fact that due to the volume increase by a factor of 845, when LH_2 is heated up to ambient conditions, the local atmosphere may change drastically. In an enclosed space, final pressure may rise to 172 MPa, which certainly overpressurizes systems to bursting.

A further temperature decrease below the boiling point eventually results in mixtures of liquid and solid hydrogen or slush hydrogen, SLH_2. Slush offers the advantages of a higher density and a prolongation of the storage time of the cryogen as the solid melts and absorbs heat. A safety risk arises from the decreasing vapour pressure even below atmospheric pressure, which demands protection against air ingress into the system. In addition, the conversion of ortho to para hydrogen connected with the release of the heat of conversion as the solid is formed needs to be taken into account [567]. The triple point finally is the temperature (13.8 K) and pressure (7.2 kPa) at which all three phases can exist in equilibrium (Fig. 216).

If hydrogen or any other fluid is maintained above its critical temperature and pressure, a single phase ‘supercritical fluid’ forms. It is gas-like in that it is compressible, it is liquid-like in that it has a comparable density, and there is some transitory state in between characterized by strong structural fluctuations causing the unusual behaviour of fluid properties near their critical point. It also exhibits higher flow rates compared with liquids. There is a strong dependence of the thermophysical properties of cryogenic hydrogen on temperature and pressure in the supercritical state. They vary strongly especially in the near-critical region. Cp has a maximum at the pseudo-critical temperature (‘thermal spike phenomenon’). Supercritical hydrogen might undergo a turbulent-to-laminar transition due to the dependence of viscosity on temperature. Heat transfer coefficients are unpredictable in the transition regime, and are much lower in the laminar regime.

Hydrogen at extreme but accessible pressures ($2–3 \times 10^5$ MPa) and temperatures (~4400 K) will make a phase transition to metallic hydrogen which may be superconducting at room temperature. This effect, predicted in 1935,

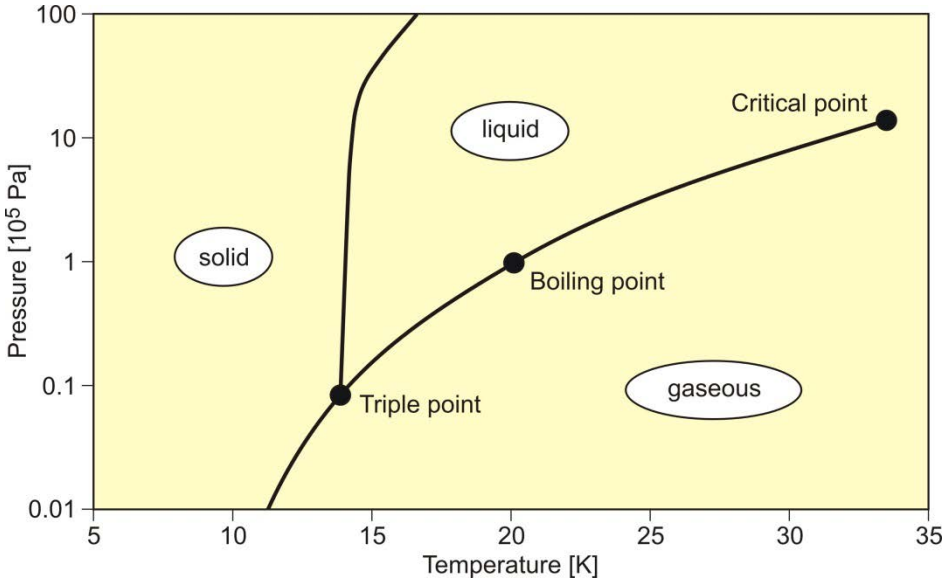

FIG. 216. Phase diagram of hydrogen.

was eventually proven in a shock compression test in 1996. Metallic hydrogen is accepted as existing in the interior of Saturn and Jupiter, but has no practical application on Earth so far.

Hydrogen is essentially an insulator in both the gaseous and the liquid phase. Only above some critical 'breakdown' voltage where ionization occurs does it becomes an electrical conductor.

A.3. CHEMICAL PROPERTIES OF HYDROGEN

Hydrogen reacts both with non-metals (high electro-negativity) and metals (low electro-negativity) to form either ionic or covalent hydrides (e.g. HCl, H_2O). The electro-negativity, a measure for the attraction of electrons to the nucleus, of hydrogen is 2.20 on the Pauling scale.

Hydrogen is able to react chemically with most other elements. In connection with oxygen, hydrogen is highly flammable over a wide range of concentrations. As a fuel it represents a clean, environmentally benign energy source. The mass-related energy density of hydrogen is very high; 1 kg of hydrogen contains 141.86 MJ (gross heat of combustion), which is approximately 2.5 times more energy than is contained in 1 kg of natural gas. The energy content of hydrogen is given as either LHV of 242 kJ/mol or as HHV of 286 kJ/mol. The difference of 15.6%, which is large compared with other gases, is due to the heat liberated upon condensation of the water vapour (which could be captured in a turbine, but not in a fuel cell).

A stoichiometric hydrogen–air mixture where all fuel is consumed upon reaction, i.e. where maximum combustion energy is released, contains 29.5 vol% of hydrogen. The combustion product of hydrogen is water vapour. It burns in a non-luminous, almost invisible pale blue, hot flame to water vapour, liberating the chemically bound energy as heat (gross heat of combustion). The flame temperature of a burning premixed and stoichiometric hydrogen–air mixture is a maximum of 2403 K.

There is a wide flammability range for hydrogen (at room temperature) between 4 and 75 vol% in air and up to 95 vol% in oxygen. The LFL, as the minimum amount of fuel that supports combustion, is usually the 'more important' limit, since it will be reached first in a continuous leakage. The flammability range widens with higher temperatures. The influence of the temperature is expressed in the modified Burgess-Wheeler equation for the LFL, which is for hydrogen at ambient pressure [568]:

$$c_{LFL} = c_{LFL}(300K) - \frac{3.14}{\Delta H_c}(T - 300) = 4.0 - 0.013(T - 300)[\text{vol\%}]$$

where

ΔH_c is the net heat of combustion;
T is the temperature, K.

The respective equation for the upper flammability limit (UFL) is [569]:

$$c_{UFL} = 74.0 + 0.026(T - 300)[\text{vol\%}]$$

valid for the temperature range 150–300 K. Measurements of upward flame propagation at higher temperatures have shown a further increase of the UFL with initial temperature reaching 87.6% at 673 K. There are still no experimental data available on the influence of moisture on the flammability limits. For the determination of the LFL and UFL of mixtures of fuels, the Le Chatelier rule is the most commonly applied method:

$$\frac{1}{L_m} = \Sigma \frac{y_i}{L_i}$$

where

y_i is the volume fraction of fuel *i*;
L_i is the flammability limit of fuel i.

Le Chatelier's rule was found to be in accurate agreement with experimental data for the system H_2–CO [570].

The potential for an explosion of a flammable hydrogen–air mixture is very high. The auto-ignition temperature, which is the minimum temperature of a hot surface that can ignite a flammable mixture, is for hydrogen in the range of 800–1000 K dependent on the experimental conditions. It is relatively high, but can be lowered by catalytic surfaces. Hydrogen gas does not have a flash point, as it is already a gas at ambient conditions. This means that cryogenic hydrogen will flash at all temperatures above its boiling point of 20 K.

The minimum ignition energy, i.e. the spark energy required to ignite the "most easily ignitable hydrogen concentration in air" (which is usually not the stoichiometric mixture), is at 0.02 mJ very low, much lower than for hydrocarbon–air mixtures. A weak spark or the electrostatic discharge from a flow of pressurized H_2 gas or from a person (~10 mJ) would suffice for an ignition; this is, however, no different from other burnable gases. The minimum ignition energy decreases further with increasing temperature, pressure or oxygen content. Of all hydrocarbons, the hot air jet ignition temperature is lowest for hydrogen and decreases further with increasing jet diameter. It is also dependent on jet velocity and mixture composition.

The maximum experimental safe gap is the maximum distance between two flat plates which still allows flame propagation through the gap; for hydrogen it is 0.08 mm. The quenching gap in air is the distance (between two flat plates) at which ignition of a flammable mixture is suppressed. It corresponds to the smallest diameter of a tube through which a flame can propagate. Faster burning gases have smaller quenching gaps. Hydrogen has a quenching gap of 0.64 mm. Because of the high explosion pressures, the maximum experimental safe gap is always smaller than the quenching gap.

The burning velocity in a flammable gas mixture, different from the flame speed, is indicative of the speed with which a smooth plane combustion wave advances into a stationary flammable mixture and is a pertinent property of the gas depending on temperature, pressure and concentration. The burning velocity of hydrogen in air (Fig. 217) at stoichiometric ambient conditions is 2.55 m/s, reaching a maximum of 3.2 m/s at a concentration of 40.1%, which would even increase to 11.75 m/s in pure oxygen. Compared with other hydrocarbon fuel–air mixtures, it is highest for hydrogen because of hydrogen's fast chemical kinetics and high diffusivity. The higher the burning velocity, the greater is the chance for a transition from deflagration to detonation (DDT). In contrast, the flame speed, which is related to a fixed observer, is much greater than the burning velocity due to the expansion of the combustion products, instabilities and turbulent deformation of the flame. The maximum possible speed of a deflagration burning flame is given by the speed of sound in the combustion products gas mixture, which is 975 m/s for a stoichiometric H_2–air mixture.

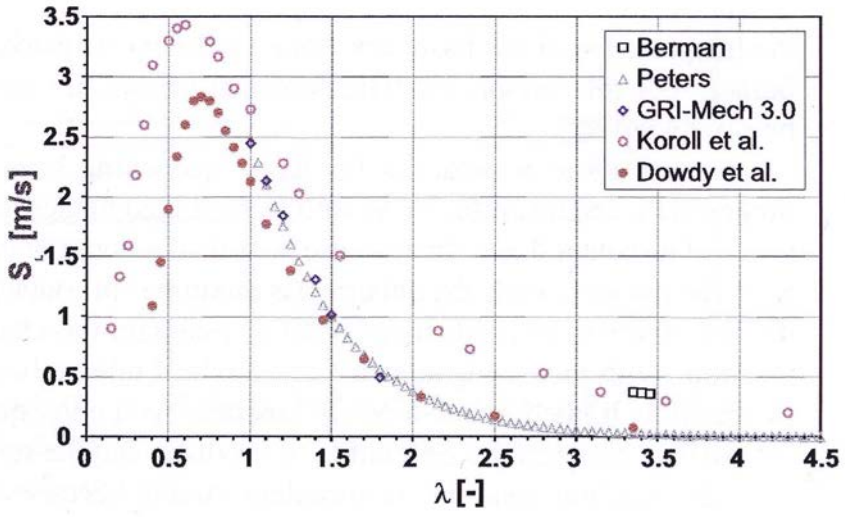

FIG. 217. Burning velocities in hydrogen–air mixtures as measured by various authors [571].

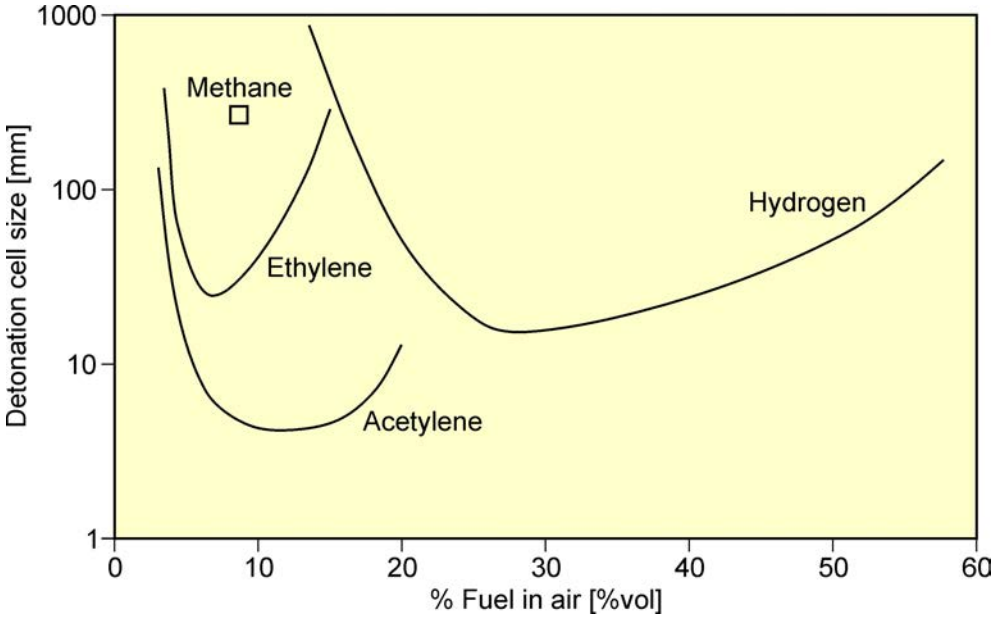

FIG. 218. Detonation cell size of hydrogen and other fuels.

The detonatability range is usually given to be 18–59 vol% of hydrogen concentration; however, the range was found to be dependent on the system size. In Ref. [572], a detonation range of 13–70% of H_2 is given for a 43 cm tube. In the Russian Federation's detonation test facility RUT, the largest of its kind, a lower detonatability limit of as low as 12.5 vol% has been observed. In pure oxygen, the detonation range is extended to 15–90% [570]. The detonation velocity in air reaches values in the range of 2000 m/s; in pure oxygen, it is up to 3500 m/s.

The size of the detonation cell is a measure of the reactivity; the smaller the cell, the more reactive is the mixture (Fig. 218). It serves to some extent as an indicator for DDT and can be measured experimentally. A stoichiometric hydrogen–air mixture with a cell size of 15 mm is highly reactive, whereas a stoichiometric methane–air mixture with a cell size of approximately 330 mm is the least sensitive of the common fuels. Cell sizes increase with increasing deviation from stoichiometry. It was in the late 1970s, when the usefulness of measurements of the detonation cell size, λ, was well acknowledged. The first step was finding a correlation between cell size and critical tube diameter ($d=13\times\lambda$). This empirical law was the basis for developing a simple

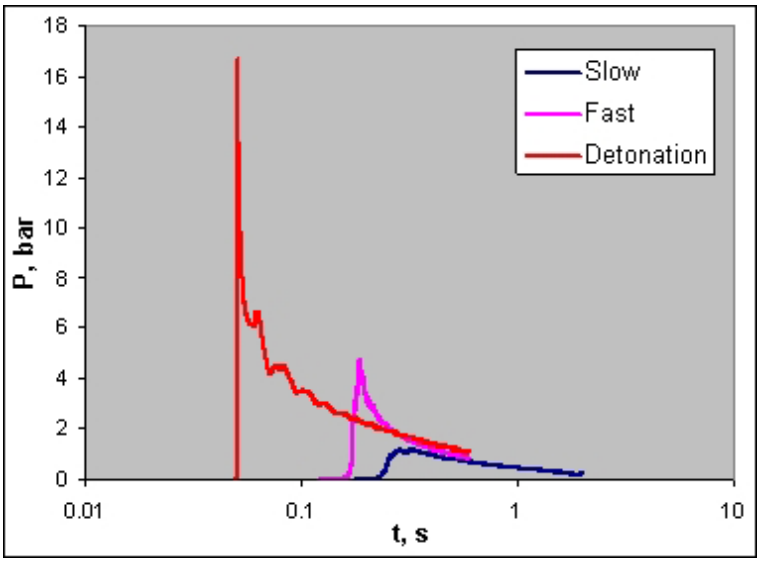

FIG. 219. Pressure signals from different hydrogen combustion modes [573].

surface energy model which allows the derivation of a critical initiation charge weight for various hydrocarbon–air mixtures in fairly good agreement with experimental data.

The critical tube diameter is the minimum diameter required for a detonation wave to emerge from a tube and become a detonation in an unconfined cloud. It is a measure of minimum dimensions of an unconfined detonable cloud. The detonation initiation energy given in mass of high explosive (TNT or tetryl) is the minimum energy necessary to initiate a spherical detonation wave; the energy content of tetryl corresponds to 4.3 MJ/kg.

The distance in which the flame front at the ignition point develops to a detonation depends on many parameters such as temperature, pressure, mixture composition, geometry (obstacles) and ignition source strength. For a stoichiometric hydrogen–air mixture to detonate, a typical ratio of tube length to diameter is approximately 100.

It is known from experience that a hydrogen–air gas cloud evolving from the inadvertent release of hydrogen upon the failure of a storage tank or pipeline liberates only a small portion of its thermal energy content in the case of an explosion, which is in the range of 0.1–10%, and in most cases <1% [405].

The explosion of a hydrogen–air mixture cloud results in the formation of a pressure wave, which is different dependent on the combustion mode, as is shown in Fig. 219. In the deflagration of a free hydrogen–air gas cloud, the maximum overpressure is in the order of 10 kPa. An overpressure of 7 kPa is still deemed not dangerous; at 7 kPa, people would fall down to the ground; at 35 kPa, damage of ear drums is expected; 240 kPa is considered a threshold value above which fatalities must be taken into account.

The thermal energy radiated from a flame corresponds to the HHV. It can be reduced due to absorption by moisture in the atmosphere. The radiation emitted from a hydrogen flame is very low due to a strong absorption by the ambient water vapour (emissivity ε <0.1) unlike hydrocarbon flames ($\varepsilon \approx 1$) [574]. Therefore despite its high flame temperature, the burning hazard is comparatively small. A major problem is given in the non-visibility of the flame, even in a dark room (unless impurities in the air are present), and therefore the difficulty of recognizing and localizing it. An advantage of hydrogen–air fires is the fact that there is no smoke generation (assuming no other material is ignited), which is important for confined areas.

A.4. ENVIRONMENTAL IMPACT OF HYDROGEN IN THE ATMOSPHERE

Currently, the major sources for hydrogen emissions to the atmosphere are the photochemical oxidation of atmospheric methane and volatile organic compounds (VOCs), estimated at 50%, and the combustion of fossil fuels and biomass, e.g. forest fires or traffic emissions (~40%). But the hydrogen content of the atmosphere is still found to be on the trace gas level. Stratospheric hydrogen is controlled by the production from methane oxidation and the destruction due to the OH reaction. In addition, hydrogen is exchanged with the troposphere. The main removal

mechanism from the atmosphere is by dry deposition and uptake in soils (~75%) or through oxidation by hydroxyl free radicals OH (~25%) [575]. Hydrogen concentrations in the troposphere and stratosphere are constant at a level of ~0.5 ppm, with a total H_2 mass of 175 million t in the atmosphere.

Hydrogen is not a direct GHG, as it does not absorb electromagnetic radiation within the infrared spectrum. An adverse effect is identified with hydrogen acting as a significant sink for OH, whose concentration further decreases with increased atmospheric concentrations of hydrogen. This in turn could increase the atmospheric lifetime of GHGs and other pollutants in the stratosphere and may reduce stratospheric ozone concentrations. On the other hand, hydrogen constitutes only about 5% of the average OH sink, and OH has a much stronger reaction to changes in reactive NO_x emissions which are believed to significantly perturb the amount of ozone in the upper troposphere and lower stratosphere region. The anticipated changes in OH levels due to changes in the atmospheric hydrogen concentration are marginal when hydrogen is atmospherically degraded in the lower stratosphere where the persistent ice (from the water) may have a cooling effect that again influences the temperature dependent ozone depletion mechanism [576].

In a global hydrogen infrastructure, emissions of molecular H_2 can occur along the whole hydrogen process chain. A realistic upper limit for the global average leak rate is 3% for the whole hydrogen energy chain [575]. Any diffusive, targeted or accidental release will emit predominantly into the atmosphere. Its oxidation results in the formation of water vapour (clouds), but it is not expected to raise considerably the overall content of water vapour in the troposphere, since also the present fossil fuel economy emits significant amounts of water vapour from combustion and cooling.

Increased water vapour concentrations in the upper troposphere can be expected if air traffic increases as projected, especially if hydrogen is used as aviation fuel. At these altitudes, increased water vapour may cause the formation of cirrus clouds, which would either increase or decrease heat radiation, depending on the height and thickness of the cloud, and so could lead to cooling or warming of the atmosphere.

It is difficult to establish reliable estimates of the potential water vapour release from aircraft, and even harder to model the effects of extra water vapour on this highly sensitive region of the atmosphere. Emissions depend strongly on engine design, and the effects will be very different depending on the altitude, air temperature, exhaust temperature and background humidity. If hydrogen combustion engines were used widely in aircraft, another source of concern could be emissions of NO_x.

There is still large uncertainty around the atmospheric budget of molecular hydrogen. Therefore, except for the expected strong reduction of CO and CO_2 emissions, no final conclusions can be made at present about the potential environmental benefits and risks of the move from a fossil fuel based to a hydrogen based energy industry [576].

A.5. HYDROGEN CHARACTERISTIC DATA

The main characteristic data of hydrogen are summarized in Table 74 [577–579].

TABLE 74. MAIN CHARACTERISTIC PROPERTIES OF HYDROGEN

Atomic weight	Standard atomic mass	1.0078225 u[a]
	Protium	1.00782503207 u[a]
	Deuterium	2.0141017778 u[a]
	Tritium	3.0160492777 u[a]
Molecular weight		2.01594 g/mol
Stoichiometric fraction in air		29.53 vol%
Boiling point (BP)		20.369 K
Melting point (MP)		14.01 K
Triple point (TP)	Temperature	13.8 K
	Pressure	7.2 kPa

TABLE 74. MAIN CHARACTERISTIC PROPERTIES OF HYDROGEN (cont.)

Critical point	Temperature	33.145 K
	Pressure	1.2964 MPa
	Density	31.263 kg/m^3
Electronegativity		2.20 Pauling scale
Density	Gas at NTP[b]	0.08376 kg/m^3
	Gas at STP[c]	0.08990 kg/m^3
	Gas at BP	1.338 kg/m^3
	Para liquid at BP	70.78 kg/m^3
	Normal[d] liquid at BP	70.96 kg/m^3
	Slush with 50 mass% solid at TP	81.48 kg/m^3
	Para solid at MP	86.50 kg/m^3
	Solid at 4 K	88.0 kg/m^3
Expansion ratio liquid/ambient		845
Diffusion coefficient	At NTP[b]	0.61×10^{-4} m^2/s
Diffusion velocity	At NTP[b]	< 0.02 m/s
Buoyant velocity		1.2–9.1 m/s
Gas constant		4124.3 J/(kg·K)
Specific heat (constant p)	Gas at NTP[b]	14.89 kJ/(kg·K)
	Gas at STP[c]	14.304
	Gas at BP	12.15
	Liquid at BP	9.69
	Slush with 50 mass% solid at TP	11.4
Ratio of specific heats c_p/c_v	At NTP	1.308
Thermal conductivity	Gas at NTP[b]	0.1897 W/(m·K)
	Gas at BP	0.01694 W/(m·K)
	Liquid at BP	0.09892 W/(m·K)
	Solid at TP	0.90 W/(m·K)
Viscosity	Gas at NTP[b]	8.948 μPa·s
	Gas at BP	1.079 μPa·s
	Liquid at BP	13.32 μPa·s
Surface tension	At BP	1.92×10^{-3} N/m
Vapour pressure	Normal[d] at TP	7200 Pa
	Para at TP	7040 Pa
	Solid at 10 K	257 Pa
Para/ortho ratio	At STP	25/75%
	At BP	99.79/0.21%
Inversion temperature	At 0.1 MPa	193 K
Heat of conversion	From ortho to para at BP	703 kJ/kg
	From normal[d] to para	527–670 kJ/kg
Heat of melting (fusion)	At MP	58.8 kJ/kg
Heat of vaporization	At BP	445.6 kJ/kg
Vaporization index[e]		8.9 K·cm^3/J
Vaporization rate (steady state) of LH_2 pool		4.2–8.3 mm/s
		25–50 mm/s [f]
Heat of sublimation		379.6 kJ/kg
Speed of sound	Gas at NTP[b]	1294 m/s
	In stoichiometric H_2-air mixture	404 m/s
	In gas at BP	355 m/s
	In liquid at BP	1093 m/s

TABLE 74. MAIN CHARACTERISTIC PROPERTIES OF HYDROGEN (cont.)

Inversion (Joule–Thomson) temperature		193 K
Flammability limits in air		4.0–75.0[g] vol%
Detonatability limits in air		13–70[h] vol%
Minimum ignition energy		1.9×10^{-5} J
	For detonation	~10 000 J
Auto-ignition temperature in air		793–1023 (858) K
Hot air jet ignition temperature		943 K
Gross heat of combustion or Higher Heating Value (HHV) at NTP [b]		141.86 MJ/kg 12.75 MJ/m^3 285.9 kJ/mol
Net heat of combustion or Lower Heating Value (LHV) at NTP [b]		119.93 MJ/kg 10.8 MJ/m^3 241.9 kJ/mol
Wobbe Index[h] (upper)		48.34 MJ/m^3
Wobbe Index[h] (lower)		40.90 MJ/m^3
Flame temperature (theoretical)		2318 K
Laminar burning velocity	Air at stoich. Maximum at 42.5 vol%	2.65 m/s 3.46 m/s
Visible laminar flame front velocity		18.6 m/s
Burning rate of LH_2 pool		0.5–1.1 mm/s
Deflagration pressure ratio		8.15
Quenching distance	At NTP[b]	0.64 mm
Maximum experimental safe gap	At NTP[b]	0.08 mm
Adiabatic flame temperature		2318 K
Emission coefficient		< 0.1
Detonation velocity		1480–2150 m/s
Chapman-Jouguet (CJ) velocity		1968 m/s
CJ detonation pressure ratio p_{CJ}/p_0		15.6
Energy release		2.82 MJ/kg mixture
Detonation cell size		15 mm
Critical tube diameter		0.2 m
Detonation initiation energy		1.1 g tetryl[k]
Detonation induction distance	At NTP[b]	length/diameter ~100
TNT equivalent		26.5 kg TNT/kg

[a] 1 u (atomic mass unit) = $1.660\,538\,782 \times 10^{-27}$ kg
[b] NTP (normal temperature and pressure): 293 K, 101325 Pa.
[c] STP (standard temperature and pressure): 273 K, 101325 Pa.
[d] 'Normal' hydrogen = 75% ortho + 25% para
[e] Indicates the relative ease of a substance to vaporize
[f] According to NASA [580].
[g] LFL is valid for upward propagation of flame. For downward propagation, LFL is 5.3 vol%.
[h] Valid for weak ignition. For a high-energy igniter, a range of 11.6–74.9 was quoted.
[i] The upper/lower Wobbe index is defined as the ratio of the HHV/LHV and the square root of the relative density, which again is the ratio of the fuel gas density to the density of dry air under the same pressure and temperature conditions.
[k] Formula: $C_7H_5N_5O_8$; IUPAC name: 2,4,6-trinitrophenyl-N-methylnitramine

REFERENCES

[1] EUROPEAN COMMISSION, Hydrogen Energy and Fuel Cells — A Vision of Our Future, High Level Group Summary Report, European Commission, Brussels (2003).

[2] FORSBERG, C.W., Sustainability by combining nuclear, fossil, and renewable energy sources, Progress in Nuclear Energy **51** (2009) 192–200.

[3] BOSSEL, U., ELIASSON, B., Energy and the hydrogen economy, 8 January 2003, http://www.afdc.energy.gov/afdc/pdfs/hyd_economy_bossel_eliasson.pdf

[4] TSUKADA, R., "Proposal for hydrogen economy", Proc. COE-INES Int. Workshop on Toward Hydrogen Economy, What Nuclear Can Contribute and How, Tokyo, 2004, THEN, Tokyo Institute of Technology (2005).

[5] NATIONAL ACADEMY OF ENGINEERING, The Hydrogen Economy — Opportunities, Costs, Barriers, and R&D Needs. Committee on Alternatives and Strategies for Future Hydrogen Production and Use, Board on Energy and Environmental Systems, Division on Engineering and Physical Sciences, National Research Council and National Academy of Engineering of the National Academies, The National Academies Press, Washington, DC (2004).

[6] INTERNATIONAL ENERGY AGENCY, Energy Technology Perspectives 2010, Scenarios & Strategies to 2050, IEA, Paris (2010).

[7] INTERNATIONAL ENERGY AGENCY, Key World Energy Statistics 2007, IEA, Paris (2008).

[8] INTERNATIONAL PANEL ON CLIMATE CHANGE, Fourth Assessment Report "Climate Change 2007", Synthesis Report, IPCC (2007).

[9] INTERNATIONALES WIRTSCHAFTSFORUM REGENERATIVE ENERGIEN, Cerina Plan, IWR, Münster (2009).

[10] MIKKELSEN, M., JOERGENSEN, M., KREBS, F.C., The teraton challenge. A review of fixation and transformation of carbon dioxide, Energy & Environmental Science **3** (2010) 43–81.

[11] SCHINDLER, J., et al., Wasserstoff und Brennstoffzellen, starke Partner erneuerbarer Energiesysteme, European Hydrogen Association (EHA) and Deutscher Wasserstoff- und Brennstoffzellen-Verband, Ludwig–Bölkow-Systemtechnik, Ottobrunn (2008).

[12] WORLD NUCLEAR ASSOCIATION, World Nuclear Power Reactors & Uranium Requirements, WNA, London (2010).

[13] INTERNATIONAL ATOMIC ENERGY AGENCY, Power Reactor Information System, IAEA, Vienna (2007).

[14] ROGNER, H.H., "Kernenergieperspektiven in der zukünftigen globalen Energieversorgung", Presentation at FZJ-STE, April 28, Research Center Jülich (2009).

[15] MADISHA, K., "Rollout strategy for hydrogen production", In: VERFONDERN, K. (Ed.), Nuclear Energy for Hydrogen Production, Schriften des Forschungszentrums Jülich, Energy Technology, Vol. 58, Research Center Jülich (2007).

[16] BAINDUR, S., Nuclear Hydrogen Production: Scoping the Safety Issues, Presentation to the Canadian Nuclear Society, January 24 (2008).

[17] FINAN, A.E., MIU, K., KADAK, A.C., "Nuclear technology and Canadian oil sands: Integration of nuclear power with in-situ oil extraction", Proc. Int. Congress on Advances in Nuclear Power Plants ICAPP'06, Reno, NV (2006) paper 6442.

[18] COUPEY, J.-P., "Recovery of unconventional oil resources", Presentation at the Post-FISA Conference on HTRs for Combined Heat/Electricity and Hydrogen Production, Luxembourg (2006).

[19] NATERER, G., et al., Recent Canadian advances in nuclear-based hydrogen production and the thermochemical Cu–Cl cycle, International Journal of Hydrogen Energy **34** (2009) 2901–2917.

[20] SADHANKAR, R.R., Leveraging nuclear research to support hydrogen economy, International Journal of Energy Research **31** (2007) 1131–1141.

[21] INTERNATIONAL ENERGY AGENCY, World Energy Outlook 2009, IEA, Paris (2009).

[22] YAN, X., INDERWILDI, O.R., KING, D.A., Biofuels and synthetic fuels in the US and China: A review of well-to-wheel energy use and greenhouse gas emissions with the impact of land-use change, Energy & Environmental Science **3** (2010) 190–197.

[23] KNOCHE, D., et al., "Advanced nuclear reactor concepts for China", Proc. Int. Youth Nuclear Congress IYNC 2008, Interlaken (2008) paper 311.

[24] EUROPEAN COMMISSION, GREEN PAPER: A European Strategy for Sustainable, Competitive and Secure Energy, Report COM(2006) 105 final, {SEC(2006) 317}, European Commission, Brussels (2006).

[25] VAN GOETHEM, V., HUGON, M., BHATNAGAR, V., MANOLATOS, P., DEFFRENNES, M., Euratom innovation in nuclear fission: Community research in reactor systems and fuel cycles, Nuclear Engineering and Design **237** (2007) 1486–1501.

[26] BASINI, V., et al., "Why HTR/VHTR? A European point of view", Proc. Int. Congress on Advances in Nuclear Power Plants ICAPP'08, Anaheim, CA (2008) paper 8433.

[27] HY-NET, Towards a European Hydrogen Energy Roadmap, Preface to HyWays – the European Hydrogen Energy Roadmap Integrated Project, Executive Report (2004).

[28] EUROPEAN COMMISSION, HyWays: The European Hydrogen Energy Roadmap, Final Report, Brussels (2008).

[29] EUROPEAN HYDROGEN AND FUEL CELL TECHNOLOGY PLATFORM, Strategic Research Agenda (2005), http://www.certh.gr/dat/91BFE801/file.pdf

[30] LE DUIGOU, A., et al., HYTHEC: An EC funded search for a long term massive hydrogen production route using solar and nuclear technologies, International Journal of Hydrogen Energy **32** (2007) 1516–1529.
[31] EUROPEAN HYDROGEN AND FUEL CELL TECHNOLOGY PLATFORM, Interim Implementation Plan, Draft report, HFP (2006),
http://hy-co.certh.gr/dat/%7Ba083028a-8db4-4919-8040-d7bf4dba91be%7D/file.pdf
[32] POITOU, S., et al., "Development programme of the SO_3 decomposer as a key component of the sulphur based thermochemical cycles: New steps towards feasibility demonstration", Proc. 17th World Hydrogen Energy Conf. WHEC'17, Brisbane, Australia (2008) paper 345.
[33] ROEB, M., et al., "HycycleS – A project on solar and nuclear hydrogen production by sulphur-based thermochemical cycles", Proc. 18th World Hydrogen Energy Conf. WHEC'18, Essen (2010).
[34] LE NAOUR, F., INNOHYP CA Final Report, INNOHYP CA –FR–CEA/07-05 (2007).
[35] COPSEY, B., et al., "The Framatome-ANP high temperature reactor concept", Proc. Int. Congress on Advances in Nuclear Power Plants ICAPP'05, Seoul (2005) paper 5254.
[36] BREUIL, E., et al., "Development of the intermediate heat exchanger (IHX) for ANTARES", Proc. Int. Congress on Advances in Nuclear Power Plants ICAPP'06, Reno, NV (2006) paper 6457.
[37] LOMMERS, L.J., SHAHROKHI, F., MAYER III, J.A., SOUTHWORTH, F.H., "AREVA HTR concept for near term deployment", Proc. 5th Int. Top. Meeting on High Temperature Reactor Technology HTR2010, Prague (2010) paper 132.
[38] GAUTHIER, J.-C., et al., Potential applications for nuclear energy besides electricity generation: A global perspective, Nuclear Engineering and Technology **39** (2007) 31–42.
[39] SINHA, R.K., KAKODKAR, A., "Indian programme related to innovative nuclear reactor technology", Proc. 13th Ann. Conf. of the Indian Nuclear Society INSAC, Mumbai (2002).
[40] FUKUDA, K., KOBAYASHI, O., OGATA, K., "A hydrogen introduction scenario in Japan", Presentation by T. Sawada at the INES-THEN, Tokyo, Nov. 5–6, 2004, Tokyo Institute of Technology (2005).
[41] NUCLEONICS WEEK, "JAERI wants to produce hydrogen in HTTR in 2010 — if money is there" January 20 (2005).
[42] KURIYAMA, N., "Millennium project", Presentation at the Int. Workshop on Fuel Cell Testing and Review of Codes & Standards Activities FCTESTNET, Ulm (2004).
[43] IWAI, Y., "Japan's approach to commercialization of fuel cell/hydrogen technology", Presentation at the 4th IPHE Steering Committee, Paris, January 26–28, International Partnership for Hydrogen and Fuel Cells in the Economy, Berlin (2005).
[44] FUEL CELL TODAY, June (2005).
[45] WATANABE, H., KAMEYAMA, H., OKAMURA, K., NISHIZAKI, K., "Commercialization of residential fuel cell systems at Tokyo Gas", Presentation at the 20th World Energy Congress, Rome (2007).
[46] GEIGER, S., Cropper M., Fuel cell market survey: Small stationary applications, Fuel Cell Today, 30 July (2003).
[47] VERFONDERN, K., NISHIHARA, T., Safety aspects of the combined HTTR/steam reforming complex for nuclear hydrogen production, Progress in Nuclear Energy **47** (2005) 527–534.
[48] KUBO, S. et al., A pilot test plant of the thermochemical water-splitting iodine–sulfur process, Nuclear Engineering and Design **233** (2004) 355–362.
[49] HINO, R., et al., R&D on hydrogen production by high temperature electrolysis of steam, Nuclear Engineering and Design **233** (2004) 363–375.
[50] SAKABA, N., KASAHARA, S., ONUKI, K., KUNITOMI K., Conceptual design of hydrogen production system with thermo–chemical water-splitting iodine–sulphur process utilizing heat from the high temperature gas-cooled reactor HTTR, International Journal of Hydrogen Energy **32** (2007) 4160–4169.
[51] SAKABA, N., HIRAYAMA, Y., "Helium chemistry in high temperature gas-cooled reactors — Chemistry control for avoiding Hastelloy XR corrosion in the HTTR-IS system", Proc. Int. Conf. on Nuclear Energy Systems for Future Generation and Global Sustainability Global 2005, Tsukuba, (2005) paper 263.
[52] SAKABA, N., SATO, H., OHASHI, H., NISHIHARA T., KUNITOMI, K., Development scenario of the iodine–sulphur hydrogen production process to be coupled with VHTR system as a conventional chemical plant, Journal of Nuclear Science and Technology **45**(9) (2008) 962–969.
[53] HINO, R., "Overview of JAERI's R&D on nuclear hydrogen production", Proc. COE-INES Int. Workshop "Towards Hydrogen Economy, What Nuclear can Contribute and How", Tokyo, 2004, THEN, Tokyo Institute of Technology (2005).
[54] YAN, X.L., et al., "GTHTR300 design variants for production of electricity, hydrogen or both", Proc. OECD/NEA 3rd Information Exchange Meeting on the Nuclear Production of Hydrogen, Oarai (2005).
[55] KUNITOMI, K., et al., JAEA's VHTR for hydrogen and electricity cogeneration: GTHTR300C, Nuclear Engineering and Technology **39** (2007) 9–20.
[56] KUNITOMI, K., Japan's future HTR — the GTHTR300, Nuclear Engineering and Design **233** (2004) 309–327.
[57] YAN, X.L., GTHTR300 design and development, Nuclear Engineering and Design **222** (2003) 247–262.
[58] MATSUYAMA, S., NISHIGUCHI, Y., SAKASHITA, Y., KASUGA, S., KAWASHIMA, M., "Steam producing plant concept of 4S for oil sand extraction", Proc. Int. Congress on Advances in Nuclear Power Plants ICAPP'09, Tokyo (2009) paper 9198.
[59] CHIKAZAWA, Y., et al., "Conceptual design of hydrogen production plant with thermochemical and electrolytic hybrid method using a sodium cooled reactor", Proc. Int. Congress on Advances in Nuclear Power Plants ICAPP'05, Seoul (2005) paper 5084.

[60] YAMADA, K., et al., “Hydrogen production with steam reforming of dimethyl ether at the temperature less than 573 K”, Proc. Int. Congress on Advances in Nuclear Power Plants ICAPP’05, Seoul (2005) paper 5138.
[61] LEE, W.J., KIM, Y.W., CHANG, J.W., Perspectives of nuclear heat and hydrogen, Nuclear Engineering and Technology **41**(4) (2009) 413–426.
[62] LEE, C.H., “Hydrogen & fuel cell activity in Korea”, Presentation at the 4th IPHE Steering Committee, Paris, January 26–28, International Partnership for Hydrogen and Fuel Cells in the Economy, Berlin (2005).
[63] CHANG, J.H., LEE, W.J., “Status of the Korean nuclear hydrogen production project” (Proc. 4th Information Exchange Meeting on the Nuclear Production of Hydrogen, Oakbrook, IL, 2009) NEA Report No. 6805, Paris (2010) 59–66.
[64] CHANG, J.H., “Challenges for production of hydrogen using nuclear energy”, Proc. IAEA Technical Meeting on Non-Electric Applications of Nuclear Energy, Daejeon (2009).
[65] PARK, J.K., “Nuclear hydrogen project in Korea”, Presentation at the Int. Congress on Advances in Nuclear Power Plants ICAPP’05, Seoul (2005).
[66] LEE, Y.J., et al., “Preliminary study on the NHDD plant configuration, a VHTR coupled to hydrogen production systems”, Proc. Int. Congress on Advances in Nuclear Power Plants ICAPP’05, Seoul (2005) paper 5315.
[67] KIM, Y.W., “Gas cooled reactor, its potential applications for process heat”, Proc. IAEA Technical Meeting on Non-Electric Applications of Nuclear Energy, Daejeon (2009).
[68] CHANG, J.H., “Current status of HTGR development in Korea”, Plenary presentation at the 5th Int. Top. Meeting on High Temperature Reactor Technology HTR2010, Prague (2010).
[69] ZVEREV D.L., et al., “Innovation technology for regional power industry based on HTGR”, Proc. Int. Conf. on Nuclear Energy Systems for Future Generation and Global Sustainability Global 2009, Paris (2009) paper 9527.
[70] ROSENERGOATOM, Experience with the Supply of Heat. Presentation, found on the Internet, October (2010).
[71] PONOMAREV-STEPNOY, N., STOLYAREVSKIY, A., KODOCHIGOV, N., “The concept of nuclear hydrogen based on MHR-T reactor”, Proc. 5th Int. Top. Meeting on High Temperature Reactor Technology HTR2010, Prague (2010) paper 237.
[72] GULEVICH, A.V., et al., “Hydrogen production and water desalination in nuclear power facilities with liquid metal coolants”, Presentation at the 12th Int. Conf. on Emerging Nuclear Energy Systems ICENES, Brussels (2005).
[73] REITSMA, F., “Technical achievements of the PBMR project in South Africa”, Proc. 5th Int. Top. Meeting on High Temperature Reactor Technology HTR2010, Prague (2010) paper 282.
[74] GREYVENSTEIN, R., CORREIA, M., KRIEL, W., South Africa’s opportunity to maximize the role of nuclear power in a global hydrogen economy, Nuclear Engineering and Design **238** (2008) 3031–3040.
[75] REITSMA, F., “Technical achievements of the PBMR project in South Africa”, Plenary presentation at the 5th Int.Top. Meeting on High Temperature Reactor Technology HTR2010, Prague (2010).
[76] CORREIA, M., GREYVENSTEIN, R., SILADY, F., PENFIELD, S., “PBMR as an ideal heat source for high temperature process heat applications”, Proc. Int. Conf. on Nuclear Engineering ICONE-14, Miami, FL (2006) paper 89473.
[77] BOLTHRUNIS, C.O., KUHR, R.W., FINAN, A.E., “Using a PBMR to heat a steam–methane reformer: Technology and economics”, Proc. 3rd Int. Top. Meeting on High Temperature Reactor Technology HTR2006, Johannesburg (2006) paper I00000118.
[78] MATZIE, R., GREYVENSTEIN, G., “Pebble bed modular reactor project status”, Proc. Int. Congress on Advances in Nuclear Power Plants ICAPP’09, Tokyo (2009) paper PN4-2.
[79] SCARLAT, R., “Preliminary safety assessment of a PBMR supplying process heat to a co-located ethylene production plant”, Proc. 5th Int. Top. Meeting on High Temperature Reactor Technology HTR2010, Prague (2010) paper 217.
[80] UNITED STATES DEPARTMENT OF ENERGY, Nuclear Energy Research and Development Roadmap, Report to Congress, USDOE Washington DC (2010).
[81] MPR, Survey of HTGR Process Energy Applications, Report MPR-3181, Rev. 0, MPR Associates, Inc., Alexandria, VA (2008).
[82] LATTIN, W.C., UTKIKAR, V.P., Transition to hydrogen economy in the United States: A 2006 status report, International Journal of Hydrogen Energy **32** (2007) 3230–3237.
[83] STOOTS, C.M., O’BRIEN, J.E., CONDIE, K.G., HERRING, J.S., “Test results from the Idaho National Laboratory 15KW high temperature electrolysis test facility”, Proc. 17th Int. Conf. on Nuclear Engineering ICONE-17, Brussels (2009) paper 75417.
[84] UNITED STATES DEPARTMENT OF ENERGY, The Impact on the Increased Use of Hydrogen on Petroleum Consumption and Carbon Dioxide Emissions, EIA/DOE-Report #SR-OIAF-CNEAF/2008-04, Appendix A, USDOE, Washington DC (2008).
[85] UNITED STATES DEPARTMENT OF ENERGY, Hydrogen Cost Goal Announcement, USDOE, Washington DC (2005), www.hydrogen.energy.gov/pdfs/h2_cost_goal.pdf
[86] UNITED STATES DEPARTMENT OF ENERGY, Nuclear Hydrogen R&D Plan, USDOE, Washington DC (2004).
[87] PARK, C.V., PATTERSON, M.W., Systematic Discrimination of Advanced Hydrogen Production Technologies, Report INL/CON-10-18411, Idaho National Laboratory, ID (2010).
[88] O’BRIEN, J., “Review of the potential of nuclear hydrogen for addressing energy security and climate change”, Proc. ST-NH2, San Diego, CA (2010).
[89] PETTI, D., The Next Generation Nuclear Plant, Report INL/EXT-08-15118, Idaho National Laboratory, ID (2009).
[90] COLLINS, J.W., Next Generation Nuclear Plant Project Technology Development Roadmaps: The Technical Path Forward, Report INL/EXT-08-15148, Idaho National Laboratory, ID (2009).

[91] MCKELLAR, M.G., HARVEGO, E.A., O'BRIEN, J.E., "Analysis of improved reference design for a nuclear-driven high temperature electrolysis hydrogen production plant", Proc. ST-NH2, San Diego, CA (2010).
[92] SHENOY, A., "Prismatic conceptual design", Presentation at the VHTR R&D FY10 Technical Review Meeting, Denver, CO (2010) paper 1–3.
[93] RICHARDS, M.B., et al., "Conceptual designs for MHR-based hydrogen production systems", Proc. Int. Conf. on Nuclear Energy Systems for Future Generation and Global Sustainability Global 2005, Tsukuba (2005) paper 190.
[94] O'BRIEN, J.E., MCKELLAR, M.G., HERRING J.S., "Commercial scale performance predictions for high temperature electrolysis plants coupled to three advanced reactor types", Proc. Int. Congress on Advances in Nuclear Power Plants ICAPP'08, Anaheim, CA (2008) paper 8244.
[95] STOOTS, C.M., CONDIE, K.G., O'BRIEN, J.E., HERRING, J.S., HARTVIGSEN, J.J., "Initial operation of the high temperature electrolysis integrated laboratory scale experiment at INL", Proc. Int. Congress on Advances in Nuclear Power Plants ICAPP'08, Anaheim, CA (2008) paper 8245.
[96] O'BRIEN, J.E., et al., Parametric study of large scale production of syngas via high temperature co-electrolysis, International Journal of Hydrogen Energy **34** (2009) 4216–4226.
[97] FORSBERG, C.W., "The ddvanced high temperature reactor: High temperature fuel, molten salt coolant, and liquid-metal reactor plant", Proc. 1st Int. Symp. on Innovative Nuclear Energy Systems for Sustainable Development of the World COE-INES, Tokyo (2004) paper 71.
[98] MOISSEYTSEV, A., Passive Load Follow Analysis of the STAR-LM and STAR-H2 Systems. Dissertation Texas A&M University, College Station, TX (2003).
[99] WADE, D., et al., "STAR-H2: Passive Load Follow/Passive Safety Coupling to the Water Cracking Balance of Plant", Presentation at the Symp. on Nuclear Energy and the Hydrogen Economy, Cambridge, MA (2003).
[100] FISCHEDICK, M., PASTOWSKI, A., "Fuel provision for early market applications" In: STOLTEN, D. (Ed.), Hydrogen and Fuel Cells — Fundamentals, Technologies and Applications, Wiley-VCH, Weinheim (2010) 149–166.
[101] SCHOLZ, W.H., Verfahren zur großtechnischen Erzeugung von Wasserstoff und ihre Umweltproblematik, Linde Berichte aus Technik und Wissenschaft **67** (1992) 13–21.
[102] PAUL SCHERRER INSTITUTE, Hopes on hydrogen: No quick fixes, PSI, Villigen, Energie-Spiegel, No. 12, November (2004).
[103] UHDE GmbH, Hydrogen, Dortmund (2003), http://www.uhde.biz/informationen/broschueren.en. html
[104] EUROPEAN HYDROGEN AND FUEL CELL TECHNOLOGY PLATFORM, Strategic Research Agenda, EHFCP (2005), https://www.hfpeurope.org/uploads/873/HFP-SRA004_V9-2004_SRA-report-final_22JUL 2005.pdf
[105] HORI, M., et al., "Synergistic hydrogen production by nuclear-heated steam reforming of fossil fuels", Proc. 1st Int. Symp. Innovative Nuclear Energy Systems for Sustainable Development of the World COE-INES, Tokyo (2004) paper 43.
[106] PETRI, M.C., KLICKMAN, A.E., HORI, M., "Hydrogen production options for water-cooled nuclear power plants" (Proc. IAEA Int. Conf. on Non-Electric Applications of Nuclear Power: Seawater Desalination, Hydrogen Production and Other Industrial Applications, Oarai, 2007), Proceedings Series IAEA-CN-152, International Atomic Energy Agency, Vienna (2009) 133–142.
[107] RANKE, H., SCHÖDEL, N., Hydrogen production technology — Status and new developments, Oil Gas European Magazine **2** (2004) 78–84.
[108] HIKITA, T., "Hydrogen from industrial processes and reforming of fossil fuels", Presentation at the COE-INES International Workshop Towards Hydrogen Economy, What Nuclear can Contribute and How, Tokyo, 2004, THEN, Tokyo Institute of Technology (2005).
[109] BARBA, D., et al., Membrane reforming in converting natural gas to hydrogen (Part 1), International Journal of Hydrogen Energy **33** (2008) 3700–3709.
[110] MUELLER-LANGER, F., TZIMAS, E., KALTSCHMITT, M., PETEVES, S., Techno–economic assessment of hydrogen production processes for the hydrogen economy for the short and medium term, International Journal of Hydrogen Energy **32**(16) (2007) 3797–3810.
[111] LI, J., Wachsman, E., "Hydrogen production and separation from carbon dioxide reforming of methane", Proc. 34th Int. Conf. and Exposition on Advanced Ceramics and Composites, Daytona Beach, FL (2010) paper ICACC-S3-018-2010.
[112] LIU, D.-J., KAUN, T.D., LIAO, H.-K., AHMED, S., Characterization of kilowatt-scale autothermal reformer for production of hydrogen from heavy hydrocarbons, International Journal of Hydrogen Energy **29** (2004) 1035–1046.
[113] PORŠ, Z., Eduktvorbereitung und Gemischbildung in Reaktionsapparaten zur autothermen Reformierung von dieselähnlichen Kraftstoffen, Schriften des Forschungszentrums Jülich, Reihe Energietechnik, Vol. 49, Research Center Jülich (2005).
[114] PASEL, J., SAMSUN, R.C., PETERS, R., STOLTEN, D., "Development of fuel cell systems for aircraft applications based on synthetic fuels", Proc. 18th World Hydrogen Energy Conf. WHEC'18, Essen (2010).
[115] RYDEN, M., LYNGFELT, A., Using steam reforming to produce hydrogen with carbon dioxide capture by chemical-looping combustion, International Journal of Hydrogen Energy **31** (2006) 1271–1283.
[116] ESWARAMOORTHI, I., DALAI, A.K., A comparative study on the performance of mesoporous SBA-15 supported Pd–Zn catalysts in partial oxidation and steam reforming of methanol for hydrogen production, International Journal of Hydrogen Energy **34** (2009) 2580–2590.

[117] FRANCK, H.-G., KNOP, A., Kohleveredlung an der Schwelle der 80er Jahre, Die Naturwissenschaften **67** (1980) 421–430.
[118] DGMK DEUTSCHE WISSENSCHAFTLICHE GESELLSCHAFT FÜR ERDÖL, ERDGAS UND KOHLE, Kohlenveredlung, Positionspapier, (http://www.dechema. de/dechema_media/Kohlenveredlung.pdf), DGMK and DECHEMA (2009).
[119] PETERS, W., Entwicklungs- und Forschungsarbeiten auf dem Gebiete der Kohletechnik, Technische Mitteilungen **71** (1978) 358–364.
[120] SCHMIEDER, H., HENRICH, E., DINJUS E., Wasserstoffgewinnung durch Wasserspaltung mit Biomasse und Kohle, Report FZKA 6556, Research Center Karlsruhe (2000).
[121] MINCHENER, A.J., Coal gasification for advanced power generation, Fuel **84** (2005) 2222–2235.
[122] TEGGERS, H., JÜNTGEN, H., Stand der Kohlevergasung zur Erzeugung von Brenngas und Synthesegas, Erdöl und Kohle — Erdgas **37** (1984) 163–174.
[123] TURNA, O., "Sasol–Lurgi fixed bed dry bottom gasification for fuels and chemicals", Presentation at the 2nd Int. Freiberg Conf. on IGCC & XtL Technologies, Freiberg (2007).
[124] VAN DYK, J.C., KEYSER, M.J., COERTZEN, M., Syngas production from South African coal using Sasol–Lurgi gasifiers, International Journal of Coal Geology **65** (2006) 243–253.
[125] KAMKA, F., JOCHMANN, A., "Development Status of BGL-Gasification", Presentation at the 1st Int. Freiberg Conf. on IGCC & XtL Technologies, Freiberg (2005).
[126] RIIS, T., HAGEN, E.F., VIE, P.J.S., ULLEBERG, Ø., Hydrogen Production — Gaps and Priorities, IEA Hydrogen Implementing Agreement (HIA). Special Report (2005), http://ieahia.org/pdfs/HIA_Production_G&P_Final_with_Rev.pdf
[127] HIGMAN, C., "European coal gasification projects", Presentation at the FutureGen Workshop, Tokyo (2008).
[128] NEDO, Clean Coal Technologies in Japan. Technological Innovation in the Coal Industry, New Energy and Industrial Technology Development Organization, Kawazaki, and Japan Coal Energy Center, Tokyo (2006).
[129] SUDIRO, M., et al., Improving process performances in coal gasification for power and synfuel production, Energy & Fuels **22** (2006) 3894–3901.
[130] GNANAPRAGASAM, N.V., REDDY, B.V., ROSEN, M.A., Hydrogen production from coal using coal direct chemical looping and syngas chemical looping combustion systems: Assessment of system operation and resource requirements, International Journal of Hydrogen Energy **34** (2009) 2606–2615.
[131] SUSTA, M.R., SEONG, K.B., "Supercritical and ultra-supercritical power plants — SEA's vision or realtity?", Presentation at the Int. Conf. POWER-GEN ASIA, Bangkok (2004).
[132] LACKNER, K.S., ZIOCK, H.-J., "The U.S. zero emission coal alliance technology" (Presentation at the VGB Conf., Essen, Germany), Report LA-UR-010423, Los Alamos National Laboratory, NM (2001).
[133] LIN, S.Y., "Progress of HyPr-RING process development for hydrogen production from fossil fuels", Proc. 16th World Hydrogen Energy Conf. WHEC'16, Lyon (2006) paper 249.
[134] WEIMER, T., BERGER, R., HAWTHORNE C., "Production of hydrogen from carbonaceous energy carriers", Proc. Int. Hydrogen Energy Congress and Exhibition IHEC, Istanbul (2005).
[135] RODDY, D.J., YOUNGER, P.L., Underground coal gasification with CCS: A pathway to decarbonising industry, Energy & Environmental Science **3** (2010) 400–407.
[136] STEINBERGER-WILCKENS, R., TRÜMPER, S.C., "Supplying the fuel — Energy resources and infrastructure", Presentation at the Roads2HyCom Research & Technology Workshop, March 5–6, Brussels (2009).
[137] JURASCIK, M., SUES, A., PTASSINSKI, K.J., Exergetic evaluation and improvement of biomass-to-synthetic natural gas conversion, Energy & Environmental Science **2** (2009) 791–801.
[138] PATEL, J., SALO, K., "CARBONA biomass gasification technology", Presentation at the Int. Conf. on Renewable Energy TAPPI, Atlanta, GA (2007).
[139] NORSK HYDRO, Hydro Electrolysers, Norway (2002).
[140] NILSEN, S., Personal Communication, Norsk Hydro (2006).
[141] IVY, J., Summary of Electrolytic Hydrogen Production, Report NREL/MP-560-36734, National Renewable Energy Laboratory, Golden, CO (2004).
[142] HERRING, J.S., et al., "Hydrogen production through high temperature electrolysis in a solid oxide cell", Proc. OECD/NEA 2nd Information Exchange Meeting on the Nuclear Production of Hydrogen, Chicago, IL (2003).
[143] HAUCH, A., EBBESEN, S.D., JENSEN, S.H., MOGENSEN, M., Highly efficient high temperature electrolysis, Journal of Materials Chemistry **18** (2008) 2331–2340.
[144] HERRING, J.S., CONDIE, K., O'BRIEN, J.E., STOOTS, C.M., HARTVIGSEN, J.J., "Hydrogen production for transportation fuels using nuclear energy", Proc. Int. Congress on Advances in Nuclear Power Plants ICAPP'08, Anaheim, CA (2008) paper 8125.
[145] FUNK, J., Thermo–chemical hydrogen production: Past and present, International Journal of Hydrogen Energy **26** (2001) 185–190.
[146] VERFONDERN, K., VON LENSA, W., "MICHELANGELO Network Recommendations on Nuclear Hydrogen Production", Proc. OECD/NEA 3rd Information Exchange Meeting on the Nuclear Production of Hydrogen, Oarai (2005).
[147] FUNK, J.E., REINSTROM, R.M., Energy requirements in the production of hydrogen from water, IEC Process Research and Development **5**(3) (1966) 336.

[148] BEGHI, G., A decade of research on thermochemical hydrogen at the Joint Research Centre Ispra, International Journal of Hydrogen Energy **11** (1986) 761–771.
[149] BESENBRUCH, G.E., et al., Report GA-A18257, General Atomics, San Diego, CA (1982).
[150] BESENBRUCH, G.E., et al., "Thermochemical hydrogen production with a high temperature gas cooled reactor", Proc. OECD/NEA 1st Information Exchange Meeting on Nuclear Production of Hydrogen, Paris (2000).
[151] VITART, X., CARLES, P., "Thermochemical production of hydrogen using nuclear heat: A survey of technical and economical issues", Proc. Int. Conf. on Nuclear Energy Systems for Future Generation and Global Sustainability Global 2005, Tsukuba (2005) paper IL008.
[152] NORMAN, J.H., et al., Thermochemical Water-Splitting Cycle, Bench-Scale Investigations and Process Engineering, Report GA-A16713, General Atomics, San Diego, CA (1982).
[153] GOLDSTEIN, S., BORGARD, J.M., VITART, X., Upperbound and best estimate of the efficiency of the IS cycle, International Journal of Hydrogen Energy **30** (2005) 619–626.
[154] BAE, K.K., et al., "A study on hydrogen production by thermochemical water-splitting IS (iodine–sulfur) process", Proc. OECD/NEA 3rd Information Exchange Meeting on the Nuclear Production of Hydrogen, Oarai (2005).
[155] NORMAN, J.H., et al., Thermochemical Water-Splitting for Hydrogen Production, Report GRI-80/0105, Gas Research Institute, Chicago, IL (1980).
[156] LANCHI, M., et al., S–I thermochemical cycle: A thermodynamic analysis of the HI–H_2O–I_2 system and design of the HI_x decomposition section, International Journal of Hydrogen Energy **34** (2009) 2121–2132.
[157] O'KEEFE, D., et al., Preliminary results from bench-scale testing of a sulfur–iodine thermochemical water-splitting cycle, International Journal of Hydrogen Energy **7** (1982) 381–392.
[158] RICHARDS, M.B., et al., H2-MHR conceptual designs based on the sulphur–iodine process and high temperature electrolysis, International Journal Nuclear Hydrogen Production and Applications **1** (2006) 36–50.
[159] KASAHARA, S., KUBO, S., ONUKI, K., NOMURA, M., Thermal efficiency evaluation of HI synthesis/concentration procedures in the thermochemical water splitting IS process, International Journal of Hydrogen Energy **29** (2004) 579–587.
[160] ZHANG, P., CHEN, S.Z., WANG, L.J., XU, J.M., Overview of nuclear hydrogen production research through iodine sulfur process at INET, International Journal of Hydrogen Energy **35**(7) (2010) 2883–2887.
[161] ONUKI, K., et al., Electro–electrodialysis of hydriodic acid in the presence of iodine at elevated temperatures, Journal of Membrane Science **192** (2001) 193–199.
[162] BRECHER, L.E., SPEWOCK, S., WARDE, C.J., The Westinghouse sulfur cycle for the thermochemical decomposition of water, International Journal of Hydrogen Energy **2** (1977) 7–15.
[163] SUMMERS, W.A., GORENSEK, M.B., BUCKNER, M.R., "The hybrid sulfur cycle for nuclear hydrogen production", Proc. Int. Conf. on Nuclear Energy Systems for Future Generation and Global Sustainability Global 2005, Tsukuba (2005) paper 097.
[164] CARLES, P., "The Westinghouse (Hybrid S) Cycle", In: VERFONDERN, K. (Ed.), Nuclear Energy for Hydrogen Production, Schriften des Forschungszentrums Jülich, Energy Technology, Vol. 58, Research Center Jülich (2007).
[165] GORENSEK, M., SUMMERS, W., Hybrid sulphur flow-sheets using PEM electrolysis and a bayonet decomposition reactor, International Journal of Hydrogen Energy **34** (2009) 4097–4114.
[166] VAN VELZEN, D., "Desulphurization and denoxing of waste gases producing hydrogen as a by-product" (Proc. 2nd IEA Technical Workshop on Hydrogen Production, Jülich) Report HUF-6, Research Center Jülich (1991) 99–111.
[167] KAMEYAMA, H., YOSHIDA, K., "Br–Ca–Fe water decomposition cycles for hydrogen production", Proc. 2nd World Hydrogen Energy Conf. WHEC'2, Zurich (1978) 829–850.
[168] LEMORT, F., LAFON, C., DEDRYVERE, R., GONBEAU, D., Physicochemical and thermodynamic investigation of the UT-3 hydrogen production cycle: A new technological assessment, International Journal of Hydrogen Energy **31** (2006) 906– 918.
[169] TEO, E.D., et al., A critical pathway energy efficiency analysis of the thermochemical UT-3 cycle, International Journal of Hydrogen Energy **30** (2005) 599–564.
[170] SCHULTZ, K.R., et al., "Production of hydrogen by nuclear energy: The enabling technology for the hydrogen economy", Presentation at America's Nuclear Energy Symp. ANES, Miami, FL (2002).
[171] LEMORT, F., LAFON, C., GIROLD, F., "Thermodynamic and technological assessment of the IS cycle", Proc. 1st European Hydrogen Energy Conf. EHEC, Grenoble (2003).
[172] NAKAYAMA, T., et al., MASCOT — A bench-scale plant for producing hydrogen by the UT-3 thermo–chemical decomposition cycle, International Journal of Hydrogen Energy **9** (1984) 187–190.
[173] LEMORT, F., LAFON, C., DEDRYVERE, R., GONBEAU D., Physiochemical and thermodynamic investigation of the UT-3 hydrogen production cycle: A new technological assessment, International Journal of Hydrogen Energy **31** (2006) 906–918.
[174] DOCTOR, R.D., et al., "Hydrogen generation using a calcium–bromine thermochemical water-splitting cycle", Proc. Symp. on Nuclear Energy and the Hydrogen Economy, Cambridge, MA (2003).
[175] DOCTOR, R.D., YANG, J.H., PANCHAL, C.B., "$CaBr_2$ hydrolysis for HBr production using a direct sparging contactor" (Proc. 4th OECD/NEA Information Exchange Meeting on Nuclear Hydrogen Production, Oakbrook, IL, 2009) NEA Report No. 6805, OECD-NEA, Paris (2010) 269–278.
[176] LEWIS, M.A., Alternative Thermochemical Cycles for Nuclear Hydrogen, USDOE Report, USDOE, Washington DC (2005).

[177] SUPPIAH, S., “Canadian Nuclear Hydrogen R&D Programme: Development of the medium temperature Cu-Cl cycle and contributions to the high temperature sulphur–iodine cycle“, Presentation at the 4th Information Exchange Meeting on the Nuclear Production of Hydrogen, Oakbrook, IL (2009).
[178] LEWIS, M.A., MASIN, J.G., VILIM, R.B., “Development of the low temperature Cu–Cl thermochemical cycle”, Proc. Int. Congress on Advances in Nuclear Power Plants ICAPP’05, Seoul (2005) paper 5425.
[179] LEWIS, M.A., FERRANDON, M.S., TATTERSON, D.F., “An overview of R&D activities for the Cu–Cl cycle with emphasis on the hydrolysis reaction” (Proc. 4th OECD/NEA Information Exchange Meeting on Nuclear Hydrogen Production, Oakbrook, IL, 2009) NEA Report No. 6805, OECD-NEA, Paris (2010) 235–242.
[180] NATERER, G., “Environmental impact comparison of steam methane reformation and thermochemical processes of hydrogen production”, Proc. 18th World Hydrogen Energy Conf. WHEC’18, Essen (2010).
[181] DOKIYA, D., KOTERA Y., Hybrid cycle with electrolysis using a Cu–Cl system, International Journal of Hydrogen Energy **1** (1976) 117–121.
[182] LEWIS, M.A., SERBAN, M., BASCO, J. K., “Generating hydrogen using a low temperature thermochemical cycle”, Proc. Int. Conf. on Nuclear Technology Global 2003, New Orleans, LA (2003).
[183] ROSEN, M., NATERER, G., SADHANKAR, R., SUPPIAH, S., “Nuclear-based hydrogen production with a thermo–chemical copper–chlorine cycle and supercritical water reactor”, Proc. Canadian Hydrogen Association Workshop, Quebec (2006).
[184] EWAN, B., ALLEN, R., Limiting thermodynamic efficiencies of thermo–chemical cycles used for hydrogen production, Green Chemistry **8** (2006) 988–994.
[185] KNOCHE, K.F., Stand der Arbeiten zur Wasserstoff-Erzeugung mit nuklearer Prozesswärme, Chemie-Ingenieur-Technik **49** (1977) 238–242.
[186] CREMER H., et al., Status report on thermochemical iron/chlorine cycles: A chemical engineering analysis of one process, International Journal of Hydrogen Energy **5** (1980) 231–252.
[187] GONZALES, R.B., LAW, V.J., PRINDLE, J.C., Analysis of the hybrid copper oxide–copper sulfate cycle for the thermochemical splitting of water for hydrogen production, International Journal of Hydrogen Energy **34** (2009) 4179–4188.
[188] SCHUSTER, P., Experimentelle Untersuchung und Bilanzierung von Vanadium/ Chlor- und Vanadium/Brom-Mehrstufenprozessen zur thermochemischen Erzeugung von Wasserstoff, Dissertation RWTH Aachen (1980).
[189] KNOCHE, K.F., SCHUSTER, P., RITTERBEX, T., Thermochemical production of hydrogen by a vanadium/chlorine cycle. Part 2: Experimental investigation of the individual reactions, International Journal of Hydrogen Energy **9** (1984) 473–482.
[190] ZHANG, P., ZHANG, L., NIE, R.J., WANG, J.C., Preparation of $CuFe_2O_4$ and its preliminary application study in two-step thermochemical water-splitting cycle, International Journal of Nuclear Hydrogen Production and Applications **1**(3) (2008) 219–228.
[191] SUBRAMANI, V., GANGWAL, S.K., “Pure hydrogen production from syngas by steam–iron process using nanoparticle iron catalyst”, Proc. 20th North American Catalysis Society Meeting, Houston, TX (2007).
[192] MURADOV, N.Z., VEZIROGLU, T.N., From hydrocarbon to hydrogen–carbon to hydrogen economy, International Journal of Hydrogen Energy **30** (2005) 225–237.
[193] BAKKEN, J.A., et al., Thermal plasma process development in Norway, Pure & Applied Chemistry **70** (1998) 1223–1228.
[194] PALM, T., BUCH, C., KRUSE, B., SAUAR, E., Green Heat and Power. Report 3, Bellona Foundation, Oslo (1999), http://www.bellona.no/imaker?id=11196=1
[195] PALUMBO, R., et al., Packaging Sunlight (2004), http://www.memagazine.org/pemar04/ pckgsun/pckgsun.html
[196] ARNASON, B., SIGFUSSON, T.I., “Application of geothermal energy to hydrogen production and storage”, Presentation at the 2nd German Hydrogen Congress, Essen (2003).
[197] KERR, W., MAJUMDAR D.P., “Aqueous homogeneous reactor for hydrogen production” (Proc. Hydrogen Economy Miami Energy Conf., Miami Beach, FL, 1974) Report Part A, New York, Plenum Press (1975) 167–181.
[198] KUGELER, K., et al., “Technical and safety aspects of processes of hydrogen production using nuclear energy”, Proc. Int. Congress on Advances in Nuclear Power Plants ICAPP’05, Seoul (2005) paper 5729.
[199] KUGELER, K., et al., The pebble-bed High Temperature Reactor as a source of nuclear process heat, Volume 4: System considerations on nuclear-heated steam reformers, Report Jül-1116-RG, Research Center Jülich (1974).
[200] SPATH, P.L., MANN, M.K., Life Cycle Assessment of Hydrogen Production via Natural Gas Steam Reforming, Report NREL/TP-570-27637, National Renewable Energy Laboratory, Golden, CO (2001).
[201] NFE, Nukleare Fernenergie, Zusammenfassender Bericht zum Projekt Nukleare Fernenergie (NFE), Report Jül-Spez-303, Research Center Jülich (1985).
[202] NIEßEN, H.F., et al., Erprobung und Versuchsergebnisse des PNP-Teströhrenspaltofens in der EVA-II-Anlage, Report Jül-2231, Research Center Jülich (1988).
[203] HARTH, R., RANGE, J., Energietransport durch EVA und ADAM, KFA Jahresbericht 1984/85, Research Center Jülich (1985) 55–62.
[204] HÖHLEIN, B., et al., Methane from synthesis gas and operation of high temperature methanation, Nuclear Engineering and Design **78** (1984) 241–250.
[205] BOLTENDAHL, U., HARTH, R., Wärmetransport auf kaltem Wege, Bild der Wissenschaft (1980) April.

[206] INAGAKI, Y., et al., “Research and development programme on HTTR hydrogen production system”, Proc. GENES4/ANP Conf., Kyoto (2003) paper 1062.
[207] HADA, K., FUJIMOTO, N., SUDO Y., “Design of steam reforming hydrogen and methanol co-production system to be connected to the HTTR” (Proc. IAEA-TCM on High Temperature Applications of Nuclear Energy, Oarai, 1992) IAEA-TECDOC-761, IAEA, Vienna (1994) 124–134.
[208] HADA, K., NISHIHARA, T., SHIBATA, T., SHIOZAWA, S., “Design of a steam reforming system to be connected to the HTTR” (Proc. 3rd JAERI Symposium on HTGR Technologies, Oarai, 1996) Report JAERI-Conf 96-010, Japan Atomic Energy Research Institute, Oarai (1996) 229–240.
[209] MIYAMOTO, Y., et al. “Overview of hydrogen production programme in HTTR” (Proc. IAEA TCM on High Temperature Gas Cooled Reactor Applications and Future Prospects, Petten) Report ECN-R-98-004, The Netherlands Energy Research Foundation (1998).
[210] OHASHI, H., et al., “Experimental and analytical study on chemical reaction loss accident with a mock-up model of HTTR hydrogen production system”, Proc. 12th Int. Conf. on Nuclear Engineering ICONE-12, Arlington (2004).
[211] HAYASHI, K., et al., “Experimental results of startup and shutdown test on HTTR hydrogen production system using mock-up test facility”, Proc. Int. Conf. on Nuclear Energy Systems for Future Generation and Global Sustainability Global 2005, Tsukuba (2005) paper 252.
[212] KARASAWA, H., et al., “Storage and hydrogen production usage of recycle materials in the flexible fuel cycle initiative”, Proc. Int. Conf. on Nuclear Energy Systems for Future Generation and Global Sustainability Global 2005, Tsukuba (2005) paper 467.
[213] YIN, H., JIANG, S., ZHANG, Y., JU H., Modeling of the helium-heated steam reformer for HTR-10, Journal of Nuclear Science and Technology **44**(7) (2007) 977–984.
[214] VAN HEEK, K.H., JÜNTGEN, H., PETERS W., Wasserdampfvergasung von Kohle mit Hilfe von Prozeßwärme aus Hochtemperatur-Kernreaktoren, Atomkernenergie/Kerntechnik **40** (1982) 225–246.
[215] KIRCHHOFF, R., VAN HEEK, K.H., JÜNTGEN, H., PETERS W., Operation of a semi-technical pilot plant for nuclear aided steam gasification of coal, Nuclear Engineering and Design **78** (1984) 233–239.
[216] FRÖHLING, W., NEEF, H.J., “Synthetisches Naturgas aus Kohle und Hochtemperatur-Reaktorwärme“, KFA Jahresbericht 1976/77, Research Center Jülich (1977) 15–24.
[217] BERG, J., Benzin und Gas aus Kohle, Bild der Wissenschaft (1978) December.
[218] JÜNTGEN, H., VAN HEEK, K.H., Gasification of coal with steam using heat from HTRs, Nuclear Engineering and Design **34** (1975) 59–63.
[219] SCHRADER, L., STRAUSS, W., TEGGERS, H., The application of nuclear process heat for hydro gasification of coal, Nuclear Engineering and. Design **34** (1975) 51–57.
[220] FLADERER, R., SCHRADER, L., Hydrierende Vergasung von Kohle – Neuere Betriebsergebnisse, Chemie-Ingenieur-Technik **54** (1982) 884–892.
[221] KLUSMANN, A., STELZER, M., “Future Applications of the High Temperature Reactor” (Proc. IAEA TCM on Gas Cooled Reactors and their Applications, Jülich, 1986) IAEA-TECDOC-436, IAEA, Vienna (1987) 473–482.
[222] BARNERT, H., Energy Alcohol from Plant Biomass plus High Temperature Heat, the CO_2-Neutral, Environmentally Benign, and Consumer Friendly Future Alternative, Report Jül-3089, Research Center Jülich (1995).
[223] MILLER, A.I., DUFFEY, R.B., “Co-generation of hydrogen from nuclear and wind: The effect on costs of realistic variations in wind capacity and power prices”, Proc. 13th Int. Conf. on Nuclear Engineering ICONE-13, Beijing (2005).
[224] NATERER, G.F., et al., Synergistic roles of off-peak electrolysis and thermochemical production of hydrogen from nuclear energy in Canada, International Journal of Hydrogen Energy **33** (2008) 6849–6857.
[225] YU, B., et al., Research advance on highly efficient hydrogen production by high temperature steam electrolysis, Science in China Series B: Chemistry **51** (2008) 289–304.
[226] YU, B., ZHANG, W.Q., XU, J.M., CHEN, J., Status and research of highly efficient hydrogen production through high temperature steam electrolysis at INET, International Journal of Hydrogen Energy **35** (2010) 2829–2835.
[227] YU, B., ZHANG, W.Q., XU, J.M., “Research progress of HTSE for hydrogen production using planar SOEC technology at INET”, Proc. 18th World Hydrogen Energy Conf. WHEC’18, Essen (2010).
[228] JENSEN, S.H., LARSEN, P.H., MOGENSEN, M., Hydrogen and synthetic fuel production from renewable energy sources, International Journal of Hydrogen Energy **32** (2007) 3253–3257.
[229] ZAHID, M., BRISSE, A., HAUCH, A., SCHILLER, G., VOGT, U., “Highly efficient, high temperature, hydrogen production by water electrolysis (Hi2H2)”, Proc. Fuel Cell Seminar & Exposition, Phoenix, AR (2008) paper RDP42a-3.
[230] YVON, P., “French activities on carbon-free hydrogen production by using nuclear energy”, Proc. IAEA Technical Meeting on Non-Electric Applications of Nuclear Energy, Daejeon (2009).
[231] LE NAOUR, F., “High temperature steam electrolysis for nuclear hydrogen production, interest, technological breakthroughs & CEA’s strategy”, Proc. IAEA Technical Meeting on Non-Electric Applications of Nuclear Energy, Daejeon (2009).
[232] DÖNITZ, W., SCHMIDBERGER, R., Concepts and design for scaling up high temperature water vapour electrolysis, International Journal of Hydrogen Energy **4** (1982) 321–330.
[233] ERDLE, E., “Hochtemperatur-Elektrolyse von Wasserdampf HOT ELLY“, Proc. BMBF Status Seminar „Wasserstoff als Energieträger“, Würzburg (1995) 1–11.

[234] MATSUNAGA K., et al., “Hydrogen production system with high temperature electrolysis for nuclear power plant”, Proc. Int. Congress on Advances in Nuclear Power Plants ICAPP’06, Reno, NV (2006) paper 6282.
[235] O’BRIEN, J.E., et al., “High temperature electrolysis for hydrogen production from nuclear energy”, Proc. 11th Int. Topical Meeting on Nuclear Reactor Thermal Hydraulics, Avignon (2005).
[236] STOOTS, C.M., et al., Integrated Laboratory Scale Test Report, Report INL/EXT-09-15283, Idaho National Laboratory, ID (2009).
[237] MAWDSLEY, J.R., CARTER, J.D., KROPF, A.J. YILDIZ, B., MARONI, V.A., Post-test evaluation of oxygen electrodes from solid oxide electrolysis stacks, International Journal of Hydrogen Energy **34** (2009) 4198–4207.
[238] STOOTS, C., SHUNN, L., O’BRIEN, J., “Integrated operation of the INL HYTEST system and high temperature steam electrolysis for synthetic natural gas production”, Proc. ST-NH2, San Diego, CA (2010).
[239] SHARMA, V.I., YILDIZ, B., Degradation mechanism in $La_{0.8}Sr_{0.2}CoO_3$ as contact layer on the solid oxide electrolysis cell anode, Journal of the Electrochemical Society **157** (2010) B441–B448.
[240] HERRING, J.S., “Hydrogen production methods”, VHTR R&D FY10 Technical Review Meeting, Denver, CO (2010) presentation 1-5.
[241] WANG, Z., et al., Comparison of different copper–chlorine thermo–chemical cycles for hydrogen production, International Journal of Hydrogen Energy **34** (2009) 3267–3276.
[242] NATERER, G., et al., Thermo–chemical hydrogen production with a copper–chlorine cycle. II: Flashing and drying of aqueous cupric chloride, International Journal of Hydrogen Energy **33** (2008) 5451–5459.
[243] KOSA, S., SHREIBER, D., The enthalpy of mixing aqueous solutions of $CdCl_2$, $CuCl_2$, $MnCl_2$ and $ZnCl_2$ with HCl at varying ionic strength at 25°C, Journal of Solution Chemistry **4** (1994) 511.
[244] KHAN, M., CHEN, Y., “Preliminary process analysis and simulation of thermochemical hydrogen generation using copper–chloride cycle”, Proc. OECD/NEA 3rd Information Exchange Meeting on the Nuclear Production of Hydrogen, Oarai (2005).
[245] ZHANG, P., CHEN, S.Z., WANG, L.J., YAO, T.Y., XU, J.M., Study on a lab-scale hydrogen production by closed cycle thermo–chemical iodine–sulfur process, International Journal of Hydrogen Energy **35** (2010) 10166–10172.
[246] CHEN, S., GUO, H., “Relationship between density and composition of HI–I_2–H_2O in I–S process”, Proc. 18th World Hydrogen Energy Conf. WHEC’18, Essen (2010).
[247] SAKURAI, M., et al., Experimental study on side-reaction occurrence condition in the iodine–sulphur thermo–chemical hydrogen production process, International Journal of Hydrogen Energy **23** (2000) 613–619.
[248] PRASAD, C.S.R., FANI, H.Z., MENON, S.B., “Heterogeneous Bunsen reaction: Analysis & experimental study of chemical absorption of sulfur dioxide and dissolution of iodine into aqueous reacting system” (Proc. IAEA Int. Conf. on Non-Electric Applications of Nuclear Power: Seawater Desalination, Hydrogen Production and Other Industrial Applications, Oarai, 2007), Proceedings Series IAEA-CN-152, IAEA, Vienna (2009) 270–277.
[249] PRASAD, C.S.R., Modeling and design of Bunsen reaction system — Issues, approaches and results (R&D on iodine–sulfur thermochemical process for hydrogen), IAEA CRP No: 13932/RO on “Advances in Nuclear Power Process Heat Applications” (2007).
[250] LIBERATORE, R., CAPUTO, G., FELICI, C., SPADONA, A., “Demonstration of hydrogen production by the sulphur–iodine cycle: realization of a 10 NL/h plant”, Proc. 18th World Hydrogen Energy Conf. WHEC’18, Essen (2010).
[251] NAKAJIMA, H., et al., “A study on a closed-cycle hydrogen production by thermochemical water-splitting IS process”, Proc. 7th Int. Conf. on Nuclear Engineering ICONE-7, Tokyo (1999) paper 7104.
[252] KASAHARA, S., et al., Flowsheet study of the thermochemical water-splitting iodine–sulfur process for effective hydrogen production, International Journal of Hydrogen Energy **32** (2007) 489–496.
[253] IMAI Y., et al., “Evaluation of required activity of SO_3 decomposition catalyst for iodine–sulfur process”, Proc. 5th Int. Topical Meeting on High Temperature Reactor Technology HTR2010, Prague (2010) paper 249.
[254] KUBO, S., NAKAJIMA, H., IMAI, Y., KASAHARA, S., ONUKI, K., “Control technology for Bunsen reaction solution to regulate process condition”, Proc. AIChE Annual Meeting, Salt Lake City, UT (2007) 357.
[255] GIACONIA, A., et al., Survey of Bunsen reaction routes to improve the sulfur–iodine thermochemical water-splitting cycle, International Journal of Hydrogen Energy **34**(9) (2009) 4041–4048.
[256] NOMURA, M., et al., Application of an electrochemical membrane reactor to the thermochemical water splitting IS process for hydrogen production, Journal of Membrane Science **240** (2004) 221–226.
[257] NOMURA, M., et al., Development of an electrochemical cell for the efficient hydrogen production through the IS process, AIChE Journal **50** (2004) 1991–1998.
[258] NOGUCHI, H., et al., “Development of sulfuric acid decomposer for thermo–chemical IS process”, Proc. Int. Congress on Advances in Nuclear Power Plants ICAPP’06, Reno, NV (2006) paper 6166.
[259] KUBO, S., et al., “A bench scale hydrogen production test by thermochemical water-splitting iodine–sulfur process”, Proc. Int. Conf. on Nuclear Energy Systems for Future Generation and Global Sustainability Global 2005, Tsukuba (2005) paper 474.
[260] KUBO, S., NAGAYA, Y., “In situ composition measurements of Bunsen reaction solution by radiation probes”, Proc. 18th World Hydrogen Energy Conf. WHEC’18, Essen (2010).

[261] NAKAGIRI, T., et al., “Development of the thermo–chemical and electrolytic hybrid hydrogen production process for sodium cooled FBR”, Proc. Int. Conf. on Nuclear Energy Systems for Future Generation and Global Sustainability Global 2005, Tsukuba (2005) paper 135.
[262] NAKAGIRI, T., CHIKAZAWA, Y., “Development of a new thermochemical and electrolytic hybrid hydrogen production process for FBR”, Presentation at the HTTR Workshop on Hydrogen Production Technology, Oarai (2004).
[263] CHO, W.C., et al., “Key technology of sulfur–iodine process in Korea”, Presentation at the IAEA Technical Meeting on Non-Electric Applications, Daejeon (2009).
[264] HONG, S.D., SEO, D.U., KIM, C.S., KIM, Y.W., PARK, G.C., “Design and analysis of a high pressure and high temperature sulfuric acid experimental system”, Proc. 5th Int. Top. Meeting on High Temperature Reactor Technology HTR2010, Prague (2010) paper 201.
[265] LEE, W.J., “Progress of nuclear hydrogen programme in Korea”, Presentation at the 3rd Nuclear Hydrogen Workshop, Jeju, Korea Atomic Energy Research Institute (2009).
[266] CHANG, J.H., et al., A study of a nuclear hydrogen production demonstration plant, Nuclear Engineering and Technology **39** (2007) 111–122.
[267] HONG, S.D., OH, D.S., LEE, W.J., CHANG, J.H., “Design of a small scale high temperature gas loop for process heat exchanger design tests”, Proc. Int. Congress on Advances in Nuclear Power Plants ICAPP’06, Reno, NV (2006) paper 6357.
[268] SHIN, Y.-J., CHOI, J.-H., TAK, N.-I., LEE, K.-Y., CHANG, J.-H., “Computational analysis of a packed column for SO_3 decomposition in sulfur–iodine process” (Proc. IAEA Int. Conf. on Non-Electric Applications of Nuclear Power: Seawater Desalination, Hydrogen Production and Other Industrial Applications, Oarai, 2007), Proceedings Series IAEA-CN-152, IAEA, Vienna (2009) 313–318.
[269] KIM, J.-H., et al., Hydrogen iodide decomposer sizing for a nuclear hydrogen production by a SI process, Transactions of the Korean Nuclear Society Autumn Meeting, Gyeongju (2009) 35–36.
[270] SHENOY, A., “Hydrogen process coupling to modular helium reactors”, Proc. 3rd Nuclear Hydrogen Workshop, Jeju, Korea Atomic Energy Research Institute (2009).
[271] RUSS, B., MOORE, R., HELIE, M., PONS, N., “Results of the sulfur iodine process integrated lab scale experiment”, Proc. ST-NH2 Conf. of the American Nuclear Society, San Diego, CA (2010).
[272] SHERMAN, S.R., “Nuclear plant/hydrogen plant safety: issues and approaches”, Proc. ST-NH2 Conf. of the American Nuclear Society, Boston, MA (2007).
[273] NAGARAJAN, V., et al., CFD modeling and experimental validation of sulfur trioxide decomposition in bayonet type heat exchanger and chemical decomposer of different packed bed designs, International Journal of Hydrogen Energy **34** (2009) 2543–2557.
[274] IDAHO NATIONAL LABORATORY, The Technical Path Forward, INL, USA (2009).
[275] MCQUILLAN, B., et al., High Efficiency Generation of Hydrogen Fuels Using Solar Thermo–Chemical Splitting of Water, Report GA-A24972, General Atomics, San Diego, CA (2002).
[276] PICKARD, P., 2005 DOE hydrogen programme review sulfur–iodine thermochemical cycle, Presentation to the USDOE, May 25 (2005).
[277] WEIRICH, W., et al., Thermochemical processes for water splitting — Status and outlook, Nuclear Engineering and Design **78** (1984) 285–291.
[278] SCHULTZ, K.R., et al., The hydrogen reaction, Nuclear Engineering International (2005) July issue.
[279] GENERATION IV INTERNATIONAL FORUM, Energy Products from Generation IV Systems, Generation IV Nuclear Energy Systems Roadmap, Energy Products Cross Cut Group, July 30 (2002).
[280] WYDLER, P., Liquid metal cooled reactors, Chimia **59** (2005) 970–976.
[281] MACPHERSON, H.G., The molten salt reactor adventure, Nuclear Science and Engineering **90** (1985) 374–380.
[282] SUPPIAH, S., “Cu–Cl cycle development for hydrogen production using Canadian SCWR”, Presentation at the IAEA Technical Advisory Meeting with Nuclear Hydrogen Experts, Vienna (2007).
[283] MOKRY, S., et al., “Conceptual thermal-design options for pressure-tube SCWRs with thermochemical co-generation of hydrogen”, Proc. 16th Int. Conf. on Nuclear Engineering ICONE-16, Orlando, FL (2008) paper 48313.
[284] INTERNATIONAL ATOMIC ENERGY AGENCY, Guidance for the Evaluation of Innovative Nuclear Reactors and Fuel Cycles, IAEA-TECDOC-1362, IAEA, Vienna (2003).
[285] HERD, E.M., LOMMERS, L.J., SOUTHWORTH, F.H., “HTGR strategies to meet process heat reliability and availability”, Proc. Int. Congress on Advances in Nuclear Power Plants ICAPP’10, San Diego, CA (2010) paper 10225.
[286] HITTNER, D., et al., “A new impetus for developing industrial process heat applications of HTR in Europe”, Proc. 4th Int. Top. Meeting on High Temperature Reactor Technology HTR2008, Washington D.C. (2008) paper 58259.
[287] IDAHO NATIONAL LABORATORY, HTGR Industrial Application Functional and Operational Requirements, Report INL/EXT-10-19706, INL, ID (2010).
[288] BROWN, L.C., et al., High Efficiency Generation of Hydrogen Fuels Using Nuclear Power, Report GA-A24285, General Atomics, San Diego, CA (2003).
[289] VON LENSA, W., VERFONDERN, K., “Wasserstoffproduktion aus Kernenergie“, Presentation at the VDI, Düsseldorf (2006).
[290] INTERNATIONAL ATOMIC ENERGY AGENCY, Status of and Prospects for Gas-cooled Reactors, Technical Report Series No. 235, IAEA, Vienna (1984).

[291] STEHLE, H., KLAS, E., “Status of the development of hot gas ducts for HTRs” (Proc. IAEA Specialists’ Meeting on Heat Exchanging Components of Gas-Cooled Reactors, Düsseldorf) Report IWGGCR-9, IAEA, Vienna (1984) paper 25.
[292] VERFONDERN, K., “Survey on 20 years of R&D on nuclear process heat applications in Germany“, Presentation at the IAEA Int. Conf. on Non-Electric Applications of Nuclear Power: Seawater Desalination, Hydrogen Production and Other Industrial Applications, Oarai (2007).
[293] FRÖHLING, W., et al., Safety concept and operational criteria of a nuclear process heat plant, Nuclear Engineering and Design **78** (1984) 167–177.
[294] DUFFEY, R.B., PIORO I.L., “Advanced high temperature concepts for pressure-tube reactors, including co-generation and sustainability”, Proc. 3rd Int. Top. Meeting on High Temperature Reactor Technology HTR2006, Johannesburg (2006) paper F00000167.
[295] ZHANG, Z.Y., et al., Current status and technical description of Chinese 2×250MW(th) HTR-PM demonstration plant, Nuclear Engineering and Design **239** (2009) 1212–1219.
[296] PRA, F., et al., Promising designs of compact heat exchangers for modular HTRs using the Brayton cycle, Nuclear Engineering and Design **238** (2008) 3160–3173.
[297] BERJON, A., et al., “Technological loops for high temperature heat exchangers”, Proc. 3rd Int. Top. Meeting on High Temperature Reactor Technology HTR2006, Johannesburg (2006) paper E00000027.
[298] SCHULTEN, R., et al., Industriekraftwerk mit Hochtemperaturreaktor PR 500 — “OTTO-Prinzip” zur Erzeugung von Prozessdampf, Report Jül-941-RG, Jülich (1973).
[299] DULERA, I.V., SINHA, R.K., “The Indian high temperature reactor programme” (Proc. IAEA Int. Conf. on Non-Electric Applications of Nuclear Power: Seawater Desalination, Hydrogen Production and Other Industrial Applications, Oarai, 2007), Proceedings Series IAEA-CN-152, IAEA, Vienna (2009) 85–93.
[300] DULERA, I.V., SINHA, R.K., High temperature reactors, Journal of Nuclear Materials **383** (2008) 183–188.
[301] TAKEDA, T., et al., “Deployment scenario of GTHTR300 cogeneration system”, Proc. Int. Conf. on Nuclear Energy Systems for Future Generation and Global Sustainability Global 2005, Tsukuba (2005) paper 325.
[302] OHASHI, H., SAKABA, N., NISHIHARA, T., TACHIBANA, Y., KUNITOMI, K., Analysis of tritium behavior in very high temperature gas-cooled reactor coupled with thermochemical iodine–sulfur process for hydrogen production, Journal of Nuclear Science and Technology **45** (2008) 1215–1227.
[303] TASHIMO, M., “FR-MR concept and its role on sustainable energy resource in 21st century”, Proc. COE-INES International Workshop on “Toward Hydrogen Economy, What Nuclear can Contribute and How”, Tokyo, 2004, THEN, Tokyo Institute of Technology (2005).
[304] SHIN, Y., et al., “An experiment on the methane–methanol–iodomethane cycle to produce nuclear hydrogen”, Proc. Int. Congress on Advances in Nuclear Power Plants ICAPP’06, Reno, NV (2006) paper 6102.
[305] PONOMAREV-STEPNOY, N., STOLYAREVSKIJ, A., KODOCHIGOV, N., “The concept of nuclear hydrogen production based on MHR-T reactor” (Proc. 4th Information Exchange Meeting on the Nuclear Production of Hydrogen, Oakbrook, IL, 2009) NEA Report No. 6805, OECD-NEA, Paris (2010) 67–75.
[306] MATZNER, D., KRIEL, W., CORREIA, M., GREYVENSTEIN, R., “Cycle configuration for a PBMR steam and electricity production plant”, Proc. Int. Congress on Advances in Nuclear Power Plants, Reno ICAPP’06, NV (2006) paper 131.
[307] KRIEL, W., “Status of PBMR process heat plant project”, Presentation at the IAEA Int. Conf. on Non-Electric Applications of Nuclear Power: Seawater Desalination, Hydrogen Production and Other Industrial Applications, Oarai (2007).
[308] RICHARDS, M., SHENOY, A., H2-MHR pre-conceptual design summary for hydrogen production, Nuclear Engineering and Technology **39** (2007) 1–8.
[309] RICHARDS, M.B., SHENOY, A., CAMPBELL, M., “Pre-conceptual hydrogen production modular helium reactor designs” (Proc. IAEA Int. Conf. on Non-Electric Applications of Nuclear Power: Seawater Desalination, Hydrogen Production and Other Industrial Applications, Oarai, 2007), Proceedings Series IAEA-CN-152, IAEA, Vienna (2009) 101–109.
[310] HERRING, J.S., et al., “Hydrogen production using high temperature electrolysis”, Presentation at the HTTR Workshop on Hydrogen Production Technology, Oarai (2004).
[311] FORSBERG, C.W., “Designing the advanced high temperature reactor for low radionuclide releases in beyond-design-basis accidents”, Proc. Int. Congress on Advances in Nuclear Power Plants ICAPP’08, Anaheim, CA (2008) paper 8025.
[312] WILLIAMS, D.F., CLARNO, K.T., “Salt selection for the LS-VHTR”, Proc. Int. Congress on Advances in Nuclear Power Plants ICAPP’06, Reno, NV (2006) paper 6160.
[313] INGERSOLL, D.T., FORSBERG, C.W., “Overview and status of the advanced high temperature reactor”, Proc. Int. Congress on Advances in Nuclear Power Plants ICAPP’06, Reno, NV (2006) paper 6264.
[314] BARDET P., et al., “Design, analysis and development of the modular PB-AHTR”, Proc. Int. Congress on Advances in Nuclear Power Plants ICAPP’08, Anaheim, CA (2008) paper 8211.
[315] OH, C.H., BARNER, R., DAVIS, C., Evaluation of working fluids in an indirect combined cycle in a very high temperature gas-cooled reactor, Nuclear Technology **156** (2006) 1–10.
[316] DUSHIN, Y.A., et al., Materials for high temperature equipment in the helium coolant of power plants, Nuclear hydrogen power and technology, Energoatomizdat (1983) Issue 5.
[317] KUGELER, K., KUGELER, M., NIESSEN, H.F., HAMMELMANN, K.H., Steam reformers heated by helium from high temperature reactors, Nuclear Engineering and Design **34** (1975) 129–145.

[318] JONES, A.R., BOX, P.O., “A very high temperature reactor (VHTR)” (Proc. Intersocietal Energy Conversion Engineering Conf., Newark, NY) Technology Record 1, USA (1975) 329–337.
[319] DEWSON, S.T., LI, X., “Selection criteria for the high temperature reactor intermediate heat exchanger”, Proc. Int. Congress on Advances in Nuclear Power Plants ICAPP’05, Seoul (2005) paper 5333.
[320] SOUTHALL, D., LE PIERRES, R., DEWSON, S.J., “Design considerations for compact heat exchangers”, Proc. Int. Congress on Advances in Nuclear Power Plants ICAPP’08, Anaheim, CA (2008) paper 8009.
[321] HEATRIC, (2006), http://www.heatric.com/compact_heat_exchangers.html
[322] SOUTHALL, D., “Innovative compact heat exchangers”, Proc. Int. Congress on Advances in Nuclear Power Plants ICAPP’10, San Diego, CA (2010) paper 10300.
[323] TOCHON, P., MAUGET, C., PRA, F., “The use of compact heat exchangers technologies for the HTRs recuperator application per proper design”, Proc. 2nd Int. Top. Meeting on High Temperature Reactor Technology HTR2004, Beijing (2004) paper E09.
[324] BUCKTHORPE, D., GENOT, J.-S., “RAPHAEL: Synthesis of achievements on materials and components and future direction”, Proc. 5th Int. Top. Meeting on High Temperature Reactor Technology HTR2010, Prague (2010) paper 029.
[325] INTERATOM, Nukleare Prozesswärmeanlagen mit Hochtemperaturreaktor-Modul zur Kohleveredlung, Technical Report ITB 78.10122.8, Kraftwerk Union AG, INTERATOM/GHT, Bergisch-Gladbach, Germany (1983).
[326] HARTH, R., JANSING, W., TEUBNER, H., Experience gained from the EVA II and KVK operation, Nuclear Engineering and Design **121** (1990) 173–182.
[327] DUMM, K., “Design requirements on HTR main components for process heat application” (Proc. IAEA Specialists’ Meeting on Heat Exchanging Components of Gas-Cooled Reactors, Düsseldorf) Report IWGGCR-9, IAEA, Vienna (1984) paper 2.
[328] CZIMCZIK, A., HIRSCHLE, G., “Development of a helium/helium intermediate heat exchanger with helical coil tube bundle” (Proc. IAEA Specialists’ Meeting on Heat Exchanging Components of Gas-Cooled Reactors, Düsseldorf) Report IWGGCR-9, IAEA, Vienna (1984) paper 5.
[329] EXNER, R., PODHORSKY, M., “Development, construction and analysis of the URKO intermediate heat exchanger” (Proc. IAEA Specialists’ Meeting on Heat Exchanging Components of Gas-Cooled Reactors, Düsseldorf) Report IWGGCR-9, IAEA, Vienna (1984) paper 8.
[330] PNP, Referenzkonzept der Prototypanlage Nukleare Prozesswärme PNP, Gesamtanlage und Kraftwerk, Bergbau-Forschung GmbH, GHT Gesellschaft für Hochtemperatur-Technik mbH, Hochtemperatur-Reaktorbau GmbH, Kernforschungsanlage Jülich GmbH, Rheinische Braunkohlenwerke AG, Germany (1981).
[331] SAITO, S., et al., Design of High Temperature Engineering Test Reactor (HTTR), Report JAERI 1332, Japan Atomic Energy Agency, Oarai (1994).
[332] GOLOVKO, V.F., KODOCHIGOV, G.N., Conceptual studies of heat transfer systems, Contribution to IAEA Coordination Research Programme (CRP-7) on Advances in Nuclear Power Process Heat Applications, Vienna (2009).
[333] MITENKOV, F.M., Designing of heat exchangers for nuclear power plants, Energoatomizdat (1988).
[334] RICHARDS M.B., et al., H2-MHR Pre-Conceptual Design Report: HTE-Based Plant, Final Technical Report for the the Period September 2002 through September 2005, Nuclear Energy Research Initiative Project 2002-196, Report GA-A25402, General Atomics, San Diego, CA (2006).
[335] RICHARDS, M.B., et al., “The H2-MHR: Nuclear hydrogen production using the Modular Helium Reactor”, Proc. Int. Congress on Advances in Nuclear Power Plants ICAPP’05, Seoul (2005) paper 5355.
[336] TALLACKSON, J.R., Thermal Radiation Transfer of Afterheat in MSBR Heat Exchangers, Report ORNL-TM-3145, Oak Ridge National Laboratory (1971).
[337] LIM, H.J., PETERSON, P.F., Conceptual Design of the Intermediate Heat Exchanger (IHX) for the PB-AHTR, Report UCBTH-09-005, University of California in Berkeley (2009).
[338] FORSBERG, C.W., “Molten-salt-reactor technology gaps”, Proc. Int. Congress on Advances in Nuclear Power Plants ICAPP’06, Reno, NV (2006) paper 6295.
[339] PIERA, M., MARTINEZ-VAL, J.M., MONTES M.J., Safety issues of nuclear production of hydrogen, Energy Conversion & Management **47** (2006) 2732–2739.
[340] TOIT, B. du, RAVENSWAAY, J. van, PLESSIS, G. du, “The impact of separation distance between reactor and process on the choice of secondary heat transport coolant for high temperature process heat applications”, Proc 3rd Int. Top. Meeting on High Temperature Reactor Technology HTR2006, Johannesburg (2006) paper I00000153.
[341] MARMIER, A., FÜTTERER, M.A., WIDER, H., “HTR with downgraded specifications for high temperature process heat applications”, Proc. Int. Congress on Advances in Nuclear Power Plants ICAPP’07, Nice (2007) paper 7058.
[342] FORSBERG, C.W., “Developments in molten salt and liquid-salt-cooled reactors”, Proc. Int. Congress on Advances in Nuclear Power Plants ICAPP’06, Reno, NV (2006) paper 6292.
[343] ZRODNIKOV, A.V., et al., Nuclear power plants based on reactor modules with SVBR-75/100, Atomic Energy **91** (2001) 957–966.
[344] MURTY, K.L. CHARIT, I., Structural materials for Gen-IV nuclear reactors: Challenges and opportunities, Journal of Nuclear Materials **383** (2008) 189–195.
[345] SAMARAS, M., et al., “Materials modeling — A key for the design of advanced high temperature reactor components”, Proc. Int. Congress on Advances in Nuclear Power Plants ICAPP’07, Nice (2007) paper 7207.

[346] BREITBACH, G., “Overview on high temperature metal development in Germany” (Proc. Soviet/German Seminar on Extraction and Utilization of High Temperature Heat from HTR, Jülich) Internal Report HTA-IB-07/90, Research Center Jülich (1990) 59–70.
[347] SAVOLAINEN, K., MONONEN, J., ILOLA, R., HÄNNINEN, H., Materials Selection for High Temperature Applications, Report TKK-MTR-4/05, Helsinki University of Technology, Espoo, Finland (2005).
[348] CABET, C., DUPREY, B., “Long term high temperature oxidation of alloys for intermediate heat exchangers”, Proc. Int. Congress on Advances in Nuclear Power Plants, San Diego ICAPP’10, CA (2010) paper 10316.
[349] MENKEN, G., et al., “Review of the gas/metal interactions in HTR helium up to 950°C”, Proc. BNES Conf. Gas Cooled Reactors Today, Bristol (1982).
[350] CABET, C., TERLAIN, A., LETT, P., GUETAZ, L., GENTZBITTEL, J.-M., High temperature corrosion of structural materials under gas-cooled reactor helium, Materials and Corrosion **57**(2) (2006) 147–153.
[351] QUADAKKERS, W.J., SCHUSTER, H., Corrosion of high temperature alloys in the primary circuit of high temperature gas cooled reactors, Part 1: Theoretical background, Materials and Corrosion **36** (1985) 141–150, Part 2: Experimental results, Materials and Corrosion **36** (1985) 335–347.
[352] NICKEL, H., SCHUBERT, F., SCHUSTER, H., Evaluation of alloys for advanced high temperature reactor systems, Nuclear Engineering and Design **78** (1984) 251–265.
[353] PENKALLA, H.J., “Material data and constitutive equations” (Proc. Workshop on Structural Design Criteria for HTR, Jülich) Report Jül-Conf-71, Research Center Jülich (1989) 185–205.
[354] HADA, K., NISHIGUCHI, I., MUTO, Y., TSUJI, H., Developments of metallic materials and a high temperature structural design code for the HTTR, Nuclear Engineering and Design **132** (1991) 1–11.
[355] KURATA, Y., OGAWA, Y., Internal stress during high temperature creep of special grade Hastelloy X alloys, Journal of Nuclear Materials **158** (1988) 42–48.
[356] HAYNER, G.O., BRATTON, R.L., MIZIA, R.E., WINDES, W.E., Next Generation Nuclear Plant Materials Research and Development Programme Plan, Report INL/EXT-06-11701, Revision 3, Idaho National Laboratory, ID (2006).
[357] REN, W., SWINDEMAN, R.W., SANTELLA, M.L., “Developing a nuclear grade of Alloy 617 for Gen IV nuclear energy systems”, Proc. Int. Congress on Advances in Nuclear Power Plants ICAPP’10, San Diego, CA (2010) paper 10068.
[358] MO, K., LOVICU, G., TUNG, H.-M., CHEN, X., STUBBINS, J.F., “High temperature aging and corrosion study on Alloy 617 and Alloy 230”, Proc. 18th Int. Conf. on Nuclear Engineering ICONE-18, Xi'an (2010) paper 30207.
[359] CERRI, G., et al., Sulfur–iodine plant for large scale hydrogen production by nuclear nower, International Journal of Hydrogen Energy **35**(9) (2010) 4002–4014.
[360] VAN HEEK, K.H., JÜNTGEN, H., “Progress in the design of a technical scale gas generator for steam gasification of coal using nuclear heat”, Proc. Int. Symp. on Gas-Cooled Reactors with Emphasis on Advanced Systems, Jülich (1975) paper IAEA-SM-200/5.
[361] KUBO, S., et al., “Corrosion test on structural materials for iodine–sulphur thermo–chemical water splitting cycle”, Presentation at the AIChE Spring National Meeting, New Orleans, LA (2003).
[362] WONG, B., et al., Construction materials development in sulfur–iodine thermochemical water-splitting process for hydrogen production, International Journal of Hydrogen Energy **32** (2007) 497–504.
[363] SHERMAN, S.R., Nuclear Reactor/Hydrogen Process Interface Including the HyPEP Model, DOE H2 Merit Review, Report INL/CON-07-12488, Idaho National Laboratory, ID (2007).
[364] SCHULTEN, R., KUGELER, K., PHLIPPEN, P.-W., Zur technischen Gestaltung von passiv sicheren Hochtemperaturreaktoren, Report Jül-2352, Research Center Jülich (1990).
[365] FORSBERG, C.W., GORENSEK, M., HERRING, S., PICKARD, P., “Safety related physical phenomena for coupled high temperature reactors and hydrogen production facilities”, Proc. 4th Int. Top. Meeting on High temperature Reactors HTR2008, Washington D.C. (2008) paper 58223.
[366] BONGARTZ, R., et al., Probabilistische Zuverlässigkeits- und Risikountersuchung der Photovoltaik-Wasserstoff-Brennstoffzellen-Demonstrationsanlage PHOEBUS Jülich, Report Jül-3176, Research Center Jülich (1996).
[367] ZHANG, Y.P., LU, L.X., NATERER, G.F., “Reliability and safety assessment of a conceptual thermochemical plant for nuclear-based hydrogen generation”, Proc. 16th Int. Conf. on Nuclear Engineering ICONE-16, Orlando, FL (2008) paper 48265.
[368] RÖLLIG, K., “Tritium — Bilanz im HTR” (Proc. Conf. on “Chemie des Hochtemperaturreaktors”, Jülich) Report Jül-Conf-43, Research Center Jülich (1981) 95–106.
[369] CORDEWINER, H.J., Numerische Berechnung des Tritium-Verhaltens von Kugelhaufenreaktoren am Beispiel des AVR-Reaktors, Report Jül-1607, Research Center Jülich (1979).
[370] MOIR, R.W., et al., Helium-Cooled Molten-Salt Fusion Breeder, Report UCID-20153, Lawrence Livermore National Laboratory (1984).
[371] STEINWARZ, W., Tritium in HTR-Anlagen, Report Jül-2138, Research Center Jülich (1987).
[372] SERPEKIAN, T., Untersuchungen an HTR-Wärmetauschermaterialien, Report Jül-1111-RG, Research Center Jülich (1974).
[373] RÖHRIG, H.D., “Überblick über die Arbeiten im IRE zur H- unnd T-Permeation und zum Tritiumverhalten in HTRs” In: BUCHKREMER, H.P. (Ed.), Überblick über die neueren Arbeiten auf dem Gebiet des Wasserstoff- und Tritiumverhaltens in Hochtemperaturreaktoren, Report Jül-1497, Research Center Jülich (1978) 5–33.
[374] RÖHRIG, H.D., et al., Neuere Ergebnisse aus der Anlage zur Untersuchung des Wasserstoffdurchtritts an Reformermaterialien (AUWARM), Atomwirtschaft **23** (1978) 339–341.

[375] HISHIDA, M., DIEHL, W., RÖHRIG, H.D., “New experimental results from the test facility "AUWARM" ” In: BUCHKREMER, H.P. (Ed.), Überblick über die neueren Arbeiten auf dem Gebiet des Wasserstoff- und Tritiumverhaltens in Hochtemperaturreaktoren, Report Jül-1497, Research Center Jülich (1978) 45–60.
[376] GAINEY, B.W., A Review of Tritium Behavior in HTGR Systems, Report GA-A13461, General Atomics, San Diego, CA (1976).
[377] KIRCH, N., SCHEIDLER, G., Stand der F+E-Arbeiten zum Tritiumpfad einer nuklearen Prozeßwärmeanlage und Bewertung im Hinblick auf eine mögliche Anhebung der Freigrenze, Internal Report KFA-HTA-IB-3/85, Research Center Jülich (1985).
[378] RÖHRIG, H.D., et al., Studies on the permeation of hydrogen and tritium in nuclear process heat installations, Nuclear Engineering and Design **34** (1975) 157–167.
[379] ESSER, H.G., Nachweis der Wasserstoffisotope H und T in verschiedenen Phasen und Konzentrationen an einer Versuchsanlage zur Untersuchung der Tritium- und Wasserstoffpermeation durch Wärmetauschermaterialien unter betriebsnahen Bedingungen (Modellversuche zu H- und T-Diffusionen), Internal Report KFA-IRE-IB-23/79, Research Center Jülich (1979).
[380] STEINWARZ, W., RÖHRIG, H.D., NIEDER, R., “Tritium behaviour in an HTR-system based on AVR-experience“ (Proc. IAEA Specialists Meeting on Coolant Chemistry, Plate-Out and Decontamination in Gas-Cooled Reactors, Jülich, 1980) Summary Report IAEA-IWGGCR/2, IAEA, Vienna (1981) 153–160.
[381] VEY, K., RESCH, G., Erste Erfahrungen mit dem Betrieb des THTR-300 aus der Sicht der Kraftwerk-Chemie, VGB Kraftwerkstechnik (1988) Issue 7 (July).
[382] EICHLER, R. Reinigung inerter Gaskreisläufe nuklearer Energieerzeugungsanlagen von Tritium und Wasserstoff, Report Jül-2008, Research Center Jülich (1985).
[383] BMU, Verordnung über den Schutz vor Schäden durch ionisierende Strahlen (Strahlenschutzverordnung – StrlSchV) in der Fassung vom 30. Juni 1989 (BGBl. I S. 1321, zuletzt geändert 1997), Bonn (1989).
[384] BMJ, Verordnung über den Schutz vor Schäden durch ionisierende Strahlen (Strahlenschutzverordnung — StrlSchV), Version of July 20, 2001, with latest changes made on August 29, 2008, Berlin (2001).
[385] INAGAKI Y., et al., Research and development on system integration technology for connection of hydrogen production system to an HTGR, Nuclear Technology **157** (2007) 111–119.
[386] VERFONDERN, K., NISHIHARA, T., Valuation of the Safety Concept of the Combined Nuclear/Chemical Complex for Hydrogen Production with HTTR, Report Jül-4135, Research Center Jülich (2004).
[387] TAKEDA, T., et al., “Study on tritium/hydrogen permeation in the HTTR hydrogen production system”, Proc. 7th Int. Conf. on Nuclear Engineering ICONE-7, Tokyo (1999).
[388] TAKEDA, T., IWATSUKI, J., Counter-permeation of deuterium and hydrogen through Inconel 600, Nuclear Technology **146** (2004) 83–95.
[389] SAKABA, N., et al., “Evaluation of permeated hydrogen through heat transfer pipes of the intermediate heat exchanger during the initial 950°C operation of the HTTR”, Proc. Int. Congress on Advances in Nuclear Power Plants ICAPP’05, Seoul (2005) paper 5159.
[390] BUCHKREMER, H.P., Entwicklung und Erprobung einer Anlage zur Untersuchung der Permeation von Wasserstoffisotopen unter nuklearen Prozessbedingungen, Report Jül-1806, Research Center Jülich (1982).
[391] RICHARDS, M., “Utilization of the JAEA HTTR to support the NGNP project”, Proc. 5th Int. Top. Meeting on High Temperature Reactor Technology HTR2010, Prague (2010) paper 039.
[392] PARK, J.H., PARK, I.K., LEE, W.J., Prediction of the tritium behavior in very high temperature gas cooled reactor using TRITGO, Bangsason Bango Hakhoe Chi (Journal of the Korean Association for Radiation Protection) **33** (2008) 113–120.
[393] RUSSIAN FEDERATION, NRB-99, Ionizing radiation, radiation safety, Norms of radiation safety, In: SP - 2.6.1., Minzdrav, Moscow (1999) 58–99.
[394] RUSSIAN FEDERATION, Sanitary rules for design and operation of nuclear plants, SANPIN 2.6.1.24-03, Moscow (2003).
[395] WICHNER, R.P., DYER, F.F., Distribution and Transport of Tritium in the Peach Bottom HTGR, Report ORNL-5497, Oak Ridge National Laboratory (1979).
[396] BURNETTE, R.D., BALDWIN, N.L., “Primary coolant chemistry of the Peach Bottom and Fort St. Vrain high temperature gas-cooled reactors” (Proc. IAEA Specialists Meeting on Coolant Chemistry, Plate-Out and Decontamination in Gas-Cooled Reactors, Jülich, 1980) Summary Report IAEA-IWGGCR/2, International Atomic Energy Agency, Vienna (1981) 132–137.
[397] CALDERONI, P., EBNER, M., PAWELKO, R., “High temperature hydrogen permeation in nickel alloys”, Proc. 5th Int. Top. Meeting on High Temperature Reactor Technology HTR2010, Prague (2010) paper 131.
[398] COMPERE, E.L., FREID, S.H., NESTOR, C.W., Distribution and Release of Tritium in High temperature Gas-Cooled Reactors as a Function of Design, Operational and Material Parameters, Report ORNL-TM-4303, Oak Ridge National Laboratory, TN (1974).
[399] GENERAL ATOMICS, Fuel Design Data Manual, Document 901866, Issue F, General Atomics, San Diego, CA (1987).
[400] MARTIN, R.C., Compilation of Fuel Performance and Fission Product Transport Models and Database for MHTGR Design, Report ORNL/NPR-91/6, Oak Ridge National Labortaory, TN (1993).
[401] OHASHI, H., SHERMAN, S.R., Tritium Movement and Accumulation in the NGNP System Interface and Hydrogen Plant, Report INL/EXT-07-12746, Idaho National Laboratory, ID (2007).

[402] KIM, E.S., OH, C.H., PATTERSON, M., “Development of tritium permeation analysis code and tritium transport in a high temperature gas-cooled reactor coupled with hydrogen production system”, Proc. Int. Congress on Advances in Nuclear Power Plants ICAPP’10, San Diego, CA (2010) paper 10207.
[403] INGERSOLL, D.T., et al., Status of Preconceptual Design of the Advanced High temperature Reactor (AHTR), Report ORNL/TM-2004/104, Oak Ridge National Laboratory, TN (2004).
[404] TNO, Green book: Methods for the Determination of Possible Damage to People and Objects Resulting from Releases of Hazardous Materials, Report CPR 16E, Voorburg, The Netherlands (1992).
[405] LIND, C.D., What causes unconfined vapor cloud explosions, Loss Prevention **9** (1975) 101–105.
[406] VAN WINGERDEN, K., Detonations in Pipes and in the Open, CMR Internal Report, Christian Michelsen Research, Bergen, Norway (1999).
[407] TIESZEN, S.R., Effect of initial conditions on combustion generated loads, Nuclear Engineering and Design **140** (1993) 81–94.
[408] TANG, M.J., BAKER, Q.A., A new set of blast curves from vapor cloud explosion, Process Safety Progress **18**(3) (1999) 235–240.
[409] CENTER FOR CHEMICAL PROCESS SAFETY, Guidelines for Evaluating the Characteristics of Vapour Cloud Explosions, Flash Fires and BLEVE’s, CCPS, American Institute of Chemical Engineers, New York (1994).
[410] MERCX, W.P.M., WEERHEIJM, J., VERHAGEN, T.L.A., Some Considerations on the Damage Criteria and Safety Distances for Industrial Explosions, HAZARDS XI — New Directions in Process Safety, UMIST, Manchester (1991).
[411] MERCX, W.P.M., Developments in vapour cloud explosion blast modeling, Journal of Hazardous Materials **71** (2000) 301–319.
[412] VAN DEN BERG, A.C., EGGEN, J.B.M., “GAME — Guidance for the application of the Multi-Energy method”, Proc. 2nd Int. Specialist Meeting on Fuel Air Explosions, Bergen (1996).
[413] VAN DEN BERG, A.C., VERSLOOT, N.H.A., The Multi-Energy critical separation distance, Journal of Loss Prevention in the Process Industries **16** (2003) 111–120.
[414] BREITUNG, W., REDLINGER, R., Containment pressure loads from hydrogen combustion in unmitigated severe accidents, Nuclear Technology **111** (1995) 395–419.
[415] FEDERAL EMERGENCY MANAGEMENT AGENCY, “Explosive blast” Chapter 4 in: Reference Manual to Mitigate Potential Terrorist Attacks against Buildings, Report FEMA426, FEMA, Washington D.C. (2003).
[416] GIESBRECHT, H., Evaluation of vapour cloud explosions by damage analysis, Journal of Hazardous Materials **17** (1988) 247–257.
[417] LI, Q.M., MENG, H., Pressure-impulse diagram for blast loads based on dimensional analysis and single-degree-of-freedom model. Journal of Engineering Mechanics **128** (2002) 87–92.
[418] PFÖRTNER, H., “Gas cloud explosions and resulting blast effects”, Proc. Int. Sem. on Extreme Load Conditions and Limit Analysis Procedures for Structural Reactor Safeguards and Containment Structures, Berlin (1975).
[419] KUMAR, R.K., et al., Carbon Monoxide–Hydrogen Combustion Characteristics in Severe Accident Containment Conditions, Final report NEA/CSNI/R(2000)10, OECD-Nuclear Energy Agency, Paris (2000).
[420] ILBAS, M., CRAYFORD, A.P., YILMAZ, I., BOWEN, P.J., SYRED, N., Laminar-burning velocities of hydrogen–air and hydrogen–methane–air mixtures: an experimental study, International Journal of Hydrogen Energy **31** (2006) 1768–1779.
[421] SINGH, Y., “Safety aspects of HTR-Module for process heat under considerations of burnable gases”, Proc. Soviet/German Seminar on Extraction and Utilization of High Temperature Heat from HTR, Jülich, Research Center Jülich (1990) 265–278.
[422] VERFONDERN, K., MOORMANN, R., BREITUNG, W., VESER, A., “Contributions to a safety analysis for a hydrogen production system with HTGR”, Proc. OECD/NEA 1st Information Exchange Meeting on Nuclear Hydrogen Production, Paris (2000).
[423] SATO, H., OHASHI, H., TAZAWA, Y., SAKABA, N., TACHIBANA, Y., “Safety evaluation of the HTTR-IS nuclear hydrogen production system”, Proc. 18th Int. Conf. on Nuclear Engineering ICONE-18, Xi'an (2010) paper 29108.
[424] MARANGON, A., et al., Safety distances: definition and values, International Journal of Hydrogen Energy **32** (2007) 2192–2197.
[425] SOCHET, I., VIOSSAT, A.-L., ROUYER, J.-L., HEMMERICH, P., “Safe hydrogen generation by nuclear HTR”, Proc. Int. Congress on Advances in Nuclear Power Plants ICAPP’04, Pittsburgh, PA (2004) paper 4261.
[426] SCHNEIDER, H., PFÖRTNER, H., Flammen- und Druckwellenausbreitung bei der Deflagration von Wasserstoff/Luft-Gemischen, Technical Note, Institute for the Chemistry of Fuels and Explosives of the Fraunhofer Gesellschaft, Pfinztal, Germany (1978).
[427] PFÖRTNER, H., et al., “Flame acceleration and pressure build up in free and partially confined hydrogen air clouds”, Proc. 9th Int. Coll. on the Dynamics of Explosions and Reactive Systems ICDERS, Poitiers (1983).
[428] PFÖRTNER, H., SCHNEIDER, H., Ballonversuche zur Untersuchung der Deflagration von Wasserstoff Luft Gemischen (Abschlussbericht), PNP-Sicherheitssofortprogrammem: “Prozessgasfreisetzung — Explosion in der Gasfabrik und Auswirkungen von Druckwellen auf das Containment”, Internal Report, Fraunhofer Institut für Chemische Technologie, Pfinztal, Germany (1983).
[429] PFÖRTNER, H., The effects of gas explosions in free and partially confined fuel/air mixtures, Propellants, Explosives, Pyrotechnics **10** (1985) 151–155.

[430] SCHNEIDER, H., PFÖRTNER, H., Explosion von Wasserstoff Luft Gemischen unter teilverdämmten Bedingungen und unter dem Einfluss einer turbulenten Strömung. PNP-Sicherheitssofortprogrammem: "Prozessgasfreisetzung — Explosion in der Gasfabrik und Auswirkungen von Druckwellen auf das Containment", Internal Report, Fraunhofer Institut für Chemische Technologie, Pfinztal, Germany (1984).
[431] SCHNEIDER, H., PFÖRTNER, H., Versuche zur Freistrahlzündung partiell verdämmter Wasserstoff Luft Gemische im Hinblick auf die Skalierbarkeit des Übergangs Deflagration Detonation, Final Report for Firma Interatom, Bergisch-Gladbach, Internal Report, Fraunhofer Institut für Chemische Technologie, Pfinztal, Germany (1984).
[432] SCHNEIDER, H., "Large scale experiments: deflagration and deflagration to detonation transition within a partial confinement similar to a lane", Proc. 1st Int. Conf. on Hydrogen Safety ICHS, Pisa (2005).
[433] BERMAN, M., A critical review of recent large scale experiments on hydrogen–air detonations, Nuclear Science and Technology **93** (2005) 321–347.
[434] MERCX, W.P.M., Extended Modelling and Experimental Research into Gas Explosions, Final Summary Report of the Project EMERGE, CEC Contract EV5VCT930274, European Commission, Directorate General XII., Brussels (1997).
[435] BMI, Bundesministerium des Innern, Bekanntmachung der Richtlinie für den Schutz von Kernkraftwerken gegen Druckwellen aus chemischen Reaktionen durch Auslegung der Kernkraftwerke hinsichtlich ihrer Festigkeit und induzierter Schwingungen sowie durch Sicherheitsabstände. Bonn, Germany, September 13 (1976).
[436] KUGELER, K., TRAGSDORF, I.M., PÖPPE, N., "Technical and Safety Aspects of Processes of Hydrogen Production using Nuclear Energy", Proc. Int. Congress on Advances in Nuclear Power Plants ICAPP'05, Seoul (2005) paper 5729.
[437] INABA, Y., NISHIHARA, T., NITTA, Y., Analytical study on fire and explosion accidents assumed in HTGR hydrogen production system, Nuclear Technology **146** (2004) 49–56.
[438] NISHIHARA, T., KUNITOMI, K., MURAKAMI, T., "Study on the separation distance in the HTGR hydrogen production system (GTHTR300C)", Proc. 3rd Int. Top. Meeting on High Temperature Reactor Technology HTR2006, Johannesburg (2006) paper I00000126.
[439] MURAKAMI, T., TERADA, A., NISHIHARA, T., INAGAKI, Y., KUNITOMI K., Analysis on characteristic of hydrogen gas dispersion and evaluation method of blast overpressure in VHTR hydrogen production system,Nihon Genshiryoku Gakkai Wabun Ronbun Shi = Transactions of the Atomic Energy Society of Japan **5**(4) (2006) 316–324. [in Japanese]
[440] KOMORI M., et al., "Safety study of hydrogen supply stations for the review of high pressure gas safety law in Japan", Proc. 1st Int. Conf. on Hydrogen Safety ICHS, Pisa (2005) paper 400081.
[441] WE-NET, Summary Report on FY 2002, Tokyo (2003).
[442] INSTITUTE OF APPLIED ENERGY, SRI INTERNATIONAL, MITSUBISHI HEAVY INDUSTRIES, "Experiments on hydrogen deflagration" (Presentation at the Research Center Karlsruhe) IAE, Tokyo (2005).
[443] RUSSIAN FEDERATION, Factoring External Natural and Man-Caused Impacts on Nuclear and Radiation Hazardous Facilities, Regulatory document NP-064-05, "Rostechnadzor" (2005).
[444] RUSSIAN FEDERATION, Rules of Design & Development of Capital Construction Projects for Nuclear Plants with Reactors of Different Types, Regulatory Document PiN AE-5.6 (1986).
[445] RUSSIAN FEDERATION, General Requirements for Explosion-Proof Conditions in the Chemical, Petrochemical and Petroleum Refining Industries, Regulatory Document PB 09-540-03 (2003).
[446] RUSSIAN FEDERATION, Safety Rules to be Observed in Production of Hydrogen by Water Electrolysis, Regulatory Document PB 03-598-03 (2003).
[447] U.S. NUCLEAR REGULATORY COMMISSION, Evaluations of Explosions Postulated to Occur on Transportation Routes Near Nuclear Power Plants, NRC Regulatory Guide 1.91, Revision 1, NRC, Washington, DC (1978).
[448] NUCLEAR NEWS, Argonne's David Wade: On the development of small modular reactors, Nuclear News (2004) August 25–28.
[449] SMITH, C., BECK, S., GALYEAN, W., "Separation requirements for a hydrogen production plant and high temperature nuclear reactor", Proc. Int. Congress on Advances in Nuclear Power Plants ICAPP'06, Reno, NV (2006) paper 6062.
[450] EDESKUTY, F.J., Critical Review and Assessment of Problems in Hydrogen Energy Delivery Systems, Report LA-7405-PR, Los Alamos Scientific Laboratory (1978).
[451] CASSUT, L.H., et al., A study of the hazards in the storage and handling of liquid hydrogen, Advances in Cryogenic Engineering **5** (1960) 55–61.
[452] BREWER, G.D., et al., Assessment of Crash Fire Hazard of LH_2-Fueled Aircraft, Final Report NASA-CR-165525, NASA Lewis Research Center (1981).
[453] URANO, Y., et al., Hazards of burning liquefied hydrogen, Part 1: Flame of stable burning, Part 2: Flame of abnormal burning, National Chemical Laboratory for Industry **81** (1986) 143–157. [In Japanese].
[454] OHASHI, H., et al., "Current status of research and development on system integration technology for connection between HTGR and hydrogen production system at JAEA", Proc. OECD/NEA 3rd Information Exchange Meeting on the Nuclear Production of Hydrogen, Oarai (2005).
[455] SAKABA, N., SATO, H., OHASHI, H., NISHIHARA, T., KUNITOMI, K., "Conceptual system design of non-nuclear grade IS process to be coupled with the HTTR" (Proc. IAEA Int. Conf. on Non-Electric Applications of Nuclear Power: Seawater Desalination, Hydrogen Production and Other Industrial Applications, Oarai, 2007), Proceedings Series IAEA-CN-152, International Atomic Energy Agency, Vienna (2009) 121–129.

[456] CHAN, S.T., Numerical simulations of LNG vapor dispersion from a fenced storage area, Journal of Hazardous Materials **30** (1992) 195–224.
[457] INTERNATIONAL ATOMIC ENERGY AGENCY, External Man-Induced Events in Relation to Nuclear Power Plant Siting, A Safety Guide, Safety Series No. 50-SG-S5, IAEA, Vienna (1981).
[458] INTERNATIONAL ATOMIC ENERGY AGENCY, External Man-Induced Events in Relation to Nuclear Power Plant Design, A Safety Guide, Safety Series No. 50-SG-D5, Revision 1, IAEA, Vienna (1996).
[459] EUROPEAN UNION, Richtlinie 82/501/EWG des Rates vom 24. Juni 1982 über die Gefahren schwerer Unfälle bei bestimmten Industrietätigkeiten (1982),
http://www.umwelt-online.de/regelwerk/eu/ 80_84/82_501a.htm
[460] EUROPEAN UNION, Seveso II Directive (96/082/EEC), (1996), http:/www.bickgreen.co.uk /risk/seveso2/ seveso2.htm (English) or Richtlinie 96/82/EG des Rates vom 9. Dezember 1996 zur Beherrschung der Gefahren beischweren Unfällen mit gefährlichen Stoffen (1996),
http://www.umwelt-online.de/regelwerk/eu/95_99/96_82a.htm
[461] EUROPEAN UNION, Directive 94/9/EC on "Equipment and Protective Systems Intended for Use in Potentially Explosive Atmospheres" ("ATEX 100a"), (1994),
http://europa.eu.int/comm/ enterprise/atex/direct/ text94-9.htm
[462] EUROPEAN UNION, Directive on "Minimum Requirements for Improving the Safety and Health Protection of Workers Potentially at Risk from Explosive Atmospheres" ("ATEX 118a"), (1999),
http://europa.eu.int/eur-lex/en/lif/dat/1999/ en_399L0092.html
[463] MAISONNIER, G., PERRIN, J., STEINBERGER-WILCKENS, R., TRÜMPER, S.C., European Hydrogen Infrastructure Atlas and Industrial Excess Hydrogen Analysis, Part II: Industrial Surplus Hydrogen and Markets and Production, Report R2H2006PU.1 of the European Integrated Project ROAD2HYCOM (2007).
[464] HIS, S., Hydrogen: An Energy Vector for the Future? Panorama 2004, IFP, Rueil-Malmaison, France (2004).
[465] WOLF, J., Die neuen Entwicklungen der Technik — Elemente der Wasserstoff-Infrastruktur von der Herstellung bis zum Tank, Medienforum Deutscher Wasserstoff-Tag, München (2003).
[466] SRI INTERNATIONAL, Liquid Hydrogen Production and Commercial Demand in the United States, SRI Project 8562, Final report, SRI International, Menlo Park, CA (1990),
http://ntrs.nasa.gov/archive/ nasa/casi.ntrs.nasa.gov/ 19910006853_1991006853.pdf
[467] SLOOP, J.L., Liquid Hydrogen as a Propulsion Fuel — 1945–1959. NASA History Office, Report NASA SP-4404, National Aeronautics and Space Administration, Washington D.C. (1978).
[468] NASA, NASA facts. FS-2001-09-015-KSC, Revised Version, Kennedy Space Center (2006).
[469] VERFONDERN, K., Safety Considerations on Liquid Hydrogen, Schriften des Forschungszentrums Jülich, Reihe Energie & Umwelt, Vol 10, Jülich (2008).
[470] INTERNATIONAL ENERGY AGENCY, Transport, Energy and CO_2, Moving towards Sustainability, IEA, Paris (2009).
[471] RUER, J., "End user requirements for nuclear process heat applications", Presentation at the Post FISA Workshop, Prague (2009).
[472] REIMERT, R., SCHAD, M., "Process heat from modularized HTR", Proc. 5th Int. Top. Meeting on High Temperature Reactor Technology HTR2010, Prague (2010) paper 186.
[473] SCHAD, M., DIDAS, U., EBELING, F., KREUZKAMP, G., RENNER, H., Project Study on Utilization of Process Heat from the HTGR in the Chemical and Related Industries, Report Lurgi GmbH, Frankfurt (1988).
[474] WORLD STEEL ASSOCIATION, Steel and Energy, Fact Sheet, WSA, Brussels (2008).
[475] YAN, X.L., HINO, R., Nuclear Hydrogen Production Handbook, CRC Press, Taylor & Francis Group, Boca Raton, FL (2011).
[476] FORSBERG, C.W., Future hydrogen markets for large scale hydrogen production systems, International Journal of Hydrogen Energy **32** (2007) 431–439.
[477] DEPARTMENT OF TRADE AND INDUSTRY, Coal Liquefaction, Technology Status Report DTIPub URN 99/1120, DTI, London (1999).
[478] VAN NIEKERK, W., "Status and future planning of the South Africa's nuclear hydrogen production programme", Proc. 3rd Nuclear Hydrogen Workshop, Jeju, Korea Atomic Energy Research Institute (2009).
[479] HARTWELL, B., ISMAIL, N., KIM, D.G., MA, J.H., Design for a Coal IGCC Plant for the Co-Production of Electricity and H_2 in Pittsburgh, PA, Report Penn State EGEE 580 Spring 2008, PA (2009).
[480] PENFIELD, S.R., BOLTHRUNIS, C.O., "Put a coalatom in your tank: The compelling case for a marriage of coal and nuclear energy", Proc. 14th Int. Conf. on Nuclear Engineering ICONE-14, Miami, FL (2006) paper 89605.
[481] FORSBERG, C.W., Assessment of Nuclear-Hydrogen Synergies with Renewable Energy Systems and Coal Liquefaction Processes, Report ORNL/TM-2006/114, Oak Ridge National Laboratory, TN (2006).
[482] BRUSSTAR, M., "Sustainable technology choices for alternative fuels" (Int. Symp. on Alcohol Fuels, San Diego, CA) ISAF XV, USA (2005).
[483] AUSFELDER, F., BAZZANELLA, A., Verwertung und Speicherung von CO_2, Discussion paper on DECHEMA (2008),
www.dechema.de/dechema_media/diskussion co2.pdf
[484] MIDDHA, P., ENGEL, D., HANSEN, O.R., "Can the addition of hydrogen to natural gas reduce the explosion risk?", Proc. 3rd Int. Conf. on Hydrogen Safety ICHS, Ajaccio (2009) paper ID114.

[485] RAUKAS, A., PUNNING, J.-M., Environmental problems in the Estonian oil shale industry, Energy & Environmental Science **2** (2009) 723–728.
[486] JONES, S., SAGD delivers healthy return on investment, Ziff Energy Group (2009).
[487] STEELE, B., HEINZEL, A., Materials for fuel cell technologies. Nature **414** (2001) 345–352.
[488] NÖLSCHER, C., Brennstoffzellen — Energiequelle für das 21. Jahrhundert? Physik in unserer Zeit **27** (1996) 52–59.
[489] FORSBERG, C.W., KAZIMI, M.S., Nuclear Hydrogen Using High temperature Electrolysis and Light-Water Reactors for Peak Electricity Production, Report MIT-NES-TR-010, Massachusetts Institute of Technology, Cambridge, MA (2009).
[490] LOKURLU, A., HÖHLEIN, B., GRUBE, T., RIENSCHE, E., "Fuel cells for stationary and mobile applications — Economic analyses and challenges", Proc. Int. Hydrogen Energy Congress and Exhibition IHEC, Istanbul (2005).
[491] NABIELEK, H., STEINBERGER-WILCKENS, R., "Fuel cell research in Europe", Proc. 1st Polish Forum Fuel Cells and Hydrogen Technologies, Zakopane (2007).
[492] MEISSNER, D., "Grundlagen der Brennstoffzelle", In: HAKE, J.-F., et al. (Ed.), (Proc. 2. Ferienkurs Energieforschung, Jülich) Konferenzen des Forschungs-zentrums Jülich, Vol. 20, Part I, Research Center Jülich (1996) 177–196.
[493] STEINBERGER-WILCKENS, R., "Overview of solid oxide fuel cell development at FZJ", Presentation at the 216th Meeting of the Electrochemical Society (ECS), Vienna (2009).
[494] HAUG, M., NEEF, H.-J., "Market introduction for hydrogen and fuel cell technologies", In: STOLTEN, D. (Ed.), Hydrogen and Fuel Cells — Fundamentals, Technologies and Applications, Wiley-VCH, Weinheim, Germany (2010) 577–596.
[495] UNITED STATES DEPARTMENT OF ENERGY, On-Board Fuel Processing Go/No Go Decision, DOE Decision Team Committee Report, USDOE, Washington DC (2004).
[496] WETZEL, F.-J., "Die keramische Brennstoffzelle als Energiewandler für die Stromerzeugung im Auto", In: Themen 2004, Wasserstoff und Brennstoffzellen — Energieforschung im Verbund, FVS Report, ForschungsVerbund Sonnenenergie, Germany (2004) 118–123.
[497] VOGLER, F., WÜRSIG, G., "Safety considerations and approval procedures for the integration of fuel cells on board of ships", Proc. 3rd Int. Conf. on Hydrogen Safety ICHS, Ajaccio (2009) paper ID 007.
[498] RYE, L., BLAKEY, S., WILSON, C.W., Sustainability of supply or the planet: A review of potential drop-in alternative aviation fuels, Energy & Environmental Science **3** (2010) 17–27.
[499] PETERS, R., "APUs for road vehicles, ships and airplanes", Proc. 18th World Hydrogen Energy Conf. WHEC'18, Essen (2010).
[500] DASA, CRYOPLANE — Deutsch-Russisches Gemeinschaftsprojekt zum Einsatz kryogener Treibstoffe in der zivilen Luftfahrt — Realisierbarkeitsstudie 1990/91/92, Feasibility study, Deutsche Aerospace Airbus GmbH, Hamburg (1992).
[501] POHL, H.-W., WILDNER, D., "Hydrogen demonstrator aircraft", Proc. 11th World Hydrogen Energy Conf. WHEC'11, Stuttgart (1996) 1779–1786.
[502] NATIONAL ACADEMIES, The Hydrogen Economy — Opportunities, Costs, Barriers and R&D Needs, NA, Washington D.C. (2004).
[503] NOU, Norges Offentlige utredninger, Hydrogen som fremtidens energibærer. Statens forvaltningstjeneste Informatiosjonsafdeling, Oslo, Norway (2004).
[504] HAIDN, O.J., et al., "Improved combustion efficiency of a H_2/O_2 steam generator for spinning reserve application", Proc. 11th World Hydrogen Energy Conf. WHEC'11, Stuttgart (1996) 1418–1427.
[505] KUSTERER, H., Scherf, H., "HYDROSS — Einsatz von Wasserstoff zur Sofort-reservebereitstellung", Proc. Status Seminar Wasserstoff als Energieträger, Jülich, Projektträger Biologie, Energie, Ökologie, Research Center Jülich (1995) 95–128.
[506] GQ-CEC, Euro–Quebec Hydro–Hydrogen Pilot Project — Phase II, Feasibility Study, Final Report, Vol. I–V, Government of Quebec, Commission of the European Communities (1991).
[507] GIACOMAZZI, G., GRETZ, J., Euro-Quebec Hydro-Hydrogen Project (EQHHPP): A challenge to cryogenic technology, Cryogenics **33** (1993) 767–771.
[508] MURASE, M., "R&D plans for WE-NET (World Energy Network) — Hydrogen and clean energy", Proc. NEDO Int. Symp., Tokyo (1995) 55–64.
[509] HIJIKATA, T., Research and development of international clean energy network using hydrogen energy (WE-NET), International Journal of Hydrogen Energy **27** (2002) 115–129.
[510] EUROPEAN HYDROGEN AND FUEL CELL TECHNOLOGY PLATFORM, Deployment Strategy, August 2005, EHFCP, Brussels (2005),
https://www.hfpeurope.org/uploads/878/HFP_ DS_Report_AUG2005.pdf
[511] CASTELLO, P., et al., Techno–Economic Assessment of Hydrogen Transmission & Distribution Systems in Europe in the Medium and Long Term, Report EUR 21586 EN, European Commission, Brussels (2005).
[512] INTERNATIONAL ROAD FEDERATION, World Road Statistics, Alexandria, VA,
http://www.irfnet.org
[513] PYE, S., et al., Cost and Environmental Effectiveness of Options for Reducing Air Pollution from Small scale Combustion Installations, AEAT/ED48256/Final Report Issue 2, AEA Technology Development, Harwell (2004).
[514] LOCKE, M., SAGE: System for Assessing Aviation's Global Emissions, US Federal Aviation Administration, Washington D.C. (2005).
[515] VANDER AREND, P.C., et al., "The liquefaction of hydrogen", In: SCOTT, R.B. et al. (Eds.), Technology and uses of liquid hydrogen, Pergamon Press Ltd, Oxford (1964) 38–105.

[516] PESCHKA, W., Liquid Hydrogen: Fuel of the Future, Springer-Verlag Wien New York (1992).
[517] STANG, J., et al., "On the design of an efficient hydrogen liquefaction plant", Proc. 16th World Hydrogen Energy Conf. WHEC'16, Lyon (2006) paper 324.
[518] MESSER-GRIESHEIM, Wasserstoff, Broschure 0.810.009, Messer-Griesheim, Krefeld (1989).
[519] TZIMAS, E., et al., Hydrogen Storage: State-of-the-Art and Future Perspective, Report EUR 20995 EN, European Commission, JRC Petten, The Netherlands (2003), http://ie.jrc.cec.eu.int/publications/scientific_publications/ 2003/P2003-81=EUR20995EN.pdf
[520] BOWMAN, The Big Chill, The Ames Laboratory, Ames, IA (1998), http://www.external.ameslab.gov/news/Inquiry/fall97/ bigchill .html
[521] FOLDEAKI, M., et al., "Material selection for magnetic refrigerator design", Proc. 7th Canadian Hydrogen Workshop, Quebec City (1995) 439–453.
[522] IWASAKI, W., A consideration of power density and hydrogen production and utilization technologies, International Journal of Hydrogen Energy **28** (2003) 1325–1332.
[523] DRNVICH, R. "Hydrogen delivery liquefaction and compression", Presentation at the Workshop on Strategic Initiatives for Hydrogen Delivery, Washington D.C. (2003).
[524] DOMASHENKO, A., et al., Production, storage and transportation of liquid hydrogen, experience of infrastructure development and operation, International Journal of Hydrogen Energy **27** (2002) 753–755.
[525] SCHLAPBACH, L., ZÜTTEL, A., Hydrogen-storage materials for mobile applications, Nature **414** (2001) 353–358.
[526] CROTOGINO, F., DONADEI, S., BÜNGER, U., LANDINGER, H., "Large scale hydrogen underground storage for securing future energy supplies", Proc. 18th World Hydrogen Energy Conf. WHEC'18, Essen (2010).
[527] BARBIER, F., "Hydrogen distribution infrastructure for an energy system: present status and perspectives of technologies, In: STOLTEN, D. (Ed.), Hydrogen and Fuel Cells — Fundamentals, Technologies and Applications, Wiley-VCH, Weinheim (2010) 121–148.
[528] SIMBECK, D., CHANG, E., Hydrogen Supply: Cost Estimate for Hydrogen Pathways — Scoping Analysis, Report NREL/SR-540-32525, National Renewable Energy Laboratory, Golden, CO (2002).
[529] EDESKUTY, F.J., STEWART, W.F., Safety in the Handling of Cryogenic Fluids, The International Cryogenics Monograph Series, Plenum Press, New York (1996).
[530] TAYLOR, J.B., Technical and economical assessment of methods for the storage of large quantities of hydrogen, International Journal of Hydrogen Energy **11** (1986) 5–22.
[531] LØVVIK, O.M., Viable storage of hydrogen in materials with off-board recharging using high temperature electrolysis, International Journal of Hydrogen Energy **34** (2009) 2679–2683.
[532] TANAKA, H., et al., Hazard assessment of complex hydrides as hydrogen storage materials, International Journal of Hydrogen Energy **34** (2009) 3210–3218.
[533] KEDING, M., REISSNER, A., SCHMID, G., TAJMAR, M., "Innovative hydrogen storage solutions for aerospace applications", Proc. 18th World Hydrogen Energy Conf. WHEC'18, Essen (2010).
[534] U.S. ENERGY INFORMATION ADMINISTRATION, The Impact of Increased Use of Hydrogen on Petroleum Consumption and Carbon Dioxide Emissions, Report SR/OIAF-CNEAF/2008-04, US-EIA, U.S. Department of Energy, Washington D.C. (2008).
[535] AIR LIQUIDE (2009), http://www.airliquide.com/en/our-offer/products/pipelines.html
[536] EDESKUTY, F.J., WILLIAMSON, K.D., Storage and handling of cryogens, Advances in Cryogenic Engineering **17** (1972) 56–68.
[537] BMBF, Icefuel, Project V3MVT100, (2006), http://www.icefuel.de
[538] MARKOWZ, G., DYLLA, A., and ELLIGER, T., "icefuel® — an infrastructure system for cryogenic hydrogen storage, distribution and decentral use", Proc. 18th World Hydrogen Energy Conf. WHEC'18, Essen (2010).
[539] PETERSEN, U., et al., Design and safety considerations for large scale sea-borne hydrogen transport, International Journal of Hydrogen Energy **19** (1994) 597–604.
[540] STUCKI, S., SCHUCAN, T., "Speicherung und Transport von Wasserstoff in Form organischer Verbindungen", In: VDI Berichte No. 1129, VDI-Verlag, Düsseldorf (1994) 175–194.
[541] EPSTEIN, M., et al., "Solar Experiments with a Tubular Reformer", Proc. 8th Int. Symp. on Solar Thermal Concentrating Technologies, Cologne (1996).
[542] NAKAGAWA K., et al., "Nippon oil's activities toward realization of hydrogen economy", Proc. 18th World Hydrogen Energy Conf. WHEC'18, Essen (2010).
[543] OGAWA, M., SHIOZAWA, S., "Evaluation of hydrogen production system with high temperature gas-cooled reactor", Proc. GENES4/ANP Conf., Kyoto (2003) paper 1055.
[544] YILDIZ, B., KAZIMI, M.S., Efficiency of hydrogen production systems using alternative nuclear energy technologies, International Journal of Hydrogen Energy **31** (2006) 77–92.
[545] FORSBERG, C.W., Nuclear Hydrogen for Peak Electricity Production and Spinning Reserve, Report ORNL/TM-2004/194, Oak Ridge National Laboratory, TN (2005).

[546] DUTTA, S., BLOCK, D.L., PORT, R.L., Economic assessment of advanced electrolytic hydrogen production, International Journal of Hydrogen Energy **15** (1990) 387–395.
[547] LIPMAN, T.E., What will Power the Hydrogen Economy? Present and Future Sources of Hydrogen Energy, Report UCD-ITS-RR-04-10, Institute of Transportation Studies, University of California at Davis (2004).
[548] SCHMATJKO, K.-J., "Electrolytic hydrogen production and present grid conditions", In: VERFONDERN, K. (Ed.), Nuclear Energy for Hydrogen Production, Schriften des Forschungszentrums Jülich, Energy Technology, Vol. 58, Research Center Jülich (2007).
[549] NUCNET Background No. 20 (2002).
[550] DELENE, J.G., et al., An Assessment of the Economics of Future Electric Power Generation Options and the Implications, ORNL Report TM-1999-2443, Oak Ridge National Laboratory, TN (1999).
[551] NATIONAL GRID COMPANY, NGC (2001), http://www.nationalgrid.com/uk/
[552] GRUHL, H., et al., In: Ullmanns Enzyklopädie der technischen Chemie, 14, 55 sqq. (1977).
[553] QUANDT, K.H., STREICHER, R., Concept and design of a 3.5 MW pilot plant for high temperature electrolysis of water vapour, International Journal of Hydrogen Energy **11** (1986) 309–315.
[554] EUROPEAN COMMISSION, External Costs — Research Results on Socio–Environmental Damages due to Electricity and Transport, Report 20198, EC, Brussels (2003).
[555] EUROPEAN COMMISSION, The Sustainable Nuclear Energy Technology Platform, Special Report EUR 22842, EC, Brussels (2007).
[556] DREIER, T., Wagner, U., Perspektiven einer Wasserstoff-Energiewirtschaft, Teil 1: Techniken und Systeme zur Wasserstofferzeugung, Brennstoff Wärme Kraft **52**(12) (2000) 41–46.
[557] SHIINA, Y., NISHIHARA, T., Cost Estimation of Hydrogen and DME Produced by Nuclear Heat Utilization System II, Report JAERI-Tech 2004-057, Japan Atomic Energy Agency, Oarai (2004).
[558] CEA-IFP-Total In-House Study, CEA Annual report (2009).
[559] ELECTRIC POWER RESEARCH INSTITUTE, High temperature Gas-Cooled Reactors for the Production of Hydrogen: An Assessment in Support of the Hydrogen Economy, Document # 1007802, EPRI, Palo Alto, CA (2003).
[560] GENERATION IV INTERNATIONAL FORUM, Cost Estimating Guidelines for Generation IV Nuclear Energy Systems, Report GIF/EMWG/2007/004, Revision 4.2, Generation IV International Forum (2007).
[561] TAYLOR, J.P., SHROPSHIRE, D., "Dynamic complexity study of nuclear reactor and process heat application integration", Proc. Int. Conf. on Nuclear Energy Systems for Future Generation and Global Sustainability Global 2009, Paris (2009) paper 9451.
[562] INTERNATIONAL ATOMIC ENERGY AGENCY, Examining the Economics of Seawater Desalination Using DEEP Code, Report IAEA-TECDOC-1186, IAEA, Vienna (2000).
[563] KHAMIS, I., "The development of hydrogen economic evaluation programmeme (HEEP)" (Proc. 4th OECD/NEA Information Exchange Meeting on Nuclear Hydrogen Production, Oakbrook, 2009) OECD-NEA Report No. 6805, Paris (2010) 281–287.
[564] KHAMIS, I., An overview of the IAEA HEEP software and international programmemes on hydrogen production using nuclear energy, International Journal of Hydrogen Energy **36** (2011) 4125–4129.
[565] HARVEGO, E.A., MCKELLAR, M.G., SOHAL, M.S., O'BRIEN, J.E., HERRING, J.S., Economic Analysis of the Reference Design for a Nuclear-Driven High temperature-Electrolysis Hydrogen Production Plant, Report INL/EXT-08-13799, Idaho National Laboratory, ID (2008).
[566] YANG, K.J., LEE, K.Y., LEE, T.H., "Preliminary cost estimates for massive hydrogen production using SI process", Proc. 4th Int. Top. Meeting on High Temperature Reactor Technology HTR2008, Washington D.C. (2008) paper 58142.
[567] SONNTAG, R., et al., Slush Hydrogen, Gelled Hydrogen, and Gelled-Slush Hydrogen, NASP Contractor Report 1027, NASA Langley Research Center, Hampton, VA (1988).
[568] ZABETAKIS, M.G., Safety with Cryogenic Fluids, Plenum Press, New York (1967).
[569] EICHERT, H., et al., Gefährdungspotential bei einem verstärkten Wasserstoff-einsatz. Study for the Büro für Technikfolgenabschätzung des Deutschen Bundestags, Deutsches Zentrum für Luft- und Raumfahrt (DLR), Stuttgart (1992).
[570] CHOUDHURI, A.R., Investigation on the Flame Extinction Limit of Fuel Blends, Combustion and Propulsion Research Laboratory at the University of Texas at El Paso, TX (2005).
[571] KROENER, M., FRITZ, J., SATTELMAYER, T., "Flashback limits for combustion induced vortex breakdown in a swirl burner", Proc. 47th ASME Int. Gas Turbine & Aeroengine Technical Congress, Amsterdam (2002).
[572] TIESZEN, S.R., et al., Detonation cell size measurements in hydrogen–air–steam mixtures, Progress in Astronautics and Aeronautics **106** (1986) 205–219.
[573] KUZNETSOV, M., et al., "Effect of pressure and temperature on flame acceleration and DDT limits for methane–air mixtures", Proc. European Combustion Meeting ECM2005, Louvain-la-Neuve (2005) paper R24-208 (1-5).
[574] ARTHUR D. LITTLE, Final Report on an Investigation of Hazards Associated with the Storage and Handling of Liquid Hydrogen, Report C-61092, Arthur D. Little Inc., Cambridge, MA (1960).
[575] SCHULTZ, M.G., DIEHL, T., BRASSEUR, G.P., ZITTEL, W., Air pollution and climate-forcing impacts of a global hydrogen economy, Science **302** (2003) 624–627.

[576] GROOß, J.-U., FECK, T., VOGEL, B., RIESE, M., “Impact of H_2 emissions of a global hydrogen economy on the stratosphere”, Proc. 18th World Hydrogen Energy Conf. WHEC’18, Essen (2010).
[577] MCCARTY, R.D., HORD, J., RODER, H.M., Selected Properties of Hydrogen (Engineering Design Data), National Bureau of Standards Monograph 168, U.S. Government Printing Office, Washington, DC (1984).
[578] PESCHKA, W., Flüssiger Wasserstoff als Energieträger, Technologie und Anwendungen, Springer Verlag (1984).
[579] INTERNATIONAL ORGANIZATION FOR STANDARDIZATION, Basic Considerations for the Safety of Hydrogen Systems, Technical Report ISO/PDTR 15916, Geneva, Switzerland (2001).
[580] NATIONAL AERONAUTICS AND SPACE ADMINISTRATION, Safety Standard for Hydrogen and Hydrogen Systems, Guidelines for Hydrogen System Design, Materials Selection, Operations, Storage, and Transportation, Office of Safety and Mission Assurance, Washington, DC (1997).

LIST OF ACRONYMS

ADAM	plant with three adiabatic methanation reactors
AFC	alkaline fuel cell
AHTR	advanced high temperature reactor (also: VHTR-LS)
AICC	adiabatic isochoric complete combustion
ANL	Argonne National Laboratory
APU	auxiliary power unit
ATR	autothermal reforming
Bbl	barrel
Btu	British thermal unit
CANDU reactor	Canada deuterium–uranium reactor
CCGT	combined cycle gas turbine
CCS	carbon capture and storage
CETS	chemical energy transmission system
CFD	computer fluid dynamics
CHP	combined heat and power
CH2P	cogeneration of hydrogen and power
CJ	Chapman–Jouguet
CLC	chemical looping combustion
CPOX	catalytic partial oxidation
CTL	coal to liquid
DDT	deflagration–detonation transition
DME	dimethyl-ether
DRI	direct reduction iron
EED	electro–electrodialysis
EPR	European pressurized water reactor

EVA	Einzelspaltrohr-Versuchsanlage (single splitting tube test facility)
FBR	fast breeder reactor
FCV	fuel cell vehicle
FH-ICT	Fraunhofer Institute for Chemical Technology
FP	Framework Programme
GFR	gas cooled fast reactor
GHG	greenhouse gas
GIF	Generation IV International Forum
GTL	gas to liquid
HEEP	hydrogen economic evaluation programme
HHV	higher heating value
HT	high temperature
HTGR	high temperature gas cooled reactor
HTSE	high temperature steam electrolysis
HTTR	high temperature engineering test reactor
HTW	Hochtemperatur Winkler (high temperature Winkler)
HyS	hybrid sulphur
ICE	internal combustion engine
IGCC	integrated gasification combined cycle
IHX	intermediate heat exchanger
I-NERI	international Nuclear Energy Research Initiative
INL	Idaho National Laboratories
IP	integrated project
IPCC	Intergovernmental Panel on Climate Change
ITM	ion transport membrane
KAERI	Korea Atomic Energy Research Institute
KIER	Korea Insitite of Energy Research

KIST	Korea Institute of Science and Technology
KVK	Komponenten-Versuchskreislauf (component test loop)
LBE	lead–bismuth eutectic
LEU	low enriched uranium
LFL	lower flammability limit
LFR	lead cooled fast reactor
LH_2	liquid hydrogen
LHV	lower heating value
LMTD	logarithmic mean temperature difference
LNG	liquefied natural gas
LOCA	loss of coolant accident
LOFC	loss of forced convection
LPG	liquid petroleum gas
LT	low temperature
MCFC	molten carbonate fuel cell
MCH	methylcyclohexane
MHR	modular helium reactor
MIT	Massachusetts Institute of Technology
MOX	mixed (U + Pu) oxide fuel
MSR	molten salt reactor
NG	natural gas
NHI	Nuclear Hydrogen Initiative
NTP	normal temperature pressure
ODS	oxide dispersion strengthened
PAFC	phosphoric acid fuel cell
PBMR	Pebble bed modular reactor
PCHX	printed circuit heat exchanger

PEFC	polymer electrolyte fuel cell
PEM	proton exchange membrane
PFHX	plate-machined heat exchanger
PHX	process heat exchanger
PMHX	plate fin heat exchanger
PNP	prototype nuclear process heat project
POX	partial oxidation
SCWR	supercritical water reactor
SDE	SO_2 depolarized electrolyser
SFR	sodium cooled fast reactor
SID	silicon carbide integrated catalytic decomposer
SMR	steam–methane reforming
SNE-TP	sustainable nuclear energy technology platform
SNG	substitute natural gas
SOEC	solid oxide electrolysis cell
SOFC	solid oxide fuel cell
SRNL	Savannah River National Laboratory
STREP	specific targeted research project
TCE	tonnes of coal equivalent
toe	tonnes of oil equivalent (= 1.428 tce = 41 868 MJ = 11 630 kW·h)
UCG	underground coal gasification
UFL	upper flammability limit
UPS	uninterrupted power supply
VHTR	very high temperature reactor
YSZ	yttria stabilized zirconia

CONTRIBUTORS TO DRAFTING AND REVIEW

Herring, S.J.	Idaho National Laboratory, United States of America
Khamis, I.	International Atomic Energy Agency
Malshe, U.D.	Bhabha Atomic Research Centre (BARC), India
Suppiah, S.	Chalk River Laboratories, Canada
Verfondern, K.	Research Centre Jülich, Germany
Yan, X.-L.	Japan Atomic Energy Agency, Japan

CONSULTANTS MEETING

Vienna, Austria: 27–30 September 2010

Structure of the IAEA Nuclear Energy Series

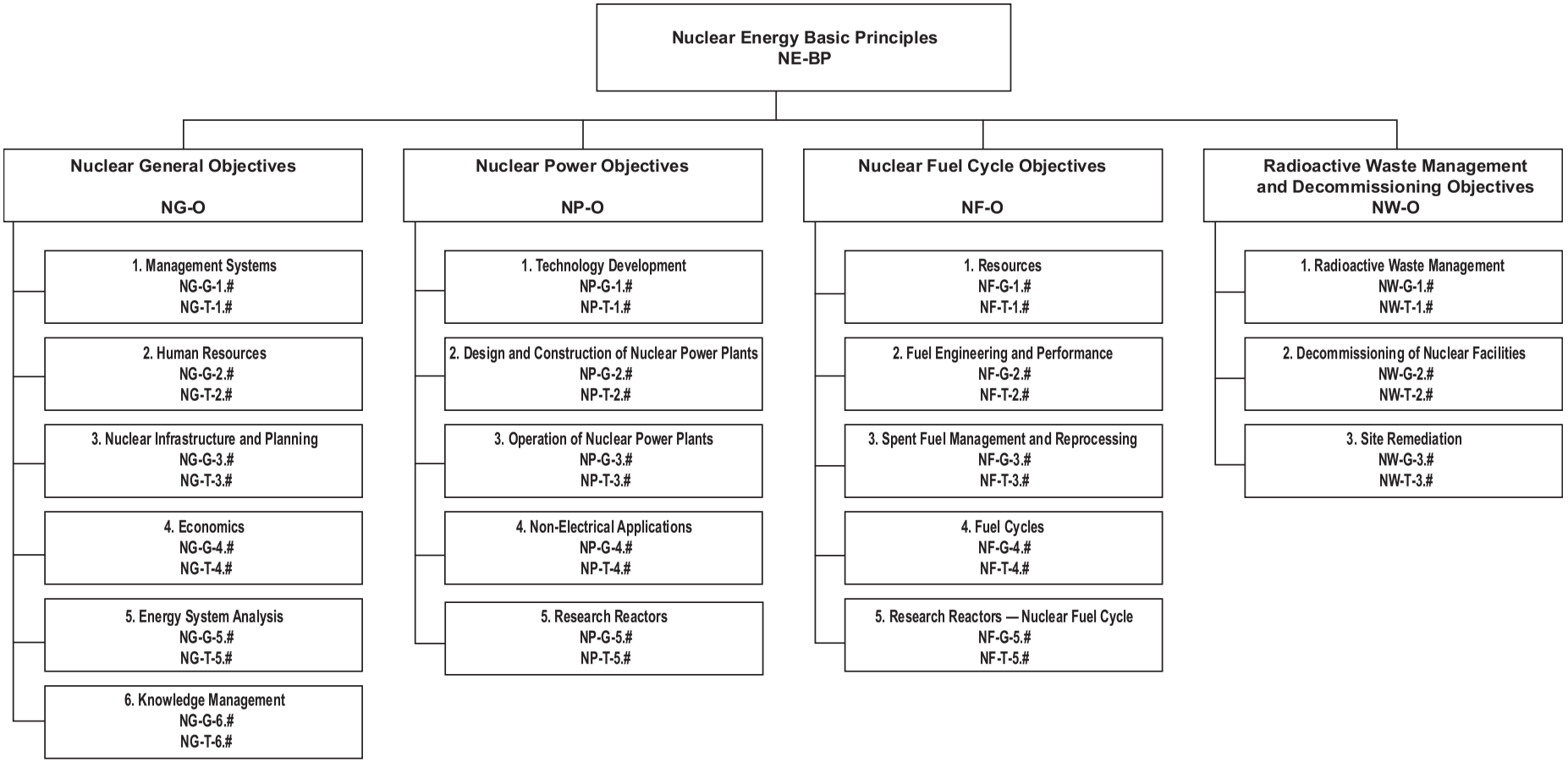

Key

BP: Basic Principles
O: Objectives
G: Guides
T: Technical Reports
Nos. 1-6: Topic designations
#: Guide or Report number (1, 2, 3, 4, etc.)

Examples

NG-G-3.1: Nuclear General (**NG**), **G**uide, Nuclear Infrastructure and Planning (topic **3**), **#1**
NP-T-5.4: Nuclear Power (**NP**), Report (**T**), Research Reactors (topic **5**), **#4**
NF-T-3.6: Nuclear Fuel (**NF**), Report (**T**), Spent Fuel Management and Reprocessing, **#6**
NW-G-1.1: Radioactive Waste Management and Decommissioning (**NW**), **G**uide, Radioactive Waste (topic **1**), **#1**

IAEA
International Atomic Energy Agency

Where to order IAEA publications

In the following countries IAEA publications may be purchased from the sources listed below, or from major local booksellers. Payment may be made in local currency or with UNESCO coupons.

AUSTRALIA
DA Information Services, 648 Whitehorse Road, MITCHAM 3132
Telephone: +61 3 9210 7777 • Fax: +61 3 9210 7788
Email: service@dadirect.com.au • Web site: http://www.dadirect.com.au

BELGIUM
Jean de Lannoy, avenue du Roi 202, B-1190 Brussels
Telephone: +32 2 538 43 08 • Fax: +32 2 538 08 41
Email: jean.de.lannoy@infoboard.be • Web site: http://www.jean-de-lannoy.be

CANADA
Bernan Associates, 4501 Forbes Blvd, Suite 200, Lanham, MD 20706-4346, USA
Telephone: 1-800-865-3457 • Fax: 1-800-865-3450
Email: customercare@bernan.com • Web site: http://www.bernan.com

Renouf Publishing Company Ltd., 1-5369 Canotek Rd., Ottawa, Ontario, K1J 9J3
Telephone: +613 745 2665 • Fax: +613 745 7660
Email: order.dept@renoufbooks.com • Web site: http://www.renoufbooks.com

CHINA
IAEA Publications in Chinese: China Nuclear Energy Industry Corporation, Translation Section, P.O. Box 2103, Beijing

CZECH REPUBLIC
Suweco CZ, S.R.O., Klecakova 347, 180 21 Praha 9
Telephone: +420 26603 5364 • Fax: +420 28482 1646
Email: nakup@suweco.cz • Web site: http://www.suweco.cz

FINLAND
Akateeminen Kirjakauppa, PO BOX 128 (Keskuskatu 1), FIN-00101 Helsinki
Telephone: +358 9 121 41 • Fax: +358 9 121 4450
Email: akatilaus@akateeminen.com • Web site: http://www.akateeminen.com

FRANCE
Form-Edit, 5, rue Janssen, P.O. Box 25, F-75921 Paris Cedex 19
Telephone: +33 1 42 01 49 49 • Fax: +33 1 42 01 90 90
Email: formedit@formedit.fr • Web site: http://www. formedit.fr

Lavoisier SAS, 145 rue de Provigny, 94236 Cachan Cedex
Telephone: + 33 1 47 40 67 02 • Fax +33 1 47 40 67 02
Email: romuald.verrier@lavoisier.fr • Web site: http://www.lavoisier.fr

GERMANY
UNO-Verlag, Vertriebs- und Verlags GmbH, Am Hofgarten 10, D-53113 Bonn
Telephone: + 49 228 94 90 20 • Fax: +49 228 94 90 20 or +49 228 94 90 222
Email: bestellung@uno-verlag.de • Web site: http://www.uno-verlag.de

HUNGARY
Librotrade Ltd., Book Import, P.O. Box 126, H-1656 Budapest
Telephone: +36 1 257 7777 • Fax: +36 1 257 7472 • Email: books@librotrade.hu

INDIA
Allied Publishers Group, 1st Floor, Dubash House, 15, J. N. Heredia Marg, Ballard Estate, Mumbai 400 001,
Telephone: +91 22 22617926/27 • Fax: +91 22 22617928
Email: alliedpl@vsnl.com • Web site: http://www.alliedpublishers.com

Bookwell, 2/72, Nirankari Colony, Delhi 110009
Telephone: +91 11 23268786, +91 11 23257264 • Fax: +91 11 23281315
Email: bookwell@vsnl.net

ITALY
Libreria Scientifica Dott. Lucio di Biasio “AEIOU”, Via Coronelli 6, I-20146 Milan
Telephone: +39 02 48 95 45 52 or 48 95 45 62 • Fax: +39 02 48 95 45 48
Email: info@libreriaaeiou.eu • Website: www.libreriaaeiou.eu

JAPAN
Maruzen Company Ltd, 1-9-18, Kaigan, Minato-ku, Tokyo, 105-0022
Telephone: +81 3 6367 6079 • Fax: +81 3 6367 6207
Email: journal@maruzen.co.jp • Web site: http://www.maruzen.co.jp

REPUBLIC OF KOREA
KINS Inc., Information Business Dept. Samho Bldg. 2nd Floor, 275-1 Yang Jae-dong SeoCho-G, Seoul 137-130
Telephone: +02 589 1740 • Fax: +02 589 1746 • Web site: http://www.kins.re.kr

NETHERLANDS
De Lindeboom Internationale Publicaties B.V., M.A. de Ruyterstraat 20A, NL-7482 BZ Haaksbergen
Telephone: +31 (0) 53 5740004 • Fax: +31 (0) 53 5729296
Email: books@delindeboom.com • Web site: http://www.delindeboom.com

Martinus Nijhoff International, Koraalrood 50, P.O. Box 1853, 2700 CZ Zoetermeer
Telephone: +31 793 684 400 • Fax: +31 793 615 698
Email: info@nijhoff.nl • Web site: http://www.nijhoff.nl

Swets and Zeitlinger b.v., P.O. Box 830, 2160 SZ Lisse
Telephone: +31 252 435 111 • Fax: +31 252 415 888
Email: infoho@swets.nl • Web site: http://www.swets.nl

NEW ZEALAND
DA Information Services, 648 Whitehorse Road, MITCHAM 3132, Australia
Telephone: +61 3 9210 7777 • Fax: +61 3 9210 7788
Email: service@dadirect.com.au • Web site: http://www.dadirect.com.au

SLOVENIA
Cankarjeva Zalozba d.d., Kopitarjeva 2, SI-1512 Ljubljana
Telephone: +386 1 432 31 44 • Fax: +386 1 230 14 35
Email: import.books@cankarjeva-z.si • Web site: http://www.cankarjeva-z.si/uvoz

SPAIN
Díaz de Santos, S.A., c/ Juan Bravo, 3A, E-28006 Madrid
Telephone: +34 91 781 94 80 • Fax: +34 91 575 55 63
Email: compras@diazdesantos.es, carmela@diazdesantos.es, barcelona@diazdesantos.es, julio@diazdesantos.es
Web site: http://www.diazdesantos.es

UNITED KINGDOM
The Stationery Office Ltd, International Sales Agency, PO Box 29, Norwich, NR3 1 GN
Telephone (orders): +44 870 600 5552 • (enquiries): +44 207 873 8372 • Fax: +44 207 873 8203
Email (orders): book.orders@tso.co.uk • (enquiries): book.enquiries@tso.co.uk • Web site: http://www.tso.co.uk

On-line orders
DELTA Int. Book Wholesalers Ltd., 39 Alexandra Road, Addlestone, Surrey, KT15 2PQ
Email: info@profbooks.com • Web site: http://www.profbooks.com

Books on the Environment
Earthprint Ltd., P.O. Box 119, Stevenage SG1 4TP
Telephone: +44 1438748111 • Fax: +44 1438748844
Email: orders@earthprint.com • Web site: http://www.earthprint.com

UNITED NATIONS
Dept. I004, Room DC2-0853, First Avenue at 46th Street, New York, N.Y. 10017, USA
(UN) Telephone: +800 253-9646 or +212 963-8302 • Fax: +212 963-3489
Email: publications@un.org • Web site: http://www.un.org

UNITED STATES OF AMERICA
Bernan Associates, 4501 Forbes Blvd., Suite 200, Lanham, MD 20706-4346
Telephone: 1-800-865-3457 • Fax: 1-800-865-3450
Email: customercare@bernan.com · Web site: http://www.bernan.com

Renouf Publishing Company Ltd., 812 Proctor Ave., Ogdensburg, NY, 13669
Telephone: +888 551 7470 (toll-free) • Fax: +888 568 8546 (toll-free)
Email: order.dept@renoufbooks.com • Web site: http://www.renoufbooks.com

Orders and requests for information may also be addressed directly to:

Marketing and Sales Unit, International Atomic Energy Agency
Vienna International Centre, PO Box 100, 1400 Vienna, Austria
Telephone: +43 1 2600 22529 (or 22530) • Fax: +43 1 2600 29302
Email: sales.publications@iaea.org • Web site: http://www.iaea.org/books

12-43111

INTERNATIONAL ATOMIC ENERGY AGENCY
VIENNA
ISBN 978–92–0–135110–4
ISSN 1995–7807